IMPACT OF THE GLIOMA MICROENVIRONMENT ON ANTITUMOR IMMUNITY

EDITED BY: Valérie Dutoit, Lukas Bunse and Payal Watchmaker
PUBLISHED IN: Frontiers in Oncology and Frontiers in Immunology

frontiers Research Topics

frontiers

ISSN 1664-8714
ISBN 978-2-88974-191-5
DOI 10.3389/978-2-88974-191-5

About Frontiers

Frontiers is more than just an open-access publisher of scholarly articles: it is a pioneering approach to the world of academia, radically improving the way scholarly research is managed. The grand vision of Frontiers is a world where all people have an equal opportunity to seek, share and generate knowledge. Frontiers provides immediate and permanent online open access to all its publications, but this alone is not enough to realize our grand goals.

Frontiers Journal Series

The Frontiers Journal Series is a multi-tier and interdisciplinary set of open-access, online journals, promising a paradigm shift from the current review, selection and dissemination processes in academic publishing. All Frontiers journals are driven by researchers for researchers; therefore, they constitute a service to the scholarly community. At the same time, the Frontiers Journal Series operates on a revolutionary invention, the tiered publishing system, initially addressing specific communities of scholars, and gradually climbing up to broader public understanding, thus serving the interests of the lay society, too.

Dedication to Quality

Each Frontiers article is a landmark of the highest quality, thanks to genuinely collaborative interactions between authors and review editors, who include some of the world's best academicians. Research must be certified by peers before entering a stream of knowledge that may eventually reach the public - and shape society; therefore, Frontiers only applies the most rigorous and unbiased reviews.
Frontiers revolutionizes research publishing by freely delivering the most outstanding research, evaluated with no bias from both the academic and social point of view. By applying the most advanced information technologies, Frontiers is catapulting scholarly publishing into a new generation.

What are Frontiers Research Topics?

Frontiers Research Topics are very popular trademarks of the Frontiers Journals Series: they are collections of at least ten articles, all centered on a particular subject. With their unique mix of varied contributions from Original Research to Review Articles, Frontiers Research Topics unify the most influential researchers, the latest key findings and historical advances in a hot research area! Find out more on how to host your own Frontiers Research Topic or contribute to one as an author by contacting the Frontiers Editorial Office: frontiersin.org/about/contact

IMPACT OF THE GLIOMA MICROENVIRONMENT ON ANTITUMOR IMMUNITY

Topic Editors:
Valérie Dutoit, Université de Genève, Switzerland
Lukas Bunse, German Cancer Research Center (DKFZ), Germany
Payal Watchmaker, University of California, San Francisco, United States

Citation: Dutoit, V., Bunse, L., Watchmaker, P., eds. (2022). Impact of the Glioma Microenvironment on Antitumor Immunity. Lausanne: Frontiers Media SA.
doi: 10.3389/978-2-88974-191-5

Table of Contents

frontiers in Oncology

MINI REVIEW
published: 15 February 2021
doi: 10.3389/fonc.2020.617385

Immunosuppression in Gliomas *via* PD-1/PD-L1 Axis and Adenosine Pathway

Thamiris Becker Scheffel[1,2], *Nathália Grave*[1,3], *Pedro Vargas*[1,3], *Fernando Mendonça Diz*[1], *Liliana Rockenbach*[1,3] *and Fernanda Bueno Morrone*[1,2,3*]

[1] *Laboratório de Farmacologia Aplicada, Escola de Ciências da Saúde e da Vida, Pontifícia Universidade Católica do Rio Grande do Sul (PUCRS), Porto Alegre, Brazil,* [2] *Programa de Pós-Graduação em Biologia Celular e Molecular, Escola de Ciências da Saúde e da Vida, Pontifícia Universidade Católica do Rio Grande do Sul (PUCRS), Porto Alegre, Brazil,* [3] *Programa de Pós-Graduação em Medicina e Ciências da Saúde, Escola de Medicina, Pontifícia Universidade Católica do Rio Grande do Sul (PUCRS), Porto Alegre, Brazil*

OPEN ACCESS

Edited by:
Payal Watchmaker, University of California, San Francisco, United States

Reviewed by:
Zoltan Vereb, University of Szeged, Hungary
Sadhak Sengupta, Triumvira Immunologics, Inc., United States

***Correspondence:**
Fernanda Bueno Morrone
fernanda.morrone@pucrs.br; fbmorrone@gmail.com

Specialty section:
This article was submitted to Cancer Immunity and Immunotherapy, a section of the journal Frontiers in Oncology

Received: *14 October 2020*
Accepted: *23 December 2020*
Published: *15 February 2021*

Citation:
Scheffel TB, Grave N, Vargas P, Diz FM, Rockenbach L and Morrone FB (2021) Immunosuppression in Gliomas via PD-1/PD-L1 Axis and Adenosine Pathway. Front. Oncol. 10:617385. doi: 10.3389/fonc.2020.617385

Glioblastoma is the most malignant and lethal subtype of glioma. Despite progress in therapeutic approaches, issues with the tumor immune landscape persist. Multiple immunosuppression pathways coexist in the tumor microenvironment, which can determine tumor progression and therapy outcomes. Research in immune checkpoints, such as the PD-1/PD-L1 axis, has renewed the interest in immune-based cancer therapies due to their ability to prevent immunosuppression against tumors. However, PD-1/PD-L1 blockage is not completely effective, as some patients remain unresponsive to such treatment. The production of adenosine is a major obstacle for the efficacy of immune therapies and is a key source of innate or adaptive resistance. In general, adenosine promotes the pro-tumor immune response, dictates the profile of suppressive immune cells, modulates the release of anti-inflammatory cytokines, and induces the expression of alternative immune checkpoint molecules, such as PD-1, thus maintaining a loop of immunosuppression. In this context, this review aims to depict the complexity of the immunosuppression in glioma microenvironment. We primarily consider the PD-1/PD-L1 axis and adenosine pathway, which may be critical points of resistance and potential targets for tumor treatment strategies.

Keywords: glioma, immunosuppression, adenosine, PD-1/PD-L1, tumor microenvironment

INTRODUCTION

Cancer is characterized by genetic instability and heterogeneity in the tumor microenvironment (TME). Currently, one of the major challenges in cancer treatment is to block the multifaceted network of tumor mechanisms that cause immunosuppression and resistance to cell death (1, 2).

Gliomas are the most aggressive primary brain tumors in adults, and are of different genetic, phenotypic, and pathological subtypes, depending on the glial lineage from which they arise (3). Glioblastoma multiforme (GBM) is the most malignant subtype of diffuse glioma, and remains the

most lethal among brain tumors (3, 4). Similar to other malignances, genetic and phenotypic variability within GBM present problems for the treatment of these tumors (5, 6).

Despite advances in modern medicine, the prognosis for malignant glioma patients remains just over a year. Therefore, several avenues, such as tumor resistance, need to be explored to improve therapeutic approaches (7, 8). Tumor resistance is related to redundant and synergic immunosuppressive pathways coexisting in the TME. Malignant and host cells create a specific niche, where cellular interactions shape the profile of cytokines and chemokines, favoring pro-tumoral activities (9).

Recent evidence has shown that tumors are proficient at evading immunostimulatory responses and resisting standard therapy by producing adenosine (ADO) and upregulating molecules like programmed cell death 1 (PD-1) that function as immune checkpoints (9, 10). Therefore, this review aims to depict the complexity of the immune system in the glioma microenvironment, including the role of the PD-1/PD-L1 axis and adenosine pathway in the maintenance of immunosuppression and resistance to glioma treatments.

IMMUNE SYSTEM IN GLIOMAS

Tumor-Associated Immunosuppression

The TME has been described as a regulator of tumor progression as well as a mediator of successful therapy. The complexity of tumor niche is shaped by a variable combination of stromal cells, endothelial cells, fibroblasts, cancer stem cells and immune system. Specially, stromal and cancer stem cells have been described by a significant involvement on glioma initiation, maintenance, and progression. In fact, cancer stem cells can suppress cytotoxic responses and modulate immune and endothelial cell functions, suggesting an important role of these cells on immunosuppressive tumor site (11, 12). Importantly, studies have demonstrated an increasing significance of the immune infiltrate and its products in the process of tumor malignancy (10, 13, 14). In GBM, resident microglia and macrophages represent up to one-third of the tumor mass and may have pro-tumorigenic functions (15).

Microglial cells are considered "plastic" due to their ability to change their functions based on environment. These cells may exhibit pro-inflammatory (M1) or immunosuppressive (M2) functions (15–17). All macrophages produce several cytokines such as tumor necrosis factor (TNF) and interleukins (IL-1, IL-6, IL-8, and IL-12), which influence the generation of effector cells and activation of lymphocytes (14). Previous data has shown that the interaction between glioma and microglia is very complex and may not be beneficial for tumor resolution. Indeed, microglia cells co-cultured with glioma cells lack phagocytic ability against tumor cells (16).

Immunosuppression in gliomas involves dynamic crosstalk between tumor and stromal cells, tumor-associated macrophages (TAMs), microglia, regulatory T cells (Tregs), and tumor-infiltrating lymphocytes (TIL) (17–19). Generally, the number of $CD4^+$ lymphocytes is lower than that of $CD8^+$ lymphocytes in a GBM environment, but it has been observed that the numbers of both $CD4^+$ and $CD8^+$ cells increase with tumor grade (20). Despite the presence of these lymphocytes in the GBM microenvironment, effector T cells do not function properly and M2 macrophages are unable to promote $CD4^+$ and $CD8^+$ polarized immune responses, which are important for the regulation of Tregs (21).

The release of chemokines such as C-C motif chemokine ligand 2 (CCL2) is critical for the recruitment of Tregs and myeloid derived suppressor cells (MDSCs). MDSCs alter the TME and suppress immune responses by blocking $CD8^+$ cells and inhibiting the function of natural killer cells (NK) (9, 19, 22). NK cells express death receptor ligands, which can induce caspase-dependent apoptosis in target cells, and can thus kill cancer cells (23). This cytotoxic action is limited by GBM-HLA-G expression, which protects tumors from T cells and NK-mediated killing. Moreover, NK cells are reduced in GBM patients (23, 24).

Studies have shown influences of effector and regulator T cells on the prognosis of cancer patients. For example, Tregs play a significant role in the immune response in the TME since they mediate immunotolerance by suppressing the function of effector T cells (9, 23). GBM patients showed an increased proportion of Tregs among $CD4^+$ cells, contributing to the reduced immune response (25). In addition, the removal of the Treg fraction from patients with GBM rescues T cell proliferation and pro-inflammatory cytokine production to standard levels. This reveals the critical role of Tregs in glioma-mediated immunosuppression (26).

The PD-1/PD-L1 Axis

Interest in immune-based treatments of cancer has been renewed after the discovery of immune checkpoint inhibitors. Recently, the co-Nobel Prize in Physiology or Medicine was awarded to Tasuko Honjo, who showed the negative regulation of T cells mediated by the PD-1 pathway (27, 28). Thus, the expression and activity of immunological checkpoints have emerged as the main immunosuppressive mechanisms in gliomas (29, 30).

The transmembrane co-receptor PD-1 (CD279), encoded by the PDCD1 gene, belongs to the family of immunoglobulins and is expressed predominantly by activated T lymphocytes (31). PD-1 is often activated by PD-L1 (B7-H1; CD274), one of the ligands known to be expressed by antigen presenting cells (APCs), B lymphocytes, and parenchymal cells. PD-L2 (B7-DC; CD273) is another ligand for PD-1 and is expressed by fewer cells than PD-L1 (31–33). In normal conditions, PD-1/PD-L engagement occurs controlling a prolonged activation of immune system, often avoiding autoimmunity processes. It is known that PD-1 interaction provides T-cell inhibitory signals. PD-1/PD-L engagement during TCR stimulation leads to tyrosine phosphorylation of the PD-1 cytoplasmic tail on high affinity sites for SH2 domain-containing phosphatase (SHP-2 and SHP-1), resulting in the dephosphorylation of proximal signaling molecules which decrease T cell proliferation and survival by attenuate PI3K and Akt pathways (31, 34).

Importantly, expression of PD-L1 has been detected in glioma (35–37). Moreover, PD-L1 expression in tumor cells is related to

levels of malignancy, and high PD-L1 expression is associated with greater invasiveness and aggressiveness of GBM cells (38, 39). Studies have shown heterogeneity of PD-L1 expression in tumor mass such that greater expression is seen at the edges of the tumor than in the core. This could also facilitate immune evasion and invasiveness of gliomas (38, 40).

The expression of PD-L1 in the TME is regulated mainly by cytokine and receptor antigen signaling (31). Interferon gamma (IFN-γ) is the major PD-L1 regulation factor in tumor cells and reflects ongoing antitumor immune activity. In addition, oncogenic mutations, such as loss of phosphatase and tensin homolog (PTEN) in glioma, can activate PD-L1 expression in tumor cells (31, 41, 42).

The PD-1/PD-L1 pathway has been appropriated by tumor cells to resist antitumor responses and facilitate tumor survival (42, 43). Influenced by hypoxia, cytokines, and oncogenes, GBM cells express PD-L1, which engages with the PD-1 receptor primarily on T cells and attenuates its functions, effectively reducing the antitumor activity of these cells (42).

A subset of lymphocytes (Tregs) has emerged as a critical target in cancer therapy. Tregs express both PD-1 and PD-L1, and the generation, immunosuppression, and interaction of Tregs with effector T cells could be, at least in part, modulated by PD-1/PD-L1 binding (44, 45). Francisco et al. have shown that PD-L1 can induce and maintain the expression of FOXP3 in induced Tregs, suggesting that PD-L1 may control Treg plasticity (46).

GBM cells were also able to upregulate PD-L1 expression in tumor-infiltrating macrophages *via* modulation of IL-10 signaling (29). Macrophages may express PD-1 and PD-L1 (47). PD-1 positive TAMs exhibit decreased phagocytic potential and PD-1 blockade improves macrophage functionalities, besides reducing tumor growth in mouse models of cancer (48).

The use of PD-1 inhibitors is becoming an effective strategy for the treatment of cancer, and several preclinical and clinical studies have been conducted for GBM (30, 49). In fact, immune checkpoint inhibitors may reverse the immunosuppressive condition and restore dysfunctional or "exhausted" T cell function in cancer (39). However, some patients remain unresponsive to PD-1/PD-L1 blockade. Therefore, fresh clinical trials to evaluate tumor resistance in PD-1/PD-L1 immunotherapy in GBM patients are required (39, 50).

Immunomodulation by Adenosine Pathway in Gliomas

Adenosine 5′-triphosphate (ATP) is the main energy molecule produced by cellular respiration. It has multiple release routes and is involved in practically all cellular responses (51). It is known that during cancer growth and progression, ATP and its main metabolite, ADO, are actively secreted or generated in the extracellular space, and accumulate to high levels in the TME (52–54).

Physiologically, extracellular ATP (eATP) functions as a "danger" signal alerting the immune system to the presence of inflammation, and is crucial for inflammasome activation and the concomitant release of cytokines (54, 55). These effects are mediated *via* P2 receptors, which are subdivided into two subfamilies: P2X ionotropic ion channel receptors (P2X1-7) and P2Y G-protein-coupled receptors ($P2Y_{1, 2, 4, 6, 11, 12, 13, 14}$) (53–55). These purinergic receptors display distinct agonist affinity and specificity, affecting both tumor and immune cells, depending on the eATP levels available in the TME (56). Different innate and adaptive immune responses are generated through activation of P2 receptors by eATP (**Table 1**). Particularly, the participation of P2X7 in inflammation is extensive, and has been better characterized compared to that of other P2 receptors (54, 55, 71–74). The direct role of P2X7 in carcinogenesis is still controversial, but it is known that cell growth or death is triggered according to the cell type that expresses P2X7 and their activation level (75).

P2 receptors are assumed to be inactive in normal physiological conditions, where ATP-dependent signaling should be at baseline levels. Ectoenzymes, such as NTPDase1 (CD39) and ecto-5′-nucleotidase (CD73), maintain levels of extracellular ATP, which is crucial to avoid P2 receptor desensitization (76).

In the TME, eATP is quickly hydrolyzed to AMP by CD39 of TILs which is then efficiently converted to the immunosuppressant ADO by CD73 expressed in glioma cells (77). ATP hydrolysis drives the immune response to collaborate with tumor growth, making the CD39/CD73 axis an important regulator of immune effector function. This is a hallmark of cancer (78–81). Interestingly, CD39 inhibition can restore TIL function, and a single nucleotide polymorphism has been identified that may predict dysfunctional $CD39^{+}$ expression in TILs in some solid tumors (81).

The suppressive role of ADO in the TME is primarily mediated by cytotoxicity, anti-inflammatory cytokine production, and restriction of immune cell infiltration (79). Adenosine effects are mediated by P1 receptors (A_1, A_{2a}, A_{2b}, and A_3). Interestingly, the pro-tumoral effects of ADO occur mainly through A2 receptors, as depicted in **Table 1**. Physiologically, ADO orchestrates tissue recovery after initial inflammation, which involves the decrease of M1 phenotype, cell proliferation, and angiogenesis. This sets the stage for tumor growth. Hence, the ADO signaling pathway may be an important therapeutic target (79, 80, 82, 83).

THE PD-1/PD-L1 AXIS AND ADENOSINE PATHWAY IN GLIOMAS

Typically, tumor growth involves disruption of the surrounding microenvironment, in which extracellular nucleotides might confer immunomodulatory properties that are critical for driving glioma immune escape. One of the main mechanisms of tumor immune evasion is the generation of high levels of ADO mediated by excessive activity of ectonucleotidases (83–85).

An effective immunosuppressive environment is maintained when the actions of ADO are synergistic or additive to other immunosuppressive mechanisms. There is growing evidence that immunosuppressive proteins, such as PD-1 and PD-L1, can be increased in the TME by the same mechanism that is implicated in hypoxia-mediated adenosinergic immunosuppression (86). Extracellular ADO increases in hypoxic conditions, concomitant with upregulation of CD39 and CD73. In addition, the oxygen

TABLE 1 | Functional immune responses triggered by nucleotides and nucleosides actions in glioblastoma microenvironment.

		Main purinergic receptors	Immune outcome	Immune cell profile	Cytokine & chemokine profile	Ref
Immunostimulatory	ATP	P2X1	**Proinflammatory response**	Chemotaxis of neutrophils; chemotaxis and phagocytosis of macrophages; release of chemokines and cytokines from eosinophils; T cell activation.	IL-2, IL-8, IL-12, TNF-α (increased)	(57–61)
		P2X4	**Proinflammatory response**	Microglia activation and proliferation; macrophages stimulation and maturation; stimulation of dendritic cells; T cell activation.	IL-2, IL-12, TNF-α (increased)	(54, 57, 59–62)
		P2X5	**Adaptative immune response**	T and B lymphocytes activation.	IL-2 (increased)	(57, 60)
		P2X7	**Proinflammatory response** **NLRP3 inflammasome activation**	Recruitment of macrophages and neutrophils; inhibition of the suppressive potential of Tregs.	IL-1β, IL-12, IL-18, IFN-γ, TNF-α, CCL-3, CXCL2 (increased)	(54, 57, 60–65)
		$P2Y_2$	**Innate immune response**	Chemotaxis of eosinophils, monocytes/macrophages, microglia, and dendritic cells; degranulation of neutrophils.	MCP-1, CCL2, IL-6, IL-8, IL-33 (increased)	(57, 66)
Immunosuppressive	ADO	A_{2a}	**Immunosuppressive response**	Macrophage differentiation into M2 phenotype; T cell anergy; increase differentiation and suppressive effect of Treg; upregulation of immune checkpoint receptors (e.g., PD-1, CTLA-4); reduction of NK cell cytotoxicity; inhibition of neutrophil and microglial chemotaxis; modulation of chemokines profile in neutrophils.	IL-10, VEGF, TGF-β (increased) IL-12, TNF-α, nitric oxide; IFN-γ (decreased)	(57, 64, 67–70)
		A_{2b}	**Anti-inflammatory response**	Macrophage differentiation into M2 phenotype; reduction of monocyte differentiation to dendritic cell; MDSCs expansion; reduction of adherence and degranulation of neutrophils.	Arginase 1, IL-10, VEGF, IL-6; TGF-β (increased) IL-12, TNF-α (decreased)	(57, 68, 70)

ATP, adenosine 5'-triphosphate; ADO, adenosine; CCL3, C-C motif chemokine ligand 3; CXCL2, C-X-C motif ligand 2; CTLA-4, cytotoxic T-lymphocyte antigen 4; IFN-γ, interferon γ; IL-, interleukine; MCP-1, monocyte chemoattractant protein-1; MDSC, myeloid-derived suppressor cell; NK, natural killer; NLRP3, sensor molecule (NOD- LRR- and pyrin domain-containing protein 3); PD-1, programmed cell death 1; TGF-β, transforming growth factor beta; TNF-α, tumor necrosis factor alpha; VEGF, vascular endothelial growth factor.

deprivation in the tumor core is related to the upregulation of immunoregulatory mechanisms such as PD-L1 expression in glioma cells, making them resistant to T cell-dependent cytotoxicity (87).

Notably, it was suggested that ADO also induces increase in PD-1 levels (88) because ADO signaling may positively regulate TGF-β levels. TGF-β is mainly involved in stopping effector T cell activation and stimulating the activity of antigen presenting cells that express PD-1 (89). In the presence of TGF-β, $CD4^+$ cell activation may predominantly generate inducible Tregs (90). These cells primarily express CD39, while GBM cells express high levels of CD73, suggesting that cancer and immune cells can cooperate to promote local adenosinergic immunosuppression. Accordingly, a vicious cycle is formed, favoring the upregulation of the PD-1/PD-L1 axis that maintains a complex synergism between the ADO pathway and immune checkpoint axis (77, 91, 92).

Additionally, ADO is involved in macrophage activation, predominantly *via* A_{2a} (A_{2a}R) and A_{2b} receptors (A_{2b}R). A_{2b}R stimulation during macrophage differentiation could skew macrophages toward the M2 phenotype. M2 macrophages can express immunoregulatory molecules such as arginase, TGF-β, and PD-1/PD-L1 proteins, resulting in the downregulation of cellular immune responses (93).

Overall, the multifaceted role of ADO in tumor immune evasion is seen in its promotion of pro-tumor rather than antitumor immune responses, dictation of Treg function, inhibition of effector T cells, modulation of anti-inflammatory cytokines, and induction of immune checkpoints as illustrated in **Figure 1** (83, 84, 86, 88, 89, 94).

Taken together, the ADO pathway and the PD-1/PD-L1 axis may act synergistically to modify the TME, favoring tumor progression. Based on this landscape, the GBM standard treatment should be multimodal, involving maximal surgical removal followed by radiotherapy (RT) and/or temozolomide (TMZ). Despite such treatments, refractoriness is often observed (95, 96).

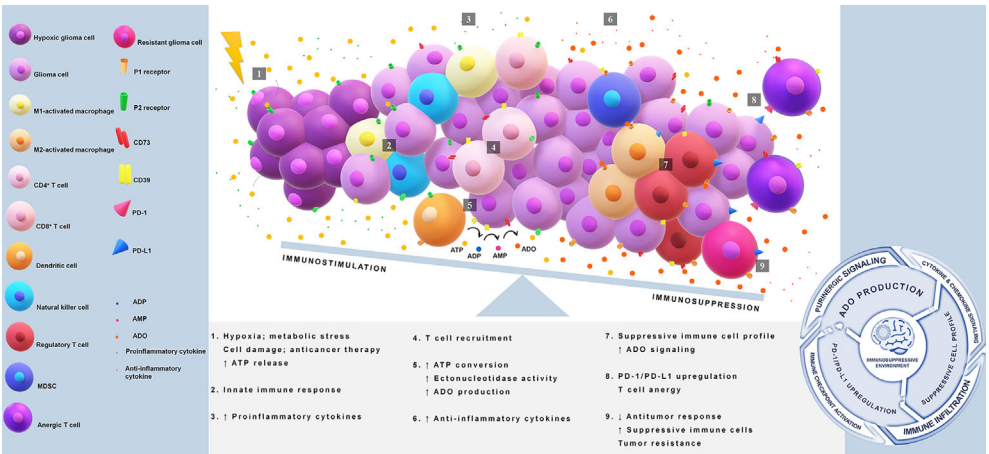

FIGURE 1 | Immunosuppression in glioblastoma *via* PD-1/PD-L1 axis and adenosine pathway. Tumor core acquires reduction in the oxygen supply causing a release of high amounts of ATP. This nucleotide acts as a damage-associated molecular pattern (DAMP) and starts immune activation. Extracellular ATP binds to P2 receptors and triggers proinflammatory responses through the induction of cytokines and chemokines. A disbalance in the ATP concentration gradient leads to an upregulation of CD39/CD73 axis, favoring adenosine production. Adenosine is a key molecule that initiates a suppressive immune cell infiltration and drives the activation of PD-1/PD-L1 axis. The immunosuppressive loop is maintained indirectly by ATP release and adenosine signaling, which avoids antitumor defenses, promotes immunosuppressive cell profile, and induces upregulation of immune checkpoints. ATP, adenosine 5′-triphosphate; ADO, adenosine; CD39 or ectonucleoside triphosphate diphosphohydrolase 1, cluster of differentiation 39; CD73 or ecto-5′-nucleotidase, cluster of differentiation 73; DAMP, damage-associated molecular pattern; MDSC, myeloid-derived suppressor cells; PD-1, programmed cell death 1; PD-L1, programmed cell death ligand 1.

TMZ and RT have several immune modulatory effects on the TME. In addition to immune activation, RT and TMZ therapy may even worsen the immunosuppressive system in GBM. This is because both interventions induce immunogenic cell death, and consequently release immunogenic factors such as ATP (97, 98). ATP binding to P2X7 purinergic receptor is a signal that primes the immune system against tumor (99). However, glioma therapy also increases the expression of CD39/CD73. Hence, it is possible that ADO rapidly rises in the TME. RT also stimulates TGF-β and chemokines that promote the recruitment of immunosuppressive cells; therefore, the activity of the PD-1/PD-L1 axis increases. In addition to Tregs recruitment, RT-induced ATP release also can be related to Treg differentiation from naïve $CD4^+$ cell *via* $A_{2b}R$ (100, 101).

Interestingly, some studies have shown irradiation-induced PD-L1 expression through an IFN-dependent pathway (102). Xia et al. (90) showed that under RT, PD-L1 expression in GBM cells is greater than that observed without radiation, and that the inhibition of PD-L1 increased radio-sensitivity in these cells (90). High PD-L1 expression was also associated with high numbers of M2 macrophages and Tregs, and low $CD8^+$ cells in the TME, favoring high levels of ADO. Consequently, the immunosuppressive TME resulting from PD-L1-induction could be an important mechanism of tumor radio-resistance (103).

PD-1/PD-L1 AXIS BLOCKADE AND PURINERGIC MODULATION THERAPY

Recently, there has been a surge in the research and development of immunotherapies in cancer, using the PD-1/PD-L1 axis blockade as a strategy to reduce tumor immune evasion (103). Anti-PD-1 immunotherapy has been shown to be successful in prolonging responses in only a fraction of patients (36, 47). There is a subset of them who fail to overcome the immunosuppression, even they can mount an antitumor response. Consequently, the focus of research has changed toward uncovering intrinsic factors that contribute to treatment failures. Currently, the ADO pathway is considered a barrier for the efficacy of immunotherapies (103, 104).

As seen in some solid tumors, alternative immunomodulatory molecules, including CD39, CD73 and $A_{2a}R$, are upregulated in response to anti-PD-1 monoclonal antibody (mAb) (88, 104). Beavis et al. showed that $CD73^+$ tumor cells restrict anti-PD-1 efficacy, and that this effect was relieved by concomitant treatment with an $A_{2a}R$ antagonist (104). Li et al. demonstrated that CD39 inhibition sensitizes tumor-resistant models to anti-PD1, and that blocking CD39 activity is associated with the enrichment of cytotoxic T cells in the TME and upregulation of inflammatory markers on these infiltrates (105).

Various clinical trials that evaluate purinergic modulation therapy along with anti-PD-1 mAb or anti-PD-L1 mAb are currently active or in the recruitment phase for multiple cancer types (**Supplementary Table S1**). In fact, simultaneous therapy using PD-1 inhibitors and targeting the adenosine pathway was more effective in improving survival, reducing tumor growth, and limiting metastasis than single therapy in some types of cancer (106–108). Furthermore, there is a rising range of anti-CD73 mAbs being tested in combination with other immunotherapies, generating encouraging results (100, 101, 109).

GBM is one of the most immunologically "cold" tumors among all cancers. The PD1/PD-L1 target characterizes a potential

strategy for conversion of the "cold" GBM microenvironment into a "hot" microenvironment to enhance the immune response to antitumor immunotherapy (110). Therefore, anti-PD-1/PD-L1 is an emerging therapeutic possibility in gliomas (111). Since PD-1/PD-L1 blockades do not significantly promote global survivor in patients with recurrent GBM compared with standard therapy, clinical trials are exploring association between anti-PD-1/PD-L1 mAb with standard radio/chemotherapy and bevacizumab or new therapies such as genetically engineered T cells and vaccines (39, 111, 112). Most studies are undergoing clinical trials evaluation and the results still have not provided decisive conclusions (**Supplementary Table S2**).

Overall, the study of alterations in "purinoma" caused by immune checkpoint inhibitors would likely provide insights for the development of interventions to overcome the immunosuppressive glioma environment and boost immune responses generated by immunotherapies.

CONCLUSION

The environment surrounding tumors directly impacts their progression. Multiple redundant and compensatory pro-tumor pathways coexist in the TME and are closely related to the success of therapeutic treatments. Immune checkpoint inhibitors help in cancer treatment, though it is not effective in some patients. Thus, immunosuppression remains a major obstacle to therapeutic success. Studies on the relationship between purinergic signaling and inflammation show that the ADO pathway and PD-1/PD-L1 axis have a close relationship and act together to create a favorable environment for tumor immune evasion. The eATP-adenosine axis has a specific role in pro-tumor immune responses including upregulating the PD-1/PD-L1 axis. The ADO pathway has been identified as the main compensatory route involved in the maintenance of immunosuppression in patients using anti-PD-1 immunotherapy, through a drop in innate or adaptive immunity. Therefore, future research should focus on concomitant disruption of the ADO pathway and PD-1/PD-L1 axis to avoid cancer resistance.

AUTHOR CONTRIBUTIONS

TS, NG, PV, FD, and LR critically appraised the literature and wrote. FM reviewed and approved final version of the manuscript.

FUNDING

The authors thank Coordenação de Aperfeiçoamento de Pessoal de Nivel Superior–Brasil [CAPES, Finance Code 001] and Conselho Nacional de Desenvolvimento Científico e Tecnológico [CNPq, project no. 310317/2018-5] for financial support.

SUPPLEMENTARY MATERIAL

The Supplementary Material for this article can be found online at: https://www.frontiersin.org/articles/10.3389/fonc.2020.617385/full#supplementary-material

REFERENCES

1. Hanahan D, Weinberg RA. Hallmarks of Cancer: The Next Generation. *Cell* (2011) 144:646–74. doi: 10.1016/j.cell.2011.02.013
2. Zugazagoitia J, Guedes C, Ponce S, Ferrer I, Molina-Pinelo S, Paz-Ares L. Current Challenges in Cancer Treatment. *Clin Ther* (2016) 38:1551–66. doi: 10.1016/j.clinthera.2016.03.026
3. Gerlinger M, Swanton C. How Darwinian models inform therapeutic failure initiated by clonal heterogeneity in cancer medicine. *Br J Cancer* (2010) 103:1139–43. doi: 10.1038/sj.bjc.6605912
4. Pawlowska E, Szczepanska J, Szatkowska M, Blasiak J. An Interplay between Senescence, Apoptosis and Autophagy in Glioblastoma Multiforme-Role in Pathogenesis and Therapeutic Perspective. *Int J Mol Sci* (2018) 19(3):889–908. doi: 10.3390/ijms19030889
5. Ostrom QT, Gittleman H, Xu J, Kromer C, Wolinsky Y, Kruchko C, et al. CBTRUS Statistical Report: Primary Brain and Other Central Nervous System Tumors Diagnosed in the United States in 2009-2013. *Neuro-Oncol* (2016) 18:v1–v75. doi: 10.1093/neuonc/now207
6. Shergalis A, Bankhead A, Luesakul U, Muangsin N, Neamati N. Current Challenges and Opportunities in Treating Glioblastoma. *Pharmacol Rev* (2018) 70:412–45. doi: 10.1124/pr.117.014944
7. Fridman WH, Zitvogel L, Sautès-Fridman C, Kroemer G. The immune contexture in cancer prognosis and treatment. *Nat Rev Clin Oncol* (2017) 14:717–34. doi: 10.1038/nrclinonc.2017.101
8. Martinez-Lage M, Lynch TM, Bi Y, Cocito C, Way GP, Pal S, et al. Immune landscapes associated with different glioblastoma molecular subtypes. *Acta Neuropathol Commun* (2019) 7:203. doi: 10.1186/s40478-019-0803-6
9. Li G, Qin Z, Chen Z, Xie L, Wang R, Zhao H. Tumor Microenvironment in Treatment of Glioma. *Open Med* (2017) 12:247–51. doi: 10.1515/med-2017-0035
10. Strepkos D, Markouli M, Klonou A, Piperi C, Papavassiliou AG. Insights in the immunobiology of glioblastoma. *J Mol Med* (2020) 98:1–10. doi: 10.1007/s00109-019-01835-4
11. Hamerlik P. Cancer Stem Cells and Glioblastoma. In: A Sedo, R Mentlein, editors. *Glioma Cell Biology*. Vienna: Springer Vienna. (2014) p. 3–22. doi: 10.1007/978-3-7091-1431-5_1
12. Ma Q, Long W, Xing C, Chu J, Luo M, Wang HY, et al. Cancer Stem Cells and Immunosuppressive Microenvironment in Glioma. *Front Immunol* (2018) 9:2924–41. doi: 10.3389/fimmu.2018.02924
13. Locarno CV, Simonelli M, Carenza C, Capucetti A, Stanzani E, Lorenzi E, et al. Role of myeloid cells in the immunosuppressive microenvironment in gliomas. *Immunobiology* (2020) 225:151853. doi: 10.1016/j.imbio.2019.10.002
14. Guadagno E, Presta I, Maisano D, Donato A, Pirrone CK, Cardillo G, et al. Role of Macrophages in Brain Tumor Growth and Progression. *Int J Mol Sci* (2018) 19(4):1005–24. doi: 10.3390/ijms19041005
15. Lee KY. M1 and M2 polarization of macrophages: a mini-review. *Med Biol Sci Eng* (2019) 2:1–5. doi: 10.30579/mbse.2019.2.1.1
16. Voisin P, Bouchaud V, Merle M, Diolez P, Duffy L, Flint K, et al. Microglia in Close Vicinity of Glioma Cells: Correlation Between Phenotype and Metabolic Alterations. *Front Neuroenerget* (2010) 2:131–46. doi: 10.3389/fnene.2010.00131
17. Watters JJ, Schartner JM, Badie B. Microglia function in brain tumors. *J Neurosci Res* (2005) 81:447–55. doi: 10.1002/jnr.20485

18. Kim R, Emi M, Tanabe K. Cancer immunosuppression and autoimmune disease: beyond immunosuppressive networks for tumour immunity. *Immunology* (2006) 119:254–64. doi: 10.1111/j.1365-2567.2006.02430.x
19. Sayour EJ, McLendon P, McLendon R, De Leon G, Reynolds R, Kresak J, et al. Increased proportion of FoxP3+ regulatory T cells in tumor infiltrating lymphocytes is associated with tumor recurrence and reduced survival in patients with glioblastoma. *Cancer Immunol Immunother CII* (2015) 64:419–27. doi: 10.1007/s00262-014-1651-7
20. Dubinski D, Wölfer J, Hasselblatt M, Schneider-Hohendorf T, Bogdahn U, Stummer W, et al. CD4+ T effector memory cell dysfunction is associated with the accumulation of granulocytic myeloid-derived suppressor cells in glioblastoma patients. *Neuro-Oncol* (2016) 18:807–18. doi: 10.1093/neuonc/nov280
21. Sica A, Larghi P, Mancino A, Rubino L, Porta C, Totaro MG, et al. Macrophage polarization in tumour progression. *Semin Cancer Biol* (2008) 18:349–55. doi: 10.1016/j.semcancer.2008.03.004
22. Iwami K, Natsume A, Wakabayashi T. Cytokine networks in glioma. *Neurosurg Rev* (2011) 34:253–63. doi: 10.1007/s10143-011-0320-y
23. Zhang X, Safonova A, Rao A, Amankulor N. Role of natural killer cells in isocitrate dehydrogenase 1/2 mutant glioma pathogenesis and emerging therapies. *Glioma* (2019) 2:133. doi: 10.4103/glioma.glioma_10_19
24. Gieryng A, Pszczolkowska D, Walentynowicz KA, Rajan WD, Kaminska B. Immune microenvironment of gliomas. *Lab Invest J Tech Methods Pathol* (2017) 97:498–518. doi: 10.1038/labinvest.2017.19
25. Woroniecka KI, Rhodin KE, Chongsathidkiet P, Keith KA. Fecci PE. T-cell Dysfunction in Glioblastoma: Applying a New Framework. *Clin Cancer Res Off J Am Assoc Cancer Res* (2018) 24:3792–802. doi: 10.1158/1078-0432.CCR-18-0047
26. Wainwright DA, Dey M, Chang A, Lesniak MS. Targeting Tregs in Malignant Brain Cancer: Overcoming IDO. *Front Immunol* (2013) 4:116. doi: 10.3389/fimmu.2013.00116
27. Ishida Y, Agata Y, Shibahara K, Honjo T. Induced expression of PD-1, a novel member of the immunoglobulin gene superfamily, upon programmed cell death. *EMBO J* (1992) 11:3887–95. doi: 10.1002/j.1460-2075.1992.tb05481.x
28. Ledford H, Else H, Warren M. Cancer immunologists scoop medicine Nobel prize. *Nature* (2018) 562:20–1. doi: 10.1038/d41586-018-06751-0
29. Bloch O, Crane CA, Kaur R, Safaee M, Rutkowski MJ, Parsa AT. Gliomas promote immunosuppression through induction of B7-H1 expression in tumor-associated macrophages. *Clin Cancer Res Off J Am Assoc Cancer Res* (2013) 19:3165–75. doi: 10.1158/1078-0432.CCR-12-3314
30. Preusser M, Lim M, Hafler DA, Reardon DA, Sampson JH. Prospects of immune checkpoint modulators in the treatment of glioblastoma. *Nat Rev Neurol* (2015) 11:504–14. doi: 10.1038/nrneurol.2015.139
31. Francisco LM, Sage PT, Sharpe AH. The PD-1 Pathway in Tolerance and Autoimmunity. *Immunol Rev* (2010) 236:219–42. doi: 10.1111/j.1600-065X.2010.00923.x
32. Flies DB, Chen L. The new B7s: playing a pivotal role in tumor immunity. *J Immunother Hagerstown Md 1997* (2007) 30:251–60. doi: 10.1097/CJI.0b013e31802e085a
33. Pedoeem A, Azoulay-Alfaguter I, Strazza M, Silverman GJ, Mor A. Programmed death-1 pathway in cancer and autoimmunity. *Clin Immunol Orlando Fla* (2014) 153:145–52. doi: 10.1016/j.clim.2014.04.010
34. Patsoukis N, Wang Q, Strauss L, Boussiotis VA. Revisiting the PD-1 pathway. *Sci Adv* (2020) 6:2712–25. doi: 10.1126/sciadv.abd2712
35. Wintterle S, Schreiner B, Mitsdoerffer M, Schneider D, Chen L, Meyermann R, et al. Expression of the B7-related molecule B7-H1 by glioma cells: a potential mechanism of immune paralysis. *Cancer Res* (2003) 63:7462–7.
36. Berghoff AS, Kiesel B, Widhalm G, Rajky O, Ricken G, Wöhrer A, et al. Programmed death ligand 1 expression and tumor-infiltrating lymphocytes in glioblastoma. *Neuro-Oncol* (2015) 17:1064–75. doi: 10.1093/neuonc/nou307
37. Nduom EK, Wei J, Yaghi NK, Huang N, Kong L-Y, Gabrusiewicz K, et al. PD-L1 expression and prognostic impact in glioblastoma. *Neuro-Oncol* (2016) 18:195–205. doi: 10.1093/neuonc/nov172
38. Yao Y, Tao R, Wang X, Wang Y, Mao Y, Zhou LF. B7-H1 is correlated with malignancy-grade gliomas but is not expressed exclusively on tumor stem-like cells. *Neuro-Oncol* (2009) 11:757–66. doi: 10.1215/15228517-2009-014
39. Xue S, Hu M, Iyer V, Yu J. Blocking the PD-1/PD-L1 pathway in glioma: a potential new treatment strategy. *J Hematol OncolJ Hematol Oncol* (2017) 10:81–91. doi: 10.1186/s13045-017-0455-6
40. Wilmotte R, Burkhardt K, Kindler V, Belkouch M-C, Dussex G, de Tribolet N, et al. B7-homolog 1 expression by human glioma: a new mechanism of immune evasion. *Neuroreport* (2005) 16:1081–5. doi: 10.1097/00001756-200507130-00010
41. Parsa AT, Waldron JS, Panner A, Crane CA, Parney IF, Barry JJ, et al. Loss of tumor suppressor PTEN function increases B7-H1 expression and immunoresistance in glioma. *Nat Med* (2007) 13:84–8. doi: 10.1038/nm1517
42. Broekman ML, Maas SLN, Abels ER, Mempel TR, Krichevsky AM, Breakefield XO. Multidimensional communication in the microenvirons of glioblastoma. *Nat Rev Neurol* (2018) 14:482–95. doi: 10.1038/s41582-018-0025-8
43. Keir ME, Butte MJ, Freeman GJ, Sharpe AH. PD-1 and its ligands in tolerance and immunity. *Annu Rev Immunol* (2008) 26:677–704. doi: 10.1146/annurev.immunol.26.021607.090331
44. Wang L, Pino-Lagos K, de Vries VC, Guleria I, Sayegh MH, Noelle RJ. Programmed death 1 ligand signaling regulates the generation of adaptive Foxp3+CD4+ regulatory T cells. *Proc Natl Acad Sci USA* (2008) 105:9331–6. doi: 10.1073/pnas.0710441105
45. Gianchecchi E, Fierabracci A. Inhibitory Receptors and Pathways of Lymphocytes: The Role of PD-1 in Treg Development and Their Involvement in Autoimmunity Onset and Cancer Progression. *Front Immunol* (2018) 9:2374. doi: 10.3389/fimmu.2018.02374
46. Francisco LM, Salinas VH, Brown KE, Vanguri VK, Freeman GJ, Kuchroo VK, et al. PD-L1 regulates the development, maintenance, and function of induced regulatory T cells. *J Exp Med* (2009) 206:3015–29. doi: 10.1084/jem.20090847
47. Cai J, Qi Q, Qian X, Han J, Zhu X, Zhang Q, et al. The role of PD-1/PD-L1 axis and macrophage in the progression and treatment of cancer. *J Cancer Res Clin Oncol* (2019) 145:1377–85. doi: 10.1007/s00432-019-02879-2
48. Gordon SR, Maute RL, Dulken BW, Hutter G, George BM, McCracken MN, et al. PD-1 expression by tumour-associated macrophages inhibits phagocytosis and tumour immunity. *Nature* (2017) 545:495–9. doi: 10.1038/nature22396
49. Schalper KA, Rodriguez-Ruiz ME, Diez-Valle R, López-Janeiro A, Porciuncula A, Idoate MA, et al. Neoadjuvant nivolumab modifies the tumor immune microenvironment in resectable glioblastoma. *Nat Med* (2019) 25:470–6. doi: 10.1038/s41591-018-0339-5
50. Zou W, Wolchok JD, Chen L. PD-L1 (B7-H1) and PD-1 Pathway Blockade for Cancer Therapy: Mechanisms, Response Biomarkers and Combinations. *Sci Transl Med* (2016) 8:328rv4. doi: 10.1126/scitranslmed.aad7118
51. Nath S, Villadsen J. Oxidative phosphorylation revisited. *Biotechnol Bioeng* (2015) 112:429–37. doi: 10.1002/bit.25492
52. Burnstock G, Di Virgilio F. Purinergic signalling and cancer. *Purinerg Signal* (2013) 9:491–540. doi: 10.1007/s11302-013-9372-5
53. Borea PA, Gessi S, Merighi S, Vincenzi F, Varani K. Pharmacology of Adenosine Receptors: The State of the Art. *Physiol Rev* (2018) 98:1591–625. doi: 10.1152/physrev.00049.2017
54. Di Virgilio F, Sarti AC, Falzoni S, De Marchi E, Adinolfi E. Extracellular ATP and P2 purinergic signalling in the tumour microenvironment. *Nat Rev Cancer* (2018) 18:601–18. doi: 10.1038/s41568-018-0037-0
55. Eltzschig HK, Sitkovsky MV, Robson SC. Purinergic signaling during inflammation. *N Engl J Med* (2012) 367:2322–33. doi: 10.1056/NEJMra1205750
56. Volonté C, Amadio S, D'Ambrosi N, Colpi M, Burnstock G. P2 receptor web: Complexity and fine-tuning. *Pharmacol Ther* (2006) 112:264–80. doi: 10.1016/j.pharmthera.2005.04.012
57. Burnstock G, Boeynaems J-M. Purinergic signalling and immune cells. *Purinerg Signal* (2014) 10:529–64. doi: 10.1007/s11302-014-9427-2
58. Lecut C, Frederix K, Johnson DM, Deroanne C, Thiry M, Faccinetto C, et al. P2X1 ion channels promote neutrophil chemotaxis through Rho kinase activation. *J Immunol Baltim Md 1950* (2009) 183:2801–9. doi: 10.4049/jimmunol.0804007
59. Woehrle T, Yip L, Elkhal A, Sumi Y, Chen Y, Yao Y, et al. Pannexin-1 hemichannel–mediated ATP release together with P2X1 and P2X4 receptors regulate T-cell activation at the immune synapse. *Blood* (2010) 116:3475–84. doi: 10.1182/blood-2010-04-277707

60. Jacob F, Novo CP, Bachert C, Van Crombruggen K. Purinergic signaling in inflammatory cells: P2 receptor expression, functional effects, and modulation of inflammatory responses. *Purinerg Signal* (2013) 9:285–306. doi: 10.1007/s11302-013-9357-4
61. Mostofa AGM, Punganuru SR, Madala HR, Al-Obaide M, Srivenugopal KS. The Process and Regulatory Components of Inflammation in Brain Oncogenesis. *Biomolecules* (2017) 7(2):34–67. doi: 10.3390/biom7020034
62. Burnstock G. P2X ion channel receptors and inflammation. *Purinerg Signal* (2016) 12:59–67. doi: 10.1007/s11302-015-9493-0
63. Hide I, Tanaka M, Inoue A, Nakajima K, Kohsaka S, Inoue K, et al. Extracellular ATP triggers tumor necrosis factor-alpha release from rat microglia. *J Neurochem* (2000) 75:965–72. doi: 10.1046/j.1471-4159.2000.0750965.x
64. Ferrari D, McNamee EN, Idzko M, Gambari R, Eltzschig HK. Purinergic Signaling During Immune Cell Trafficking. *Trends Immunol* (2016) 37:399–411. doi: 10.1016/j.it.2016.04.004
65. Kan LK, Williams D, Drummond K, O'Brien T, Monif M. The role of microglia and P2X7 receptors in gliomas. *J Neuroimmunol* (2019) 332:138–46. doi: 10.1016/j.jneuroim.2019.04.010
66. Rayah A, Kanellopoulos JM, Di Virgilio F. P2 receptors and immunity. *Microbes Infect Inst Pasteur* (2012) 14:1254–62. doi: 10.1016/j.micinf.2012.07.006
67. Campos-Contreras ADR, Díaz-Muñoz M, Vázquez-Cuevas FG. Purinergic Signaling in the Hallmarks of Cancer. *Cells* (2020) 9:1612–36. doi: 10.3390/cells9071612
68. Di Virgilio F, Vuerich M. Purinergic signaling in the immune system. *Auton Neurosci* (2015) 191:117–23. doi: 10.1016/j.autneu.2015.04.011
69. Leone RD, Lo Y-C, Powell JD. A2aR antagonists: Next generation checkpoint blockade for cancer immunotherapy. *Comput Struct Biotechnol J* (2015) 13:265–72. doi: 10.1016/j.csbj.2015.03.008
70. Vigano S, Alatzoglou D, Irving M, Ménétrier-Caux C, Caux C, Romero P, et al. Targeting Adenosine in Cancer Immunotherapy to Enhance T-Cell Function. *Front Immunol* (2019) 10:925–55. doi: 10.3389/fimmu.2019.00925
71. De Marchi E, Orioli E, Pegoraro A, Sangaletti S, Portararo P, Curti A, et al. The P2X7 receptor modulates immune cells infiltration, ectonucleotidases expression and extracellular ATP levels in the tumor microenvironment. *Oncogene* (2019) 38:3636–50. doi: 10.1038/s41388-019-0684-y
72. Wiley JS, Sluyter R, Gu BJ, Stokes L, Fuller SJ. The human P2X7 receptor and its role in innate immunity. *Tissue Antigens* (2011) 78:321–32. doi: 10.1111/j.1399-0039.2011.01780.x
73. Rassendren F, Buell GN, Virginio C, Collo G, North RA, Surprenant A. The permeabilizing ATP receptor, P2X7. Cloning and expression of a human cDNA. *J Biol Chem* (1997) 272:5482–6. doi: 10.1074/jbc.272.9.5482
74. Monif M, Reid CA, Powell KL, Smart ML, Williams DA. The P2X7 receptor drives microglial activation and proliferation: a trophic role for P2X7R pore. *J Neurosci Off J Soc Neurosci* (2009) 29:3781–91. doi: 10.1523/JNEUROSCI.5512-08.2009
75. de Andrade Mello P, Coutinho-Silva R, Savio LEB. Multifaceted Effects of Extracellular Adenosine Triphosphate and Adenosine in the Tumor-Host Interaction and Therapeutic Perspectives. *Front Immunol* (2017) 8:1526. doi: 10.3389/fimmu.2017.01526
76. Di Virgilio F. Purinergic mechanism in the immune system: A signal of danger for dendritic cells. *Purinerg Signal* (2005) 1:205–9. doi: 10.1007/s11302-005-6312-z
77. Xu S, Shao Q-Q, Sun J-T, Yang N, Xie Q, Wang D-H, et al. Synergy between the ectoenzymes CD39 and CD73 contributes to adenosinergic immunosuppression in human malignant gliomas. *Neuro-Oncol* (2013) 15:1160–72. doi: 10.1093/neuonc/not067
78. Bastid J, Regairaz A, Bonnefoy N, Déjou C, Giustiniani J, Laheurte C, et al. Inhibition of CD39 enzymatic function at the surface of tumor cells alleviates their immunosuppressive activity. *Cancer Immunol Res* (2015) 3:254–65. doi: 10.1158/2326-6066.CIR-14-0018
79. Vijayan D, Young A, Teng MWL, Smyth MJ. Targeting immunosuppressive adenosine in cancer. *Nat Rev Cancer* (2017) 17:709–24. doi: 10.1038/nrc.2017.86
80. Hammami A, Allard D, Allard B, Stagg J. Targeting the adenosine pathway for cancer immunotherapy. *Semin Immunol* (2019) 42:101304. doi: 10.1016/j.smim.2019.101304
81. Gallerano D, Ciminati S, Grimaldi A, Piconese S, Cammarata I, Focaccetti C, et al. Genetically driven CD39 expression shapes human tumor-infiltrating CD8+ T-cell functions. (2020) *Int J Cancer* 147(9):2597–610. doi: 10.1002/ijc.33131
82. Haskó G, Linden J, Cronstein B, Pacher P. Adenosine receptors: therapeutic aspects for inflammatory and immune diseases. *Nat Rev Drug Discovery* (2008) 7:759–70. doi: 10.1038/nrd2638
83. Antonioli L, Blandizzi C, Pacher P, Haskó G. Immunity, inflammation and cancer: a leading role for adenosine. *Nat Rev Cancer* (2013) 13:842–57. doi: 10.1038/nrc3613
84. Stagg J, Smyth MJ. Extracellular adenosine triphosphate and adenosine in cancer. *Oncogene* (2010) 29:5346–58. doi: 10.1038/onc.2010.292
85. Beavis PA, Stagg J, Darcy PK, Smyth MJ. CD73: a potent suppressor of antitumor immune responses. *Trends Immunol* (2012) 33:231–7. doi: 10.1016/j.it.2012.02.009
86. Ohta A, Kini R, Ohta A, Subramanian M, Madasu M, Sitkovsky M. The development and immunosuppressive functions of CD4+ CD25+ FoxP3+ regulatory T cells are under influence of the adenosine-A2A adenosine receptor pathway. *Front Immunol* (2012) 3:190–202. doi: 10.3389/fimmu.2012.00190
87. Ohta A. Oxygen-dependent regulation of immune checkpoint mechanisms. *Int Immunol* (2018) 30(8):335–43. doi: 10.1093/intimm/dxy038
88. Allard B, Pommey S, Smyth MJ, Stagg J. Targeting CD73 Enhances the Antitumor Activity of Anti-PD-1 and Anti-CTLA-4 mAbs. *Clin Cancer Res* (2013) 19:5626–35. doi: 10.1158/1078-0432.CCR-13-0545
89. Zarek PE, Huang C-T, Lutz ER, Kowalski J, Horton MR, Linden J, et al. A2A receptor signaling promotes peripheral tolerance by inducing T-cell anergy and the generation of adaptive regulatory T cells. *Blood* (2008) 111:251–9. doi: 10.1182/blood-2007-03-081646
90. Xia W, Zhu J, Tang Y, Wang X, Wei X, Zheng X, et al. PD-L1 Inhibitor Regulates the miR-33a-5p/PTEN Signaling Pathway and Can Be Targeted to Sensitize Glioblastomas to Radiation. *Front Oncol* (2020) 10:821–33. doi: 10.3389/fonc.2020.00821
91. Bavaresco L, Bernardi A, Braganhol E, Cappellari AR, Rockenbach L, Farias PF, et al. The role of ecto-5'-nucleotidase/CD73 in glioma cell line proliferation. *Mol Cell Biochem* (2008) 319:61–8. doi: 10.1007/s11010-008-9877-3
92. Ceruti S, Abbracchio M. Adenosine Signaling in Glioma Cells. *Adv Exp Med Biol* 986:13–30. doi: 10.1007/978-3-030-30651-9_2
93. Csóka B, Selmeczy Z, Koscsó B, Németh ZH, Pacher P, Murray PJ, et al. Adenosine promotes alternative macrophage activation via A2A and A2B receptors. *FASEB J Off Publ Fed Am Soc Exp Biol* (2012) 26:376–86. doi: 10.1096/fj.11-190934
94. Sek K, Mølck C, Stewart GD, Kats L, Darcy PK, Beavis PA. Targeting Adenosine Receptor Signaling in Cancer Immunotherapy. *Int J Mol Sci* (2018) 19:3837–60. doi: 10.3390/ijms19123837
95. Stupp R, Mason WP, van den Bent MJ, Weller M, Fisher B, Taphoorn MJB, et al. Radiotherapy plus concomitant and adjuvant temozolomide for glioblastoma. *N Engl J Med* (2005) 352:987–96. doi: 10.1056/NEJMoa043330
96. Fernandes C, Costa A, Osório L, Lago RC, Linhares P, Carvalho B, et al. Current Standards of Care in Glioblastoma Therapy, in: *Glioblastoma*. Brisbane (AU): Codon Publications. Available at: http://www.ncbi.nlm.nih.gov/books/NBK469987/ (Accessed August 6, 2020).
97. Martins I, Tesniere A, Kepp O, Michaud M, Schlemmer F, Senovilla L, et al. Chemotherapy induces ATP release from tumor cells. *Cell Cycle* (2009) 8:3723–8. doi: 10.4161/cc.8.22.10026
98. Golden EB, Frances D, Pellicciotta I, Demaria S, Helen Barcellos-Hoff M, Formenti SC. Radiation fosters dose-dependent and chemotherapy-induced immunogenic cell death. *Oncoimmunology* (2014) 3:e28518. doi: 10.4161/onci.28518
99. Ma Y, Kepp O, Ghiringhelli F, Apetoh L, Aymeric L, Locher C, et al. Chemotherapy and radiotherapy: cryptic anticancer vaccines. *Semin Immunol* (2010) 22:113–24. doi: 10.1016/j.smim.2010.03.001
100. Hay CM, Sult E, Huang Q, Mulgrew K, Fuhrmann SR, McGlinchey KA, et al. Targeting CD73 in the tumor microenvironment with MEDI9447. *Oncoimmunology* (2016) 5(8):e1208875–85. doi: 10.1080/2162402X.2016.1208875
101. Siu LL, Burris H, Le DT, Hollebecque A, Steeghs N, Delord J-P, et al. Abstract CT180: Preliminary phase 1 profile of BMS-986179, an anti-CD73 antibody,

in combination with nivolumab in patients with advanced solid tumors. *Cancer Res* (2018) 78:CT180–0. doi: 10.1158/1538-7445.AM2018-CT180
102. Dovedi SJ, Adlard AL, Lipowska-Bhalla G, McKenna C, Jones S, Cheadle EJ, et al. Acquired resistance to fractionated radiotherapy can be overcome by concurrent PD-L1 blockade. *Cancer Res* (2014) 74:5458–68. doi: 10.1158/0008-5472.CAN-14-1258
103. Jang B-S, Kim IA. A Radiosensitivity Gene Signature and PD-L1 Status Predict Clinical Outcome of Patients with Glioblastoma Multiforme in The Cancer Genome Atlas Dataset. *Cancer Res Treat Off J Korean Cancer Assoc* (2020) 52:530–42. doi: 10.4143/crt.2019.440
104. Beavis PA, Milenkovski N, Henderson MA, John LB, Allard B, Loi S, et al. Adenosine Receptor 2A Blockade Increases the Efficacy of Anti-PD-1 through Enhanced Antitumor T-cell Responses. *Cancer Immunol Res* (2015) 3:506–17. doi: 10.1158/2326-6066.CIR-14-0211
105. Li X-Y, Moesta AK, Xiao C, Nakamura K, Casey M, Zhang H, et al. Targeting CD39 in cancer reveals an extracellular ATP and inflammasome driven tumor immunity. *Cancer Discovery* (2019) 9(12):1754–73. doi: 10.1158/2159-8290.CD-19-0541
106. Mittal D, Young A, Stannard K, Yong M, Teng MWL, Allard B, et al. Antimetastatic effects of blocking PD-1 and the adenosine A2A receptor. *Cancer Res* (2014) 74:3652–8. doi: 10.1158/0008-5472.CAN-14-0957
107. Leone RD, Sun I-M, Oh M-H, Sun I-H, Wen J, Englert J, et al. Inhibition of the adenosine A2a receptor modulates expression of T cell coinhibitory receptors and improves effector function for enhanced checkpoint blockade and ACT in murine cancer models. *Cancer Immunol Immunother CII* (2018) 67:1271–84. doi: 10.1007/s00262-018-2186-0
108. Steingold JM, Hatfield SM. Targeting Hypoxia-A2A Adenosinergic Immunosuppression of Antitumor T Cells During Cancer Immunotherapy. *Front Immunol* (2020) 11:570041–48. doi: 10.3389/fimmu.2020.570041
109. Barnhart BC, Sega E, Yamniuk A, Hatcher S, Lei M, Ghermazien H, et al. Abstract 1476: A therapeutic antibody that inhibits CD73 activity by dual mechanisms. *Cancer Res* (2016) 76:1476–6. doi: 10.1158/1538-7445.AM2016-1476
110. Pardoll DM. The blockade of immune checkpoints in cancer immunotherapy. *Nat Rev Cancer* (2012) 12:252–64. doi: 10.1038/nrc3239
111. Shu C, Li Q. Current advances in PD-1/PD-L1 axis-related tumour-infiltrating immune cells and therapeutic regimens in glioblastoma. *Crit Rev Oncol Hematol* (2020) 151:102965. doi: 10.1016/j.critrevonc.2020.102965
112. Wang X, Guo G, Guan H, Yu Y, Lu J, Yu J. Challenges and potential of PD-1/PD-L1 checkpoint blockade immunotherapy for glioblastoma. *J Exp Clin Cancer Res CR* (2019) 37:87–100. doi: 10.1186/s13046-019-1085-3

Conflict of Interest: The authors declare that the research was conducted in the absence of any commercial or financial relationships that could be construed as a potential conflict of interest.

frontiers in Immunology

ORIGINAL RESEARCH
published: 16 February 2021
doi: 10.3389/fimmu.2021.628966

PDIA5 is Correlated With Immune Infiltration and Predicts Poor Prognosis in Gliomas

Hao Zhang[1†], Jialin He[2†], Ziyu Dai[1], Zeyu Wang[1], Xisong Liang[1], Fengqiong He[1,3], Zhiwei Xia[4], Songshan Feng[1], Hui Cao[5], Liyang Zhang[1,3,6] and Quan Cheng[1,3,6,7*]*

[1] Department of Neurosurgery, Xiangya Hospital, Central South University, Changsha, China, [2] Department of Neurology, The Second Xiangya Hospital, Central South University, Changsha, China, [3] Clinical Diagnosis and Therapy Center for Glioma of Xiangya Hospital, Central South University, Changsha, China, [4] Department of Neurology, Hunan Aerospace Hospital, Changsha, China, [5] Department of Psychiatry, The Second People's Hospital of Hunan Province, The Hospital of Hunan University of Chinese Medicine, Changsha, China, [6] National Clinical Research Center for Geriatric Disorders, Xiangya Hospital, Central South University, Changsha, China, [7] Department of Clinical Pharmacology, Xiangya Hospital, Central South University, Changsha, China

Gliomas are the most common and lethal primary malignant tumor of the brain. Routine treatment including surgical resection, chemotherapy, and radiotherapy produced limited therapeutic effect, while immunotherapy targeting the glioma microenvironment has offered a novel therapeutic option. PDIA5 protein is the member of PDI family, which is highly expressed in glioma and participates in glioma progression. Based on large-scale bioinformatics analysis, we discovered that PDIA5 expression level is upregulated in aggressive gliomas, with high PDIA5 expression predicting poor clinical outcomes. We also observed positive correlation between PDIA5 and immune infiltrating cells, immune related pathways, inflammatory activities, and other immune checkpoint members. Patients with high PDIA5 high-expression benefited from immunotherapies. Additionally, immunohistochemistry revealed that PDIA5 and macrophage biomarker CD68 were upregulated in high-grade gliomas, and patients with low PDIA5 level experienced favorable outcomes among 33 glioma patients. Single cell RNA sequencing exhibited that PDIA5 was in high level presenting in neoplastic cells and macrophages. Cell transfection and co-culture of glioma cells and macrophages revealed that PDIA5 in tumor cells mediated macrophages exhausting. Altogether, our findings indicate that PDIA5 overexpression is associated with immune infiltration in gliomas, and may be a promising therapeutic target for glioma immunotherapy.

Keywords: gliomas, PDIA5, immune infiltration, immunotherapy, scRNA-seq

OPEN ACCESS

Edited by:
Valérie Dutoit, Université de Genève, Switzerland

Reviewed by:
Tobias Weiss, University Hospital Zürich, Switzerland
Juan Manuel Sepulveda Sanchez, University Hospital October 12, Spain

***Correspondence:**
Quan Cheng
chengquan@csu.edu.cn
Liyang Zhang
zhangliyang@csu.edu.cn

[†]These authors have contributed equally to this work

Specialty section:
This article was submitted to Cancer Immunity and Immunotherapy, a section of the journal Frontiers in Immunology

Received: *13 November 2020*
Accepted: *04 January 2021*
Published: *16 February 2021*

Citation:
Zhang H, He J, Dai Z, Wang Z, Liang X, He F, Xia Z, Feng S, Cao H, Zhang L and Cheng Q (2021) PDIA5 is Correlated With Immune Infiltration and Predicts Poor Prognosis in Gliomas. Front. Immunol. 12:628966. doi: 10.3389/fimmu.2021.628966

INTRODUCTION

Gliomas are the most common primary malignant tumor of the central nervous system in adults and are responsible for most of the deaths caused by primary brain tumors (1, 2), among which glioblastoma multiforme (GBM) is the deadliest subtype. Comprehensive therapy including surgery, radiotherapy, and chemotherapy fails to achieve satisfactory therapeutic effect, and poor survival of GBM patients is associated with the high infiltration of tumor cells and persistence of chemotherapy-resistant cells (3, 4). Recent studies demonstrate that infiltration of immune cells into tumor regions contributes to the development of metastasis and resistance to cancer therapies in gliomas (5, 6). Therefore, to explore other effective treatment options, more work on immunotherapy targeting the glioma microenvironment is being conducted (7–9), and single cell sequencing is providing a new approach to identify immune biomarkers of gliomas (10). Currently, human gliomas are diagnosed using morphological and molecular biomarker criteria according to the 2016 World Health Organization (WHO) classification of central nervous system (CNS) tumors (11). Therefore, further exploration of novel biomarkers to dissect glioma subtypes may help to clarify the molecular mechanisms and promote therapeutic strategies.

Protein disulfide isomerase (PDI), first discovered in 1963, is a 57-kDa dithiol-disulfide oxidoreductase with isomerase and chaperone functions (12, 13). The human PDI gene family currently comprises 21 genes, which have different biochemical characteristics, but share a common structural feature, the TRX-like domain. PDI family proteins are largely expressed in the endoplasmic reticulum (ER) (14, 15), where they play an important regulatory role in protein homeostasis, but also may participate in tumor progression. Previous studies have shown that PDI family protein overexpression correlates with the occurrence, invasion, and metastasis of a variety of malignant tumors (16–20). Consequently, PDI family proteins are likely prognostic factors and therapeutic targets for related tumors (21, 22). Two recent studies have demonstrated that the PDI family may serve as potential prognostic signature in gliomas (16, 23), and PDIA6 (17), P4HB, and PDIA3 (24) have all been proven to be involved in glioma progression. Moreover, high P4HB level contributes significantly to temozolomide resistance (25).

Protein disulfide isomerase A5 (PDIA5), also known as protein disulfide isomerase-related protein (PDIR), is a member of the PDI gene family and also exhibits chaperone-like activity. PDIA5 was first identified in 1995 and was found to be expressed in the brain, liver, kidney, and lungs (26). In gliomas, PDIA5 had significantly increased expression in gliomas compared with normal brain tissues (16).

Currently, the role of PDI proteins in tumor progression mainly lies in their ability to improve tumor apoptosis resistance (19, 27), while other molecular mechanism remains largely unclear. PDIA5 regulates the unfolded protein response (UPR) signaling pathway by activating ATF6α (28), whereby UPR regulates tumor cell survival. Other research has found that PDI inhibition could impair tumorigenic T cells and enhance normal T cell function (29). Based on the aforementioned findings, we speculated that PDIA5 correlated with histopathology grades and immune infiltration of gliomas, and could be a potential prognostic molecule.

In the present study, we comprehensively analyzed the PDIA5 expression pattern in gliomas. We conducted large-scale bioinformatics analyses, using gene expression data downloaded from existing databases, including single cell RNA-sequencing databases. We also performed PDIA5 over-expression and siRNA on U251 then co-culturing with HMC3 *in vitro* to mimic the infiltration of residential immune cells in glioma microenvironment. Additionally, we systematically evaluated the prognostic value of PDIA5 in gliomas. PDIA5 was found to be upregulated in gliomas and related to the suppressive tumor microenvironment by recruiting M2 macrophages, indicating that PDIA5 might be a potential prognostic biomarker or therapy target in the clinical treatment of gliomas.

MATERIALS AND METHODS

Ethics Statement

The experiments were undertaken with the understanding and written consent of each subject. The study methodologies conformed to the standards set by the Declaration of Helsinki, and the study methodologies were approved by the Ethics Committee of Xiangya Hospital, Central South University.

Clinical Specimens and Data Collection

Archived paraffin embedded glioma tissues (WHO grades I–IV) were collected from patients (n= 31) who underwent surgery in the Department of Neurosurgery, Xiangya Hospital of Central South University. Normal brain tissue samples (n = 3) were gathered from severe traumatic brain injury patients who underwent partial resection of the normal brain.

We obtained data for 1,013 samples from Chinese Glioma Genome Atlas (CGGA) database (http://www.cgga.org.cn/) and 672 samples from The Cancer Genome Atlas (TCGA) database (https://portal.gdc.cancer.gov/). PDIA5 expression data in

Abbreviations: GBM, glioblastoma multiforme; WHO, World Health Organization; CNS, central nervous system; PDI, protein disulfide isomerase; ER, endoplasmic reticulum; PDIA5, protein disulfide isomerase A5; PDIR, protein disulfide isomerase-related protein; UPR, unfolded protein response; CGGA, Chinese Glioma Genome Atlas; TCGA, The Cancer Genome Atlas; GEO, Gene Expression Omnibus; LGG, low grade glioma; IHC, immunohistochemical; scRNA-seq, single-cell RNA sequencing; OS, overall survival; DSS, disease specific survival; HRs, hazard ratios; CI, confidence intervals; PFI, progression-free interval; CNVs, somatic copy variations; ESTIMATE, Estimation of Stromal and Immune cells in Malignant Tumor tissues using Expression; GSVA, gene set variation analysis; GEP, gene expression profile; CYT, cytolytic activity; PCA, principal component analysis; GSEA, gene set enrichment analysis; GO, gene ontology; KEGG, Kyoto Encyclopedia of Genes and Genomes; ROI, region of interest; IDH, isocitrate dehydrogenase; MGMT, O6-methylguanine DNA methyltransferase; CL, classical; ME, mesenchymal; NE, neural; PN, proneural; CE, control enhanced; BLCA, bladder urothelial carcinoma; CESC, cervical and endocervical cancers; KIRP, kidney renal papillary cell carcinoma; LUSC, lung squamous cell carcinoma; MESO, mesothelioma; THCA, thyroid carcinoma; Treg, regulatory T cells; MDSCs, myeloid-derived suppressor cells; OPCs, oligodendrocyte precursor cells.

different radiographical regions of normal brain and GBM were obtained from the Gill dataset (30). RNA-seq data about specific tumor anatomy in GBM was downloaded from the Ivy Glioblastoma Atlas Project (http://glioblastoma.alleninstitute.org/). Single-cell expression matrices were acquired from the Gene Expression Omnibus (GEO; https://www.ncbi.nlm.nih.gov/geo/) GSE138794 (31), and eight single-cell RNA sequencing (scRNA-seq) datasets including both low grade glioma (LGG) and GBM were selected for analysis. Data of immunotherapeutic cohorts was downloaded from IMvigor210 (http://research-pub.Gene.com/IMvigor210CoreBiologies) (32) and GSE78220 in GEO (33).

Survival Analysis in Kaplan-Meier Plotter

Kaplan-Meier Plotter (https://kmplot.com/analysis/) was used to evaluate the correlation between PDIA5 and survival in across cancer types (34). Briefly, the patient samples were divided into two cohorts according to the cut-off expression of the gene (high *vs*. low expression) for the purpose of assessing prognostic value of PDIA5. We analyzed the relationship of PDIA5 expression with overall survival (OS) and disease specific survival (DSS) in each available cancer type (total number = 33). Hazard ratios (HRs) with 95% confidence intervals (CI) and log-rank P values were calculated.

Bioinformatics Analysis

The cut-off point was calculated using the R package survminer for OS, progression-free interval (PFI), and DSS. Somatic copy number variations (CNVs) and somatic mutations were downloaded from the TCGA database. CNVs associated with PDIA5 expression were analyzed using GISTIC 2.0 (35). Correlation analysis of PDIA5 was performed for gene expression profiles available in the TCGA and CGGA datasets using the R language. ESTIMATE (Estimation of Stromal and Immune cells in Malignant Tumor tissues using Expression) algorithm was performed as previously reported (36) to evaluate the presence of stromal cells and the infiltration of immune cells in tumor samples. Gene set variation analysis (GSVA) analysis was performed as described in the previous study (37). Briefly, the differential expression in immune cell lineages, GO terms of immune related biological process and inflammatory metagenes from TCGA and CGGA samples were analyzed *via* GSVA. Besides, T cell-inflamed gene expression profile (GEP) levels, cytolytic activity (CYT) was also analyzed through GSVA as described by Ye et al. (38).

Single-Cell RNA Sequencing

scRNA-seq was performed as described in previous studies (39, 40). The single-cell data expression matrix was processed with the R package Seurat. First, the data was normalized using the "NormalizeData" function, then the function "FindVariableGenes" was used to identify 2,000 highly variable genes. Next, "FindIntergrationAnchors" and "Integratedata" functions were used to merge eight glioma sample datasets. Afterward, the "RunPCA" function was performed and a K-nearest neighbor graph was constructed based on principal component analysis (PCA) using the "FindNeighbors" function, and then the "FindClusters" function was used to alternately combine cells together at the best resolution. Finally, "UMAP" was used for visualization. The "Single R" R package was used to identify the cell types. We chose a glioma dataset in GEO (GSE84465) and data in the Human Primary Cell Atlas Data as a reference. "FeaturePlot" and "VlnPlot" were used to further visualize gene expression. Single-cell pseudotime trajectories reconstruction and analysis was conducted using Monocle according to Pang et al. (41). Briefly, Single cells were projected onto low-dimensional space and ordered into a trajectory with branch points and cells in the same segment of the trajectory were classified as having the same "state". Additionally, functional annotations by gene set enrichment analysis (GSEA) for PDIA5 in each 'state' was constructed. Gene ontology (GO) enrichment analysis and pathway analysis based on Kyoto Encyclopedia of Genes and Genomes (KEGG) was also carried out.

Immunohistochemistry

Immunohistochemical (IHC) staining was performed as previously described (42). Briefly, sections were obtained from formalin-fixed, paraffin-embedded tissues of normal brains and different grades of human gliomas (WHO grades I–IV). After antigen retrieval and blocking endogenous HRP activity, the slides were blocked with 10% normal goat serum and incubated with primary antibody (anti-PDIA5 antibody human reactivity (D225376, 1:200, Sangon Biotech, China), anti-CD68 E11 human reactivity (SC-17832, 1:400, Santa Cruz, US) at 4°C overnight. Then the signal was visualized using standard protocols. For negative controls, sections were incubated with antibody dilution solution. Slides were counterstained with hematoxylin, and representative images were obtained using an Olympus inverted microscope. H-score of each sample was calculated.

Cell Transfection and Co-Cultured Organoids

U251 VCT/PDIA5 and U251 siNC/siPDIA5 were co-cultured with HMC3 GFP in 3D condition. In brief, PDIA5 over expression and Vector (VCT) plasmids were transfected *via* Lipofectamine 3000 (Invitrogen, US). Simultaneously. siNC and siPDIA5 RNA transfections were performed *via* RNA Max (Invitrogen, US). Two days post-transfection, tumor, and HMC3 GFP cells were genteelly digested and counted at 5x10'/each, then mixing in 200 µl organoids medium. U251 VCT/PDIA5-HMC3 GFP and U251 siNÇ/siPDIA5-HMC3 GFP in organoids medium were divided and planted 40 ul/droplet. Three days post-plantation, droplets were monitored and imaged by EVOS M5000 (Invitrogen, US). The second timepoint of monitoring was scheduled at 10 days post-plantation. Diameter and region of interest (ROI) (ImageJ, US) of organoids were measured.

Statistical Analysis

Correlations between continuous variables were assessed *via* Spearman correlation analysis, while between rank variables were analyzed by Kendall test. The Student t-test, one-way ANOVA, and Pearson's chi-squared test were used to evaluate

differences in variables between groups. The survival probability was analyzed using Kaplan–Meier survival curves and the statistical significance was evaluated by the log-rank test. All statistical analyses were performed using R (version 3.6.1, https://www.r-project.org/). The Bonferroni correction was applied to correct nominal p-values in the subgroup analysis of checkpoint inhibitor immunotherapy reference to Hoshida et al. (43). A P-value < 0.05 was considered statistically significant. All statistical tests were two-sided.

RESULTS

Clinical and Molecular Characteristics of PDIA5 in Gliomas

The flow diagram of this study was shown in **Figure 1A**. PDIA5 expression in GBM and LGG tissues was higher than in normal tissues (**Figure 1B**). We found no significant correlation between gender and PDIA5 expression in CGGA dataset and TCGA dataset (**Supplementary Figure S1A**), and PDIA5 level was significantly higher in recurrent gliomas and secondary gliomas compared to primary gliomas in the CGGA dataset (**Supplementary Figure S1B**). Additionally, when compared to complete remission/response, PDIA5 expression levels were significantly elevated in patients who experienced progressive disease in response to therapy, whereas no differences were found between other groups (**Supplementary Figure S1C**).

It is well-known that several molecular biomarkers, such as isocitrate dehydrogenase (IDH) mutation, 1p/19q codeletion status and O6-methylguanine DNA methyltransferase (MGMT) promoter methylation are related to the malignancy of gliomas (3, 44). Therefore, these molecular biomarkers were also included into the analysis in addition to WHO grade. PDIA5 expression level was higher in GBM (WHO grade IV) compared to LGG (WHO grade II and grade III) (**Figure 1C**), and it was elevated in malignant histopathologic gliomas (**Supplementary Figure S1D**). In the CGGA dataset, we found that the expression of PDIA5 was higher in the IDH wild-type compared to IDH mutant tumors among different WHO grades (**Figure 1D**). We also found that the PDIA5 expression level was positively associated with 1p/19q non-codeletion status in LGG patients (**Supplementary Figure S1E**). Moreover, PDIA5 expression was upregulated in the MGMT promoter non-methylated samples of pan-glioma patients (**Supplementary Figure S1F**). In summary, our results revealed that PDIA5 expression is upregulated in aggressive gliomas.

Currently, molecular subclasses provides a new perspective to predict disease outcomes (45), and gliomas can be classified into four subtypes: classical (CL), mesenchymal (ME), neural (NE), and pro-neural (PN), among which CL and ME subtypes are more aggressive (46). We detected PDIA5 expression in GBM and pan-gliomas samples from the TCGA dataset and found that increased PDIA5 expression was associated with the CL and ME molecular subtypes (**Supplementary Figure S1G**). Additionally, we evaluated the distribution of PDIA5 expression in GBM and normal tissues using radiographic methods. PDIA5 was found to be highly expressed in control enhanced (CE) regions (**Figure 1E**), which represented tumor cell infiltration. Furthermore, in the IVY GBM dataset, high PDIA5 level was enriched in hyperplastic blood vessels, microvascular proliferation, and peri-necrotic zones compared with other areas (**Figure 1F**).

Protein levels of PDIA5 were examined *via* IHC staining in the gliomas and normal brain tissue samples from Xiangya Hospital (n=34). Demographics and clinical characteristics of these patients are shown in **Supplementary Table S1**. The expression of PDIA5 was higher in GBM (WHO grade IV) compared to LGG (WHO grade II–III) and normal brain tissues (**Figures 1G, H**). Notably, glioma patients with low PDIA5 level experienced favorable outcomes among the glioma patients (**Figure 1I**). These results suggest that PDIA5 is significantly increased in gliomas and high PDIA5 expression may play an important role in invasive processes of gliomas.

Multifaceted Prognostic Value of PDIA5 in Cancers

Since PDIA5 is overexpressed in tumor tissues, we set out to investigate the prognostic value of PDIA5 across cancer types. Patients with high levels of PDIA5 expression experienced shorter OS in bladder urothelial carcinoma (BLCA), cervical and endocervical cancers (CESC), kidney renal papillary cell carcinoma (KIRP), lung squamous cell carcinoma (LUSC), mesothelioma (MESO), and thyroid carcinoma (THCA) (**Figures 2A–G**), and those patients with higher PDIA5 expression levels also experienced shorter DSS (**Figure 2H**, **Supplementary Figures S2A–F**). These findings revealed that high PDIA5 expression predicts poor clinical outcomes in multiple cancers.

We further assessed the prognostic value of PDIA5 in glioma patients from TCGA and CGGA. Among pan-glioma, LGG, and GBM in the TCGA dataset, patients with higher PDIA5 levels presented shorter OS (**Figure 2I**), DSS (**Supplementary Figure S2G**), and PFI (**Supplementary Figure S2H**) compared to patients expressing low levels of PDIA5, with the exception of GBM which was not statistically significant for OS. Similarly, high PDIA5 expression was significantly associated with poor prognosis in the CGGA dataset (**Supplementary Figure S2I**).

Subsequently, we analyzed the effect of PDIA5 on the prognosis of gliomas in the context of different molecular biomarkers and treatments. Regardless of whether IDH was mutated, 1p19q was co-deleted, and MGMT promoter was methylated, low PDIA5 expression was related to a favorable outcome (**Supplementary Figures S3A–F**), and the same results were obtained in the analysis of chemotherapy and radiotherapy (**Supplementary Figures S3G–I**). Analysis of the prognostic significance of PDIA5 in different types of gliomas under the 2016 WHO classification of CNS tumors demonstrated that patients with low PDIA5 expression experienced longer OS regardless of the subtypes (**Supplementary Figures S3J–R**).

PDIA5 Expression Is Correlated With Distinct Genomic Alterations

To explore the relationship between PDIA5 expression levels and specific genomic alterations in gliomas, CNVs and somatic

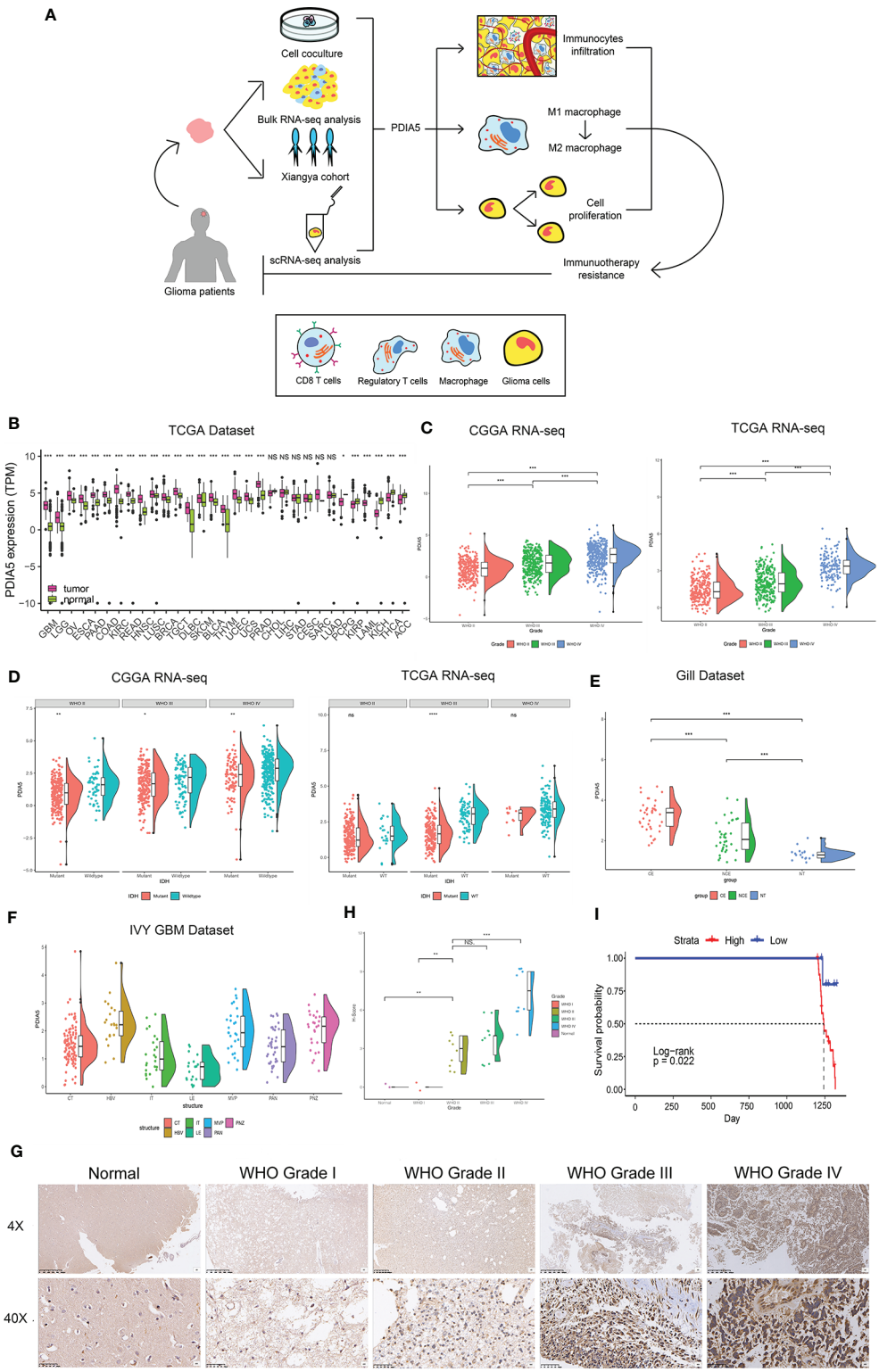

FIGURE 1 | Continued

FIGURE 1 | Clinical and molecular characteristics of PDIA5 in gliomas. **(A)** The flow diagram of this research. **(B)** Expression of PDIA5 in multiple human cancers from the The Cancer Genome Atlas (TCGA) dataset. GBM, glioblastoma multiforme; LGG, brain lower grade glioma; OV, ovarian serous cystadenocarcinoma; ESCA, esophageal carcinoma; PAAD, pancreatic adenocarcinoma; COAD, colon adenocarcinoma; KIRC, kidney renal clear cell carcinoma; READ, rectum adenocarcinoma; HNSC, head and neck squamous cell carcinoma; LUSC, lung squamous cell carcinoma; BRCA, breast invasive carcinoma; TGCT, testicular germ cell tumors; DLBC, lymphoid neoplasm diffuse large B-cell lymphoma; SKCM, skin cutaneous melanoma; BLCA, bladder urothelial carcinoma; THYM, thymoma; UCEC, uterine corpus endometrial carcinoma; UCS, uterine carcinosarcoma; PRAD, prostate adenocarcinoma; CHOL, cholangiocarcinoma; LIHC, liver hepatocellular carcinoma; STAD, stomach adenocarcinoma; CESC, cervical squamous cell carcinoma and endocervical adenocarcinoma; SARC, sarcoma; LUAD, lung adenocarcinoma; PCPG, pheochromocytoma and paraganglioma; KIRP, kidney renal papillary cell carcinoma; LAML, acute myeloid leukemia; KICH, kidney chromophobe; THCA, thyroid carcinoma; ACC, adrenocortical carcinoma. **(C)** The expression levels of PDIA5 increased with WHO grade in the Chinese Glioma Genome Atlas (CGGA) and TCGA datasets. **(D)** PDIA5 expression was upregulated in isocitrate dehydrogenase (IDH) wild-type compared with IDH mutant gliomas in CGGA and TCGA datasets. **(E)** PDIA5 expression levels in different radiographical regions of glioblastoma multiforme (GBM) and normal brain from the Gill dataset. **(F)** PDIA5 expression was detected in different locations in the IVY GBM dataset. CT, cellular tumor; HBV, hyperplastic blood vessels; IT, infiltrating tumor; LE, leading edge; MVP, microvascular proliferation; PAN, pseudopalisading cells around necrosis; PNZ, perinecrotic zone. **(G)** Representative images of IHC staining for PDIA5 in normal brain tissue and different WHO grades of glioma [scale bar=625*μm* (upper), 50*μm* (lower)]. **(H)** Quantification (H-score) of PDIA5 IHC staining in normal brain (n=3) and different pathological grades of gliomas (n=31). **(I)** Kaplan-Meier survival curves comparing the high and low expression of PDIA5 in glioma patients from Xiangya Hospital. *P <.05, **P <.01, ***P <.001, ns. p>.05.

mutations from the TCGA dataset were analyzed. CNV was investigated between high PDIA5 expression group (n=158) and low PDIA5 expression group (n=158). Amplification of chr7 and deletion of chr10 consistently appeared in gliomas with high PDIA5 expression. Additionally, 1p/19q codeletion more frequently occurred in gliomas with low PDIA5 expression (**Supplementary Figure S4A**), and 63 and 30 significant genomic events were discovered in the high and low PDIA5 groups respectively (**Supplementary Figure S4B**). In the high PDIA5 group, focal amplification peaks, including driver oncogenes such as PIK3C2B (1q32.1), PDGFRA (4q12), EGFR (7p11.2), and CDK4 (12q14.1) were found accompanied by focal deletion peaks for tumor suppressor genes such as CHD5 (1p36.31), CDKN2A/CDKN2B (9p21.3), and PTEN (10q23.31). In the low PDIA5 group, 4q12 amplification peak was observed, but the G score was evidently lower than the high PDIA5 group. Moreover, 19p13.3 amplification peak was also detected, while deletion peaks occurred in 1p32.3, 14q24.2, and 19q13.41. In regards to somatic mutations, mutation in TP53 (41%), TTN (25%), PTEN (23%), and EGFR (22%) were identified in the high PDIA5 group, while IDH1 (89%), CIC (45%), and FUBP1 (22%) were detected in the low PDIA5 group (**Supplementary Figure S4C**).

We also analyzed the correlation between PDIA5 expression and PDIA5 gene copy number, and found that GBM with PDIA5 copy number loss expressed significantly lower levels of PDIA5 mRNA (**Supplementary Figure S5A**). Moreover, in combination analysis of LGG and GBM, we observed PDIA5 expression was higher in the PDIA5 copy number gain group relative to the other two groups (**Supplementary Figure S5B**). These results suggest that PDIA5 expression may be controlled by chromosomal changes in gliomas.

PDIA5 Is Involved in Immunity Pathways and Inflammatory Activities in Gliomas

Previous studies have shown that the extent of immune infiltration in the tumor microenvironment is closely related to prognosis (47), and the aforementioned results support that PDIA5 could be a prognostic signature across cancers. Therefore, we analyzed the correlation between PDIA5 expression and immune infiltration using ESTIMATE, and discovered positive correlation between PDIA5 expression and stromal score, immune score, and ESTIMATE score in pan-glioma (**Figure 3A**) and GBM patients (**Figure 3B**).

Then we continued to conduct correlation analysis between PDIA5 and immunity pathways in gliomas using GO (**Supplementary Table S2**). In GBM patients, PDIA5 was positive associated with regulation of B cell mediated immunity, positive regulation of regulatory T cell differentiation, T cell apoptotic process, T helper2 cell differentiation, negative regulation of CD4 positive alpha beta T cell activation, regulation of T cell differentiation, positive regulation of T cell cytokine production, T helper1 cell differentiation, negative regulation of activated T cell proliferation, negative regulation of T cell receptor signaling pathway, T helper1 cell cytokine production, macrophage inflammatory protein 1 alpha production, fibroblast activation, and natural killer cell mediated immune response to tumor cells in both CGGA and TCGA datasets (**Figures 3C, D**). Similar results were obtained from the analysis of pan-glioma patients (**Supplementary Figures S5C, D**). These findings indicate that PDIA5 may take part in regulating the tumor immune environment of gliomas.

Inflammation response is another essential component of the tumor microenvironment (48). Consequently, we analyzed the association between PDIA5 and seven inflammatory metagenes. PDIA5 expression was positively correlated with interferon, STAT1, MHC-I, MHC-II, HCK and LCH, but negatively correlated with IgG in GBM patients from the CGGA dataset (**Figure 3E**). In the TCGA dataset, PDIA5 was positively correlated with MHC-I, HCK and LCH, and negatively correlated with IgG (**Figure 3F**). Additionally, in pan-glioma patients, there was a positive correlation between PDIA5 expression and six metagenes other than IgG (**Supplementary Figures S5E, F**). These results suggest that PDIA5 is likely to be enriched in signal transduction of T cells and antigen presenting and activation of macrophages, but negatively associated with B lymphocytes in gliomas.

PDIA5 Is Relevant to Stromal and Immune Cell Infiltration in Gliomas

To investigate the specific mechanism of PDIA5 overexpression promoting immune infiltration, we further explored the correlation between PDIA5 expression and detailed immune cell

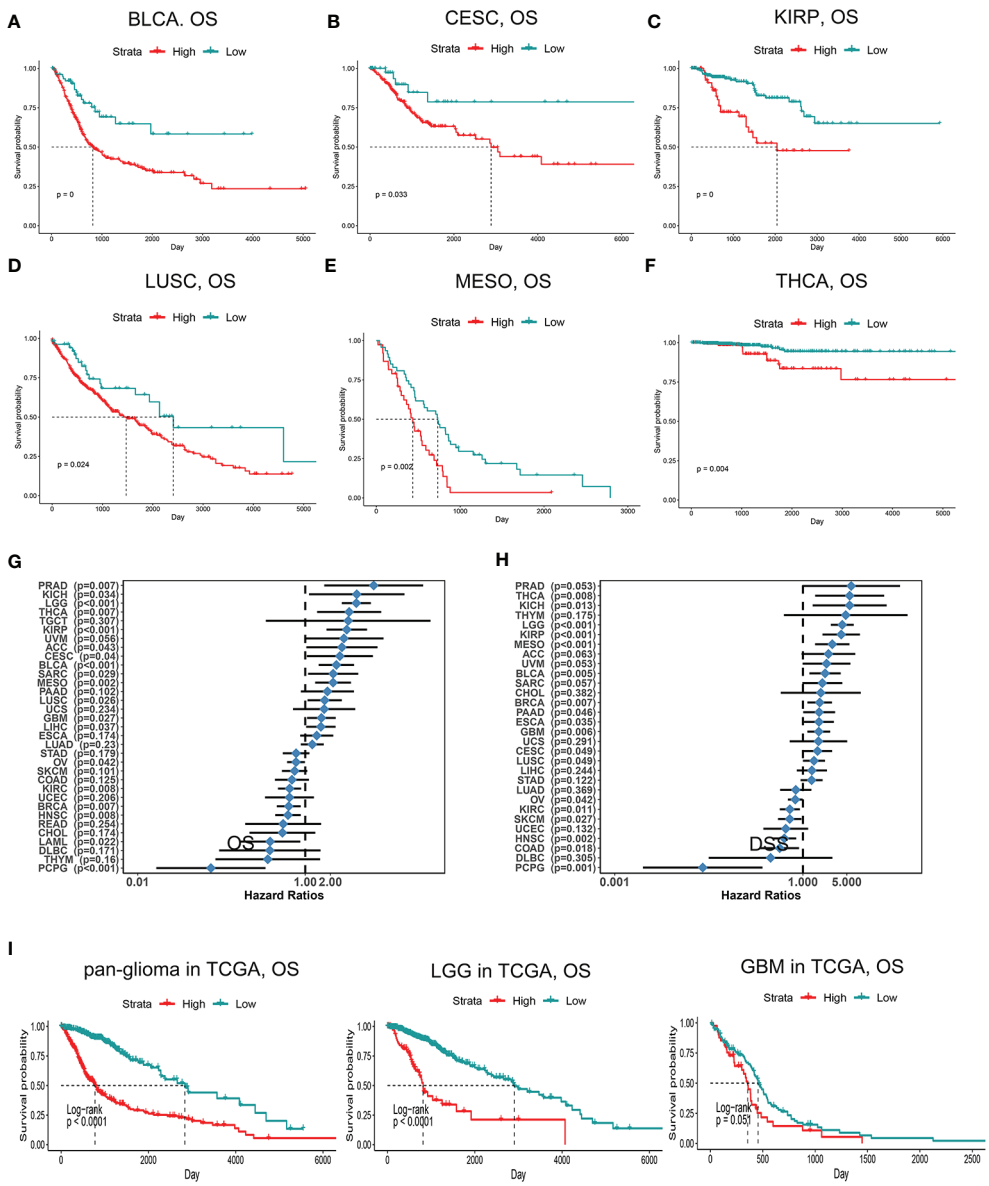

FIGURE 2 | Kaplan-Meier survival curves comparing high and low expression of PDIA5 in different cancers. OS of bladder urothelial carcinoma (BLCA) **(A)**, cervical and endocervical cancers (CESC) **(B)**, kidney renal papillary cell carcinoma (KIRP) **(C)**, lung squamous cell carcinoma (LUSC) **(D)**, mesothelioma (MESO) **(E)**, and thyroid carcinoma (THCA) **(F)**. Correlation of PDIA5 expression with OS **(G)** and DSS **(H)** in 33 types of cancer. OS, overall survival. DSS; disease specific survival. **(I)** Kaplan-Meier analysis of OS based on high *vs*. low expression of PDIA5 in pan-glioma, LGG, and GBM patients in the TCGA dataset. Red curve represents patients with high expression of PDIA5, and blue curve represents low PDIA5.

types in 33 cancer types, and found that PDIA5 was positively correlated with multiple immune cell infiltrates in most cancers including GBM, LGG, and others (**Supplementary Figure S6A**).

We then examined the relationship between PDIA5 and 28-immune cell lineage genes in GBM and pan-glioma, and found that the vast majority immune cells, including various types of T cells, B cells, macrophages, myeloid-derived suppressor cells (MDSCs), neutrophils, and natural killer cells, were enriched in the high PDIA5 group of GBM (**Figures 4A, B**) and pan-glioma (**Supplementary Figures S6B, C**). Taken together, these results suggest that high PDIA5 expression level was relevant to stromal and immune cell infiltration in the tumor microenvironment of gliomas.

We also assessed the difference in the expression value of 22 immune cells between high and low expression of PDIA5 group in both CGGA and TCGA dataset using CIBERSORT, and discovered that the differences in macrophages was statistically significant, with M2 macrophages being the most significant (**Supplementary Figures S7A, B**). Positive correlation was also

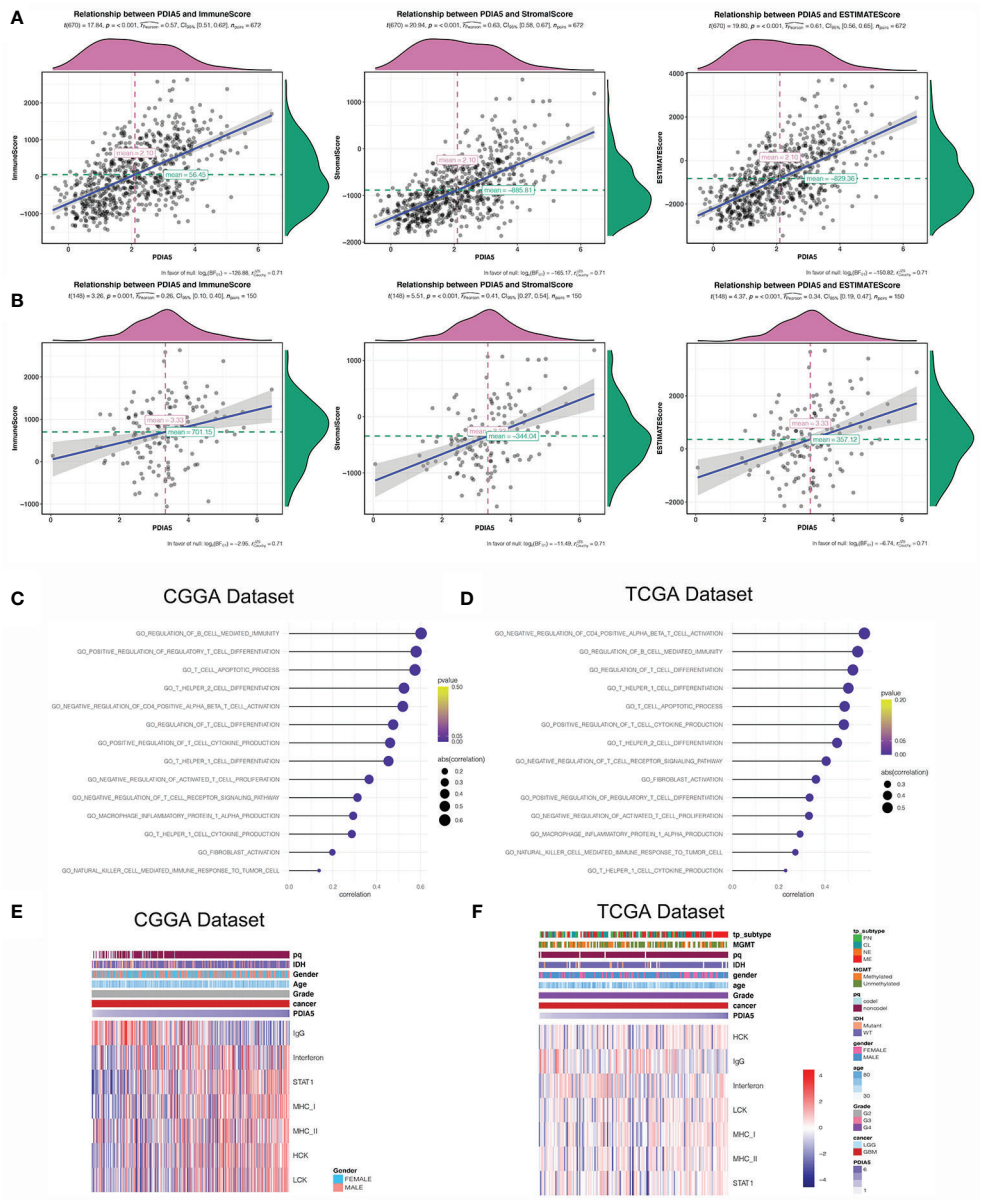

FIGURE 3 | PDIA5 is associated with immunity pathways and inflammatory activities in GBM. PDIA5 expression was positively correlated with immune score, stromal score, and ESTIMATE score in pan-gliomas **(A)** and GBM patients (**B**). Correlation of PDIA5 and immunity pathways in CGGA **(C)** and TCGA **(D)** datasets. The relationship between PDIA5 and inflammatory activities in the CGGA **(E)** and TCGA **(F)** datasets. Expression values are z-transformed and are highlighted in red for high expression and blue for low expression as indicated in the scale bar.

found in the correlation analysis of PDIA5 and macrophage biomarkers (**Supplementary Figures S7C–F**). Consequently, we detected macrophage biomarker CD68 in gliomas and normal brain tissue samples from Xiangya Hospital using IHC staining and found that the number of CD68 positive cells was positively correlated with the WHO grade of gliomas (**Figures 4C, D**). Moreover, a positive relationship was observed in correlation analysis between PDIA5 and CD68 in gliomas patients from TCGA dataset (**Supplementary Figure S8A**). Similarly, the positive correlation between PDIA5 and CD68 was also displayed in the IHC staining samples from Xiangya Hospital (**Figure 4E**). Finally, patients with high PDIA5 and CD68, high combined expression of PDIA5 and CD68 group, and high ratio of PDIA5 to CD68 group experienced shorter OS (**Supplementary Figures S8B–D**). The above findings verify the positive correlation between PDIA5 and macrophage, especially M2, infiltration in gliomas.

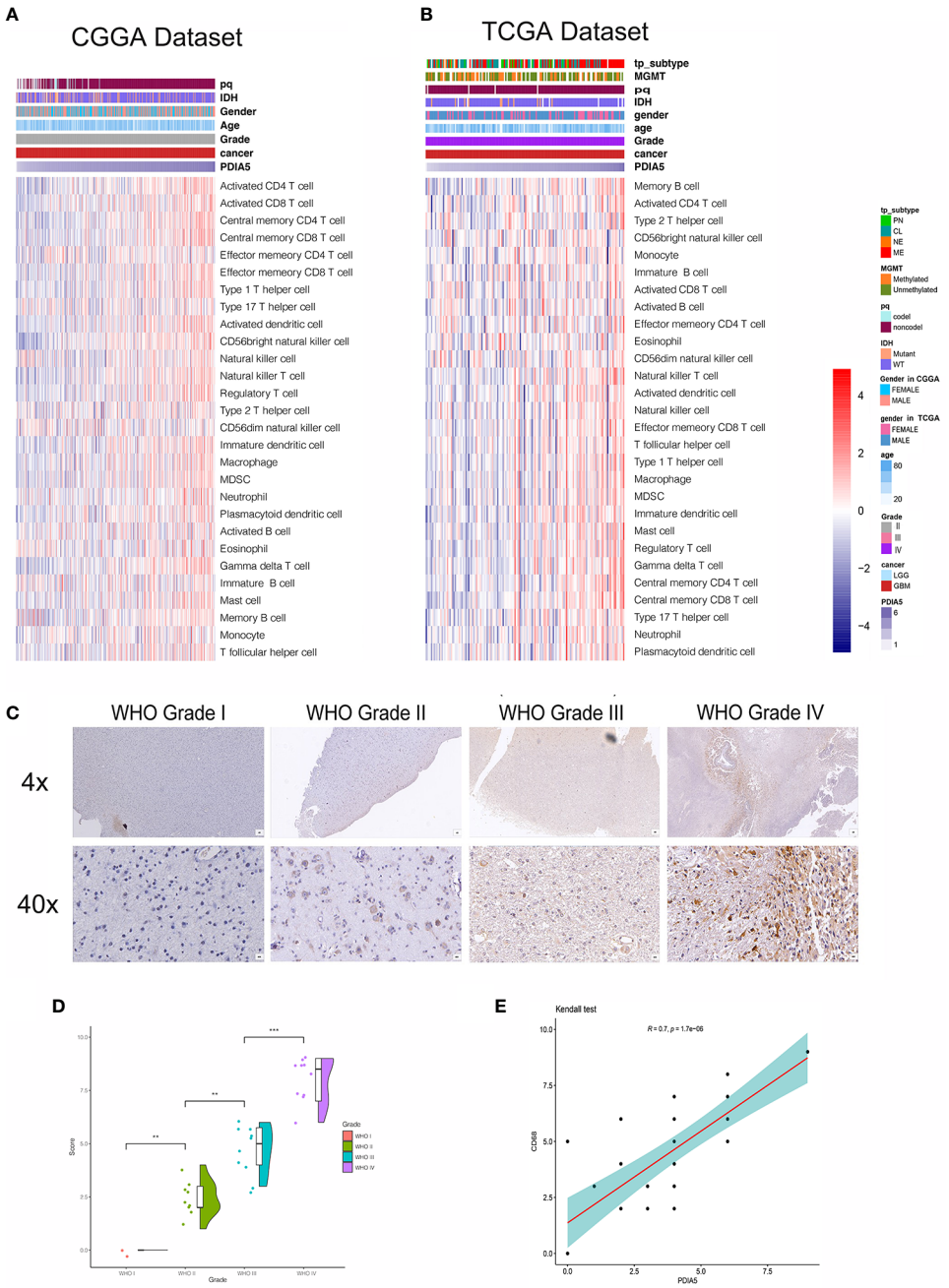

FIGURE 4 | Correlation between PDIA5 expression and immune cell infiltration in gliomas. Correlation of PDIA5 and 28-immune cell lineage genes in glioblastoma multiforme (GBM) from the Chinese Glioma Genome Atlas (CGGA) **(A)** and The Cancer Genome Atlas (TCGA) **(B)** datasets. Expression values are z-transformed and are highlighted in red for high expression and blue for low expression as indicated in the scale bar. **(C)** Representative images of immunohistochemical (IHC) staining for CD68 in different WHO grades of gliomas [scale bar=625*μm* (upper), 50*μm* (lower)]. **(D)** Quantification (H-score) of CD68 IHC staining in normal brain (n=3) and different pathological grades of gliomas (n=31). **(E)** Correlations analysis between PDIA5 and CD68 of IHC staining. **P <.01, ***P <.001.

Neoplastic Cells and Macrophages Exhibit High PDIA5 Expression in scRNA-Seq of Gliomas

To further elucidate the immune infiltrating role of PDIA5, we also analyzed the expression of PDIA5 in gliomas using scRNA-seq. The representative merged image showing the data from 8 glioma samples is displayed in **Supplementary Figure S8E**. Eight clusters of cells, including neoplastic cells, oligodendrocyte precursor cells (OPCs), astrocytes, macrophages, oligodendrocytes, vascular endothelial cells, neurons, and T cells were identified from the eight glioma samples (**Supplementary Figure S8F**). The expression of PDIA5 in all eight clusters of cells is visualized

in **Figure 5A**. We subsequently analyzed the expression level of PDIA5 in the 8 glioma samples. PDIA5 was richly expressed in neoplastic cells, macrophages, and OPCs (**Supplementary Figure S8G**). Additionally, the analysis of the expression level of PDIA5 in different cell clusters further confirmed that PDIA5 was highly correlated with neoplastic cells, macrophages, and OPCs (**Figure 5B**).

We further analyzed the Single-cell pseudotime trajectories and functional annotations of neoplastic cells and macrophages in gliomas. In both neoplastic cells and macrophages, a trajectory was reconstructed by Monocle, which mainly contained two branch points (denoted "1" and "2") and grouped cells into five states (**Figures 5C, D**). High PDIA5 expression level was observed in state 3 and 4 of neoplastic cells, and particularly higher in state 4 and 5 of macrophages. We further identified 100 genes with branch-dependent expression for branch point 1 of neoplastic cells, the differentially expressed genes before and after branch point 1 and related clustering are visualized in **Supplementary Figure S9A**. The top 12 genes are shown in **Supplementary Figure S9B**. Moreover, 100 differentially expressed genes with branch-dependent expression for branch point 2 of macrophages were also ascertained (**Supplementary Figure S10A**). The top 12 genes are displayed in **Supplementary Figure S10B**. GSEA for neoplastic cells and macrophages for PDIA5 in each "state" is shown in **Supplementary Figures S9C** and **S10C**, respectively. Notably, PDIA5 in state 4 of macrophage was uniformly positively correlated with immune pathways. Finally, the results of GO enrichment analysis (**Supplementary Table S3**, **S4**, **S5**) and KEGG pathway analysis (**Supplementary Table S6**, **S7**, **S8**) in regards to PDIA5 in neoplastic cells and macrophages is shown in **Supplementary Figures S9D–F** and **S10D–F**.

PDIA5 in Tumor Cells Mediates Tumor Cells Proliferation and Macrophages Exhausting

Accumulating evidence of the correlation between PDIA5 and macrophages in glioma microenvironment drove us to investigate the in-depth mechanisms involved in the interconnection among PDIA5, glioma cells, and macrophages. Microglia, the common consensus of residential immune cells in cerebral microenvironment performances essentially as functional macrophages. To investigate PDIA5 functions in glioma, the PDIA5 over-expression plasmid (VCT/PDIA5 plasmid) and siRNA (siNC/siPDIA5) were generated and transfected into U251. Subsequently, PDIA5 relative U251 lines were co-cultured with HMC3 GFP. The dimension of organoid was increased in co-culturing with U251 PDIA5 at 10 days post-transplantation, while dramatically decreased in co-culturing with U251 siPDIA5 (**Figure 6A**). Statistical evaluations of GFP ROIs presenting the HMC3 viabilities was dynamic in co-culturing with U251 siPDIA5

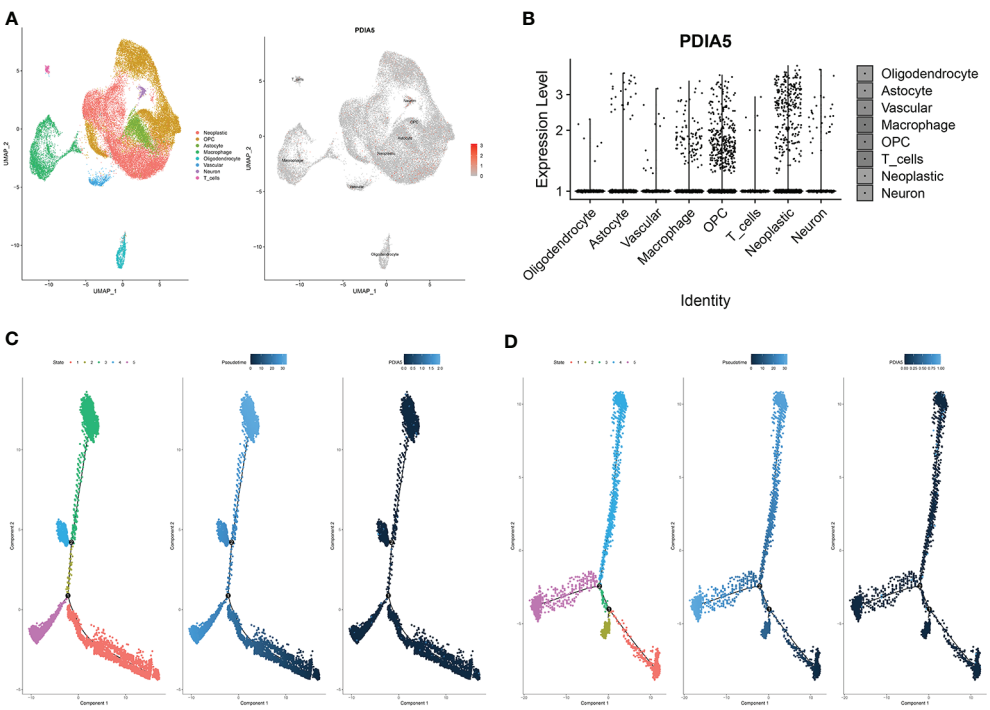

FIGURE 5 | scRNA-seq results for PDIA5 in gliomas. **(A)** The cells were categorized into eight clusters (left). Scatter plots of PDIA5 expression distribution of different cell clusters (right). Gray areas represent the whole cell clusters. The red dots represent cell with PDIA5 expression. **(B)** Violin plot of PDIA5 expression distribution of different cell clusters. **(C)** The single-cell trajectory of neoplastic cells contains four main branches. Cells are colored based on state (left), pseudotime (middle), and PDIA5 (right). **(D)** The single-cell trajectory of macrophages contained four main branches. Cells are colored based on state (left), pseudotime (middle), and PDIA5 (right).

comparing significantly to co-culturing with U251 PDIA5 (**Figure 6B**). Histological sections demonstrated cell types of co-culturing organoids (**Figure 6C**). In co-culturing with U251 siPDIA5, HMC3 was obviously monitored comparing to other organoids. Accordingly, these results demonstrated that PDIA5 high glioma cells functionally promoted tumor cell proliferation and exhausted immune cells (HMC3). Furthermore, knock-down PDIA5 presented the malignant behavior decreasing of glioma cells in immune cells exhausting.

Immunotherapy Is More Practical for High PDIA5 Patients

In recent years, immunotherapies, which target the immune checkpoint molecules including CTLA-4, PD-1, and PD-L1/2 have offered new treatment opportunities and improved survival in hard-to-treat tumors (7, 8). To assess the correlation between PDIA5 and immune checkpoints, we selected several well-known immune checkpoints, including LAG3, HAVCR2 (TIM-3), CD274 (PD-L1), CD276 (B7-H3), CD80, PDCD1LG2 (PD-L2), PDCD1 (PD-1), and IDO1 for correlation analysis. In CGGA dataset, PDIA5 expression was positively associated with CD276, CD274, PDCD1LG2, and HAVCR2 in pan-glioma and LGG patients, and positively correlated with CD276, PDCD1, CD274, PDCD1LG2, and HAVCR2 in GBM patients. In TCGA datasets, there was positive correlation between PDIA5 and CD276 or PDCD1LG2 in pan-glioma patients, and PDIA5 expression was positively associated with CD276, PDCD1LG2 and HAVCR2 in LGG patients. However, in GBM patients, PDIA5 only demonstrated a strong positive correlation with CD276 (**Figures 7A, B**). Altogether, our results imply that PDIA5 has positive correlation with clinically relevant immune checkpoint molecules in gliomas.

Subsequently, we investigated whether PDIA5 could predict glioma patients' responses to checkpoint inhibitor

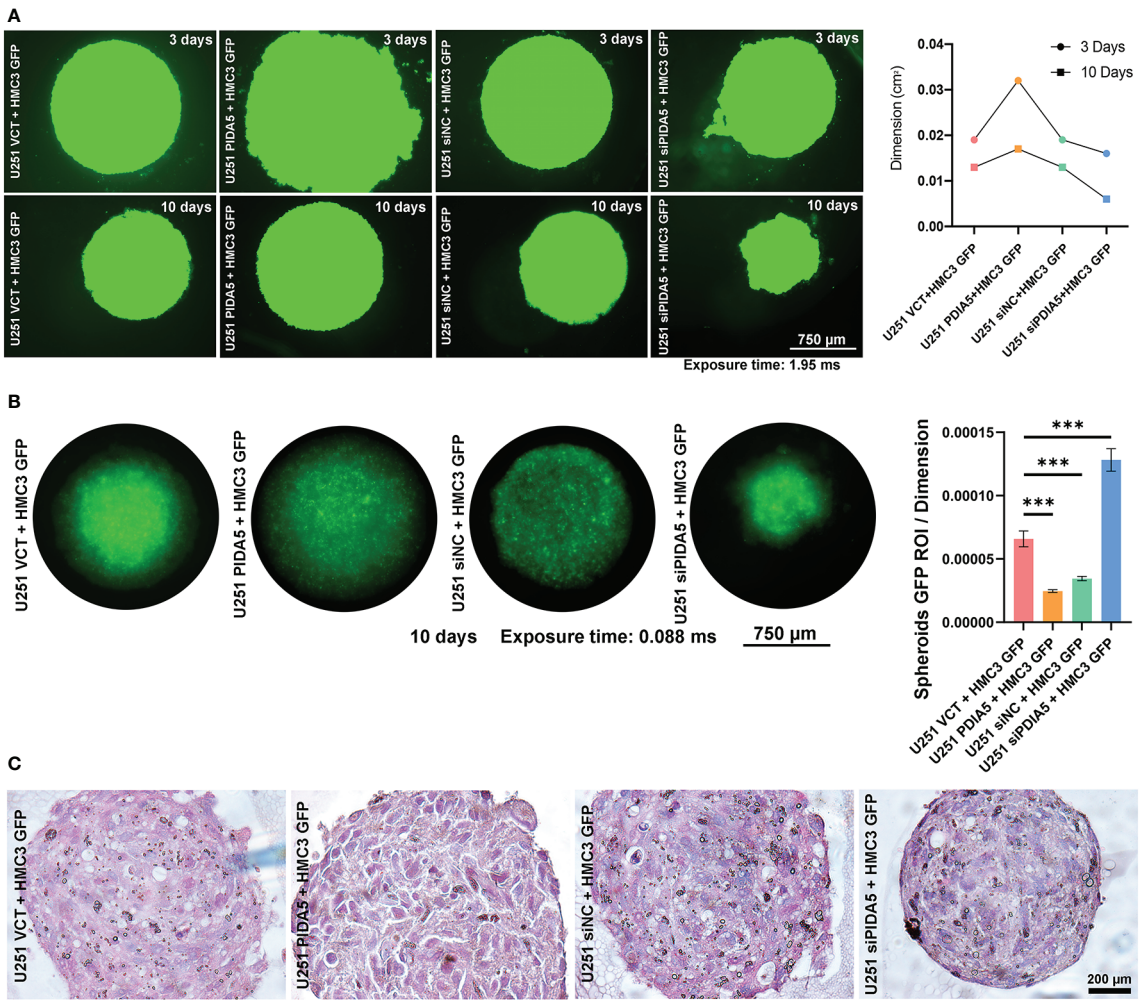

FIGURE 6 | PDIA5 high expression tumor cells exhausted immune cells (HMC3) activation. **(A)** PDIA5 relative U251 lines were co-cultured with HMC3 GFP in organoids medium and monitored and quantified at 3/10 days-post droplets implantation (exposure time: 1.95 ms). **(B)** GFP ROI per dimension measurements valued the viabilities of HMC3 in each co-culturing (exposure time: 0.888 ms). **(C)** HE stained co-cultured organoids demonstrated cell types. Note: figure panel pairs in **(A–C)** represent images captured at differing magnifications; magnification scale bars: panel **(A, B)** *4×amplification: 750 μm;* panel **(C)** *10×amplification: 200 μm.* ***P <.001.

immunotherapy in anti-CTLA-4 and anti-PD-1 based on CGGA and TCGA datasets, and found that compared with low PDIA5 group, high PDIA5 group was expected to respond better to immunotherapies (**Figure 7C**). Previous work indicates that GEP and CYT are able to enhance anti-tumor activity and associated with the response to PD-1 inhibitor (49, 50). Therefore, we further explored the relationship between PDIA5 and GEP as well as CYT. PDIA5 was found to be positively associated with GEP and CYT (**Figures 7D, E**).

Then we continued to analyze the predictive value of PDIA5 regarding the response of anti-PD-L1 (IMvigor210) and anti-PD-1 (GSE78220) therapy for urothelial cancer and metastatic melanoma cohorts, respectively. In the anti-PD-L1 cohort (IMvigor210), we observed that patients with high PDIA5 experienced significant clinical survival benefits (**Figure 8A**). The significant treatment strengths and response to anti-PD-L1 immunotherapy in high PDIA5 group compared to the low PDIA5 group were also verified (**Figures 8B–E**). In the anti-PD-L1 cohort, the percentages of complete response (CR) and progressive disease (PD) were 19.35 and 39.44% in the high PDIA5 group, respectively, and 6.7 and 58.64% in the low PDIA5 group, respectively. And the proportion of high PDIA5 expression in CR group and PD group were 35.93 and 11.56%, respectively. Additionally, the high PDIA5 group exhibited high expression of CD274 (PD-L1), which resulted in good response to anti-PD-L1 therapy (**Figure 8F**). Similarly, notable favorable outcome of the high PDIA5 group was also observed in the anti-PD-1 cohort (GSE78220) (**Figure 8G**). The frequencies of CR, PD, and partial response (PR) were 15.99, 42.25, and 41.77% in the high PDIA5 group, respectively, and 0%, 77.53, and 22.47% in the low PDIA5 group, respectively (**Figure 8H**). And the proportion of high PDIA5 expression in CR group, PD group, and PR group were 100, 84.35, and 94.84%, respectively (**Figure 8I**). The difference is not statistically significant possibly due to the small sample size. The above findings suggest that patients with high PDIA5 have high anti-tumor immune activity and may benefit from immunotherapies.

DISCUSSION

Based on large-scale bioinformatic analysis, we are the first to comprehensively analyze PDIA5 expression profiles in gliomas according to the WHO grading system, histopathology, molecular biomarkers, and molecular subclasses. PDIA5 expression levels were elevated in malignant gliomas ground on the above different categories. PDIA5 overexpression was also found in the areas of infiltrating tumor cells according to radiology imaging. Importantly, our results show that high levels of PDIA5 expression predict poor outcomes based on survival analysis of different subgroups.

Genomic alterations in gliomas are able to predict disease classification and prognosis (51). In CNV analysis, we found focal amplification peaks for oncogenes in the high PDIA5 group and focal deletion peaks for tumor suppressor genes. Several common somatic mutations in GBM including TP53, TTN, PTEN, and EGFR (52), were also present in the high PDIA5 group. These results suggest that high PDIA5 expression plays an important role in glioma infiltration. Investigating the detailed mechanism of PDIA5 promotion of glioma development may help to develop new therapeutic strategies.

High-grade gliomas progress rapidly, and cause short survival of patients, among which GBM harbors the most severe malignancy. The role of the immune microenvironment in the progression of gliomas has become increasingly well-known (53). Previous research has shown that the tumor immune microenvironment influences gene expression of tumor tissues and the degree of stromal and immune cell infiltration contribute notably to prognosis (54). Stromal score, immune score, and ESTIMATE score, which are based on ESTIMATE algorithm, were shown to be negatively correlated with the prognosis of GBM (47), glioma, oligodendroglioma, melanoma (55), and gastric cancer (56). In our research, we found these three ESTIMATE algorithm scores were increased along with PDIA5, indicating that high expression level of PDIA5 is positively correlated with immune infiltration in gliomas.

Infiltrating immune cells in glioma tumor microenvironment are comprised of microglia/macrophages, CD4+ T cells, regulatory T cells (Tregs), MDSCs, and granulocytes, among which microglia and MDSC are the most frequent (53), contributing to ineffective immune activation in GBM (57). Our results revealed that multiple immune cell types were enriched in high PDIA5 patients. And the correlation between PDIA5 and T cells as well as macrophages in gliomas was presented in the subsequent specific analysis.

So far, no previous studies have focused on the interaction between PDIA5 and tumor immunity, but a few studies on PDI and immune cells have demonstrated that PDI can elicit CD8+ T-cells in leishmaniasis (58, 59). Caorsi et al. have shown PDIA3 induced proliferation of autologous CD4 and CD8 T cells in colorectal cancer, accompanied by PDIA3-specific Th1 effector cell accumulation in tumor tissue (60). Besides, the other member of PDI family has also been identified to be relevant to the activation and function of macrophages (61). Most of the functions of PDIA5 remains unclear, but the b-type domain of PDIA5 has a binding region for PDIA3 (62), suggesting the possibility that PDIA5 may be related to some biological functions of PDIA3. However, basic research is needed to further investigate the specific interactions between PDIA5 and the immune system in gliomas.

Gliomas, especially GBM, can escape anti-tumor immunity and cause severe T cell dysfunction, which includes the apoptosis of effector T cells and the activation of Tregs (63). Our correlation analysis of immune pathways showed that PDIA5 was positively associated with the differentiation of regulatory T cell and the apoptotic process of T cells, while negative correlated with CD4+ T cell activation and proliferation. Besides, the investigation about inflammatory activity suggested that PDIA5 was also enriched in the biological process of T cells. The above indicating that PDIA5 may be associated with abnormal T cell function in gliomas.

Additionally, growing evidence have identified that tumor-associated macrophages (TAMs) played a key role in the

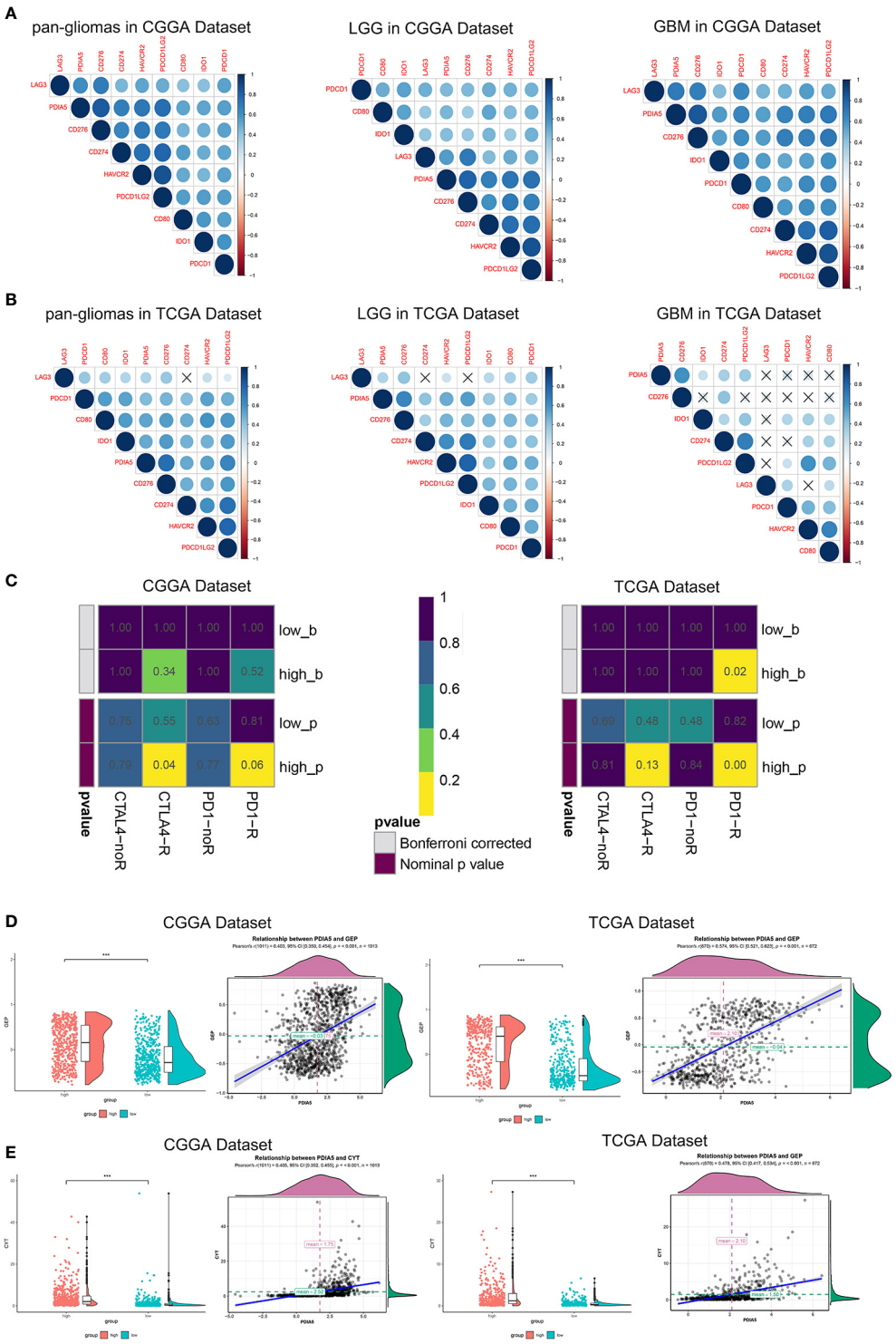

FIGURE 7 | Immunotherapy is more practical for high PDIA5 patients. Correlation between PDIA5 and immune checkpoint members in pan-gliomas, low grade glioma (LGG), and glioblastoma multiforme (GBM) from the Chinese Glioma Genome Atlas (CGGA) **(A)** and The Cancer Genome Atlas (TCGA) **(B)** datasets. **(C)** Submap analysis of the response of anti-CTLA-4 and anti-PD-1 therapy in the CGGA and TCGA datasets. low_b, or high_b was the value obtained from low_p, or high_p multiplied by 8 (2 *4) based on Bonferroni correction, respectively. **(D)** The relationship between PDIA5 and T cell-inflamed gene expression profile (GEP) level in the CGGA and TCGA datasets. **(E)** The relationship between PDIA5 and cytolytic activity (CYT) in the CGGA and TCGA datasets. ***P <.001.

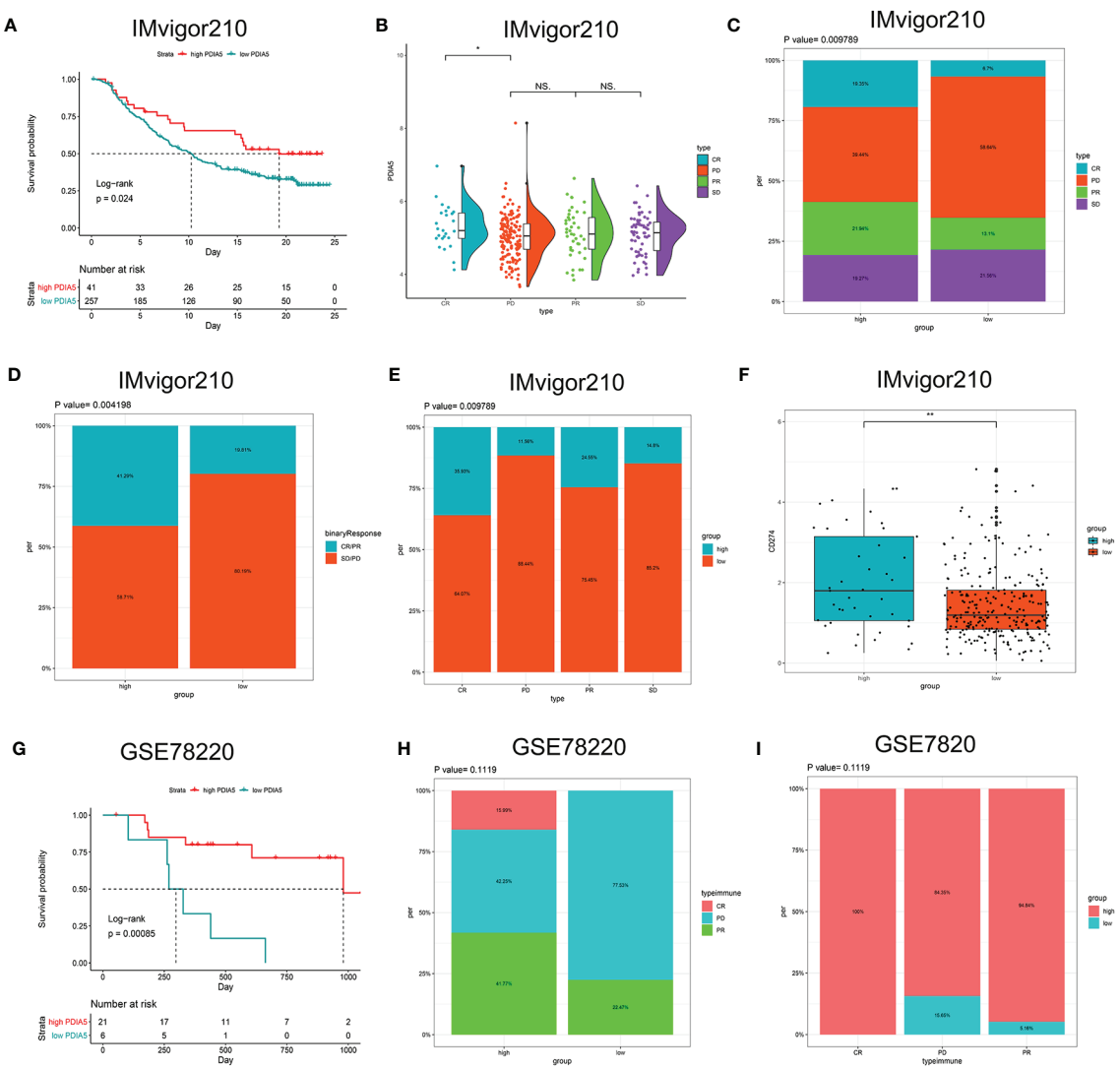

FIGURE 8 | The role of PDIA5 in predicting the therapeutic value of checkpoint blockade immunotherapy. **(A)** Kaplan–Meier survival plot showed a significant survival benefit in the high PDIA5 group of IMvigor210 cohort. **(B)** Distribution of PDIA5 in the distinct anti-PD-L1 clinical response group. *p <.05, ns, p >.05. **(C)** The proportions of clinical response to anti-PD-L1 immunotherapy in the high and low PDIA5 groups. **(D)** The proportions of clinical binary response to anti-PD-L1 immunotherapy in the high and low PDIA5 groups. **(E)** The proportions of the high and low PDIA5 groups in the anti-PD-L1 immunotherapy clinical response. **(F)** Differences in CD274 (PD-L1) expression in the high and low PDIA5 groups in the IMvigor210 cohort. **(G)** Kaplan–Meier survival plot showed a significant survival benefit in the high PDIA5 group of GSE78220 cohort. **(H)** The proportions of clinical response to anti-PD-1 immunotherapy in the high and low PDIA5 groups. **(I)** The proportions of the high and low PDIA5 groups in the anti-PD-1 immunotherapy clinical response. **p < .01.

progression and metastasis of tumor cells (64–66). As the result of the impact of metabolites of malignant cells, TAMs in the tumor microenvironment make corresponding metabolic changes, leading to functional reprogramming of TAMs which includes the M2 polarization of macrophages, and alterations of cytokines and angiogenic factors secretion. These above changes are conducive to the migration and invasion of tumors (67, 68). Our immunohistochemistry results found that the number of macrophages increased with the WHO grade of gliomas, which was consistent with previous studies. Further analysis attested the positive correlation between PDIA5 and macrophage, especially M2, infiltration in gliomas. Therefore, we deduced that high expression of PDIA5 may induce macrophage associated immunity, and contribute to M2 polarization of macrophage in gliomas.

To learn more about the role of PDIA5 in macrophage associated immunity and malignant cell proliferation of gliomas, scRNA-seq analysis and gain of function as well as loss of function assay were performed. To date, scRNA-seq has exhibited great potential in screening therapeutic targets for antitumor immunity. Several studies have analyzed the gene expression of immune cells in gliomas using scRNA-seq data. Goswami et al. identified CD73 as a specific immunotherapy target which enhances the antitumor immune response to

immune checkpoint therapy in GBM using scRNA-seq (69), and Cheng et al. identified 31 genes that could be biomarkers for GBM tumor cells based on single cell sequencing (70). Additionally, pseudotime trajectories analysis is capable of capturing and dissecting transcriptional changes in cells during glioma progression. Therefore, it can be used to evaluate the relationship between genes and development of specific cell lineages in gliomas (41). In the present study, using scRNA-seq data, we found that high PDIA5 expression existed in neoplastic cells and macrophages of gliomas, further research on pseudotime trajectories and functional annotations emphasized the correlation between PDIA5 and macrophage infiltration as well as progression in gliomas. Moreover, cell transfection and co-culture of glioma cells and macrophages based on organoids revealed that PDIA5 in tumor cells mediated glioma cells proliferation and macrophages exhausting, which further confirmed the crucial role of PDIA5 in regulating immune activity in the tumor microenvironment of glioma.

Nevertheless, the overexpression of PDIA5 resulted in the ultimate exhaustion of macrophage in our *in vitro* experiments, which was contrary to the findings that PDIA5 was positively correlated with macrophage infiltration in our previous bioinformatic analysis. This phenomenon can be attributed to the fact that the glioma cells with high expression of PDIA5 secrete certain cytokines to recruit M2 macrophages, which interact with glioma cells (67) and potentially ended with apoptosis and degradation. And the consumed macrophages can be continuously replenished from the peripheral blood and resident microglia in brain *in vivo* (68), while the number of macrophages in the co-culture system is constant, eventually led to the exhaustion of macrophages. Therefore, the high level of PDIA5 expression in gliomas indeed contribute to recruiting macrophages and probably mediating the polarization of macrophages to M2. Taken together, our findings demonstrate that PDIA5 overexpression correlates with immune infiltration and inflammation in gliomas, which may lead to poor prognosis in glioma patients.

Immune checkpoint refers to specific molecular interactions at the interface between T cells and antigen presenting cells, and exhibits the ability to inhibition T cell function (63). Targeting immune checkpoint, which enhances anti-tumor immune responses, has brought about remarkable clinical advances and offered new targets for tumor therapy (7). Each immune checkpoint has its own unique molecular characteristics, and several immune checkpoints may interact with each other. The prominent PD-1/PD-L1 axis, can promote invasion of GBM cells in brain tissue (71). Additionally, PD-1 has also proven to be correlated with other immune checkpoints including IDO1, LAG3, TIM-3, and B7-H3 (72). Li et al. found that glioma patients had higher TIM-3 expression on peripheral innate immunocytes, which further contributed to immune disorders (73). B7H3 has been reported to play a pivotal role in cell differentiation and carcinogenesis of glioma by Zhang et al. (74), And PD-L2, another ligand of PD-1, can evade antitumor immunity through modulating T cell response and proliferation in gliomas (75). We found tight correlations between PDIA5 and B7-H3, PD-L2, and TIM-3, suggesting that PDIA5 probably plays a synergistic role with those immune checkpoints in the progression of glioma. Further predictive analysis based on the existing databases showed that patients with high PDIA5 had high anti-tumor immune activity and were more likely to benefit from immunotherapies in gliomas as well as other tumor types, indicating that inhibition of combined PDIA5 and these immune checkpoints could improve the clinical management of gliomas.

Hsowever, there are still some limitations regarding this study, which are expected to be improved on in subsequent studies. Firstly, the relationship between PDIA5 and B cells is unclear or even seems to be contradictory in different analyses relative to macrophages and T cells. Despite the negative association between PDIA5 and IgG indicate PDIA5 inhibition of IgG activity, which might only represent part of the B cells, PDIA5 promotion of malignancy attract more immune cells including B cells in the tumor microenvironment of gliomas. Secondly, the high anti-tumor activity and poor clinical outcomes are another discrepancy among patients with high PDIA5. Prior evidence implicated that high PD-L1 contributed to immunosuppression but enhanced the response rate to anti-PD-1 therapy in metastatic melanomas and breast cancer (76, 77). The authors suggested that pre-treatment high level of PD-L1 may be related to its role in immune dysfunction and T cell exhaustion, while the increased PD-L1 level in on-treatment patients was caused by the reinvigoration of T cells. And the loss of PD-L1 inhibition effect on T cells was due to the interaction between PD-L1 and PD-1 blocked by anti-PD-1 therapy. Similar interplay patterns potentially exist between PDIA5 and certain immune checkpoint, like PD-1 and CTLA-4, giving rise to better responses to checkpoint inhibitor immunotherapy. Generally, existing data regarding the action mechanism of PDIA5 to interfere with the immune system is relatively lacking, and more wet experiments are needed to further interpret the role of PDIA5 in gliomas immunology.

In summary, our findings demonstrate that PDIA5 is upregulated in multiple types of malignant gliomas, and has multifaceted prognostic value in cancers. It is particularly noteworthy that PDIA5 overexpression correlates with immune infiltration and is associated with poor prognosis in glioma patients. And patients with high PDIA5 are more likely to benefit from immunotherapies. Overall, these findings indicate that PDIA5 could be a promising target for glioma immunotherapy.

DATA AVAILABILITY STATEMENT

The datasets analyzed during the current study are available in the Gene Expression Omnibus (https://www.ncbi.nlm.nih.gov/geo/), TCGA data source (https://xena.ucsc.edu) and CGGA data portal (http://www.cgga.org.cn).

ETHICS STATEMENT

The studies involving human participants were reviewed and approved by the Ethics Committee of Xiangya Hospital, Central South University. The patients/participants provided their written informed consent to participate in this study.

AUTHOR CONTRIBUTIONS

HZ and JH designed the study and interpreted data. QC and LZ provided foundation support and supervised the study. HZ, JH, ZD, and ZW acquired and analyzed data. HZ, JH, QC, HC, ZX, FH, and SF drafted the manuscript and revised for submission quality. All authors contributed to the article and approved the submitted version.

FUNDING

This work was supported by the National Natural Science Foundation of China (No. 82073893, No.81703622, No.81402249, No.81903015); China Postdoctoral Science Foundation (No.2018M633002); Natural Science Foundation of Hunan Province (No.2018JJ3838, No. S2019JJQNJJ1625); Hunan Provincial Health and Health Committee Foundation of China (C2019186); and Xiangya Hospital Central South University postdoctoral foundation.

SUPPLEMENTARY MATERIAL

The Supplementary Material for this article can be found online at: https://www.frontiersin.org/articles/10.3389/fimmu.2021.628966/full#supplementary-material

REFERENCES

1. Weller M, Wick W, Aldape K, Brada M, Berger M, Pfister SM, et al. Glioma. *Nat Rev Dis Primers* (2015) 1:15017. doi: 10.1038/nrdp.2015.17
2. Zhang H, Wang R, Yu Y, Liu J, Luo T, Fan F. Glioblastoma Treatment Modalities besides Surgery. *J Cancer* (2019) 10(20):4793–806. doi: 10.7150/jca.32475
3. Jiang T, Mao Y, Ma W, Mao Q, You Y, Yang X, et al. CGCG clinical practice guidelines for the management of adult diffuse gliomas. *Cancer Lett* (2016) 375(2):263–73. doi: 10.1016/j.canlet.2016.01.024
4. Zeng F, Wang K, Liu X, Zhao Z. Comprehensive profiling identifies a novel signature with robust predictive value and reveals the potential drug resistance mechanism in glioma. *Cell Commun Signal* (2020) 18(1):2. doi: 10.1186/s12964-019-0492-6
5. Audia A, Conroy S, Glass R, Bhat KPL. The Impact of the Tumor Microenvironment on the Properties of Glioma Stem-Like Cells. *Front Oncol* (2017) 7:143. doi: 10.3389/fonc.2017.00143
6. Ma Q, Long W, Xing C, Chu J, Luo M, Wang HY, et al. Cancer Stem Cells and Immunosuppressive Microenvironment in Glioma. *Front Immunol* (2018) 9:2924. doi: 10.3389/fimmu.2018.02924
7. Romani M, Pistillo MP, Carosio R, Morabito A, Banelli B. Immune Checkpoints and Innovative Therapies in Glioblastoma. *Front Oncol* (2018) 8:464. doi: 10.3389/fonc.2018.00464
8. Sharma P, Allison JP. The future of immune checkpoint therapy. *Science* (2015) 348(6230):56–61. doi: 10.1126/science.aaa8172
9. Hodges TR, Ott M, Xiu J, Gatalica Z, Swensen J, Zhou S, et al. Mutational burden, immune checkpoint expression, and mismatch repair in glioma: implications for immune checkpoint immunotherapy. *Neuro Oncol* (2017) 19(8):1047–57. doi: 10.1093/neuonc/nox026
10. Gibellini L, De Biasi S, Porta C, Lo Tartaro D, Depenni R, Pellacani G, et al. Single-Cell Approaches to Profile the Response to Immune Checkpoint Inhibitors. *Front Immunol* (2020) 11:490. doi: 10.3389/fimmu.2020.00490
11. Louis DN, Perry A, Reifenberger G, von Deimling A, Figarella-Branger D, Cavenee WK, et al. The 2016 World Health Organization Classification of Tumors of the Central Nervous System: a summary. *Acta Neuropathol* (2016) 131(6):803–20. doi: 10.1007/s00401-016-1545-1
12. Xu S, Liu Y, Yang K, Wang H, Shergalis A, Kyani A, et al. Inhibition of protein disulfide isomerase in glioblastoma causes marked downregulation of DNA repair and DNA damage response genes. *Theranostics* (2019) 9(8):2282–98. doi: 10.7150/thno.30621
13. Ferrari DM, Söling HD. The protein disulphide-isomerase family: unravelling a string of folds. *Biochem J* (1999) 339(Pt 1):1–10. doi: 10.1042/0264-6021:3390001
14. Galligan JJ, Petersen DR. The human protein disulfide isomerase gene family. *Hum Genomics* (2012) 6:6. doi: 10.1186/1479-7364-6-6
15. Wang Z, Zhang H, Cheng Q. PDIA4: The basic characteristics, functions and its potential connection with cancer. *BioMed Pharmacother* (2020) 122:109688. doi: 10.1016/j.biopha.2019.109688
16. Peng Z, Chen Y, Cao H, Zou H, Wan X, Zeng W, et al. Protein disulfide isomerases are promising targets for predicting the survival and tumor progression in glioma patients. *Aging (Albany NY)* (2020) 12(3):2347–72. doi: 10.18632/aging.102748
17. Horibe T, Torisawa A, Masuda Y, Kawakami K. Functional analysis of protein disulfide isomerase P5 in glioblastoma cells as a novel anticancer target. *Oncol Rep* (2019) 41(2):961–72. doi: 10.3892/or.2018.6868
18. Ramos FS, Serino LT, Carvalho CM, Lima RS, Urban CA, Cavalli IJ, et al. PDIA3 and PDIA6 gene expression as an aggressiveness marker in primary ductal breast cancer. *Genet Mol Res* (2015) 14(2):6960–7. doi: 10.4238/2015.June.26.4
19. Tufo G, Jones AWE, Wang Z, Hamelin J, Tajeddine N, Esposti DD, et al. The protein disulfide isomerases PDIA4 and PDIA6 mediate resistance to cisplatin-induced cell death in lung adenocarcinoma. *Cell Death Differ* (2014) 21(5):685–95. doi: 10.1038/cdd.2013.193
20. Silva Z, Verissimo T, Videira PA, Novo C. Protein disulfide isomerases: Impact of thapsigargin treatment on their expression in melanoma cell lines. *Int J Biol Macromol* (2015) 79:44–8. doi: 10.1016/j.ijbiomac.2015.04.029
21. Xu S, Sankar S, Neamati N. Protein disulfide isomerase: a promising target for cancer therapy. *Drug Discov Today* (2014) 19(3):222–40. doi: 10.1016/j.drudis.2013.10.017
22. Lee E, Lee D. Emerging Roles of Protein Disulfide Isomerase in Cancer. *BMB Rep* (2017) 50(8):401–10. doi: 10.5483/bmbrep.2017.50.8.107
23. Hu Q, Huang K, Tao C, Zhu X. Protein disulphide isomerase can predict the clinical prognostic value and contribute to malignant progression in gliomas. *J Cell Mol Med* (2020) 24(10):5888–900. doi: 10.1111/jcmm.15264
24. Zou H, Wen C, Peng Z, Shao Y, Hu L, Li S, et al. P4HB and PDIA3 are associated with tumor progression and therapeutic outcome of diffuse gliomas. *Oncol Rep* (2018) 39(2):501–10. doi: 10.3892/or.2017.6134
25. Sun S, Lee D, Ho AS, Pu JK, Zhang XQ, Lee NP, et al. Inhibition of prolyl 4-hydroxylase, beta polypeptide (P4HB) attenuates temozolomide resistance in malignant glioma via the endoplasmic reticulum stress response (ERSR) pathways. *Neuro Oncol* (2013) 15(5):562–77. doi: 10.1093/neuonc/not005
26. Hayano T, Kikuchi M. Molecular cloning of the cDNA encoding a novel protein disulfide isomerase-related protein (PDIR). *FEBS Lett* (1995) 372(2-3):210–4. doi: 10.1016/0014-5793(95)00996-m
27. Kuo TF, Chen TY, Jiang ST, Chen KW, Chiang YM, Hsu YJ, et al. Protein disulfide isomerase a4 acts as a novel regulator of cancer growth through the procaspase pathway. *Oncogene* (2017) 36(39):5484–96. doi: 10.1038/onc.2017.156
28. Higa A, Taouji S, Lhomond S, Jensen D, Fernandez-Zapico ME, Simpson JC, et al. Endoplasmic reticulum stress-activated transcription factor ATF6α requires the disulfide isomerase PDIA5 to modulate chemoresistance. *Mol Cell Biol* (2014) 34(10):1839–49. doi: 10.1128/MCB.01484-13
29. Hurst KE, Lawrence KA, Reyes Angeles L, Ye Z, Zhang J, Townsend DM, et al. Endoplasmic Reticulum Protein Disulfide Isomerase Shapes T Cell Efficacy for Adoptive Cellular Therapy of Tumors. *Cells* (2019) 8(12):1514. doi: 10.3390/cells8121514

30. Gill BJ, Pisapia DJ, Malone HR, Goldstein H, Lei L, Sonabend A, et al. MRI-localized biopsies reveal subtype-specific differences in molecular and cellular composition at the margins of glioblastoma. *Proc Natl Acad Sci U S A* (2014) 111(34):12550–5. doi: 10.1073/pnas.1405839111
31. Wang L, Babikir H, Müller S, Yagnik G, Shamardani K, Catalan F, et al. The Phenotypes of Proliferating Glioblastoma Cells Reside on a Single Axis of Variation. *Cancer Discov* (2019) 9(12):1708–19. doi: 10.1158/2159-8290.cd-19-0329
32. Mariathasan S, Turley SJ, Nickles D, Castiglioni A, Yuen K, Wang Y, et al. TGFbeta attenuates tumour response to PD-L1 blockade by contributing to exclusion of T cells. *Nature* (2018) 554(7693):544–8. doi: 10.1038/nature25501
33. Hugo W, Zaretsky JM, Sun L, Song C, Moreno BH, Hu-Lieskovan S, et al. Genomic and Transcriptomic Features of Response to Anti-PD-1 Therapy in Metastatic Melanoma. *Cell* (2016) 165(1):35–44. doi: 10.1016/j.cell.2016.02.065
34. Ni M, Liu X, Wu J, Zhang D, Tian J, Wang T, et al. Identification of Candidate Biomarkers Correlated With the Pathogenesis and Prognosis of Non-small Cell Lung Cancer via Integrated Bioinformatics Analysis. *Front Genet* (2018) 9:469. doi: 10.3389/fgene.2018.00469
35. Mermel CH, Schumacher SE, Hill B, Meyerson ML, Beroukhim R, Getz G. GISTIC2.0 facilitates sensitive and confident localization of the targets of focal somatic copy-number alteration in human cancers. *Genome Biol* (2011) 12(4):R41. doi: 10.1186/gb-2011-12-4-r41
36. Yoshihara K, Shahmoradgoli M, Martínez E, Vegesna R, Kim H, Torres-Garcia W, et al. Inferring tumour purity and stromal and immune cell admixture from expression data. *Nat Commun* (2013) 4(1):2612. doi: 10.1038/ncomms3612
37. Hänzelmann S, Castelo R, Guinney J. GSVA: gene set variation analysis for microarray and RNA-seq data. *BMC Bioinformatics* (2013) 14:7. doi: 10.1186/1471-2105-14-7
38. Ye Y, Jing Y, Li L, Mills GB, Diao L, Liu H, et al. Sex-associated molecular differences for cancer immunotherapy. *Nat Commun* (2020) 11(1):1779. doi: 10.1038/s41467-020-15679-x
39. Stuart T, Butler A, Hoffman P, Hafemeister C, Papalexi E, Mauck III WM, et al. Comprehensive Integration of Single-Cell Data. *Cell* (2019) 177(7):1888–902.e21. doi: 10.1016/j.cell.2019.05.031
40. Aran D, Looney AP, Liu L, Wu E, Fong V, Hsu A, et al. Reference-based analysis of lung single-cell sequencing reveals a transitional profibrotic macrophage. *Nat Immunol* (2019) 20(2):163–72. doi: 10.1038/s41590-018-0276-y
41. Pang B, Xu J, Hu J, Guo F, Wan L, Cheng M, et al. Single-cell RNA-seq reveals the invasive trajectory and molecular cascades underlying glioblastoma progression. *Mol Oncol* (2019) 13(12):2588–603. doi: 10.1002/1878-0261.12569
42. Xu J, Zhang Z, Qian M, Wang S, Qiu W, Chen Z, et al. Cullin-7 (CUL7) is overexpressed in glioma cells and promotes tumorigenesis via NF-kappaB activation. *J Exp Clin Cancer Res* (2020) 39(1):59. doi: 10.1186/s13046-020-01553-7
43. Hoshida Y, Brunet JP, Tamayo P, Golub TR, Mesirov JP. Subclass mapping: identifying common subtypes in independent disease data sets. *PloS One* (2007) 2(11):e1195. doi: 10.1371/journal.pone.0001195
44. Eckel-Passow JE, Lachance DH, Molinaro AM, Walsh KM, Decker PA, Sicotte H, et al. Glioma Groups Based on 1p/19q,IDH, andTERTPromoter Mutations in Tumors. *N Engl J Med* (2015) 372(26):2499–508. doi: 10.1056/NEJMoa1407279
45. Verhaak RGW, Hoadley KA, Purdom E, Wang V, Qi Y, Wilkerson MD, et al. Integrated Genomic Analysis Identifies Clinically Relevant Subtypes of Glioblastoma Characterized by Abnormalities in PDGFRA, IDH1, EGFR, and NF1. *Cancer Cell* (2010) 17(1):98–110. doi: 10.1016/j.ccr.2009.12.020
46. Phillips HS, Kharbanda S, Chen R, Forrest WF, Soriano RH, Wu TD, et al. Molecular subclasses of high-grade glioma predict prognosis, delineate a pattern of disease progression, and resemble stages in neurogenesis. *Cancer Cell* (2006) 9(3):157–73. doi: 10.1016/j.ccr.2006.02.019
47. Jia D, Li S, Li D, Xue H, Yang D, Liu Y. Mining TCGA database for genes of prognostic value in glioblastoma microenvironment. *Aging (Albany NY)* (2018) 10(4):592–605. doi: 10.18632/aging.101415
48. Lepore F, D'Alessandro G, Antonangeli F, Santoro A, Esposito V, Limatola C, et al. CXCL16/CXCR6 Axis Drives Microglia/Macrophages Phenotype in Physiological Conditions and Plays a Crucial Role in Glioma. *Front Immunol* (2018) 9:2750. doi: 10.3389/fimmu.2018.02750
49. Ayers M, Lunceford J, Nebozhyn M, Murphy E, Loboda A, Kaufman DR, et al. IFN-gamma-related mRNA profile predicts clinical response to PD-1 blockade. *J Clin Invest* (2017) 127(8):2930–40. doi: 10.1172/JCI91190
50. Rooney MS, Shukla SA, Wu CJ, Getz G, Hacohen N. Molecular and genetic properties of tumors associated with local immune cytolytic activity. *Cell* (2015) 160(1-2):48–61. doi: 10.1016/j.cell.2014.12.033
51. McNulty SN, Cottrell CE, Vigh-Conrad KA, Carter JH, Heusel JW, Ansstas G, et al. Beyond sequence variation: assessment of copy number variation in adult glioblastoma through targeted tumor somatic profiling. *Hum Pathol* (2019) 86:170–81. doi: 10.1016/j.humpath.2018.12.004
52. Segura-Collar B, Gargini R, Tovar-Ambel E, Hernandez-SanMiguel E, Epifano C, Perez de Castro I, et al. The EGFR-TMEM167A-p53 Axis Defines the Aggressiveness of Gliomas. *Cancers (Basel)* (2020) 12(1):208. doi: 10.3390/cancers12010208
53. Gieryng A, Pszczolkowska D, Walentynowicz KA, Rajan WD, Kaminska B. Immune microenvironment of gliomas. *Lab Invest* (2017) 97(5):498–518. doi: 10.1038/labinvest.2017.19
54. Winslow S, Lindquist KE, Edsjo A, Larsson C. The expression pattern of matrix-producing tumor stroma is of prognostic importance in breast cancer. *BMC Cancer* (2016) 16(1):841. doi: 10.1186/s12885-016-2864-2
55. Liu W, Ye H, Liu Y, Xu C, Zhong Y, Tian T, et al. Transcriptome-derived stromal and immune scores infer clinical outcomes of patients with cancer. *Oncol Lett* (2018) 15(4):4351–7. doi: 10.3892/ol.2018.7855
56. Wang H, Wu X, Chen Y. Stromal-Immune Score-Based Gene Signature: A Prognosis Stratification Tool in Gastric Cancer. *Front Oncol* (2019) 9:1212. doi: 10.3389/fonc.2019.01212
57. Marvel D, Gabrilovich DI. Myeloid-derived suppressor cells in the tumor microenvironment: expect the unexpected. *J Clin Invest* (2015) 125(9):3356–64. doi: 10.1172/JCI80005
58. Amit A, Vijayamahantesh, Dikhit MR, Singh AK, Kumar V, Suman SS, et al. Immunization with Leishmania donovani protein disulfide isomerase DNA construct induces Th1 and Th17 dependent immune response and protection against experimental visceral leishmaniasis in Balb/c mice. *Mol Immunol* (2017) 82:104–13. doi: 10.1016/j.molimm.2016.12.022
59. Amit A, Dikhit MR, Mahantesh V, Chaudhary R, Singh AK, Singh A, et al. Immunomodulation mediated throughLeishmania donovaniprotein disulfide isomerase by eliciting CD8+ T-cell in cured visceral leishmaniasis subjects and identification of its possible HLA class-1 restricted T-cell epitopes. *J Biomol Struct Dyn* (2016) 35(1):128–40. doi: 10.1080/07391102.2015.1134349
60. Caorsi C, Niccolai E, Capello M, Vallone R, Chattaragada MS, Alushi B, et al. Protein disulfide isomerase A3-specific Th1 effector cells infiltrate colon cancer tissue of patients with circulating anti-protein disulfide isomerase A3 autoantibodies. *Transl Res* (2016) 171:17–28.e1-2. doi: 10.1016/j.trsl.2015.12.013
61. Xiao Y, Li C, Gu M, Wang H, Chen W, Luo G, et al. Protein Disulfide Isomerase Silence Inhibits Inflammatory Functions of Macrophages by Suppressing Reactive Oxygen Species and NF-κB Pathway. *Inflammation* (2018) 41(2):614–25. doi: 10.1007/s10753-017-0717-z
62. Vinaik R, Kozlov G, Gehring K. Structure of the non-catalytic domain of the protein disulfide isomerase-related protein (PDIR) reveals function in protein binding. *PloS One* (2013) 8(4):e62021. doi: 10.1371/journal.pone.0062021
63. Woroniecka KI, Rhodin KE, Chongsathidkiet P, Keith KA, Fecci PE. T-cell Dysfunction in Glioblastoma: Applying a New Framework. *Clin Cancer Res* (2018) 24(16):3792–802. doi: 10.1158/1078-0432.CCR-18-0047
64. Wang D, Wang X, Si M, Yang J, Sun S, Wu H, et al. Exosome-encapsulated miRNAs contribute to CXCL12/CXCR4-induced liver metastasis of colorectal cancer by enhancing M2 polarization of macrophages. *Cancer Lett* (2020) 474:36–52. doi: 10.1016/j.canlet.2020.01.005
65. Yang D, Liu K, Fan L, Liang W, Xu T, Jiang W, et al. LncRNA RP11-361F15.2 promotes osteosarcoma tumorigenesis by inhibiting M2-Like polarization of tumor-associated macrophages of CPEB4. *Cancer Lett* (2020) 473:33–49. doi: 10.1016/j.canlet.2019.12.041
66. Sa JK, Chang N, Lee HW, Cho HJ, Ceccarelli M, Cerulo L, et al. Transcriptional regulatory networks of tumor-associated macrophages that

drive malignancy in mesenchymal glioblastoma. *Genome Biol* (2020) 21 (1):216. doi: 10.1186/s13059-020-02140-x
67. Netea-Maier RT, Smit JWA, Netea MG. Metabolic changes in tumor cells and tumor-associated macrophages: A mutual relationship. *Cancer Lett* (2018) 413:102–9. doi: 10.1016/j.canlet.2017.10.037
68. Zhou W, Ke SQ, Huang Z, Flavahan W, Fang X, Paul J, et al. Periostin secreted by glioblastoma stem cells recruits M2 tumour-associated macrophages and promotes malignant growth. *Nat Cell Biol* (2015) 17(2):170–82. doi: 10.1038/ncb3090
69. Goswami S, Walle T, Cornish AE, Basu S, Anandhan S, Fernandez I, et al. Immune profiling of human tumors identifies CD73 as a combinatorial target in glioblastoma. *Nat Med* (2020) 26(1):39–46. doi: 10.1038/s41591-019-0694-x
70. Cheng Q, Li J, Fan F, Cao H, Dai ZY, Wang ZY, et al. Identification and Analysis of Glioblastoma Biomarkers Based on Single Cell Sequencing. *Front Bioeng Biotechnol* (2020) 8:167. doi: 10.3389/fbioe.2020.00167
71. Litak J, Mazurek M, Grochowski C, Kamieniak P, Roliński J. PD-L1/PD-1 Axis in Glioblastoma Multiforme. *Int J Mol Sci* (2019) 20(21):5347. doi: 10.3390/ijms20215347
72. Liu S, Wang Z, Wang Y, Fan X, Zhang C, Ma W, et al. PD-1 related transcriptome profile and clinical outcome in diffuse gliomas. *Oncoimmunology* (2018) 7(2): e1382792. doi: 10.1080/2162402X.2017.1382792
73. Li X, Wang B, Gu L, Gao L, Ma C, Liang X, et al. Tim-3 expression predicts the abnormal innate immune status and poor prognosis of glioma patients. *Clin Chim Acta* (2018) 476:178–84. doi: 10.1016/j.cca.2017.11.022
74. Zhang J, Wang J, Marzese DM, Wang X, Yang Z, Li C, et al. B7H3 regulates differentiation and serves as a potential biomarker and theranostic target for human glioblastoma. *Lab Invest* (2019) 99(8):1117–29. doi: 10.1038/s41374-019-0238-5
75. Wang Z, Li G, Wang Q, Bao Z, Wang Z, Zhang C, et al. PD-L2 expression is correlated with the molecular and clinical features of glioma, and acts as an unfavorable prognostic factor. *OncoImmunology* (2018) 8(2):e1541535. doi: 10.1080/2162402x.2018.1541535
76. Chen G, Huang AC, Zhang W, Zhang G, Wu M, Xu W, et al. Exosomal PD-L1 contributes to immunosuppression and is associated with anti-PD-1 response. *Nature* (2018) 560(7718):382–6. doi: 10.1038/s41586-018-0392-8
77. Cortes J, Cescon DW, Rugo HS, Nowecki Z, Im S-A, Yusof MM, et al. Pembrolizumab plus chemotherapy versus placebo plus chemotherapy for previously untreated locally recurrent inoperable or metastatic triple-negative breast cancer (KEYNOTE-355): a randomised, placebo-controlled, double-blind, phase 3 clinical trial. *Lancet* (2020) 396(10265):1817–28. doi: 10.1016/s0140-6736(20)32531-9

Conflict of Interest: The authors declare that the research was conducted in the absence of any commercial or financial relationships that could be construed as a potential conflict of interest.

frontiers in Immunology

ORIGINAL RESEARCH
published: 25 March 2021
doi: 10.3389/fimmu.2021.627650

Association of Isocitrate Dehydrogenase (IDH) Status With Edema to Tumor Ratio and Its Correlation With Immune Infiltration in Glioblastoma

Daniel Dubinski[1], Sae-Yeon Won[1], Maximilian Rauch[2], Bedjan Behmanesh[1], Lionel D. C. Ngassam[1], Peter Baumgarten[1], Christian Senft[1], Patrick N. Harter[3], Joshua D. Bernstock[4], Thomas M. Freiman[1], Volker Seifert[1] and Florian Gessler[1]*

[1] Department of Neurosurgery, Goethe University Hospital, Frankfurt, Germany, [2] Institute of Neuroradiology, Goethe University, Frankfurt, Germany, [3] Neurological Institute (Edinger Institute), Goethe University, Frankfurt, Germany, [4] Department of Neurosurgery, Brigham and Women's Hospital, Harvard Medical School, Boston, MA, United States

OPEN ACCESS

Edited by:
Lukas Bunse, German Cancer Research Center (DKFZ), Germany

Reviewed by:
Susanna Mandruzzato, University Hospital of Padua, Italy
Michael O. Breckwoldt, German Cancer Research Center (DKFZ), Germany

***Correspondence:**
Daniel Dubinski
danieldubinski@gmail.com

Specialty section:
This article was submitted to Cancer Immunity and Immunotherapy, a section of the journal Frontiers in Immunology

Received: 09 November 2020
Accepted: 09 March 2021
Published: 25 March 2021

Citation:
Dubinski D, Won S-Y, Rauch M, Behmanesh B, Ngassam LDC, Baumgarten P, Senft C, Harter PN, Bernstock JD, Freiman TM, Seifert V and Gessler F (2021) Association of Isocitrate Dehydrogenase (IDH) Status With Edema to Tumor Ratio and Its Correlation With Immune Infiltration in Glioblastoma. Front. Immunol. 12:627650. doi: 10.3389/fimmu.2021.627650

Purpose: The extent of preoperative peritumoral edema in glioblastoma (GBM) has been negatively correlated with patient outcome. As several ongoing studies are investigating T-cell based immunotherapy in GBM, we conducted this study to assess whether peritumoral edema with potentially increased intracranial pressure, disrupted tissue homeostasis and reduced local blood flow has influence on immune infiltration and affects survival.

Methods: A volumetric analysis of preoperative imaging (gadolinium enhanced T1 weighted MRI sequences for tumor size and T2 weighted sequences for extent of edema (including the infiltrative zone, gliosis etc.) was conducted in 144 patients using the Brainlab® software. Immunohistochemical staining was analyzed for lymphocytic- (CD 3+) and myelocytic (CD15+) tumor infiltration. A retrospective analysis of patient-, surgical-, and molecular characteristics was performed using medical records.

Results: The edema to tumor ratio was neither associated with progression-free nor overall survival (p=0.90, p=0.74). However, GBM patients displaying IDH-1 wildtype had significantly higher edema to tumor ratio than patients displaying an IDH-1 mutation (p=0.01). Immunohistopathological analysis did not show significant differences in lymphocytic or myelocytic tumor infiltration (p=0.78, p=0.74) between these groups.

Conclusion: In our cohort, edema to tumor ratio had no significant correlation with immune infiltration and outcome. However, patients with an IDH-1wildtype GBM had a significantly higher edema to tumor ratio compared to their IDH-1 mutated peer group. Further studies are necessary to elucidate the underlying mechanisms.

Keywords: immune infiltration, glioma microenvironment, dexamethasone, peritumoral edema, peritumoral edema zone

INTRODUCTION

Glioblastoma (GBM) patients frequently present with peritumoral edema as diagnosed with preoperative imaging, such as T2 or FLAIR MRI scan. Peritumoral edema in turn often causes severe neurological impairment and remains a challenging factor throughout treatment (1). The peritumoral edema in GBM is considered to be vasogenic and caused by increased vascular permeability as hypoxia induced capillary formations lack functional tight junctions, contain fenestration and irregular basal membrane endothelia (2). The disrupted blood brain barrier (BBB) leads to the extravasation of plasma into the brain parenchyma surrounding the lesion.

Furthermore, the hypoxic core of the GBM, often containing necrosis, results in VEGF secretion which in turn is a crucial mediator of peritumoral edema and disrupted tissue hemostasis. Although several studies have identified the synthetic corticosteroid dexamethasone (DEX) as unbeneficial in terms of survival for edema treatment in GBM, it is still routinely used in clinics for peritumoral edema treatment in GBM (3, 4).

Peritumoral edema has been described as a strong propagator of malignant cell infiltration and several studies have confirmed the negative prognostic impact of high edema to tumor ratios in GBM, although the mechanisms remain unclear (5, 6). Perfusion-weighted imaging has been used to demonstrate 50% reduced regional cerebral blood- volume and flow in peritumoral edema compared to the contralateral white matter (7). We therefore postulated that increased edema (including the infiltrative zone, gliosis etc.) to tumor ratio would influence the lymphocytic and myelocytic tumor infiltration in patients with GBM and could therefore be associated with a poor prognosis.

MATERIAL AND METHODS

Patients and Data Collection

For this retrospective analysis an ethical approval was obtained from the ethics committee of the University Hospital Frankfurt, Germany, (Identification number: 20-676). As a non-interventional single-center study no patient consent was necessary.

Cohort

In total, 162 GBM patients that were treated at the authors' institution between September 2008 and January 2013 were retrospectively analyzed. The inclusion criteria were tumor resection (stereotactic biopsies were excluded) with the histological confirmation of WHO IV GBM without previous treatment such as radio- chemotherapy for low grade astrocytoma. Further inclusion criteria were the availability of a preoperative cranial MRI with gadolinium enhanced T1 sequences and T2 sequences.

Patient medical charts were analyzed by two neurosurgeons (D.D. and S-Y.W.) and blinded to the preoperative radiological data. Tumor and edema volume were analyzed by an experienced neuroradiologist (M.R.) and two neurosurgeons (P.B. and B.B.) who were blinded to the medical chart data. Patient characteristics that were extracted from the medical chart including the preoperative Karnofsky performance scale (KPS), date of surgery, date of death or date of last contact, date of tumor progression that was defined as the date of cranial MRI with progressive disease according to the RANO (8) criteria and/or the determination of the local interdisciplinary neurooncological tumor board.

Magnetic Resonance Imaging

Preoperative MRI scans were performed in the department of neuroradiology, Goethe University Hospital Frankfurt at a 3 Tesla Siemens Verio scanner. Gd-DO3A-butrol (Gadovist®, Bayer Vital GmbH) was administered intravenously (0.2 ml/kg, 0.5-1 ml/sec) and imaging started 9 seconds after administration of the contrast agent.

Image Analysis

Image analysis was performed by a neuroradiologist (M.R.) and two neurosurgeons (P.B. and B.B.) that were blinded to patients' molecular characteristics. Pre- and postoperative tumor and edema volumes were analyzed by semi-automatic segmentation with IPlannet 3 (Cranial planning software, Brainlab AG, Feldkirchen, Germany). A representative analysis is displayed in **Figure 1**. All tumor segmentations were done semi-automatically with the 'Smartbrush' tool of the Brainlab Elements software. A two-dimensional segmentation was drawn in the axial image and a second two-dimensional segmentation was drawn in a coronal slide. These two segmentations automatically generated a three-dimensional graphic of the tumor. The three-dimensional graphic was then manually corrected by adding or erasing certain areas. A total of 144 segmentations were performed in this manner. Tumor volume was delineated on contrast enhanced T1-weighted images and necrotic areas were spared. Edema volume was measured on a non-enhancing T2-hyperintense image set in the same procedure. The extent of resection was calculated by the pre- and postoperative tumor volume. Gross total resection (GTR) was defined as complete removal (100%) of contrast-enhancing tissue.

Tissue Specimen and Processing

For this analysis the formalin-fixed and paraffin-embedded (FFPE) tissue samples from 26 patients of a recently published cohort were used (4). Paraffin full mounts were processed as follows: 1. cutting into 3µm thick slices using a microtome (Leica Microsystems, Nussloch GmbH, Nussloch, Germany), 2. placing on microscope slides (SuperFrost, Thermo Scientific, Dreieich, Germany), 3. heating to 40°C for 20min and 4. storage in an incubator overnight (37°C). For staining, standardized protocols for the automated IHC slide staining system BOND-III (Leica Biosystems, Nussloch GmbH, Nussloch, Germany) were used including the following antibodies: CD3 (A0452; 1:500; Dako), CD15 (M3631; 1:2000; Dako). After hematoxylin-counterstaining slides were mounted, lymphocytic (myelocytic) infiltration was assessed by counting CD3 (CD15) positive stained cells, in a defined tumor bearing area, using a Zeiss microscope (Axiophot, Carl Zeiss Microscopy GmbH, Jena,

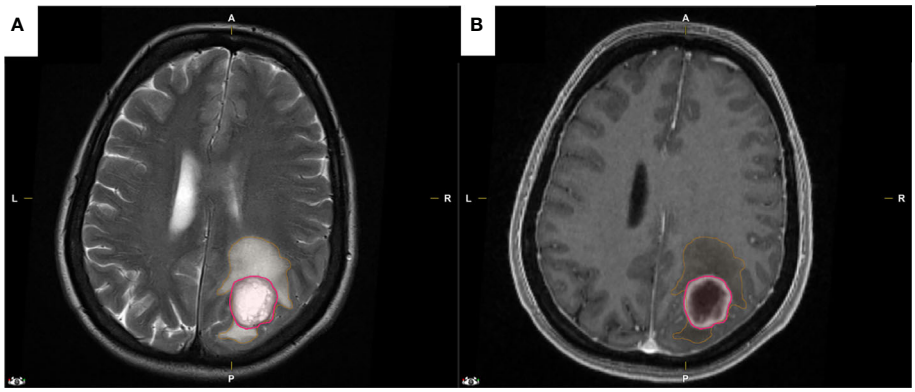

FIGURE 1 | Representative MRI images that were used for the semi-automatic segmentation with IPlannet 3 software by Brainlab®. **(A, B)** Preoperative axial T2 and gadolinium enhanced T1 weighted MRI of a GBM patient with peritumoral edema encircled in orange and with tumor enhancement encircled in pink.

Germany) with a Stereo Investigator (Version 4.34 software from MicroBrightField Inc.), subsequently obtaining the ratio of positive stained cells per mm^2 (9). A representative analysis is displayed in **Figure 2**.

Statistics

Data analysis was performed with IBM SPSS Statistics Version 23.0 (SPSS Inc., IBM Corp., Armonk, NY, USA). For patients and tumor characteristics, descriptive statistics were used. Fisher's exact test was used for the comparison of categorical variables between the cohorts. For continuous parameters, the Wilcoxon-Mann-Whitney test was used. To assess the impact of the variables, odds ratio (OR) with 95% confidence intervals (CI) were calculated. Results with $p \leq 0.05$ were considered statistically relevant. To estimate the survival rates, the Kaplan-Meier analysis was used. The differences between curves were assessed using the log-rank test. Progression free survival (PFS) was defined as the time from diagnosis to first recurrence or death. Overall survival (OS) was defined as the time of first presentation to death.

RESULTS

Patient Characteristics

A total of 144 patients with primary GBM were treated at the authors' institution between September 2008 and January 2013. Of those, 18 patients were excluded due to a lack of radiological data, loss to follow-up, and/or lack of molecular data. Of the analyzed cohort, 64 patients (44%) were female and 80 patients (56%) were male. Of all patients, 64 patients (44%) were under 60 years of age. In total, 63 patients had a Karnofsky performance scale (KPS) of less than 80 (44%). Preoperative dexamethasone treatment was observed in 57 patients (39%). Gross total resection (GTR) was achieved in 89 patients (62%). O (6)-methylguanine-DNA methyltransferase (MGMT) promotor methylation was detected in 68 patients (47%) and an isocitrate dehydrogenase (IDH) (IDH1R132H-mutation) mutation was observed in 19 patients (13%). The median tumor volume on T1 + contrast preoperative MRI was 29.75 cm^3 (IQR: 36.6) and median edema volume on T2 was 114 cm^3 (IQR: 120.8). Median progression free survival (PFS) was 9 months (IQR: 11.5) and overall survival was 17 months (IQR: 19.5). Of the 144 patients with complete diagnostic histopathological analysis, 26 FFPE's were available for further immunohistochemical analysis. Of those, median tumor infiltration (CD3+) were 0.18/mm^2 (IQR: 0.15) for lymphocytic (CD3+) cells and 0.08/mm^2 (IQR: 0.66) for myelocytic (CD15+) cells (see **Table 1**).

Association of Edema to Tumor Ratio With Patient Characteristics

According to the median preoperative MRI edema to tumor volume, patients were stratified into the high or low edema to tumor ratio groups. Patients of the high edema to tumor ratio group had 57% (n=41) female patients compared to 54% (n= 39) in the low edema to tumor cohort. No significant differences regarding sex were observed between both groups (p=0.86; 95%CI: 0.57-2.16; OR 1.1). In the high edema to tumor cohort, 35 (49%) patients were under the age of 60 compared to 29 (40%) patients in the low edema to tumor cohort. No significant differences regarding age were observed between both groups. Moreover, 31 (43%) patients with a high edema to tumor ratio and 32 patients (44%) with a low edema to tumor ratio presented with a median preoperative Karnofsky performance scale (KPS) of less than 80. The preoperative KPS was not associated with edema to tumor ratio (p=0.99; 95%CI:0.48-1.82; OR: 0.9); see **Table 2**.

Preoperative Dexamethasone Administration and Edema to Tumor Ratio

Patient medical charts showed preoperative dexamethasone (DEX) administration present in 26 patients (36%) in the high edema to tumor ratio cohort vs. 31 patients (43%) in the low edema to tumor ratio cohort. Preoperative presence of DEX was not associated with a high edema to tumor ratio (p=0.49; 95%CI: 0.38-1.47; OR: 0.7; **Table 2**).

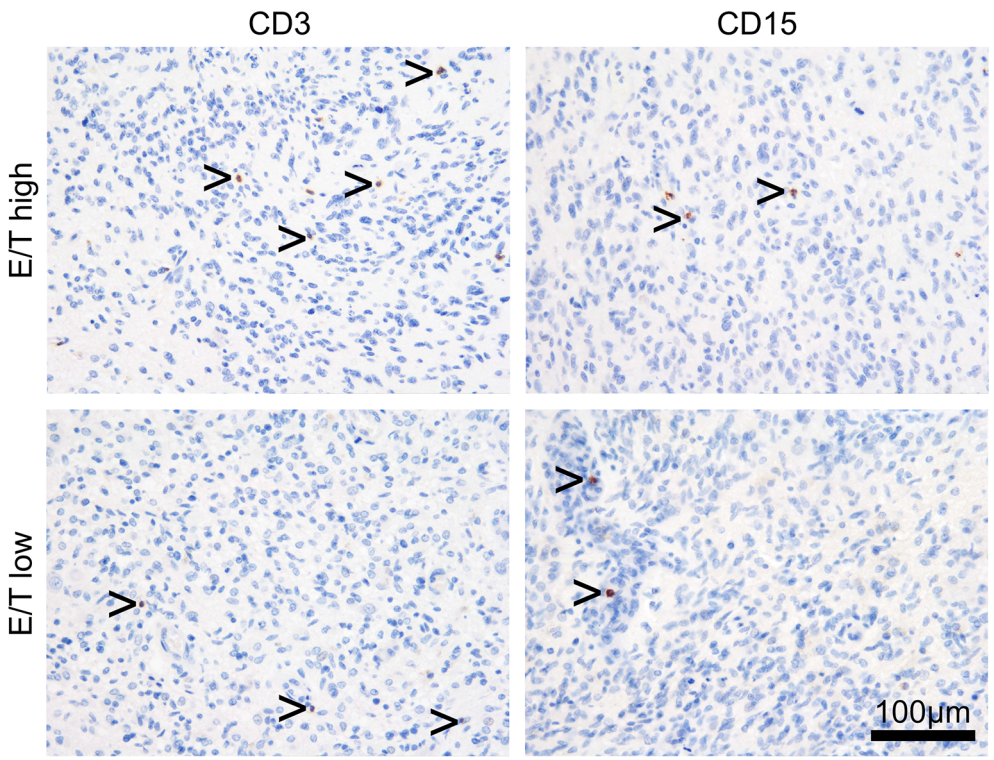

FIGURE 2 | Representative immunohistochemistry slides with anti-CD3 (lymphocytic) and anti-CD15 (myelocytic) tumor infiltration in GBM patients allocated according to high vs low edema to tumor ratio.

TABLE 1 | Patient characteristics.

n=144	Number(%)
Gender	
Male	80 (56)
Female	64 (44)
Age (years)	
<60	64 (44)
≥60	80 (56)
Karnofsky performance scale	
<80	63 (44)
≥80	81(56)
Dexamethasone preoperative	
yes	57 (39)
no	87 (61)
Surgical Charactersitic	
Gross total resection	89 (62)
Partial resection	55 (38)
Tumor Charactersitic	
MGMT+	68 (47)
MGMT-	76 (53)
IDH-1mut	19 (13)
IDH-1wt	125 (87)
MRI Charactersitic	
Median tumor volume (T1+contrast)	29.75 (IQR: 36.6)
Median edema volume (T2)	114 (IQR: 120.8)
Edema/Tumor Ratio <3	72 (50)
Edema/Tumor Ratio >3	72 (50)
Immunologica l Charactersitic (n=26)	
Lymphocytic infiltration (median/mm2)	0.18 (IQR: 0.15)
Granulocytic infiltration (median/mm2)	0.08 (IQR: 0.66)

Association of Edema to Tumor Ratio With Operative Results

Gross total resection (GTR) was achieved in 45 patients (62%) in the high edema to tumor cohort and 44 patients (61%) in the low edema to tumor cohort. The operative result was independent of preoperative edema to tumor ratio (p=0.99; 95% 0.54-2.07; OR: 1.0; **Table 2**).

Association of Edema to Tumor Ratio With Molecular Characteristics

In patients with a high edema to tumor ratio, the MGMT promotor was methylated (+) in 38 patients (53%) and in 30 patients (42%) of the low edema to tumor ratio cohort (p=0.40; 95%CI: 0.36-1.37; OR: 07). The MGMT promotor status was not significantly correlated with edema to tumor ratio. Isocitrate dehydrogenase 1 wildtype (IDH-1 wt) was observed in 68 patients (94%) with a high edema to tumor ratio and in 57 patients (79%) with a low edema to tumor ratio (p=0.01; 95%CI: 0.07-0.71, OR: 0.2 in univariate and p=0.03; 95%CI: 0.13-0.90, OR: 4.6 in multivariate analysis. (**Table 2**).

Survival Analysis Depending on Edema to Tumor Volume

Volumetric analysis displayed a median tumor size of 29.75cm^3 (IQR: 37.52). Patients with a tumor smaller than 29.75cm^3 were defined as low tumor volume and patients with tumor size larger than 29.75cm^3 as high tumor volume. Patients with low tumor volume had a median OS of 17 months (IQR: 19) and a PFS of 9

months (IQR: 12) compared to 16 months OS (IQR: 19.25) and 8 months PFS (IQR:11.75) in patients with large tumors, respectively. Preoperative volumetric tumor size was not associated with PFS (p=0.734) or OS (0.925; **Figure 3A, B**).

For the volumetric analysis of peritumoral edema, a median of 116.3cm^3 (IQR: 120.8) was detected. Patients with peritumoral edema smaller than 116.3cm^3 were defined as low edema volume and had a median OS of 16 months (IQR: 19.75) and a PFS of 8 months (IQR: 10.75) whereas patients with high edema volume had a median OS of 19 months (IQR: 19) and a median PFS of 9.5 months (IQR: 11). The volume of peritumoral edema was not associated with either PFS (p=0.55) or OS (p=0.40; **Figure 3C, D**).

To analyze the edema to tumor ratio, edema/tumor was calculated and a median of 3 was observed. Thus, patients with ratios under 3 were counted as having a low edema to tumor ratio and above 3 as having a high edema to tumor ratio. Patients with low edema to tumor ratio had a median PFS of 8 months (IQR: 12), compared to the PFS of 9 months (IQR: 11) in patients with high preoperative edema to tumor ratio (p=0.401). In terms of OS, patients with a low preoperative edema to tumor ratio displayed a median survival of 15 months (IQR: 21) compared with 19 months (IQR: 18) in patients with a high edema to tumor ratio (p=0.551; **Figures 3E, F**).

Leukocytic Tumor Infiltration in Dependence of Edema to Tumor Ratio

In our cohort of 144 patients, immunohistochemistry was available in a total of 26 patients. In the high edema to tumor ratio group (n=9), median lymphocytic infiltration was 0.15 cells/mm^2 (IQR: 0.18) vs. 0.21 cells/mm^2 (IQR: 0.13) in the low edema to tumor ratio group (n=17) indicating that the lymphocytic tumor infiltration was not significantly correlated with edema to tumor ratio (p=0.78; 95%CI: 0.38-0.50; OR: 0.06). Furthermore, median myelocytic tumor infiltration was 0.06 cells/mm^2 (IQR: 0.16) in the high edema to tumor ratio group vs. 0.08 cells/mm^2 (IQR: 0.05) in the low edema to tumor ratio group. The myelocytic tumor infiltration was therefore not associated with edema to tumor ratio (p=0.74; 95% CI: 0.10-0.14; OR 0.02) (**Table 2**).

DISCUSSION

The major finding of our study is the significant correlation between IDH-1 status and the edema to tumor ratio. Patients harboring an IDH-1 wildtype glioblastoma presented with an increased preoperative edema to tumor ratio; however, further translational investigations are warranted to elucidate the underlaying mechanism. Furthermore, our immunohistochemistry analysis and its correlation with the edema to tumor ratio revealed that edema to tumor ratio had no significant association with lymphocytic and/or myelocytic tumor infiltration.

The interplay between cancer and immune cells is a major determinant in cancer progression and the immune system is emerging as a powerful prognostic marker and therapeutic target in neuro-oncology (10). Additionally, peritumoral edema frequently leads to neurological impairment and remains a challenging factor throughout treatment (3). Our study therefore analyzed a potential interaction between these factors.

Regarding the preoperative dexamethasone (DEX) treatment our study found no significant correlation between the extent of edema and DEX administration. Although dosage

TABLE 2 | Uni- and multivariate analysis of juxtaposed characteristics according to edema to tumor ratio.

Variable(%)	Edema/Tumor ratio		Univariate			Multivariate		
	high *(n = 72)*	low *(n=72)*	*P* value	95% CI	OR	*P* value	95% CI	OR
Gender								
Male	41(57)	39 (54)	0.86	0.57-2.16	1.1	0.32	0.96-1.03	0.9
Female	31(43)	33 (46)	0.86	0.46-1.71	0.8			
Age (years)								
<60	35 (49)	29 (40)	0.40	0.72-2.71	1.4	1.01	0.98-1.01	0.9
≥60	37 (51)	43 (60)	0.40	0.36-1.37	0.7			
Karnofsky performance scale								
<80	31(43)	32 (44)	0.99	0.48-1.82	0.9	0.6	0.98-1.21	1.0
≥80	41(57)	40 (56)	0.99	0.54-2.04	1.0			
Dexamethasone preoperative								
yes	26 (36)	31 (43)	0.49	0.38-1.47	0.7	0.95	0.55-15.69	0.9
no	46 (64)	41 (57)	0.49	0.68-2.61	1.3			
Surgical Charactersitic								
Gross total resection	45 (62)	44 (61)	0.99	0.54-2.07	1.0	0.87	0.45-1.26	0.4
Partial resection	27 (38)	28 (39)	0.99	0.48-1.84	0.9			
Molecular Charactersitic								
MGMT+	38 (53)	30 (42)	0.40	0.36-1.37	0.7	0.85	0.57-1.92	1.0
MGMT-	34 (47)	42 (58)	0.40	0.72-2.72	1.4			
IDH-1mut	4 (6)	15 (21)	0.01	0.07-0.71	0.2	0.03	0.13-0.90	0.34
IDH-1wt	68 (94)	57 (79)	0.01	1.40-14.23	1.4			
Immunological Charactersitic (n=26)	*n=9*	*n=7*						
Median lymphocytic infiltration per mm2	0.15 (IQR: 0.18)	0.21(IQR: 0.13)	0.78	0.38-0.50	0.06			
Median granulocytic infiltration per mm2	0.06 (IQR: 0.16)	0.08 (IQR: 0.05)	0.74	0.10-0.14	0.02			

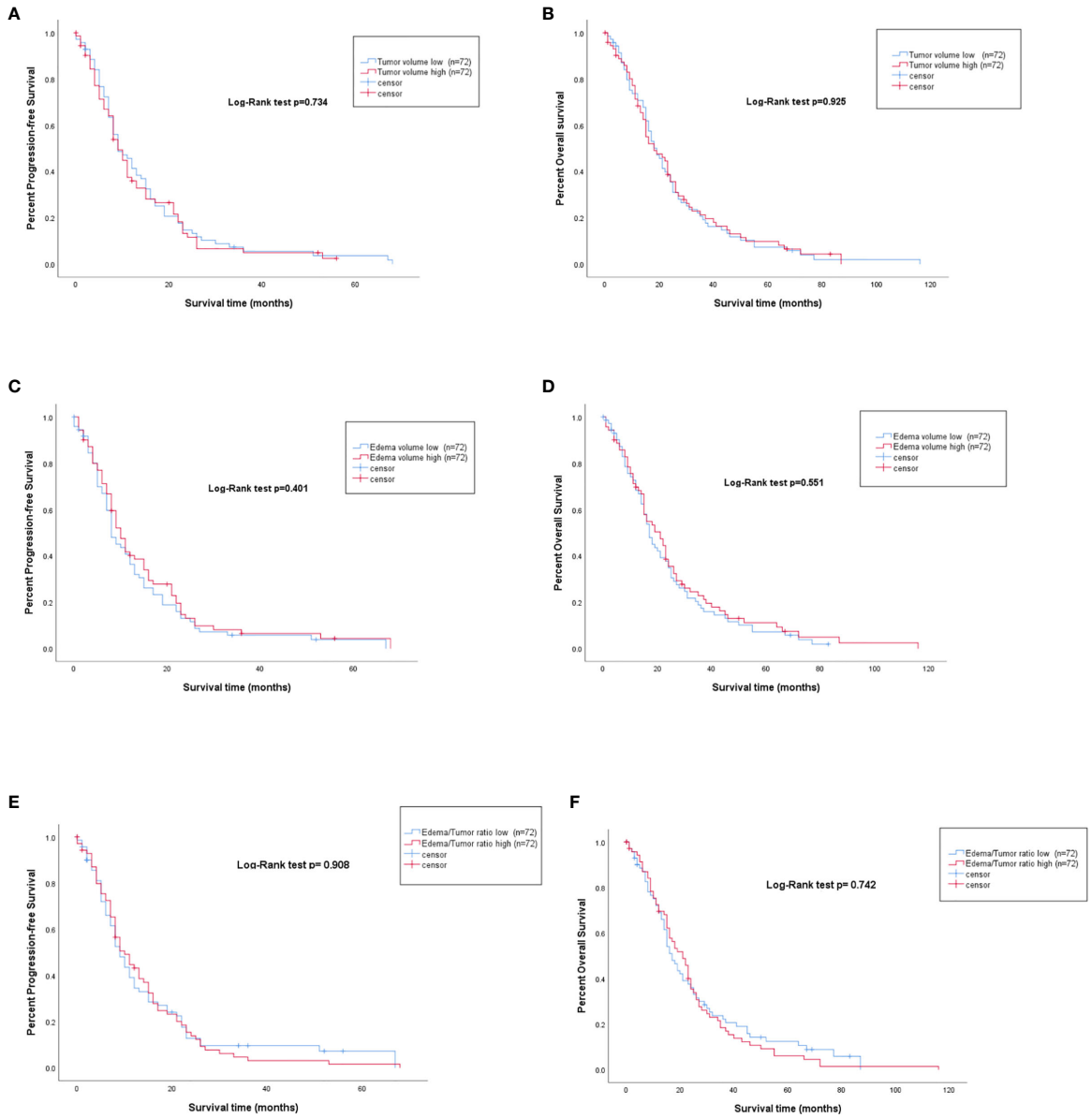

FIGURE 3 | PFS and OS represented by Kaplan-Meier curves for high vs. low preoperative tumor volume **(A, B)**, high vs. low preoperative edema volume **(C, D)**, and high vs. low edema to tumor ratio **(E, F)**.

recommendations are lacking, the routinely used synthetic corticoid DEX is clinically established for edema treatment (11, 12). However, recent studies identified several mechanisms indicating that administration of DEX in patients with GBM may be not be beneficial; in fact, it may worsen the prognosis, decrease radiosensitivity, and decreased immune infiltration is certain subtypes of GBM (3, 4, 13). Considering the missing association between the extent of tumor-edema and DEX dosage in our study, this finding supports the critical review of DEX administration in GBM patients, even more so in lesions that are not strategically located (motor or sensory cortex, language cortex, insula or basal ganglia), since several recently discovered mechanisms explain the unbeneficial impact of DEX on the outcome in GBM (3, 13).

Our study did not find a significant association between peritumoral edema or edema to tumor ratio with the extent of resection. Wu et al. recently described the negative impact of the extent of peritumoral edema (≥1 cm from tumor margin on axial MRI) on survival (6). Extensive peritumoral edema can lead to intraoperative challenges as it may obscure anatomical landmarks and complicate resection, which in turn contributes to poor survival (14, 15). Our finding does not support this proposal, since resection status was not associated with edema or edema to tumor ratio in our

cohort. An important bias which could obscure our results is the inhomogeneous surgical management (5-ALA, intraoperative MRI etc.) paired with differences in surgeon experience. However, since we included the postoperative results in terms of gross vs subtotal resection we ensured to exclude a significant impact of this potential confounder.

One of the major findings of our analysis is the positive correlation between IDH-1 wildtype and a higher edema to tumor ratio. A few studies have investigated the association of IDH-1 status with morphological MRI analysis in low grade gliomas (16). IDH-1 mutated tumors present frequently with a unilateral pattern of growth, sharply defined tumor margins, homogeneous signal intensity, and less contrast enhancement on MRI. All these factors might contribute to the improved prognosis of patients with this subtype of GBM; however, an association between edema and IDH-1 is not described in the literature (16). The IDH-1 mutation leads to neo-enzymatic activity of the IDH-1 enzyme which drives the conversion of isocitrate into 2-hydroxyglutarate (2-HG), leading to a genome-wide histone- and DNA methylation alternations (17, 18). One of these consequences is the increased hypoxia-inducible factor 1-alpha (HIF-1α) that is frequently detected in patients with an IDH-1 mutation (19, 20). On the contrary, the proliferation rate (Ki-67) and vascular endothelial growth factor (VEGF) levels are significantly lower in IDH-1 mutated tumors (21, 22). However, little is known about the affinity for vasogenic edema in IDH-1 wildtype GBM (23). Our findings encourage further translational investigations into the mechanism of peritumoral edema in GBM wildtype.

Several studies have investigated the extent of peritumoral edema and correlated it with patient's outcome but the results were conflicting and a consistent conclusion is therefore absent (1, 6, 24). In a multicenter analysis, Schoeneggers et al. identified edema as an independent prognostic factor for poor outcome in GBM (1). On the contrary, Lacroix et al. published their results including more than 400 GBM patients where the extent of peritumoral edema was not found to be an independent prognostic factor (25). In our study, neither tumor size, nor edema or a high edema to tumor ratio were associated with outcome. A possible explanation is the high-level of heterogeneity within the peritumoral edema tissue. Since the majority (>90%) of the tumors relapse in the peritumoral zone, the microenvironment with alternated tissue hemostasis may play a crucial role in recurrence, and the currently standardized quantitative measurements (T1+, T2, FLAIR etc.) do no capture molecular alternations in the peritumoral edema (26, 27). Radiomic approaches may complement current MRI imaging in future studies and elucidate pathological processes in peritumoral edema tissue.

Within this study, we addressed the effects of edema on immune infiltration (2). The assessment of immune infiltration is of paramount importance since the introduction of T cells with the expression of chimeric antigen receptors (CARs) directed against specific antigens (EGFRvIII-, HER2- and IL-13 Rα2 CAR T-cells) have initiated the era of personalized immunotherapy in GBM; and the results of several ongoing studies are eagerly anticipated (10, 28, 29). Berghoff et al. published their findings on CNS metastasis, where a high density of tumor-infiltrating lymphocytes (TIL) was more frequently observed in patients with low peritumoral edema, as compared to patients with high peritumoral edema; however, studies analysing this issue in GBMs are absent (30). In our analysis neither myelocytic nor lymphocytic infiltration was correlated with peritumoral edema. A possible explanation could be that the peritumoral microenvironment in brain tumor patients contains an array of other non-neoplastic cells, including vascular and other glial cells, all of which could contribute to edema formation (27). Although immunotherapy in general and CAR T administration in specific carries a risk of cerebral edema as a dreadful complication, our data implies that patients with a high edema to tumor ratio should not be excluded from further immunological studies (31, 32).

We did analyze a large number of patients with extensive radiological and immunohistological parameters, whereas histopathological analysis was only available in nearly 20% of the cases. As a limitation, the investigated cohort is from 2008-2013. Although all patients in our cohort received the temozolomide based radio-chemotherapy which still is the standard of care, novel therapies such as TTFields could not have been investigated. Our cohort is representative of GBM patients since the molecular profile is congruent with the literature (~10% IDH mutated GBM in the literature and in 13% in our cohort) (18). As further limitation and potentially introducing a bias, this investigation was a single centre study and of retrospective design.

In conclusion, the present study found no association between the extent of edema and immunogenic infiltration; however, IDH wildtype GBM was found to be more likely associated with extensive peritumoral edema than IDH mutant GBM. Further translational investigations are necessary to evaluate the underlying mechanism and the clinical relevance of this observation.

DATA AVAILABILITY STATEMENT

The raw data supporting the conclusions of this article will be made available by the authors, without undue reservation.

ETHICS STATEMENT

For this retrospective analysis, an ethical approval was obtained from the ethics committee of the University Hospital Frankfurt, Germany, (Identification number: 20-676). As a non-interventional single-center study, no patient consent was necessary.

AUTHOR CONTRIBUTIONS

DD collected the data and wrote the first draft. FG supervised the manuscript. All authors supplied additional information, edited the manuscript and contributed to critical review and revision of the manuscript. All authors contributed to the article and approved the submitted version.

REFERENCES

1. Schoenegger K, Oberndorfer S, Wuschitz B, Struhal W, Hainfellner J, Prayer D, et al. Peritumoral edema on MRI at initial diagnosis: an independent prognostic factor for glioblastoma? *Eur J Neurol* (2009) 16:874–8. doi: 10.1111/j.1468-1331.2009.02613.x
2. Stummer W. Mechanisms of tumor-related brain edema. *Neurosurg Focus* (2007) 22(5):E8. doi: 10.3171/foc.2007.22.5.9
3. Dubinski D, Hattingen E, Senft C, Seifert V, Peters KG, Reiss Y, et al. Controversial roles for dexamethasone in glioblastoma – Opportunities for novel vascular targeting therapies. *J Cereb Blood Flow Metab* (2019) 39 (8):0271678X1985984. doi: 10.1177/0271678X19859847
4. Dubinski D, Won S-Y, Gessler F, Quick-Weller J, Behmanesh B, Bernatz S, et al. Dexamethasone-induced leukocytosis is associated with poor survival in newly diagnosed glioblastoma. *J Neurooncol* (2018) 137:503–10. doi: 10.1007/s11060-018-2761-4
5. Yan JL, Li C, Boonzaier NR, Fountain DM, Larkin TJ, Matys T, et al. Multimodal MRI characteristics of the glioblastoma infiltration beyond contrast enhancement. *Ther Adv Neurol Disord* (2019) 12. doi: 10.1177/1756286419844664
6. Wu C-X, Lin G-S, Lin Z-X, Zhang J-D, Liu S-Y, Zhou C-F. Peritumoral edema shown by MRI predicts poor clinical outcome in glioblastoma. *World J Surg Oncol* (2015) 13:97. doi: 10.1186/s12957-015-0496-7
7. Uematsu H, Maeda M, Itoh H. Peritumoral brain edema in intracranial meningiomas evaluated by dynamic perfusion-weighted MR imaging: A preliminary study. *Eur Radiol* (2003) 13:758–62. doi: 10.1007/s00330-002-1559-z
8. Wen PY, Macdonald DR, Reardon DA, Cloughesy TF, Sorensen AG, Galanis E, et al. Updated response assessment criteria for high-grade gliomas: Response assessment in neuro-oncology working group. *J Clin Oncol* (2010) 28:1963–72. doi: 10.1200/JCO.2009.26.3541
9. Golub VM, Brewer J, Wu X, Kuruba R, Short J, Manchi M, et al. Neurostereology protocol for unbiased quantification of neuronal injury and neurodegeneration Stereology protocol for neuron counting. *Front Aging Neurosci* (2015) 7:196. doi: 10.3389/fnagi.2015.00196
10. Chuntova P, Downey KM, Hegde B, Almeida ND, Okada H. Genetically engineered T-cells for malignant glioma: Overcoming the barriers to effective immunotherapy. *Front Immunol* (2019) 9:3062. doi: 10.3389/fimmu.2018.03062
11. Dietrich J, Rao K, Pastorino S, Kesari S. Corticosteroids in brain cancer patients: benefits and pitfalls. *Expert Rev Clin Pharmacol* (2011) 4:233–42. doi: 10.1586/ecp.11.1
12. Kostaras X, Cusano F, Kline GA, Roa W, Easaw J. Use of dexamethasone in patients with high-grade glioma: a clinical practice guideline. *Curr Oncol* (2014) 21:e493–503. doi: 10.3747/co.21.1769
13. Pitter KL, Tamagno I, Alikhanyan K, Hosni-Ahmed A, Pattwell SS, Donnola S, et al. Corticosteroids compromise survival in glioblastoma. *Brain* (2016) 139:1458–71. doi: 10.1093/brain/aww046
14. Marcus HJ, Williams S, Hughes-Hallett A, Camp SJ, Nandi D, Thorne L. Predicting surgical outcome in patients with glioblastoma multiforme using pre-operative magnetic resonance imaging: development and preliminary validation of a grading system. *Neurosurg Rev* (2017) 40:621–31. doi: 10.1007/s10143-017-0817-0
15. Buckner JC. Factors Influencing Survival in High-Grade Gliomas. *Semin Oncol (WB Saunders)* (2003) 10–4. doi: 10.1053/j.seminoncol.2003.11.031
16. Dunn GP, Andronesi OC, Cahill DP. From genomics to the clinic: Biological and translational insights of mutant IDH1/2 in glioma. *Neurosurg Focus* (2013) 34:1–15. doi: 10.3171/2012.12.FOCUS12355
17. Xu W, Yang H, Liu Y, Yang Y, Wang P, Kim SH, et al. Oncometabolite 2-hydroxyglutarate is a competitive inhibitor of α-ketoglutarate-dependent dioxygenases. *Cancer Cell* (2011) 19:17–30. doi: 10.1016/j.ccr.2010.12.014
18. Cohen AL, Holmen SL, Colman H. IDH1 and IDH2 mutations in gliomas. *Curr Neurol Neurosci Rep* (2013) 13:1–7. doi: 10.1007/s11910-013-0345-4
19. Sulkowski PL, Corso CD, Robinson ND, Scanlon SE, Purshouse KR, Bai H, et al. 2-Hydroxyglutarate produced by neomorphic IDH mutations suppresses homologous recombination and induces PARP inhibitor sensitivity. *Sci Transl Med* (2017) 9:eaal2463. doi: 10.1126/scitranslmed.aal2463
20. Chowdhury R, Yeoh KK, Tian YM, Hillringhaus L, Bagg EA, Rose NR, et al. The oncometabolite 2-hydroxyglutarate inhibits histone lysine demethylases. *EMBO Rep* (2011) 12:463–9. doi: 10.1038/embor.2011.43
21. Zeng A, Hu Q, Liu Y, Wang Z, Cui X, Li R, et al. IDH1/2 mutation status combined with Ki-67 labeling index defines distinct prognostic groups in glioma. *Oncotarget* (2015) 6:30232–8. doi: 10.18632/oncotarget.4920
22. Polívka J, Pešta M, Pitule P, Hes O, Holubec L, Polívka J, et al. IDH1 mutation is associated with lower expression of VEGF but not microvessel formation in glioblastoma multiforme. *Oncotarget* (2018) 9:16462–76. doi: 10.18632/oncotarget.24536
23. Huang LE. Friend or foe-IDH1 mutations in glioma 10 years on. *Carcinogenesis* (2019) 40:1299–307. doi: 10.1093/carcin/bgz134
24. Hammoud MA. Prognostic significance of preoperative MRI scans in glioblastoma multiforme. *J Neurooncol* (1996) 27:65–73. doi: 10.1007/BF00146086
25. Lacroix M, Abi-Said D, Fourney DR, Gokaslan ZL, Shi W, DeMonte F, et al. A multivariate analysis of 416 patients with glioblastoma multiforme: Prognosis, extent of resection, and survival. *J Neurosurg* (2001) 95:190–8. doi: 10.3171/jns.2001.95.2.0190
26. Aubry M, de Tayrac M, Etcheverry A, Clavreul A, Saikali S, Menei P, et al. From the core to beyond the margin: A genomic picture of glioblastoma intratumor heterogeneity. *Oncotarget* (2015) 6:12094–109. doi: 10.18632/oncotarget.3297
27. Chen Z, Hambardzumyan D. Immune microenvironment in glioblastoma subtypes. *Front Immunol* (2018) 9:01004. doi: 10.3389/fimmu.2018.01004
28. *Pilot Study of Autologous Anti-EGFRvIII CAR T Cells in Recurrent Glioblastoma Multiforme - Full Text View - ClinicalTrials.gov* . Available at: https://clinicaltrials.gov/ct2/show/NCT02844062 (Accessed April 13, 2020).
29. Bagley SJ, Desai AS, Linette GP, June CH, O'Rourke DM. CAR T-cell therapy for glioblastoma: recent clinical advances and future challenges. *Neuro Oncol* (2018) 20:1429–38. doi: 10.1093/neuonc/noy032
30. Berghoff AS, Fuchs E, Ricken G, Mlecnik B, Bindea G, Spanberger T, et al. Density of tumor-infiltrating lymphocytes correlates with extent of brain edema and overall survival time in patients with brain metastases. *Oncoimmunology* (2016) 5:2162–402X. doi: 10.1080/2162402X.2015.1057388
31. Gust J, Taraseviciute A, Turtle CJ. Neurotoxicity Associated with CD19-Targeted CAR-T Cell Therapies. *CNS Drugs* (2018) 32:1091–101. doi: 10.1007/s40263-018-0582-9
32. Torre M, Solomon IH, Sutherland CL, Nikiforow S, DeAngelo DJ, Stone RM, et al. Neuropathology of a Case With Fatal CAR T-Cell-Associated Cerebral Edema. *J Neuropathol Exp Neurol* (2018) 77:877–82. doi: 10.1093/jnen/nly064

Conflict of Interest: The authors declare that the research was conducted in the absence of any commercial or financial relationships that could be construed as a potential conflict of interest.

frontiers in Immunology

ORIGINAL RESEARCH
published: 16 April 2021
doi: 10.3389/fimmu.2021.656541

The Predictive Value of Monocytes in Immune Microenvironment and Prognosis of Glioma Patients Based on Machine Learning

Nan Zhang[1,2†], Ziyu Dai[1†], Wantao Wu[3,4], Zeyu Wang[1], Hui Cao[5], Yakun Zhang[2], Zhanchao Wang[6], Hao Zhang[1] and Quan Cheng[1,4*]*

[1] Department of Neurosurgery, Xiangya Hospital, Central South University, Changsha, China, [2] College of Bioinformatics Science and Technology, Harbin Medical University, Harbin, China, [3] Department of Oncology, Xiangya Hospital, Central South University, Changsha, China, [4] National Clinical Research Center for Geriatric Disorders, Xiangya Hospital, Central South University, Changsha, China, [5] Department of Psychiatry, The Second People's Hospital of Hunan Province, The Hospital of Hunan University of Chinese Medicine, Changsha, China, [6] Department of Orthopaedics, Changzheng Hospital, Naval Medical University, Shanghai, China

OPEN ACCESS

Edited by:
Valérie Dutoit,
Université de Genève, Switzerland

Reviewed by:
Ranran Sun,
Zhengzhou University, China
Peng Luo,
The University of Hong Kong, Hong Kong
Joseph Chen,
University of Louisville, United States

***Correspondence:**
Quan Cheng
chengquan@csu.edu.cn
Hao Zhang
haozhang@csu.edu.cn

[†]These authors have contributed equally to this work

Specialty section:
This article was submitted to Cancer Immunity and Immunotherapy, a section of the journal Frontiers in Immunology

Received: 21 January 2021
Accepted: 19 March 2021
Published: 16 April 2021

Citation:
Zhang N, Dai Z, Wu W, Wang Z, Cao H, Zhang Y, Wang Z, Zhang H and Cheng Q (2021) The Predictive Value of Monocytes in Immune Microenvironment and Prognosis of Glioma Patients Based on Machine Learning. Front. Immunol. 12:656541. doi: 10.3389/fimmu.2021.656541

Gliomas are primary malignant brain tumors. Monocytes have been proved to actively participate in tumor growth. Weighted gene co-expression network analysis was used to identify meaningful monocyte-related genes for clustering. Neural network and SVM were applied for validating clustering results. Somatic mutation and copy number variation were used for defining the features of identified clusters. Differentially expressed genes (DEGs) between the stratified groups after performing elastic regression and principal component analyses were used for the construction of risk scores. Monocytes were associated with glioma patients' survival and exhibited high predictive value. The prognostic value of risk score in glioma was validated by the abundant expression of immune checkpoint and metabolic profile. Additionally, high risk score was positively associated with the expression of immunogenic and antigen presenting factors, which indicated high immune infiltration. A prognostic model based on risk score demonstrated high accuracy rate of receiver operating characteristic curves. Compared with previous studies, our research dissected functional roles of monocytes from large-scale analysis. Findings of our analyses strongly support an immune modulatory and prognostic role of monocytes in glioma progression. Notably, monocyte could be an effective predictor for therapy responses of glioma patients.

Keywords: monocyte, glioma microenvironment, immune infiltration, machine learning, immunotherapy, prognostic model

INTRODUCTION

Gliomas are one of the most malignant solid cancer types, which grade 2 and grade 3 glioma are defined as diffuse lower-grade glioma (LGG) and grade 4 glioma is defined as glioblastoma (GBM) based on the WHO 2016 classification (1). GBM, with the highest incidence rate (3.23 per 100,000 population) in United states, accounted for the majority of gliomas (57.7%) (2). The 10-year survival

rate of LGG is 47% whereas the median overall survival (OS) time of GBM is less than 3 years (3). Recently, increasing molecular markers have been identified for prediction of glioma patient survival rate, including mutational status, and DNA methylation (4, 5). Given that, WHO proposed an updated grading system for CNS tumors integrating molecular diagnosis (6). However, the inevitable tumor recurrence and drug resistance due to the high heterogeneity of gliomas make it still urgent to identify novel biomarkers to help illustrate the pathological mechanism of gliomas and develop the corresponding therapeutic strategies.

Tumor microenvironment (TME), consisting of noncancerous cells and tumor associated biomolecules, have become increasingly attractive as potential targets for the treatment of gliomas (7). Accumulating evidence has demonstrated the immunosuppressive context in TME of gliomas, such as tumor associated macrophages (TAMs), regulatory T cells (Tregs), cancer associated fibroblasts (CAFs), myeloid derived suppressor cells (MDSCs), and monocytes (7, 8). Monocytes, emerged as important regulators of cancer progression, are innate immune cells of the mononuclear phagocyte system. Monocytes perform diverse functions that contribute to both pro- and antitumoral immunity during cancer development, including phagocytosis, secreting tumoricidal mediators, promoting of angiogenesis, remodeling extracellular matrix, and recruiting lymphocytes (8). Monocytes comprise as many as 30–50% of all cells in GBM microenvironment (9). Previous study has proved that monocytes closely adhere to GBM via vascular cell adhesion molecule-1 (*VCAM-1*) (10). Notably, monocytes also serve as the important source of TAMs and dendritic cells (DCs) that shape a more permissive TME (11). Moreover, monocyte-mediated nano drug delivery in GBM has been proposed and proved with effective cancer cell damage. Although several studies have highlighted the potential roles of monocytes in tumor growth, the in-depth mechanism of monocytes in TME and its overall prognostic value in gliomas has not been fully elucidated due to its eventual destiny of differentiation.

Weighted gene co-expression network analysis (WGCNA) has been known for its ability to explore the specific genes related to clinical traits. In this study, WGCNA was employed to identify meaningful monocyte-related gene modules in glioma patients. Genes within the identified module were extracted for clustering. Machine learning including neural network and Support Vector Machines (SVM) was used to validate the clustering results. Significant differentially expressed genes (DEGs) between the stratified groups after performing elastic regression and Principal component analyses (PCA) were used for the construction of risk scores. Risk scores could also predict immunotherapeutic efficiency. These results are expected to promote the development of novel therapeutic targets based on monocytes and provide the basis for future research on monocytes in gliomas. Besides, given the current shortcoming in diagnostic and therapeutic options in GBM, the remarkable prognostic value of monocytes can better achieve precise medicine and promote the clinical management of GBM patients.

Abbreviations: CDF, cumulative distribution function; CGGA, Chinese Glioma Genome Atlas; CNA, copy number alternations; CNV, copy number variation; GBM, glioblastoma; GEO, Gene Expression Omnibus; GO, gene ontology; GSEA, gene set enrichment analysis; GSVA, gene set variation analysis; KEGG, Kyoto Encyclopaedia of Genes and Genomes; LGG, low grade glioma; PCA, principal component analysis; TGF-β, tumor growth factor-β; SNP, single-nucleotide polymorphism; SNV, single-nucleotide variant; TAM, tumor associated macrophage; TCGA, The Cancer Genome Atlas; TME, tumor microenvironment; WGCNA, weighted gene co-expression network analysis; PD-L1, programmed cell death 1 ligand; DEG, differentially expressed genes; VCAM-1, vascular cell adhesion molecule-1; DC, dendritic cell; PAM, partition around medoids; MSI, microsatellite instability; HRD, homologous recombination deficiency; CTA, cancer testis antigen.

METHODS

Patient and Cohort Inclusion

2405 diffuse glioma samples were collected from three databases: The Cancer Genome Atlas (TCGA), Chinese Glioma Genome Atlas (CGGA), and Gene Expression Omnibus (GEO). For the TCGA cohort (672 glioma samples), the RNA-seq data and corresponding clinical information were retrieved from TCGA database (http://cancergenome.nih.gov/). Three CGGA validation cohorts were employed in this study, including two RNA-seq cohorts (CGGA325 and CGGA693) and a microarray cohort (CGGAarray). The RNA-seq and microarray data, clinical and survival information were downloaded from the CGGA database (http://www.cgga.org.cn). Expression matrices of GSE108474 (414 glioma samples) were obtained from the GEO database (https://www.ncbi.nlm.nih.gov/geo/).

WGCNA Identifying Monocytes Related Genes

The WGCNA package in R version 3.6.1 was used to perform WGCNA. The association between individual genes and monocyte densities was quantified by gene significance, and the correlation between module eigengenes and gene expression profiles was represented by module membership. A power of $\beta = 2$ and a scale-free $R2 = 0.89$ were set as soft-threshold parameters to ensure a scale-free topology network. A total of seven modules were generated, and turquoise module showing the strongest correlation was used for further analysis. Genes within the turquoise module were thus chosen for GO (gene ontology) and KEGG (Kyoto Encyclopaedia of Genes and Genomes) functional enrichment analyses. Metascape (https://metascape.org/) was also used for functional annotation of turquoise module genes.

Delineation and Validation of Immune Subtypes

Based on the 806 genes extracted from turquoise module, we applied consensus clustering algorithm of partition around medoids (PAM) to identify robust clusters of TCGA patients (12). The cumulative distribution function (CDF) and consensus heatmap were used to assess the optimal *K* value of 2. To validate

the immune subtypes in three CGGA cohorts, we trained a neural network classifier in the discovery cohort to predict the immune subtypes for patients in the validation cohort based on 300 overlapped module-derived genes in TCGA and three CGGA cohorts using R package Rcpp, RSNNS, and "e1071". Among the three learning functions (Quickprop, BackpropBatch, SCG), Quickprop was used for the training. The clustering results were further validated by SVM using R package caret and "e1071". Three types of models (C-classification, nu-classification, one-classification) and four types of kernels (linear, polynomial, radial, sigmoid) in SVM were analyzed. The combination of C-classification and radial was found with the highest accuracy.

Genomic Alterations in Immune Subtypes

Somatic mutations and somatic copy number alternations (CNAs) which corresponded to the cases with RNA-seq data, were downloaded from the TCGA database. GISTIC analysis was performed to determine the genomic event enrichment. CNAs associated with the two clusters and the threshold copy number at alteration peaks were obtained using GISTIC 2.0 analysis (https://gatk.broadinstitute.org).

Annotation of the Immune Infiltrating Microenvironment

ESTIMATE was performed to evaluate the immune cell infiltration level (immune scores) and stromal content (stromal scores) for each sample. The enrichment levels of 64 immune signatures were quantified by the xCell algorithm (13). The relative fraction of 22 immune cell types in tumor tissues were estimated using CIBERSORT algorithm (14). Gene set variation analysis (GSVA) was performed to study GO pathways, and GO items with p value < 0.05 were identified. Seven types of classified immune checkpoints signaling pathways were investigated from two previous published studies (15, 16).

Identification of an Immune-Related Signature

Univariate Cox regression analysis was performed to determine the differentially expressed immune genes with prognostic significance with a p value < 0.05 between subtypes. Elastic regression analysis and PCA were further used to calculate the risk scores of patients. The extracted principal component 1 served as the signature score. The risk score of each patient after the prognostic value of gene signature score was obtained by the following calculation: ΣPC1i - ΣPC1j, where i represented the expression of genes with HR>1, and j the expression of genes with HR<1.

Prediction of Immunotherapy Response

The IMvigor210 cohort, which is an urothelial carcinoma cohort treated with the anti-*PD-L1* antibody atezolizumab was used for prediction of patient response to immunotherapy (16). Based on the Creative Commons 3.0 License, complete expression data and clinical data were downloaded from http://research-pub.Gene.com/IMvigor210CoreBiologies. Raw data were then normalized using the DEseq2 R package, and the count value was transformed into the TPM value.

Construction and Validation of a Prognostic Model

Ultimately, nomogram is a form of visualized multi-factor regression analysis commonly used for cancer survival rate prediction. Variables selected for construction of the nomogram included the calculated prognostic scores, ages, pathological stages of glioma and mutation status. Univariate and multivariate regression analyses were also used to evaluate the prognostic value of these factors.

Statistical Analysis

Kaplan-Meier curves with log-rank test were used to assess survival difference between groups. The univariate and multivariate Cox regression analyses were performed to detect the prognostic factors. Pearson correlation and distance correlation analyses were used to calculate correlation coefficients. Contingency tables were analyzed by χ^2 contingency test. The OS and risk scores were calculated using the R package survival and cutoff values determined. Based on the dichotomized risk scores, patients were grouped as with high or low risk score in each data set, and the computational batch effect was reduced by the R package sva. Data were visualized using the R package ggplot2. OncoPrint was used to delineate the mutation landscape of TCGA by the maftools R package (17). All survivorship curves were generated using R package survminer. Heatmaps were generated based on pheatmap. All statistical analyses were conducted using R software. $P < 0.05$ was considered statistically significant.

RESULTS

Identification of Monocyte Density as a Potential Prognostic Marker

The flow chart of our study design was shown in **Figure S1A**. We sought to determine the prognostic value of monocytes in glioma by studying the monocyte-related genes using WGCNA. After stratifying patients by high and low median levels of monocytes, survival analysis revealed a clear distinction between the two subtypes in LGG, GBM, and pan-gliomas from TCGA, respectively (**Figure S1B**). The expression level of monocyte could also stratify patients in CGGAarray, CGGA325, and CGGA693, respectively (**Figure S1C**). To evaluate the potential prognostic value of monocytes, we performed WGCNA for monocyte-specific genes. A power β=2 was selected as the software threshold for a scale-free network construction. Seven modules were identified by clustering dendrogram (**Figure 1A**). Tomplot depicting the random 400 genes within the clustering dendrogram (**Figure 1B**). The correlation between the turquoise module and xCell-defined monocytes was 0.58, indicating a selective expression of the turquoise module in monocytes (**Figures 1C, D**). Once established the turquoise module as the

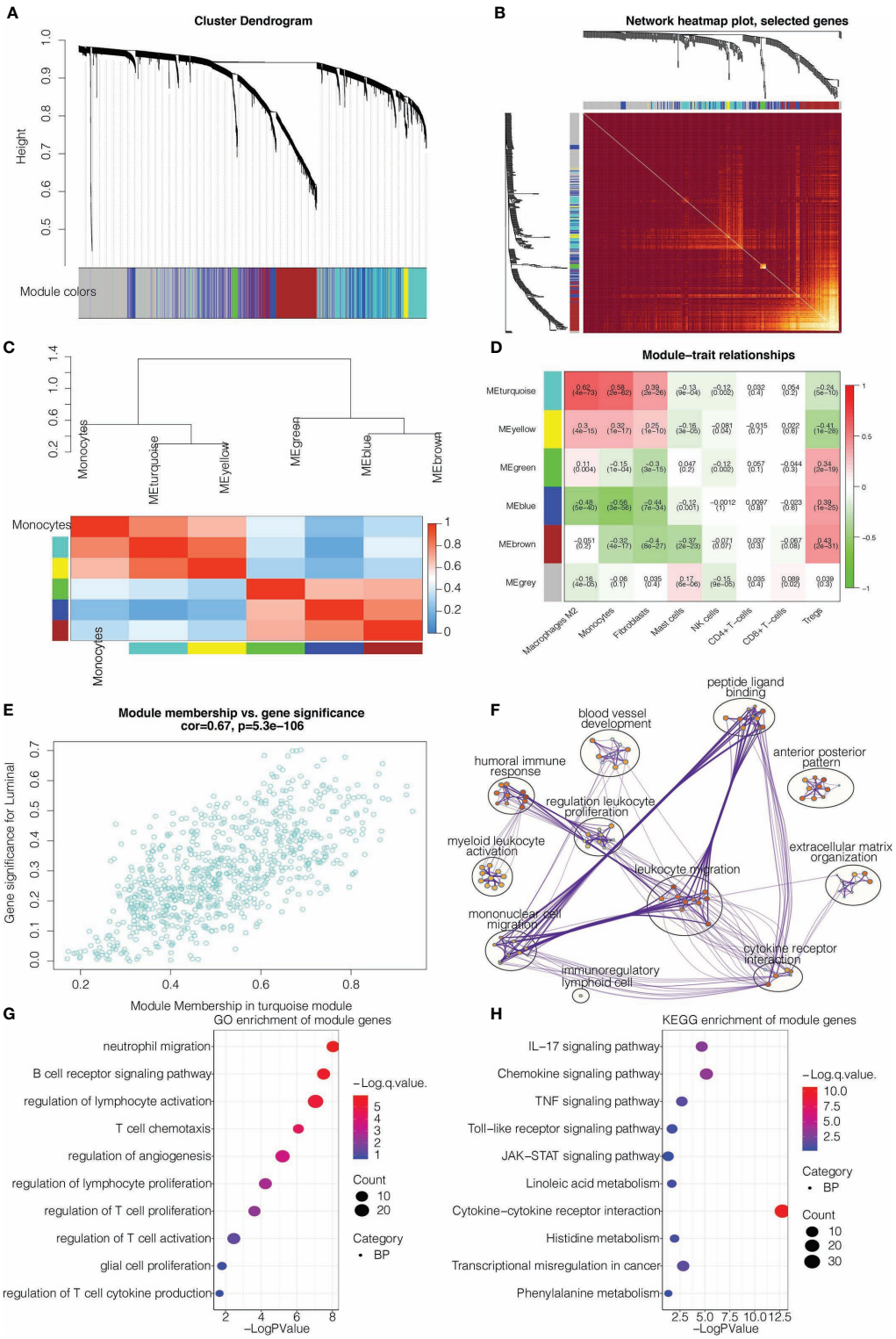

FIGURE 1 | WGCNA for the monocyte-related genes. **(A)** Cluster dendrogram generating gene modules. **(B)** Tomplot depicting the random 400 genes. **(C)** Hierarchical clustering dendrogram of module. **(D)** Correlation analysis of modules and cell types. **(E)** Scatterplot demonstrating the correlation of intramodular connectivity and monocytes. **(F)** Metascape for the functional annotation of key genes in module turquoise. **(G)** GO functional enrichment analysis of key genes in module turquoise. **(H)** KEGG functional enrichment analysis of key genes in module turquoise.

one with the highest significance, we investigated the correlation between the intramodular connectivity and monocytes, which reached 0.67 (**Figure 1E**). Metascape revealed that turquoise-derived genes were enriched in leukocyte migration and mononuclear cell migration (**Figure 1F**). GO functional enrichment analysis found that the genes were concentrated in pathways involving neutrophil migration and regulation of lymphocyte activation (**Figure 1G**). KEGG analysis showed that the genes were enriched in the cytokine-receptor interaction (**Figure 1H**).

We subsequently extracted 806 genes from module turquoise by WGCNA. PAM was performed for glioma patients with the corresponding gene expression profiles in TCGA cohort (**Figure 2A**). The optimal number of clusters was evaluated by ConsensusClusterPlus package (**Figure S2A**). Clustering results were most stable when the number was set to two (K=2). The delineated groups based on the 806 genes showed distinct patterns of clinical traits and monocyte levels with statistical significance (**Figure 2A**). Survival analyses of the two clusters confirmed an obviously lower survival probability curve for cluster 1 (**Figure 2B**). PCA managed to differentiate the samples from the TCGA dataset (**Figure 2C**). Subsequently, combining the gene expression profiles from three CGGA cohorts, 300 genes were identified from these 806 genes by neural network to validate the clustering results (**Figure 2D**). Samples were then clustered into two groups with high or low death risk by pamr in three CGGA cohorts, respectively (**Figures S2B-D**). SVM was performed for validation of the clustering as well, which the contingency table showed the consistency in clustering results among SVM and neural network (**Figure 2E**). Survival analyses of the two clusters confirmed an obviously lower survival probability curve for cluster 1 (**Figures S2E–G**). PCA also managed to differentiate the samples from three individual datasets (**Figures S2H–J**).

Clinical traits and TME Characteristics of the Monocyte-Stratified Groups

We then proceeded to investigate the TME characteristics of the two clusters. The expression difference of the levels of 64 cell types in two defined subtypes were investigated in TCGA and three CGGA cohorts (**Figures 3A** and **S3A**). It was found that increased cells such as fibroblasts, DCs, M2 macrophages and monocytes were related to cluster 1 with worse survival probability. Moreover, CIBERSORT algorithm showed that the expression of several types of immune cells including M0/1/2 macrophages, DCs, and neutrophils were higher in cluster 1 in TCGA, CGGAarray, CGGA325, and CGGA693, respectively (**Figures S3B**, **S4A**, **S5A**, **S6A**). The association between ESTIMATE scores of the immune infiltrating microenvironment, an indicator of the cancer biological behaviour, and clusters, as well as levels of immune cells was examined in TCGA and three CGGA cohorts (**Figures 3B** and **S4B**, **S5B**, **S6B**). ESTIMATEScores, ImuneScores and StromalScores were all higher in cluster 1 than in cluster 2 (**Figures 3B** and **S4B**, **S5B**, **S6B**). We then compared the levels of several series of immune checkpoint molecules related to antigen presentation, cell surface receptor, coinhibition, ligand and cell adhesion between the two clusters. Immune checkpoint markers tended to be overexpressed in cluster 1 (**Figures 3C** and **S4C**, **S5C**, **S6C**).

The pathological gradings of glioma were also significantly different between clusters 1 and 2 (p<2.2e-16), with a higher gradings in cluster 1 in TCGA and three CGGA cohorts (**Figure S7A**). The proportions of samples with *IDH* wildtype *(*WT) and chromosome 1p/19q codeletion in cluster 1 were higher than those in cluster 2 (**Figures S7B, S7C**), also indicating a more malignant propensity in cluster 1. Results regarding the proportion of patients with *MGMT* promoter methylation were less universal, with data from the TCGA database showing the most significant difference while data from the other three databases statistically insignificant difference (**Figure S7D**). The proportions of the four GBM subtypes in clusters 1 and 2 were significantly different in TCGA (p<2.2e-16), showing that the more malignant CL and ME subtypes accounted for the majority of cluster 1 samples (**Figure S7E**).

The expression differences of hypoxia pathways in two clusters were explored using GSVA. Investigated pathways included cell response regulation, hypoxia-induced intrinsic apoptosis, Hypoxia-Inducible Factor 1α (HIF1A) and others. These pathways were found to be more activated in cluster 1 in TCGA and three CGGA cohorts, suggesting a tendency for cell hypoxia, which is a universal marker for malignant tumor proliferation, in this group (**Figures S8A–D**). We also interrogated the relationship between metabolic pathways, such as pyrimidine synthesis and sulfur metabolism, and subtypes. The metabolic pathways were overrepresented in cluster 1, proving a more active proliferation of glioma cells in these samples (**Figures S8A–D**).

Monocyte-Enriched Group Showed More Malignant Genomic Features

Somatic mutation analysis and copy number variation (CNV) were performed using the TCGA dataset to explore genomic traits of the two clusters (**Table S1**). A global CNV profile was obtained by comparing the two clusters (**Figure 4A** and **Table S2**). According to somatic mutation analysis, mutations in *EGFR* (28%), *TP53* (28%), *PTEN* (23%) and *TTN* (23%) were most highly enriched in cluster 1 (**Figure 4B**). In comparison, *IDH1* (92%), *TP53* (52%), *ARTX* (38%) and *CIC* (25%) mutations were enriched in cluster 2 (**Figure 4C**). Missense mutation was the predominant gene alteration type in all these genes except for *ATRX*, in which frame-shifting deletion was the most common type.

Different types of somatic mutations, including the single-nucleotide variant (SNV), single-nucleotide polymorphism (SNP), insertion, deletion and intergenic region (IGR), were analyzed using the R package. Silent, nonsense, missense, intronic, 5' and 3' UTR mutations were more common in cluster 1 than in cluster 2 (**Figure 5A**). Among the detected SNVs, C>T appeared to be the most common mutation in cluster 1 (**Figure 5B**). The T to A, C to T and C to A mutations occurred more frequently in cluster 1 than in cluster 2. While the frequencies of insertion and deletion were not statistically

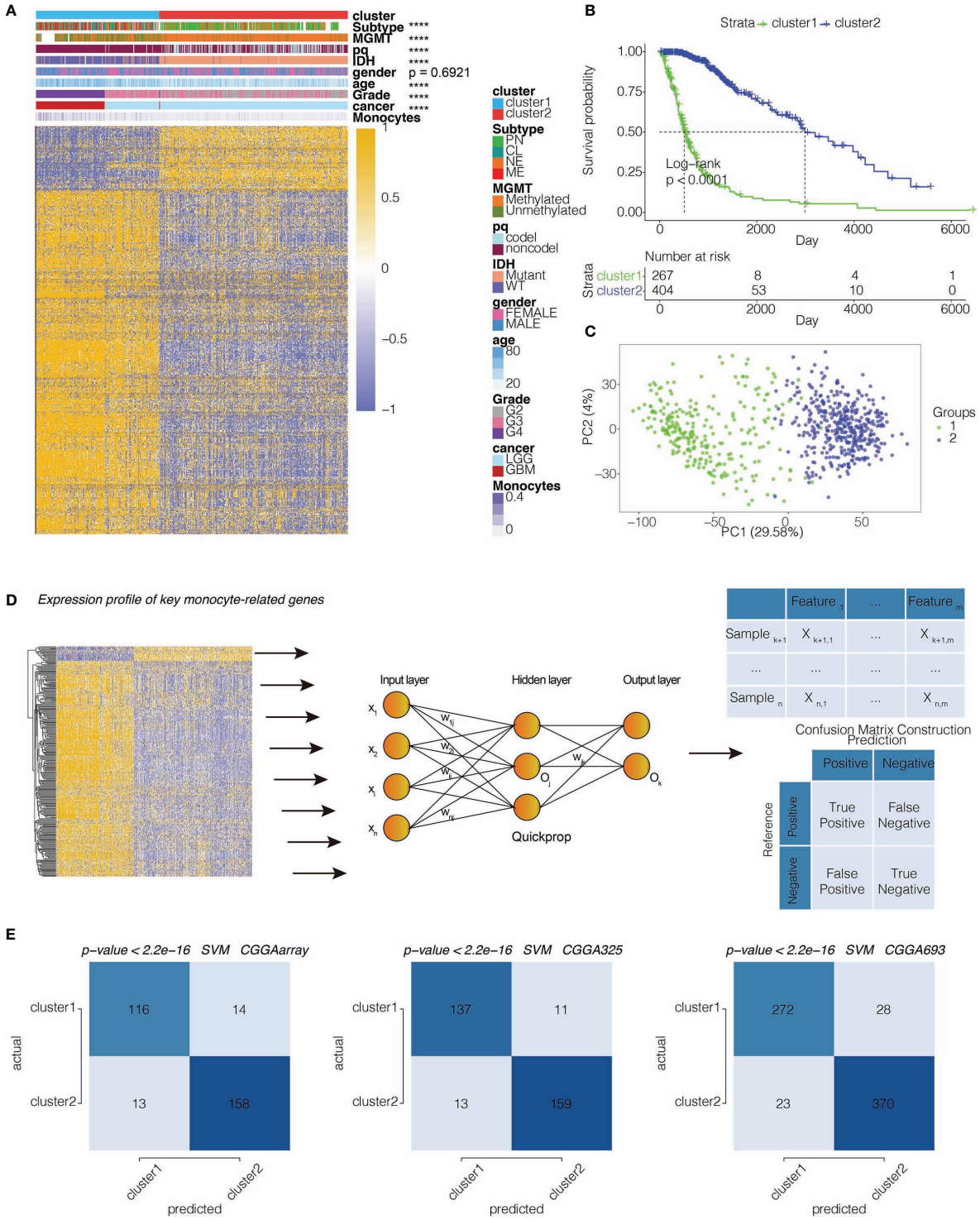

FIGURE 2 | Machine learning for validation of clustering based on monocyte-related genes. **(A)** Clustering dendrogram demonstrating good separation of the two clusters by traits. ****P < 0.0001. **(B)** Kaplan-Meier survival analysis of the two clusters. **(C)** Sample clustering by PCA in the TCGA dataset. **(D)** Construction of clustering in CGGAarray, CGGA325, and CGGA693 based on the clustering in TCGA by neural network learning function of Quickprop. Schematic diagram of the neural network. **(E)** Validation of clustering by SVM algorithm in CGGAarray, CGGA325, and CGGA693. Contingency tables showing the high consistency between predicted clusters from SVM and actual clusters from neural network.

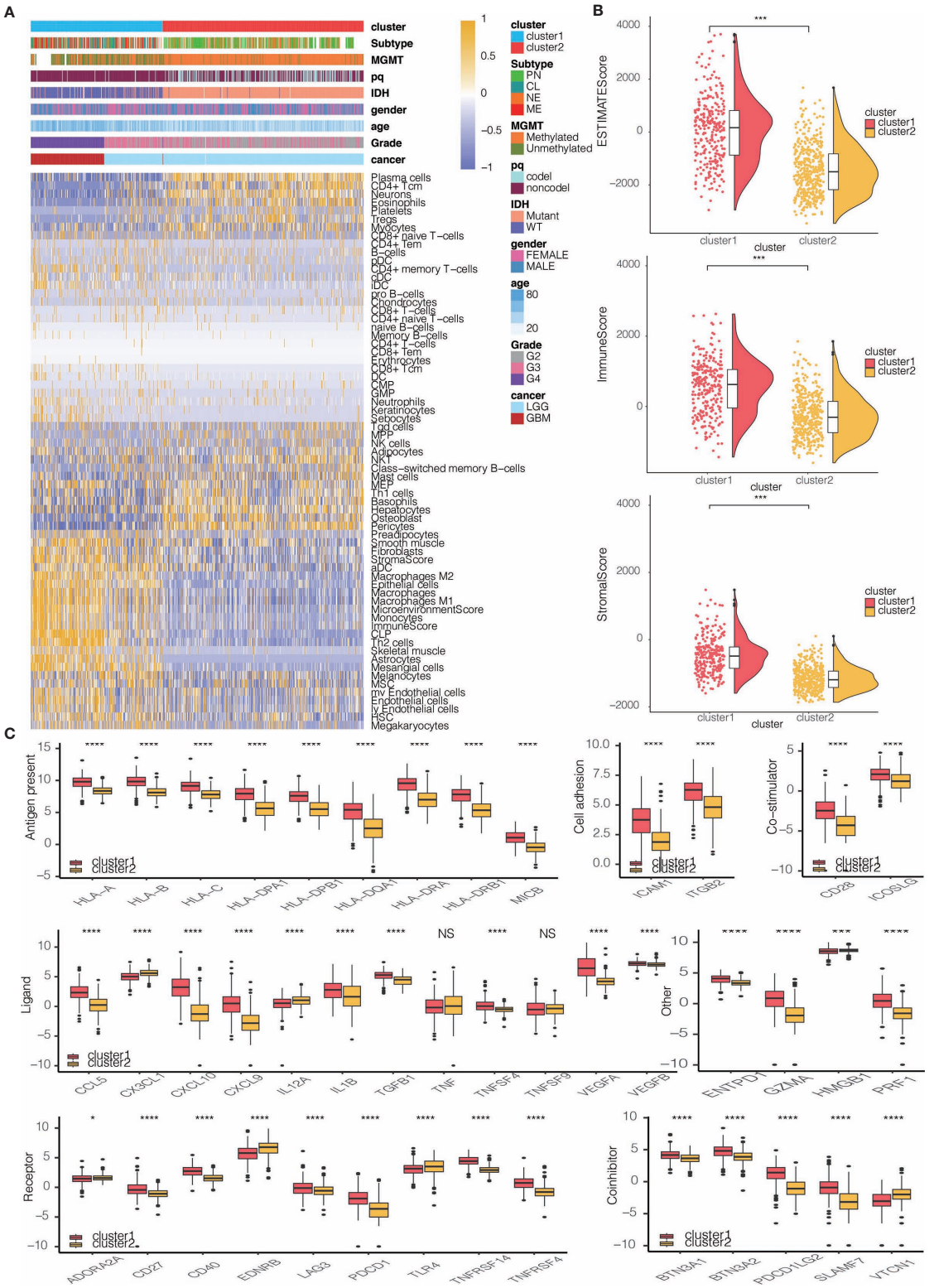

FIGURE 3 | Immune characteristics of the two clusters. **(A)** Dendrogram correlating the levels of 64 cell types calculated by xCell and clusters in TCGA. **(B)** ESTIMATEScores, ImmuneScores and StromalScores of the two clusters in TCGA. **(C)** Molecule levels of seven types of immune checkpoints in two clusters in TCGA. *P < 0.05, ***P < 0.001, ****P < 0.0001. NS, not statistically significant.

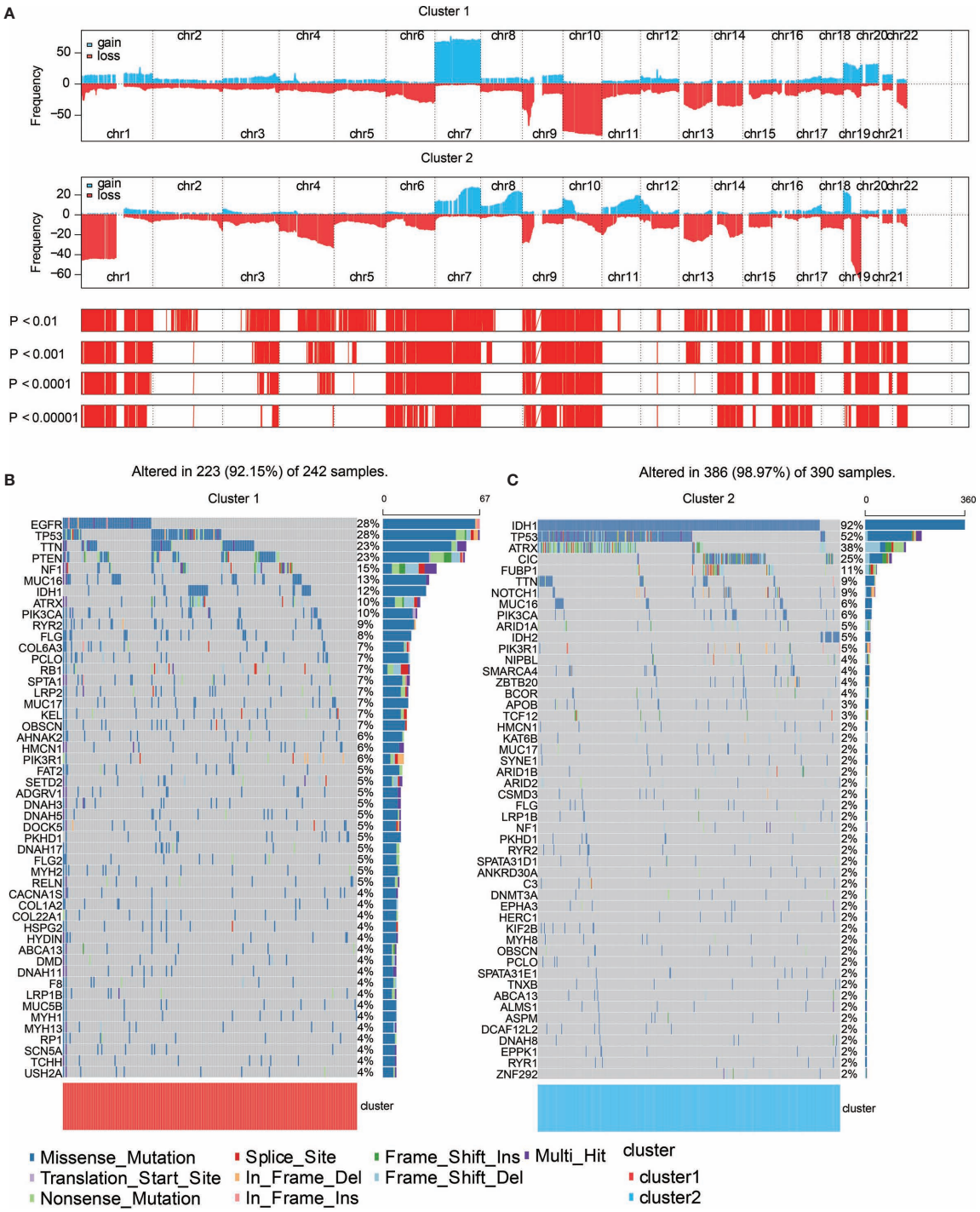

FIGURE 4 | Genomic features of the two clusters. **(A)** Distribution of gain or loss of function mutation in the 22 human chromosomes in the two clusters. Amplification of genes is marked in blue. Deletion of genes is marked in red. **(B)** List of the most frequently altered genes in clusters 1. **(C)** List of the most frequently altered genes in clusters 2. Nine mutation types were exhibited.

different between the two clusters, SNPs were significantly more common in cluster 1 (**Figure 5C**). The top 33 most mutated cancer-related genes were listed in **Figure 5D**. Common carcinogenic pathways were more active in cluster 1 (**Figure 5E**). The strongest co-occurrent pairs of gene alteration in cluster 1 were *ATRX-TP53* and *ATRX-IDH1*, which was in accordance

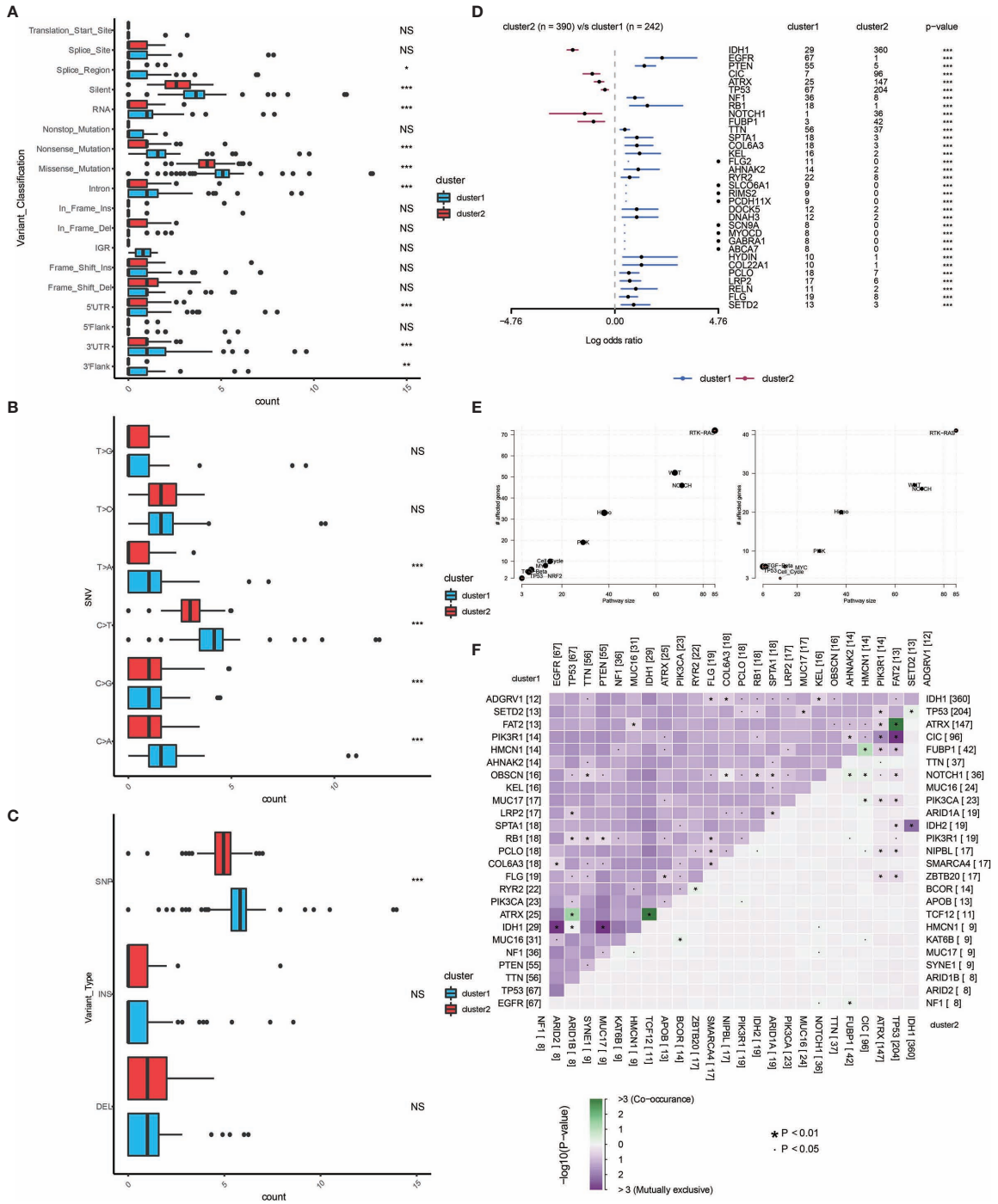

FIGURE 5 | Genomic alterations in the two clusters. Frequency comparison according to types of mutation **(A)**, SNV **(B)**, INDEL and SNV **(C)** between the two clusters. **(D)** The Forest plot listing the top 17 most mutated genes between the two clusters. **(E)** Demonstration of the pathways involved in cancer biology in the two clusters. **(F)** The heatmap showing the concurrence or mutual exclusivity of the top 25 most mutated genes in the two clusters. *p < 0.05, *p < 0.01, ***P < 0.001, ****P < 0.0001. NS, not statistically significant.

with previous reports (18–20). It was suggested that acquisition of a second cancer-related gene alteration may dictate the development of certain tumor types, and that *TP53*, *IDH1*, *ATRX* are functionally linked (**Figure 5F**) (20, 21). On the other hand, the most mutually exclusive pairs were *PTEN-IDH1* and *EGFR-IDH1* (**Figure 5F**).

Generation of Risk Score and Its Functional Annotation

By performing elastic net regression analysis and PCA algorithm (**Figure S9A**), 33 monocyte-related genes were derived from the 300 genes and their coefficients were obtained (**Figure 6A**). The monocyte-related gene signature was used to calculate risk scores by PCA. Sankey plot revealed a high consistency between monocyte-related clusters and risk scores (**Figure S9B**). The correlation of the expression levels of 64 cell types and risk scores was then evaluated. There was a positive correlation between the scores and the levels of fibroblasts, M2 macrophages, DCs, and monocytes (**Figure 6B**). Pathways related to macrophage activation and migration, dendritic cell differentiation and negative regulation of T cell proliferation were more active in the samples with higher scores (**Figure 6C**). In the TGCA dataset, survival analysis demonstrated a good separation of patients with different death risks by high and low risk scores (**Figure 6D**). The prognostic value of risk scores was further validated in CGGAarray, CGGA325, CGGA693, and GSE108474 datasets (**Figure S9C**). The receiver operating characteristic (ROC) analyses with the Area Under the Curve (AUC) of 0.878 and 0.845 confirmed that risk score was a prognostic biomarker in predicting 3 years and 5 years survival status of glioma patients (**Figure 6E**).

Construction of a Prognostic Nomogram Based on Risk Scores

After establishing monocyte density as a suitable marker for survival prediction of gliomas, we further investigated its prediction efficiency by developing a prognostic nomogram. Combing prognostic factors, including risk scores, patient ages, tumor grades, *IDH* mutation, and chromosome 1p/19q codeletion, a prognostic nomogram was developed (**Figure S10A**). In TCGA dataset, the Kaplan-Meier survival curve demonstrated a good discrimination of survival probabilities of the two clusters ($p<0.0001$) (**Figure S10B**). The ROC curve confirmed the discriminative ability of this nomogram (AUC=0.802, **Figure S10C**). Predicted probabilities corresponded well with the actual one- to five-year overall survival rates of glioma patients (**Figure S10D**). The efficiency of the prognostic model was validated in CGGA 693 cohort. The Kaplan-Meier survival curve demonstrated a good discrimination of survival probabilities of the two clusters ($p<0.0001$) (**Figure S10E**). The ROC curve confirmed the discriminative ability of this nomogram (AUC=0.737, **Figure S10F**). Predicted probabilities corresponded well with the actual four-year overall survival rates of glioma patients (**Figure S10G**).

Monocyte-Stratified Groups Predicted Response to Immunotherapies

High risk scores were associated with several immune checkpoint molecules including PDCD1, PDCD1LG2, and LAG3 (**Figure 7A**). Except for immune checkpoint molecules, the intrinsic immune escape mechanism was reported to include tumor immunogenicity and antigen presentation capacity (22). Factors associated with tumor immunogenicity was first assessed in glioma samples from TCGA (23). High risk score group exhibited lower microsatellite instability (MSI) and higher level of intratumor heterogeneity (**Figures 7B, C**, respectively). High risk score group presented higher silent mutation rate, number of segements, homologous recombination deficiency (HRD), aneuploidy score, and fraction altered that were all crucial indicators for genomic alterations (**Figures S11A–E**). Cancer testis antigen (CTA) and neoantigens were vital sources of tumor-specific antigens, and they were both higher in high risk score group (**Figures S11F, S11G**). Further, high risk score group exhibited higher level of macrophage regulation, lymphocyte infiltration signature score, leukocyte fraction, TCR Shannon, and TCR richness, all of which were significant indicators for antigen presentation capacity (**Figures S11H–L**). Six immune subtypes including Wound Healing, IFN-γ Dominant, Inflammatory, Lymphocyte Depleted, Immunologically Quiet, and tumor growth factor-β (TGF-β) Dominant have been previously identified across cancer types (23). Lymphocyte Depleted, representing an immune cold microenvironment, was more frequently observed in high risk score group (**Figure 7D**). We evaluated whether risk scores were able to predict therapeutic effects of immune blockade treatment. High and low risk scores succeed in stratifying patients by survival probability from the IMvigor210 cohort ($p=0.012$, **Figure 7E**). Nevertheless, when further stratifying the patients according to immunotherapeutic response types, the progressive disease, stable disease and partial response groups showed different risk scores (**Figure 7F**). We also grouped the therapeutic response in a binary mode, and found that the complete/partial response group had a higher percentage of high scores than the stable/progressive disease group (**Figure 7G**). Besides, glioma patients with high risk score were less likely to benefit from chemotherapy or radiotherapy (**Figures 7H, I**, respectively).

DISCUSSION

In the present study, monocyte density was explored as a marker for glioma prognosis by using WGCNA for the first time. Genes derived from the module of WGCNA were used for glioma patient grouping. Machine learning including neural network and SVM were applied for validating the clustering results based on monocyte. An extensive annotation of tumor genomics, TME, clinical traits, metabolism, and hypoxia was performed for monocyte-related patient groups. A risk score based on the DEGs between monocyte -related clusters was generated by PCA, with biological functions, immune subtypes, and immunotherapeutic response associated with the risk score being explored.

As a major population of innate immune cells, monocyte exert its two-sided roles in facilitating tumor growth (24) and inhibiting metastatic spread of tumor (25). Notably, monocytes could primarily differentiate into tumorigenic TAMs, yet monocytes could also differentiate into DCs responsible for effective adaptive immune responses. TAMs are recruited early during tumor formation of GBM and contribute to tumor

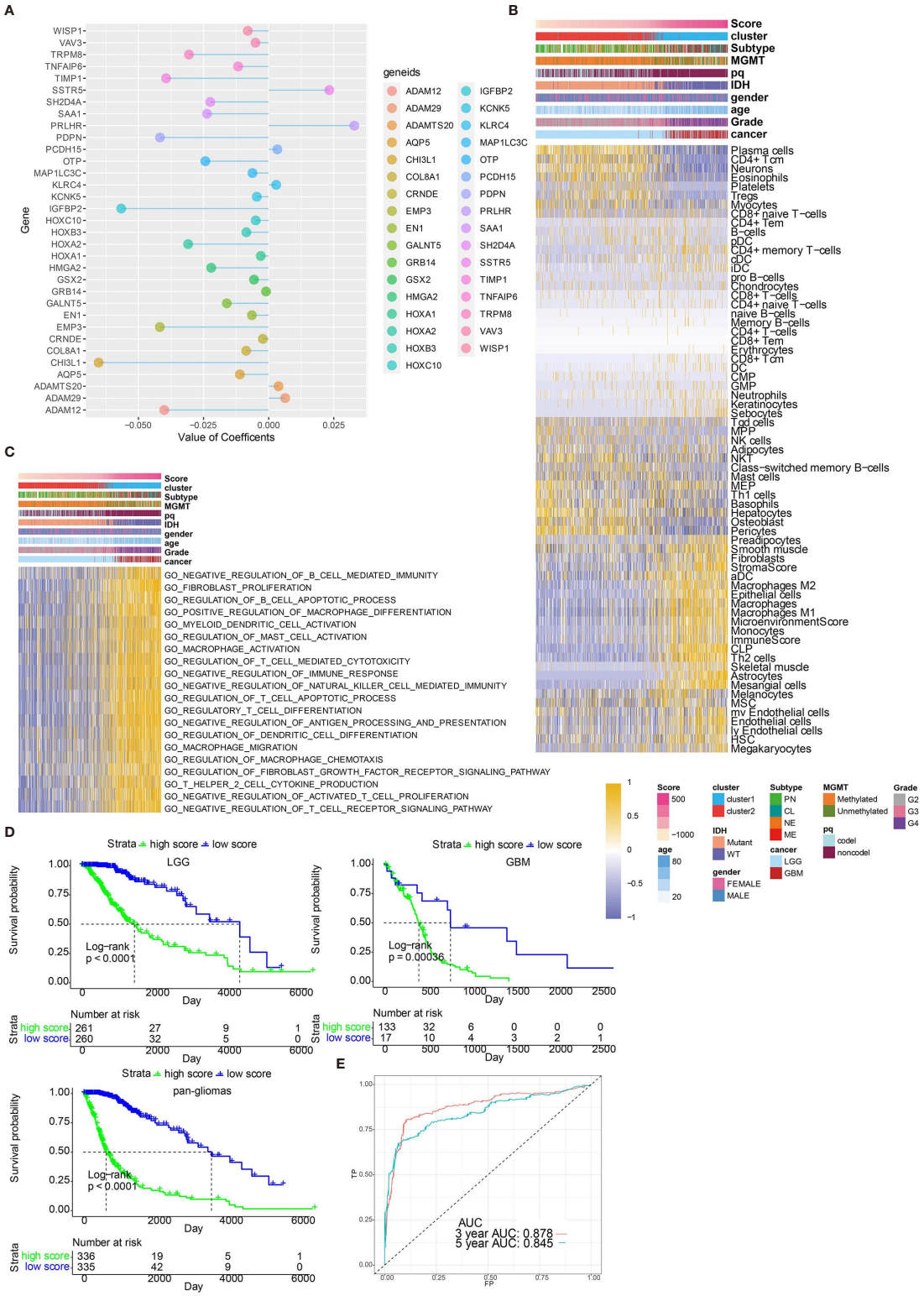

FIGURE 6 | Functional annotation of risk scores. **(A)** Elastic net regression analysis and PCA obtained 33 monocyte-related genes and their coefficients. **(B)** Dendrogram correlating the risk score and 64 cell types. **(C)** GO functional enrichment analysis correlating different immune regulatory processes with risk score. **(D)** Survival analyses of risk scores in pan-glioma, LGG and GBM groups from TCGA. D, Hazard ratios of risk scores in different cancer types. **(E)** ROC curve measuring the sensitivity of risk score in predicting patient's 3 years and 5 years survival status. The area under the ROC curve was 0.878 and 0.845, respectively.

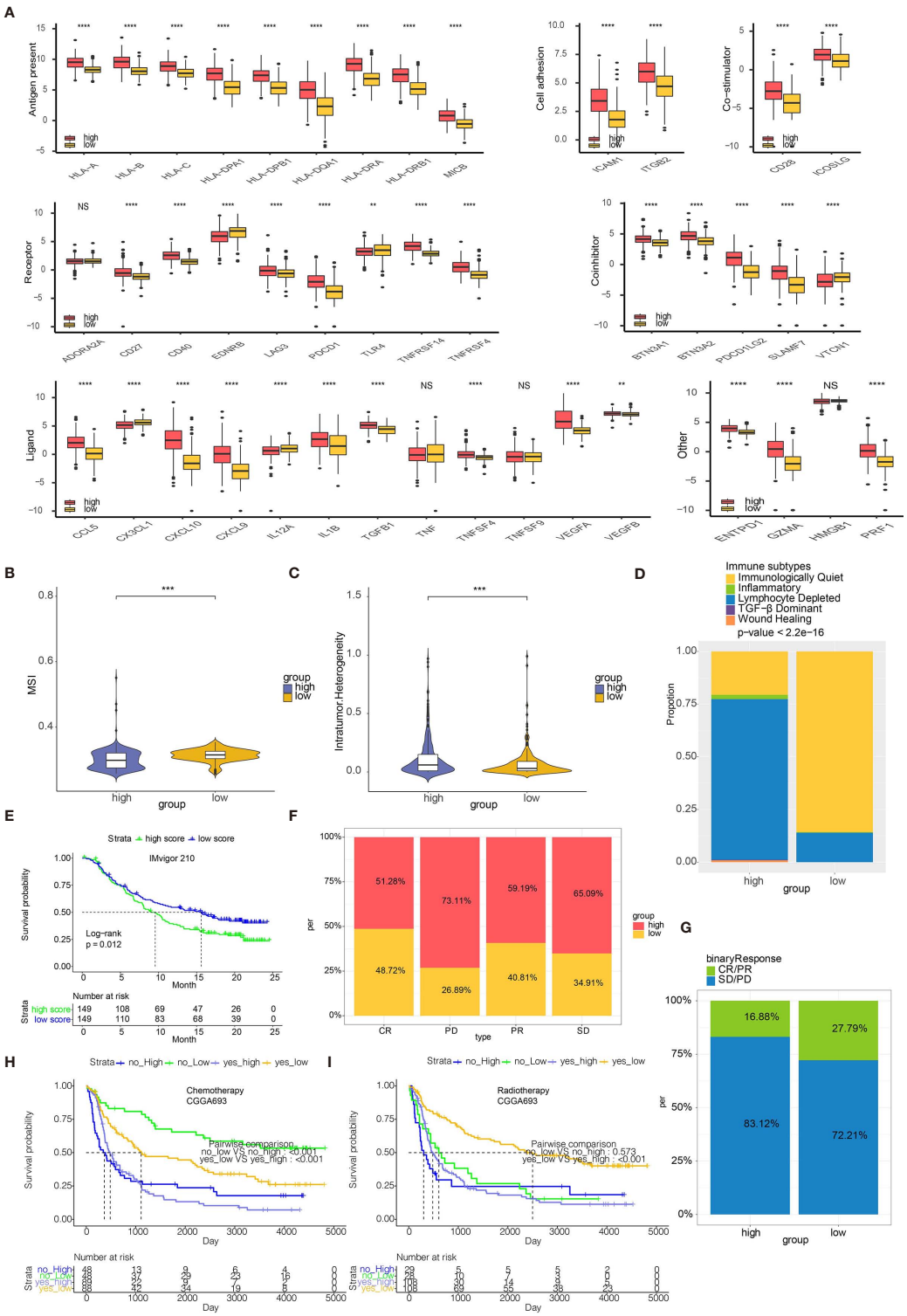

FIGURE 7 | Risk scores predict immunotherapy response. **(A)** Molecule levels of immune checkpoints in two risk score groups in TCGA. **(B)** MSI in high and low risk score. **(C)** Intratumor Heterogeneity in high and low risk score. **(D)** Distribution of six immune subtypes in two risk score groups in TCGA. **(E)** Kaplan-Meier curve of high and low risk score groups in IMvigor210 cohort. **(F)** The bar chart showing proportions of high and low risk scores. **(G)** The bar chart showing proportions of CR/PR and SD/PD patients in high and low risk score groups. **(H)** Kaplan-Meier curve of high and low risk score groups in patients receiving chemotherapy from CGGA693. **(I)** Kaplan-Meier curve of high and low risk score groups in patients receiving radiotherapy from CGGA693. **P < 0.01, ***P < 0.001, ****P < 0.0001. NS, not statistically significant.

development (26). Dendritic Cell-based Vaccination has been proved with potential therapeutic effect on GBM patient survival (27). Moreover, monocytes closely adhere to GBM via *VCAM-1* and promotes tumor invasion activity (10). In summary, monocytes could both directly or indirectly mediate the tumor growth and invasion of gliomas.

To explore and confirm the predictive value of monocyte in gliomas, monocyte entity is defined by the consensus-based xCell algorithm in the present study. The WGCNA-derived monocyte-related genes clustered glioma patients into two groups with distinctive clinical traits and immune characteristics. It should be noted that even though almost all GBM patients fell in cluster 1, some LGG patients also fell in cluster 1. Therefore, the clustering results are more likely to reflect the similar molecular characteristics of GBM and LGG. Patients in Cluster 1, with worse survival, had higher level of *IDH* WT, 1p19q noncodeletion, and *MGMT* promoter unmethylation that all correlated with a more malignant phenotype of glioma. Further, patients in cluster 1 was more associated with hypoxia and hypermetabolism, both of which correlated with the malignancy of cancer. Immune infiltrating cells such as fibroblasts, M2 macrophages, and DCs had higher expression in Cluster 1. Classical immune checkpoint molecules such as *PD1*, *PDCD1LG2*, *LAG3*, and *VTCN1* all had higher expression in cluster 1. Additionally, patients in cluster 1 had higher ESTIMATE scores. Taken together, monocyte served as an effective factor stratifying glioma patients with diverse clinical features and outcomes.

The genomic alteration related to monocyte entity was then investigated. The *IDH* missense mutations confer better survival outcome in glioma patients. Nevertheless, LGGs carrying the *IDH* mutations are more prone to develop into secondary GBMs, especially when tertiary genetic alterations in oncogenes like *PIK3CA* and *PDGFRA* occur in the same patient (28). The present study finds that the *IDH1* missense mutations are overrepresented in the cluster 2 (92%) compared with the cluster 1 (12%), in accordance with previous findings that *IDH* mutations are more enriched in LGGs than in high grade ones (29). Likewise, *EGFR*, which is the most enriched mutated gene in cluster 1 (28%) as identified by somatic mutation analysis, has been reported to be frequently activated in GBM (30).

Based on the DEGs identified between two clusters, a risk score calculated by 33 monocyte related genes was reached. Monocyte related risk score showed high efficiency in predicting patients' 3 years and 5 years survival probability. A nomogram incorporating monocyte further confirmed the efficacy of monocyte as a prognostic marker.

In recent years, acumulating evidence proved that the tumor immune microenvironment played an important role in cancer development (31). Central nervous system was long considered as an "immune privileged" organ due to the existence of blood brain barrier. Currently, the discovery of lymphatic vessels has subverted this opinion, in which immune cells could infiltrate into the brain during tumor progression as a part of the tumor immune microenvironment (32). We next tried to establish a robust relationship between risk score and tumor immune microenvironment. Glioma cells secret *CCL-2* to promote the activity of tumor-associated macrophages which suppressed the activities of cytotoxic T cells (33). Besides, glioma cells increase the expression of programmed cell death 1 ligand (*PD-L1*), a classical immune checkpoint molecule, which induces the immunosuppressive context and mediates the immune escape of tumor cells (34). High risk score group tended to correlate with more immune infiltrating cells, such as macrophages and fibroblasts. High risk score group also expressed more immune checkpoint molecules including *PDCD1* and chemokines *CCL-5*, *CXCL10*, and *CXCL9*. Functional annotation of risk score further revealed that macrophage activation, fibroblast proliferation, and regulation of T cell apoptotic process were more frequently occurred in glioma patients with high risk score. A series of factors associated with tumor immunogenicity and antigen presentation capacity such as MSI, intratumor heterogeneity, and neoantigens were found to be highly expressed in high risk score group. MSI has been recently reported to predict patients' responses to immunotherapy, and has been proposed as a promising biomarker for anti-PD-L1 therapy (35). Likewise, intratumor heterogeneity has also been proved to influence the outcome of immunotherapy (36). It is noteworthy that therapeutic approaches based on neoantigens, another biomarker in cancer immunotherapy, have been proposed to selectively enhance T cell reactivity (22). Besides, *IFN-γ*Dominant and Lymphocyte Depleted immune subtypes were more observed in high risk score group. The above findings indicated that risk score was associated with an immunosuppressive and tumorigenic microenvironment.

Immunotherapy, represented by anti-*PD-1* therapy, has been regarded as a promising therapeutic option in melanoma and urothelial cancer (37–41). So far, clinical trials of immunotherapy have not demonstrated satisfactory results in glioma patients. Based on the IMvigor210 cohort, our analyses showed that the high risk score group had more frequent stable/progressive disease patients than responsive patients, representing a worse response to immunotherapies. Based on the CGGA693 cohort, high risk score group receiving chemotherapy or radiotherapy was associated with worse survival. Therefore, we hypothesized that monocyte could be an effective factor in predicting glioma patients' response to immunotherapy and classical chemoradiotherapy.

In conclusion, our analyses identified a monocyte gene signature consisting of 33 monocyte-specific genes, and established its prognostic value in glioma. Our findings strongly supported a modulatory role of monocytes in glioma progression and proved that monocyte served as an effective factor stratifying glioma patients' survival probability. One major limitation of this study was the lack of external real-world data to confirm and support our findings. Another limitation was the lack of GBM cohort for predicting the immunotherapy response, which the tumor microenvironment in urothelial carcinoma might be different from that in GBM. Thus, a GBM cohort was expected to validate the efficacy of monocyte-derived risk score in predicting immunotherapy response in the future. Moreover, the in-depth mechanisms such as governing the differentiation of

monocytes into protumoral or antitumoral cells in TME of gliomas remained undermined and needed further experiment for validation. Additionally, the underlying regulatory role of monocyte in immune responses remained to be elucidated.

DATA AVAILABILITY STATEMENT

All data used in this work can be acquired from the Cancer Genome Atlas (TCGA) datasets (https://xenabrowser.net/), the Chinese Glioma Genome Atlas (CGGA) datasets (http://www.cgga.org.cn/), and GSE108474 from the GEO database (https://www.ncbi.nlm.nih.gov/geo/).

AUTHOR CONTRIBUTIONS

HZ, QC, WW, NZ, YZ, HC, and ZD designed and drafted the manuscript. HZ wrote figure legends and revised the manuscript. QC, HZ, and NZ conducted data analysis. All authors contributed to the article and approved the submitted version.

FUNDING

Financial support was provided by the National Natural Science Foundation of China (NO. 82073893), China Postdoctoral Science Foundation (NO. 2018M633002), Hunan Provincial Natural Science Foundation of China (NO.2018JJ3838), Hunan Provincial Health Committee Foundation of China (C2019186). Xiangya Hospital Central South University postdoctoral foundation.

SUPPLEMENTARY MATERIAL

The Supplementary Material for this article can be found online at: https://www.frontiersin.org/articles/10.3389/fimmu.2021.656541/full#supplementary-material

REFERENCES

1. Zhang H, Wang R, Yu Y, Liu J, Luo T, Fan F. Glioblastoma Treatment Modalities besides Surgery. *J Cancer* (2019) 10:4793–806. doi: 10.7150/jca.32475
2. Ostrom QT, Patil N, Cioffi G, Waite K, Kruchko C, Barnholtz-Sloan JS. CBTRUS Statistical Report: Primary Brain and Other Central Nervous System Tumors Diagnosed in the United States in 2013-2017. *Neuro Oncol* (2020) 22:iv1–iv96. doi: 10.1093/neuonc/noaa200
3. Ostrom QT, Cioffi G, Gittleman H, Patil N, Waite K, Kruchko C, et al. CBTRUS Statistical Report: Primary Brain and Other Central Nervous System Tumors Diagnosed in the United States in 2012-2016. *Neuro Oncol* (2019) 21:v1–v100. doi: 10.1093/neuonc/noz150
4. Parsons DW, Jones S, Zhang X, Lin JC, Leary RJ, Angenendt P, et al. An integrated genomic analysis of human glioblastoma multiforme. *Science* (2008) 321:1807–12. doi: 10.1126/science.1164382
5. Ludwig K, Kornblum HI. Molecular markers in glioma. *J Neurooncol* (2017) 134:505–12. doi: 10.1007/s11060-017-2379-y
6. Louis DN, Perry A, Reifenberger G, von Deimling A, Figarella-Branger D, Cavenee WK, et al. The 2016 World Health Organization Classification of Tumors of the Central Nervous System: a summary. *Acta Neuropathol* (2016) 131:803–20. doi: 10.1007/s00401-016-1545-1
7. Zhang H, Zhou Y, Cui B, Liu Z, Shen H. Novel insights into astrocyte-mediated signaling of proliferation, invasion and tumor immune microenvironment in glioblastoma. *BioMed Pharmacother* (2020) 126:110086. doi: 10.1016/j.biopha.2020.110086
8. Olingy CE, Dinh HQ, Hedrick CC. Monocyte heterogeneity and functions in cancer. *J Leukoc Biol* (2019) 106:309–22. doi: 10.1002/JLB.4RI0818-311R
9. Charles NA, Holland EC, Gilbertson R, Glass R, Kettenmann H. The brain tumor microenvironment. *Glia* (2012) 60:502–14. doi: 10.1002/glia.21264
10. Liu YS, Lin HY, Lai SW, Huang CY, Huang BR, Chen PY, et al. MiR-181b modulates EGFR-dependent VCAM-1 expression and monocyte adhesion in glioblastoma. *Oncogene* (2017) 36:5006–22. doi: 10.1038/onc.2017.129
11. Guilliams M, Ginhoux F, Jakubzick C, Naik SH, Onai N, Schraml BU, et al. Dendritic cells, monocytes and macrophages: a unified nomenclature based on ontogeny. *Nat Rev Immunol* (2014) 14:571–8. doi: 10.1038/nri3712
12. Wilkerson MD, Hayes DN. ConsensusClusterPlus: a class discovery tool with confidence assessments and item tracking. *Bioinformatics* (2010) 26:1572–3. doi: 10.1093/bioinformatics/btq170
13. Aran D, Hu Z, Butte AJ. xCell: digitally portraying the tissue cellular heterogeneity landscape. *Genome Biol* (2017) 18:220. doi: 10.1186/s13059-017-1349-1
14. Newman AM, Liu CL, Green MR, Gentles AJ, Feng W, Xu Y, et al. Robust enumeration of cell subsets from tissue expression profiles. *Nat Methods* (2015) 12:453–7. doi: 10.1038/nmeth.3337
15. Schreiber RD, Old LJ, Smyth MJ. Cancer immunoediting: integrating immunity's roles in cancer suppression and promotion. *Science* (2011) 331:1565–70. doi: 10.1126/science.1203486
16. Zhang M, Wang X, Chen X, Zhang Q, Hong J. Novel Immune-Related Gene Signature for Risk Stratification and Prognosis of Survival in Lower-Grade Glioma. *Front Genet* (2020) 11:363. doi: 10.3389/fgene.2020.00363
17. Gu Z, Eils R, Schlesner M. Complex heatmaps reveal patterns and correlations in multidimensional genomic data. *Bioinformatics* (2016) 32:2847–9. doi: 10.1093/bioinformatics/btw313
18. Network CGAR, Brat DJ, Verhaak RG, Aldape KD, Yung WK, Salama SR, et al. Comprehensive, Integrative Genomic Analysis of Diffuse Lower-Grade Gliomas. *N Engl J Med* (2015) 372:2481–98. doi: 10.1056/NEJMoa1402121
19. Liu XY, Gerges N, Korshunov A, Sabha N, Khuong-Quang DA, Fontebasso AM, et al. Frequent ATRX mutations and loss of expression in adult diffuse astrocytic tumors carrying IDH1/IDH2 and TP53 mutations. *Acta Neuropathol* (2012) 124:615–25. doi: 10.1007/s00401-012-1031-3
20. Xie Y, Tan Y, Yang C, Zhang X, Xu C, Qiao X, et al. Omics-based integrated analysis identified ATRX as a biomarker associated with glioma diagnosis and prognosis. *Cancer Biol Med* (2019) 16:784–96. doi: 10.20892/j.issn.2095-3941.2019.0143
21. Ichimura K. Molecular pathogenesis of IDH mutations in gliomas. *Brain Tumor Pathol* (2012) 29:131–9. doi: 10.1007/s10014-012-0090-4
22. Schumacher TN, Schreiber RD. Neoantigens in cancer immunotherapy. *Science* (2015) 348:69–74. doi: 10.1126/science.aaa4971
23. Thorsson V, Gibbs DL, Brown SD, Wolf D, Bortone DS, Ou Yang TH, et al. The Immune Landscape of Cancer. *Immunity* (2018) 48:812–30.e14. doi: 10.1016/j.immuni.2018.03.0233
24. Qian BZ, Li J, Zhang H, Kitamura T, Zhang J, Campion LR, et al. CCL2 recruits inflammatory monocytes to facilitate breast-tumour metastasis. *Nature* (2011) 475:222–5. doi: 10.1038/nature10138
25. Hanna RN, Cekic C, Sag D, Tacke R, Thomas GD, Nowyhed H, et al. Patrolling monocytes control tumor metastasis to the lung. *Science* (2015) 350:985–90. doi: 10.1126/science.aac9407
26. Chen Z, Feng X, Herting CJ, Garcia VA, Nie K, Pong WW, et al. Cellular and Molecular Identity of Tumor-Associated Macrophages in Glioblastoma. *Cancer Res* (2017) 77:2266–78. doi: 10.1158/0008-5472.CAN-16-2310
27. Mitsuya K, Akiyama Y, Iizuka A, Miyata H, Deguchi S, Hayashi N, et al. Alpha-type-1 Polarized Dendritic Cell-based Vaccination in Newly Diagnosed High-grade Glioma: A Phase II Clinical Trial. *Anticancer Res* (2020) 40:6473–84. doi: 10.21873/anticanres.14669

28. Wakimoto H, Tanaka S, Curry WT, Loebel F, Zhao D, Tateishi K, et al. Targetable signaling pathway mutations are associated with malignant phenotype in IDH-mutant gliomas. *Clin Cancer Res* (2014) 20:2898–909. doi: 10.1158/1078-0432.CCR-13-3052
29. Yan H, Parsons DW, Jin G, McLendon R, Rasheed BA, Yuan W, et al. IDH1 and IDH2 mutations in gliomas. *N Engl J Med* (2009) 360:765–73. doi: 10.1056/NEJMoa0808710
30. Network CGAR. Comprehensive genomic characterization defines human glioblastoma genes and core pathways. *Nature* (2008) 455:1061–8. doi: 10.1038/nature07385
31. Quail DF, Joyce JA. The Microenvironmental Landscape of Brain Tumors. *Cancer Cell* (2017) 31:326–41. doi: 10.1016/j.ccell.2017.02.009
32. Louveau A, Smirnov I, Keyes TJ, Eccles JD, Rouhani SJ, Peske JD, et al. Structural and functional features of central nervous system lymphatic vessels. *Nature* (2015) 523:337–41. doi: 10.1038/nature14432
33. Zhang J, Sarkar S, Cua R, Zhou Y, Hader W, Yong VW. A dialog between glioma and microglia that promotes tumor invasiveness through the CCL2/CCR2/interleukin-6 axis. *Carcinogenesis* (2012) 33:312–9. doi: 10.1093/carcin/bgr289
34. Bloch O, Crane CA, Kaur R, Safaee M, Rutkowski MJ, Parsa AT. Gliomas promote immunosuppression through induction of B7-H1 expression in tumor-associated macrophages. *Clin Cancer Res* (2013) 19:3165–75. doi: 10.1158/1078-0432.CCR-12-3314
35. Luchini C, Bibeau F, Ligtenberg MJL, Singh N, Nottegar A, Bosse T, et al. ESMO recommendations on microsatellite instability testing for immunotherapy in cancer, and its relationship with PD-1/PD-L1 expression and tumour mutational burden: a systematic review-based approach. *Ann Oncol* (2019) 30:1232–43. doi: 10.1093/annonc/mdz116
36. Li J, Byrne KT, Yan F, Yamazoe T, Chen Z, Baslan T, et al. Tumor Cell-Intrinsic Factors Underlie Heterogeneity of Immune Cell Infiltration and Response to Immunotherapy. *Immunity* (2018) 49:178–93.e7. doi: 10.1016/j.immuni.2018.06.006
37. Zhang H, Zhou Y, Cheng Q, Dai Z, Wang Z, Liu F, et al. PDIA3 correlates with clinical malignant features and immune signature in human gliomas. *Aging (Albany NY)* (2020) 12:15392–413. doi: 10.18632/aging.103601
38. Zhang H, Fan F, Yu Y, Wang Z, Liu F, Dai Z, et al. Clinical characterization, genetic profiling, and immune infiltration of TOX in diffuse gliomas. *J Transl Med* (2020) 18:305. doi: 10.1186/s12967-020-02514-6
39. Zhang H, Cui B, Zhou Y, Wang X, Wu W, Wang Z, et al. B2M overexpression correlates with malignancy and immune signatures in human gliomas. *Sci Rep* (2021) 11:5045. doi: 10.1038/s41598-021-84465-6
40. Zhang H, He J, Dai Z, Wang Z, Liang X, He F, et al. PDIA5 is Correlated With Immune Infiltration and Predicts Poor Prognosis in Gliomas. *Front Immunol* (2021) 12:628966. doi: 10.3389/fimmu.2021.628966
41. Wang Z, Zhang H, Cheng Q. PDIA4: The basic characteristics, functions and its potential connection with cancer. *BioMed Pharmacother* (2020) 122:109688. doi: 10.1016/j.biopha.2019.109688

Conflict of Interest: The authors declare that the research was conducted in the absence of any commercial or financial relationships that could be construed as a potential conflict of interest.

frontiers in Oncology

REVIEW
published: 10 May 2021
doi: 10.3389/fonc.2021.672508

Making a Cold Tumor Hot: The Role of Vaccines in the Treatment of Glioblastoma

Stephen C. Frederico[1†], *John C. Hancock*[1†], *Emily E. S. Brettschneider*[1,2], *Nivedita M. Ratnam*[1], *Mark R. Gilbert*[1] *and Masaki Terabe*[1*]

[1] *Neuro-Oncology Branch, CCR, NCI, National Institutes of Health, Bethesda, MD, United States,* [2] *Ludwig Institute for Cancer Research, University of Oxford, Oxford, United Kingdom*

OPEN ACCESS

Edited by:
Payal Watchmaker, University of California, San Francisco, United States

Reviewed by:
Christopher Jackson, Johns Hopkins University, United States
Wei Chen, Stanford University, United States

***Correspondence:**
Masaki Terabe
terabe@mail.nih.gov

[†]*These authors have contributed equally to this work and share first authorship*

Specialty section:
This article was submitted to Cancer Immunity and Immunotherapy, a section of the journal Frontiers in Oncology

Received: *25 February 2021*
Accepted: *19 April 2021*
Published: *10 May 2021*

Citation:
Frederico SC, Hancock JC, Brettschneider EES, Ratnam NM, Gilbert MR and Terabe M (2021) Making a Cold Tumor Hot: The Role of Vaccines in the Treatment of Glioblastoma. Front. Oncol. 11:672508. doi: 10.3389/fonc.2021.672508

The use of immunotherapies for the treatment of brain tumors is a topic that has garnered considerable excitement in recent years. Discoveries such as the presence of a glymphatic system and immune surveillance in the central nervous system (CNS) have shattered the theory of immune privilege and opened up the possibility of treating CNS malignancies with immunotherapies. However, despite many immunotherapy clinical trials aimed at treating glioblastoma (GBM), very few have demonstrated a significant survival benefit. Several factors for this have been identified, one of which is that GBMs are immunologically "cold," implying that the cancer does not induce a strong T cell response. It is postulated that this is why clinical trials using an immune checkpoint inhibitor alone have not demonstrated efficacy. While it is well established that anti-cancer T cell responses can be facilitated by the presentation of tumor-specific antigens to the immune system, treatment-related death of GBM cells and subsequent release of molecules have not been shown to be sufficient to evoke an anti-tumor immune response effective enough to have a significant impact. To overcome this limitation, vaccines can be used to introduce exogenous antigens at higher concentrations to the immune system to induce strong tumor antigen-specific T cell responses. In this review, we will describe vaccination strategies that are under investigation to treat GBM; categorizing them based on their target antigens, form of antigens, vehicles used, and pairing with specific adjuvants. We will review the concept of vaccine therapy in combination with immune checkpoint inhibitors, as it is hypothesized that this approach may be more effective in overcoming the immunosuppressive milieu of GBM. Clinical trial design and the need for incorporating robust immune monitoring into future studies will also be discussed here. We believe that the integration of evolving technologies of vaccine development, delivery, and immune monitoring will further enhance the role of these therapies and will likely remain an important area of investigation for future treatment strategies for GBM patients.

Keywords: glioblastoma, vaccine, dendritic cells, peptide, tumor antigen, neoantigen, T cells, heat shock protein

INTRODUCTION

Glioblastoma (GBM) is one of the most lethal primary brain malignancies, with a median overall survival of 14-17 months despite intervention with both surgery and chemo-radiation therapy (1, 2). In recent years, there has been hope that immunotherapy would be a promising new approach to treat this devastating disease. Since 2011, a new wave of immune checkpoint inhibitors (ICIs) such as anti-CTLA-4 and anti-PD-1/PD-L1 monotherapies have been approved for melanoma, non-small cell lung cancer, and other solid malignancies outside of the CNS (3). The hypothesis of immune privilege in the CNS has begun to weaken, making immunotherapy a possibility for the treatment of GBM and other CNS cancers (4–6). Early murine studies conducted to test the efficacy of anti-PD-1, anti-PD-L1, and anti-CTLA-4 using orthotopic, syngeneic GBM models were very promising, demonstrating long-term tumor eradication using single-agent therapy and a cure rate of 75% when combining anti-CTLA-4 with anti-PD-1 (7). These results led to CheckMate 143: the first major clinical trial for immunotherapy in GBM (1). This phase III trial tested the survival benefit of anti-PD-1 monotherapy in 369 patients with recurrent GBM (8). Unfortunately, the outcome of the trial was disappointing as no significant difference was found between patients receiving treatment with anti-PD-1 in comparison to those receiving the standard of care (8). To date, immune checkpoint monotherapy has not been proven to be successful in the treatment of GBM clinically (1). Also, no phase III clinical trial with any immunotherapy approach has demonstrated benefit in GBM patients (9). One of the primary reasons for this failure is the ability of GBM tumor cells to induce immune suppression (1, 9, 10), which is why combination of different therapies may yield better results (1, 9). A call to action has now been made to develop new therapies that can provide patients with improved OS.

The mechanisms of GBM immunosuppression are multifaceted, with effects propagated both locally and systemically. At the local level, tumors can recruit regulatory T cells and induce tumor-associated macrophages to cause T cell apoptosis (4). Immunosuppressive cytokines such as IL-10, TGF-beta, and CCL2 are also secreted (11). GBM uses metabolites such as kynurenine to polarize macrophages to an anti-inflammatory phenotype (1). These mechanisms result in the majority of immune cell infiltrates being composed of immunosuppressive MDSCs and tumor-associated macrophages (11). On a systemic level, intracranial tumors can cause sequestration of T cells in the bone marrow (12). It is speculated that this is induced through the loss of the sphingosine-1-phosphate receptor 1 (S1P1) from the T cell surface, a G-protein-coupled receptor that plays a vital role in lymphocyte trafficking (12). Furthermore, recent evidence has identified meningeal lymphatic drainage that lies between the brain parenchyma and cervical lymph nodes: the "glymphatic system" (13, 14). Meningeal lymphatics play a role in the control of immune surveillance of the CNS (15). It is possible that GBM disrupts this drainage and thus hinders antigen flow and immune cell trafficking (13, 15, 16). GBMs are thus known as "cold" tumors, which have few or no lymphocyte infiltrates (11). One promising strategy to "heat up" a cold tumor is to promote a robust anti-tumor T cell response through the use of vaccines.

In 1953, observations in radiation oncology highlighted a phenomenon that has become known as the abscopal effect (17, 18). The idea refers to the systemic regression of tumors and metastases in non-radiated areas outside of the primary localized radiation field (17, 18). It is hypothesized that radiation induces the release of tumor antigens which then prime the immune system for an anti-tumor response (17). This observation inspires the possibility of stimulating the immune system using exogenously introduced antigens and is the basis for the generation and use of anti-cancer vaccines. Ideally, systemic induction of an anti-cancer T cell response by vaccines can lead to increased trafficking to the tumor site. One could theoretically "heat up" an immunologically "cold" tumor. Thus in the case of cancer, vaccinations are therapeutic rather than prophylactic (9).

It has become clear that GBMs are complex and heterogeneous, evolving before, during, and after treatment (4). Given the vast inter- and intra-tumoral heterogeneity and multiple facets of immunosuppression provided by GBM, a single target approach may not be effective. The pooled mechanisms of multiple distinct therapies will be required. One important observation in GBM is that increased levels of inflammation in and around the tumor site induces increased PD-L1 expression (10). Thus, it is anticipated that the combination of vaccines and PD-1/PD-L1 targeted therapy would be synergistic in overcoming GBM immunosuppression. Combinations of ICIs with other therapies is increasingly being tested in clinical trials (1).

This review will highlight the most promising vaccines capable of treating GBM. In addition to discussing how these vaccines are made and their success in clinical trials, we will also explore pairing these vaccines with different adjuvants to enhance overall effect. Each vaccine trial will be categorized based on their target antigens, antigenic forms, vehicles used, as well as adjuvant pairings (see **Figure 1**). We hope that by highlighting the most promising vaccines and adjuvants, as well as discussing the need for robust immune monitoring in future clinical trials, this review can be used as a guide for designing novel vaccine-based approaches for treating GBM.

Abbreviations: CNS, central nervous system; GBM, glioblastoma; MDSC, myeloid-derived suppressor cell; HLA, human leukocyte antigen; IDH, isocitrate dehydrogenase; WT1, Wilms tumor 1; TERT, telomerase reverse transcriptase; MHC, major histocompatility complex; PFS, progression-free survival; OS, overall survival; EGFR, epidermal growth factor receptor; CMV pp65, cytomegalovirus phosphoprotein 65; DC, dendritic cell; GSC, glioma stem cell; HSP, heat shock protein; HSPPC, heat shock protein-peptide complex; TLR, toll-like receptor; PET, positron emission tomography; BBB, blood-brain barrier; TME, tumor microenvironment; ICI, immune checkpoint inhibitors.

TARGET ANTIGENS

Antigen targets for vaccines are broadly classified as either tumor-associated or tumor-specific. Tumor-associated antigens are proteins expressed in many cells throughout the body in limited quantities, but are overexpressed in tumors (9, 19). Examples of these proteins in the case of GBM include survivin and Wilms

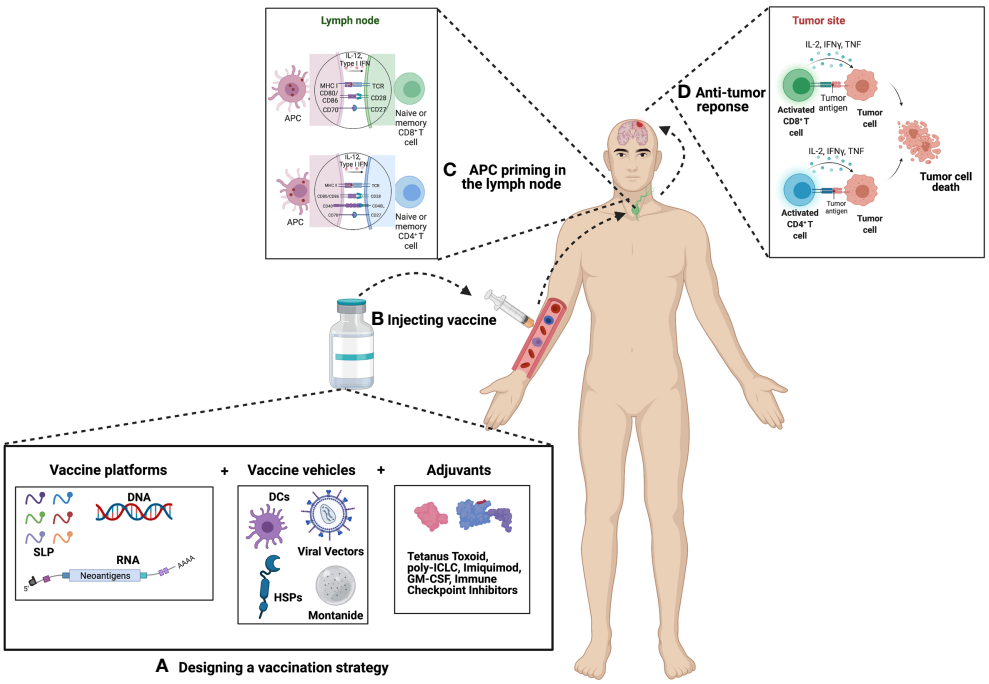

FIGURE 1 | Principle of Cancer Vaccination. **(A)** Vaccine selection and preparation – Upon selection of suitable candidates a vaccine platform is chosen which includes either peptides, DNA or RNA. This platform is then packaged into a vehicle which includes either dendritic cells (DCs), viral vectors, heat shock proteins (HSPs), or montanide. The vaccine is then combined or paired with an adjuvant in an effort to boost the efficacy of the vaccine. Common choices of adjuvants include tetanus toxoid, poly-ICLC, imiquimod, GM-CSF, immune checkpoint inhibitors, as well as many others. **(B)** Vaccines can be administered intra-venously, intra-nodally, intra-dermally, or intra-muscularly. **(C)** Antigens are then presented by APCs to naïve or memory T cells in the lymph node. For GBM, presentation most commonly occurs in the deep-seated cervical lymph node. **(D)** Primed T cells migrate to the site of the tumor where they mount an anti-tumor immune response.

tumor 1 (WT1). Tumor-specific antigens on the other hand include mutant proteins exclusively expressed by tumor cells (19). Examples include EGFRvIII and isocitrate dehydrogenase (IDH) R132H in the context of GBM and grade 4 astrocytoma, respectively (19). Generally, tumor-specific antigens are considered as ideal targets for a vaccine since they are selectively expressed on tumor cells and not in normal tissue. One of the challenges of GBM is the ability to find a tumor-specific antigen that is expressed uniformly within the tumor, is shared between patients, and is present after the widespread changes that occur with disease recurrence (1, 11).

Neoantigens are proteins that arise from mutations within a tumor cell and vary from cell to cell and person to person (20). Personalized neoantigen vaccines use sequencing data from the whole exome and RNA of a patient's tumor to identify specific mutations particular to that individual (1). Most of these are "passenger mutations," which derive from genomic instability within the tumor and do not play a role in tumorigenesis (20). The process of developing a neoantigen vaccine starts with DNA and RNA sequencing of the patient's normal cells and the tumor (21). Analysis identifies mutational differences between the two, followed by RNA sequencing data which predicts the expression level of those mutations (21). MHC or human leukocyte antigen (HLA) typing is critical because the peptide that can be presented by MHC depends on MHC/HLA haplotype (21).

The activation of neoantigen-specific T cell responses requires T cell receptor recognition and binding to a specific epitope on the MHC. Upon transcription and translation of the neoantigen, the protein is cleaved into short peptide sequences that can be presented on class I MHC on tumor cells or class II MHC on antigen presenting cells (20). In the class I MHC pathway, intracellular protein fragments are transported into the endoplasmic reticulum *via* the TAP protein to be bound to MHC (21). Antigen presenting cells endocytose antigens that are cleaved by proteases in endosomes and then load these onto class II MHC (21). A large number of computational algorithms have been developed to predict the neoantigens that will undergo each step of this process and successfully lead to T cell activation (21). For example, predictions can be made to identify mutations that will lead to immunogenic neoantigens that are capable of binding to MHC molecules with high affinity (20). However, the prediction algorithm continues to be optimized and currently there is no standard (22).

Two phase I trials in 2019 tested the use of a personalized neoantigen vaccine strategy in newly diagnosed GBM patients (23, 24). The study by Keskin et al. (24) tested the approach in MGMT-unmethylated GBM patients after they had undergone surgery and standard radiation. Development of the vaccine first used whole-exome sequencing to compare data from the tumor samples to normal tissue. Specific single-nucleotide mutations were identified as candidates, RNA sequencing confirmed expression, and then predictions were made for the binding affinity of the neoantigens with the patient's specific MHC/HLA alleles.

The study enrolled 10 patients and the sequencing data identified a median of 116 somatic single-nucleotide mutations per tumor, which included genes such as *PTEN*, *EGFR*, and *RB1*. Interestingly, only patients who had not received dexamethasone during vaccine administration developed $CD4^+$ and $CD8^+$ T cell responses specific to the neoantigen of interest. These T cells could be detected in the peripheral blood, and the median PFS was 7.6 months alongside the median OS of 16.8 months. Unfortunately, each of the patients experienced relapse with progressive disease and the tumor-associated T cells showed an exhausted phenotype after vaccination. Thus, the authors noted that the therapy may be more effective in combination with ICIs.

A second study (GAPVAC-101) conducted by Hilf et al. (23) tested the concurrent administration of both a tumor-associated and a tumor-specific vaccine. APVAC1 was a tumor-associated vaccine with 5-10 unmutated peptides identified by expression profiling that most highly associated with the individual's tumor (19, 23). APVAC2 was a personalized vaccine with 1-2 mutated neoepitopes (19, 23). The vaccines were given in conjunction with standard radiation and temozolomide and the authors concluded that administration of the vaccine with unmutated peptides led to prolonged central memory $CD8^+$ T cell responses, while the personalized neoepitope vaccine primarily induced a Th1 $CD4^+$ T cell response (23). The authors suggested that studies would be required to confirm these preliminary results (23).

These initial clinical trials have now led to two on-going clinical trials that combine a personalized neoantigen vaccine with immune checkpoint blockade. The first (NCT02287428) study is using a vaccine strategy that targets 20 mutant peptides directly expressed on the patient's tumor (19, 25) in combination with pembrolizumab (anti-PD-1 antibody) and radiation therapy in newly diagnosed patients with MGMT-unmethylated GBM (25). This study divides patients into three different cohorts where vaccine and ICI is administered at different timepoints in relation to one another along with radiation therapy (25). This is important since it allows the study personnel to investigate if the timing of administration of pembrolizumab enhances efficacy of the vaccine (25). The second clinical trial (NCT03422094) uses a similar vaccine in newly diagnosed patients with MGMT-unmethylated GBM (26). However, the investigators in this trial combined treatment with nivolumab (yet another anti-PD-1 antibody) with the CTLA-4 antagonist, ipilimumab (26). Since anti-CTLA-4 and anti-PD-1 therapies have different mechanisms of action (27), this second trial will provide interesting insights with regard to the treatment of GBM.

VACCINE PLATFORMS

Peptides

Peptide vaccines are composed of short chains of amino acids to induce activation of T cells. The presentation of these peptides by dendritic cells (DCs) in the draining lymph nodes prime antigen-specific T cells. Work done in human papillomavirus-associated cervical cancer first identified the enhanced efficacy of a 35 amino acid long-peptide vaccine (28). Longer peptides induced efficacious tumor immunity in mice and humans superior to minimal epitope peptides that fit MHC class I exactly because they were more likely to be processed and presented by professional antigen presenting cells, DCs (28, 29). Peptide vaccines are some of the most commonly used vaccines tested for the treatment of GBM and are composed of single or multiple antigens. Peptides tested as a single-antigen have included EGFRvIII, CMV pp65, TERT, IDH1, survivin, and WT1. These include epitopes of tumor-associated or GBM-specific antigens.

The GBM-specific EGFRvIII is a truncated mutant of the epidermal growth factor receptor (EGFR) (11, 30, 31). It is present in 20-30% of GBM patients and is expressed heterogeneously throughout the tumor (30, 31). The loss of exons 2-7 in the extracellular domain of the protein leads to the continuous activation of the growth factor signaling pathway (30). A peptide of 14 amino acids, which includes the novel epitope created by the deletion, was conjugated to keyhole limpet hemocyanin and formed the Rindopepimut vaccine (30). ACT IV was a multicenter phase III clinical trial that investigated the OS of patients receiving the Rindopepimut vaccine administered with temozolomide. This trial enrolled 745 patients with newly diagnosed GBM (11, 30). Despite the vaccine producing a notable humoral response, there was no significant survival benefit compared to control (30). The median OS of the Rindopepimut group was 20.1 months and the median OS of the control group was 20.0 months (11). The failure of this trial illustrates the limitation of the single antigen approach (11). EGFRvIII is expressed heterogeneously in 37-86% of tumor cells. Therefore, the successful induction of immune responses will allow the expansion of antigen negative tumor cells because they are not recognized by T cells activated by the vaccine, a process that is called immune selection (11, 32). In both arms of the study, around half of patients had loss of EGFRvIII expression upon recurrence (19). The randomized phase II ReACT trial explored the efficacy of Rindopepimut together with the anti-angiogenic bevacizumab in 72 patients with relapsed EGFRvIII-positive GBM (31, 33). PFS at 6 months favored the experimental group, suggesting that combination treatments may show promise despite previous monotherapy vaccine failures (31, 33).

Another potentially important antigen is cytomegalovirus (CMV) phosphoprotein 65 (pp65). Cytomegalovirus infects a large majority of adults and CMV proteins are expressed on greater than 90% of GBMs, with 50-70% of them positive for pp65 (34). Importantly, CMV proteins are suitable tumor-specific antigens since they are only found on GBMs and are not present on normal brain parenchyma (34). Preclinical studies have shown that CMV-reactive T cells effectively kill GBM cells positive for the pp65 antigen (19). A phase I trial is currently underway called PRiME (NCT03299309) which is testing the peptide vaccine PEP-CMV in malignant glioma and medulloblastoma patients (35). The therapy contains Component A which is a 26 amino acid peptide of the human pp65 CMV antigen and the study is actively recruiting patients ages 3-35 years old (35).

Two other tumor-specific antigens of note for single-antigen GBM vaccines include TERT and IDH1. Each plays an important

role in the molecular classification of CNS tumors (36, 37). Promoter mutations of TERT (telomerase reverse transcriptase) are commonly present in GBM and expression of the protein is enhanced in many different cancer types (31). UCPVax is a peptide vaccine derived from TERT epitopes that induce Th1 $CD4^+$ T cell responses (38, 39). A phase I/II clinical trial (NCT04280848) is currently evaluating this approach in GBM patients (38). Peptide vaccines for the IDH1 R132H mutation have also been developed for grade II and III gliomas (11). Around 80% of these low-grade tumors have an IDH mutation, of which the IDH1 R132H substitution is the most common (30). The benefit of this tumor-specific target is that it is present on every tumor cell (11). An IDH1 vaccine created in 2014 also had peptide that can be presented by class II MHC and induced a Th1 $CD4^+$ T cell response (40). Two phase I clinical trials that have studied IDH1R132H peptide vaccines include NOA-16 (NCT02454634) and RESIST (NCT02193347) (41, 42). Each vaccine contains a peptide that includes the IDH1 R132H mutated sequence and administration was combined with temozolomide (41, 42). NOA-16 is completed and enrolled 33 patients with grade III and IV gliomas and the RESIST trial is still enrolling patients with grade II tumors (41–43). NOA-16 was shown to be safe and immunogenic with 93.3% of patients having IDH1 R132H-specific T cells (identified by ELISPOT or ELISA) that were not present before vaccination (43).

Tumor-associated antigens that have been tested in single-target GBM vaccines include survivin and WT1. Survinin prevents apoptosis in cells by inhibiting caspase activation and is highly expressed in GBM and other cancers (34). SurVaxM is a peptide vaccine of amino acids 53 through 67 of the protein, conjugated with keyhole limpet hemocyanin (44). A phase II study (NCT02455557) is currently investigating the treatment of 64 newly diagnosed GBM patients with temozolomide and the SurVaxM vaccine (34, 45). Early results indicate high titers of survivin antibodies and CD8 T cells after administration of the vaccine (46). The data also point to improvement in PFS and OS compared to historical controls (46). WT1 is a transcription factor, with DNA-binding that promotes oncogenesis (34). The peptide vaccine for WT1 has also shown to be effective inducing humoral and cytotoxic $CD8^+$ T lymphocyte responses (47). A phase II study in 21 patients demonstrated a 9.5% clinical response rate and a PFS at 6 months of 33.3% (48). An additional peptide vaccine under investigation that induces WT1-specific T cell responses is DSP-7888 (49). It has been tested in multiple types of advanced malignancies (NCT02498665) (50), pediatric high grade glioma (NCT02750891) (51), and in combination with bevacizumab for the treatment of recurrent or progressive GBM (NCT03149003) (52). Importantly, another clinical trial (NCT03311334) is underway in other solid tumors that combines DSP-7888 with immune checkpoint inhibition (53).

Peptide vaccines have also been developed that include multiple antigens. One such example combined three tumor-associated antigens overexpressed in childhood gliomas (survivin, IL-13 receptor alpha 2, and EphA2) (54). Preliminary evidence with enzyme-linked immunosorbent spot analysis showed that 13 of 21 patients mounted positive responses to at least one of the antigens (54). IMA950 is a vaccine with 11 different tumor-associated antigens (one of which is survivin) and each antigen was found present on HLA in GBM tissue samples (55). Nine of the peptides bound class I MHC, two bound class II MHC, and each was chosen based on ability to activate $CD4^+$ and $CD8^+$ T cells (55). A phase I/II study tested the vaccine in newly diagnosed GBM patients which found that it elicited $CD8^+$ and Th1 $CD4^+$ T cell responses and led to a median survival of 19 months (56). A current clinical trial (NCT03665545) is combining the IMA950 vaccine with pembrolizumab (57). Strategies such as this with multiple antigens or combinatorial approaches will be necessary to outcompete the heterogeneity and immunosuppression of GBM.

Nucleic Acids

The development of DNA vaccines is a recent strategy that is being tested in patients with GBM. Bacterial DNA plasmids that encode tumor-associated antigens and immune-stimulating cytokines are inserted into host cells, thus enhancing the expression of these molecules (58). One major benefit of DNA vaccines is that once the plasmid is in the nucleus, the antigens can be presented on both class I and class II MHC (58). The expressed antigens can activate the normal cytotoxic $CD8^+$ T lymphocyte and Th1 $CD4^+$ T cell responses that normally play a role in combating intracellular pathogens or malignancies (58, 59). The technique also activates the innate immune response through the recognition of bacterial CpG motifs and double-stranded DNA-sensing receptors (58, 59). Electroporation, a commonly used method for plasmid delivery into the nucleus of host cells, delivers brief, high intensity electricity to induce increased membrane permeability (59). The process also has a pro-inflammatory benefit with the release of cytokines that increase immune cell concentrations to the site of delivery (59). Recent progress in the field of DNA vaccines has drastically increased their efficacy by optimizing the codons used and untranslated RNA transport elements (60, 61). A phase I/II clinical trial (NCT03491683) is currently investigating the efficacy of the DNA vaccines INO-5401 and INO-9012 combined with the PD-1 antagonist cemiplimab in newly diagnosed GBM patients (62, 63). INO-5401 expresses the tumor-associated antigens WT1, PSMA (prostate specific membrane antigen), and TERT, while INO-9012 encodes the p35 and p40 subunits of IL-12 (62, 63). Both of the vaccines are administered with an intramuscular injection with subsequent electroporation (62, 63). The study is still ongoing, but interim analysis identified that the therapy is safe, immunologically effective, and may lead to an encouraging survival advantage (64). A similar DNA vaccine phase I trial (NCT04015700) with 6 participants is also underway using a personalized neoantigen DNA vaccine, INO-9012, and electroporation (65).

RNA vaccines are in the early stages of development as a potential treatment of GBM patients. The idea behind this approach is that a desired mRNA can be injected in the form of a vaccine and the subsequent proteins are expressed in the cells of the patient (66, 67). The mRNA will encode the antigen of interest, 5' and 3' untranslated regions, a 5' cap, and a poly A tail (66). Translation occurs in the cytosol without the need for

transport to a specific organelle, and then normal degradation decreases the chance for toxicity (66). Only recently have protocols been developed which have allowed the stable, efficient delivery of mRNA *in vivo* (66, 67). Many of the benefits of the mRNA approach over other vaccines include its safety and manufacturing (66). Messenger RNA is not an infectious agent, will not insert into the human DNA genome, and manufacturing can be quickly and inexpensively increased (66). Downsides of RNA vaccines continue to be storage and lifetime, but efforts are being made to combat these problems (66). A phase I/II RNA vaccine study (NCT04573140) is underway in GBM patients in the form of lipid particles that are loaded with the mRNA (68). Given the benefits of RNA vaccines, it is anticipated that the number of GBM vaccine trials with this approach will continue to increase.

VACCINE VEHICLES

Dendritic Cells

DC are professional antigen presenting cells (APCs) with the ability to capture and present exogenous antigens (69). The ability of DCs to stimulate $CD8^+$ T cells with peripheral antigens *via* class I MHC molecules makes them ideal vehicles for administering GBM vaccines. DCs loaded with glioma antigens *ex vivo* can be administered to patients for activation of T cells and induction of robust cytotoxic activity (69). Antigen-loaded DCs must migrate to the lymphoid organs to activate T cells (69). Once activated, T cells that successfully traffic to the tumor site can exert cytotoxic effects on antigen-expressing tumor cells, provided that the tumor microenvironment (TME) is not overly immunosuppressive.

Though classical DCs are undetected in healthy brain parenchyma, they are present in proximal vascular-rich tissues including the choroid plexus and meninges (70). Additionally, in pathological conditions, DCs are capable of migrating to the brain through the afferent lymphatics or the high endothelial venules, and are readily recruited to parenchymal inflammatory lesions (69, 70). This suggests that DCs are capable of recognizing and presenting brain-derived antigens in order to stimulate effector T cells to combat brain tumors. However, compared to other organs, drainage of brain tumor antigens is inefficient and trafficking of immune cells to the brain is attenuated. Viewed optimistically, the native limitations of CNS DCs indicate great potential for therapeutic interventions capable of promoting DC-mediated presentation of glioma antigens to peripheral T cells.

The current generation of DC vaccines are derived from specific subsets of freshly isolated, patient-derived DCs from peripheral blood cultured *ex vivo* with a maturation cocktail of proinflammatory cytokines such as PGE1, TNF-alpha, and IL-1beta (70, 71). Before administration to patients, DC vaccines are pulsed with antigens from a variety of sources, including peptides, tumor lysates, tumor RNA, vectors expressing tumor-associated antigens, and tumor-derived exosomes (69, 70). The most common route of DC vaccine administration in GBM patients has been intradermal, although intravenous, intranodal and intramuscular routes are also possible (69, 70). Though autoimmune reactions caused by DC vaccines are a potential concern, DC vaccines have demonstrated minimal to low toxicity in over 10 phase I/II trials in GBM patients (30).

DCs as vehicles for administration of GBM antigens have been explored in a variety of clinical trials. The first major category of DC vaccines are those expressing single tumor antigens, with most in early stages of clinical investigation. A phase I trial of newly diagnosed GBM patients receiving DCs pulsed with EGFRvIII conjugated to keyhole limpet hemocyanin was demonstrated to be immunogenic in 10 of 12 patients with no serious adverse events (72). A phase I trial in which patients with recurrent glioma received DCs pulsed with WT1 also reported no serious adverse events, and 6 of 10 patients showed a two-fold or greater increase in WT1-specific cytotoxic T lymphocytes by tetramer analysis (73). The phase I/II ADDIT-GLIO trial (NCT02649582) is currently investigating the effectiveness of autologous WT1 mRNA-loaded DCs in combination with TMZ (74). The ICT-121 vaccine targets the cancer stem cell antigen CD133 and is comprised of autologous DCs loaded with two HLA-A2 restricted CD133 epitopes (75). ICT-121 was demonstrated to be safe and to generate immune responses in a phase I trial of patients with recurrent GBM (75). A small phase I trial of patients with recurrent glioma also demonstrated safety and immunogenicity of DCs pulsed with IL-13 receptor alpha 2-derived peptides (76).

In addition to these studies, a number of trials have investigated the usage of DCs pulsed with mRNA encoding the immunodominant CMV pp65 antigen (77, 78). Pooling results from multiple trials utilizing CMV pp65 DC vaccines, it was recently reported that nearly a third of patients receiving treatment have survived beyond 5 years, indicating high promise for these treatments (79). A phase II clinical trial investigating TMZ plus CMV pp65-LAMP mRNA-pulsed DCs administered with GM-CSF and tetanus-diphtheria toxoid is ongoing in patients with newly diagnosed GBM (NCT02465268) (80). Additionally, the Phase I AVERT study (NCT02529072) of pp65-LAMP mRNA-pulsed DCs combined with nivolumab has been completed in patients with recurrent gliomas and additional phase II studies are anticipated (81).

A benefit of using DC vaccines over therapies, such as adoptive transfer of chimeric antigen receptor (CAR) T cells is that they can be used to generate responses to a multiplicity of antigens. The second major category of DC vaccines are pulsed with multiple selected antigens, creating an opportunity to activate $CD8^+$ T cells specific for a variety of targets, which may be a beneficial strategy for combating the heterogeneity of GBM. Ideally, DCs pulsed with multiple common glioma antigens, such as WT1, EGFRvIII, and survivin, could serve as "off-the-shelf" therapies capable of treating a variety of GBM patients (69). However, a downside of this approach is the potential misallocation of immune "resources," (*i.e.* generation of activated T cells specific for antigens not actually expressed on a particular patient's tumor) as this may dilute the effects of vaccination against expressed antigens (70).

The most extensively studied multi-peptide pulsed DC vaccine is ICT-107, which consists of autologous DCs pulsed with six synthetic peptides: HLA-A1-restricted melanoma-associated antigen-1 (MAGE-1) and antigen isolated from immunoselected melanoma-2 (AIM-2), as well as HLA-A2-restricted human EGFR-2 (Her2/neu), tyrosine-related protein-2 (TRP-2), glycoprotein 100 (gp100), and IL-13 receptor alpha 2 (82). In a randomized phase II trial of newly diagnosed HLA-$A1^+$ and/or HLA-$A2^+$ patients receiving the ICT-107 vaccine, no significant difference in OS was observed in the treatment group as compared to controls (82). However, PFS significantly favored the treatment group by 2.2 months. Additional analyses revealed that while over 90% of patients expressed all the HLA-A2 antigens, only 38% of patients expressed the HLA-A1 antigens, and for HLA-$A2^+$ patients with a methylated MGMT promoter, median PFS was 24.1 months for the ICT-107 treatment group compared to a median PFS of 8.5 months for the controls (82). A phase III trial of ICT-107 plus TMZ restricted to HLA-$A2^+$ GBM patients was underway but has been suspended due to a lack of funding (31).

A third approach to DC vaccination involves pulsing DCs with autologous whole-tumor lysate. This class of DC vaccines has been the most extensively studied to date and offers the advantage of being personalized to each patient's unique tumor profile. It also allows for presentation of a comprehensive repertoire of heterogeneously expressed TAAs and neoantigens without a need for identifying them (70). However, such indiscriminate antigen presentation may be capable of driving extraneous or even harmful responses against non-tumor antigens, though a large number of clinical trials have demonstrated minimal toxicity of this approach (69).

DC-VaxL is a tumor-lysate pulsed DC vaccine and is the only phase III DC vaccine trial with published interim results at this time (83). At the interim analysis, the median OS for the intent-to-treat population was 23.1 months from surgery, with 46.6% of patients with methylated MGMT surviving three years (83). While this data appears exciting, the unblinded survival data and immunological results remain highly anticipated. However, a different tumor-lysate-pulsed DC vaccine (Audencel) evaluated in a randomized, controlled phase II study of patients with newly diagnosed GBM (GBM-Vax) showed no significant difference in OS between the treatment and control groups (84).

There are also a number of non-controlled phase II trials of tumor-lysate pulsed DCs with or without temozolomide that have been completed in patients with *de novo* GBM. These trials have shown immunoreactivity in 25-40% of patients (where reported) and patient OS ranging between 18.3 to 28 months (85–88), with MGMT methylated patients showing a median OS of 32.8 months in one study (88). In a phase II study of 23 patients with recurrent GBM and 11 patients with newly diagnosed GBM receiving tumor lysate-pulsed DCs, 50% of patients had positive vaccine responses as indicated by a 1.5 or more fold enhancement of IFN-gamma production compared to pre-vaccination levels. Vaccine responders had significantly longer median OS compared to non-responders (642 vs. 430 days) (89). A number of additional phase I and II clinical trials involving autologous tumor-lysate pulsed DCs in GBM are currently ongoing, including phase I trials investigating new adjuvant therapies such as topical imiquimod, cyclophosphamide + nivolumab/ipilimumab, and pembrolizumab + Poly-ICLC (NCT01808820) (NCT03879512) (NCT04201873) (31).

Another approach to DC vaccination gaining interest in recent years involves pulsing DCs with glioma stem cells (GSC) components. In a phase I clinical trial of 7 GBM patients receiving DCs pulsed with mRNA-derived from autologous GSC cultures, PFS was 1.9 years and increased lymphocyte proliferation in response to GSC lysate exposure *in vivo* was observed in all 3 patients with testable material (90). Additional trials involving GSC DC vaccines are ongoing (NCT01567202) (NCT02010606) (NCT02820584).

A recent meta-analysis of randomized controlled studies using GBM DC vaccines demonstrated that DC vaccination was associated with significantly improved overall survival in GBM patients (91). However, only six studies were included in this analysis due to strict inclusion criteria and the lack of randomized, controlled studies. This highlights the need for larger, thoughtfully-designed studies evaluating DC vaccine efficacy. Further research into the optimization of DC vaccines, including optimal adjuvant strategy, tumor antigens, pulsing scheme, and combinatorial treatments are needed.

Because the success of DC vaccines ultimately lies in the ability of DC-activated T cells to successfully exert cytotoxic effects, it is important that the GBM microenvironment does not suppress $CD8^+$ T cell activity. In this context, the combination of DC vaccines with checkpoint inhibitors such as nivolumab warrants more thorough investigation. Checkpoint inhibitors have the ability to combat T cell exhaustion, thus facilitating more effective T cell mediated anti-tumor lytic activity. The immunosuppressive microenvironment of gliomas may greatly hamper the impact of a DC vaccine in the absence of combinatorial therapies, and may be the reason that DC vaccines have had limited success in clinical trials thus far.

Heat Shock Proteins

Heat shock proteins (HSP) are critical in cell survival as the production of these proteins becomes upregulated whenever a cell is undergoing a stressful event. These stressful conditions can range from the cell being too hot or cold, undergoing UV radiation, having an osmolarity that is too high or low, or an abnormal acid-base status (92). HSPs were originally discovered by observing cells that were overheated, hence how the name "heat shock" originally came about. Once a cell undergoes stressful event, this can either result in the halting of protein production, or more commonly the misfolding of proteins. These misfolded proteins then begin to aggregate within the cell, which can eventually lead to cell death. The cell employs HSPs to prevent these deleterious events from happening by limiting the number of misfolded proteins within the cell in two different ways. If the misfolded protein can be refolded so that the protein gains functionality, the HSP will serve as a chaperone and bind to hydrophobic regions of the misfolded protein to help it fold properly (92). If the HSP cannot refold a misfolded protein due

to significant misfolding, the HSP will assist in degradation by shuttling the protein to the proteosome.

HSPs are of great interest to the oncology community because their production is upregulated in cancer patients as tumors have an increased expression of misfolded or abnormal protein products. To avoid cell death as a result of an aggregation of misfolded proteins, it is believed that tumors increase the production of HSPs (93). In patients with GBM specifically, it has been reported throughout the literature that these patients have an increased expression of HSP27, HSP72, HSP73, and HSP90 (93, 94). It has also been reported that HSP27, HSP60, HSP70, and HSP90 are present within exosomes released by GBM tumors (93, 95). However, using HSPs alone to prime the immune system in order to evoke an anti-tumor immune response would not be successful as a vaccine platform as HSPs alone are unable to evoke immune responses. Alternatively, when HSPs and peptides are brought together into complexes (HSPPCs), these can elicit class I MHC -based $CD8^+$ cytotoxic T lymphocyte responses (96). This is important because exogenous antigens are typically presented by class II MHC molecules leading to $CD4^+$ T helper cell responses, yet HSPPCs induce robust $CD8^+$ T cell responses (97). The key to having these HSPPC-derived peptides presented on class I MHC molecules is the CD91 receptor on antigen presenting cells, which allows for the uptake of HSPPCs into the cell (97). Once these complexes are inside the cell, they will ultimately be broken down *via* proteosomes, and then shuttled to the endoplasmic reticulum to be loaded onto class I MHC molecules (98). While the majority of the internalized protein follows the pathway mentioned prior, it is also important to note that some of the internalized HSPPC can be loaded into an acidic compartment which allows for loading onto class II MHC (93). This finding is pivotal as it shows that HSPPCs can stimulate both $CD8^+$ and $CD4^+$ T cells, a major benefit for using HSPPCs in anti-cancer vaccines.

HSPPCs can also interact with a variety of receptors that allow for activation of the NF-κB pathway (93). Additionally, it has been observed in macrophages that these HSPPCs can upregulate the secretion of pro-inflammatory cytokines such as TNF-alpha as well as IL-12 (99). Given that HSPPCs are capable of inducing pro-inflammatory responses in multiple different ways, it is clear why they are being used in vaccines. HSPPCs are capable of providing more than one antigen for presentation (100). Given the heterogeneity of tumors such as GBM, having a vaccine which accounts for more than one antigenic target is a far more improved approach.

The vast majority of HSP vaccines have used HSPPC-96 because of observed safety and minimal toxicity. The HSPPC-96 vaccine is created by isolating HSPs from patient tumor specimens. The HSPs are expected to be bound with proteins including tumor antigens made by tumor cells. Once enrichment is complete, the purified HSPs are given to patients on a weekly schedule for the first month and then on a bi-weekly schedule until the vaccine supply has been fully depleted (101). Overall, the vaccine has been well tolerated by patients with GBM in phase I trials. In a phase II trial that enrolled patients with recurrent GBM, 90.2% of patients receiving the HSPPC-96 vaccine were alive at 6 months following treatment, whereas 29.3% of patients receiving the HSPPC-96 vaccine were alive at 12 months following treatment. The median OS for patients receiving the HSPPC-96 vaccine was 42.6 weeks (93, 102). An exciting trial that is currently ongoing (NCT03018288) is treating newly diagnosed GBM with radiation therapy and temozolomide while combining pembrolizumab with or without HSPPC-96 (103). One of the goals of this trial is to determine if combining pembrolizumab with HSPPC-96 provides a synergistic effect. This is being compared to the immune response of patients receiving only radiation therapy, temozolomide, and pembrolizumab (103). Clinical trials have demonstrated that HSPPC vaccines promote a survival benefit in patients with GBM. While this may appear promising, far more clinical trials are needed to determine if pairing this vaccine platform with different adjuvants such as ICIs will promote long-term survival in patients with GBM.

ADJUVANTS

Unsuccessful vaccine trials in GBM are thought, in large part, the result of the intense immunosuppression caused by the disease (19). A combination of vaccines paired with adjuvants may be able to overcome these immunosuppresive mechanisms (19). Adjuvants are given in addition to the vaccine to enhance the immune response to a particular antigen (30). This is accomplished by either promoting the ideal presentation of the antigen, inducing the expression of co-stimulatory molecules, or prompting the release of cytokines by antigen presenting cells (104). The most successful and commonly used adjuvants in GBM vaccine trials include montanide, tetanus toxoid, poly-ICLC, imiquimod, CpG nucleotides, and GM-CSF. It is anticipated that the success seen with ICIs in other cancers will also translate over to GBM when used as a vaccine adjuvant.

Montanide is the clinical-grade of Incomplete Freund's Adjuvant (Complete Freund's Adjuvant without the *Mycobateria tuberculosis*) (104). As a water-in-oil emulsion, the adjuvant enhances the length of antigen presentation by retaining and slowly releasing the antigen at the site of vaccination (104). Two preparations of Montanide used as an adjuvant in human vaccine trials include Montanide ISA 51 and Montanide ISA 720 (105). Each uses a mannide monooleate surfactant, the difference being that Montanide ISA 51 uses a mineral oil and Montanide 720 a nonmineral vegetable oil (105).

In 2003 it was noted that the tetanus-diphtheria toxoid could improve the efficacy of DC vaccines in GBM patients (78). Mitchell et al. primed the vaccine site with a dose of the toxoid prior to vaccinating with CMV pp65-pulsed DCs (78). This significantly improved DC migration to lymph nodes and improved OS and PFS (78). Thus, two current clinical trials (NCT02366728) and (NCT03927222) are studying this pre-conditioning technique with the tetanus-diphtheria toxoid in the context of the CMV pp65 DC vaccine (106, 107).

Poly-ICLC, Imiquimod, and CpG oligonucleotides each activate the innate immune system by binding and activating toll-like receptors (TLRs): poly-ICLC to TLR3, Imiquimod to TLR7/8, and CpG to TLR9 (104). Poly-ICLC, also known as Hiltonol, is a stable double-stranded RNA derivative of poly I:C (polyinosine-polycytidylic acid) (104). Imiquimod is a synthetic imidazoquinoline that mostly activates TLR7, while resiquimod acts on TLR7 and TLR8 (104). TLRs 7 and 8 are each activated by single-stranded RNA and upregulate costimulatory molecules (CD80/86 and CD40), increase cytokine production (IFN-alpha, TNF-alpha, and IL-12), and enhance lymph node DC migration (104). An active phase II clinical trial (NCT01204684) is comparing the efficacy of imiquimod/resiquimod versus poly-ICLC in a tumor-lysate pulsed autologous DC vaccine (108). Lastly, TLR9 is activated by unmethylated CpG nucleotides, a pathogen-associated molecular pattern indicative of bacterial DNA (104, 109). These CpG nucleotides stimulate professional antigen presenting cells such as B cells and DCs leading to Th1-specific responses (109). These innate system agonists may prove pivotal in the challenge to surmount the multiple mechanisms of immunosuppression in GBM.

GM-CSF, or granulocyte-macrophage colony stimulating factor, is a cytokine growth factor that stimulates the activity and enhances the production of neutrophils, monocytes, and eosinophils (104, 110). Vaccine studies have shown that the adjuvant leads to DC maturation and recruitment, and macrophage, NK cell, and neutrophil activation (104). GM-CSF can not only be used as a recombinant protein, but also expressed by transfected tumor cells in a vaccine known as GVAX (111). To date, no clinical trial has used GVAX in GBM.

ICIs provide a promising approach for general activation of the immune system (19). CTLA-4 and PD-1 are both negative regulators of immune cell function (27). CTLA-4 acts early in the immune response in lymphoid tissues by preventing the binding of B7 on the antigen presenting cell to the T cell costimulatory molecule CD28 (27). PD-1 on T cells acts later in the peripheral tissue by initiating an inhibitory signal after binding to PD-L1 on tumor cells (27). ICIs are not limited to PD-1, CTLA-4, and PD-L1. Studies have shown promise with the antagonism of TIM3, LAG3, and VISTA (32, 112). Another possible inhibitory receptor to target is TIGIT (113). In addition, approaches to agonize molecules that activate T cells have also been used. The costimulatory molecule OX40 (CD134) is a part of the tumor necrosis factor superfamily and binds with the OX40 ligand (CD252) on antigen presenting cells (114). Expression is only present after antigen stimulation, thus OX40 co-stimulation is a late signal to enhance effector T cell survival (114). A preclinical study combined an OX40 agonist with an irradiated GL261 tumor cell GVAX vaccine (115). The result was increased survival by 14 days compared to controls, as well as Th1 responses and CD8 to T regulatory cell ratio (115). The authors also noted that combination therapy improved T cell exhaustion phenotypes with decreased expression of PD-1, TIM-3, and LAG-3 (115). An additional costimulatory molecule that has been studied in GBM vaccine trials is CD27. The monoclonal antibody varlilumab is an agonist of CD27, mimicking the physiological interaction with CD70 on antigen presenting cells which initiates T cell proliferation and activation (116). The ongoing DERIVe clinical trial (NCT03688178) is investigating a CMV pp65 DC vaccine together with varlilumab (117). The study will continue the previously discussed work of pre-conditioning by comparing groups treated with the tetanus-diphtheria toxoid and control prior to administering the vaccination (117).

A final immune checkpoint target that has shown efficacy in preclinical models of GBM treatment is the CD47-SIRP-alpha axis. CD47 is an antiphagocytic transmembrane protein that is upregulated on tumor cells to initiate immune escape (118). CD47 binding to the inhibitory signal regulatory protein-alpha (SIRP-alpha) on myeloid cells initiates a "don't eat me" signal and prevents macrophage phagocytosis (119). Hu5F9-G4 is a humanized anti-CD47 antibody that showed clinical efficacy in mouse xenograft models of patient-derived pediatric brain tumors (119). Inhibition of the CD47-SIRP-alpha axis in combination with autophagy inhibitors increased macrophage infiltration, tumor cell apoptosis, and median survival in mouse models of GBM (118). Despite promising preclinical results, blockade of this checkpoint target has yet to be tested in a clinical trial for GBM. Anti-CD47 treatment has shown to play an important role in enhancing macrophage phagocytosis of GBM and promoting an anti-tumor phenotype (120). Considering that tumor-associated macrophages are one of the major players of GBM mediated immunosuppression, clincal trials combining vaccination with an anti-CD47 adjuvant could prove to be quite efficacious.

ICIs have had broad success in many cancer types, thus it might be the most promising adjuvant to use in combination with vaccines. It is important to note that while the vast majority of research is focused around PD-1, PD-L1, and CTLA-4, the immune checkpoint repertoire is not restricted to this small subset. Trials into the future can continue to investigate proven strategies such as agonists for the innate immune system, or one of the novel immune checkpoints such as OX40 or CD27.

CLINICAL TRIALS

Unfortunately, no vaccine targeted to GBM has met primary endpoints in a phase III clinical trial. The failure of these clinical studies, modeled after marked success of the approaches used in pre-clinical settings supports a re-evaluation of the clinical trial designs used to test immunotherapy in brain tumors. In most clinical trials for GBM there is a lack of robust immune monitoring. Rather, many of these trials evaluate only for OS and PFS and if the trial does not meet its endpoint for one of these indicators, the intervention is often labeled a failure. The cause for why the intervention failed is often not known. For example, in the ACT IV Rindopepimut clinical trial, the patients receiving the vaccine did not experience a survival benefit and hence the study was deemed unsuccessful. Retrospectively, it was identified that the patients did experience an enhancement of anti-EGFRvIII antibody titers as a result of the vaccine, indicating that the intervention performed its desired biological function but this was not sufficient to impact survival (121).

This finding reinforces the concept that GBM is both a heterogeneous and immunosuppressive disease thereby decreasing the likelihood that one intervention can target a sufficient number of cancer cells to result in a long-term survival benefit. Future treatment protocols for patients with GBM will most likely involve patients receiving a cocktail therapy targeted to multiple aspects of the tumor. However, evaluation of immunotherapeutic strategies must go beyond just determining the efficacy of an intervention by measuring OS or PFS. Robust immune monitoring must be incorporated into the design of clinical trials enabling the identification of interventions that enhance anti-tumor immunity. Frequent and longitudinal evaluations will help determine optimal timing of interventions and the duration of the immune response.

Immune monitoring can be incorporated into clinical trials using clinical imaging, blood correlative studies, and tissue analysis. Imaging studies are often capable of showing whether patients are experiencing a response to the intervention. However, imaging in brain tumor studies can be complicated as it can be quite difficult to distinguish between tumor progression and response to therapy (pseudo-progression) (122). Therefore, incorporating other imaging studies such as positron emission tomography (PET) into brain tumor immunotherapy clinical trials may be complementary and help confirm patient response to treatment (123–125). Radiomics is an additional imaging technique that may be advantageous to incorporate into clinical studies when evaluating for patient response to immunotherapy. This technique can take sets of clinical images and use computer algorithms to analyze differences in tumor shape as well as spatial orientation and structure (126). The results of this analysis can then be used to inform clinical teams about prognosis as well as whether the disease is progressing. While this technique has been used in studies to predict OS for patients with GBM, coupling radiomics with machine learning is needed to provide an objective indicator to differentiate between tumor progression and patient response to treatment (126).

Measuring patient response using peripheral blood is promising. Most T cell activation takes place in the periphery, when naïve T cells interact with APCs that present tumor antigens. Subsequently these T cells migrate to the site of the tumor in the brain where they may be subject to additional stimulation or suppression from the tumor cells or other factors in the TME. Therefore, it is likely that GBM patients who demonstrate a response to immunotherapy, first display a systemic effect. Activation of peripheral T cells would suggest a response to the intervention. Previous studies have shown that looking at peripheral markers of immune response such as the clonal expansion of T cells, expression of specific chemokine receptors, and levels of IFN-gamma can potentially determine whether a patient is experiencing a response to immunotherapy (122). In patients with GBM, it has been observed that an enhanced expression of IFN-gamma has been associated with better patient outcomes, while the IL-6 axis specifically has been associated with both increased tumor growth and expression of an M2-like myeloid phenotype (32, 122, 127). If patients experience an immune response as shown by markers within the peripheral blood yet fail to meet the primary endpoints of a trial, additional treatments may be needed to enhance either the trafficking of peripheral immune cells to the brain tumor or suppress the hostile TME.

Patient response to immunotherapy can also be evaluated through analyzing different expression levels of intra-tumoral markers. Specifically, intra-tumoral TCR diversity and clonality can be used. Cloughesy and colleagues observed that baseline increases in the TCR repertoire in patients with GBM may be associated with a survival benefit (128). This finding is new to the field as most studies have focused on how increased clonal size of T cells may promote a survival benefit as opposed to an increase in the overall TCR repertoire. Whether an increase in the TCR repertoire promotes a survival benefit in patients with GBM is still up for debate, however studies by Li and colleagues (who treated patients with a HSPPC-96 vaccine) observed the opposite (129). In fact, they noted that long term survivors with GBM expressed a lower amount of TCR diversity and a higher amount of TCR clonal expansion (129). While the benefit that TCR repertoire expansion provides to patients is still debated, clinical trials such as this have demonstrated that increased TCR clonal expansion promotes a survival benefit in patients with GBM. Evaluating for increased intra-tumoral TCR clonal expansion in patients with GBM may be worthwhile to help research teams understand whether patients are experiencing robust intra-tumoral immune responses to the intervention they are receiving.

In addition to incorporating robust immune monitoring into clinical trials of the future, there is a clear need for limiting the administration of immunosuppressive corticosteroids to patients enrolled in brain tumor clinical trials. Dexamethasone (a type of corticosteroid) is commonly given to newly diagnosed brain tumor patients in order to alleviate cerebral edema. However, it has been well documented by our group that dexamethasone upregulates the presence of CTLA-4, as well as blocks CD28-mediated cell cycle entry and naïve T cell differentiation (130). This results in an overall decrease in naïve T cell proliferation and differentiation. However, in pre-clinical models of GBM, it has been seen that treatment with anti-CTLA-4 or stimulation of T cells with strong activators such as CD28, prior to dexamethasone exposure can rescue T cells from the detrimental effects of this corticosteroid (130). A study by Reardon and colleagues demonstrated that dexamethasone administration concurrent with anti-PD-1 therapy reduced the survival of tumor-bearing mice in a dose dependent manner (131). It was also observed in this study that dexamethasone enabled an overall decrease in the number of T-cells as a result of increased T cell apoptosis (131). Lymphocytes that did not undergo apoptosis displayed a significant decrease in their overall function (131). The authors also note that dexamethasone reduced the number of myeloid and natural killer cell populations as well. While the studies showing the negative impacts dexamethasone has for brain tumor immunotherapy patients are still limited at this time, it may be worth considering using alternatives to dexamethasone in brain tumor immunotherapy trials of the future as dexamethasone may impact outcomes for brain tumor patients receiving immunotherapy.

One possible alternative to dexamethasone that should be considered for clinical trials of the future is mannitol. Mannitol is a sugar alcohol that reduces cerebral edema by creating an

osmotic gradient within the brain that allows for movement of water from the parenchyma to the intravascular space which allows for a reduction in brain tissue volume as well as a lowering of intracranial pressure (132). While mannitol can decrease brain edema without causing immune suppression, it has been noted that increased doses of mannitol can lead to adverse events which is why more clinical trials are needed to determine the safety in using mannitol to manage edema in brain tumor patients (132). However, only a limited number of patients suffering from cerebral edema may benefit from receiving mannitol. It has been noted in the literature that using mannitol is problematic when treating patients with chronic cerebral edema (133). In addition to mannitol requiring IV infusion when treating chronic edema, mannitol diffuses into the brain over time which limits the effectiveness of this approach (133, 134). While mannitol may be effective in treating some patients with

TABLE 1 | Summary of all vaccine-based clinical trials discussed in this review.

Clinical Trial Number	Target antigen	Platform	Vehicle	Adjuvant	Reference
NCT02287428	Personalized neoantigen	Peptide		Poly-ICLC	(24)
NCT02149225	Personalized neoantigen	Peptide		Poly-ICLCGM-CSF	(23)
NCT02287428	Personalized neoantigen	Peptide		Pembrolizumab	(25)
NCT03422094	Personalized neoantigen	Peptide		Poly-ICLC Nivolumab Ipilimumab	(26)
NCT01480479	EGFRvIII	Peptide		Keyhole limpet hemocyanin GM-CSF	
NCT01498328	EGFRvIII	Peptide		Bevacizumab	(33)
NCT03299309	pp65 CMV	Peptide		Tetanus-diphtheria toxoid Montanide ISA 51	(35)
NCT04280848	TERT	Peptide		Montanide ISA 51	(38)
NCT02454634	IDH1 R132H	Peptide		Montanide Imiquimod	(41, 43)
NCT02193347	IDH1 R132H	Peptide		Tetanus-diphtheria toxoid	(42)
NCT02455557	Survivin	Peptide		Keyhole limpet hemocyanin Montanide ISA 51 GM-CSF	(45)
	WT1	Peptide		Montanide ISA 51	(48)
NCT02498665	WT1 DSP-7888	Peptide			(50)
NCT02750891	WT1 DSP-7888	Peptide			(51)
NCT03149003	WT1 DSP-7888	Peptide		Bevacizumab	(52)
NCT01130077	Survivin IL-13 receptor alpha 2 EphA2	Peptide		Poly-ICLC	(54)
NCT01222221	IMA950	Peptide		GM-CSF	(55)
NCT01920191	IMA950	Peptide		Poly-ICLC	(56)
NCT03665545	IMA950	Peptide		Poly-ICLC Pembrolizumab	(57)
NCT03491683	WT1 PSMA TERT	DNA		IL-12 Cemiplimab	(62–64)
NCT04015700	Personalized neoantigen	DNA		IL-12	(65)
NCT04573140	Tumor mRNA pp65 CMV	RNA			(68)
	EGFRvIII	Peptide	DCs	Keyhole limpet hemocyanin	(72)
	WT1 Tumor lysate	Peptide	DCs	OK-432	(73)
NCT02649582	WT1	RNA	DCs		(74)
NCT02049489	CD133	Peptide	DCs		(75)
	IL-13 receptor alpha 2	Peptide	DCs		(76)
NCT00639639	pp65 CMV	RNA	DCs	GM-CSF	(77)
NCT00639639	pp65 CMV	RNA	DCs	Tetanus-diphtheria toxoid CCL3	(78)
NCT02465268	pp65 CMV	RNA	DCs	GM-CSF Tetanus-diphtheria toxoid	(80)
NCT02529072	pp65 CMV	RNA	DCs	Nivolumab	(81)
NCT01280552	ICT-107	Peptide	DCs		(82)
NCT02546102	ICT-107	Peptide	DCs		(31)
NCT00045968	Tumor lysate	Peptide	DCs		(83)
2009-015979-27 (EudraCT)	Tumor lysate	Peptide	DCs		(84)
2006-002881-20 (EudraCT)	Tumor lysate	Peptide	DCs		(85)
NCT00323115	Tumor lysate	Peptide	DCs		(86)
NCT01006044	Tumor lysate	Peptide	DCs		(87)
2008-005035-15 (EudraCT)	Tumor lysate	Peptide	DCs		(88)
	Tumor lysate	Peptide	DCs		(89)
NCT01808820	Tumor lysate	Peptide	DCs	Imiquimod	(31)
NCT03879512	Tumor lysate	Peptide	DCs	Cyclophosphamide Nivolumab Ipilimumab	(31)
NCT04201873	Tumor lysate	Peptide	DCs	Pembrolizumab Poly-ICLC	(31)
NCT00846456	Glioma stem cells	RNA	DCs		(90)
NCT01567202	Glioma stem cells	Peptide	DCs		
NCT02010606	Glioma stem cells	Peptide	DCs		
NCT02820584	Glioma stem cells	Peptide	DCs		
NCT00293423	Tumor lysate	Peptide	HSPs		(102)
NCT03018288	Tumor lysate	Peptide	HSPs	Pembrolizumab	(103)
NCT02366728	pp65 CMV	RNA	DCs	Tetanus-diphtheria toxoid Basiliximab	(106)
NCT03927222	pp65 CMV	RNA	DCs	GM-CSF Tetanus-diphtheria toxoid	(107)
NCT01204684	Tumor lysate	Peptide	DCs	Imiquimod/Resiquimod Poly-ICLC	(108)
NCT03688178	pp65 CMV	RNA	DCs	Varlilumab Tetanus-diphtheria	(117)

cerebral edema, its time-limited efficacy restricts use for short term or acute situations.

Bevacizumab has been proposed as an alternative to dexamethasone for combatting cerebral edema as it specifically targets vascular endothelial growth factor A (VEGF-A) which promotes both angiogenesis and vascular permeability (135). This finding suggests that VEGF-A plays a critical role in the increased brain edema that has been observed in patients with brain tumors (135). Bevacizumab sequesters VEGF-A thereby preventing binding to its receptors which allows for a reduction in cerebral edema as observed by Xiangying and colleagues (135) but does not extend survival in patients with GBM (136). However, with a prolonged plasma half-life and sustained inhibition of wound healing, the use of bevacizumab, while effective in reducing cerebral edema in patients with brain tumors, raises concerns in this patient population. Specifically, Bota and colleagues found that the optimum time for patients to stop receiving bevacizumab prior to tumor resection was four weeks (137). Additionally, the research team found that patients should not undergo treatment with bevacizumab for at least two weeks following surgery (137). The cessation of bevacizumab prior to surgery and wait time prior to re-initiating this treatment following surgery is necessary for patients to avoid surgical complications, thereby limiting widespread use of this agent as a substitute for corticosteroids.

Control of tumor-related cerebral edema remains a challenge. In the context of clinical trials, alternatives to corticosteroid use such as short-term mannitol and bevacizumab can be prospectively evaluated so that guidelines can be established to enable testing of immune therapies in this patient population where response is not further compromised by iatrogenic factors.

DISCUSSION

In this review, some of the most promising vaccines that are currently under investigation for the treatment of GBM were discussed including the rationale for their use and the clinical trial results thus far (see **Table 1**). Additionaly strategies such as the use of adjuvants and the importance of immune monitoring thereby enhancing the information obtained from clinical trials were also discussed. Hopefully, this review serves as a guide or provides an outline for investigators and clinicians as they seek to design and implement different vaccine-based approaches to treat patients suffering from GBM. While many vaccines targeted to GBM can stimulate the immune system, the benefit of this stimulation is often transient, failing to be sufficient enough to increase OS and/or PFS. The heavily immunosuppressive nature of GBM contributes to the failure for most immunotherapeutic strategies as does the heterogenous nature of GBM. Targeting multiple antigens, perhaps some commonly occurring in most GBMs such as EGFRvIII, IL-13 receptor alpha 2, or WT1 in combination with vaccines targeting antigens more specific to individual patients may increase the efficacy of this treatment modality. In addition, combining multiple therapeutic strategies such as a combination of vaccination and treatment with ICIs may also overcome the challenge of tumor-immune escape. Given the challenges inherent in treating GBM, a multifaceted approach will likely be necessary to ultimately generate effective immune therapies for this disease.

AUTHOR CONTRIBUTIONS

All authors wrote and edited the article and approved the submitted version.

FUNDING

This research was partly supported by the Intramural Research Program of the NIH, National Cancer Institute, and the Center for Cancer Research. EB is supported by a Marshall Scholarship from the Marshall Aid Commemoration Commission and the NIH-Oxford-Cambridge-Scholars Program.

ACKNOWLEDGMENTS

This research was supported by the Intramural Research Program of the NIH, National Cancer Institute, the Center for Cancer Research, and the NIH Medical Research Scholars Program (a public-private partnership supported jointly by the NIH and contributions to the Foundation for the NIH from the Doris Duke Charitable Foundation, Genentech, the American Association for Dental Research, and the Colgate-Palmolive Company). We would like to thank Kristin Odom for her assistance in processing the figure for this manuscript.

REFERENCES

1. Medikonda R, Dunn G, Rahman M, Fecci P, Lim M. A Review of Glioblastoma Immunotherapy. *J Neurooncol* (2020) 151:41–53. doi: 10.1007/s11060-020-03448-1
2. Molinaro AM, Taylor JW, Wiencke JK, Wrensch MR. Genetic and Molecular Epidemiology of Adult Diffuse Glioma. *Nat Rev Neurol* (2019) 15:405–17. doi: 10.1038/s41582-019-0220-2
3. Ottaviano M, De Placido S, Ascierto PA. Recent Success and Limitations of Immune Checkpoint Inhibitors for Cancer: A Lesson From Melanoma. *Virchows Arch* (2019) 474:421–32. doi: 10.1007/s00428-019-02538-4
4. Aldape K, Brindle KM, Chesler L, Chopra R, Gajjar A, Gilbert MR, et al. Challenges to Curing Primary Brain Tumours. *Nat Rev Clin Oncol* (2019) 16:509–20. doi: 10.1038/s41571-019-0177-5
5. Louveau A, Smirnov I, Keyes TJ, Eccles JD, Rouhani SJ, Peske JD, et al. Structural and Functional Features of Central Nervous System Lymphatic Vessels. *Nature* (2015) 523:337–41. doi: 10.1038/nature14432
6. Ratnam NM, Gilbert MR, Giles AJ. Immunotherapy in CNS Cancers: The Role of Immune Cell Trafficking. *Neuro Oncol* (2019) 21:37–46. doi: 10.1093/neuonc/noy084
7. Reardon DA, Gokhale PC, Klein SR, Ligon KL, Rodig SJ, Ramkissoon SH, et al. Glioblastoma Eradication Following Immune Checkpoint Blockade in

an Orthotopic, Immunocompetent Model. *Cancer Immunol Res* (2016) 4:124–35. doi: 10.1158/2326-6066.CIR-15-0151
8. Reardon DA, Brandes AA, Omuro A, Mulholland P, Lim M, Wick A, et al. Effect of Nivolumab vs Bevacizumab in Patients With Recurrent Glioblastoma: The CheckMate 143 Phase 3 Randomized Clinical Trial. *JAMA Oncol* (2020) 6:1003–10. doi: 10.1001/jamaoncol.2020.1024
9. McGranahan T, Therkelsen KE, Ahmad S, Nagpal S. Current State of Immunotherapy for Treatment of Glioblastoma. *Curr Treat Options Oncol* (2019) 20:24. doi: 10.1007/s11864-019-0619-4
10. Filley AC, Henriquez M, Dey M. Recurrent Glioma Clinical Trial, CheckMate-143: The Game is Not Over Yet. *Oncotarget* (2017) 8:91779–94. doi: 10.18632/oncotarget.21586
11. Rahman M, Sawyer WG, Lindhorst S, Deleyrolle LP, Harrison JK, Karachi A, et al. Adult Immuno-Oncology: Using Past Failures to Inform the Future. *Neuro Oncol* (2020) 22:1249–61. doi: 10.1093/neuonc/noaa116
12. Chongsathidkiet P, Jackson C, Koyama S, Loebel F, Cui X, Farber SH, et al. Sequestration of T Cells in Bone Marrow in the Setting of Glioblastoma and Other Intracranial Tumors. *Nat Med* (2018) 24:1459–68. doi: 10.1038/s41591-018-0135-2
13. Hu X, Deng Q, Ma L, Li Q, Chen Y, Liao Y, et al. Meningeal Lymphatic Vessels Regulate Brain Tumor Drainage and Immunity. *Cell Res* (2020) 30:229–43. doi: 10.1038/s41422-020-0287-8
14. Razavi SM, Lee KE, Jin BE, Aujla PS, Gholamin S, Li G. Immune Evasion Strategies of Glioblastoma. *Front Surg* (2016) 3:11. doi: 10.3389/fsurg.2016.00011
15. Louveau A, Herz J, Alme MN, Salvador AF, Dong MQ, Viar KE, et al. CNS Lymphatic Drainage and Neuroinflammation are Regulated by Meningeal Lymphatic Vasculature. *Nat Neurosci* (2018) 21:1380–91. doi: 10.1038/s41593-018-0227-9
16. Song E, Mao T, Dong H, Boisserand LSB, Antila S, Bosenberg M, et al. Vegf-C-driven Lymphatic Drainage Enables Immunosurveillance of Brain Tumours. *Nature* (2020) 577:689–94. doi: 10.1038/s41586-019-1912-x
17. Frey B, Rubner Y, Wunderlich R, Weiss EM, Pockley AG, Fietkau R, et al. Induction of Abscopal Anti-Tumor Immunity and Immunogenic Tumor Cell Death by Ionizing Irradiation - Implications for Cancer Therapies. *Curr Med Chem* (2012) 19:1751–64. doi: 10.2174/092986712800099811
18. Mole RH. Whole Body Irradiation; Radiobiology or Medicine? *Br J Radiol* (1953) 26:234–41. doi: 10.1259/0007-1285-26-305-234
19. Weller M, Roth P, Preusser M, Wick W, Reardon DA, Platten M, et al. Vaccine-Based Immunotherapeutic Approaches to Gliomas and Beyond. *Nat Rev Neurol* (2017) 13:363–74. doi: 10.1038/nrneurol.2017.64
20. Dunn GP, Cloughesy TF, Maus MV, Prins RM, Reardon DA, Sonabend AM. Emerging Immunotherapies for Malignant Glioma: From Immunogenomics to Cell Therapy. *Neuro Oncol* (2020) 22:1425–38. doi: 10.1093/neuonc/noaa154
21. Richters MM, Xia H, Campbell KM, Gillanders WE, Griffith OL, Griffith M. Best Practices for Bioinformatic Characterization of Neoantigens for Clinical Utility. *Genome Med* (2019) 11:56. doi: 10.1186/s13073-019-0666-2
22. Wells DK, van Buuren MM, Dang KK, Hubbard-Lucey VM, Sheehan KCF, Campbell KM, et al. Key Parameters of Tumor Epitope Immunogenicity Revealed Through a Consortium Approach Improve Neoantigen Prediction. *Cell* (2020) 183:818–834.e13. doi: 10.1016/j.cell.2020.09.015
23. Hilf N, Kuttruff-Coqui S, Frenzel K, Bukur V, Stevanović S, Gouttefangeas C, et al. Actively Personalized Vaccination Trial for Newly Diagnosed Glioblastoma. *Nature* (2019) 565:240–5. doi: 10.1038/s41586-018-0810-y
24. Keskin DB, Anandappa AJ, Sun J, Tirosh I, Mathewson ND, Li S, et al. Neoantigen Vaccine Generates Intratumoral T Cell Responses in Phase Ib Glioblastoma Trial. *Nature* (2019) 565:234–9. doi: 10.1038/s41586-018-0792-9
25. *Personalized NeoAntigen Cancer Vaccine W RT Plus Pembrolizumab for Patients With MGMT Unmethylated, Newly Diagnosed Gbm*. Available at: https://ClinicalTrials.gov/show/NCT02287428.
26. *Neoantigen-Based Personalized Vaccine Combined With Immune Checkpoint Blockade Therapy in Patients With Newly Diagnosed, Unmethylated Glioblastoma*. Available at: https://ClinicalTrials.gov/show/NCT03422094.
27. Buchbinder EI, Desai A. CTLA-4 and PD-1 Pathways: Similarities, Differences, and Implications of Their Inhibition. *Am J Clin Oncol* (2016) 39:98–106. doi: 10.1097/COC.0000000000000239
28. Zwaveling S, Ferreira Mota SC, Nouta J, Johnson M, Lipford GB, Offringa R, et al. Established Human Papillomavirus Type 16-Expressing Tumors are Effectively Eradicated Following Vaccination With Long Peptides. *J Immunol* (2002) 169:350–8. doi: 10.4049/jimmunol.169.1.350
29. Kenter GG, Welters MJ, Valentijn AR, Lowik MJ, Berends-van der Meer DM, Vloon AP, et al. Vaccination Against HPV-16 Oncoproteins for Vulvar Intraepithelial Neoplasia. *N Engl J Med* (2009) 361:1838–47. doi: 10.1056/NEJMoa0810097
30. Kong Z, Wang Y, Ma W. Vaccination in the Immunotherapy of Glioblastoma. *Hum Vaccin Immunother* (2018) 14:255–68. doi: 10.1080/21645515.2017.1388481
31. Lim M, Xia Y, Bettegowda C, Weller M. Current State of Immunotherapy for Glioblastoma. *Nat Rev Clin Oncol* (2018) 15:422–42. doi: 10.1038/s41571-018-0003-5
32. Sampson JH, Gunn MD, Fecci PE, Ashley DM. Brain Immunology and Immunotherapy in Brain Tumours. *Nat Rev Cancer* (2020) 20:12–25. doi: 10.1038/s41568-019-0224-7
33. Reardon DA, Desjardins A, Vredenburgh JJ, O'Rourke DM, Tran DD, Fink KL, et al. Rindopepimut With Bevacizumab for Patients With Relapsed Egfrviii-Expressing Glioblastoma (React): Results of a Double-Blind Randomized Phase Ii Trial. *Clin Cancer Res* (2020) 26:1586–94. doi: 10.1158/1078-0432.CCR-18-1140
34. Cuoco JA, Benko MJ, Busch CM, Rogers CM, Prickett JT, Marvin EA. Vaccine-Based Immunotherapeutics for the Treatment of Glioblastoma: Advances, Challenges, and Future Perspectives. *World Neurosurg* (2018) 120:302–15. doi: 10.1016/j.wneu.2018.08.202
35. *Pep-CMV in Recurrent Medulloblastoma/Malignant Glioma*. Available at: https://ClinicalTrials.gov/show/NCT03299309.
36. Louis DN, Perry A, Reifenberger G, von Deimling A, Figarella-Branger D, Cavenee WK, et al. The 2016 World Health Organization Classification of Tumors of the Central Nervous System: A Summary. *Acta Neuropathol* (2016) 131:803–20. doi: 10.1007/s00401-016-1545-1
37. Louis DN, Wesseling P, Aldape K, Brat DJ, Capper D, Cree IA, et al. cIMPACT-NOW Update 6: New Entity and Diagnostic Principle Recommendations of the cIMPACT-Utrecht Meeting on Future CNS Tumor Classification and Grading. *Brain Pathol* (2020) 30:844–56. doi: 10.1111/bpa.12832
38. *Anticancer Therapeutic Vaccination Using Telomerase-Derived Universal Cancer Peptides in Glioblastoma*. Available at: https://ClinicalTrials.gov/show/NCT04280848.
39. Dosset M, Godet Y, Vauchy C, Beziaud L, Lone YC, Sedlik C, et al. Universal Cancer Peptide-Based Therapeutic Vaccine Breaks Tolerance Against Telomerase and Eradicates Established Tumor. *Clin Cancer Res* (2012) 18:6284–95. doi: 10.1158/1078-0432.CCR-12-0896
40. Schumacher T, Bunse L, Pusch S, Sahm F, Wiestler B, Quandt J, et al. A Vaccine Targeting Mutant IDH1 Induces Antitumour Immunity. *Nature* (2014) 512:324–7. doi: 10.1038/nature13387
41. *Phase I Trial of IDH1 Peptide Vaccine in IDH1R132H-mutated Grade III-IV Gliomas*. Available at: https://ClinicalTrials.gov/show/NCT02454634.
42. *Idh1 Peptide Vaccine for Recurrent Grade II Glioma*. Available at: https://ClinicalTrials.gov/show/NCT02193347.
43. Platten M, Schilling D, Bunse L, Wick A, Bunse T, Riehl D, et al. A Mutation-Specific Peptide Vaccine Targeting IDH1R132H in Patients With Newly Diagnosed Malignant Astrocytomas: A First-in-Man Multicenter Phase I Clinical Trial of the German Neurooncology Working Group (Noa-16). *J Clin Oncol* (2018) 36:2001–1. doi: 10.1200/JCO.2018.36.15_suppl.2001
44. Fenstermaker RA, Ciesielski MJ, Qiu J, Yang N, Frank CL, Lee KP, et al. Clinical Study of a Survivin Long Peptide Vaccine (SurVaxM) in Patients With Recurrent Malignant Glioma. *Cancer Immunol Immunother* (2016) 65:1339–52. doi: 10.1007/s00262-016-1890-x
45. *Survaxm Vaccine Therapy and Temozolomide in Treating Patients With Newly Diagnosed Glioblastoma*. Available at: https://ClinicalTrials.gov/show/NCT02455557.
46. Ahluwalia M, Reardon D, Abad A, Curry W, Wong E, Peereboom D, et al. ATIM-41. PHASE II TRIAL OF A SURVIVIN VACCINE (Survaxm) For Newly Diagnosed Glioblastoma. *Neuro-Oncology* (2018) 20:vi10–1. doi: 10.1093/neuonc/noy148.036
47. Oji Y, Hashimoto N, Tsuboi A, Murakami Y, Iwai M, Kagawa N, et al. Association of WT1 Igg Antibody Against WT1 Peptide With Prolonged

Survival in Glioblastoma Multiforme Patients Vaccinated With WT1 Peptide. *Int J Cancer* (2016) 139:1391–401. doi: 10.1002/ijc.30182
48. Izumoto S, Tsuboi A, Oka Y, Suzuki T, Hashiba T, Kagawa N, et al. Phase II Clinical Trial of Wilms Tumor 1 Peptide Vaccination for Patients With Recurrent Glioblastoma Multiforme. *J Neurosurg* (2008) 108:963–71. doi: 10.3171/JNS/2008/108/5/0963
49. Winograd EK, Ciesielski MJ, Fenstermaker RA. Novel Vaccines for Glioblastoma: Clinical Update and Perspective. *Immunotherapy* (2016) 8:1293–308. doi: 10.2217/imt-2016-0059
50. *A Study of DSP-7888 Dosing Emulsion in Adult Patients With Advanced Malignancies*. Available at: https://ClinicalTrials.gov/show/NCT02498665.
51. *A Study of DSP-7888 in Pediatric Patients With Relapsed or Refractory High Grade Gliomas*. Available at: https://ClinicalTrials.gov/show/NCT02750891.
52. *A Study of DSP-7888 Dosing Emulsion in Combination With Bevacizumab in Patients With Recurrent or Progressive Glioblastoma Following Initial Therapy*. Available at: https://ClinicalTrials.gov/show/NCT03149003.
53. *A Study of DSP-7888 Dosing Emulsion in Combination With Immune Checkpoint Inhibitors in Adult Patients With Advanced Solid Tumors*. Available at: https://ClinicalTrials.gov/show/NCT03311334.
54. Pollack IF, Jakacki RI, Butterfield LH, Hamilton RL, Panigrahy A, Potter DM, et al. Antigen-Specific Immune Responses and Clinical Outcome After Vaccination With Glioma-Associated Antigen Peptides and Polyinosinic-Polycytidylic Acid Stabilized by Lysine and Carboxymethylcellulose in Children With Newly Diagnosed Malignant Brainstem and Nonbrainstem Gliomas. *J Clin Oncol* (2014) 32:2050–8. doi: 10.1200/JCO.2013.54.0526
55. Rampling R, Peoples S, Mulholland PJ, James A, Al-Salihi O, Twelves CJ, et al. A Cancer Research UK First Time in Human Phase I Trial of IMA950 (Novel Multipeptide Therapeutic Vaccine) in Patients With Newly Diagnosed Glioblastoma. *Clin Cancer Res* (2016) 22:4776–85. doi: 10.1158/1078-0432.CCR-16-0506
56. Migliorini D, Dutoit V, Allard M, Grandjean Hallez N, Marinari E, Widmer V, et al. Phase I/II Trial Testing Safety and Immunogenicity of the Multipeptide IMA950/poly-ICLC Vaccine in Newly Diagnosed Adult Malignant Astrocytoma Patients. *Neuro Oncol* (2019) 21:923–33. doi: 10.1093/neuonc/noz040
57. *Pembrolizumab in Association With the IMA950/Poly-ICLC for Relapsing Glioblastoma*. Available at: https://ClinicalTrials.gov/show/NCT03665545.
58. Lopes A, Vandermeulen G, Préat V. Cancer DNA Vaccines: Current Preclinical and Clinical Developments and Future Perspectives. *J Exp Clin Cancer Res* (2019) 38:146. doi: 10.1186/s13046-019-1154-7
59. Herrada AA, Rojas-Colonelli N, González-Figueroa P, Roco J, Oyarce C, Ligtenberg MA, et al. Harnessing DNA-induced Immune Responses for Improving Cancer Vaccines. *Hum Vaccin Immunother* (2012) 8:1682–93. doi: 10.4161/hv.22345
60. Felber BK, Valentin A, Rosati M, Bergamaschi C, Pavlakis GN. Hiv DNA Vaccine: Stepwise Improvements Make a Difference. *Vaccines (Basel)* (2014) 2:354–79. doi: 10.3390/vaccines2020354
61. Flingai S, Czerwonko M, Goodman J, Kudchodkar SB, Muthumani K, Weiner DB. Synthetic DNA Vaccines: Improved Vaccine Potency by Electroporation and Co-Delivered Genetic Adjuvants. *Front Immunol* (2013) 4:354. doi: 10.3389/fimmu.2013.00354
62. *INO-5401 and INO-9012 Delivered by Electroporation (EP) in Combination With Cemiplimab (REGN2810) in Newly-Diagnosed Glioblastoma (GBM)*. Available at: https://ClinicalTrials.gov/show/NCT03491683.
63. Reardon D, Nagpal S, Soltys S, Brem S, Omuro A, Fuente MDL, et al. Abstract CT114: Ino-5401 and INO-9012 Delivered by Electroporation (EP) in Combination With Cemiplimab (REGN2810) in Newly-Diagnosed Glioblastoma (GBM) (NCT03491683). *Cancer Res* (2019) 79:CT114–4. doi: 10.1158/1538-7445.AM2019-CT114
64. Reardon DA, Brem S, Desai AS, Bagley SJ, Kurz SC, Fuente MIDL, et al. Ino-5401 and INO-9012 Delivered Intramuscularly (IM) With Electroporation (EP) in Combination With Cemiplimab (REGN2810) in Newly Diagnosed Glioblastoma (GBM): Interim Results. *J Clin Oncol* (2020) 38:2514–4. doi: 10.1200/JCO.2020.38.15_suppl.2514
65. *Neoantigen-based Personalized DNA Vaccine in Patients With Newly Diagnosed, Unmethylated Glioblastoma*. Available at: https://ClinicalTrials.gov/show/NCT04015700.
66. Pardi N, Hogan MJ, Porter FW, Weissman D. mRNA Vaccines - a New Era in Vaccinology. *Nat Rev Drug Discovery* (2018) 17:261–79. doi: 10.1038/nrd.2017.243
67. Pardi N, Hogan MJ, Weissman D. Recent Advances in mRNA Vaccine Technology. *Curr Opin Immunol* (2020) 65:14–20. doi: 10.1016/j.coi.2020.01.008
68. *A Study of RNA-lipid Particle (RNA-LP) Vaccines for Newly Diagnosed Pediatric High-Grade Gliomas (pHGG) and Adult Glioblastoma (GBM)*. Available at: https://ClinicalTrials.gov/show/NCT04573140.
69. Reardon DA, Mitchell DA. The Development of Dendritic Cell Vaccine-Based Immunotherapies for Glioblastoma. *Semin Immunopathol* (2017) 39:225–39. doi: 10.1007/s00281-016-0616-7
70. Srivastava S, Jackson C, Kim T, Choi J, Lim M. A Characterization of Dendritic Cells and Their Role in Immunotherapy in Glioblastoma: From Preclinical Studies to Clinical Trials. *Cancers (Basel)* (2019) 11:537–69. doi: 10.3390/cancers11040537
71. Garg AD, Coulie PG, Van den Eynde BJ, Agostinis P. Integrating Next-Generation Dendritic Cell Vaccines Into the Current Cancer Immunotherapy Landscape. *Trends Immunol* (2017) 38:577–93. doi: 10.1016/j.it.2017.05.006
72. Sampson JH, Archer GE, Mitchell DA, Heimberger AB, Herndon 2JE, Lally-Goss D, et al. An epidermal growth factor receptor variant III-targeted vaccine is safe and immunogenic in patients with glioblastoma multiforme. *Mol Cancer Ther* (2009) 8:2773–9. doi: 10.1158/1535-7163.MCT-09-0124
73. Sakai K, Shimodaira S, Maejima S, Udagawa N, Sano K, Higuchi Y, et al. Dendritic Cell-Based Immunotherapy Targeting Wilms' Tumor 1 in Patients With Recurrent Malignant Glioma. *J Neurosurg* (2015) 123:989–97. doi: 10.3171/2015.1.JNS141554
74. *Adjuvant Dendritic Cell-immunotherapy Plus Temozolomide in Glioblastoma Patients*. Available at: https://ClinicalTrials.gov/show/NCT02649582.
75. Rudnick JD, Fink KL, Landolfi JC, Markert J, Piccioni DE, Glantz MJ, et al. Immunological Targeting of CD133 in Recurrent Glioblastoma: A Multi-Center Phase I Translational and Clinical Study of Autologous CD133 Dendritic Cell Immunotherapy. *J Clin Oncol* (2017) 35:2059–9. doi: 10.1200/JCO.2017.35.15_suppl.2059
76. Iwami K, Shimato S, Ohno M, Okada H, Nakahara N, Sato Y, et al. Peptide-Pulsed Dendritic Cell Vaccination Targeting interleukin-13 Receptor α2 Chain in Recurrent Malignant Glioma Patients With HLA-A*24/A*02 Allele. *Cytotherapy* (2012) 14:733–42. doi: 10.3109/14653249.2012.666633
77. Batich KA, Reap EA, Archer GE, Sanchez-Perez L, Nair SK, Schmittling RJ, et al. Long-term Survival in Glioblastoma with Cytomegalovirus pp65-Targeted Vaccination. *Clin Cancer Res* (2017) 23:1898–909. doi: 10.1158/1078-0432.CCR-16-2057
78. Mitchell DA, Batich KA, Gunn MD, Huang MN, Sanchez-Perez L, Nair SK, et al. Tetanus toxoid and CCL3 improve dendritic cell vaccines in mice and glioblastoma patients. *Nature* (2015) 519:366–9. doi: 10.1038/nature14320
79. Batich KA, Mitchell DA, Healy P, Herndon 2JE, Sampson JH. Once, Twice, Three Times a Finding: Reproducibility of Dendritic Cell Vaccine Trials Targeting Cytomegalovirus in Glioblastoma. *Clin Cancer Res* (2020) 26:5297–303. doi: 10.1158/1078-0432.CCR-20-1082
80. *Vaccine Therapy for the Treatment of Newly Diagnosed Glioblastoma Multiforme*. Available at: https://ClinicalTrials.gov/show/NCT02465268.
81. *Nivolumab With DC Vaccines for Recurrent Brain Tumors*. Available at: https://ClinicalTrials.gov/show/NCT02529072.
82. Wen PY, Reardon DA, Armstrong TS, Phuphanich S, Aiken RD, Landolfi JC, et al. A Randomized Double-Blind Placebo-Controlled Phase II Trial of Dendritic Cell Vaccine Ict-107 in Newly Diagnosed Patients With Glioblastoma. *Clin Cancer Res* (2019) 25:5799–807. doi: 10.1158/1078-0432.CCR-19-0261
83. Liau LM, Ashkan K, Tran DD, Campian JL, Trusheim JE, Cobbs CS, et al. First Results on Survival From a Large Phase 3 Clinical Trial of an Autologous Dendritic Cell Vaccine in Newly Diagnosed Glioblastoma. *J Transl Med* (2018) 16:142. doi: 10.1186/s12967-018-1507-6
84. Buchroithner J, Erhart F, Pichler J, Widhalm G, Preusser M, Stockhammer G, et al. Audencel Immunotherapy Based on Dendritic Cells Has No Effect on Overall and Progression-Free Survival in Newly Diagnosed Glioblastoma: A Phase II Randomized Trial. *Cancers (Basel)* (2018) 10:372–86. doi: 10.3390/cancers10100372

85. Ardon H, Van Gool SW, Verschuere T, Maes W, Fieuws S, Sciot R, et al. Integration of Autologous Dendritic Cell-Based Immunotherapy in the Standard of Care Treatment for Patients With Newly Diagnosed Glioblastoma: Results of the HGG-2006 Phase I/II Trial. *Cancer Immunol Immunother* (2012) 61:2033–44. doi: 10.1007/s00262-012-1261-1
86. Fadul CE, Fisher JL, Hampton TH, Lallana EC, Li Z, Gui J, et al. Immune Response in Patients With Newly Diagnosed Glioblastoma Multiforme Treated With Intranodal Autologous Tumor Lysate-Dendritic Cell Vaccination After Radiation Chemotherapy. *J Immunother* (2011) 34:382–9. doi: 10.1097/CJI.0b013e318215e300
87. Inogés S, Tejada S, de Cerio AL, Gállego Pérez-Larraya J, Espinós J, Idoate MA, et al. A Phase II Trial of Autologous Dendritic Cell Vaccination and Radiochemotherapy Following Fluorescence-Guided Surgery in Newly Diagnosed Glioblastoma Patients. *J Transl Med* (2017) 15:104. doi: 10.1186/s12967-017-1202-z
88. Pellegatta S, Eoli M, Cuccarini V, Anghileri E, Pollo B, Pessina S, et al. Survival Gain in Glioblastoma Patients Treated With Dendritic Cell Immunotherapy is Associated With Increased NK But Not CD8(+) T Cell Activation in the Presence of Adjuvant Temozolomide. *Oncoimmunology* (2018) 7:e1412901. doi: 10.1080/2162402X.2017.1412901
89. Wheeler CJ, Black KL, Liu G, Mazer M, Zhang XX, Pepkowitz S, et al. Vaccination Elicits Correlated Immune and Clinical Responses in Glioblastoma Multiforme Patients. *Cancer Res* (2008) 68:5955–64. doi: 10.1158/0008-5472.CAN-07-5973
90. Vik-Mo EO, Nyakas M, Mikkelsen BV, Moe MC, Due-Tønnesen P, Suso EM, et al. Therapeutic Vaccination Against Autologous Cancer Stem Cells With mRNA-transfected Dendritic Cells in Patients With Glioblastoma. *Cancer Immunol Immunother* (2013) 62:1499–509. doi: 10.1007/s00262-013-1453-3
91. Lv L, Huang J, Xi H, Zhou X. Efficacy and Safety of Dendritic Cell Vaccines for Patients With Glioblastoma: A Meta-Analysis of Randomized Controlled Trials. *Int Immunopharmacol* (2020) 83:106336. doi: 10.1016/j.intimp.2020.106336
92. Stetler RA, Gan Y, Zhang W, Liou AK, Gao Y, Cao G, et al. Heat Shock Proteins: Cellular and Molecular Mechanisms in the Central Nervous System. *Prog Neurobiol* (2010) 92:184–211. doi: 10.1016/j.pneurobio.2010.05.002
93. Ampie L, Choy W, Lamano JB, Fakurnejad S, Bloch O, Parsa AT. Heat Shock Protein Vaccines Against Glioblastoma: From Bench to Bedside. *J Neurooncol* (2015) 123:441–8. doi: 10.1007/s11060-015-1837-7
94. Hermisson M, Strik H, Rieger J, Dichgans J, Meyermann R, Weller M. Expression and Functional Activity of Heat Shock Proteins in Human Glioblastoma Multiforme. *Neurology* (2000) 54:1357–65. doi: 10.1212/WNL.54.6.1357
95. Graner MW, Cumming RI, Bigner DD. The Heat Shock Response and Chaperones/Heat Shock Proteins in Brain Tumors: Surface Expression, Release, and Possible Immune Consequences. *J Neurosci* (2007) 27:11214–27. doi: 10.1523/JNEUROSCI.3588-07.2007
96. Blachere NE, Li Z, Chandawarkar RY, Suto R, Jaikaria NS, Basu S, et al. Heat Shock Protein–Peptide Complexes, Reconstituted In Vitro, Elicit Peptide-Specific Cytotoxic T Lymphocyte Response and Tumor Immunity. *J Exp Med* (1997) 186:1315–22. doi: 10.1084/jem.186.8.1315
97. Binder RJ, Srivastava PK. Essential Role of CD91 in Re-Presentation of gp96-chaperoned Peptides. *Proc Natl Acad Sci USA* (2004) 101:6128–33. doi: 10.1073/pnas.0308180101
98. Basu S, Binder RJ, Ramalingam T, Srivastava PK. CD91 is a Common Receptor for Heat Shock Proteins gp96, hsp90, hsp70, and Calreticulin. *Immunity* (2001) 14:303–13. doi: 10.1016/S1074-7613(01)00111-X
99. Heimbach JK, Reznikov LL, Calkins CM, Robinson TN, Dinarello CA, Harken AH, et al. TNF Receptor I is Required for Induction of Macrophage Heat Shock Protein 70. *Am J Physiol Cell Physiol* (2001) 281:C241–7. doi: 10.1152/ajpcell.2001.281.1.C241
100. Ji N, Zhang Y, Liu Y, Xie J, Wang Y, Hao S, et al. Heat Shock Protein Peptide complex-96 Vaccination for Newly Diagnosed Glioblastoma: A Phase I, Single-Arm Trial. *JCI Insight* (2018) 3:e99145. doi: 10.1172/jci.insight.99145
101. Meng SD, Song J, Rao Z, Tien P, Gao GF. Three-Step Purification of gp96 From Human Liver Tumor Tissues Suitable for Isolation of gp96-bound Peptides. *J Immunol Methods* (2002) 264:29–35. doi: 10.1016/S0022-1759(02)00093-5
102. Bloch O, Crane CA, Fuks Y, Kaur R, Aghi MK, Berger MS, et al. Heat-Shock Protein Peptide Complex–96 Vaccination for Recurrent Glioblastoma: A Phase II, Single-Arm Trial. *Neuro-Oncology* (2013) 16:274–9. doi: 10.1093/neuonc/not203
103. *Radiation Therapy Plus Temozolomide and Pembrolizumab With and Without HSPPC-96 in Newly Diagnosed Glioblastoma (GBM)*. Available at: https://ClinicalTrials.gov/show/NCT03018288.
104. Khong H, Overwijk WW. Adjuvants for Peptide-Based Cancer Vaccines. *J Immunother Cancer* (2016) 4:56. doi: 10.1186/s40425-016-0160-y
105. Aucouturier J, Dupuis L, Deville S, Ascarateil S, Ganne V. Montanide ISA 720 and 51: A New Generation of Water in Oil Emulsions as Adjuvants for Human Vaccines. *Expert Rev Vaccines* (2002) 1:111–8. doi: 10.1586/14760584.1.1.111
106. *DC Migration Study for Newly-Diagnosed GBM*. Available at: https://ClinicalTrials.gov/show/NCT02366728.
107. *Immunotherapy Targeted Against Cytomegalovirus in Patients With Newly-Diagnosed WHO Grade IV Unmethylated Glioma*. Available at: https://ClinicalTrials.gov/show/NCT03927222.
108. *Dendritic Cell Vaccine for Patients With Brain Tumors*. Available at: https://ClinicalTrials.gov/show/NCT01204684.
109. Bode C, Zhao G, Steinhagen F, Kinjo T, Klinman DM. Cpg DNA as a Vaccine Adjuvant. *Expert Rev Vaccines* (2011) 10:499–511. doi: 10.1586/erv.10.174
110. Griffin JD, Cannistra SA, Sullivan R, Demetri GD, Ernst TJ, Kanakura Y. The Biology of GM-CSF: Regulation of Production and Interaction With its Receptor. *Int J Cell Cloning* (1990) 8 Suppl 1:35–44. doi: 10.1002/stem.5530080705
111. Nemunaitis J. Vaccines in Cancer: GVAX, a GM-CSF Gene Vaccine. *Expert Rev Vaccines* (2005) 4:259–74. doi: 10.1586/14760584.4.3.259
112. Lines JL, Pantazi E, Mak J, Sempere LF, Wang L, O'Connell S, et al. VISTA is an Immune Checkpoint Molecule for Human T Cells. *Cancer Res* (2014) 74:1924–32. doi: 10.1158/0008-5472.CAN-13-1504
113. Manieri NA, Chiang EY, Grogan JL. Tigit: A Key Inhibitor of the Cancer Immunity Cycle. *Trends Immunol* (2017) 38:20–8. doi: 10.1016/j.it.2016.10.002
114. Ishii N, Takahashi T, Soroosh P, Sugamura K. Ox40-OX40 Ligand Interaction in T-cell-mediated Immunity and Immunopathology. *Adv Immunol* (2010) 105:63–98. doi: 10.1016/S0065-2776(10)05003-0
115. Jahan N, Talat H, Curry WT. Agonist OX40 Immunotherapy Improves Survival in Glioma-Bearing Mice and is Complementary With Vaccination With Irradiated GM-CSF-expressing Tumor Cells. *Neuro Oncol* (2018) 20:44–54. doi: 10.1093/neuonc/nox125
116. Ansell SM, Flinn I, Taylor MH, Sikic BI, Brody J, Nemunaitis J, et al. Safety and Activity of Varlilumab, a Novel and First-in-Class Agonist anti-CD27 Antibody, for Hematologic Malignancies. *Blood Adv* (2020) 4:1917–26. doi: 10.1182/bloodadvances.2019001079
117. *DC Migration Study to Evaluate TReg Depletion In GBM Patients With and Without Varlilumab*. Available at: https://ClinicalTrials.gov/show/NCT03688178.
118. Zhang X, Chen W, Fan J, Wang S, Xian Z, Luan J, et al. Disrupting Cd47-Sirpα Axis Alone or Combined With Autophagy Depletion for the Therapy of Glioblastoma. *Carcinogenesis* (2018) 39:689–99. doi: 10.1093/carcin/bgy041
119. Gholamin S, Mitra SS, Feroze AH, Liu J, Kahn SA, Zhang M, et al. Disrupting the CD47-Sirpα Anti-Phagocytic Axis by a Humanized anti-CD47 Antibody is an Efficacious Treatment for Malignant Pediatric Brain Tumors. *Sci Transl Med* (2017) 9:eaaf2968. doi: 10.1126/scitranslmed.aaf2968
120. Zhang M, Hutter G, Kahn SA, Azad TD, Gholamin S, Xu CY, et al. Anti-Cd47 Treatment Stimulates Phagocytosis of Glioblastoma by M1 and M2 Polarized Macrophages and Promotes M1 Polarized Macrophages In Vivo. *PloS One* (2016) 11:e0153550. doi: 10.1371/journal.pone.0153550
121. Weller M, Butowski N, Tran DD, Recht LD, Lim M, Hirte H, et al. Rindopepimut With Temozolomide for Patients With Newly Diagnosed, EGFRvIII-expressing Glioblastoma (ACT IV): A Randomised, Double-Blind, International Phase 3 Trial. *Lancet Oncol* (2017) 18:1373–85. doi: 10.1016/s1470-2045(17)30517-x
122. Ratnam NM, Frederico SC, Gonzalez JA, Gilbert MR. Clinical Correlates for Immune Checkpoint Therapy: Significance for CNS Malignancies. *Neuro-Oncol Adv* (2020) 3. doi: 10.1093/noajnl/vdaa161

123. Chiba Y, Kinoshita M, Okita Y, Tsuboi A, Isohashi K, Kagawa N, et al. Use of (11)C-Methionine PET Parametric Response Map for Monitoring WT1 Immunotherapy Response in Recurrent Malignant Glioma. *J Neurosurg* (2012) 116:835–42. doi: 10.3171/2011.12.JNS111255
124. Rashidian M, Ingram JR, Dougan M, Dongre A, Whang KA, LeGall C, et al. Predicting the Response to CTLA-4 Blockade by Longitudinal Noninvasive Monitoring of CD8 T Cells. *J Exp Med* (2017) 214:2243–55. doi: 10.1084/jem.20161950
125. Vrabec M, Van Cauter S, Himmelreich U, Van Gool SW, Sunaert S, De Vleeschouwer S, et al. MR Perfusion and Diffusion Imaging in the Follow-Up of Recurrent Glioblastoma Treated With Dendritic Cell Immunotherapy: A Pilot Study. *Neuroradiology* (2011) 53:721–31. doi: 10.1007/s00234-010-0802-6
126. Rizzo S, Botta F, Raimondi S, Origgi D, Fanciullo C, Morganti AG, et al. Radiomics: The Facts and the Challenges of Image Analysis. *Eur Radiol Exp* (2018) 2:36. doi: 10.1186/s41747-018-0068-z
127. Buerki RA, Chheda ZS, Okada H. Immunotherapy of Primary Brain Tumors: Facts and Hopes. *Clin Cancer Res* (2018) 24:5198–205. doi: 10.1158/1078-0432.CCR-17-2769
128. Cloughesy TF, Mochizuki AY, Orpilla JR, Hugo W, Lee AH, Davidson TB, et al. Neoadjuvant anti-PD-1 Immunotherapy Promotes a Survival Benefit With Intratumoral and Systemic Immune Responses in Recurrent Glioblastoma. *Nat Med* (2019) 25:477–86. doi: 10.1038/s41591-018-0337-7
129. Zhang Y, Mudgal P, Wang L, Wu H, Huang N, Alexander PB, et al. T Cell Receptor Repertoire as a Prognosis Marker for Heat Shock Protein Peptide complex-96 Vaccine Trial Against Newly Diagnosed Glioblastoma. *Oncoimmunology* (2020) 9:1749476. doi: 10.1080/2162402X.2020.1749476
130. Giles AJ, Hutchinson MND, Sonnemann HM, Jung J, Fecci PE, Ratnam NM, et al. Dexamethasone-Induced Immunosuppression: Mechanisms and Implications for Immunotherapy. *J Immunother Cancer* (2018) 6:51. doi: 10.1186/s40425-018-0371-5
131. Iorgulescu JB, Gokhale PC, Speranza MC, Eschle BK, Poitras MJ, Wilkens MK, et al. Concurrent Dexamethasone Limits the Clinical Benefit of Immune Checkpoint Blockade in Glioblastoma. *Clin Cancer Res* (2021) 27:276–87. doi: 10.1158/1078-0432.CCR-20-2291
132. Jha SK. Cerebral Edema and its Management. *Med J Armed Forces India* (2003) 59:326–31. doi: 10.1016/S0377-1237(03)80147-8
133. Peng Y, Liu X, Wang A, Han R. The Effect of Mannitol on Intraoperative Brain Relaxation in Patients Undergoing Supratentorial Tumor Surgery: Study Protocol for a Randomized Controlled Trial. *Trials* (2014) 15:165. doi: 10.1186/1745-6215-15-165
134. Wakai A, McCabe A, Roberts I, Schierhout G. Mannitol for Acute Traumatic Brain Injury. *Cochrane Database Syst Rev* (2013) 2013:Cd001049. doi: 10.1002/14651858.CD001049.pub5
135. Meng X, Zhao R, Shen G, Dong D, Ding L, Wu S. Efficacy and Safety of Bevacizumab Treatment for Refractory Brain Edema: Case Report. *Medicine* (2017) 96:e8280. doi: 10.1097/MD.0000000000008280
136. Gilbert MR, Dignam JJ, Armstrong TS, Wefel JS, Blumenthal DT, Vogelbaum MA, et al. A Randomized Trial of Bevacizumab for Newly Diagnosed Glioblastoma. *N Engl J Med* (2014) 370:699–708. doi: 10.1056/NEJMoa1308573
137. Abrams DA, Hanson JA, Brown JM, Hsu FP, Delashaw JBJr., Bota DA. Timing of Surgery and Bevacizumab Therapy in Neurosurgical Patients With Recurrent High Grade Glioma. *J Clin Neurosci* (2015) 22:35–9. doi: 10.1016/j.jocn.2014.05.054

Conflict of Interest: The authors declare that the research was conducted in the absence of any commercial or financial relationships that could be construed as a potential conflict of interest.

frontiers in Oncology

ORIGINAL RESEARCH
published: 20 May 2021
doi: 10.3389/fonc.2021.646060

Immune-Related Gene SERPINE1 Is a Novel Biomarker for Diffuse Lower-Grade Gliomas *via* Large-Scale Analysis

Xiaoming Huang[1], Fenglin Zhang[1], Dong He[2], Xiaoshuai Ji[1], Jiajia Gao[1], Wenqing Liu[1], Yunda Wang[3], Qian Liu[4] and Tao Xin[1,5,6]**

[1] Department of Neurosurgery, Shandong Provincial Qianfoshan Hospital, Cheeloo College of Medicine, Shandong University, Jinan, China, [2] Department of Neurosurgery, Shandong Provincial Hospital, Cheeloo College of Medicine, Shandong University, Jinan, China, [3] Department of Neurosurgery, Shandong Provincial Qianfoshan Hospital, Shandong First Medical University & Shandong Academy of Medical Sciences, Jinan, China, [4] Department of Histology and Embryology, School of Basic Medical Sciences, Cheeloo College of Medicine, Shandong University, Jinan, China, [5] Department of Neurosurgery, Jiangxi Provincial People's Hospital Affiliated to Nanchang University, Nanchang, Jiangxi, China, [6] Shandong Medicine and Health Key Laboratory of Neurosurgery, The First Affiliated Hospital of Shandong First Medical University & Shandong Provincial Qianfoshan Hospital, Jinan, China

OPEN ACCESS

Edited by:
Valérie Dutoit,
Université de Genève, Switzerland

Reviewed by:
Marta Domenech,
Catalan Institute of Oncology, Spain
Montserrat Lara-Velazquez,
University of Wisconsin-Madison, United States

***Correspondence:**
Tao Xin
drxintao@yeah.net
Qian Liu
cardioqian@sdu.edu.cn

Specialty section:
This article was submitted to Cancer Immunity and Immunotherapy, a section of the journal Frontiers in Oncology

Received: *24 December 2020*
Accepted: *28 April 2021*
Published: *20 May 2021*

Citation:
Huang X, Zhang F, He D, Ji X, Gao J, Liu W, Wang Y, Liu Q and Xin T (2021) Immune-Related Gene SERPINE1 Is a Novel Biomarker for Diffuse Lower-Grade Gliomas via Large-Scale Analysis. Front. Oncol. 11:646060. doi: 10.3389/fonc.2021.646060

Background: Glioma is one of the highly fatal primary tumors in the central nervous system. As a major component of tumor microenvironment (TME), immune cell has been proved to play a critical role in the progression and prognosis of the diffuse lower-grade gliomas (LGGs). This study aims to screen the key immune-related factors of LGGs by investigating the TCGA database.

Methods: The RNA-sequencing data of 508 LGG patients were downloaded in the TCGA database. ESTIMATE algorithm was utilized to calculate the stromal, immune, and ESTIMATE scores, based on which, the differentially expressed genes (DEGs) were analyzed by using "limma" package. Cox regression analysis and the cytoHubba plugin of Cytoscape software were subsequently applied to screen the survival-related genes and hub genes, the intersection of which led to the identification of SERPINE1 that played key roles in the LGGs. The expression patterns, clinical features, and regulatory mechanisms of SERPINE1 in the LGGs were further analyzed by data mining of the TCGA database. What's more, the above analyses of SERPINE1 were further validated in the LGG cohort from the CGGA database.

Result: We found that stromal and immune cell infiltrations were strongly related to the prognosis and malignancy of the LGGs. A total of 54 survival-related genes and 46 hub genes were screened out in the DEGs, within which SERPINE1 was identified to be significantly overexpressed in the LGG samples compared with the normal tissues. Moreover, the upregulation of SERPINE1 was more pronounced in the gliomas of WHO grade III and IDH wild type, and its expression was correlated with poor prognosis in the LGG patients. The independent prognostic value of SERPINE1 in the LGG patients was also confirmed by Cox regression analysis. In terms of the functions of SERPINE1,

the results of enrichment analysis indicated that SERPINE1 was mainly enriched in the immune-related biological processes and signaling pathways. Furthermore, it was closely associated with infiltrations of immune cells in the LGG microenvironment and acted synergistically with PD1, PD-L1, PD-L2.

Conclusion: These findings proved that SERPINE1 could serve as a prognostic biomarker and potential immunotherapy target of LGGs.

Keywords: SERPINE1, LGG, TME, biomarker, immune checkpoint, prognosis

INTRODUCTION

Glioma is the most common type of primary brain tumors in the central nervous system (CNS), originated from the transformed progenitor cells or neural stem cells (1). According to the WHO Classification of CNS tumors revised in 2016, gliomas are divided into four grades from WHO grade I to WHO grade IV and comprise two major subtypes: diffuse gliomas and gliomas and non-diffuse gliomas (2, 3). Among them, diffuse low-grade (WHO grade II) and intermediate-grade (WHO grade III) gliomas are collectively referred to as lower-grade gliomas (LGGs) (4). Compared with glioblastoma (WHO grade IV), LGGs are relatively benign and have a favorable prognosis. However, LGGs commonly exhibit diffuse and infiltrative nature, which makes it extremely difficult to be completely resected. As a matter of fact, most LGGs eventually progress to the secondary tumors with higher grades (4, 5). Despite ongoing advances in surgical operation and postoperative adjuvant chemoradiotherapy, the prognosis of gliomas has not been dramatically improved over the past decades (6, 7). Therefore, more effective therapeutic strategies for LGGs need to be further explored.

The tumor microenvironment (TME), which consists of large and diverse amounts of immune cells, stromal cells and other non-tumor components, plays pivotal roles in tumor initiation and progression (8, 9). For instance, tumor-associated macrophages (TAM) affect the development of tumors mainly through proliferation, local infiltration, angiogenesis and immunosuppression (10, 11). Other immune cells, including effector T cells, regulatory T cells, B cells, natural killer (NK) cells, dendritic cells (DCs), and N1-polarized neutrophils, have also been reported to serve various functions in the TME (12). In recent years, tumor immunotherapies that target tumor or immune cells have evolved to the most promising therapeutic approaches to treat cancers (13, 14). Immune checkpoint inhibitors, such as programmed cell death receptor 1 (PD-1) inhibitor, programmed death-ligand 1 (PD-L1) inhibitor, have made tremendous progress in the clinical treatment of melanoma, non–small cell lung cancer (NSCLC), and urothelial carcinoma (UC) (15–17). However, immune suppression and evasion that also exist in the TME remain the formidable challenges to effective immunotherapies in some tumor patients (18). For example, under induction of CSF-1, CCL2, IL-4, IL-6, IL-10, tumor-associated macrophages (TAMs) in the glioma microenvironment differentiate into M2-type macrophages (19, 20), which contribute to establishing an immunosuppressive microenvironment due to lack of costimulatory factors such as CD40, CD80, and CD86 (21, 22). Hence, further investigation of the immune status of the TME remains particularly needed.

Serpin family E member 1 (SERPINE1), encoding plasminogen activator inhibitor 1 (PAI-1), serves as the primary inhibitor of uridylyl phosphate adenosine (uPA) and tissue plasminogen activator (tPA) (23). Previous researches have predominantly focused on its function in thrombosis (24). With the recent development of high-throughput sequencing technology, the abnormal expression of SERPINE1 has been detected in various tumors and its role in tumors has attracted great attention. SERPINE1 has been reported to induce tumor migration, invasion, angiogenesis and thereby promote the progression and metastasis of tumors (24, 25). For example, SERPINE1 was reported to be elevated in the gastric adenocarcinoma tissues and its upregulation enhanced the invasive and proliferative capacities of tumor cells by regulating epithelial-mesenchymal transition (EMT) (26). Moreover, SERPINE1 was identified as a regulator of glioblastoma cell dispersal and downregulation of SERPINE1 limited the proliferation and invasion of glioma cells (27). However, the specific molecular mechanisms underlying these phenotypes caused by SERPINE1 in gliomas still remain obscure.

In this study, the LGG cohort data from the TCGA database was mined to screen the prognostic immune-related genes for the LGGs. SERPINE1 was finally determined as our research objective. The association between the expressions and clinical features of SERPINE1were analyzed *via* using the LGG RNA-seq data from the TCGA and CGGA database. To better elucidate the biological mechanisms of SERPINE1, we carried out the gene co-expression analysis, GSEA, immune-cell infiltration correlation analysis, and immune checkpoints correlation analysis in the LGG cohort. Finally, we proved that SERPINE1 served as an oncogene in the LGGs and might be a novel potential target for glioma immunotherapy.

MATERIALS AND METHODS

Data Collection and Processing

The TCGA RNA-seq data and corresponding phenotype data of LGG samples were downloaded from UCSC Xena website (http://xena.ucsc.edu/). Samples with incomplete information and duplicates were removed. Stromal scores and immune scores were calculated by the ESTIMATE algorithm for each sample

(28). RNA-seq data and corresponding clinical information used for further validation were downloaded from the CGGA database (29, 30). Batch effects were removed using the "sva" Bioconductor package (31). We extracted the following clinical characteristics for this study: gender, age, survival status, survival time, tumor grade, IDH status. The glioma tissue chip was purchased from the Shanghai Outdo Biotech Co. Ltd (Shanghai, China), which contained 30 LGG cases (Lot No.: XT16-017).

Screening Differentially Expressed Genes (DEGs)

All LGG patients were divided into high/low groups according to the immune scores and stromal scores. We screened the DEGs between the high and low score groups using the "limma" R package, with the thresholds of p-value<0.05 and log2|fold change|> 1 (32). The intersections of these DEG sets were showed by Venn diagram (http://bioinformatics.psb.ugent.be/webtools/Venn/).

Functional Enrichment Analysis

Kyoto Encyclopedia of Genes and Genomes (KEGG) analysis and gene ontology (GO) analysis were performed using the Bioconductor package "clusterProfiler" to identify the possible pathways and functions of the DEGs (33). GO analysis included three categories: cellular component (CC), biological process (BP), and molecular function (MF). Metascape database was utilized to conduct functional enrichment analysis for the top 500 SERPINE1 positively correlated genes (34). The terms with p-value<0.05 were considered statistically significant.

PPI Network, GSEA, GSVA, and ROC

The protein-protein interaction (PPI) network was constructed using the STRING online tool (35) and visualized by Cytoscape software (V3.7.1) (36). Gene set enrichment analysis (GSEA) was performed using GSEA software (V 4.1.0). The false discovery rate (FDR)<0.05 was considered statistically significant. Gene set variation analysis (GSVA) was performed *via* R software (37). The receiver operating characteristic (ROC) curves were constructed using "survivalROC" package (38).

Tumor-Infiltrating Immune Cells

To calculate the abundance of 22 immune cell types in each LGG sample, we submitted the gene expression data to the CIBERSORT website (https://cibersort.stanford.edu/) and performed the CIBERSORT deconvolution algorithm (39). The results with p-value<0.05 were considered statistically significant.

Immunohistochemistry (IHC)

PAI-1 and cell markers were detected by immunohistochemistry (ICH) that was conducted with the standard protocol. Rabbit anti-PAI1 antibody was purchased from ZEN-BIOSCIENCE (Chengdu, Sichuan, China), and other primary antibodies were purchased from Affinity Biosciences LTD. Secondary antibody (HRP conjugated Goat Anti-Rabbit IgG) was purchased from Servicebio Technology Co. Ltd (Wu Han, China). Primary antibodies and secondary antibody were respectively diluted at a ratio of 1:50 and 1:200. The staining intensity of each staining area was categorized into four-level: negative staining (scored 0), weak staining (scored 1), moderate staining (scored 2), strong staining (scored 3). And the area of each staining intensity was measured respectively. We quantified the results of tissue microarray immunohistochemistry staining using histochemistry score (H-score). H-score = (percentage of weak staining area ×1) + (percentage of moderate staining area ×2) + (percentage of strong staining area ×3).

Statistical Analysis and Plot Generation

The R software (Version 4.0.3), GraphPad Prism 8 software (Version 8.0.2), and Adobe Illustrator software (Version 24.0.2) were used to perform statistical analysis and generate figures. Kaplan-Meier survival analysis was performed using the "survival" (https://CRAN.R-project.org/package=survival) and "survminer" (Version: 0.4.8) R packages. Wilcoxon rank-sum test was used to compare the median values between the variables. The Cox regression model was used for univariate and multivariate analyses. We calculated the correlations between the different variables *via* the Spearman correlation test. In all statistical tests, p-value<0.05 was considered statistically significant. The plots were generated by R packages: "ggplot2" (Version: 3.3.2), "ggpubr" (Version: 0.4.0), "pheatmap" (Version: 1.0.12), "VennDiagram" (Version: 1.6.20), "enrichplot" (40), "survivalROC" (Version: 1.0.3), "vioplot" (Version: 0.3.5), "corrplot" (Version: 0.84).

RESULTS

Relationship Between The Immune, Stromal, ESTIMATE Scores and the Clinical Characteristics of the LGG Patients

The gene expression profiling data and clinical information of 533 LGG samples were downloaded from the TCGA database (https://www.cancer.gov/tcga). Three samples, including TCGA-TQ-A7RS-01A, TCGA-CS-5390-01A, and TCGA-R8-A6YH-01A, were excluded from our study cohort for lack of complete clinical information. Since 18 patients in the cohort corresponded to multiple sample information, we thus merged these repeated gene expression profiles after taking the average. Ultimately, a total of 508 LGG patients were enrolled in our study, and their clinical informations were presented in **Table 1**. Based on the ESTIMATE algorithm, the immune scores varied from -1676.002 to 2477.026, the stromal scores ranged from -1769.170 to 1710.690, and the ESTIMATE scores (ESTIMATE score is the sum of the immune score and stromal score of each sample, which reflects the purity of the tumor. The higher the ESTIMATE score, the lower the purity of the tumor.) were distributed between -3422.599 and 3762.907 (**Supplementary Table 1**). We subsequently sorted the 508 LGG cases into high-score and low-score groups according to the median value of these scores. Kaplan-Meier analysis indicated that the cases with low immune (p=0.004), stromal (p=0.001), and ESTIMATE (p=0.007) scores exhibited longer overall survival than those with high scores (**Figures 1A–C**). We further analyzed the associations between these scores and the clinical characteristics of

TABLE 1 | Demographic and clinicopathologic characteristics of the LGG patients enrolled in this study.

		TCGA dataset	CGGA dataset
Total		508	575
Gender			
	male	282	334
	female	226	241
Event			
	alive	382	245
	dead	126	330
Age			
	age ≤ 41	265	323
	age >41	243	252
Grade			
	WHO II	247	271
	WHO III	261	304
Radiotherapy			
	yes	286	430
	no	176	128
	unknown	46	17
Chemotherapy (TMZ)			
	yes	–	359
	no	–	200
	unknown	–	16
Corticosteroids			
	non-treatment	211	–
	treatment	149	–
	unknown	148	–
IDH status			
	wild type	34	130
	mutation	91	411
	unknown	383	34
1p19q status			
	non-codeletion	–	366
	codeletion	–	175
	unknown	–	34
MGMTp status			
	methylated	–	279
	un-methylated	–	194
	unknown	–	102
KPS			
	KPS≥90	196	–
	70≤KPS<90	81	–
	KPS<70	22	–
	unknown	209	

KPS, Karnofsky performance score; TMZ, temozolomide; MGMTp, MGMT promoter.

the LGG patients. The results showed that the WHO grade III and IDH wild-type LGG patients exhibited higher immune, stromal, and ESTIMATE scores, although the immune score was not statistically significant between the IDH groups (**Figures 1D–I**). No significant differences also appeared in age and gender subgroups (**Supplementary Figures 1A-F**).

Identification of the Differentially Expressed Genes (DEGs) Based on the Immune and Stromal Scores of the LGGs

To identify the DEGs, the LGG patients were classified into the high-score and low-score groups based on the immune and stromal scores above. The DEGs were subsequently screened by comparing the gene expression profiles of the high-score and low-score groups, with a threshold of the absolute value of fold change > 2 (FDR<0.05). A total of 1264 up-regulated genes and 1028 down-regulated genes were selected in the high immune score group (**Figure 2C** and **Supplementary Table 2**). 1513 up-regulated genes and 518 down-regulated genes were chosen in the high stromal score group (**Figure 2D** and **Supplementary Table 2**). The "pheatmap" package was then employed to plot the heatmap, which exhibited the expression distribution of the DEGs between the high-score and low-score groups (**Figures 2A, B**). The intersected genes that were upregulated or downregulated in both immune and stromal groups were selected for further investigation (**Figures 2E, F**). Ultimately, a total of 1113 up-regulated genes and 463 down-regulated genes were included for the subsequent research.

To validate the potential functions of these 1576 DEGs, we performed Gene Ontology (GO) and Kyoto Encyclopedia of Genes and Genome (KEGG) pathway analyses. As presented in the bubble plot, the top GO terms enriched by these DEGs included T cell activation (BP), regulation of lymphocyte activation (BP), external side of plasma membrane (CC), and immune receptor activity (MF) (**Figure 2G**). On the other hand, the KEGG enrichment analysis indicated that the 1576 DEGs were predominantly enriched in the pathways of cytokine-cytokine receptor interaction, phagosome, and chemokine signaling pathway (**Figure 2H**). From the enrichment analysis results above, these DEGs were mainly involved in a varied range of biological processes and pathways associated with immune responses. Considering that these DEGs were obtained based on the immune and stromal cell scores, we thus identified the 1576 DEGs as immune-related genes (IRGs).

Screening of Target Genes

Initially, to gain the hub genes within the 1576 DEGs, the protein-protein interaction (PPI) network was constructed using the STRING database and visualized by Cytoscape software (v3.7.2) (**Supplementary Figure 2**). 46 hub genes in the network were identified by two algorithms (Stress and Betweenness) in the cytoHubba plugin of Cytoscape software (**Figures 3A, B**). Secondly, we conducted a univariate Cox regression analysis for the TCGA cohort to identify the genes correlated with the overall survival of the LGG patients. Of the 1576 DEGs that were analyzed, 54 genes were significantly associated with the prognosis of the LGG patients ($p<0.001$) (**Figure 3C**). Finally, the intersection of the 54 prognostic genes and the 46 hub genes led to the identification of SERPINE1 and TIMP1 (**Figure 3D**). Based on the online GEPIA2 database (http://gepia2.cancer-pku.cn/#index), the expression of TIMP1 was not significantly different between the LGG and normal brain tissues (**Supplementary Figure 3A**), which implied a minor role of TIMP1 as a biomarker for the LGGs. Therefore, SERPINE1 was selected as the target gene for the later study.

The Expressions of SERPINE1 Increased With the Grades of Gliomas and Was Upregulated in the IDH Wild-Type LGGs

The analysis based on the GEPIA2 database indicated that SERPINE1 was significantly upregulated in the LGG samples compared with the normal brain tissues (**Supplementary Figure 3B**). We subsequently examined the

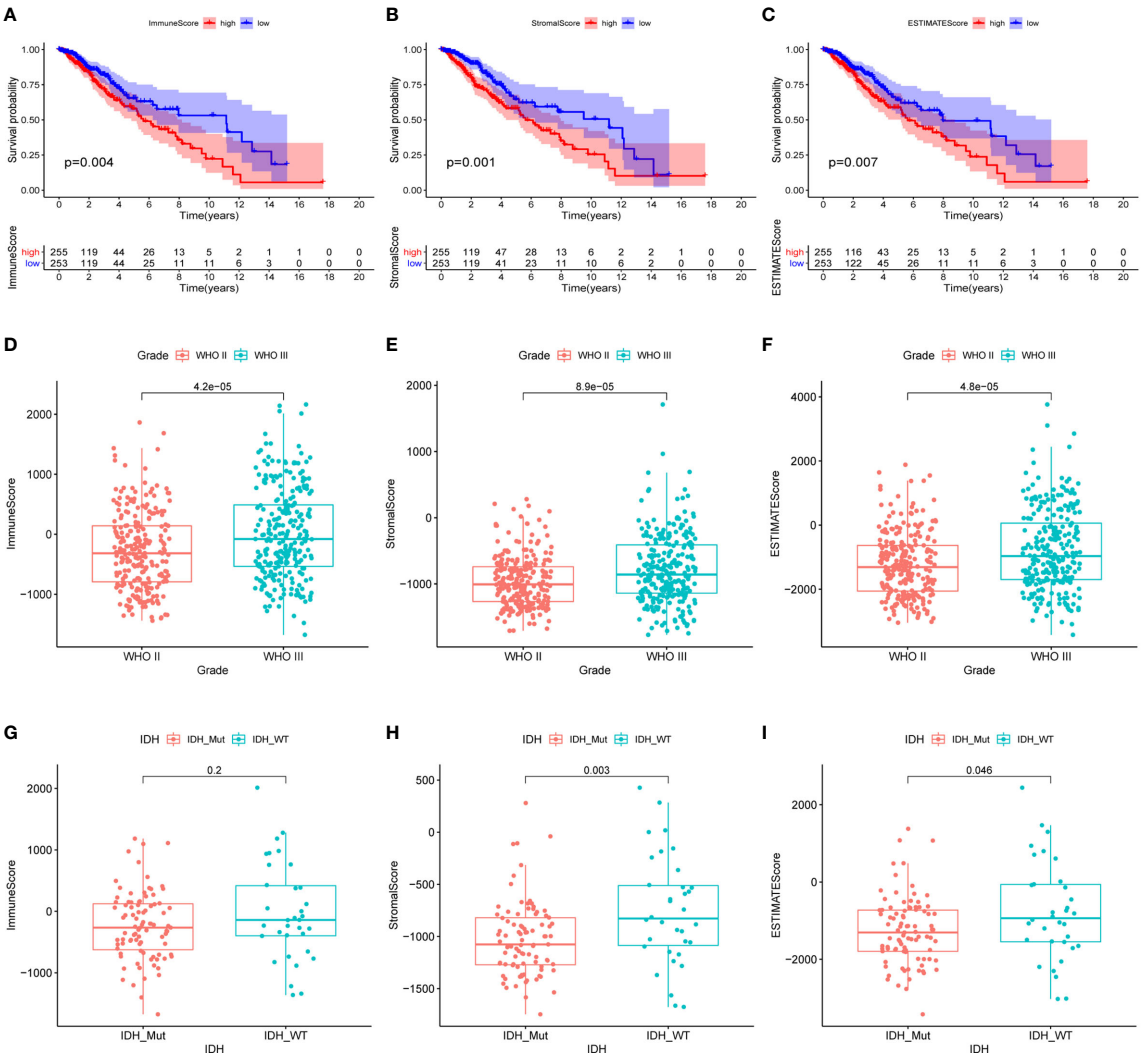

FIGURE 1 | Relationship between the immune, stromal, ESTIMATE scores and the clinical characteristics of the LGG patients. **(A)** Kaplan-Meier survival analysis of LGG patients in high and low immune-score groups. **(B)** Kaplan-Meier survival analysis of LGG patients in high and low stromal-score groups. **(C)** Kaplan-Meier survival analysis of LGG patients in high and low ESTIMATE-score groups. **(D–F)** The distribution of immune score, stromal score, ESTIMATE score in tumor grades. **(G–I)** The distribution of immune score, stromal score, ESTIMATE score in IDH status. P-value < 0.05 was considered statistically significant.

expression patterns of SERPINE1 in the LGGs using the RNA-seq data from the TCGA database, which was further validated by the RNA-seq data in the CGGA database. The CGGA RNA-seq datasets that included 693 and 325 glioma samples were collected and merged after the batch effects by the "sva" package were removed (**Supplementary Figure 3C**). We ultimately selected the 575 LGG samples with the complete follow-up information from the merged dataset for our research (**Table 1**).

We found that the expression of SERPINE1 was comparatively higher in higher-grade tumors and patients of more advanced age. In the TCGA and CGGA cohorts, WHO grade III gliomas showed higher levels of SERPINE1 mRNA than WHO grade II gliomas (p<0.001, respectively) (**Figures 4A, C**). The older LGG patients tended to express higher levels of SERPINE1 mRNA (**Supplementary Figure 3D**) but failed to be validated in the CGGA cohort (**Supplementary Figure 3F**). It is well known that IDH status influences the prognosis of gliomas, among which IDH wild-type gliomas often associated with a worse survival rate (41). We thus determined the expression patterns of SERPINE1 based on IDH status. The results showed that the expression of SERPINE1 was significantly upregulated in the IDH wild-type gliomas in comparison to the IDH-mutant gliomas (**Figures 4B, D**). No significant difference in SERPINE1 mRNA levels was indicated by gender (**Supplementary Figures 3E, G**). In a word, the above results suggested that the expression of SERPINE1 was positively correlated with the malignancy of gliomas.

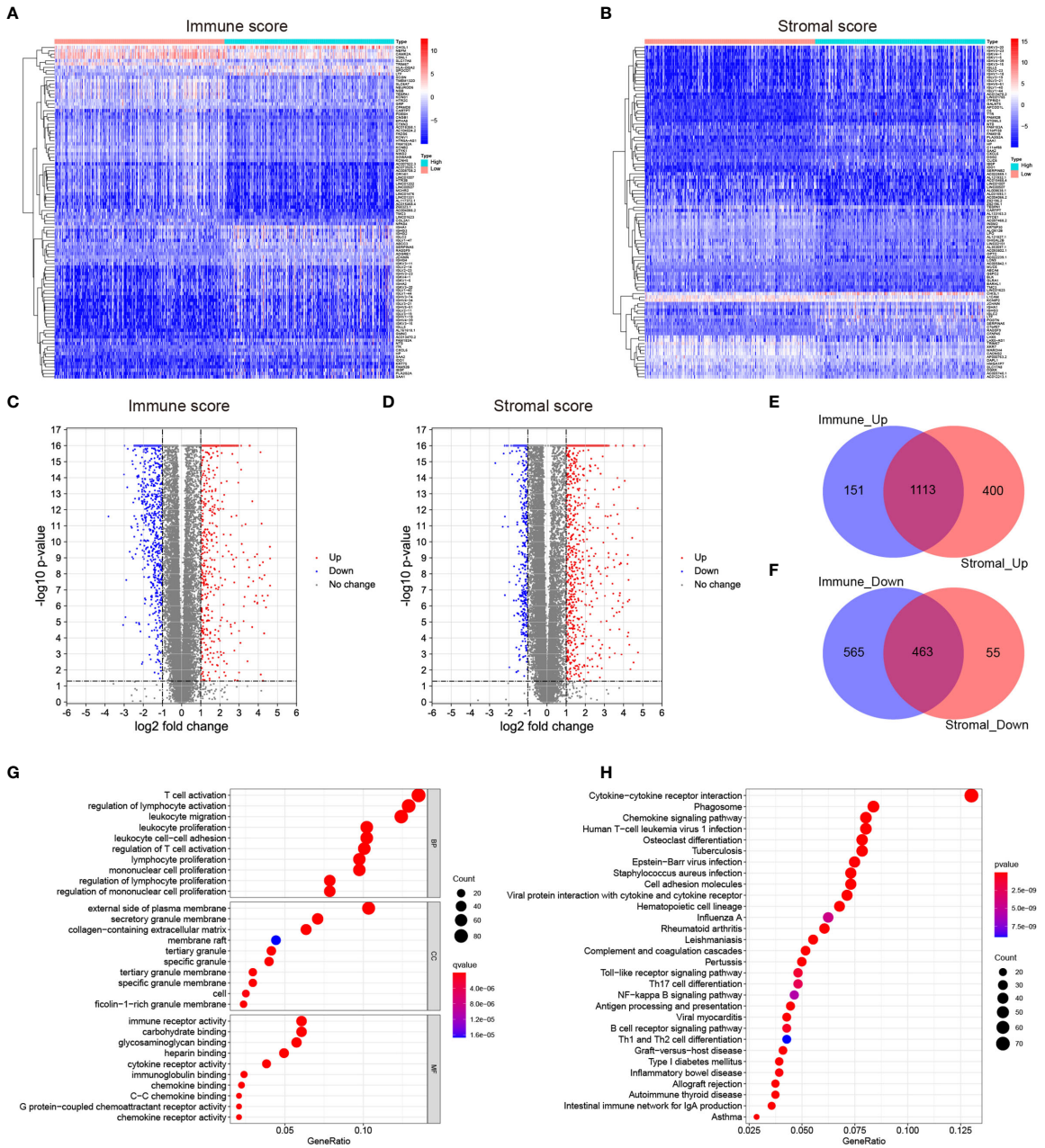

FIGURE 2 | Identification of the differentially expressed genes (DEGs) based on the immune and stromal scores of the LGGs. **(A, B)** Heatmaps showing the distribution patterns of differentially expressed genes based on immune and stromal scores. The darker the red color, the higher the gene expression was. The deeper the blue color, the lower the gene expression was. **(C, D)** Volcano plots of significantly differentially expressed genes based on immune and stromal scores (|lg FC|>1, $p < 0.05$). Blue dots represented significantly down-regulated genes, and red dots represented significantly up-regulated genes. **(E, F)** Venn plots showing the overlapping DEGs between immune and stromal groups. **(G)** Bubble plot of GO enrichment analysis of DEGs. **(H)** Bubble plot of KEGG enrichment analysis of DEGs. Node size represented the number of DEGs contained in the corresponding GO/KEGG term, and the node color denoted the p-value. P-value<0.05 was considered statistically significant.

SERPINE1 High Expression Predicted an Unfavorable Prognosis in the LGG Patients

To investigate the prognostic value of SERPINE1 for LGG patients, we collected the clinical and gene expression profile data from the TCGA and CGGA databases. The baseline of the patient characteristics was presented in **Table 1**. Firstly, the patients were divided into high and low expression groups based on the median value of SERPINE1 mRNA. The subsequent

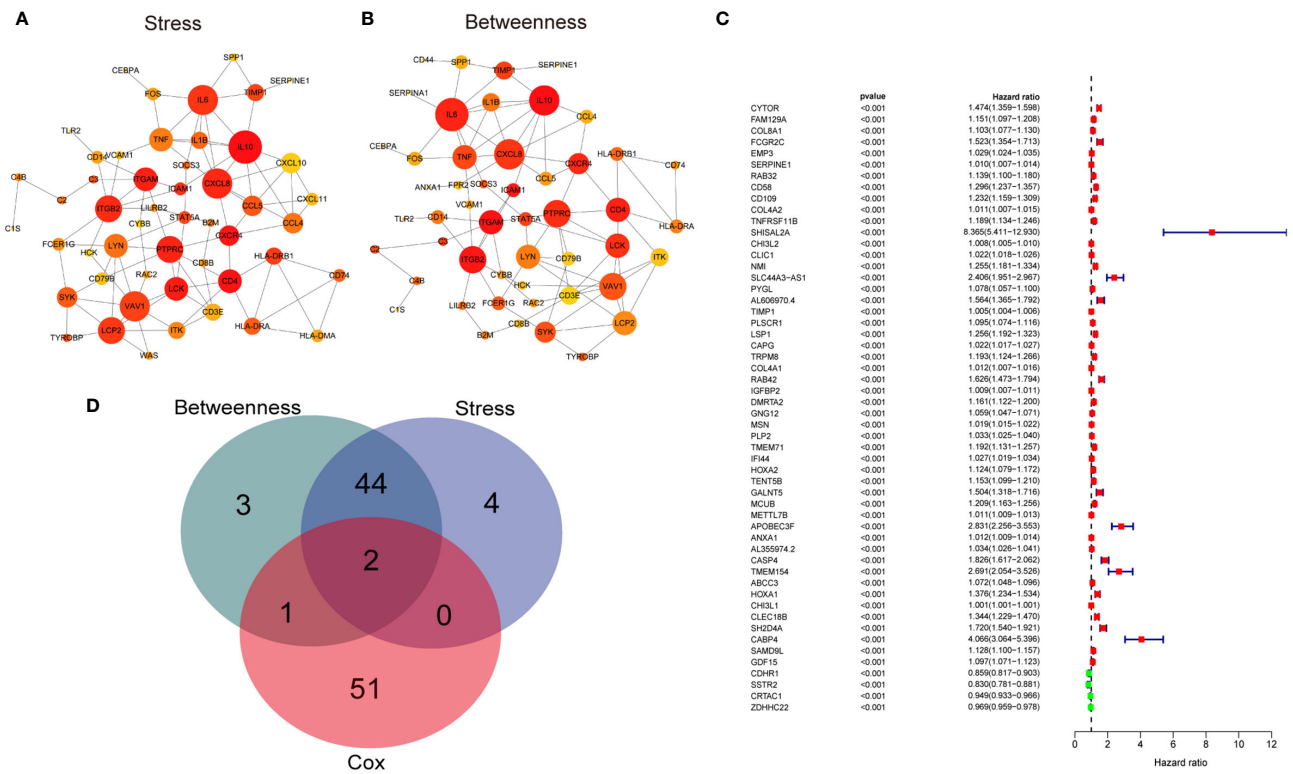

FIGURE 3 | Screening target genes. **(A)** The network of top 50 hub genes screened by CytoHubba Stress algorithm. **(B)** The network of top 50 hub genes screened by CytoHubba Betweenness algorithm. Node size indicated its connectivity (the larger the node, the more proteins interacted). Node color indicated gene ranking (top-ranked genes colored by relatively darker color). **(C)** Forest plot showing hazard ratios with p-values and 95% CI measured by univariate Cox regression analysis. The dashed line marked hazard ratio=1. Red boxes represented unfavorable prognosis genes, and blue boxes remarked favorable prognosis genes. CI, confidence interval. **(D)** Venn plots showing the intersected genes between hub genes and survival-related genes.

Kaplan-Meier analysis indicated that the high SERPINE1 expression group had shorter overall survival in all the LGG patients (P<0.001) (**Figure 5A**). Similar results were achieved in the WHO grade II patients (P=0.011) and WHO grade III patients (P<0.001) from the TCGA cohort (**Figures 5B, C**). In line with the results from the TCGA dataset, the patients with higher SERPINE1 expression also exhibited shorter overall survival in the CGGA dataset (P<0.001 for all LGGs, P=0.042 for WHO grade II gliomas, and P<0.001 for WHO grade III gliomas) (**Figures 5D–F**). Additionally, the univariate and multivariate Cox analysis of the TCGA and CGGA cohorts indicated that age, tumor grade, corticosteroids treatment, IDH status, 1p19q status, as well as SERPINE1 expression could serve as independent prognostic factors in patients with LGG (**Table 2**). Moreover, we performed receiver operating characteristic (ROC) curve analysis to assess the predictive ability (1-, 3-, 5-year overall survival) of SERPINE1 in LGG. The areas under the ROC curve (AUC) for 1-year survival were 0.819 in the TCGA cohort, 0.654 in the CGGA cohort; 3-year survival were 0.753 in the TCGA cohort, 0.697 in the CGGA cohort; 5-year survival were 0.677 in the TCGA cohort, 0.688 in the CGGA cohort (**Figures 5G, H**). All in all, the above results suggested that SERPINE1 could be an important prognostic biomarker for LGG patients.

The Potential Functions of SERPINE1

To better understand the potential functions of SERPINE1, we examined the correlation between SERPINE1 and other genes in the LGG gene expression profile through the online database LinkedOmics (**Figure 6A** and **Supplementary Table 3**) (42). The top 500 positively correlated genes were selected to perform enrichment analysis through the Metascape online tools. As presented in **Figures 6B–D**, these genes were primarily enriched in extracellular matrix organization, myeloid leukocyte activation, blood vessel development, response to wounding, and T cell activation, some of which exhibited immunologic characteristics.

Gene set enrichment analysis (GSEA) was subsequently utilized to distinguish the signaling pathways involved in the LGGs between the high and low SERPINE1 expression groups. Significant difference was demonstrated (FDR<0.05) in the MSigDB collection enrichment (c2.Cp.Keg.v7.2.symbols). As shown in Figures, antigen processing and presentation, B cell receptor signaling pathway, chemokine signaling pathway, cytokine cytokine receptor interaction, natural killer cell mediated cytotoxicity, primary immunodeficiency, T cell receptor signaling pathway, and Toll-like receptor signaling pathway were enriched in the SERPINE1 high expression group from the TCGA cohort (**Figure 6E** and **Supplementary Table 4**). Similar results were

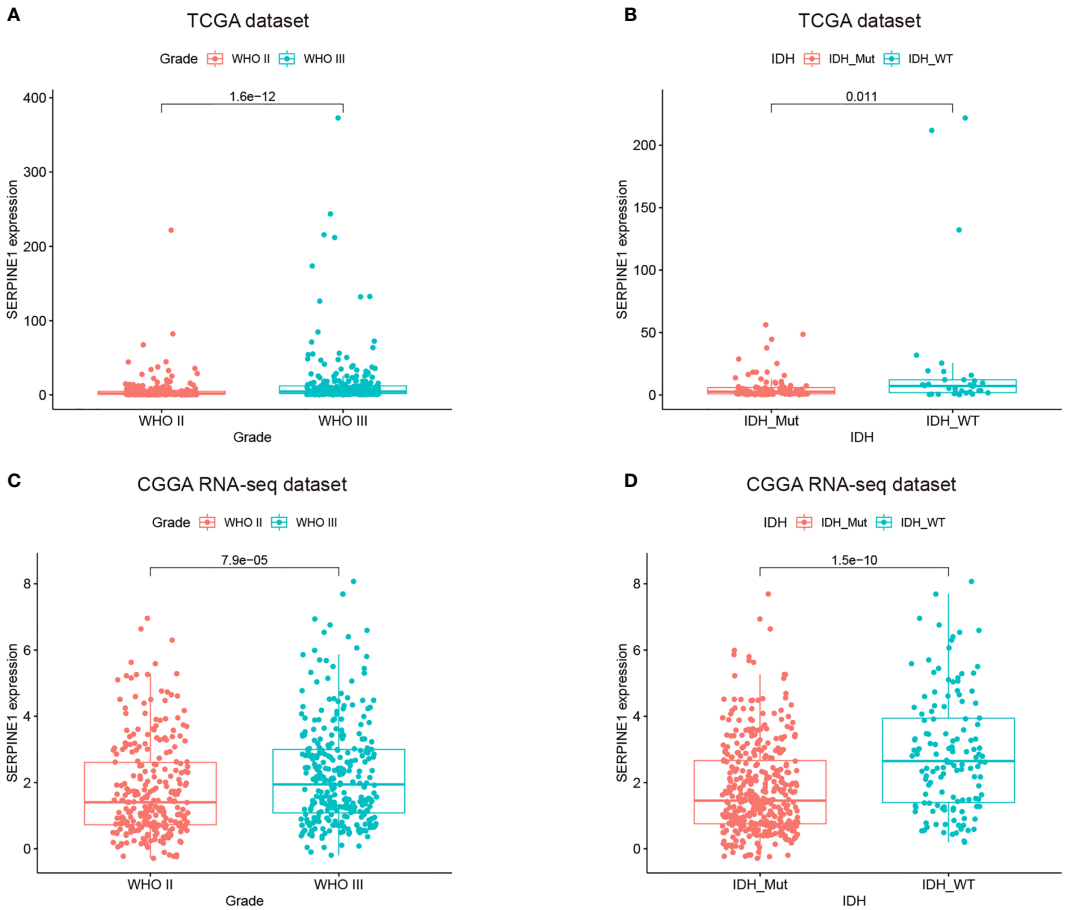

FIGURE 4 | The expressions of SERPINE1 increased with the grades of gliomas and was upregulated in the IDH wild-type LGGs. **(A, C)** SERPINE1 was highly expressed in WHO grade III glioma. **(B, D)** SERPINE1 was significantly elevated in IDH wild-type glioma.

obtained in the CGGA dataset (**Figure 6F** and **Supplementary Table 4**), evidently suggesting that SERPINE1 might serve as a crucial factor in regulating immune-related biological processes and pathways in the glioma microenvironment.

SERPINE1 Regulated the Infiltration of Immune Cells in the LGGs

Considering that SERPINE1 might play a role in regulating immune-related responses in the LGGs, the abundance of 22 types of infiltrating immune cells in the TCGA (**Figure 7A**) and CGGA datasets (**Figure 7C**) were examined *via* using the CIBERSORT algorithm. The results showed that NK cells, monocytes, and macrophages accounted for a reasonably large proportion of the 22 immune cell types, which might suggest close involvements of these three cell types in the development of LGGs. And the correlations among 22 types of infiltrating immune cells were weak to moderate in the LGG cohort. Clearly, M2 macrophages presented highly negative correlations with activated mast cells, and eosinophils positively correlated with activated mast cells (**Supplementary Figures 4A, B**). By comparing the proportion of each immune cell type between high- and low-SERPINE1 expression groups, we found that the groups with high-SERPINE1 expression in both of the TCGA and CGGA datasets exhibited relatively low level of monocytes infiltration and high level of infiltration of M0 macrophages and naive CD4+ T cells (**Figures 7B, D**). In addition, Spearman correlation analysis found that SERPINE1 expression was significantly associated with the infiltration of several immune cell types in LGG. In both of TCGA and CGGA datasets, SERPINE1 expression was positively correlated with the infiltration of M0 macrophages (**Figures 7E, I**), neutrophils (**Figures 7F, J**), follicular helper T-cells (**Figures 7G, K**), and negatively correlated with the infiltration of monocytes (**Figures 7H, L**). **Supplementary Figures 4C-J** presented other immune cells related to SERPINE1 expression. Then, we performed ICH staining to identify the content of TAMs (CD68, CD163), neutrophils (CD66b, MPO), monocytes (HLA-DR, CD14), and follicular helper T-cells (CXCR5, ICOS) in LGG tissues. The results showed that the content of TAMs and neutrophils in the PAI-1 high expression group was significantly higher than that in the PAI-1 low expression group (**Supplementary Figures 5A, B**). Between the two groups, there was no significant difference in the

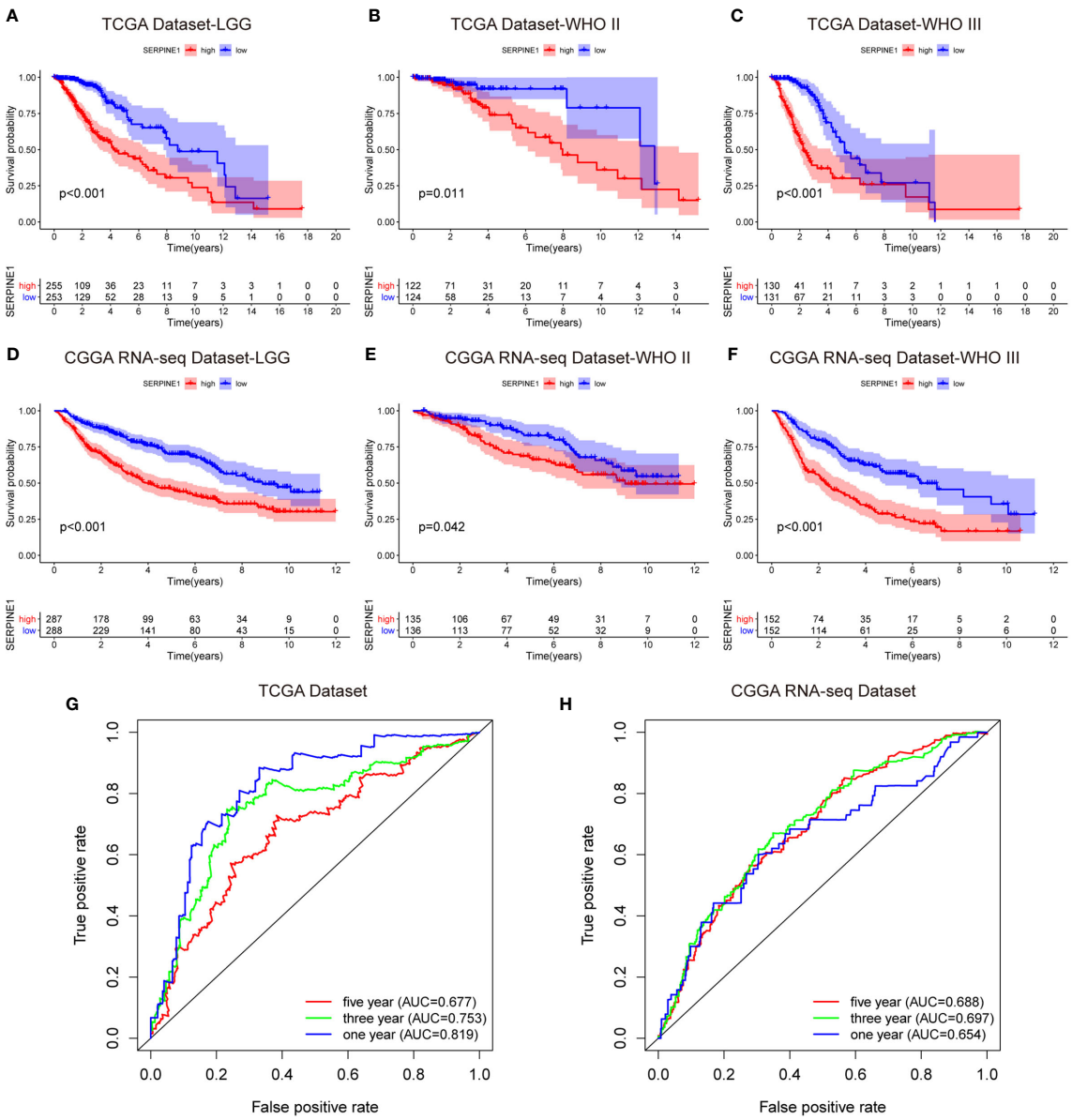

FIGURE 5 | SERPINE1 high expression predicted an unfavorable prognosis in the LGG patients. **(A, D)** Kaplan-Meier overall survival analysis of SERPINE1 expression in all LGG patients. **(B, E)** Kaplan-Meier overall survival analysis of SERPINE1 expression in patients with grade II glioma. **(C, F)** Kaplan-Meier overall survival analysis of SERPINE1 expression in patients with grade III glioma. **(G, H)** ROC curve analysis of SERPINE1 in LGG patients. P-value < 0.05 was considered statistically significant.

infiltration of monocytes and follicular helper T-cells (**Supplementary Figures 5C, D**). Altogether, it was suggested that SERPINE1 expression did influence the immune cell infiltration in the LGG microenvironment, especially the macrophages and neutrophils.

SERPINE1-Related Inflammatory Responses

Considering the important role of inflammation in host immune reaction to the tumor as well as tumor immunotherapy, we further analyzed the associations between SERPINE1 and different inflammatory responses. Therefore, seven clusters of metagenes (**Supplementary Table 6**), representing different types of inflammatory and immune responses, were selected to analyze the association between SERPINE1 and different inflammatory responses (43). The expression pattern of these metagenes in the TCGA dataset was presented in the **Figure 8A**. As showcased in the heatmap, SERPINE1 expression positively correlates with HCK-, Interferon-, LCK-, MHC_I-, MHC_II-, and STAT1-related genes but negatively with IgG-related genes.

TABLE 2 | Univariate analysis and multivariate analysis of overall survival in the LGG cohort.

Datasets	Characteristic	Univariate			Multivariate		
		HR	95%CI	P.value	HR	95%CI	P.value
TCGA	Age	3.311	2.245-4.883	<0.001	3.110	2.090-4.627	0.009
	Gender	0.901	0.632-1.284	0.565	–	–	–
	Grade	3.434	2.323-5.076	<0.001	1.265	0.199-8.030	0.803
	Radiotherapy	2.001	1.289-3.131	0.002	14.639	0.821-261.099	0.068
	Corticosteroids	1.622	1.046-2.516	0.031	80.121	4.702-136.525	0.002
	IDH status	0.181	0.067-0.484	<0.001	0.067	0.008-0.516	0.009
	SERPINE1	1.010	1.006-1.014	<0.001	1.009	1.002-1.016	0.029
CGGA	Age	1.189	0.943-1.500	0.143	–	–	–
	Gender	1.112	0.881-1.404	0.372	–	–	–
	Grade	2.878	2.231-3.714	<0.001	3.177	2.418-4.175	<0.001
	Radiotherapy	1.011	0.756-1.351	0.943	–	–	–
	Chemotherapy	1.275	0.990-1.643	0.060	–	–	–
	IDH status	0.435	0.338-0.560	<0.001	0.694	0.525-0.917	0.001
	1p19q status	0.275	0.199-0.378	<0.001	0.319	0.226-0.449	<0.001
	MGMT status	0.795	0.618-1.024	0.075	–	–	–
	SERPINE1	1.008	1.006-1.011	<0.001	1.004	1.001-1.007	0.023

To verify the result of heatmap analysis, we convert the expression data of these metagenes into enrichment scores *via* Gene set variation analysis (GSVA). Then, the correlogram was used to display the correlation between seven inflammatory metagene signatures and SERPINE1 (**Figure 8C**). This analysis showed that SERPINE1 was positively related with the signature of HCK, Interferon, LCK, MHC_I, MHC_II, and STAT1 but was negatively associated with IgG, a marker for B lymphocytes activities. Moreover, the analysis based on the CGGA dataset gave identical results (**Figures 8B, D**).

Correlation Analysis Between SERPINE1 and Immune Checkpoints

According to the above study, SERPINE1 was not only identified as an immune-related gene but might affect the infiltration of immune cells in the TME. Considering that suppressive mechanisms in the TME exerted a critical role in the immune evasion of glioma cells (19), we took a step further to explore the potential association between SERPINE1 and some crucial immune checkpoints. Spearman correlation analysis was used to analyze the correlation between SERPINE1 and the immune checkpoint-related genes, including PD-1, PD-L1, PD-L2, CTLA4, TIM-3, IDO1, B7-H4, and LAG3. Correlation matrix plots indicated that SERPINE1 was correlated significantly with several immune checkpoints in the TCGA (**Figure 9A**) and CGGA dataset (**Figure 9B**). Notably, SERPINE1 showed significant positive relationships with PD-1, PD-L1, and PD-L2 both in TCGA and CGGA datasets. Moreover, Kaplan-Meier survival analysis demonstrated that LGG patients with low levels of SERPINE1 and PD1 exhibited appreciably longer overall survival than those with high levels of SERPINE1 and PD1 expression (**Figures 9C, F**). Similar results were obtained in the analysis of SERPINE1 combined with PD-L1(**Figures 9D, G**) and PD-L2(**Figures 9E, H**). In short, these results indicated that SERPINE1 and some immune checkpoints such as PD-1, PD-L1, PD-L2 might act synergistically in the progression of LGGs.

DISCUSSION

Treatments of LGGs have remained a huge challenge to clinicians due to the aggressive nature and high risk of recurrence (44). Although tremendous efforts have been made to improve the clinical outcome, the prognosis of LGG patients has not been substantially improved in the last decades (45, 46). Therefore, it is necessary to develop novel treatment strategies for glioma patients. In recent years, immunotherapy for gliomas has attracted increasing attention to scientists, based on the continuous in-depth research on the immune TME. For example, some studies have corroborated that combination of PD-1 blockade and local radiotherapy prolonged the survival time of an orthotopic glioma mouse model (47). However, due to the immunosuppressive microenvironment in glioblastoma, PD-1/PD-L1 checkpoint blockades have not made breakthroughs in glioblastoma treatment (48). And the detailed molecular mechanisms of the immune responses in the glioma microenvironment have not been clarified, which greatly limits the development of effective immunotherapies to treat gliomas. This study investigated the TME of LGGs and screened out the prognosis-related immune genes based on the TCGA and CGGA databases, which may provide a new perspective to find potential therapeutic targets for gliomas.

In the screening phase, we used the ESTIMATE algorithm to calculate the immune cell and stromal cell scores for each LGG sample from the TCGA database. We found that high immune or stromal scores tended to predict poor prognosis. WHO grade III or IDH wild-type gliomas, as expected, had higher immune and stromal scores. Similar results were observed in the research of glioblastoma and osteosarcoma (49, 50). These results evidently confirmed that the infiltrative level of immune and stromal cells was correlated with tumor malignancy and prognosis. Subsequently, based on the immune and stromal scores, 1576 differentially expressed genes were screened out. GO and KEGG pathway enrichment analyses further verified a close involvement of these DEGs in the immunologic processes. Additionally, out of

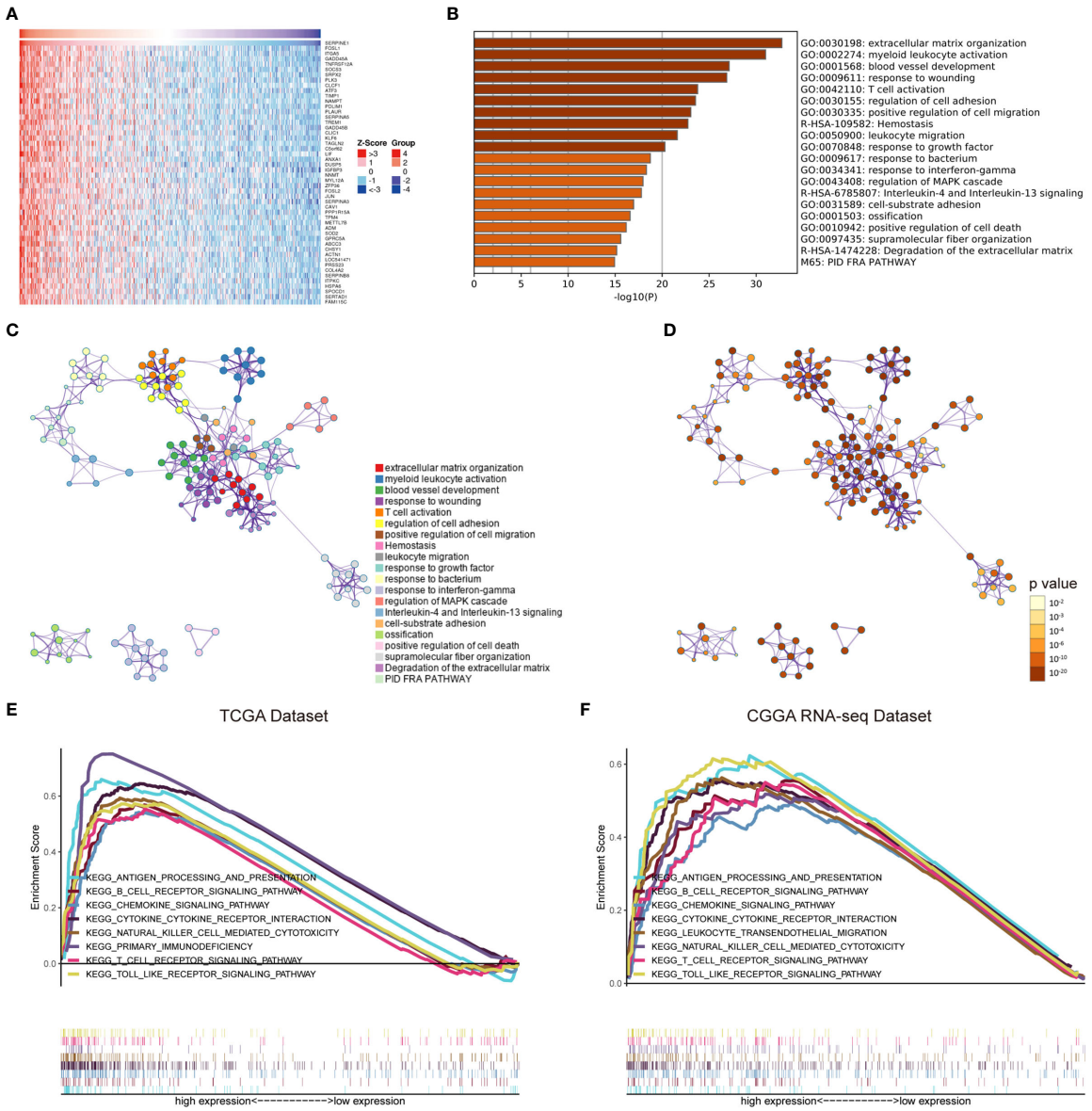

FIGURE 6 | The potential functions of SERPINE1. **(A)** Heatmap of SERPINE1 positively correlated genes. **(B)** Bar graph showing the top 20 enriched terms of SERPINE1 positively correlated genes. The color depth denoted the p-value. Network plot of enriched terms: **(C)** each node represented one enriched term colored by its cluster ID; **(D)** colored by p-value. GSEA enrichment analysis of SERPINE1 in LGG datasets: **(E)** the KEGG pathways enriched in high SERPINE1 expression group of TCGA dataset; **(F)** CGGA dataset. P-value < 0.05 was considered statistically significant.

the 1576 DEGs, 54 survival-related genes were obtained by the univariate Cox regression analysis, and 46 hub genes were filtered out through the cytoHubba plugin in Cytoscape software. In this way, the target gene SERPINE1 was ultimately selected at the intersection of the survival-related genes and hub genes.

SERPINE1 encodes plasminogen activator inhibitor type 1 (PAI-1), which serves as the primary inhibitor of urokinase plasminogen activator (uPA) and tissue-type plasminogen activator (tPA) (23). Previous studies have primarily focused on its role in thrombosis. However, in recent years, high-throughput sequencing results showed that SERPINE1 was aberrantly overexpressed in various types of tumors. It has also been reported that SERPINE1 was mainly produced by stromal cells in the TME and thus might exert its tumor-promoting function by regulating the interactions between tumor cells and the microenvironment (51). Currently, SERPINE1 as a tumor-promoting factor has been studied in breast cancer, gastric cancer, and head and neck squamous cell carcinoma. For instance, Yang et al. reported that SERPINE1 was an independent predictor of poor prognosis for gastric

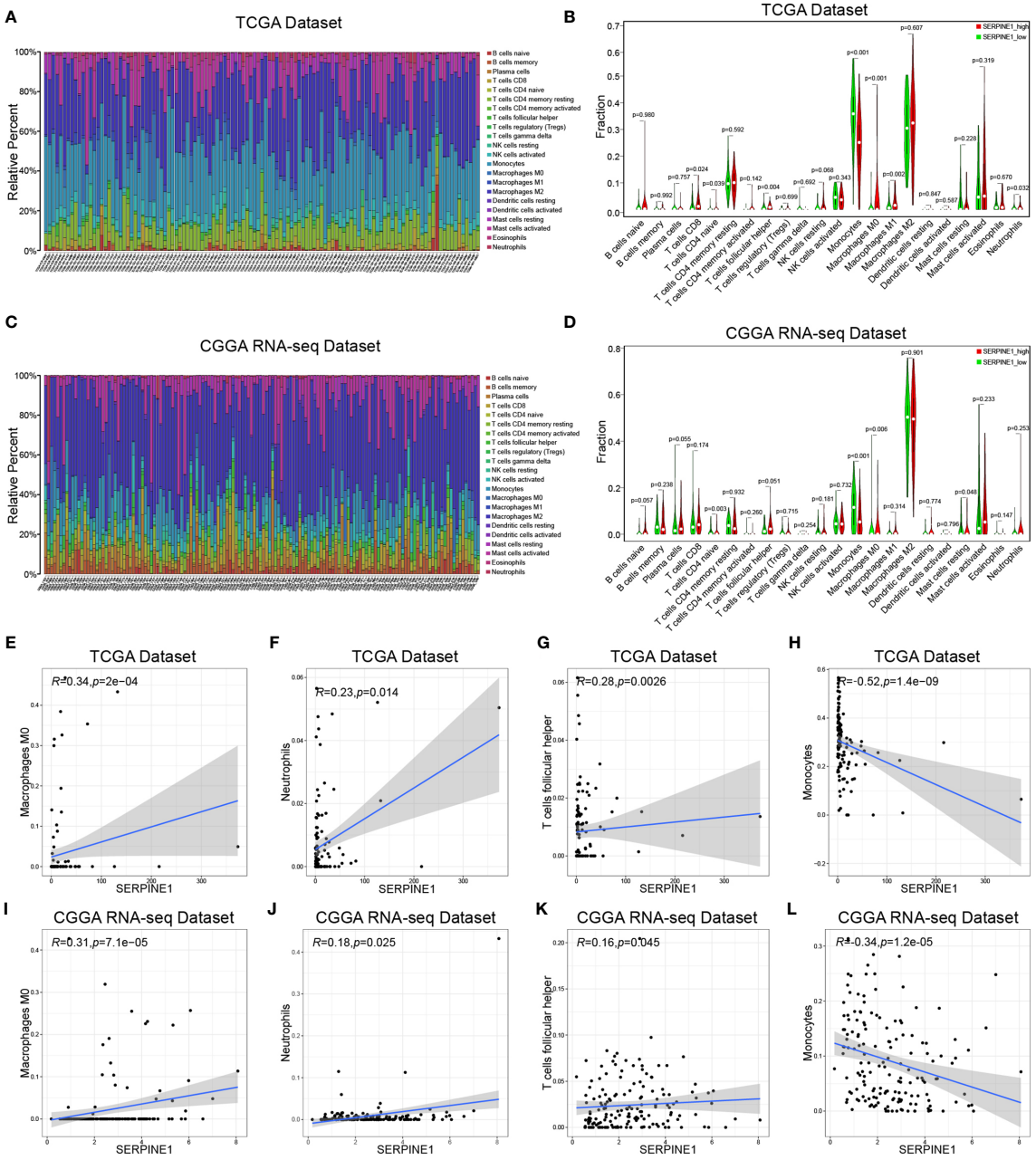

FIGURE 7 | SERPINE1 regulated the infiltration of immune cells in the LGGs. The immune infiltration landscape of LGGs: **(A, C)** bar plots showing the proportion of 22 immunocyte types in TCGA dataset and CGGA dataset. **(B, D)** Violin plots showing the differences in the proportion of 22 immunocyte types between SERPINE1 high and low expression groups. Red colors represented the group with SERPINE1 high expression; green color represented the group with SERPINE1 low expression. The SERPINE1 expression was positively correlated with the infiltration of M0-type macrophages **(E, I)**, neutrophils **(F, J)**, follicular helper T cells **(G, K)**, and negatively associated with monocytes **(H, L)**. P-value < 0.05 was considered statistically significant.

adenocarcinoma and it promoted tumor cell proliferation, migration, and invasion by regulating epithelial-mesenchymal transition (EMT) (26). Likewise, both *in vivo* and *in vitro* experiments confirmed that SERPINE1 knock-down could inhibit glioma growth and invasiveness (27). Nevertheless, the molecular mechanisms of SERPINE1 were still obscure in gliomas, particularly its regulatory mechanisms in the TME of gliomas.

We subsequently analyzed the expression characteristics of SERPINE1 in the LGGs based on the TGCA, CGGA, and GEPIA2 databases. Compared with the normal brain tissues, SERPINE1 was significantly upregulated in the LGGs. Besides, the expression levels of SERPINE1 were higher in the WHO grade III or IDH wild-type gliomas. According to the previous studies, high grade or IDH wild-type gliomas are often associated

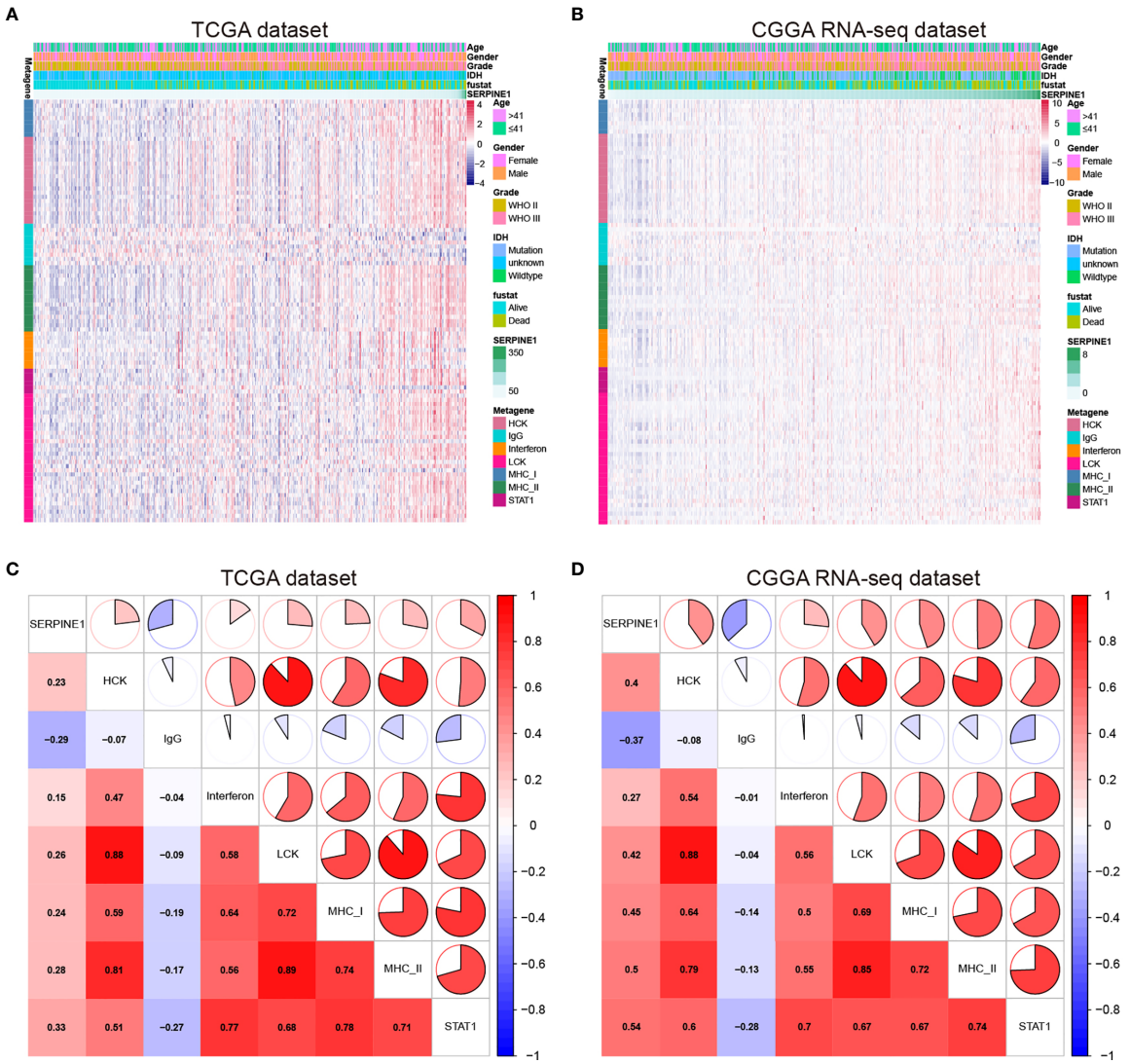

FIGURE 8 | SERPINE1-related inflammatory responses in LGG. **(A, C)** Heatmaps showing the relationship between SERPINE1 and seven metagenes in TCGA and CGGA datasets. **(B, D)** Correlogram showing the correlation between SERPINE1 and seven metagenes in TCGA and CGGA datasets.

with poor prognosis (52). As a result, it was rational to hypothesize that SERPINE1 was a tumor-promoting factor and positively correlated with the malignancy of LGGs. Kaplan-Meier analysis indeed indicated that higher SERPINE1 expression predicted shorter overall survival in the LGG patients. ROC analysis further revealed that SERPINE1 could function as a sensitive indicator predicting one-year, three-year, and five-year survival rates for the LGG patients. Moreover, we found that SERPINE1 was an independent prognostic factor for overall survival using the Cox multivariate analysis. Taken together, we speculated that SERPINE1 was a valuable prognostic biomarker for the LGGs.

To further investigate the potential mechanisms of SERPINE1 in the LGGs, we examined the top 500 genes positively related to SERPINE1 in the LGGs *via* the LinkedOmics website. These related genes were mainly enriched in immune-response related processes, such as myeloid leukocyte activation (GO:0002274), T cell activation (GO:0042110). Besides, gene set enrichment analysis (GSEA) was performed to investigate the biological functions of SERPINE1 in the LGGs based on the TCGA and CGGA database. Likewise, the GSEA results demonstrated that many immune-response related processes existed in the group with high SERPINE1 expression. Taken together, SERPINE1 was an immune-related gene and was involved in the immune processes in the TME of the LGGs. Considering that immune-related genes often conducted their functions by regulating immune cell behaviors, we utilized the CIBERSORT algorithm to assess the proportions of 22 types of immune cells in the microenvironment of LGGs. The results showed that SERPINE1 affected immune cell infiltrations. The group with high

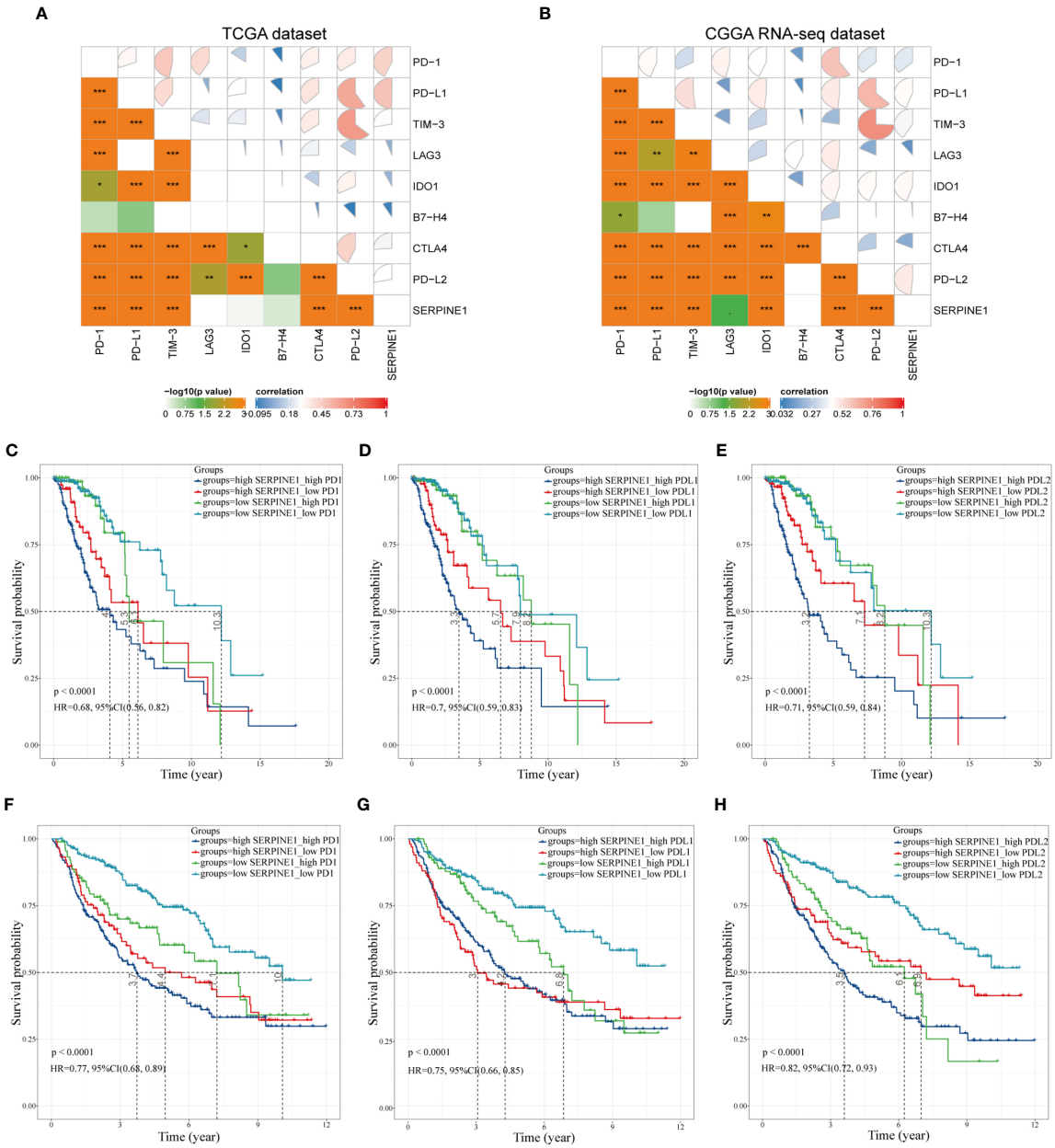

FIGURE 9 | Correlation analysis between SERPINE1 and immune checkpoints. **(A, B)** Correlation matrix plots of SERPINE1 and major immune checkpoints in the TCGA dataset and CGGA dataset. **(C, F)** Kaplan–Meier survival analysis in LGG patients stratified by SERPINE1 and PD-1 expression. **(D, G)** Kaplan–Meier survival analysis in LGG patients stratified by SERPINE1 and PD-L1 expression. **(E, H)** Kaplan–Meier survival analysis in LGG patients stratified by SERPINE1 and PD-L2 expression. P-value < 0.05 was considered statistically significant. *p-value ≤ 0.05; **p-value ≤ 0.01; ***p-value ≤ 0.001.

expression of SERPINE1 harbored a higher proportion of T cells follicular helper, neutrophils, macrophages M0, and a lower proportion of monocytes. Moreover, we confirmed through ICH staining that TAMs and neutrophils were highly infiltrated in LGG with high PAI-1 expression. As we all know, immune cells are critical components of the TME and have been confirmed to influence tumor behavior and patient prognosis (53). Although tumor-associated microglia/macrophages (TAMs) accounted for the higher proportion of all infiltrating immune cells in the glioma TME, their capacities were not sufficient to cause antitumor immune responses (54). On the other hand, they could secrete copious amounts of anti-inflammatory cytokines to develop an immunosuppressive microenvironment (54, 55). Likewise, neutrophil was known to activate immune response and mediate tissue damage in the inflammatory response, however, tumor-associated neutrophils

(TANs) exerted an immunosuppressive role in the TME (56). The activation and recruitment of neutrophils could directly or indirectly affect the recruitment and differentiation of the TAMs, which was important for tumor progression and the maintenance of the TME (57). Moreover, there was initial evidence suggesting that PAI-1 can affect the biological behavior of inflammatory cells. For example, Sakamoto et al. (58) found that PAI-1 that abnormally elevated in esophageal squamous cell carcinoma (ESCC) could promote macrophage infiltration by the Akt and Erk1/2 signaling pathways. And studies indicated that PAI-1 could assist IL-8-mediated neutrophil infiltration *via* inhibiting IL-8/Heparan Sulfate/Syndecan-1 Complex shedding on endothelial cell surfaces (59). In the analysis of SERPINE1 and seven immune metagenes, we found that SERPINE1 expression was particularly correlated with macrophage- and T-cell-related, but not B cell-related immune responses. These results suggested that SERPINE1 is a negative prognostic factor for LGG and plays an important role in the regulation of immune responses. Thus, we speculated that the negative effects of SERPINE1 on the LGGs might be associated with the infiltrations of macrophages and neutrophils.

In this study, SERPINE1, as an immune-related gene, was screened out and was confirmed to affect immune cell infiltrations in the LGG microenvironment. Given the importance of immunotherapy in gliomas, we took a step further to analyze the correlation between SERPINE1 and immune checkpoint genes in the TCGA- and CGGA-LGG datasets. Indeed, SERPINE1 exhibited significant correlations with the immune checkpoints, especially PD-1, PD-L1, and PD-L2, and might synergize with them. It has been demonstrated that the interaction of PD-1 and PD-L1 was a critical mechanism for tumor cells to evade immune surveillance. Blockade of PD-1/PD-L1 could enhance the anti-tumoral T cell immune responses (60). Pembrolizumab and nivolumab, the PD-1 immune checkpoint inhibitors, have received FDA approval for the treatment of metastatic melanoma and non-small-cell lung cancer (61). Moreover, ACT001, which directly targeted PAI-1, has been reported to suppress glioma cell proliferation, migration, and invasion *via* inhibiting the PI3K/AKT pathway (62). Whether ACT001 and pembrolizumab/nivolumab have synergistic effects in the treatment of gliomas will be the subject of our future research.

In summary, we screened SERPINE1 in the immune-related differential genes and further explored its expression features and biological functions in the LGG cohorts through bioinformatic analysis. The results indicated that SERPINE1 could not only act as a prognostic biomarker but also function as a potential therapeutic target for gliomas.

DATA AVAILABILITY STATEMENT

The datasets presented in this study can be found in online repositories. The names of the repository/repositories and accession number(s) can be found in the article/**Supplementary Material**.

AUTHOR CONTRIBUTIONS

XH designed this study and drafted the manuscript. XH, FZ, and DH collected and performed data analysis. XJ, JG, WL, and YW contributed to figures and tables. QL and TX reviewed and edited the manuscript. All authors contributed to the article and approved the submitted version.

FUNDING

This work was supported by Natural Science Foundation of China (Grant NO. 81972340, No.81871196, No.81471517), Science and Technology Project of Jinan city (Grant NO. 201907048), Key Projects of Natural Science Foundation of Jiangxi Province (Grant NO. 20192ACB20011), Shandong Provincial Natural Science Foundation, China (Grant No. ZR2018MH005), Shandong Province Key Research and Development Program (Grant No. 2019GSF107046).

SUPPLEMENTARY MATERIAL

The Supplementary Material for this article can be found online at: https://www.frontiersin.org/articles/10.3389/fonc.2021.646060/full#supplementary-material

Supplementary Figure 1 | Relationship between the immune, stromal, ESTIMATE scores and the clinical characteristics of the LGG patients. **(A–C)** The distribution of immune score, stromal score, ESTIMATE score at different ages. **(D–F)** The distribution of immune score, stromal score, ESTIMATE score in different genders. P-value<0.05 was considered statistically significant.

Supplementary Figure 2 | Protein-protein interaction (PPI) network of DEGs visualized by Cytoscape software (v3.7.2) (Confidence score=0.97). Node size indicated its connectivity (the larger the node, the more proteins interacted). Red nodes represented upregulated genes, while blue nodes downregulated genes.

Supplementary Figure 3 | (A) The difference in TIMP1 expression between LGG samples and normal brain samples was not statistically significant. **(B)** SERPINE1 expression was significantly higher in LGG samples than in normal brain samples. (*represent p-value<0.05) **(C)** The batch effect between mRNAseq_693 dataset and mRNAseq_325 dataset from the CGGA database was removed by the "sva" R package. **(D, F)** The expression level of SERPINE1 mRNA in LGG at different ages. **(E, G)** The expression level of SERPINE1 mRNA in LGG in different genders. P-value<0.05 was considered statistically significant.

Supplementary Figure 4 | (A, B) Correlation matrix plots of 22 immunocyte types in TCGA dataset and CGGA dataset. **(C–E)** Immune cells related to SERPINE1 expression in TCGA dataset. **(F–J)** Immune cells related to SERPINE1 expression in CGGA dataset. P-value<0.05 was considered statistically significant.

Supplementary Figure 5 | (A) The biomarkers of TAMs (CD68, CD163) were detected by immunohistochemistry staining in LGG samples. **(B)** The biomarkers of neutrophils (CD66b, MPO) were detected by immunohistochemistry staining in LGG samples. **(C)** The biomarkers of monocytes (CD14, HLA-DR) were detected by immunohistochemistry staining in LGG samples. **(D)** The biomarkers of follicular helper T-cells (CXCR5, ICOS) were detected by immunohistochemistry staining in LGG samples.

REFERENCES

1. Ilkhanizadeh S, Lau J, Huang M, Foster DJ, Wong R, Frantz A, et al. Glial Progenitors as Targets for Transformation in Glioma. *Adv Cancer Res* (2014) 121:1–65. doi: 10.1016/b978-0-12-800249-0.00001-9
2. Louis DN, Perry A, Reifenberger G, von Deimling A, Figarella-Branger D, Cavenee WK, et al. The 2016 World Health Organization Classification of Tumors of the Central Nervous System: A Summary. *Acta Neuropathol* (2016) 131(6):803–20. doi: 10.1007/s00401-016-1545-1
3. Wesseling P, Capper D. Who 2016 Classification of Gliomas. *Neuropathol Appl Neurobiol* (2018) 44(2):139–50. doi: 10.1111/nan.12432
4. Cancer Genome Atlas Research N, Brat DJ, Verhaak RG, Aldape KD, Yung WK, Salama SR, et al. Comprehensive, Integrative Genomic Analysis of Diffuse Lower-Grade Gliomas. *New Engl J Med* (2015) 372(26):2481–98. doi: 10.1056/NEJMoa1402121
5. Kiran M, Chatrath A, Tang X, Keenan DM, Dutta A. A Prognostic Signature for Lower Grade Gliomas Based on Expression of Long non-Coding Rnas. *Mol Neurobiol* (2019) 56(7):4786–98. doi: 10.1007/s12035-018-1416-y
6. Feng E, Liang T, Wang X, Du J, Tang K, Wang X, et al. Correlation of Alteration of HLA-F Expression and Clinical Characterization in 593 Brain Glioma Samples. *J Neuroinflamm* (2019) 16(1):33. doi: 10.1186/s12974-019-1418-3
7. Sun Z, Li Y, Wang Y, Fan X, Xu K, Wang K, et al. Radiogenomic Analysis of Vascular Endothelial Growth Factor in Patients With Diffuse Gliomas. *Cancer Imaging Off Publ Int Cancer Imaging Soc* (2019) 19(1):68. doi: 10.1186/s40644-019-0256-y
8. Arneth B. Tumor Microenvironment. *Med (Kaunas Lithuania)* (2019) 56(1). doi: 10.3390/medicina56010015
9. Ribeiro Franco PI, Rodrigues AP, de Menezes LB, Pacheco Miguel M. Tumor Microenvironment Components: Allies of Cancer Progression. *Pathol Res Pract* (2020) 216(1):152729. doi: 10.1016/j.prp.2019.152729
10. Noy R, Pollard JW. Tumor-Associated Macrophages: From Mechanisms to Therapy. *Immunity* (2014) 41(1):49–61. doi: 10.1016/j.immuni.2014.06.010
11. Sica A, Larghi P, Mancino A, Rubino L, Porta C, Totaro MG, et al. Macrophage Polarization in Tumour Progression. *Semin Cancer Biol* (2008) 18(5):349–55. doi: 10.1016/j.semcancer.2008.03.004
12. Lei X, Lei Y, Li JK, Du WX, Li RG, Yang J, et al. Immune Cells Within the Tumor Microenvironment: Biological Functions and Roles in Cancer Immunotherapy. *Cancer Lett* (2020) 470:126–33. doi: 10.1016/j.canlet.2019.11.009
13. Chin SM, Kimberlin CR, Roe-Zurz Z, Zhang P, Xu A, Liao-Chan S, et al. Structure of the 4-1BB/4-1BBL Complex and Distinct Binding and Functional Properties of Utomilumab and Urelumab. *Nat Commun* (2018) 9(1):4679. doi: 10.1038/s41467-018-07136-7
14. Li L, Goedegebuure SP, Gillanders WE. Preclinical and Clinical Development of Neoantigen Vaccines. *Ann Oncol Off J Eur Soc Med Oncol* (2017) 28 (suppl_12):xii11–xii7. doi: 10.1093/annonc/mdx681
15. Aguiar PNJr., De Mello RA, Barreto CMN, Perry LA, Penny-Dimri J, Tadokoro H, et al. Immune Checkpoint Inhibitors for Advanced non-Small Cell Lung Cancer: Emerging Sequencing for New Treatment Targets. *ESMO Open* (2017) 2(3):e000200. doi: 10.1136/esmoopen-2017-000200
16. Gellrich FF, Schmitz M, Beissert S, Meier F. Anti-PD-1 and Novel Combinations in the Treatment of Melanoma-An Update. *J Clin Med* (2020) 9(1). doi: 10.3390/jcm9010223
17. Koshkin VS, Grivas P. Emerging Role of Immunotherapy in Advanced Urothelial Carcinoma. *Curr Oncol Rep* (2018) 20(6):48. doi: 10.1007/s11912-018-0693-y
18. Qin H, Yu H, Sheng J, Zhang D, Shen N, Liu L, et al. Pi3kgamma Inhibitor Attenuates Immunosuppressive Effect of Poly(l-Glutamic Acid)-Combretastatin A4 Conjugate in Metastatic Breast Cancer. *Advanced Sci (Weinheim Baden-Wurttemberg Germany)* (2019) 6(12):1900327. doi: 10.1002/advs.201900327
19. Ma Q, Long W, Xing C, Chu J, Luo M, Wang HY, et al. Cancer Stem Cells and Immunosuppressive Microenvironment in Glioma. *Front Immunol* (2018) 9:2924. doi: 10.3389/fimmu.2018.02924
20. Wu A, Wei J, Kong LY, Wang Y, Priebe W, Qiao W, et al. Glioma Cancer Stem Cells Induce Immunosuppressive Macrophages/Microglia. *Neuro-oncology* (2010) 12(11):1113–25. doi: 10.1093/neuonc/noq082
21. Panni RZ, Linehan DC, DeNardo DG. Targeting Tumor-Infiltrating Macrophages to Combat Cancer. *Immunotherapy* (2013) 5(10):1075–87. doi: 10.2217/imt.13.102
22. Yang L, Zhang Y. Tumor-Associated Macrophages: From Basic Research to Clinical Application. *J Hematol Oncol* (2017) 10(1):58. doi: 10.1186/s13045-017-0430-2
23. Huang J, Sabater-Lleal M, Asselbergs FW, Tregouet D, Shin SY, Ding J, et al. Genome-Wide Association Study for Circulating Levels of PAI-1 Provides Novel Insights Into its Regulation. *Blood* (2012) 120(24):4873–81. doi: 10.1182/blood-2012-06-436188
24. Li S, Wei X, He J, Tian X, Yuan S, Sun L. Plasminogen Activator Inhibitor-1 in Cancer Research. *Biomed Pharmacother Biomed Pharmacother* (2018) 105:83–94. doi: 10.1016/j.biopha.2018.05.119
25. Dellas C, Loskutoff DJ. Historical Analysis of PAI-1 From its Discovery to its Potential Role in Cell Motility and Disease. *Thromb Haemostasis* (2005) 93 (4):631–40. doi: 10.1160/th05-01-0033
26. Yang JD, Ma L, Zhu Z. SERPINE1 as a Cancer-Promoting Gene in Gastric Adenocarcinoma: Facilitates Tumour Cell Proliferation, Migration, and Invasion by Regulating EMT. *J Chemother (Florence Italy)* (2019) 31(7-8):408–18. doi: 10.1080/1120009x.2019.1687996
27. Seker F, Cingoz A, Sur-Erdem İ, Erguder N, Erkent A, Uyulur F, et al. Identification of SERPINE1 as a Regulator of Glioblastoma Cell Dispersal With Transcriptome Profiling. *Cancers* (2019) 11(11). doi: 10.3390/cancers11111651
28. Yoshihara K, Shahmoradgoli M, Martínez E, Vegesna R, Kim H, Torres-Garcia W, et al. Inferring Tumour Purity and Stromal and Immune Cell Admixture From Expression Data. *Nat Commun* (2013) 4:2612. doi: 10.1038/ncomms3612
29. Liu X, Li Y, Qian Z, Sun Z, Xu K, Wang K, et al. A Radiomic Signature as a non-Invasive Predictor of Progression-Free Survival in Patients With Lower-Grade Gliomas. *NeuroImage Clin* (2018) 20:1070–7. doi: 10.1016/j.nicl.2018.10.014
30. Zhao Z, Meng F, Wang W, Wang Z, Zhang C, Jiang T. Comprehensive RNA-seq Transcriptomic Profiling in the Malignant Progression of Gliomas. *Sci Data* (2017) 4:170024. doi: 10.1038/sdata.2017.24
31. Leek JT, Johnson WE, Parker HS, Jaffe AE, Storey JD. The Sva Package for Removing Batch Effects and Other Unwanted Variation in High-Throughput Experiments. *Bioinf (Oxford England)* (2012) 28(6):882–3. doi: 10.1093/bioinformatics/bts034
32. Ritchie ME, Phipson B, Wu D, Hu Y, Law CW, Shi W, et al. Limma Powers Differential Expression Analyses for RNA-sequencing and Microarray Studies. *Nucleic Acids Res* (2015) 43(7):e47. doi: 10.1093/nar/gkv007
33. Yu G, Wang LG, Han Y, He QY. clusterProfiler: An R Package for Comparing Biological Themes Among Gene Clusters. *Omics J Integr Biol* (2012) 16 (5):284–7. doi: 10.1089/omi.2011.0118
34. Zhou Y, Zhou B, Pache L, Chang M, Khodabakhshi AH, Tanaseichuk O, et al. Metascape Provides a Biologist-Oriented Resource for the Analysis of Systems-Level Datasets. *Nat Commun* (2019) 10(1):1523. doi: 10.1038/s41467-019-09234-6
35. Szklarczyk D, Gable AL, Lyon D, Junge A, Wyder S, Huerta-Cepas J, et al. String v11: Protein-Protein Association Networks With Increased Coverage, Supporting Functional Discovery in Genome-Wide Experimental Datasets. *Nucleic Acids Res* (2019) 47(D1):D607–d13. doi: 10.1093/nar/gky1131
36. Shannon P, Markiel A, Ozier O, Baliga NS, Wang JT, Ramage D, et al. Cytoscape: A Software Environment for Integrated Models of Biomolecular Interaction Networks. *Genome Res* (2003) 13(11):2498–504. doi: 10.1101/gr.1239303
37. Hänzelmann S, Castelo R, Guinney J. GSVA: Gene Set Variation Analysis for Microarray and RNA-seq Data. *BMC Bioinf* (2013) 14:7. doi: 10.1186/1471-2105-14-7
38. Heagerty PJ, Lumley T, Pepe MS. Time-Dependent ROC Curves for Censored Survival Data and a Diagnostic Marker. *Biometrics* (2000) 56(2):337–44. doi: 10.1111/j.0006-341x.2000.00337.x
39. Newman AM, Liu CL, Green MR, Gentles AJ, Feng W, Xu Y, et al. Robust Enumeration of Cell Subsets From Tissue Expression Profiles. *Nat Methods* (2015) 12(5):453–7. doi: 10.1038/nmeth.3337
40. Yu G. Gene Ontology Semantic Similarity Analysis Using Gosemsim. *Methods Mol Biol (Clifton NJ)* (2020) 2117:207–15. doi: 10.1007/978-1-0716-0301-7_11

41. Cohen AL, Holmen SL, Colman H. IDH1 and IDH2 Mutations in Gliomas. *Curr Neurol Neurosci Rep* (2013) 13(5):345. doi: 10.1007/s11910-013-0345-4
42. Vasaikar SV, Straub P, Wang J, Zhang B. LinkedOmics: Analyzing Multi-Omics Data Within and Across 32 Cancer Types. *Nucleic Acids Res* (2018) 46 (D1):D956–d63. doi: 10.1093/nar/gkx1090
43. Rody A, Holtrich U, Pusztai L, Liedtke C, Gaetje R, Ruckhaeberle E, et al. T-Cell Metagene Predicts a Favorable Prognosis in Estrogen Receptor-Negative and HER2-positive Breast Cancers. *Breast Cancer Res BCR* (2009) 11(2):R15. doi: 10.1186/bcr2234
44. Delgado-López PD, Corrales-García EM, Martino J, Lastra-Aras E, Dueñas-Polo MT. Diffuse Low-Grade Glioma: A Review on the New Molecular Classification, Natural History and Current Management Strategies. *Clin Trans Oncol Off Publ Fed Spanish Oncol Societies Natl Cancer Institute Mexico* (2017) 19(8):931–44. doi: 10.1007/s12094-017-1631-4
45. Claus EB, Walsh KM, Wiencke JK, Molinaro AM, Wiemels JL, Schildkraut JM, et al. Survival and Low-Grade Glioma: The Emergence of Genetic Information. *Neurosurg Focus* (2015) 38(1):E6. doi: 10.3171/2014.10.FOCUS12367
46. Youland RS, Schomas DA, Brown PD, Parney IF, Laack NNI. Patterns of Care and Treatment Outcomes in Older Adults With Low Grade Glioma: A 50-Year Experience. *J Neuro-Oncol* (2017) 133(2):339–46. doi: 10.1007/s11060-017-2439-3
47. Zeng J, See AP, Phallen J, Jackson CM, Belcaid Z, Ruzevick J, et al. Anti-PD-1 Blockade and Stereotactic Radiation Produce Long-Term Survival in Mice With Intracranial Gliomas. *Int J Radiat Oncol Biol Phys* (2013) 86(2):343–9. doi: 10.1016/j.ijrobp.2012.12.025
48. Wang X, Guo G, Guan H, Yu Y, Lu J, Yu J. Challenges and Potential of PD-1/PD-L1 Checkpoint Blockade Immunotherapy for Glioblastoma. *J Exp Clin Cancer Res* (2019) 38(1):87. doi: 10.1186/s13046-019-1085-3
49. Hong W, Yuan H, Gu Y, Liu M, Ji Y, Huang Z, et al. Immune-Related Prognosis Biomarkers Associated With Osteosarcoma Microenvironment. *Cancer Cell Int* (2020) 20:83. doi: 10.1186/s12935-020-1165-7
50. Jia D, Li S, Li D, Xue H, Yang D, Liu Y. Mining TCGA Database for Genes of Prognostic Value in Glioblastoma Microenvironment. *Aging* (2018) 10 (4):592–605. doi: 10.18632/aging.101415
51. Placencio VR, DeClerck YA. Plasminogen Activator Inhibitor-1 in Cancer: Rationale and Insight for Future Therapeutic Testing. *Cancer Res* (2015) 75 (15):2969–74. doi: 10.1158/0008-5472.Can-15-0876
52. Weller M, Wick W, Aldape K, Brada M, Berger M, Pfister SM, et al. Glioma. *Nat Rev Dis Primers* (2015) 1:15017. doi: 10.1038/nrdp.2015.17
53. Yan S, Fang J, Zhu Y, Xie Y, Fang F. Comprehensive Analysis of Prognostic Immune-Related Genes Associated With the Tumor Microenvironment of Pancreatic Ductal Adenocarcinoma. *Oncol Lett* (2020) 20(6):366. doi: 10.3892/ol.2020.12228
54. Gieryng A, Pszczolkowska D, Walentynowicz KA, Rajan WD, Kaminska B. Immune Microenvironment of Gliomas. *Lab Investigation J Tech Methods Pathol* (2017) 97(5):498–518. doi: 10.1038/labinvest.2017.19
55. Xu Y, Liao C, Liu R, Liu J, Chen Z, Zhao H, et al. IRGM Promotes Glioma M2 Macrophage Polarization Through P62/TRAF6/NF-κb Pathway Mediated IL-8 Production. *Cell Biol Int* (2019) 43(2):125–35. doi: 10.1002/cbin.11061
56. Nagaraj S, Schrum AG, Cho HI, Celis E, Gabrilovich DI. Mechanism of T Cell Tolerance Induced by Myeloid-Derived Suppressor Cells. *J Immunol (Baltimore Md 1950)* (2010) 184(6):3106–16. doi: 10.4049/jimmunol.0902661
57. Kim J, Bae JS. Tumor-Associated Macrophages and Neutrophils in Tumor Microenvironment. *Mediators Inflammation* (2016) 2016:6058147. doi: 10.1155/2016/6058147
58. Sakamoto H, Koma Y-I, Higashino N, Kodama T, Tanigawa K, Shimizu M, et al. PAI-1 Derived From Cancer-Associated Fibroblasts in Esophageal Squamous Cell Carcinoma Promotes the Invasion of Cancer Cells and the Migration of Macrophages. *Lab Investigation J Tech Methods Pathol* (2021) 101(3):353–68. doi: 10.1038/s41374-020-00512-2
59. Marshall LJ, Ramdin LSP, Brooks T, Dphil PC, Shute JK. Plasminogen Activator Inhibitor-1 Supports IL-8-mediated Neutrophil Transendothelial Migration by Inhibition of the Constitutive Shedding of Endothelial IL-8/heparan Sulfate/Syndecan-1 Complexes. *J Immunol (Baltimore Md 1950)* (2003) 171(4):2057–65. doi: 10.4049/jimmunol.171.4.2057
60. Xue S, Hu M, Iyer V, Yu J. Blocking the PD-1/PD-L1 Pathway in Glioma: A Potential New Treatment Strategy. *J Hematol Oncol* (2017) 10(1):81. doi: 10.1186/s13045-017-0455-6
61. Kamran N, Alghamri MS, Nunez FJ, Shah D, Asad AS, Candolfi M, et al. Current State and Future Prospects of Immunotherapy for Glioma. *Immunotherapy* (2018) 10(4):317–39. doi: 10.2217/imt-2017-0122
62. Xi X, Liu N, Wang Q, Chu Y, Yin Z, Ding Y, et al. ACT001, a Novel PAI-1 Inhibitor, Exerts Synergistic Effects in Combination With Cisplatin by Inhibiting PI3K/AKT Pathway in Glioma. *Cell Death Dis* (2019) 10(10):757. doi: 10.1038/s41419-019-1986-2

Conflict of Interest: The authors declare that the research was conducted in the absence of any commercial or financial relationships that could be construed as a potential conflict of interest.

frontiers in Immunology

ORIGINAL RESEARCH
published: 24 May 2021
doi: 10.3389/fimmu.2021.637053

Programmed Cell Death 10 Mediated CXCL2-CXCR2 Signaling in Regulating Tumor-Associated Microglia/Macrophages Recruitment in Glioblastoma

Quan Zhang[1,2†], Junwen Wang[1†], Xiaolong Yao[1,3], Sisi Wu[1], Weidong Tian[1,4], Chao Gan[1], Xueyan Wan[1], Chao You[1], Feng Hu[1], Suojun Zhang[1], Huaqiu Zhang[1], Kai Zhao[1], Kai Shu[1*] and Ting Lei[1]*

[1] Department of Neurosurgery, Tongji Hospital, Tongji Medical College, Huazhong University of Science and Technology, Wuhan, China, [2] Department of Neurosurgery, Beijing Tiantan Hospital, Capital Medical University, Beijing, China, [3] Department of Neurosurgery, The Third People's Hospital of Hubei Province, Wuhan, China, [4] Department of Neurosurgery, First Affiliated Hospital of Medical College, Shihezi University, Xinjiang, China

OPEN ACCESS

Edited by:
Valérie Dutoit, Université de Genève, Switzerland

Reviewed by:
Lisa Sevenich, Georg Speyer Haus, Germany
Bozena Kaminska, Nencki Institute of Experimental Biology (PAS), Poland

***Correspondence:**
Kai Zhao
zhaokai@tjh.tjmu.edu.cn
Kai Shu
kshu@tjh.tjmu.edu.cn

[†]These authors have contributed equally to this work

Specialty section:
This article was submitted to Cancer Immunity and Immunotherapy, a section of the journal Frontiers in Immunology

Received: *02 December 2020*
Accepted: *06 May 2021*
Published: *24 May 2021*

Citation:
Zhang Q, Wang J, Yao X, Wu S, Tian W, Gan C, Wan X, You C, Hu F, Zhang S, Zhang H, Zhao K, Shu K and Lei T (2021) Programmed Cell Death 10 Mediated CXCL2-CXCR2 Signaling in Regulating Tumor-Associated Microglia/Macrophages Recruitment in Glioblastoma. Front. Immunol. 12:637053. doi: 10.3389/fimmu.2021.637053

Background: Programmed cell death 10 (PDCD10) plays a crucial role in regulating tumor phenotyping, especially in glioblastoma (GBM). Glioma-associated microglia/macrophages (GAMs) in tumor pathological microenvironment contribute to GBM progression. We previously found that the infiltration of GAMs was associated with PDCD10 expression in GBM patients. The present study aims to further explore the regulation of PDCD10 on GAMs in GBM.

Methods: Overexpression of *PDCD10* in human- and murine-GBM cells was established by lentiviral transduction. Cell behaviors and polarization of primary microglia, microglia- and macrophage-like cells were investigated through indirect co-culture with GBM cells *in vitro* respectively. The PDCD10-induced release of chemokines was identified by a chemokine protein array. The cross-talk between GBM and microglia as well as macrophages was further studied using selective antagonist SB225002. Finally, an orthotopic homograft mouse model was employed to verify the results of *in vitro* experiments.

Results: Indirect co-culture with *PDCD10*-overexpressed GBM cells promoted proliferation and migration of microglia- and macrophage-like cells, and stimulated pro-tumorigenic polarization of primary microglia, microglia- and macrophage-like cells. *Pdcd10*-upregulated GBM cells triggered a nearly 6-fold increase of CXC motif chemokine ligand 2 (CXCL2) release, which in turn activated CXC chemokine receptor 2 (CXCR2) and downstream Erk1/2 and Akt signaling in primary microglia, microglia- and macrophage-like cells. The blockage of CXCR2 signaling with specific inhibitor (SB225002) abolished microglia- and macrophage-like cell migration induced by *PDCD10*-upregulated GBM cells. Moreover, *Pdcd10*-upregulated GL261 cells promoted GAMs recruitment and tumor growth *in vivo*.

Conclusion: Our study demonstrates that overexpression of *PDCD10* in GBM recruits and activates microglia/macrophages, which in turn promotes tumor progression. CXCL2-CXCR2 signaling mediated by PDCD10 is potentially involved in the crosstalk between GBM cells and GAMs.

Keywords: glioblastoma, CXCR2, CXCl2, SB225002, tumor-associated microglia/macrophages (TAM), programmed cell death 10 (PDCD10)

INTRODUCTION

Glioblastoma (GBM) is the most common primary malignant tumor in central nervous system, accounting for 57.3% of gliomas with poor prognosis (1). Five-year survival rate is only 6.8% despite the combine application of aggressive surgical resection, chemotherapy and radiation (2). Characterized as a heterogeneous neoplasm, tumor microenvironment (TME) in GBM consists of various types of cells including tumor cells, endothelial cells, tumor-associated microglia/macrophages (TAMs) and numerous soluble factors like cytokines. TAMs, which are also named as glioma- associated microglia/macrophages (GAMs), account for up to 30% of tumor mass in human GBM (3). The interaction between tumor cells and TME modulated tumor progression (4). GAMs are composed of resident microglia and monocyte-derived macrophages (MDMs) which enter the brain through the compromised blood brain barrier under pathologic status (5). Accumulating evidences suggest that TAMs play a crucial role in tumorigenesis and progression (6, 7). The accumulation and activation of GAMs in GBM niche promoted tumor growth and invasion, while depletion of GAMs inhibited tumor growth (8, 9). Novel therapeutic strategies targeting TAMs have achieved a curative effect in various cancers *in vitro* (10, 11). However, these medications did not improve the patient prognosis (7). The infiltration of TAMs in tumors was mediated by numerous chemotactic factors produced by tumor cells and TME cells including C-C motif ligand 2 (CCL2), CX3C chemokine ligand 1 (CX3CL1), stromal cell-derived factor-1 (SDF-1), colony-stimulating factor-1 (CSF-1) and periostin (POSTN) etc. (12). These facts raised our consideration to define a novel therapeutic approach targeting the interaction of tumors and GAMs.

Programmed cell death 10 *(PDCD10)*, originally named TF-1 cell apoptosis related gene 15, is also known as cerebral cavernous malformation 3 (*CCM3*) (13). Mutations of CCM3 resulted in human familial cerebral cavernous malformation. PDCD10 is widely expressed in various types of cells, such as astrocyte, neuron, endothelial cells and tumor cells. PDCD10 is the component of striatin-interacting phosphatase and kinase (STRIPAK) complex, plays an important role in the modulation of germinal center kinases III activity, vascular endothelial-derived growth factor receptor 2 (VEGF-R2) internalization, Golgi assembly and cell polarity (14). Endothelial loss of *PDCD10* promoted cell proliferation, migration, sprouting and tube formation (13). In central nerve system, PDCD10 played a critical role in neuron-glial unit and neo-neuron migration (15, 16). *Pdcd10*-deficiency in gut epithelium augmented CCM formation in a mouse model, indicating the PDCD10 function in a gut-brain axis (17). Altered expression of *PDCD10* had been reported in various tumors including breast cancer, prostate cancer, bladder cancer etc., playing dual function in tumor progression and chemo-therapy resistance (18–20).

The function of PDCD10 in GBM is still unclear. Previous report indicated that loss of *PDCD10* in GBM activated tumor cell behaviors and mediated chemotherapy resistance (21). However, clinical data from The Cancer Genome Atlas (TCGA) shows that *PDCD10* is upregulated in GBM patients, revealing a positive correlation with poor prognosis (**Figure S1**). We focused on PDCD10 function and reported previously a paracrine mechanism triggered by endothelial-PDCD10 (22). Most recently, we found that GAMs infiltration was positively correlated with PDCD10-positive staining in specimens generated from GBM patients, which was consistent with the findings from TIMER database described in **Figure S2**. Taken together, we assumed that PDCD10 in GBM played a role in the recruitment and activation of GAMs. To this end, we performed indirect co-culture experiments and employed an orthotopic homograft mouse model to investigate the underlying mechanism. As a result, we demonstrate overexpression of PDCD10 in GBM recruits and activates microglia/macrophages, which in turn promotes tumor progression. CXC motif chemokine ligand 2/CXC motif chemokine receptor 2 (CXCL2-CXCR2) signaling mediated by PDCD10 is potentially involved in the crosstalk between GBM cells and GAMs.

MATERIAL AND METHODS

GBM Patients' Samples

Thirty-four specimens were obtained from patients who underwent surgical treatments from 2015 to 2018 in Tongji Hospital and histologically confirmed as GBM postoperatively. This study was approved by Ethical Committee of Tongji Hospital, Tongji Medical College, Huazhong University of Science and Technology in accordance with the Helsinki Criteria. Informed consent was obtained from all individual patients included in this study.

Animals

C57BL/6J mice used for isolation of primary microglia or for orthotopic homograft implantation were purchased from SPF Biotechnology Co. Ltd., Beijing, China. C57BL/6J mice of mixed sex were bred and kept in the animal center of Tongji Medical College, Huazhong University of Science and Technology. All the experiments were performed following the ARRIVE

(Animals in research reporting *in vivo* experiments) Guidelines and were approved by the Committee on Animal Research of Tongji Medical College, Huazhong University of Science and Technology.

Cell Culture and Mouse Primary Microglial Isolation

Murine GBM cell line GL261 (National Cancer Institute, Frederick, USA), microglia-like cell line BV2 and human GBM cell lines U251 (China Center for Type Culture Collection, CCTCC, Wuhan, China), murine monocyte/macrophage cell line RAW264.7 and human GBM cell lines U373 (American Type Culture Collection, ATCC, Manassas, USA) were cultured in Dulbecco's modified Eagle's medium (DMEM, Gibco, Carlsbad, USA) supplemented with 10% fetal bovine serum (FBS, Gibco), 200 mM glutamine, 50 units/ml penicillin and 50 μg/ml streptomycin. Human monocyte cell line THP1 (ATCC) were cultured in RPMI1640 (Gibco) with 10% FBS and 200 mM glutamine. To perform following experiments, THP1 was pretreated with phorbol myristate acetate (PMA, Sigma-Aldrich, St. Louis, USA) 100 ng/ml for 2 days, to obtain differentiated macrophage-like cells (THP1-mac).

Mouse primary microglia was isolated from neonatal C57BL/6J mice. Briefly, the forebrains were completely digested by 0.125% trypsin and DNase (Sigma) and centrifuged at 1500 rpm for 15 min. The cell pellet was suspended in culture medium and filtrated with a 40 μm cell filter (Millipore, Darmstadt, Germany). Then, the cell mixture was incubated in a poly-L-lysine pre-coated flask for 14 days. Microglia detached after shaking flask at 220 rpm for 1 h at 37 °C. The supernatant containing microglia was collected and centrifuged (1000 rpm for 5 min). Then, microglia were routinely cultured in DMEM with10% FBS. Iba1 staining was used for verification of isolated primary microglia.

Human *PDCD10* and Murine *Pdcd10* -Upregulated GBM Cell Line Generation

The lentiviral vectors for human *PDCD10* (ox*PDCD10*, Cat#29650-13) and murine *Pdcd10* (ox*Pdcd10*, Cat#43748) and corresponding empty vectors (LVCON238 for human species, Ch and LVCON254 for murine, Cm) were purchased from GenePharma, Shanghai, China. The infection of lentiviral-*PDCD10/Pdcd10* and corresponding controls in human (U251 and U373) and murine GBM cell lines (GL261) was respectively performed according to manufacturer's instructions. After selection by 2 μg/μl puromycin (Sigma), the PDCD10 upregulation was confirmed by RT^2-PCR and Western Blot.

Cell Proliferation, Migration and Cell Morphology Study

The conditioned medium (CM) and control medium (C) were prepared from ox*PDCD10*/ox*Pdcd10* and corresponding empty vectors transducted GBM cells respectively. Briefly, the same number of GBM cells was incubated in culture dishes with equal volume of DMEM supplemented with 10% of FBS and 200 mM glutamine for 48 hours. Then, the media were harvested, centrifuged and used for the following experiments. Cell behavior studies were performed by incubation with CM or control medium. For cell proliferation assay, 5.0×10^3 cells were seeded into 96-well-plate with respective media derived from GBM cells. After 72 hours incubation, the cell proliferation was detected by CCK8 reagent (Boster Biological Technology, Pleasanton, USA). To perform scratch assay, 5.0×10^5 cells were seeded in 6-well-plate overnight. A thin stripe was scratched by a pipette tip. Then, cells were incubated with CM or control medium for 24 hours. The migrated area was photographed by a microscope (Olympus Corporation, Tokyo, Japan). For transwell assay, 3×10^6 *PDCD10/Pdcd10*-upregulated- or control-GBM cells with corresponding medium was added into 24-well-plate. Then, 1.0×10^5 cells were suspended and seeded in the inserts of transwell system (8 μm pore, Corning Life Sciences, NY, USA), which was placed in 24-well-plate. After 48 hours incubation, migrated cells were fixed with 4% of formalin and stained with crystal violet. The numbers of migrated cells were counted. The morphology of cells including primary microglia, microglia- and macrophage-like cells was observed through regular microscope. The number of spindle-shaped cells and the average length of cellular processes were measured using Image J software. To determine whether inhibition of CXCR2 signaling suppressed microglia- and macrophage-like cell migration induced by ox*PDCD10*-GBM cells, SB225002 (Cat#S7651, Selleck Chemicals, Houston, USA), a selective CXCR2 antagonist, was used with optimized concentrations. Generally, each *in vitro* experiment was performed for at least 3 times with 3 technical replicates.

RT^2-PCR and Western Blot

RNA extraction was performed using Axygen AxyPrep Kit (Corning Life Sciences) according to the manufacture's protocol. cDNA was synthesized using PrimeScript RT Kit (Takara Bio Inc., Shiga, Japan). The PCR reaction was performed using TB Green kit (Takara Bio Inc.) with standard procedure in CFX Systems (Bio-Rad, Hercules, USA). Sequences of human and mouse primers were shown in **Supplemental Data** (**Table S1**). Relative expression of target genes was quantified using 2^{-ddCt} method, normalized to the reference gene.

Protein extraction and Western blot were carried out as previous description (22). The following antibodies was used: PDCD10, GAPDH (each 1:1000 dilution, Abcam, Cambridge, UK), Iba1 (1:500, Abcam), CXCR2 (1:500, Abclonal, Wuhan, China), p-Erk1/2, Erk1/2, p-Akt and Akt (each 1:1000 dilution, Cell signaling technology, Danvers, USA).

Protein Array

The protein array was carried out using a mouse chemokines array kit (Cat#: ARY020, R&D Systems, Minneapolis, USA). Two identical membranes precoated with antibodies against 25 different chemokines were incubated with media derived from ox*Pdcd10*- and control-GL261 cells respectively. The following procedure was performed according to the manufacturer's instructions. The semi-quantification of the dots was analyzed by ImageJ software.

Immunohistochemical (IHC) and Immunofluorescent (IF) Staining

IHC and IF staining were respectively performed according to the protocols described in our previous publication (22). We did use PBS and related lysis buffer to perfuse blood cells before IHC and IF for GAMs. For IHC-staining, the sections were incubated with primary antibodies as follows: PDCD10 (1:200) and anti-Iba1 (1:200). Images were acquired by an Olympus microscope. To perform double-IF staining, the following primary antibodies mixtures were applied on the sections: PDCD10 (anti-rabbit, 1:200) and Iba1 (anti-goat, 1:200); CXCR2 (anti-rabbit, 1:100) and Iba1 (anti-goat, 1:200). Negative control sections were incubated with nonimmune IgG. Slides were counterstained with DAPI (1:500). The images were acquired using a confocal microscope (LSM800, Carl Zeiss, Jena, Germany).

Orthotopic Homograft Mouse Model

An orthotopic homograft model was employed by using 6-8 weeks old and mixed sex C57BL/6J mice (20-25 g). Mice were given ox*Pdcd10*- (ox*Pdcd10*) or control-GL261 cells (C) by cerebral orthotopic injection using mouse intracranial stereotactic injection system (RWD, Shenzhen, China). Briefly, mice were anesthetized and immobilized by a head holder. After skin incision, the skull was drilled at the point which located at 1mm anterior and 1.5 mm lateral to the bregma. Then, 2 μl cell suspension containing 3 x 10^5 cells was slowly injected into the brain by a microsyringe. The needle was slowly retracted and the skin was sutured by a surgical histoacryl. To evaluate whether inhibition of CXCR2 signaling reduced *in vivo* microglia/macrophages recruitments induced by oxPDCD10-GL261 cells, mice were intraperitoneally injected with SB225002 (5 mg/kg, Selleck Chemicals) daily, beginning on the eighth day after implantation for a whole period of 21 days. Twenty-eight days after implantation, the mice were sacrificed. The brain containing homograft tumors were totally removed and prepared for further studies. Iba1-positive cells were quantified using Image J software in high magnification images.

Statistical Analysis

The statistical analysis was performed using IBM SPSS 23.0 software. Data was described as mean and standard deviation (Means ± SD). Student's t-test and ANOVA were respectively used for analyzing the differences between two groups and multiple groups. Pearson's correlation analysis was used to determine the correlation between two groups. Statistical significance was established as $p<0.05$.

RESULTS

PDCD10 Overexpression in GBM Patients Was Positively Correlated With Infiltration of GAMs

The PDCD10 and Iba1 expression in human GBM specimens was detected by Western Blot. The semi-quantification of the blots demonstrated a positive correlation between PDCD10 and Iba1 expression ($p<0.01$) (**Figure 1A**). Moreover, IHC-staining on adjacent slices from different GBM patients showed that Iba1-labelled cells were dominantly observed in those patients with high expression of PDCD10 (**Figure 1B**). Scatter plot analysis indicated a positive correlation between the quantification of PDCD10- and Iba1-positive cells ($p<0.05$) (**Figure 1B**). In addition, the altered expression of PDCD10 in different areas of single slice was also observed by IF-staining (**Figure 1C** left panel). Notably, the Iba1-labelled GAMs were dominantly detected in the area with massive PDCD10 expression (**Figure 1C** middle and right panel).

Cultured Medium From *PDCD10*-Upregulated GBM Cells Activated Microglia and Macrophages *In Vitro*

To explore the effect of PDCD10 in GBM on microglia and macrophages *in vitro*, two *PDCD10*-overexpressed human GBM cell lines was established (ox*PDCD10*-U251 and ox*PDCD10*-U373) (**Figures 2A, B**). THP1-mac cells cultured with CM derived from ox*PDCD10*-U251 ($p<0.001$) and ox*PDCD10*-U373 ($p<0.01$) showed a significantly higher proliferation rate than that with the corresponding control media (**Figure 2C**). Increase of migration ability in THP1-mac cells mediated by ox*PDCD10*-U251 ($p<0.01$ and $p<0.001$ respectively) and ox*PDCD10*-U373 ($p<0.05$, respectively) were identified by scratch assay (**Figure 2D**) and transwell assay (**Figure 2E**) respectively. After incubation with medium derived from ox*PDCD10*-GBM cells, most THP1-mac cells displayed a morphological change (**Figure 2F, G**), revealing a spindle-shaped cell type as well as a longer cellular process in THP1 cells ($p<0.001$, respectively). Further studies shown in **Figure 2H** revealed that a significant increase in *IL-10, IL-6, arg-1* ($p<0.001$) and *NOS2* ($p<0.05$) was detected in CM-treated THP1-mac cells, indicating a pro-tumorigenic polarization induced by ox*PDCD10*-CM.

Subsequently, we performed similar experiments using murine cells. Upregulation of *Pdcd10* was established by lentiviral-*Pdcd10* transduction in murine GBM cell line GL261 (**Figure 3A, B**). A significant increase of cell proliferation was detected in BV2 and RAW264.7 after incubation with medium derived from ox*Pdcd10*-GL261 cells for 72 hours ($p<0.01$, respectively) (**Figure 3C**). Scratch assay reveled a 1.8- and 1.4-fold increase of migrated area in BV2 and RAW264.7 cells treated with ox*Pdcd10*-CM compared with the corresponding controls ($p<0.01$, respectively) (**Figure 3D**). Furthermore, more migrated cells were detected in ox*Pdcd10*-CM treated BV2 and RAW264.7 cells in comparison with control medium treated cells by transwell assay ($p<0.001$, respectively) (**Figure 3E**). To evaluate the morphological and functional change in microglia and macrophages, mouse primary microglia and macrophage-like cells (RAW264.7) were respectively incubated with culture medium (Blank), control GL261-medium (C) and ox*Pdcd10*-GL261 medium (ox*Pdcd10*) for 24 hours. Unstimulated primary microglial and RAW264.7 cells in blank group displayed a round-shape without protrusions (left panel of **Figures 3F, G**). In comparison with blank group, more spindle-shaped cells with

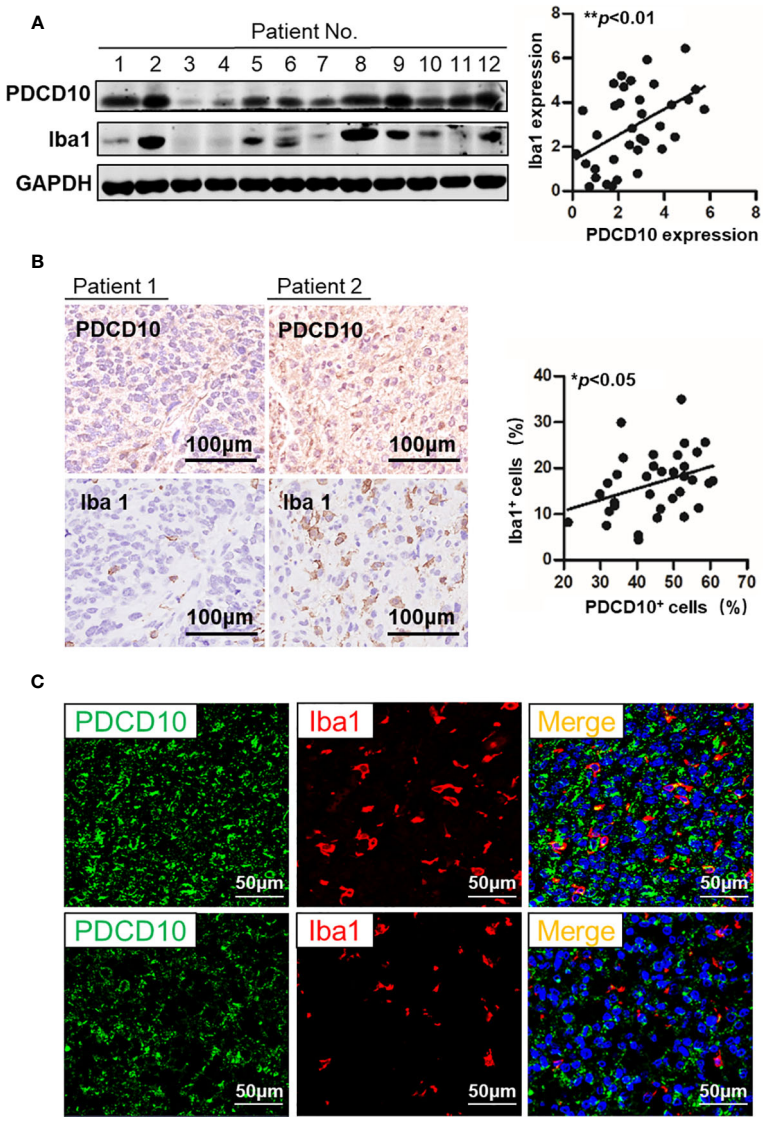

FIGURE 1 | The expression of PDCD10 in glioblastoma (GBM) patients displayed a positive correlation with the infiltration of glioma-associated microglia/macrophages (GAMs). **(A)** Western blot of PDCD10 and Iba1 in GBM patients. Representative blots showed the expression of PDCD10 and Iba1 in GBM patients. Semi-quantification of the blots revealed a positive correlation between PDCD10 and Iba1 expression. **(B)** Immunohistochemical staining of PDCD10 and Iba1 on the adjacent sections of GBM patients. Quantitative analysis revealed that the number of GAMs was positively correlated with that of PDCD10-positive staining cells. **(C)** Immunofluorescent staining of PDCD10 and Iba1 in representative GBM patient. The altered immunoreactivity of PDCD10 (left panel) and Iba-1 (middle panel) were identified in various tumor regions. As shown in double staining (right panel), a massive number of Iba1-labelled GAMs (red) was observed in high PDCD10-immunoreactivity (green) areas. *p< 0.05; **p< 0.01.

longer process were observed in control- and ox*Pdcd10*-groups (p<0.001, respectively). In particular, medium generated from ox*Pdcd10*-GL261 induced a more visible morphological change in both primary microglia and RAW264.7 than that in corresponding control groups (p<0.001) (**Figure 3F**). IF-staining of Iba1 in primary microglia suggested a similar cell morphological change after treatment by medium from ox*Pdcd10*-GL261 (**Figure 3G**). As shown in **Figure 3H**, a heat-map was used to illustrate the change of the related markers in murine primary microglia, BV2 and RAW264.7 cells. In detail, *IL-10*, *IL-6* and a*rg-1* were significantly elevated after ox*Pdcd10*-CM treatment in comparison with control (p<0.05).

Upregulation of *Pdcd10* in GBM Increased Microglia/Macrophages Recruitment and Promoted Tumor Growth *In Vivo*

GL261 (C) and ox*Pdcd10*-GL261 cells (ox*Pdcd10*) were orthotopically implanted into mice brain. Stable overexpression of PDCD10 *in vivo* was confirmed by Western blot (p<0.01) (**Figure 4A**), IHC- (**Figure 4B**) and IF-staining of PDCD10

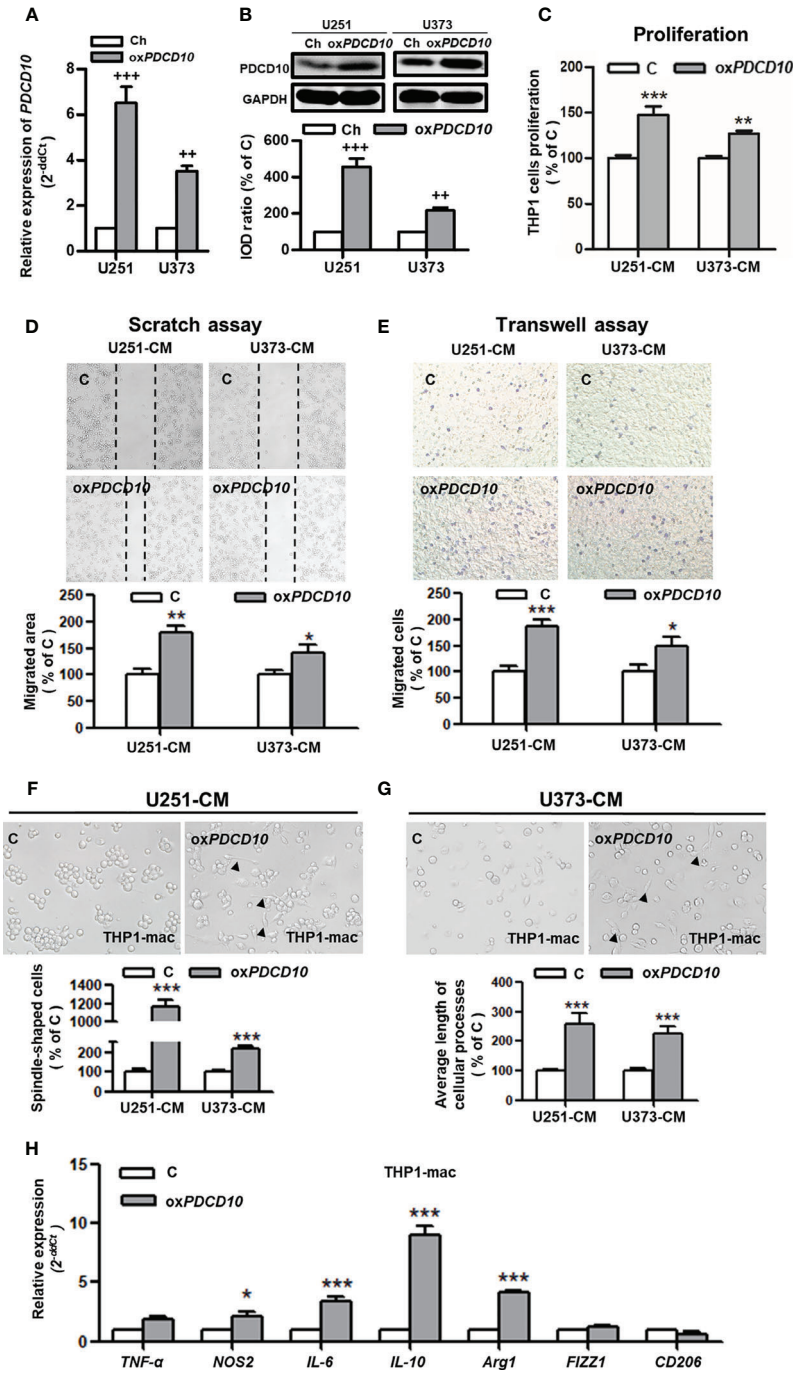

FIGURE 2 | Overexpression of *PDCD10* in human GBM cells activated macrophages *in vitro*. Human GBM cell lines (U251 and U373) were transducted by lentivirus vectors containing human *PDCD10* (ox*PDCD10*) and empty vector (Ch) respectively. **(A, B)** PDCD10 overexpression was confirmed by RT^2-PCR **(A)** and Western blot **(B)**. Macrophage-like cells (THP1-mac) were generated by the treatment of human THP1 cells with 100 ng/ml prorbol myristate acetate. Then, cells were incubated with conditioned medium (CM) and control medium derived from ox*PDCD10*- (ox*PDCD10*) and control-GBM cells **(C)** respectively. **(C)** Cell proliferation was detected by CCK-8 assay. **(D, E)** Cell migration was measured by scratch assay and transwell assay. For scratch assay **(D)**, migrated area of THP1-mac cells was measured 48 hours after scratching. To perform transwell assay **(E)**, THP1-mac cells were seeded into the insert of transwell system with serum-free medium. CM or control medium was added into the lower chamber. After incubation for 24 hours, the migrated cells were counted after crystal violet staining in a high magnification. **(F, G)** THP1-mac cell morphology study. After incubation with medium derived from ox*PDCD10*-U251 **(F)** or ox*PDCD10*-U373 **(G)** GBM cells, most THP1-mac cells displayed a morphological change including a higher percentage of spindle-shaped cell type as well as a longer cellular process (arrowheads). **(H)** The relative gene expressions in THP1-mac cells were detected by RT^2-PCR. $^{++}p<0.01$ and $^{+++}p<0.001$, compared with Ch; $^{*}p<0.05$, $^{**}p < 0.01$ and $^{***}p < 0.001$, compared with **(C)**.

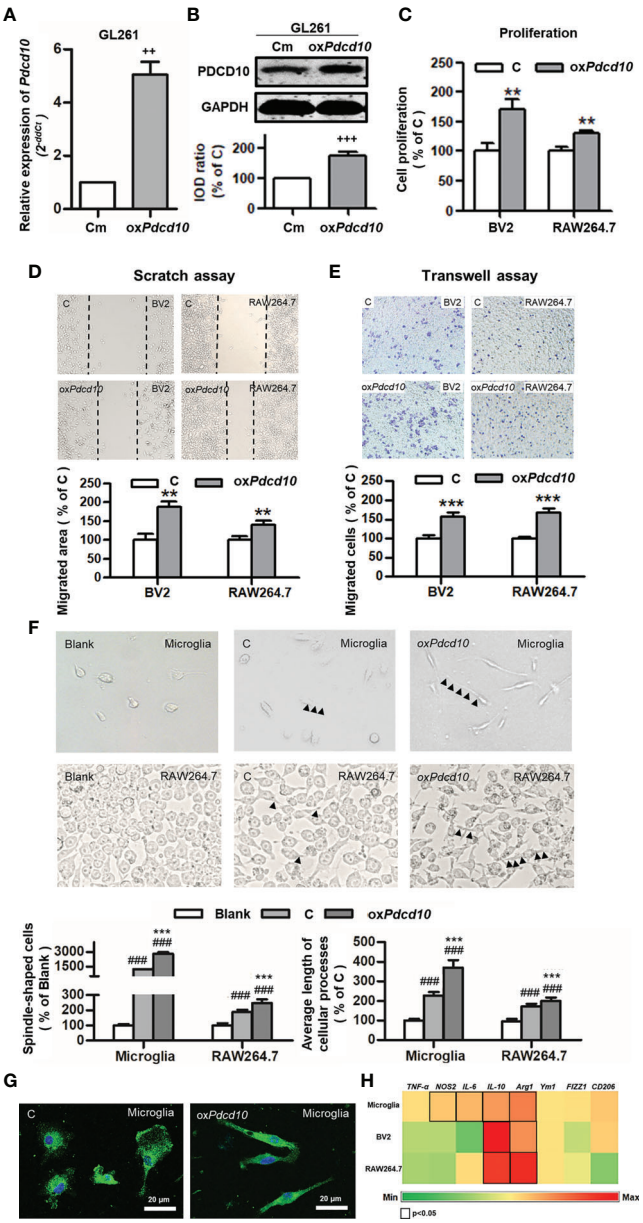

FIGURE 3 | Overexpression of *Pdcd10* in murine GBM cells activated microglia and macrophages *in vitro*. **(A, B)** Stable upregulation of *Pdcd10* in murine GBM cell line GL261 (ox*Pdcd10*) was established by the transduction of lentivirus vector. The control cells (Cm) were transducted with empty vector. The PDCD10 upregulation was confirmed at mRNA **(A)** and protein levers **(B)**. The murine microglia-like cell line (BV2), macrophage-like cell line (RAW264.7) and primary microglia (microglia) were used in the following experiments. **(C)** Medium derived from ox*Pdcd10*-GL261 cells (CM) promoted cell proliferation in BV2 and RAW264.7 cells. Cell proliferation was detected by CCK-8 assay. **(D, E)** CM activated cell migration in BV2 and RAW264.7 cells. For scratch assay **(D)**, BV2 and RAW264.7 cells was seeded in a 6-well-plate followed by media replacement with CM and control medium **(C)** retrospectively. 48 hours after scratching, the migrated area was automatic calculated by image J software. The transwell assay **(E)** was performed using BV2 and RAW264.7 cells. Cells were suspended with serum-free media and seeded into upper insert. CM or control medium was added into the lower chamber. **(F)** The morphological features of primary microglia and RAW264.7 cells. Primary microglia mostly displayed a round-shaped morphology with short cellular processes (left panel). Both CM and control medium induced a spindle-shaped morphologic transformation in both primary microglia and RAW264.7 cells (middle and right panel). In particular, significantly more spindle-shaped cells and longer cellular processes (arrowheads) were identified in both primary microglia and RAW264.7 cells incubated with CM. **(G).** Immunofluorescent staining of Iba1 in microglia showing morphological change induced by CM treatment More spindle-shape microglia were observed in CM-treated group. Scar bar = 20 μm. **(H)** CM induced phenotype polarization in primary microglia, BV2 and RAW264.7 cells. Various gene expressions were detected by RT^2-PCR and showed in a heat-map (black box indicated statistic difference). $^{++}p < 0.01$ and $^{+++}p < 0.001$, compared with Cm; $^{**}p < 0.01$ and $^{***}p < 0.001$, compared with C; $^{###}p < 0.001$, compared with blank.

(**Figure 4E**). At 28 days after implantation, the maximum diameter of tumor mass was larger in ox*Pdcd10*-mice than that in control mice (p<0.01) (**Figure 4C**). To evaluate the microglia/macrophage recruitment, two sectional areas of interest including tumor edge (**Figure 4D**) and tumor core (**Figure 4E**) were examined. Of note, IF-staining of Iba1 (green) revealed a significantly more microglia/macrophage infiltration in peri-tumor area and tumor edge (p<0.001, respectively) (**Figure 4D**) in ox*Pdcd10*-group, suggesting a potential chemotaxis effect mediated by PDCD10 on microglia/macrophages which migrated from normal brain tissue towards homograft tumors. As shown in **Figure 4E**, the number of infiltrated microglia/macrophages in tumor core was larger in ox*Pdcd10*-group than that in control group (p<0.001), and a positive correlation was revealed between PDCD10 expression and infiltration of microglia/macrophages, which was consistent with our findings in GBM patients. Intriguingly, the aggressive tumor growth and increase of microglia/macrophage recruitments induced by

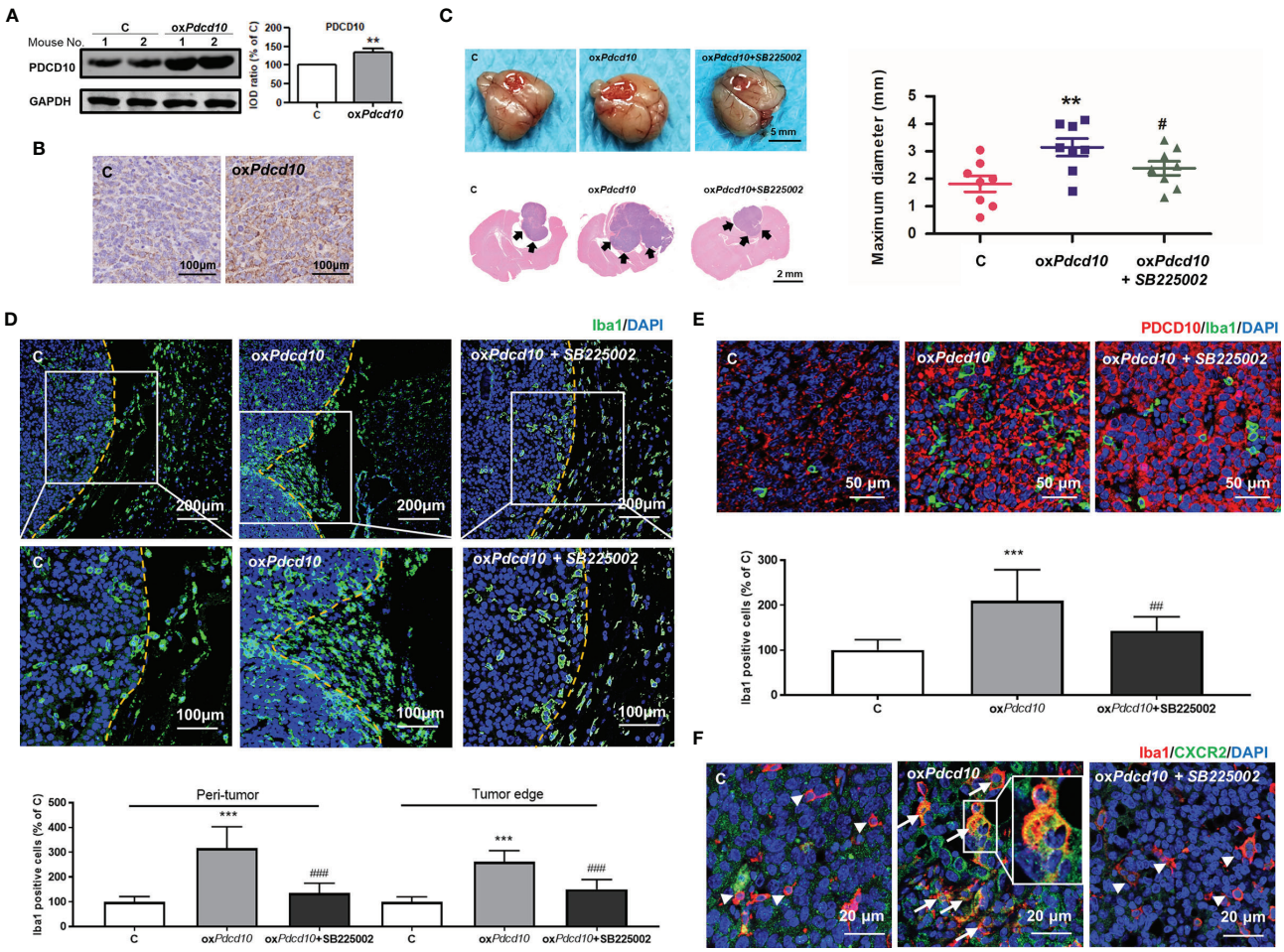

FIGURE 4 | Overexpression of *Pdcd10* in murine GBM cells recruited microglia/macrophages and promoted tumor growth *in vivo*. Mice were cerebral orthotopic implanted with ox*Pdcd10*- (ox*Pdcd10*) or control-GL261 cells **(C)** (n = 8 for each group). The whole brain was removed 28 days after implantation. **(A)** The stable PDCD10 overexpression was confirmed by Western blot. **(B)** Immunohistochemical staining demonstrated PDCD10 overexpression in homograft tumors. Scale bar = 100 μm. **(C)** Overexpression of *Pdcd10* promoted homograft tumor growth, which was reversed by SB225002 treatment. Representative photos showed the homograft tumors (dot-line) in control-, ox*Pdcd10*-mice, and SB225002 treated ox*Pdcd10*-mice. Scale bar = 5 mm. HE-staining demonstrated that homograft tumor (arrows) in ox*Pdcd10* group was larger than that in control group. After treatment with SB225002, the increase of tumor volume was reduced. **(D)** *Pdcd10* overexpression in GL261 cells recruited microglia/macrophages, which was attenuated by SB225002 treatment. Substantial Iba1-positive cells (green) were detected in tumor edge and peri-tumor area (dot-line indicated tumor margin). The lower photos were the enlargement of white box in the upper images respectively. **(E)** Microglia/macrophages infiltration in tumor core induced by *Pdcd10* overexpression was also attenuated by SB225002 application. Double-staining of PDCD10- (red) and Iba1 (green) in tumor core. Scar bar = 50 μm. **(F)** CXCR2 activation in microglia/macrophages mediated by *Pdcd10* upregulation was abolished by SB225002 treatment. Immunoreactivity of CXCR2 (green) was merely detected in cells without Iba1-staining (red, arrowheads) in control mice. Co-labelling of Iba1 and CXCR2 (orange, arrows) was significantly detected in ox*Pdcd10*-tumors. The box (middle photo) was magnified to show the co-localization of CXCR2 and Iba1. Scar bar = 20 μm. **p<0.01 and ***p<0.001, compared with C, $^{\#}p < 0.05$, $^{\#\#}p < 0.01$ and $^{\#\#\#}p < 0.001$, compared with ox*Pdcd10*.

Pdcd10 upregulation were reversed by the treatment with SB225002 (**Figures 4C–E**).

Upregulation of *PDCD10* in GBM Cells Promoted CXCL2 Release, Which in Turn Activated CXCR2 Signaling in Microglia and Macrophages

To explore the underlying mechanism of PDCD10 in GBM on microglia and macrophages, a mouse chemokine protein array kit including 25 chemokines was used. The dot-blots reflecting protein expression were shown in **Figure 5A**. After semi-quantification, eleven detected chemokines were listed in **Figure 5B**. Among them we outlined that CXCL2 was the one of greatest upregulated chemokines. Then, we further examined the expression of CXCR2 in primary microglia, microglia- and macrophage-like cells. Notably, a significant upregulation in both mRNA (**Figure 5C**) and protein levels (**Figure 5D**) of CXCR2 were detected in mouse microglia, BV2 and RAW264.7 cells treated with medium from ox*Pdcd10*-GL261 cells. Similarly, CXCR2 expression in human THP1-mac cells was upregulated after incubation with ox*PDCD10*-CM than that with control medium (**Figures 5E, F**). Additionally, double-staining of Iba1 and CXCR2 in sections generated from homograft tumors demonstrated an increased expression of CXCR2 on microglia/macrophages in ox*Pdcd10*-tumors than control (**Figure 4F**), while this effect was reversed by SB225002 application (**Figure 4F**).

Treatment of SB225002 Suppressed CXCR2 Activation and Cell Migration of Microglia and Macrophages Induced by PDCD10-Upregulated GBM Cells

Murine BV2 and RAW264.7 cells were co-cultured with media from ox*Pdcd10*-GL261 (ox*Pdcd10*) and control GL261 cells (C) respectively. SB225002, a selective CXCR2 antagonist, was applied to BV2 and RAW264.7 cells with optimized concentrations. As a result, the migrated area induced by *oxPdcd10*-CM was reduced by 27% in BV2 cells ($p<0.05$) and 43% in RAW264.7 cells ($p<0.01$) after the administration of 80 nM SB225002 (**Figure 6A**). For transwell assay, both 40 nM and 80 nM of SB225002 were applied. As shown in **Figure 6B**, the number of migrated cells induced by ox*Pdcd10*-CM was significantly reduced by SB225002 treatment (BV2:$p<0.05$ and $p<0.01$, RAW264.7: $p<0.001$ and $p<0.001$, for 40 nM and 80 nM SB225002 application respectively). Additionally, human THP1-mac cells treated with medium from ox*PDCD10*-GBM cells also showed a significant increase of migration ability ($p<0.001$, respectively), which was attenuated by the application of optimized concentration of SB225002 respectively ($p<0.05$, respectively) (**Figures 6C, D**).

Moreover, the signaling pathway was verified by Western blot. As shown in **Figures 6E, F**, the upregulated CXCR2 expression mediated by ox*Pdcd10*/ox*PDCD10*-GBM cells was identified in primary microglia, microglia- and macrophage-like cells respectively, which were abolished upon SB225002 treatment in different concentrations. Following the activation of CXCR2, the phosphorylation of Erk1/2 and Akt were significantly elevated, which was subsequently reversed following the SB225002 application in a dose-dependent manner.

DISCUSSION

In the past few years, the role of PDCD10 in regulating endothelial angiogenesis and apoptosis were well studied (13). However, there was remarkable controversy regarding the role of PDCD10 in human malignant tumors. Previous reports revealed that PDCD10 in malignant tumors exerted dual functions through a cell-type dependent manner (23, 24). Until now, the role of PDCD10 in GBM is still not clear. A recent publication demonstrates that loss of PDCD10 in GBM promotes cellular behaviors and tumor progression (21). However, the TCGA data raise obvious controversy revealing that *PDCD10* is upregulated in GBM, and associated with poor prognosis (**Figure S1**). PDCD10 triggered a paracrine manner, which in turn affects GBM cells (22), indicating an important role of PDCD10 in pathological TME. It is well known that accumulative evidence demonstrates that TAMs play a pivotal role in regulation of tumor progression. Based on the paracrine mechanism and the direct interaction between tumor cells and TAMs, our present study aimed to explore the potential impact of *PDCD10* in GBM on GAMs and the underlying mechanism. In summary, our study revealed that ①upregulation of PDCD10 is positively correlated with GAMs infiltration in GBM patients; ②upregulation of PDCD10 in GBM cells recruits and activates murine primary microglia, microglia- and macrophage-like cells *in vitro* and promotes tumor growth *in vivo*; ③PDCD10-overexpressed GBM cells increases the release of CXCL2, which activates CXCR2 and downstream Akt and Erk1/2 signaling in primary microglia, microglia- and macrophage-like cells.

GAMs are mainly composed of resident microglia and MDMs. Most previous publications demonstrated that cellular distribution and function of resident microglia and MDMs are similar, and accordingly it was difficult to discriminate them (25, 26). However, recent studies revealed tiny differences in their distributions. MDMs occupy a dominant proportion and are observed in all areas of tumor mass with an extremely high distribution in close proximity to vessels, while resident microglia are often confined to tumor border areas and absent from the tumor core in GBM. These reports also employed flow cytometry or histology to discriminate GAMs by using different markers, such as P2ry12, Tmem119 for microglia and Emilin2, Mertk for MDMs (25, 27, 28). In the present study, we performed indirect co-culture experiments by using various human and murine cells to understand the possible interaction between GBM and microglia and macrophages. Considering the possible differences between residual microglial and MDMs, to avoid the bias, we used macrophage-like (THP1-mac and RAW264.7 from human and murine respectively) and microglia-like cell lines (BV2 from murine) as well as murine primary microglia to confirm our consumption. For instance, the following interaction groups including two human ox*PDCD10*-GBM cell lines (U251 and U373) and THP1-mac, murine ox*Pdcd*-GBM cell line (GL261) and three microglia as well as macrophages (primary microglia,

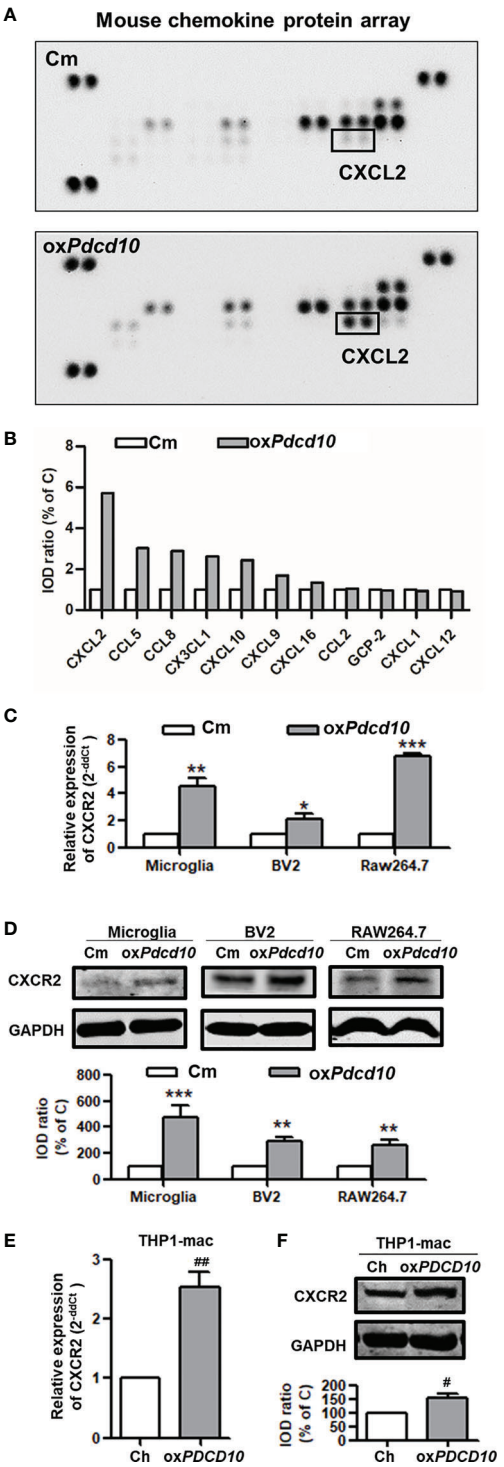

FIGURE 5 | Upregulation of *Pdcd10* in murine GBM cells triggered the release of CXCL2 that in turn activated CXCR2 on microglia and macrophages. **(A)** Different expression of various chemokines in media derived from *Pdcd10*-overexpressed or control-GL261 cells (ox*Pdcd10* or C) was detected by a mouse chemokine array kit. **(B)** Semi-quantification of the dot-blots. CXCL2 was demonstrated as a nearly 6-fold increase in ox*Pdcd10*-medium than that in control medium. **(C, D)** Detection of CXCR2 in murine BV2, RAW264.7 and primary microglia. **(C)** RT^2-PCR and **(D)** Western blot demonstrated that CXCR2 was upregulated in murine primary microglia, BV2 and RAW264.7 in ox*Pdcd10*-group. **(E, F)** CXCR2 in human THP1-mac cells was detected at mRNA **(E)** and protein levels **(F)**. $^{*}p < 0.05$, $^{**}p < 0.01$ and $^{***}p < 0.001$, compared with Cm. $^{\#}p < 0.05$ and $^{\#\#}p < 0.01$, compared with Ch.

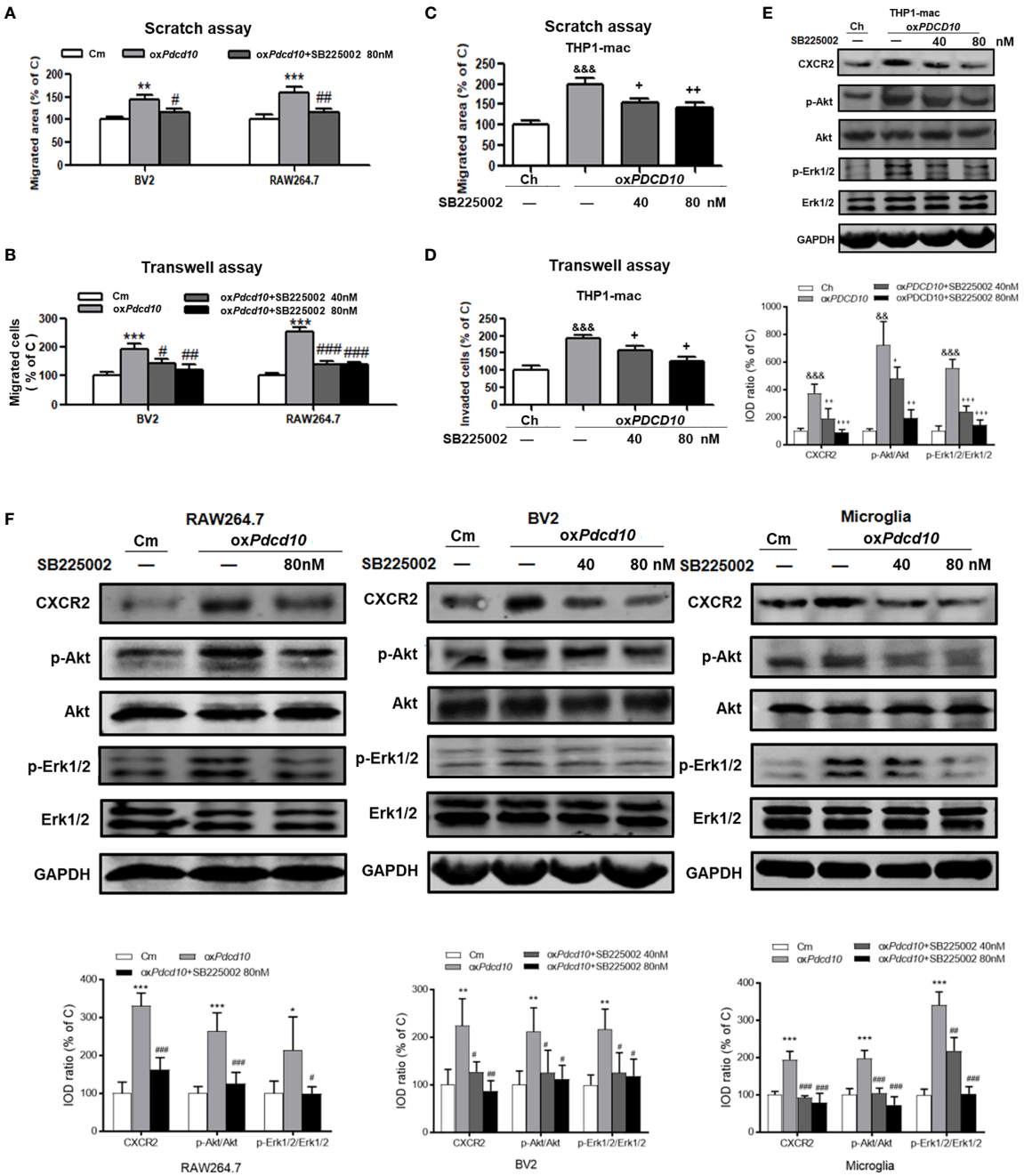

FIGURE 6 | SB225002 treatment suppressed CXCR2 activation and cell migration in microglia and macrophages induced by PDCD10-upregulated GBM cells. Cell migration was detected in murine BV2 and RAW264.7 cells **(A, B)** and in human THP1-mac cells **(C, D)**. For scratch assay **(A, C)**, cells were treated with 40 nM or 80 nM SB225002 for 48 hours. To perform transwell assay **(B, D)**, 40 nM or 80 nM SB225002 was used for cell treatment for 24 hours. CXCR2 and downstream signaling pathways in human THP1-mac **(E)** murine primary microglia, BV2 and RAW264.7 cells **(F)** were detected by Western blot. *$p < 0.05$, **$p < 0.01$ and ***$p < 0.001$, compared with Cm; SB225002 treatment suppressed CXCR2 activation and cell migration in $^{\#}p < 0.05$, $^{\#\#}p < 0.01$ and $^{\#\#\#}p < 0.001$, compared with oxPdcd10; $^{\&\&}p < 0.01$, $^{\&\&\&}p < 0.001$, compared with Ch; $^{+}p < 0.05$, $^{++}p < 0.01$ and $^{+++}p < 0.001$ compared with oxPDCD10.

BV2 and RAW264.7), were used to perform multiple cellular behavior studies. Intriguingly, incubation of microglia- and macrophage-like cells with medium derived from *PDCD10*/*Pdcd10*-upregulated GBM cells promoted cell proliferation and migration *in vitro*. The GAMs polarization and the related morphological change were still uncertain. Generally, M0 morphological status of microglia/macrophage displays a round-shape with little protrusions without any stimuli. Amoeboid- and spindle-shape with elongated cellular processes is characterized as M1 or M2 polarization (29–32). GAMs in GBM are usually polarized

into M2-phenotype, exerting anti-inflammatory function and promoting tumor progression (33). However, some previous reports indicated that co-cultures with GBM cells resulted in an amoeboid shape change in most microglia cells, which in turn play anti-inflammatory function like M2 macrophage (34, 35). In our study, we demonstrated that ox*PDCD10*-CM induced a larger number of M2-phenotype cells than that induced by control medium. Additionally, a significantly increased transcription of M2-markers, such as *IL-10, IL-6* and *arg-1* was detected in ox*PDCD10*-CM cultured primary microglia, microglia- and macrophage-like cells, suggesting that overexpression of *PDCD10* in GBM triggered a pro-tumorigenic phenotype polarization. Subsequently, we employed an orthotopic homograft mouse model to evaluate the impact of GBM PDCD10 on microglia/macrophages *in vivo*. Compared with subcutaneous tumor model, this model provides similar cerebral microenvironment for tumor growth *in vivo* mimicking pathological status in patients. Moreover, this model also avoided the inflammatory reaction induced by xenograft-tumor, which might influence the evaluation of microglia/macrophages recruitment and activation as well as xenograft tumor growth. As a result, PDCD10 expression in homograft tumor was positively associated with the number of infiltrated microglia/macrophages in both tumor edge and tumor core. Since the cellular function of microglia and MDMs possibly differs, the discrimination and respectively functional analysis of them are urged in our further study. In addition, we found that *oxPdcd10*-mice raised a much bigger tumor mass, suggesting that the recruitment of microglia/macrophages might contribute to GBM growth.

Numerous chemotactic factors in tumor pathological circumstance were identified to function in tumor progression. By binding to corresponding receptors, they activate various types of cells including TAMs, endothelial and tumor cells etc. Previous reports demonstrated that TAMs recruitment and activation by various chemotactic factors are crucial process in tumor progression (12, 36). In the present study, we demonstrated that ox*Pdcd10*-GL261 cells facilitated more than 2-fold release of CCL8, CX3CL1, CXCL10, CCL5 and CXCL2. Of them, CXCL2 was dominantly increased by nearly 6-fold, which attracted our attention to focus on the related signaling pathways. CXCL2 mediates biological functions by interacting with corresponding receptor CXCR2 and activates downstream signaling, such as PI3K/Akt, PLC/PKC, MAPK/p38, ras/Erk1/2 and STAT3 etc (37). CXCR2 is dominantly expressed on TAMs, and plays a role in tumor progression through paracrine manner (10, 38). However, CXCR2 mediated autocrine loop is also demonstrated in tumor pathology. In our study, we found that CXCR2 and its downstream signaling, both Akt and Erk1/2, were activated in both microglia and macrophages after the treatment of ox*PDCD* and ox*Pdcd* GBM medium, resulting in a significant increase of cell migration. The related enhancements could be abolished by specific CXCR2 inhibitor application. Moreover, IF-staining of CXCR2 demonstrated that the activation of CXCR2 was identified not only in ox*Pdcd10*-GBM recruited microglia/macrophages but also in ox*Pdcd10*-GBM cells. More intriguingly, treatment of mice with SB225002 inhibited CXCR2 signaling in both microglia/macrophages and tumor cells (**Figure 4F**). Thus, we assumed that CXCL2-CXCR2 resulted in tumor growth *in vivo* might through both autocrine and paracrine manner.

Taken together, PDCD10 in GBM promotes microglia/macrophages recruitment by increasing cell migration ability, and induces pro-tumorigenic polarization through a paracrine CXCL2-CXCR2 signaling pathway. All these effects finally contribute to an aggressive tumor progression. Thus, our study provides evidence that PDCD10 might be an oncogene which highly involved in GBM pathology.

DATA AVAILABILITY STATEMENT

The raw data supporting the conclusions of this article will be made available by the authors, without undue reservation.

ETHICS STATEMENT

The studies involving human participants were reviewed and approved by Ethical Committee of Tongji Hospital, Tongji Medical College, Huazhong University of Science and Technology. The patients/participants provided their written informed consent to participate in this study. The animal study was reviewed and approved by Committee on Animal Research of Tongji Medical College, Huazhong University of Science and Technology.

AUTHOR CONTRIBUTIONS

QZ, JW, XY, SW and WT performed the *in vitro*, *in vivo* experiments and Western blot. HF and SZ carried out the immunofluorescent and immunohistochemical staining as well as image acquisition. CY performed PCR analysis. CG and XW were involved in data acquisition. KZ took part in project concept and study design. QZ, JW and KZ participated in statistical analysis and took part in manuscript preparation. HZ, KS and TL took part in critical revision of the manuscript for important intellectual content. KZ, JW, HF and XW obtained funding. All authors contributed to the article and approved the submitted version.

FUNDING

This work was supported by National Nature Science Foundation of China under Grant 81602204 (KZ), 81702478 (JW) and 81602202 (FH) and by the Scientific Research Starting Foundation for Returned Overseas Chinese Scholars from Tongji hospital, Tongji Medical College, Huazhong University of Science and Technology (2020HGRY009).

SUPPLEMENTARY MATERIAL

The Supplementary Material for this article can be found online at: https://www.frontiersin.org/articles/10.3389/fimmu.2021.637053/full#supplementary-material

REFERENCES

1. Ostrom QT, Cioffi G, Gittleman H, Patil N, Waite K, Kruchko C, et al. CBTRUS Statistical Report: Primary Brain and Other Central Nervous System Tumors Diagnosed in the United States in 2012-2016. *Neuro Oncol* (2019) 21: v1–v100. doi: 10.1093/neuonc/noz150
2. Khosla D. Concurrent Therapy to Enhance Radiotherapeutic Outcomes in Glioblastoma. *Ann Transl Med* (2016) 4(3):54. doi: 10.3978/j.issn.2305-5839.2016.01.25
3. Szulzewsky F, Arora S, de Witte L, Ulas T, Markovic D, Schultze JL, et al. Human Glioblastoma-Associated Microglia/Monocytes Express a Distinct RNA Profile Compared to Human Control and Murine Samples. *Glia* (2016) 64(8):1416–36. doi: 10.1002/glia.23014
4. Hinshaw DC, Shevde LA. The Tumor Microenvironment Innately Modulates Cancer Progression. *Cancer Res* (2019) 79(18):4557–66. doi: 10.1158/0008-5472.CAN-18-3962
5. Hambardzumyan D, Gutmann DH, Kettenmann H. The Role of Microglia and Macrophages in Glioma Maintenance and Progression. *Nat Neurosci* (2016) 19(1):20–7. doi: 10.1038/nn.4185
6. Amici SA, Dong J, Guerau-de-Arellano M. Molecular Mechanisms Modulating the Phenotype of Macrophages and Microglia. *Front Immunol* (2017) 8:1520. doi: 10.3389/fimmu.2017.01520
7. Gutmann DH, Kettenmann H. Microglia/Brain Macrophages as Central Drivers of Brain Tumor Pathobiology. *Neuron* (2019) 104(3):442–9. doi: 10.1016/j.neuron.2019.08.028
8. Vinnakota K, Hu F, Ku MC, Georgieva PB, Szulzewsky F, Pohlmann A, et al. Toll-Like Receptor 2 Mediates Microglia/Brain Macrophage MT1-MMP Expression and Glioma Expansion. *Neuro Oncol* (2013) 15(11):1457–68. doi: 10.1093/neuonc/not115
9. Hu F, a Dzaye OD, Hahn A, Yu Y, Scavetta RJ, Dittmar G, et al. Glioma-Derived Versican Promotes Tumor Expansion Via Glioma-Associated Microglial/Macrophages Toll-like Receptor 2 Signaling. *Neuro Oncol* (2015) 17(2):200–10. doi: 10.1093/neuonc/nou324
10. Di Mitri D, Mirenda M, Vasilevska J, Calcinotto A, Delaleu N, Revandkar A, et al. Re-Education of Tumor-Associated Macrophages by CXCR2 Blockade Drives Senescence and Tumor Inhibition in Advanced Prostate Cancer. *Cell Rep* (2019) 282156-2168(8):e2155. doi: 10.1016/j.celrep.2019.07.068
11. Lu Z, Zou J, Li S, Topper MJ, Tao Y, Zhang H, et al. Epigenetic Therapy Inhibits Metastases by Disrupting Premetastatic Niches. *Nature* (2020) 579 (7798):284–90. doi: 10.1038/s41586-020-2054-x
12. Roesch S, Rapp C, Dettling S, Herold-Mende C.). When Immune Cells Turn Bad-Tumor-Associated Microglia/Macrophages in Glioma. *Int J Mol Sci* (2018) 19(2):436–55. doi: 10.3390/ijms19020436
13. You C, Sandalcioglu IE, Dammann P, Felbor U, Sure U, Zhu Y. Loss of CCM3 Impairs DLL4-Notch Signalling: Implication in Endothelial Angiogenesis and in Inherited Cerebral Cavernous Malformations. *J Cell Mol Med* (2013) 17 (3):407–18. doi: 10.1111/jcmm.12022
14. Hwang J, Pallas DC. STRIPAK Complexes: Structure, Biological Function, and Involvement in Human Diseases. *Int J Biochem Cell Biol* (2014) 47:118–48. doi: 10.1016/j.biocel.2013.11.021
15. Louvi A, Chen L, Two AM, Zhang H, Min W, Gunel M. Loss of Cerebral Cavernous Malformation 3 (Ccm3) in Neuroglia Leads to CCM and Vascular Pathology. *Proc Natl Acad Sci USA* (2011) 108(9):3737–42. doi: 10.1073/pnas.1012617108
16. Louvi A, Nishimura S, Gunel M. Ccm3, a Gene Associated With Cerebral Cavernous Malformations, is Required for Neuronal Migration. *Development* (2014) 141(6):1404–15. doi: 10.1242/dev.093526
17. Tang AT, Sullivan KR, Hong CC, Goddard LM, Mahadevan A, Ren A, et al. Distinct Cellular Roles for PDCD10 Define a Gut-Brain Axis in Cerebral Cavernous Malformation. *Sci Transl Med* (2019) 11(520):eaaw3521-53. doi: 10.1126/scitranslmed.aaw3521
18. Fu X, Zhang W, Su Y, Lu L, Wang D, Wang H. MicroRNA-103 Suppresses Tumor Cell Proliferation by Targeting PDCD10 in Prostate Cancer. *Prostate* (2016) 76(6):543–51. doi: 10.1002/pros.23143
19. Wu K, Mu XY, Jiang JT, Tan MY, Wang RJ, Zhou WJ, et al. miRNA26a5p and miR26b5p Inhibit the Proliferation of Bladder Cancer Cells by Regulating PDCD10. *Oncol Rep* (2018) 40(6):3523–32. doi: 10.3892/or.2018.6734
20. Tan P, He L, Zhou Y. TRIM59 Deficiency Curtails Breast Cancer Metastasis Through SQSTM1-Selective Autophagic Degradation of PDCD10. *Autophagy* (2019) 15(4):747–9. doi: 10.1080/15548627.2019.1569951
21. Wan X, Saban DV, Kim SN, Weng Y, Dammann P, Keyvani K, et al. Pdcd10-Deficiency Promotes Malignant Behaviors and Tumor Growth Via Triggering Ephb4 Kinase Activity in Glioblastoma. *Front Oncol* (2020) 10:1377–88. doi: 10.3389/fonc.2020.01377
22. Zhu Y, Zhao K, Prinz A, Keyvani K, Lambertz N, Kreitschmann-Andermahr I, et al. Loss of Endothelial Programmed Cell Death 10 Activates Glioblastoma Cells and Promotes Tumor Growth. *Neuro Oncol* (2016) 18(4):538–48. doi: 10.1093/neuonc/nov155
23. Ma X, Zhao H, Shan J, Long F, Chen Y, Chen Y, et al. PDCD10 Interacts With Ste20-related Kinase MST4 to Promote Cell Growth and Transformation Via Modulation of the ERK Pathway. *Mol Biol Cell* (2007) 18(6):1965–78. doi: 10.1091/mbc.e06-07-0608
24. Urfali-Mamatoglu C, Kazan HH, Gunduz U. Dual Function of Programmed Cell Death 10 (PDCD10) in Drug Resistance. *BioMed Pharmacother* (2018) 101:129–36. doi: 10.1016/j.biopha.2018.02.020
25. Bowman RL, Klemm F, Akkari L, Pyonteck SM, Sevenich L, Quail DF, et al. Macrophage Ontogeny Underlies Differences in Tumor-Specific Education in Brain Malignancies. *Cell Rep* (2016) 17(9):2445–59. doi: 10.1016/j.celrep.2016.10.052
26. Sevenich L. Brain-Resident Microglia and Blood-Borne Macrophages Orchestrate Central Nervous System Inflammation in Neurodegenerative Disorders and Brain Cancer. *Front Immunol* (2018) 9:697. doi: 10.3389/fimmu.2018.00697
27. Friebel E, Kapolou K, Unger S, Nunez NG, Utz S, Rushing EJ, et al. Single-Cell Mapping of Human Brain Cancer Reveals Tumor-Specific Instruction of Tissue-Invading Leukocytes. *Cell* (2020) 1811626-1642(7):e1620. doi: 10.1016/j.cell.2020.04.055
28. Klemm F, Maas RR, Bowman RL, Kornete M, Soukup K, Nassiri S, et al. Interrogation of the Microenvironmental Landscape in Brain Tumors Reveals Disease-Specific Alterations of Immune Cells. *Cell* (2020) 1811643-1660(7): e1617. doi: 10.1016/j.cell.2020.05.007
29. Michelucci A, Heurtaux T, Grandbarbe L, Morga E, Heuschling P. Characterization of the Microglial Phenotype Under Specific Pro-Inflammatory and Anti-Inflammatory Conditions: Effects of Oligomeric and Fibrillar Amyloid-Beta. *J Neuroimmunol* (2009) 210(1-2):3–12. doi: 10.1016/j.jneuroim.2009.02.003
30. Chen W, Zhao Y, Li XC, Kubiak JZ, Ghobrial RM, Kloc M. Rho-Specific Guanine Nucleotide Exchange Factors (Rho-GEFs) Inhibition Affects Macrophage Phenotype and Disrupts Golgi Complex. *Int J Biochem Cell Biol* (2017) 93:12–24. doi: 10.1016/j.biocel.2017.10.009
31. Quail DF, Joyce JA. Molecular Pathways: Deciphering Mechanisms of Resistance to Macrophage-Targeted Therapies. *Clin Cancer Res* (2017) 23 (4):876–84. doi: 10.1158/1078-0432.CCR-16-0133
32. Wosik J, Chen W, Qin K, Ghobrial RM, Kubiak JZ, Kloc M. Magnetic Field Changes Macrophage Phenotype. *Biophys J* (2018) 114(8):2001–13. doi: 10.1016/j.bpj.2018.03.002
33. Umemura N, Saio M, Suwa T, Kitoh Y, Bai J, Nonaka K, et al. Tumor-Infiltrating Myeloid-Derived Suppressor Cells Are Pleiotropic-Inflamed Monocytes/Macrophages That Bear M1- and M2-type Characteristics. *J Leukoc Biol* (2008) 83(5):1136–44. doi: 10.1189/jlb.0907611
34. Sliwa M, Markovic D, Gabrusiewicz K, Synowitz M, Glass R, Zawadzka M, et al. The Invasion Promoting Effect of Microglia on Glioblastoma Cells Is Inhibited by Cyclosporin a. *Brain* (2007) 130(Pt 2):476–89. doi: 10.1093/brain/awl263
35. Walentynowicz KA, Ochocka N, Pasierbinska M, Wojnicki K, Stepniak K, Mieczkowski J, et al. In Search for Reliable Markers of Glioma-Induced Polarization of Microglia. *Front Immunol* (2018) 9:1329–41. doi: 10.3389/fimmu.2018.01329
36. Zhang X, Guo R, Kambara H, Ma F, Luo HR. The Role of CXCR2 in Acute Inflammatory Responses and its Antagonists as Anti-Inflammatory Therapeutics. *Curr Opin Hematol* (2019) 26(1):28–33. doi: 10.1097/MOH.0000000000000476
37. Grepin R, Guyot M, Giuliano S, Boncompagni M, Ambrosetti D, Chamorey E, et al. The CXCL7/CXCR1/2 Axis Is a Key Driver in the Growth of Clear Cell Renal Cell Carcinoma. *Cancer Res* (2014) 74(3):873–83. doi: 10.1158/0008-5472.CAN-13-1267

38. Acker G, Zollfrank J, Jelgersma C, Nieminen-Kelha M, Kremenetskaia I, Mueller S, et al. The CXCR2/CXCL2 Signalling Pathway - An Alternative Therapeutic Approach in High-Grade Glioma. *Eur J Cancer* (2020) 126:106–15. doi: 10.1016/j.ejca.2019.12.005

Conflict of Interest: The authors declare that the research was conducted in the absence of any commercial or financial relationships that could be construed as a potential conflict of interest.

frontiers in Immunology

REVIEW
published: 31 May 2021
doi: 10.3389/fimmu.2021.679954

Glioma-Derived Extracellular Vesicles – Far More Than Local Mediators

*Stoyan Tankov and Paul R. Walker**

Center for Translational Research in Onco-Hematology, Geneva University Hospitals and University of Geneva, Geneva, Switzerland

Extracellular vesicle (EV) secretion is a ubiquitous cellular process with both physiologic and pathologic consequences. EVs are small lipid bilayer vesicles that encompass both microvesicles and exosomes and which are secreted by virtually all cells including cancer cells. In this review, we will focus on the roles of EVs in mediating the crosstalk between glioblastoma (GBM) cells and innate and adaptive immune cells and the potential impact on glioma progression. Glioma-derived EVs contain many bioactive cargoes that can broaden and amplify glioma cell mediated immunosuppressive functions and thereby contribute to shaping the tumor microenvironment. We will discuss evidence demonstrating that the low oxygen (hypoxia) in the GBM microenvironment, in addition to cell-intrinsic effects, can affect intercellular communication through EV release, raising the possibility that properties of the tumor core can more widely impact the tumor microenvironment. Recent advances in glioma-derived EV research have shown their importance not only as message carriers, but also as mediators of immune escape, with the capacity to reprogram tumor infiltrating immune cells. Exploring EV function in cancer-immune crosstalk is therefore becoming an important research area, opening up opportunities to develop EV monitoring for mechanistic studies as well as novel diagnostic glioma biomarker applications. However, robust and reproducible EV analysis is not always routinely established, whether in research or in clinical settings. Taking into account the current state of the art in EV studies, we will discuss the challenges and opportunities for extending the many exciting findings in basic research to a better interpretation of glioma and its response to current and future immunotherapies.

Keywords: glioma, tumor microenvironment, immunosuppression, hypoxia, extracellular vesicles, biomarkers

OPEN ACCESS

Edited by:
Lukas Bunse, German Cancer Research Center (DKFZ), Germany

Reviewed by:
Mir Munir Rahim, University of Windsor, Canada
Andrea Zendrini, University of Brescia, Italy

***Correspondence:**
Paul R. Walker
Paul.Walker@unige.ch

Specialty section:
This article was submitted to Cancer Immunity and Immunotherapy, a section of the journal Frontiers in Immunology

Received: *12 March 2021*
Accepted: *30 April 2021*
Published: *31 May 2021*

Citation:
Tankov S and Walker PR (2021) Glioma-Derived Extracellular Vesicles – Far More Than Local Mediators. Front. Immunol. 12:679954. doi: 10.3389/fimmu.2021.679954

INTRODUCTION

Since the first comprehensive histomorphological description of glioblastoma multiforme (GBM) by Rudolf Virchow in the 19th century, it still remains a challenge not only to comprehensively describe its "multiforme" features, but also to develop effective treatments. Extensive research in brain cancer, particularly the most aggressive primary brain cancer GBM, has led to only modest progress in prolonging the median lifespan of patients from the time of diagnosis. GBM forms a complex and

heterogeneous microenvironment that is composed of both cancerous and non-cancerous cells including endothelial cells, immune cells, glioma stem-like cells (GSCs), and astrocytes. The complexity of the GBM tumor microenvironment (TME) is further enhanced by hallmark features of solid tumors, such as low oxygenation (hypoxia). Tumor hypoxia drives malignancy by promoting chemo- and radiotherapy resistance, an immunosuppressive microenvironment, cancer cell stemness, angiogenesis, and metabolic modulation (1–3). These features most likely contribute to the tumor recurrence in most patients receiving standard-of-care consisting of surgical resection followed by chemo-radiotherapy (4). Indeed, *in silico* analyses showed that high expression of a recently defined hypoxia signature was highly correlated with poor prognosis of GBM patients (5).

Cells comprising GBM tumors use different communication routes that facilitate tumor progression. They include direct cell interactions through membrane receptors and their ligands, and the release of soluble factors, such as cytokines, chemokines, and metabolites. Recently, extracellular vesicles (EVs), as a new means of intercellular communication, have drawn much attention due to their ability to carry various bioactive molecules that are responsible for altering expression of tumor promoting and tumor suppressing genes in recipient cells. In this review, we will look at the spectrum of research that has established EVs as prominent actors in the pathophysiology of GBM, focusing on GBM-derived EV influence on immune cells of the tumor microenvironment. We will discuss how these findings could be extrapolated to a better interpretation of GBM and its response to current and future immunotherapies. We will also consider how EVs can be implicated in novel diagnostic, prognostic, and predictive glioma biomarker applications.

BIOGENESIS, RELEASE, CARGO AND UPTAKE

EVs are defined as phospholipid-bilayer enclosed extracellular spherical structures that can vary in size from 30 nm to a few μm. EVs are secreted by multiple cell types and are involved in intercellular communication between neighboring or distant cells through the transfer of their cargo from the donor to recipient cells. EV release is generally constitutive, but it can also be influenced by pathological conditions such as cancer, and by immune responses. Two important mechanisms influence not only the subtype of the vesicles secreted, but also their cargo composition. The first mechanism is used by cells to secrete exosomes or small vesicles (30-150nm) and starts with the formation of early endosomes (**Figure 1**). Early endosomes, during their maturation towards late endosomes or multi-vesicular bodies (MVBs), start to accumulate intraluminal vesicles (ILV) through endosomal membrane invaginations. Late endosomes or MVBs subsequently fuse with lysosomes and thus promote ILV destruction, or they can fuse with the cell membrane, releasing ILVs into the extracellular space. The second mechanism of EV formation is through direct budding of the plasma membrane straight to the extracellular space. The vesicles formed by this mechanism are called microvesicles or medium/large vesicles (100–1,000 nm). Although microvesicles are released by many cell types during normal and pathological processes, there are still many unanswered questions regarding their functions. A size based categorization is useful to simplify the study of EVs, but further analysis of EV subpopulations is needed in order to identify their biological properties. Indeed, there are other vesicles that are formed in a similar way that do not fall in the category of microvesicles or exosomes, but which are considered as an important mediator of extracellular interactions. Apoptotic bodies (50–2,000 nm), released from cells entering apoptosis, contain proteins, fragments of DNA, mRNAs and non-coding RNAs (6, 7). A separate class of EVs, oncosomes and large oncosomes, has also been described. They are defined as cancer cell-derived EVs that contain cancer specific molecules, such as oncogenic proteins or nucleic acids. Whether these EVs are indeed different type of vesicles is a question that needs to be answered by investigating their biogenesis and detailed functions. EV nomenclature is controversial, since there are no totally specific markers to clearly distinguish each EV biogenesis pathway, although presence of tetraspanin proteins CD63, CD9 and CD81 has been used for general characterization (8). Therefore, following the recommendations stated by the positional paper of the International Society for Extracellular Vesicles (ISEV) in 2018, EVs should rather be named according to their size: small EVs (<100 nm or <200 nm) and medium/large EVs (>200 nm) (9). Whether vesicle classification by biogenesis pathway rather than by size has a stronger biological basis or functional relevance remains to be determined. We propose that one way to resolve this is to link biogenesis pathways with cargo composition or delivery efficiency. This would give more precise EV systematization and even enable us to describe novel subtypes or distinguish targeted EVs from randomly secreted ones. However, this will be only achieved with enhanced isolation techniques, better EV structural analysis and functional analyses.

However, size matters, and the specific differences in EV size and surface molecules can impact their recognition and uptake by recipient cells. There are three major mechanisms that cells are using to take up EVs nonspecifically; endocytosis, phagocytosis and micropinocytosis. Additionally, EVs can be taken up by cell specific receptor-ligand interaction (clathrin or caveolin-mediated) (10, 11). EVs may also deliver their cargo by simple fusion with the plasma membrane (12). Once the vesicle is internalized, its cargo can be released into the cytoplasm or transported to the nucleus or the cell membrane. Nevertheless, EV internalization is not obligatory for EV functionality, since surface proteins can interact with receptors of the recipient cell plasma membrane that may lead to direct or indirect stimulation of intracellular signaling cascades. All of these specific and nonspecific mechanisms of EV uptake and interactions represent the array of possibilities for EV-mediated intercellular communication that can induce epigenetic modifications in the recipient cells by transfer of bioactive molecules. Overall, EVs are a ubiquitous communication system used by many cell types in many different organisms; however, the processes involved, and the messages carried, are highly individual. In the case of malignancy, it is becoming apparent that EV mediated communication can work

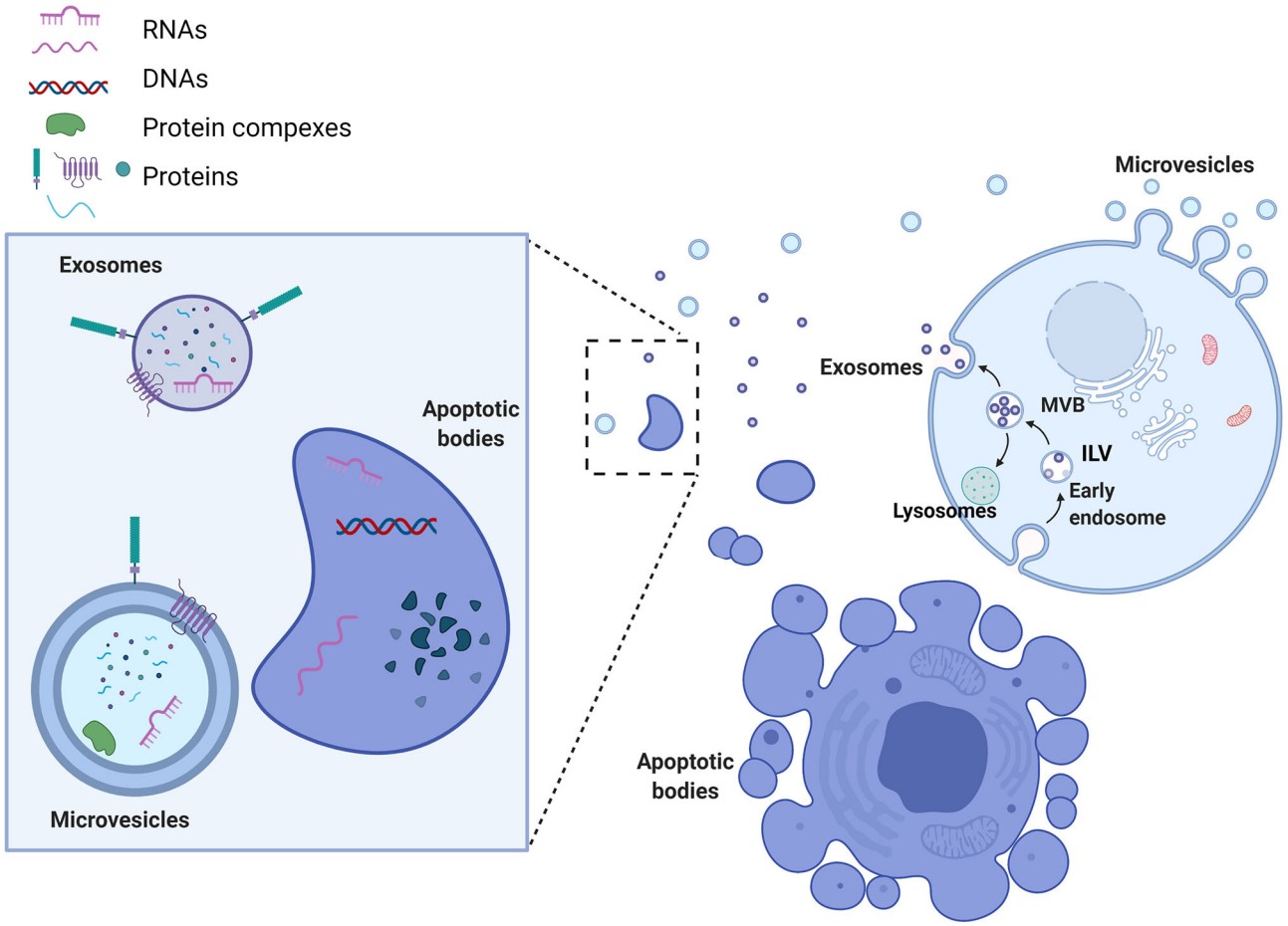

FIGURE 1 | Extracellular vesicle biogenesis and types. Microvesicles are formed by direct budding of the plasma membrane and release into the extracellular space. Exosome biogenesis begins with the formation of early endosomes. Early endosomes accumulate intraluminal vesicles (ILVs) through membrane shedding, leading to the formation of multivesicular bodies (MVBs). Subsequently, late endosomes/MVBs either fuse with lysosomes, in which case the ILVs will be destroyed, or else they fuse directly with the cell membrane, releasing exosomes into the extracellular space. Apoptotic bodies are shed directly into the extracellular environment by apoptotic cells. Each of these types of EVs can carry different cargos that are loaded on their membrane (proteins, glycoproteins) or packed in their lumen (proteins, DNA and RNAs). EV cargo composition can reflect donor cells (apoptotic bodies) or harbor more specifically sorted biomolecules (exosomes).

alongside the mutated protein network and other oncogenic mechanisms to enable cancer cells to proliferate and sculpt their environment to facilitate tumor progression.

ROLE OF EVS IN GLIOMA. WHAT CAN THEY DO?

The GBM microenvironment consists of diverse cellular populations which have different functions and origins. It is well known that GBM cells interact with surrounding non-cancer cells to maintain a microenvironment that favors tumor proliferation, invasion of the brain, angiogenesis and immunosuppression. Multiple modes of communication are involved in this phenomenon, such as soluble factors, cell-cell (contact) interactions, metabolic disruption (nutrient utilization), and EVs. We will describe key findings showing how EVs released by GBM cells can specifically impact immune cells.

EVs are involved in the mechanisms of tumor progression and invasion in different types of cancers. In the light of these data, their relevance in GBM is being explored as a potential factor contributing to malignancy. It was calculated that a single GBM cell secretes as many as 10,000 EVs over a 48 hour period (13); the potential biological significance of this is highlighted by the fact that as few as 1,000 GBM EVs are sufficient to inhibit cytotoxicity of one T cell (our unpublished *in vitro* data). Of course, we should consider that *in vivo* the number, size and cargo of GBM EVs can vary depending on patients' treatments (14) and local conditions in the TME, such as hypoxia (15). The EVs of GBM cells carry different molecules than those of normal glial cells (16). These molecules include cancer effector molecules (e.g., mutant oncoproteins, oncogenic transcripts and oncomiRs) and can directly or indirectly support tumor progression and immune

evasion (13, 17). This can lead to physiological transformation of the cancer and the stromal cells, creating a permissive environment in which the tumor can thrive (**Figure 2**).

To increase the viability of tumor cells, GBM EVs can interfere with signaling pathways through the coding and non-coding RNAs they contain. The most studied RNA species transferred by EVs are the miRNAs although many other types are found (18). miRNAs are short sequence single-stranded RNAs with a major role in gene regulation (19). Several *in vitro* studies using microarray have shown the involvement of miRNAs (including miR-21, mir-29 miR-210, miR-148, and many others) in enhancing proliferation and inhibiting tumor cell apoptosis in GBM (20–25). mir-21 has been mostly studied as a major GBM cell regulator (26) and has also been shown to be transferred in the cargo of GBM EVs (27). *In vitro* suppression of miR-21 decreased proliferation and increased apoptosis in GBM cells (28). Additionally, plasma levels of mir-21 (cell-free and potentially EV-derived) were shown to correlate with glioma grade, and GBM patients with high EV associated miR-21 levels in cerebrospinal fluid (CSF) had poor prognosis (29). In addition to miRNAs, other non-coding RNA can also be transported by the EVs and can potentially affect recipient cells (18). Human GBM cells that were resistant to temozolomide transferred long non-coding RNA SBF2-AS1 *via* EVs to neighboring GBM cells; this endowed temozolomide resistance in the recipient cells (30). Induction of hypoxia and hypoxia induced pathways in GBM are considered as a major influence on treatment failure and strongly regulate many genes including those encoding miRNA (31, 32). Notably, many miRNAs, including miR-21, are shown to be upregulated by hypoxia in GBM (33, 34) and are proposed as potential biomarkers (35, 36).

EV cargos are not limited to coding and non-coding RNAs. EVs can be involved in protein transport or they can dysregulate the lipid balance in the cells that internalize them. EGFRvIII, PDGFR and human epidermal growth factor receptor 2 (HER2) are some of the key receptors involved in the molecular pathogenesis of GBM. GBM cells are shown to secret these proteins with EVs and transfer them to another cancer cell population, thereby promoting a malignant phenotype (17). Furthermore, EVs released by GBM cell lines were demonstrated to carry the chloride intracellular channel-1

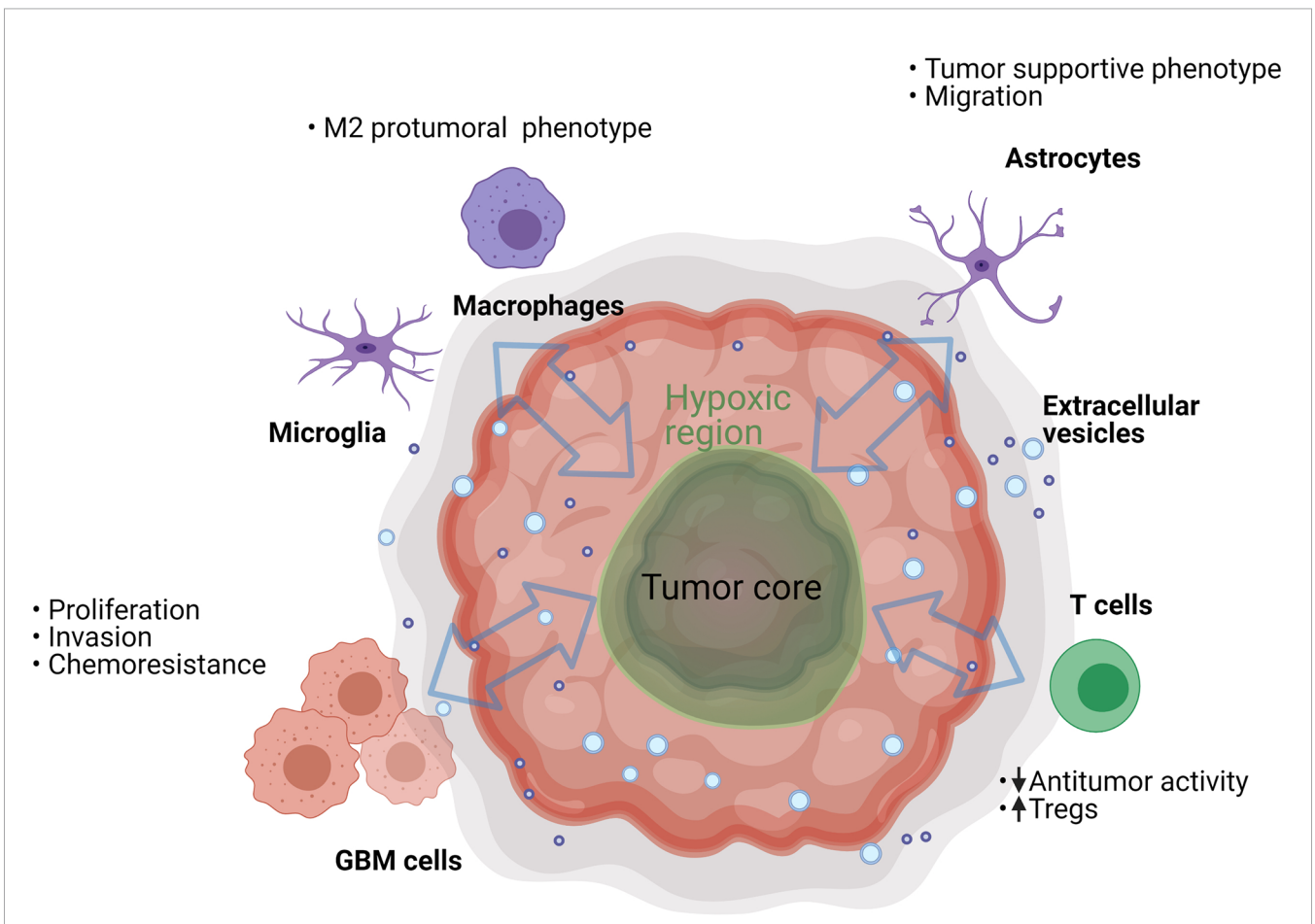

FIGURE 2 | GBM EVs can trigger various processes in the cells present in the tumor microenvironment. They can have an effect on neighboring cancer cells, resident brain cells (astrocytes and microglia), and on infiltrating immune cells (T cells and macrophages). However, the process is bidirectional and many of the EV-recipient tumor-suppressive cells can also secrete EVs that further suppress the antitumor functions of immune infiltrating cells and support GBM cell proliferation.

(CLIC1) protein (37), which is important for cell cycle regulation and was reported to be associated with poor prognosis in GBM patients when highly expressed (38).

Additionally, GBM EVs were shown to modulate *in vitro* and *in vivo* migration patterns and morphology of the surrounding astrocytes, which supports the invasion and progression of GBM (39, 40). Nevertheless, EV-mediated GBM interactions with cells in the microenvironment are reciprocal in nature. For example, endothelial cell-derived EVs isolated from a GBM tumor promoted glioma cell migration (15). Similarly, GBM associated fibroblasts secreted EVs that were taken up by tumor cells to promote glycolysis (41).

An important source of EVs in the tumor is the small population of GSCs that are playing a significant role in GBM progression. Indeed, the resistance to standard-of-care chemotherapy (42) and radiotherapy (43) in GBM is facilitated by GSCs. The capacity of GSCs to thrive in harsh, hypoxic microenvironmental niches is achieved by their self-renewal and differentiation potential (44). GSCs are also involved in modulating the expression of the key components that promote tumor proliferation and survival in hypoxic and perinecrotic regions. Notably, GSCs are exerting some of these functions by a high EV secretion capacity and these EVs have substantial differences in their protein cargo profiles and activities (45). One of the mechanisms by which GSCs regulate other cells is through EV-mediated transfer of Notch1 protein that is highly enriched in their EVs (46), or by transfer of the pro-angiogenic and immunosuppressive factor VEGF-A (47). Regarding GSC chemoresistance, this is facilitated by high expression levels of specific ABC drug transporters and is also linked to their EV secretion patterns (48, 49).

ROLE OF EVS IN THE CROSSTALK BETWEEN CANCER CELLS AND INNATE AND ADAPTIVE IMMUNE CELLS

Effects on Innate Immune Cells

Innate immune cells present in GBM are represented by NK cells and myeloid cells. GBM EVs were shown *in vitro* to inhibit NK cell expression of NKG2D activating receptor, which could potentially limit NK anti-tumor reactivity (50). For myeloid cells these comprise around one third of cells of the GBM tumor mass and include dendritic cells (DCs) monocytes, macrophages and microglia. The proportion of these tumor-associated cells has been shown to correlate with clinical outcome in GBM and other solid cancers (51). Of particular interest are macrophages that can acquire different phenotypes according to cytokines and signaling molecules of the microenvironment. Classically activated M1 macrophages are capable of phagocytosis, cytotoxicity, antigen presentation and secretion of inflammatory cytokines. In solid cancers, including GBM, it is believed that many macrophages acquire an alternatively activated M2 polarization, resulting in production of angiogenic factors, EVs, immunosuppressive molecules, and chemokines, cytokines and growth factors favoring tumor progression (52). However recent observations in GBM suggest that a non-polarized M0 status of the so-called glioma associated macrophages (GAMs) can also be identified (53). Evidence from the last few years shows that EVs released by GBM cells promote a tumor-supportive macrophage phenotype. EVs derived from GBM cell lines (U87MG) were able to modify blood-derived monocytes to M2-like macrophages *in vitro* (54). Moreover, functional delivery of miR-451/miR-21 contained in GBM EVs to microglia and macrophages *in vitro*, as well as to macrophages *in vivo*, led to downregulation of miR-21 targeted c-Myc mRNA (21). Interestingly, the transcription factor c-Myc is suggested to be upregulated in M2 macrophages and to regulate murine tumor-associated macrophage (TAM) polarization (55). However, downregulation of c-Myc by GBM EV-derived miR-21 might promote a more global transition of the microglia/macrophage phenotype that leads to the expression of a distinct transcriptional program rather than modulation of just one gene. This was later confirmed *in vivo* using the GL261 mouse glioma model in which EV-delivered miR-21 was able to downregulate BTG2 cell cycle progression regulator, particularly in microglia cells (27). These data suggest that *in vivo* downregulation of the anti-proliferative effects of *Btg2* by EV-delivered miR-21 could increase microglia proliferation, promote tumor growth and formation of a hypoxic microenvironment. Additionally, the release of EVs from the hypoxic zones of GBM tumors was shown to induce M2 macrophage polarization *in vitro*, which subsequently promoted glioma proliferation, migration and invasion. This was demonstrated to be the result of EV-mediated delivery of miR-1246 that polarized macrophages towards M2 by inhibiting NF-κB and activating the STAT3 pathway (56), which could serve as a polarization switch, as suggested for other cancers (57). Nevertheless, some of the most important mechanisms leading to tumor immune escape and tumor growth in many solid tumors, potentially including GBM, are the immune checkpoints and their ligand interactions. One such immune checkpoint molecule is Tim-3 that could be engaged by Galectin-9 (Gal-9) and lead to immunoregulatory effects (58). Indeed, EVs from CSF of patients with GBM were shown to be enriched in Gal-9, particularly in high grade gliomas; these EVs were shown to decrease antigen presenting abilities of DCs *in vitro* in a Tim-3 dependent manner (59). This data highlights the interest of CSF sampling to interrogate EV immunoregulatory functions, but also raises questions about the cellular origin of the EVs, which needs to be clarified in order to understand their potential roles in the *in vivo* tumor microenvironment. Furthermore GSC-derived EVs can potentially skew tumor infiltrating monocytes towards immunosuppressive M2 macrophages by transferring axonal guidance signaling proteins, which leads to M2-like polarization (60). The programmed cell death ligand-1 (PD-L1) expression of these M2 macrophages clearly has potential for major effects on programmed cell death 1 (PD1) expressing tumor infiltrating T cells, as discussed below.

Effects on T Cells

T cell infiltration of tumors positively correlates with better clinical outcome in many cancers [reviewed in (61)]. However, in GBM, increased inflammation, immune infiltration and activation was reported to be associated with shorter overall survival (62). Although the brain environment certainly limits effective antitumor immunity, the GBM tumor and the TME further

compromises T cell functionality. One of the first studies on GBM EVs (63) reported that mouse GBM EVs promoted *in vivo* tumor growth and inhibited $CD8^+$ T cell cytolytic activity. Similarly, GBM EVs from low passage GBM cell lines were shown to decrease IFN-γ secretion and migration capacities in peripheral blood mononuclear cells (PBMCs) from healthy donors (64). Indeed GSCs *in vitro* were shown to secrete EVs that contain tenascin-C that disrupts mTOR signaling in PBMCs (65), which is a key mechanism for integrating signaling from DCs during antigen presentation. Furthermore, it was shown that human GSC EVs inhibited T cell activation and proliferation through direct PD-L1/PD1 interactions (66). This indicates that PD-L1 expression on GBM EVs can suppress T cell-mediated antitumor functions and potentially contribute to the immunosuppressive environment. PD-L1 belongs to the family of immune checkpoint molecules, and has a direct consequence on effector T cell function in the tumor microenvironment through binding PD1 expressed on T cells. The PD-L1, expressed by GBM cells and myeloid cells (67), induces inhibitory signals in PD1 expressing T cells, blocking effector responses and allowing cancer cells to evade immune attack. Additionally, other proteins with immunosuppressive functions (FasL, CTLA-4 and CD39) were identified in GBM EVs from several human cell lines. In $CD4^+$ T cells, these EVs suppressed T cell activation, measured by diminished CD69 expression, and in $CD8^+$ T cells they induced apoptosis and reduced IFN-γ and TNF-α production (50). These effects were at least partially mediated by FasL, suggesting that FasL expressing GBM cells not only inhibit T cell functions by cell-cell contact (68), but also by releasing $FasL^+$ EVs. Since the local concentration, distribution and the specific cellular source of EVs *in vivo* is not well defined, to what extent these *in vitro* results are representative of direct EV mediated GBM/T cell interactions *in vivo* remains to be determined. Nevertheless, extrapolating from findings in other cancer indications (69–71), this mechanism of immunosuppression, i.e., direct interaction of cancer cell-derived EVs with T cells in the TME, is certainly feasible. However, EV-mediated T cell inhibition in GBM can also be myeloid cell dependent (72, 73). EV modulation of T cell function in solid tumors does not necessarily arise directly from cancer cell-derived EVs; myeloid cells that are coerced to support GBM progression such as TAMs and myeloid-derived suppressor cells (MDSCs) can represent a rich source of EVs in the TME. Paradoxically, the EVs from such immunosuppressive cells do not necessarily recapitulate the functions of the donor cells, as demonstrated for myeloid cell-derived EVs in the MC38 colorectal model, which had a stimulatory effect on T cells (74).

LOCAL, REGIONAL AND SYSTEMIC RELEASE OF EVS AND THEIR USE AS BIOMARKERS

The ubiquitous presence of EVs in the TME is a factor to consider when assessing the impact of immunotherapy. Based on *in vitro* data, high concentrations of GBM EVs can deactivate T cells and push macrophages towards an immunoinhibitory phenotype (56, 64). This raises the possibility of a differential effect of GBM-derived EVs on recipient cells depending on their proximity. Using a chick embryo chorioallantoic membrane model, which allows rapid vascularization, survival and development of tumor cells or tissues placed on its surface, it was shown that GBM cells can export molecules from the tumor core to the leading edge of the tumor, promoting invasion (75). An interesting question to be addressed is whether GBM EVs could promote functional export of some of the immunosuppressive features of the GBM TME, such as hypoxia or acidification, by transferring proteins or miRNA that are induced by these microenvironmental features in donor cells.

Therapy responses in GBM are mostly assessed radiologically, since brain tumor tissue is rarely available. Non-invasive biopsies would be an attractive option, if they can provide information on the underlying biology of the tumor. EVs released by the GBM tumor into the blood circulation or CSF are interesting candidates for biomarkers of the tumor status. Analysis of EV-based "liquid biopsies" has shown that EVs secreted by GBM cells differ from those secreted by normal glial cells, based on their cargo content, their quantity, and their size profile; this information could be exploited for monitoring therapy outcome or even for diagnosing patients with brain tumors. Indeed, plasma or CSF-derived EVs have already furnished information about the molecular subtype of GBM (76), hypoxic status (77) and therapy responsiveness (78). Many of the reported GBM EVs are enriched in oncogenic proteins (EGFRvIII), angiogenic factors, and RNAs (coding and non-coding). A comprehensive cargo characterization would be interesting from a research perspective but would require application of multiple technologies to achieve this (**Table 1**). Therefore, careful selection of the most tumor-specific EV markers would be necessary for clinical biomarker applications. Taken together, these advances in EV analysis highlight the precious information that can be obtained about a highly inaccessible brain tumor through plasma or CSF sampling. This of course opens up many possibilities of not just enhancing our understanding of the mechanisms of GBM progression, but also of improving on existing radiological monitoring. However, almost one third of the patients show imaging changes on brain MRI that are interpreted as tumor progression, eventually leading to therapy change or suspension, but which is in fact due to so-called pseudoprogression. According to response assessment in neuro-oncology criteria (RANO) pseudoprogression is a transient MRI pattern mimicking tumor progression but not necessarily accompanied by worsening of the clinical outcome (87). The process is generally observed within the first 3 months of completion of radiotherapy, but may occur later (88). The detailed causes of pseudoprogression are not fully determined, but mechanisms may include enhanced permeability of the tumor vasculature from chemotherapy and radiation, or immune cell infiltration (89). Pseudoprogression is an important issue in GBM and correct diagnosis could be very important in patients undergoing immunotherapy, for which immune infiltration is likely to be a necessary event for therapy

TABLE 1 | Categories of EV cargos detected in liquid biopsies in patients with GBM.

EV associated molecules	Biological source	Method of detection	Reference
RNAs			
miRNA-21	CSF	qPCR array	(29, 79)
RNU6-1 (small noncoding RNA)	serum	qPCR and PCR array	(12)
miR-320	serum	qPCR and PCR array	(12, 80)
HOTAIR (long noncoding RNA)	serum	qPCR	(81)
EGFRvIII mRNA	serum	qPCR	(13)
miRNA signature (10 miRNAs)	serum	qRT-PCR and arrays	(82)
DNA			
PD-L1	serum and plasma	droplet PCR	(66)
Proteins			
protein signature (five proteins)	Cavitron Ultrasonic Surgical Aspirator (CUSA)	MS	(83)
PTRF (Polymerase I and transcript release factor)	serum	Western blot	(84)
TrkB (Tropomyosin receptor kinase B)	plasma	Western blot	(85)
Semaphorin3A	serum	Electron microscopy Flow cytometry	(86)

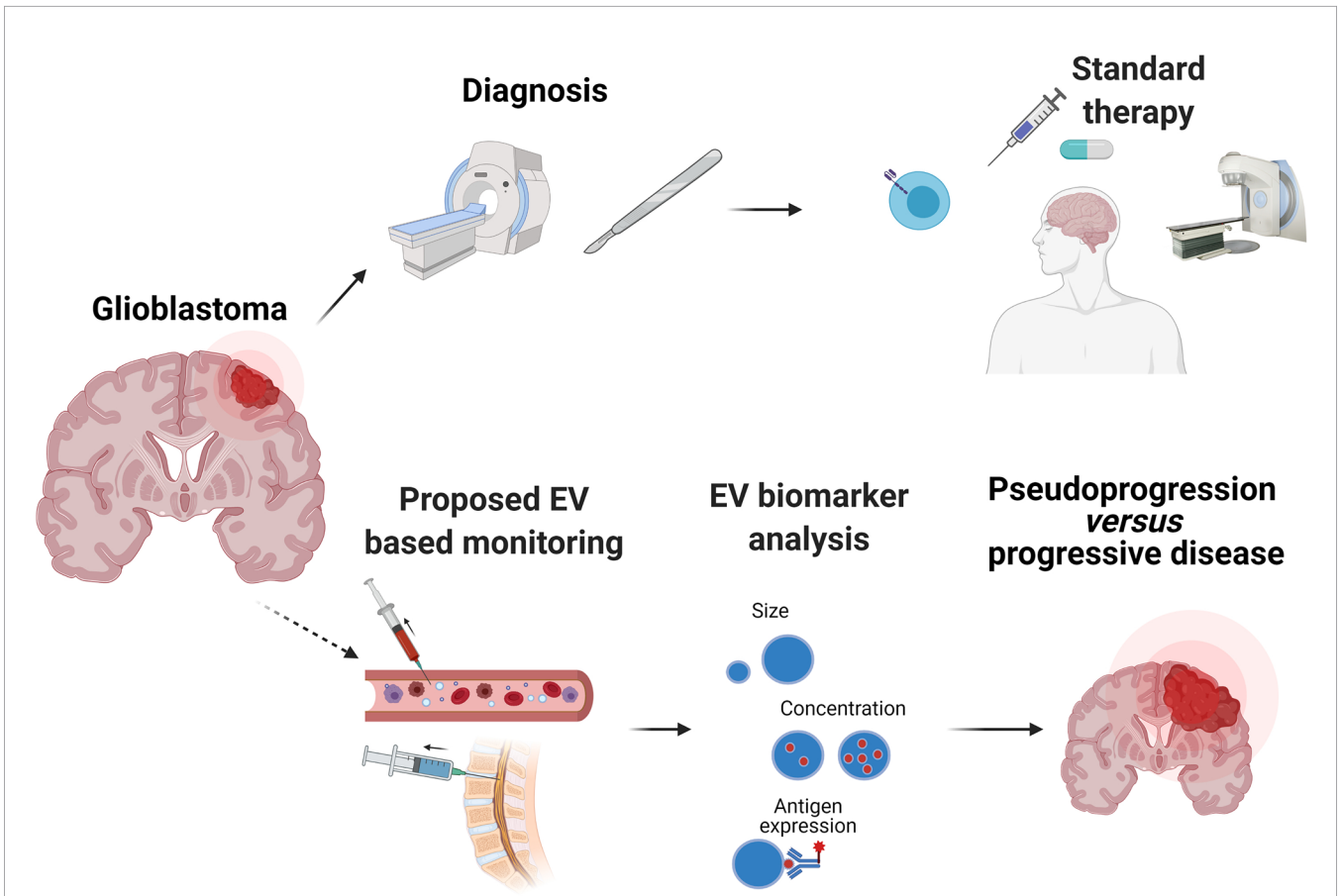

FIGURE 3 | Potential of EVs as a non-invasive clinical biomarker in GBM. Diagnosis of GBM usually comprises magnetic resonance imaging (MRI) and histopathological analysis of a tumor biopsy. Most patients receive treatment composed of surgery, followed by radiation and chemotherapy with temozolomide. Despite this treatment, GBM recurrence generally occurs. However, radiological distinction between tumor progression and pseudoprogression is often difficult, particularly after experimental treatments such as immunotherapy (immunomodulatory antibodies, vaccines, chimeric antigen receptor T cells). Methodologically, EVs can be rapidly characterized by nanoparticle tracking analysis (NTA) that can detect size and concentration, as well as surface expression of EV and tumor associated antigens with the use of fluorochrome-conjugated antibodies. EVs and their cargo detected in patients' plasma or CSF offer great potential as a biomarker that can improve diagnosis and treatment decisions.

response. Development and validation of EV-based biomarkers could therefore address this unmet clinical need for non-invasive biomarkers (**Figure 3**).

CONCLUDING REMARKS

The release of EVs by cancer cells and other cells within the GBM microenvironment, as well as their presence in plasma or CSF, is now established as an incontrovertible feature of GBM biology. Nevertheless, the field merits further research efforts to understand and to potentially profit from the presence of GBM-derived EVs. The list of possible functional properties of EVs that we have discussed now needs to be put back in the context of GBM *in vivo*. The biologically active concentrations of EVs that actually reach different areas of the tumor (hypoxic, perinecrotic or leading edge regions) remain to be determined. This is an important issue, in order to understand the very different cellular interactions (e.g. between cancer cells and immune cells induced by therapy) occurring in these different sites. Manipulating EV function will be challenging, but identifying the producer cell might offer opportunities to modulate EV release or cargo composition, such as a bioactive proteins or miRNAs. For the latter approach, the cargo molecule to therapeutically target would need to be chosen based on rigorous functional testing of recipient cell responses, ultimately *in vivo*. Finally, EV characterization from plasma or CSF, benefitting from sophisticated research platforms, has established the proof of principle of using EVs as liquid biopsy biomarkers. More widespread application for the unmet clinical need of non-invasive monitoring of treatment response, notably in immunotherapy clinical trials, should now be envisaged, with appropriate use of precise and robust EV and cargo characterization.

AUTHOR CONTRIBUTIONS

ST and PW conceived and wrote the manuscript. All authors contributed to the article and approved the submitted version.

ACKNOWLEDGMENTS

Figures were created with BioRender.com. PW acknowledges the support of Carigest Foundation.

REFERENCES

1. Tredan O, Galmarini CM, Patel K, Tannock IF. Drug Resistance and the Solid Tumor Microenvironment. *J Natl Cancer Inst* (2007) 99(19):1441–54. doi: 10.1093/jnci/djm135
2. Wei J, Wu A, Kong LY, Wang Y, Fuller G, Fokt I, et al. Hypoxia Potentiates Glioma-Mediated Immunosuppression. *PloS One* (2011) 6(1):e16195. doi: 10.1371/journal.pone.0016195
3. Vaupel P. Hypoxia and Aggressive Tumor Phenotype: Implications for Therapy and Prognosis. *Oncologist* (2008) 13 Suppl 3:21–6. doi: 10.1634/theoncologist.13-S3-21
4. Stupp R, Mason WP, van den Bent MJ, Weller M, Fisher B, Taphoorn MJ, et al. Radiotherapy Plus Concomitant and Adjuvant Temozolomide for Glioblastoma. *N Engl J Med* (2005) 352(10):987–96. doi: 10.1056/NEJMoa043330
5. Calvo Tardon M, Marinari E, Migliorini D, Bes V, Tankov S, Charrier E, et al. An Experimentally Defined Hypoxia Gene Signature in Glioblastoma and Its Modulation by Metformin. *Biol (Basel)* (2020) 9(9):264. doi: 10.3390/biology9090264
6. Holmgren L, Szeles A, Rajnavolgyi E, Folkman J, Klein G, Ernberg I, et al. Horizontal Transfer of DNA by the Uptake of Apoptotic Bodies. *Blood* (1999) 93(11):3956–63. doi: 10.1182/blood.V93.11.3956.411k05_3956_3963
7. Pavlyukov MS, Yu H, Bastola S, Minata M, Shender VO, Lee Y, et al. Apoptotic Cell-Derived Extracellular Vesicles Promote Malignancy of Glioblastoma Via Intercellular Transfer of Splicing Factors. *Cancer Cell* (2018) 34(1):119–135 e10. doi: 10.1016/j.ccell.2018.05.012
8. Lotvall J, Hill AF, Hochberg F, Buzas EI, Di Vizio D, Gardiner C, et al. Minimal Experimental Requirements for Definition of Extracellular Vesicles and Their Functions: A Position Statement From the International Society for Extracellular Vesicles. *J Extracell Vesicles* (2014) 3:26913. doi: 10.3402/jev.v3.26913
9. Thery C, Witwer KW, Aikawa E, Alcaraz MJ, Anderson JD, Andriantsitohaina R, et al. Minimal Information for Studies of Extracellular Vesicles 2018 (MISEV2018): A Position Statement of the International Society for Extracellular Vesicles and Update of the MISEV2014 Guidelines. *J Extracell Vesicles* (2018) 7(1):1535750. doi: 10.1080/20013078.2018.1461450
10. Tian T, Zhu YL, Zhou YY, Liang GF, Wang YY, Hu FH, et al. Exosome Uptake Through Clathrin-Mediated Endocytosis and Macropinocytosis and Mediating miR-21 Delivery. *J Biol Chem* (2014) 289(32):22258–67. doi: 10.1074/jbc.M114.588046
11. Horibe S, Tanahashi T, Kawauchi S, Murakami Y, Rikitake Y. Mechanism of Recipient Cell-Dependent Differences in Exosome Uptake. *BMC Cancer* (2018) 18(1):47. doi: 10.1186/s12885-017-3958-1
12. Montecalvo A, Larregina AT, Shufesky WJ, Stolz DB, Sullivan ML, Karlsson JM, et al. Mechanism of Transfer of Functional microRNAs Between Mouse Dendritic Cells Via Exosomes. *Blood* (2012) 119(3):756–66. doi: 10.1182/blood-2011-02-338004
13. Skog J, Wurdinger T, van Rijn S, Meijer DH, Gainche L, Sena-Esteves M, et al. Glioblastoma Microvesicles Transport RNA and Proteins That Promote Tumour Growth and Provide Diagnostic Biomarkers. *Nat Cell Biol* (2008) 10(12):1470–6. doi: 10.1038/ncb1800
14. Andre-Gregoire G, Bidere N, Gavard J. Temozolomide Affects Extracellular Vesicles Released by Glioblastoma Cells. *Biochimie* (2018) 155:11–5. doi: 10.1016/j.biochi.2018.02.007
15. Kucharzewska P, Christianson HC, Welch JE, Svensson KJ, Fredlund E, Ringner M, et al. Exosomes Reflect the Hypoxic Status of Glioma Cells and Mediate Hypoxia-Dependent Activation of Vascular Cells During Tumor Development. *Proc Natl Acad Sci USA* (2013) 110(18):7312–7. doi: 10.1073/pnas.1220998110
16. Ma C, Chen H, Zhang S, Yan Y, Wu R, Wang Y, et al. Exosomal and Extracellular HMGB1 Have Opposite Effects on SASH1 Expression in Rat Astrocytes and Glioma C6 Cells. *Biochem Biophys Res Commun* (2019) 518(2):325–30. doi: 10.1016/j.bbrc.2019.08.057
17. Al-Nedawi K, Meehan B, Micallef J, Lhotak V, May L, Guha A, et al. Intercellular Transfer of the Oncogenic Receptor EGFRvIII by Microvesicles Derived From Tumour Cells. *Nat Cell Biol* (2008) 10(5):619–24. doi: 10.1038/ncb1725
18. Wei Z, Batagov AO, Schinelli S, Wang J, Wang Y, El Fatimy R, et al. Coding and Noncoding Landscape of Extracellular RNA Released by Human Glioma Stem Cells. *Nat Commun* (2017) 8(1):1145. doi: 10.1038/s41467-017-01196-x
19. O'Brien J, Hayder H, Zayed Y, Peng C. Overview of MicroRNA Biogenesis, Mechanisms of Actions, and Circulation. *Front Endocrinol (Lausanne)* (2018) 9:402. doi: 10.3389/fendo.2018.00402
20. Zhong F, Huang T, Leng J. Serum miR-29b as a Novel Biomarker for Glioblastoma Diagnosis and Prognosis. *Int J Clin Exp Pathol* (2019) 12(11):4106–12.

21. van der Vos KE, Abels ER, Zhang X, Lai C, Carrizosa E, Oakley D, et al. Directly Visualized Glioblastoma-Derived Extracellular Vesicles Transfer RNA to Microglia/Macrophages in the Brain. *Neuro Oncol* (2016) 18(1):58–69. doi: 10.1093/neuonc/nov244
22. Zottel A, Samec N, Kump A, Raspor Dall'Olio LR, Puzar Dominkus P, Romih R, et al. Analysis of miR-9-5p, miR-124-3p, miR-21-5p, miR-138-5p, and miR-1-3p in Glioblastoma Cell Lines and Extracellular Vesicles. *Int J Mol Sci* (2020) 21(22):8491. doi: 10.3390/ijms21228491
23. Chan JA, Krichevsky AM, Kosik KS. MicroRNA-21 is an Antiapoptotic Factor in Human Glioblastoma Cells. *Cancer Res* (2005) 65(14):6029–33. doi: 10.1158/0008-5472.CAN-05-0137
24. Sana J, Busek P, Fadrus P, Besse A, Radova L, Vecera M, et al. Identification of microRNAs Differentially Expressed in Glioblastoma Stem-Like Cells and Their Association With Patient Survival. *Sci Rep* (2018) 8(1):2836. doi: 10.1038/s41598-018-20929-6
25. Kim J, Zhang Y, Skalski M, Hayes J, Kefas B, Schiff D, et al. microRNA-148a is a Prognostic Oncomir That Targets MIG6 and BIM to Regulate EGFR and Apoptosis in Glioblastoma. *Cancer Res* (2014) 74(5):1541–53. doi: 10.1158/0008-5472.CAN-13-1449
26. Masoudi MS, Mehrabian E, Mirzaei H. Mir-21: A Key Player in Glioblastoma Pathogenesis. *J Cell Biochem* (2018) 119(2):1285–90. doi: 10.1002/jcb.26300
27. Abels ER, Maas SLN, Nieland L, Wei Z, Cheah PS, Tai E, et al. Glioblastoma-Associated Microglia Reprogramming Is Mediated by Functional Transfer of Extracellular Mir-21. *Cell Rep* (2019) 28(12):3105–3119 e7. doi: 10.1016/j.celrep.2019.08.036
28. Gaur AB, Holbeck SL, Colburn NH, Israel MA. Downregulation of Pdcd4 by mir-21 Facilitates Glioblastoma Proliferation In Vivo. *Neuro Oncol* (2011) 13 (6):580–90. doi: 10.1093/neuonc/nor033
29. Shi R, Wang PY, Li XY, Chen JX, Li Y, Zhang XZ, et al. Exosomal Levels of miRNA-21 From Cerebrospinal Fluids Associated With Poor Prognosis and Tumor Recurrence of Glioma Patients. *Oncotarget* (2015) 6(29):26971–81. doi: 10.18632/oncotarget.4699
30. Zhang Z, Yin J, Lu C, Wei Y, Zeng A, You Y. Exosomal Transfer of Long non-Coding RNA Sbf2-AS1 Enhances Chemoresistance to Temozolomide in Glioblastoma. *J Exp Clin Cancer Res* (2019) 38(1):166. doi: 10.1186/s13046-019-1139-6
31. Volinia S, Calin GA, Liu CG, Ambs S, Cimmino A, Petrocca F, et al. A microRNA Expression Signature of Human Solid Tumors Defines Cancer Gene Targets. *Proc Natl Acad Sci USA* (2006) 103(7):2257–61. doi: 10.1073/pnas.0510565103
32. Bhandari V, Hoey C, Liu LY, Lalonde E, Ray J, Livingstone J, et al. Molecular Landmarks of Tumor Hypoxia Across Cancer Types. *Nat Genet* (2019) 51 (2):308–18. doi: 10.1038/s41588-018-0318-2
33. Agrawal R, Pandey P, Jha P, Dwivedi V, Sarkar C, Kulshreshtha R. Hypoxic Signature of microRNAs in Glioblastoma: Insights From Small RNA Deep Sequencing. *BMC Genomics* (2014) 15:686. doi: 10.1186/1471-2164-15-686
34. Hermansen SK, Nielsen BS, Aaberg-Jessen C, Kristensen BW. Mir-21 Is Linked to Glioma Angiogenesis: A Co-Localization Study. *J Histochem Cytochem* (2016) 64(2):138–48. doi: 10.1369/0022155415623515
35. Lai NS, Wu DG, Fang XG, Lin YC, Chen SS, Li ZB, et al. Serum microRNA-210 as a Potential Noninvasive Biomarker for the Diagnosis and Prognosis of Glioma. *Br J Cancer* (2015) 112(7):1241–6. doi: 10.1038/bjc.2015.91
36. Lan F, Yue X, Xia T. Exosomal microRNA-210 is a Potentially non-Invasive Biomarker for the Diagnosis and Prognosis of Glioma. *Oncol Lett* (2020) 19 (3):1967–74. doi: 10.3892/ol.2020.11249
37. Setti M, Osti D, Richichi C, Ortensi B, Del Bene M, Fornasari L, et al. Extracellular Vesicle-Mediated Transfer of CLIC1 Protein is a Novel Mechanism for the Regulation of Glioblastoma Growth. *Oncotarget* (2015) 6(31):31413–27. doi: 10.18632/oncotarget.5105
38. Wang L, He S, Tu Y, Ji P, Zong J, Zhang J, et al. Elevated Expression of Chloride Intracellular Channel 1 is Correlated With Poor Prognosis in Human Gliomas. *J Exp Clin Cancer Res* (2012) 31:44. doi: 10.1186/1756-9966-31-44
39. Hallal S, Mallawaaratchy DM, Wei H, Ebrahimkhani S, Stringer BW, Day BW, et al. Extracellular Vesicles Released by Glioblastoma Cells Stimulate Normal Astrocytes to Acquire a Tumor-Supportive Phenotype Via p53 and MYC Signaling Pathways. *Mol Neurobiol* (2019) 56(6):4566–81. doi: 10.1007/s12035-018-1385-1
40. Gao X, Zhang Z, Mashimo T, Shen B, Nyagilo J, Wang H, et al. Gliomas Interact With Non-glioma Brain Cells Via Extracellular Vesicles. *Cell Rep* (2020) 30(8):2489–2500 e5. doi: 10.1016/j.celrep.2020.01.089
41. Zhao H, Yang L, Baddour J, Achreja A, Bernard V, Moss T, et al. Tumor Microenvironment Derived Exosomes Pleiotropically Modulate Cancer Cell Metabolism. *Elife* (2016) 5:e10250. doi: 10.7554/eLife.10250
42. Chen J, Li Y, Yu TS, McKay RM, Burns DK, Kernie SG, et al. A Restricted Cell Population Propagates Glioblastoma Growth After Chemotherapy. *Nature* (2012) 488(7412):522–6. doi: 10.1038/nature11287
43. Bao S, Wu Q, McLendon RE, Hao Y, Shi Q, Hjelmeland AB, et al. Glioma Stem Cells Promote Radioresistance by Preferential Activation of the DNA Damage Response. *Nature* (2006) 444(7120):756–60. doi: 10.1038/nature05236
44. Singh SK, Hawkins C, Clarke ID, Squire JA, Bayani J, Hide T, et al. Identification of Human Brain Tumour Initiating Cells. *Nature* (2004) 432 (7015):396–401. doi: 10.1038/nature03128
45. Spinelli C, Montermini L, Meehan B, Brisson AR, Tan S, Choi D, et al. Molecular Subtypes and Differentiation Programmes of Glioma Stem Cells as Determinants of Extracellular Vesicle Profiles and Endothelial Cell-Stimulating Activities. *J Extracell Vesicles* (2018) 7(1):1490144. doi: 10.1080/20013078.2018.1490144
46. Sun Z, Wang L, Zhou Y, Dong L, Ma W, Lv L, et al. Glioblastoma Stem Cell-Derived Exosomes Enhance Stemness and Tumorigenicity of Glioma Cells by Transferring Notch1 Protein. *Cell Mol Neurobiol* (2020) 40(5):767–84. doi: 10.1007/s10571-019-00771-8
47. Treps L, Perret R, Edmond S, Ricard D, Gavard J. Glioblastoma Stem-Like Cells Secrete the Pro-Angiogenic VEGF-A Factor in Extracellular Vesicles. *J Extracell Vesicles* (2017) 6(1):1359479. doi: 10.1080/20013078.2017.1359479
48. Garnier D, Meehan B, Kislinger T, Daniel P, Sinha A, Abdulkarim B, et al. Divergent Evolution of Temozolomide Resistance in Glioblastoma Stem Cells is Reflected in Extracellular Vesicles and Coupled With Radiosensitization. *Neuro Oncol* (2018) 20(2):236–48. doi: 10.1093/neuonc/nox142
49. Lucero R, Zappulli V, Sammarco A, Murillo OD, Cheah PS, Srinivasan S, et al. Glioma-Derived Mirna-Containing Extracellular Vesicles Induce Angiogenesis by Reprogramming Brain Endothelial Cells. *Cell Rep* (2020) 30(7):2065–2074 e4. doi: 10.1016/j.celrep.2020.01.073
50. Azambuja JH, Ludwig N, Yerneni S, Rao A, Braganhol E, Whiteside TL. Molecular Profiles and Immunomodulatory Activities of Glioblastoma-Derived Exosomes. *Neurooncol Adv* (2020) 2(1):vdaa056. doi: 10.1093/noajnl/vdaa056
51. Zhang QW, Liu L, Gong CY, Shi HS, Zeng YH, Wang XZ, et al. Prognostic Significance of Tumor-Associated Macrophages in Solid Tumor: A Meta-Analysis of the Literature. *PloS One* (2012) 7(12):e50946. doi: 10.1371/journal.pone.0050946
52. Komohara Y, Ohnishi K, Kuratsu J, Takeya M. Possible Involvement of the M2 Anti-Inflammatory Macrophage Phenotype in Growth of Human Gliomas. *J Pathol* (2008) 216(1):15–24. doi: 10.1002/path.2370
53. Gabrusiewicz K, Rodriguez B, Wei J, Hashimoto Y, Healy LM, Maiti SN, et al. Glioblastoma-Infiltrated Innate Immune Cells Resemble M0 Macrophage Phenotype. *JCI Insight* (2016) 1(2):e85841. doi: 10.1172/jci.insight.85841
54. de Vrij J, Maas SL, Kwappenberg KM, Schnoor R, Kleijn A, Dekker L, et al. Glioblastoma-Derived Extracellular Vesicles Modify the Phenotype of Monocytic Cells. *Int J Cancer* (2015) 137(7):1630–42. doi: 10.1002/ijc.29521
55. Pello OM, Chevre R, Laoui D, De Juan A, Lolo F, Andres-Manzano MJ, et al. In Vivo Inhibition of c-MYC in Myeloid Cells Impairs Tumor-Associated Macrophage Maturation and Pro-Tumoral Activities. *PloS One* (2012) 7(9): e45399. doi: 10.1371/journal.pone.0045399
56. Qian M, Wang S, Guo X, Wang J, Zhang Z, Qiu W, et al. Hypoxic Glioma-Derived Exosomes Deliver microRNA-1246 to Induce M2 Macrophage Polarization by Targeting TERF2IP Via the STAT3 and NF-kappaB Pathways. *Oncogene* (2020) 39(2):428–42. doi: 10.1038/s41388-019-0996-y
57. Mu X, Shi W, Xu Y, Xu C, Zhao T, Geng B, et al. Tumor-derived lactate induces M2 macrophage polarization via the activation of the ERK/STAT3 signaling pathway in breast cancer. *Cell Cycle* (2018) 17(4):428–38. doi: 10.1080/15384101.2018.1444305
58. Wada J, Kanwar YS. Identification and Characterization of galectin-9, a Novel Beta-Galactoside-Binding Mammalian Lectin. *J Biol Chem* (1997) 272 (9):6078–86. doi: 10.1074/jbc.272.9.6078

59. Wang M, Cai Y, Peng Y, Xu B, Hui W, Jiang Y. Exosomal LGALS9 in the Cerebrospinal Fluid of Glioblastoma Patients Suppressed Dendritic Cell Antigen Presentation and Cytotoxic T-cell Immunity. *Cell Death Dis* (2020) 11(10):896. doi: 10.1038/s41419-020-03042-3
60. Gabrusiewicz K, Li X, Wei J, Hashimoto Y, Marisetty AL, Ott M, et al. Glioblastoma Stem Cell-Derived Exosomes Induce M2 Macrophages and PD-L1 Expression on Human Monocytes. *Oncoimmunology* (2018) 7(4): e1412909. doi: 10.1080/2162402X.2017.1412909
61. Fridman WH, Zitvogel L, Sautes-Fridman C, Kroemer G. The Immune Contexture in Cancer Prognosis and Treatment. *Nat Rev Clin Oncol* (2017) 14(12):717–34. doi: 10.1038/nrclinonc.2017.101
62. Marinari E, Allard M, Gustave R, Widmer V, Philippin G, Merkler D, et al. Inflammation and Lymphocyte Infiltration are Associated With Shorter Survival in Patients With High-Grade Glioma. *Oncoimmunology* (2020) 9 (1):1779990. doi: 10.1080/2162402X.2020.1779990
63. Liu ZM, Wang YB, Yuan XH. Exosomes From Murine-Derived GL26 Cells Promote Glioblastoma Tumor Growth by Reducing Number and Function of CD8+T Cells. *Asian Pac J Cancer Prev* (2013) 14(1):309–14. doi: 10.7314/APJCP.2013.14.1.309
64. Hellwinkel JE, Redzic JS, Harland TA, Gunaydin D, Anchordoquy TJ, Graner MW. Glioma-Derived Extracellular Vesicles Selectively Suppress Immune Responses. *Neuro Oncol* (2016) 18(4):497–506. doi: 10.1093/neuonc/nov170
65. Mirzaei R, Sarkar S, Dzikowski L, Rawji KS, Khan L, Faissner A, et al. Brain Tumor-Initiating Cells Export Tenascin-C Associated With Exosomes to Suppress T Cell Activity. *Oncoimmunology* (2018) 7(10):e1478647. doi: 10.1080/2162402X.2018.1478647
66. Ricklefs FL, Alayo Q, Krenzlin H, Mahmoud AB, Speranza MC, Nakashima H, et al. Immune Evasion Mediated by PD-L1 on Glioblastoma-Derived Extracellular Vesicles. *Sci Adv* (2018) 4(3):eaar2766. doi: 10.1126/sciadv.aar2766
67. Berghoff AS, Kiesel B, Widhalm G, Rajky O, Ricken G, Wohrer A, et al. Programmed Death Ligand 1 Expression and Tumor-Infiltrating Lymphocytes in Glioblastoma. *Neuro Oncol* (2015) 17(8):1064–75. doi: 10.1093/neuonc/nou307
68. Saas P, Walker PR, Hahne M, Quiquerez AL, Schnuriger V, Perrin G, et al. Fas Ligand Expression by Astrocytoma In Vivo: Maintaining Immune Privilege in the Brain? *J Clin Invest* (1997) 99(6):1173–8. doi: 10.1172/JCI119273
69. Wieckowski EU, Visus C, Szajnik M, Szczepanski MJ, Storkus WJ, Whiteside TL. Tumor-Derived Microvesicles Promote Regulatory T Cell Expansion and Induce Apoptosis in Tumor-Reactive Activated CD8+ T Lymphocytes. *J Immunol* (2009) 183(6):3720–30. doi: 10.4049/jimmunol.0900970
70. Maybruck BT, Pfannenstiel LW, Diaz-Montero M, Gastman BR. Tumor-Derived Exosomes Induce CD8(+) T Cell Suppressors. *J Immunother Cancer* (2017) 5(1):65. doi: 10.1186/s40425-017-0269-7
71. Czystowska-Kuzmicz M, Sosnowska A, Nowis D, Ramji K, Szajnik M, Chlebowska-Tuz J, et al. Small Extracellular Vesicles Containing Arginase-1 Suppress T-cell Responses and Promote Tumor Growth in Ovarian Carcinoma. *Nat Commun* (2019) 10(1):3000. doi: 10.1038/s41467-019-10979-3
72. Iorgulescu JB, Ivan ME, Safaee M, Parsa AT. The Limited Capacity of Malignant Glioma-Derived Exosomes to Suppress Peripheral Immune Effectors. *J Neuroimmunol* (2016) 290:103–8. doi: 10.1016/j.jneuroim.2015.11.025
73. Domenis R, Cesselli D, Toffoletto B, Bourkoula E, Caponnetto F, Manini I, et al. Systemic T Cells Immunosuppression of Glioma Stem Cell-Derived Exosomes Is Mediated by Monocytic Myeloid-Derived Suppressor Cells. *PloS One* (2017) 12(1):e0169932. doi: 10.1371/journal.pone.0169932
74. Cianciaruso C, Beltraminelli T, Duval F, Nassiri S, Hamelin R, Mozes A, et al. Molecular Profiling and Functional Analysis of Macrophage-Derived Tumor Extracellular Vesicles. *Cell Rep* (2019) 27(10):3062–3080 e11. doi: 10.1016/j.celrep.2019.05.008
75. Pace KR, Dutt R, Galileo DS. Exosomal L1CAM Stimulates Glioblastoma Cell Motility, Proliferation, and Invasiveness. *Int J Mol Sci* (2019) 20(16):3982. doi: 10.3390/ijms20163982
76. Lane R, Simon T, Vintu M, Solkin B, Koch B, Stewart N, et al. Cell-Derived Extracellular Vesicles can be Used as a Biomarker Reservoir for Glioblastoma Tumor Subtyping. *Commun Biol* (2019) 2:315. doi: 10.1038/s42003-019-0560-x
77. Indira Chandran V, Welinder C, Goncalves de Oliveira K, Cerezo-Magana M, Mansson AS, Johansson MC, et al. Global Extracellular Vesicle Proteomic Signature Defines U87-MG Glioma Cell Hypoxic Status With Potential Implications for non-Invasive Diagnostics. *J Neurooncol* (2019) 144(3):477–88. doi: 10.1007/s11060-019-03262-4
78. Panzarini E, Tacconi S, Carata E, Mariano S, Tata AM, Dini L. Molecular Characterization of Temozolomide-Treated and Non Temozolomide-Treated Glioblastoma Cells Released Extracellular Vesicles and Their Role in the Macrophage Response. *Int J Mol Sci* (2020) 21(21):8353. doi: 10.3390/ijms21218353
79. Qu K, Lin T, Pang Q, Liu T, Wang Z, Tai M, et al. Extracellular miRNA-21 as a Novel Biomarker in Glioma: Evidence From Meta-Analysis, Clinical Validation and Experimental Investigations. *Oncotarget* (2016) 7(23):33994–4010. doi: 10.18632/oncotarget.9188
80. Dong L, Li Y, Han C, Wang X, She L, Zhang H. miRNA Microarray Reveals Specific Expression in the Peripheral Blood of Glioblastoma Patients. *Int J Oncol* (2014) 45(2):746–56. doi: 10.3892/ijo.2014.2459
81. Tan SK, Pastori C, Penas C, Komotar RJ, Ivan ME, Wahlestedt C, et al. Serum Long Noncoding RNA HOTAIR as a Novel Diagnostic and Prognostic Biomarker in Glioblastoma Multiforme. *Mol Cancer* (2018) 17(1):74. doi: 10.1186/s12943-018-0822-0
82. Akers JC, Ramakrishnan V, Kim R, Phillips S, Kaimal V, Mao Y, et al. miRNA Contents of Cerebrospinal Fluid Extracellular Vesicles in Glioblastoma Patients. *J Neurooncol* (2015) 123(2):205–16. doi: 10.1007/s11060-015-1784-3
83. Mallawaaratchy DM, Hallal S, Russell B, Ly L, Ebrahimkhani S, Wei H, et al. Comprehensive Proteome Profiling of Glioblastoma-Derived Extracellular Vesicles Identifies Markers for More Aggressive Disease. *J Neurooncol* (2017) 131(2):233–44. doi: 10.1007/s11060-016-2298-3
84. Huang K, Fang C, Yi K, Liu X, Qi H, Tan Y, et al. The Role of PTRF/Cavin1 as a Biomarker in Both Glioma and Serum Exosomes. *Theranostics* (2018) 8 (6):1540–57. doi: 10.7150/thno.22952
85. Pinet S, Bessette B, Vedrenne N, Lacroix A, Richard L, Jauberteau MO, et al. TrkB-containing Exosomes Promote the Transfer of Glioblastoma Aggressiveness to YKL-40-inactivated Glioblastoma Cells. *Oncotarget* (2016) 7(31):50349–64. doi: 10.18632/oncotarget.10387
86. Treps L, Edmond S, Harford-Wright E, Galan-Moya EM, Schmitt A, Azzi S, et al. Extracellular Vesicle-Transported Semaphorin3A Promotes Vascular Permeability in Glioblastoma. *Oncogene* (2016) 35(20):2615–23. doi: 10.1038/onc.2015.317
87. Wen PY, Chang SM, Van den Bent MJ, Vogelbaum MA, Macdonald DR, Lee EQ. Response Assessment in Neuro-Oncology Clinical Trials. *J Clin Oncol* (2017) 35(21):2439–49. doi: 10.1200/JCO.2017.72.7511
88. Radbruch A, Fladt J, Kickingereder P, Wiestler B, Nowosielski M, Baumer P, et al. Pseudoprogression in Patients With Glioblastoma: Clinical Relevance Despite Low Incidence. *Neuro Oncol* (2015) 17(1):151–9. doi: 10.1093/neuonc/nou129
89. Lieberman F. Glioblastoma Update: Molecular Biology, Diagnosis, Treatment, Response Assessment, and Translational Clinical Trials. *F1000Res* (2017) 6:1892. doi: 10.12688/f1000research.11493.1

Conflict of Interest: The authors declare that the research was conducted in the absence of any commercial or financial relationships that could be construed as a potential conflict of interest.

frontiers in Oncology

REVIEW
published: 08 June 2021
doi: 10.3389/fonc.2021.631037

Genetic Alterations in Gliomas Remodel the Tumor Immune Microenvironment and Impact Immune-Mediated Therapies

*Maria B. Garcia-Fabiani[1,2], Santiago Haase[1,2], Andrea Comba[1,2], Stephen Carney[1,2], Brandon McClellan[1,3], Kaushik Banerjee[1,2], Mahmoud S. Alghamri[1,2], Faisal Syed[1,2], Padma Kadiyala[1,2], Felipe J. Nunez[4], Marianela Candolfi[5], Antonela Asad[5], Nazareno Gonzalez[5], Marisa E. Aikins[6,7], Anna Schwendeman[6,7], James J. Moon[6,7,8], Pedro R. Lowenstein[1,2] and Maria G. Castro[1,2]**

[1] Department of Neurosurgery, University of Michigan Medical School, Ann Arbor, MI, United States, [2] Department of Cell and Developmental Biology, University of Michigan Medical School, Ann Arbor, MI, United States, [3] Immunology graduate program, University of Michigan Medical School, Ann Arbor, MI, United States, [4] Leloir Institute Foundation, Buenos Aires, Argentina, [5] Instituto de Investigaciones Biomédicas (INBIOMED, UBA-CONICET), Facultad de Medicina, Universidad de Buenos Aires, Buenos Aires, Argentina, [6] Department of Pharmaceutical Sciences, University of Michigan, Ann Arbor, MI, United States, [7] Biointerfaces Institute, University of Michigan, Ann Arbor, MI, United States, [8] Department of Biomedical Engineering, University of Michigan, Ann Arbor, MI, United States

OPEN ACCESS

Edited by:
Valérie Dutoit, Université de Genève, Switzerland

Reviewed by:
Mirco Friedrich, German Cancer Research Center (DKFZ), Germany
Gregor Hutter, University Hospital of Basel, Switzerland

***Correspondence:**
Maria G. Castro
mariacas@med.umich.edu

Specialty section:
This article was submitted to Cancer Immunity and Immunotherapy, a section of the journal Frontiers in Oncology

Received: *19 November 2020*
Accepted: *06 May 2021*
Published: *08 June 2021*

Citation:
Garcia-Fabiani MB, Haase S, Comba A, Carney S, McClellan B, Banerjee K, Alghamri MS, Syed F, Kadiyala P, Nunez FJ, Candolfi M, Asad A, Gonzalez N, Aikins ME, Schwendeman A, Moon JJ, Lowenstein PR and Castro MG (2021) Genetic Alterations in Gliomas Remodel the Tumor Immune Microenvironment and Impact Immune-Mediated Therapies. Front. Oncol. 11:631037. doi: 10.3389/fonc.2021.631037

High grade gliomas are malignant brain tumors that arise in the central nervous system, in patients of all ages. Currently, the standard of care, entailing surgery and chemo radiation, exhibits a survival rate of 14-17 months. Thus, there is an urgent need to develop new therapeutic strategies for these malignant brain tumors. Currently, immunotherapies represent an appealing approach to treat malignant gliomas, as the pre-clinical data has been encouraging. However, the translation of the discoveries from the bench to the bedside has not been as successful as with other types of cancer, and no long-lasting clinical benefits have been observed for glioma patients treated with immune-mediated therapies so far. This review aims to discuss our current knowledge about gliomas, their molecular particularities and the impact on the tumor immune microenvironment. Also, we discuss several murine models used to study these therapies pre-clinically and how the model selection can impact the outcomes of the approaches to be tested. Finally, we present different immunotherapy strategies being employed in clinical trials for glioma and the newest developments intended to harness the immune system against these incurable brain tumors.

Keywords: glioma, immune microenviroment, immunotherapy, mouse model, clinical trial

Abbreviations: CNS, Central nervous system; GBM, Glioblastoma; HGG, High grade glioma; ICI, Immune checkpoint inhibitors; LGG, Low grade glioma; MDSC Myeloid-derived suppre,ssor cells; MS, Median survival; OS, Overall Survival; OVs. Oncolytic Viruses; PFS, Progression Free Survival; PBMCs, peripheral blood mononuclear cells; SOC, Standard of care; TAA, Tumor-associated antigen; TILs, Tumor-infiltrating lymphocytes; TME, Tumor microenvironment; TMZ, Temozolomide; Tregs, Regulatory T cells; TSA, Tumor-specific antigen.

INTRODUCTION

Malignant tumors of the central nervous system (CNS) have an annual rate mortality of 9.01 per 100,000 adults in the US (1). Gliomas are brain tumors which clinically can present as grades II–IV in relation to their malignancy. Glioblastoma, the most aggressive type of glioma (high-grade glioma, WHO grade IV), accounts for the majority of gliomas and the highest incidence rate for malignant tumors of the CNS in adults (3.21 per 100,000 population) (1). This type of aggressive tumor has been subjected to extensive research due to the dismal outcomes of the current standard of care (SOC) therapies (maximal safe surgery, followed by radiation and chemotherapy with Temozolomide), and the lack of improvement in the median survival post-diagnosis (14-17 months) (2).

There are several aspects of this type of tumor that makes it difficult to treat (3), such as its anatomical location and the presence of a blood-brain barrier, which hampers the delivery of therapeutics (4); its intrinsic infiltrative nature, that makes it a tumor virtually impossible to resect completely (3, 5); and the presence of an immunosuppressive micro-environment, that impedes the natural development of an anti-tumor immune response (6–11). In spite of these challenges, in the last decade, there has been an expansion in the therapies aimed to harness the immune system to direct it against malignant glioma (12). So far, pre-clinical data has demonstrated the effectiveness of immune-stimulatory or anti-immunosuppressive strategies, and many clinical trials are currently ongoing to test their efficacy in the clinical arena (12).

This review aims to discuss several aspects related to the glioma immune-microenvironment and the newest strategies that could emerge as a result of the latest pre-clinical investigations. Firstly, we will present the available clinical data regarding the immune microenvironment in glioma and its particularities in terms of tumor classification and molecular features (7, 13–15), as well as the current immune-mediated strategies being tested in the pre-clinical field (16). Also, we will overview the present immune-stimulatory therapeutic modalities being tested in clinical trials (8, 17). Finally, we will discuss the latest pre-clinical developments related to anti-glioma therapies that could enhance the immune system to develop long-lasting anti-tumor immunity (18–24).

We believe that this review will bring to light the latest improvements in the strategies being developed to treat high-grade gliomas aimed to stimulate an anti-tumor immune response, broadening the spectrum of possibilities to be tested in the clinical setting and bringing new concepts for fighting this devastating tumor.

GLIOMA CLASSIFICATION

Adult Gliomas

Glioma involves a heterogeneous group of primary brain tumors originated from neural precursor cells (25), and represent thirty percent of the CNS tumors (1, 26). They can be divided in diffuse gliomas and non-diffuse gliomas, which refer to tumors with a circumscribed growth pattern, including ependymomas and other astrocytic tumors (27, 28). The majority of adult gliomas are diffuse, distinguished by an infiltrative pattern of growth within the CNS parenchyma, and have been typically classified according to histological features and grade of malignancy (27–29). The histological analysis of surgical specimens allows the identification different glioma subtypes: oligodendroglioma, characterized by uniformly rounded nuclei; astrocytoma, with nuclear irregularities and hyperchromasia; and oligoastrocytoma, which is a rare mixed glioma (30). Additionally, based on the grade of anaplasia it is possible to further divide gliomas into four World Health Organization (WHO) subtypes, ranging from WHO grade I to WHO grade IV. WHO grade I gliomas correspond to tumors with slow development and better prognosis; WHO grade II gliomas are defined as low grade gliomas; WHO grade III gliomas are used to describe anaplastic gliomas; and WHO grade IV encompass glioblastoma (27, 28, 31). Usually, high grade gliomas (HGG) include WHO III and IV gliomas.

The revised 2016 WHO CNS classification includes, for the first time, distinctive genetic/epigenetic alterations to define several groups of gliomas (28, 32). The presence and distribution of genetic alterations in brain tumors, such as alterations in *PI3K, PDGFR, PTEN, TP53, IDH, EGFR, H3F3A, ATRX* and *TERT* (33–35), are now a criteria used to differentiate glioma subtypes (28, 36, 37). Each molecular glioma subtype is related to a histologic tumor-class and a particular WHO grade of malignancy (33, 34, 38–40). The hallmark genetic alteration in adult diffuse gliomas, that promoted the incorporation of molecular features in their classification, is the mutation in isocitrate dehydrogenase 1 (IDH1). This alteration, usually at arginine 132 (IDH1-R132H), is highly frequent in diffuse low-grade gliomas (LGGs; WHO grade II), in anaplastic astrocytomas (WHO grade III), and also in a smaller proportion of HGG originated from LGGs (secondary glioblastomas; WHO grade IV) (28, 40–42). IDH1-R132H (mIDH1) catalyzes the production of 2-hydroxyglutarate, eliciting epigenetic reprogramming of gene expression (33, 40, 43, 44) and is associated with better prognosis in glioma patients (33, 39, 40, 45). In addition, the loss of 1p/19q chromosomal segments define mIDH1-1p/19q-codel and mIDH1-noncodel glioma subtypes. Mutant IDH1-noncodel typically co-occurs with loss-of-function mutations in *ATRX* and *TP53* genes, which are associated with astrocytoma and oligoastrocytoma subtypes (28). Mutant IDH1 1p/19q-codel gliomas are usually oligodendrogliomas and frequently co-express mutations in *TERT* promoter (*TERT*p) and *CIC* (28, 39–41). In adults, diffuse wild type (wt) IDH1 gliomas appear principally in patients over 50 years old and commonly are HGG, WHO grade IV of malignancy (28, 31, 39). These HGG generally harbor mutations in *TP53* and *TERT*p, with retention of ATRX function. They can also present alterations in the chromosomes 7 and 10, deletions in *CDKN2A/B*, and changes in genes involved in the RTK-RAS-PI3K signaling cascade, such as *PTEN* mutation or loss or EGFR amplification (28, 31, 32, 34). Importantly, the DNA methylation, which typically occurs at

cytosines followed by a guanine separated by a phosphate group (CpG site), emerges as a distinctive parameter to refine tumor classification with clinical implications, especially in cases with ambiguous histology. The CpG-island methylator phenotype (G-CIMP) is closely related with IDH1 mutation and is associated with better prognosis in gliomas (46, 47). On the other hand, demethylation in CXCR4, TBX18, SP5, and TMEM22, genes have been linked with initiation and progression of glioblastoma (48). DNA methylation profiling has been shown to be highly robust and reproducible. In diffuse glioma TCGA patients, Ceccarelli et al., identified glioma DNA methylation clusters (LGm1–LGm6) linked to different molecular glioma subtypes (40). More recently, Capper et al, developed a DNA methylation-based classification system, which allowed to define five categories of methylation classes of CNS tumors, which resulted in a change of diagnosis in up to 12% of prospective cases analyzed (49); and in the positioning of this method as a powerful tool to improve glioma classification. In addition, the analysis of DNA methylation profiles has utility in therapeutic decisions. The presence of methylated CpG islands in the O6-methylguanine-DNA methyltransferase (MGMT) promoter is a molecular marker of better response to DNA alkylating agents (50), indicating that the methylation status of MGMT promoter is a critical feature to design glioma treatment.

In summary, adult gliomas are classified by histological features and by molecular lesions, that define distinctive tumor entities, which are associated with different grades of malignancy. This classification is relevant for diagnosis, prognosis and clinical decisions. In addition, the updated CNS-WHO classification for brain tumors is a valuable source to improve and conduct accurate studies of gliomas, considering the intrinsic biological features of the different glioma subtypes.

Currently, the adult glioma SOC includes maximal safe surgery when is possible; chemotherapy, generally with temozolomide (TMZ); and focal radiation (17, 51). However, in spite of intense investigation for years, no substantial clinical improvements have been observed (51). This unfortunate fact encourages the development novel therapeutic approaches for a wide spectrum of glioma patients who are waiting for an effective treatment.

Pediatric Gliomas

High grade gliomas comprise ~ 15% of all central nervous system (CNS) pediatric tumors (52), and have an incidence of approximately 0.85 per 100,000 children (26). Pediatric high grade gliomas (pHGG) and diffuse intrinsic pontine gliomas (DIPG) (recently included into the classification of Diffuse midline glioma (DMG)) are highly aggressive gliomas, which, unlike the adult counterparts, occur throughout the CNS anatomy. The prognosis for pHGG is dismal, with an overall median survival of 9-15 months and a 5-year survival rate of less than 20% (53).

Brainstem gliomas are more prevalent in childhood, whereas hemispheric pHGG, are more prevalent in adolescents (54). Several characteristics distinguish pHGG from adult gliomas, such as molecular (genetic and epigenetic), and clinical features (55). Particularly, advancements in molecular high-throughput profiling over the last few years improved our understanding of pHGG and led to the identification of unique genetic and epigenetic features of these tumors. Most notably, the discovery of recurrent mutations in the genes encoding histone variants H3.3 (*H3F3A*) and H3.1 (*HIST1H3B/C*), and other genes associated with epigenetic mechanisms, demonstrated the unique biology of pediatric brain tumors (53, 56, 57). Three somatic mutations resulting in the replacement of a lysine with a methionine at residue 27 of histones H3.1 and H3.3 (K27M) in brainstem/midline pHGG, or the replacement of a glycine to arginine or valine at residue 34 (G34R/V) of the histone H3.3 in hemispheric pHGG were found to be characteristic of these tumors (53, 57). These mutations rewire the epigenome, resulting in global hypomethylation and disrupt critical regulatory sites of post-translational histone modifications (56). These mutations are exclusive, are found at specific anatomical locations, within distinct age groups and patients harboring these tumors have different survival outcomes (38, 56).

The WHO classifies pHGGs as anaplastic astrocytoma (WHO grade III) and glioblastoma (GBM; WHO grade IV) (28). Among midline pHGG, the updated 2016 WHO classification of tumors of the CNS classifies the DMG H3-K27M-mutant as an independent entity, WHO grade IV (58). DMG H3 K27M-mutant arises in all midline CNS structures, are astrocytic tumors, and represent the majority of infiltrative brainstem glioma (59).

The histological characteristics of pHGG include hypercellularity, nuclear atypia, abnormally high mitotic activity, and increased angiogenesis and/or necrosis, the latter two associated primarily with GBM morphology (60). Due to their proliferative nature, HGG have shorter duration between symptom onset and diagnosis compared to tumors of lower grade, precluding the clinical advantages of early detection (61, 62). Surgical intervention of non-brainstem pHGG patients includes tumor resection and biopsy, although total tumor resection is often impossible in pHGG, particularly for midline pHGG, as these infiltrative tumors often progress into normal tissue beyond surgical margins (58). However, the extent of resection is one of the few significant prognostic markers for overall survival (OS) in pediatric patients with pHGG (63). Although surgery is the primary intervention for treatment of non-brainstem pHGGs, it is not curative. Standard of care also includes radiation therapy for pHGG patients above three years of age, typically 50-60 Gy delivered over 3-6 weeks (61). Currently, no chemotherapeutic treatments are involved in the SOC for pHGG; however, various are being tested in clinical trials (64). Despite immense efforts, there are no effective treatment options and pHGG has become the leading cause of cancer related death in children and adolescents under the age of 19 years (26, 60).

There is a diversity of molecular alterations driving pHGG and therapies must be accordingly diverse and specific. Highly targetable molecular alterations are found in different subtypes of non-brainstem pHGG. For example, pHGG often carry genetic alterations in the TP53, PTEN/PI3K/Akt, PDGF or Ras pathways, which include targets that can be druggable (65). However, immunotherapies specifically designed for pediatric brain tumors have been understudied. Pre-clinical models for

pHGG and the testing of immune-mediated therapeutic approaches are starting to emerge (66, 67), which open new avenues for the treatment of these aggressive pediatric brain tumors.

GLIOMA IMMUNE MICROENVIRONMENT

Crosstalk Between the Healthy CNS and the Immune System

The brain has for long been considered an immune privileged site due to the absence of immune response after the heterotopic transplantation of skin xenografts (68). However, in the same set of experiments, Medawar et al. observed that if the immune system had been previously exposed to the tissue graft in any other site of the body and then the transplantation was done in the brain, a powerful immune response invaded the CNS, causing grafting breakdown and rejection (68). These data showed that the CNS in not immune-isolated and that even though an immune response against xenografts cannot be easily started in the brain parenchyma, it can reach this site in a pre-immunized state.

Due to anatomical particularities, the crosstalk between the CNS and the immune system differs from the immune response mounted in any other organ of the body (69–72). For instance, the passage of molecules and cells, such as immune cells, to the brain parenchyma is subjected to a strict control by the endothelial blood-brain barrier (BBB) (69). Also, the absence of classic lymphatic drainage in the CNS was considered to be the cause of the lack of an afferent arm of the immune system; i.e. the route of antigen transportation from the site of infection/trauma to the nearby lymphatic node (69). However, maintaining the brain as an immune-isolated tissue would be dangerous, thus many efforts had been destined to understand the mechanism by which the immune system surveils the CNS. There are two types of fluids in the CNS: the cerebrospinal fluid (CSF), in the ventricles and the subarachnoid space; and the interstitial fluid in the brain parenchyma. Even though both types of fluids drain to the cervical and lumbar lymphatic nodes, they do it through separate routes: while the CSF drains across the cribriform plate and the dura mater lymphatics, the interstitial fluid drains via perivascular channels into the lymph nodes or the CSF (69, 71). This narrow space does not allow the passage of cells, but it permits antigen transportation to the nearest lymph node, where adaptive immune response could be started. In contrast, the drainage pathways of the CSF allow cell trafficking and this fluid has a more active crosstalk with the immune system (69, 73). In fact, healthy individuals contain up to 700,000 cells in total in the CSF (70). Around 80-90 % of these cells are T cells, majority of which are memory T cells (70, 73). Also, a small proportion DCs has been found in the CNS, and there is evidence that DC can scan the CSF for foreign antigens and reach the lymphoid organs to activate T cells in the periphery (70, 72).

Even though these data demonstrate the interconnection between the immune system and the healthy CNS, this site usually remains quiescent and immunosuppressed due to the presence of factors derived from neural cells (70, 73). For instance, the brain parenchyma contains only one type of immune cell: the microglia. These cells are tissue resident macrophages, but they originate from a different embryonic layer than circulating macrophages (73, 74). These cells are kept in an inactivated state through the interaction of the CD200 receptor in neural cells and CD200 ligand in microglia (75). Even though these cells are capable of antigen presentation, the levels of MHC in microglia and other astrocytes remains low (73). However, in response to an infection, microglial cells become activated and produce an array of pro-inflammatory mediators, to facilitate the recruitment and activation of innate and adaptive immune cells (76). After an inflammatory stimulus, the immune privilege of the brain switches, increasing the permeability of the BBB and the infiltration of myeloid cells and activated T cells, as well as the proliferation of microglial cells (73, 76–78). This state causes phenotypic changes as well, such as CD11c, MHCII and co-stimulatory molecules' upregulation (73, 78).

Immune Microenvironment in Brain Tumors: General Concepts

The shift in the dogma of the CNS as an immune inert site, prompted the development of immunotherapies against glioma. Glioblastoma is one of the deadliest type of tumor and currently patients succumb to this disease even after their treatment with SOC (79). Thus, researchers have been devoted to find therapeutic alternatives to harness the immune system and direct it against this tumor. Today, there are several ongoing clinical trials testing different type of immunotherapies, but the results obtained so far have not been as encouraging as the effects observed in pre-clinical models and the great majority have not been tested in Phase III yet (12, 79).

There are several aspects related to the biology of gliomas that make them difficult to treat by immunotherapies. For instance, these tumors tend to have high intra-tumoral heterogeneity, so that finding a tumor specific antigen as a target for immune mediated therapies is difficult and usually approaches involving tumor antigens require the inclusion of more than one target to prevent antigen scape (80–82). Also, the intact BBB prevents the readily penetration of chemotherapeutics to the brain parenchyma, though its permeability can be affected in an inflammatory state (83). Finally, the immune microenvironment of these tumors tends to be immunosuppressive, hijacking the efficacy of immune mediated strategies (6, 8, 9, 12, 78).

Glioma tumor immune microenvironment (TME), refers to all those immune cells infiltrating the tumor mass. Even though the diversity of cell infiltration can vary depending on the type of brain tumor (revised below), glioma TME has usually been found to be immunosuppressive (6, 7, 11, 84). Animal models as well as the analysis of human samples have shed light on the characteristics of glioma TME. Myeloid cells are the major type of immune cell in glioma's TME, with macrophages representing more than 30% of the tumor mass (6, 85). This group encompasses bone-marrow derived macrophages and tissue-resident derived macrophages (13, 74). It is not clear if these two populations have different functions in glioma or if they are associated with tumor progression, but they have been

encountered at different locations: while microglial cells were found at the tumor border, bone-marrow derived macrophages were detected at the tumor core (86). These two types of cells are generally known as tumor-associated macrophages (TAMs). Also, infiltrating monocyte-derived macrophages constitute 85% of the total macrophage population in glioma and it has been observed that prevention of monocyte infiltration extended de median survival of tumor-bearing animals (86). There have been detected expression markers and differential transcriptional landscapes that can be used to distinguish these two populations (86–88). For instance, resident microglia express P2Y12, TMEM19, and are CD45 low, whereas macrophages express CD44, CD169 and are CD45 high (87). More importantly, these two cells' subclasses have been identified in human samples, in which intratumoral blood-derived macrophages displayed a more immunosuppressive transcriptional program and their presence correlated with tumor malignancy (86).

Myeloid-derived suppressor cells (MDSC) are a type of immature myeloid cells that are known to have immunosuppressive functions via different mechanisms that ultimately inhibit T cell functions (9, 11, 13). These cells have been found in the blood of glioma patients and in the tumor mass, and they have also been characterized in animal models (9, 15, 89, 90). Usually, MDSCs are divided phenotypically in monocytic MDSCs (M-MDSCs) and polymorphonuclear MDSCs (PMN-MDSCs). In humans, M-MDSCs are characterized by CD11b +HLA-DR−CD14+CD15−CD33high, whereas PMN-MDSCs express CD11b+CD66b+CD15+CD14−/dimCD33dimHLA-DR− [PMCID: PMC6447515]. In mouse, MDSCs characterization entails less markers: M-MDSC are defined as CD45+/CD11b+Ly6G-Ly6C+ and PMN-MDSCs as Cd45+/CD11b+Ly6G+Ly6C- (91). It has been observed that the quantity and activation status of MDSC inversely correlates with patient survival and that they can be a predictor of WHO tumor grade (90). Moreover, whilst MDSC infiltration after surgery has been associated with poor prognosis, MDSC decrease correlated with better prognosis and an increase in DC infiltration (90).

Lastly, tissue hypoxia, which is common in GBM due to the inefficient neovascularization (10), induces regulatory T cells (Tregs) activation and tumor-promoting phenotype of tumor associated macrophages (10, 92). The presence of Tregs can suppress cytotoxic T cell activities, leading to tumor progression. Moreover, tumor cells as well as immunosuppressive tumor infiltrating immune cells, secrete an array of cytokines that promote and maintain the immunosuppressive microenvironment, not only affecting tumor infiltration, but also cellular differentiation at the bone marrow level (10, 84). Some of the cytokines encountered in the TME are IL-10, TGFβ and IL-6. These are related to NK and T-cell activities inhibition and their expression is related to glioma progression (93).

Immune Infiltration Patterns in Brain Tumors With Different Genetic Landscapes: Lessons From The Clinic and Animal Models

It is clear that immunosuppression is a common feature of gliomas that enables tumor progression and malignancy. However, the composition of the immune cell infiltrate varies among the type of tumor and certain immune cells are associated with particular genetic alterations usually found in gliomas, such as mutations in *IDH1* (94).

The transcriptional landscape of GBM has been classified at least in three different types: proneural, classical and mesenchymal, which correlate with the presence of different genetic alterations (95, 96). This classification not only describes inter-tumor differences, but also intra-tumoral variability, as samples taken from distinct regions and at different times thought-out treatment showed diverse transcriptional signatures. With the emergence of Single cell RNA-Seq (scRNA-Seq), the cellular composition of glioblastoma was found to be even more complex. It has been observed that tumor cells can exist in four different phenotypes: mesenchymal-like, astrocyte-like, oligodendrocytic precursor cell-like and neural progenitor cell-like (80). These different cellular states are correlated with different genetic mutations and with the transcriptional signatures defined previously, with neural progenitor cell-like and oligodendrocytic precursor cell-like cells associated with the proneural subtype; mesenchymal-like cells with mesenchymal subtype; and mesenchymal subtype and astrocyte-like cells associated with classical subtype (80). This complexity in the phenotype of gliomas has been found to have a correlation with the composition of immune cell infiltrate (7).

Tumor microenvironment composition in adult glioma has been lately characterized. Luoto et al. performed a regression-based gene expression deconvolution to estimate the proportions of particular immune cell types based on RNA-Seq analysis of 156 primary GBM samples generated by The Cancer Genome Atlas (97). They found that cases could be grouped into three immune-response groups which were the following: negative, humoral and cellular-like. They also found that differences in adaptive immune response could be associated with the specific subtypes of HGG defined above. They describe that the "negative" subgroup, which is associated with the negative regulation of lymphocyte response, encompass the proneural subtype, including those samples with *CDK4-MARCH9* locus amplification and *IDH1* mutation. The mesenchymal subtype was more prevalent in the "humoral" subgroup, in which gene signature was related to B-cell and humoral response components. Finally, the "cellular-like" subgroup was more populated with classical subtype samples, as well as with samples with *EGFR* amplification. Also, they observed that immune-related responses correlated with the presence of specific genetic alterations. Samples with *CDK4* locus amplification or *IDH1* mutations were found to be less infiltrated by macrophages, and to have less CD4+ components. On the contrary, samples with *NF1* inactivation had a higher macrophage content. This observation has been confirmed in the study of Wang et al. (98). Even though none of the cell components described in the work by Luoto *et al.* correlated with patient survival, the presence of high activity related to the "antigen presentation and interferon response" cluster was a positive predictor of longer OS. Similarly, Caleb Rutledge W. et al., also found a correlation between tumor-

infiltrating lymphocytes (TILs) and GBM transcriptional subclasses and they show that TILs were enriched in the mesenchymal class compared with all other classes (99). Also, they did not observe a correlation between *IDH1* mutation and TIL presence, nor did they with patient OS (99).

The correlation of *IDH1* status and TME composition has been extensively characterized (94). In general, as presented above, *IDH1*-mutant (mIDH1) gliomas tend to be less populated with TILs when compared to *IDH1*-wt tumors. Specifically, less CD8+ cytotoxic T cells have been found in mIDH1 gliomas and this could be explained by the reduced expression of chemoattractant cytokines to T cells by mIDH1 glioma cells (100, 101). Also, and in correlation to what Luoto *et al.* found, mIDH1 gliomas tend to have less macrophages than wt-IDH1 tumors (97). Moreover, in an animal model of mIDH1 glioma in the context of *ATRX* and *TP53* mutations, it has been observed that the presence of this mutation reprograms the tumor cell transcriptome, which affects not only immune cell infiltration but also the bone marrow differentiation of the granulocytic lineage (15). This effect was found to be mediated by G-CSF secretion by mIDH1 glioma cells, which prompted the expansion of pre-neutrophils, while reducing the immunosuppressive phenotype of the granulocytes encountered in mIDH1 tumors' TME (15).

Tumor microenvironment in pediatric gliomas has been less characterized than the adult counterpart, in part because of the small amount of samples available. Thus, it is difficult to correlate molecular subtypes of pediatric tumors with TME infiltration patterns. However, the data gathered so far in the pediatric population show differences in relation to the immune infiltrate characteristics observed in adult patients. In the study of Plant et al., they analyzed 22 pediatric brain tumor tissue samples of mixed diagnoses and they observed no correlation between the amount of T cells and the aggressiveness of the tumor or the patient survival (102). Griesinger et al., analyzed different types of pediatric brain tumors, which consisted in 7 pilocytic astrocytomas (PA), 19 ependymomas (EPN), 5 GBM, 6 medulloblastomas (MED), and 5 non-tumor brain (NT) control samples. They show PA and EPN to be the most enriched tumors in myeloid cells, with GBM at the third place, but still with more myeloid cells than the NT samples (103). These cells expressed makers for both, immune activation (HLA-DR and CD64) and immunosuppression (CD206 and CD163). T cell infiltration was also evaluated and GBM had more T cells than the NT control (0.79% vs 0.02%), exhibiting a 46-fold and 26-fold increase in CD8 and CD4 T cells, respectively. Also, the average CD8/CD4 ratio, which was shown to be a prognostic factor in other types of cancer, was elevated in GBM with respect to NT controls: 2.83 vs 0.83, respectively (103). Moreover, Lieberman et al., studied the TME in DIPG, a pediatric high grade glioma that occurs in the pons. They conclude that the TME of these tumors do not show strong evidence of immunosuppression or inflammation, so that immune-directed therapies against these tumors should focus on immune cell recruitment to the tumor site (104). In this regard, Mendez et al. demonstrated the efficacy of an immunestimulatory gene therapy in increasing the median survival of tumor bearing mice in a pre-clinical mouse model for DIPG harboring mutant *ACVR1* gene (66). They show that this therapy was effective in promoting the activation and the infiltration of anti-tumor CD8 T cells (66). Lastly, using a model for pediatric HGG harboring the H3.3-G34R mutation it has been demonstrated that these tumor exhibit a more permissive TME with respect to the control group without the mutated histone (105, 106). Researchers show that H3.3-G34R tumors are less populated with MDSC and that these cells are not immunosuppressive. Also they observed an increased infiltration of T cells, DCs and M1 macrophages; and an increased sensitivity of glioma cells to IFNγ-induced apoptosis (105, 106).

In conclusion, these data gathered from clinical samples and pre-clinical models highlight the complexity of the immune cell infiltrate in brain tumors and the importance of taking into account the particularities of each type of glioma when considering the application of immune-mediated therapies.

MOUSE MODELS TO STUDY GLIOMA IMMUNE MICROENVIRONMENT AND POSSIBLE THERAPIES

The dismal prognosis of glioma patients demonstrates the need to faithfully model the formation and the biology of this tumor type to enable successful anti-glioma therapies. Immunotherapy has emerged as a promising approach to treat growing number of cancers (107, 108), but none has been effective in improving the survival of GBM patients (59, 109, 110). However, researchers working on GBM believe that immunotherapy could establish successful treatment regimens where other treatments have not been successful (111, 112).

Genetic, histological and physiological modifications are involved in the evolution of glioma's malignancy and invasive phenotype. A good glioma animal model would enable the identification of signaling pathways which are related to tumor initiation, invasion, malignancy and therapeutic resistance. Ideally, the model should accurately resemble histologically and genetically the human disease. It should also display the cellular heterogeneity observed in glioma patients. Most glioma tumors have been previously modeled either in immunodeficient (113–115) or immunosuppressed (116) animals. However, these models have important drawbacks in terms of the lack of interactions with the adaptive immunity, which is key to fight this tumor. Also, tumors in immunocompetent mice exhibit characteristics similar to clinical pathophysiology in patients with glioma, characterized by immune infiltration and strong neovascularization, which are absent in brain tumors developed in immunodeficient mice (117).

Preclinical syngeneic murine glioma models are crucial to determine the immune response of novel therapies prior to its human clinical trial. The use of animal models of malignant glioma shed light on the composition of the TME, its influence on disease progression and outcomes, as well as on new therapeutic targets for treatment (118). The method widely

used in glioma biomedical research is intracranial or subcutaneous injection of tumor cells like C6, 9L or GL261 into mice or rats. These syngeneic models are used to study the biology of glioma or new therapeutic agents. Also, there are other syngeneic murine glioma models, such as SMA560, GL26, CT-2A, 4C8 mouse models and 9L, RG-2, F98 and CNS-1 rat glioma models which maintain the immunological interaction between the tumor cells and the host (16).

GL261 model is perhaps the most extensively used syngeneic mouse model of GBM. This model is reported to recapitulate histologic and biological characteristics of GBM (16). Furthermore, this model employs immunocompetent mice, and thus is suitable to analyze GBM tumor immunology and to perform immunotherapeutic research (119). Among the reported pre-clinical applications of this model, we can mention: the use of adoptive T cell transfers to restore and induce long-term immunity; the use of antibodies to improve antitumor T cell activity via augmentation of costimulatory signals; the abrogation of survival advantages of Tregs; and the enhancement of tumor immunogenicity using IL12 based gene therapy to stimulate robust cytotoxic T cell responses (119), as GL261 express unique tumor antigens which can induce a specific T cell responses (120). Moreover, this model has been employed to study the immunosuppressive effects of TGFβ, which promotes Treg activity (121). Also, GL261 has been used to test the efficacy of a peptide vaccine using GL261-specific antigens and a TGFβ neutralizing antibody (1D11) (122). In another study, GL261-based DC vaccines have been curative and preventive of tumor engraftment (119). Thus, these results have helped to validate GL261 as one of the model of choice for investigating immunotherapeutic treatment modalities against GBM. Likewise, GL26 model enables the study of immunotherapies. GL26 tumors express melanoma associated antigens gp100 and tyrosinase-related protein 2, both of which can be used to pulse DCs, which would in turn stimulate cytotoxic T cell-mediated robust antitumor immune response (123). Other immune-mediated strategies tested with GL26 model include Treg depletion using PC61, which is an antibody directed against CD25, one of the primary markers for Tregs (124).

SMA-560 tumors are an excellent model of anaplastic astrocytoma with low S-100 expression and high expression of glial fibrillary acid protein (GFAP) and glutamine synthetase, providing a representative model of glial tumors of astrocytic lineage (125). These tumors lack MHC Class II molecules, but do express MHC Class I at low levels which highlights their potential for antigenic recognition by traditional effector T cells (126). They also express TGF-β which lends great value to this model (126). SMA-560 model has been used to test the efficacy of the induction of secretion of selected cytokines such as IL2, IL4, IL3, IL6 or TNFα, which resulted in an increase in MS of VM/Dk mice (126). Another study also showed that the over-expression of a soluble form of CD70 ligand in SMA-560 tumor cells, reduced tumor growth rate and increased host animal survival (127). Also, this model was used to investigate DC and CAR-T cell based therapies' outcomes for radio-resistant glioma cells (128).

Histologically, CT-2A tumors show features of high-grade astrocytomas, including pleomorphism and high cellular density, and can undergo malignant transformation with evidence of pseudopalisading necrosis (129). Compared to established glioma cell lines, CT-2A cells are significantly more proliferative and invasive (130), but less invasive than other mouse brain tumors (131). CT-2A share similarities with neural stem cells, like primary human GBMs grown *ex-vivo*, and express stem cell markers such as CD133, Oct and Nestin (132). Overall, the CT-2A model is considered to accurately represent several GBM characteristics including intra-tumoral heterogeneity, *in vivo* migratory patterns, radio-resistance, and chemo-resistance (129). By virtue of its brain tumor stem cell-like properties, the CT-2A model could provide a resource for studying the role of tumor stem cells in the immunological landscape of gliomas. Moreover, since CT-2A is deficient in PTEN and this deficiency contributes to tumor induced immunosuppression (133), this model can be utilized to devise strategies for mitigating PTEN deficiency-associated immune effects (134).

4C8-B6D2F1 tumor model was developed to address the shortcomings observed with other glial tumors (135). The 4C8 cells adopt oligodendrocytic characteristics *in vitro*, but convert to GFAP+ astrocytes when exposed to serum (136). Implantation of 4C8 into B6D2F1 mice produces pleomorphic, highly cellular tumors with extensive invasion into ventricles and meninges (135). They also express components of MHC I and II molecules (137). Intratumoral injections with vaccines and viruses engineered to secrete IL-12, have shown to promote significant anti-tumor activity, with detected immune cell infiltration, and minimal toxicity (138).

The RCAS/*tv-a* system is a model that allows the somatic transfer of oncogenes driving glioma development, enabling the development of tumor *in situ*. This method has been used to initiate tumors in newborn mice, by the introduction of genetic alterations into brain cells engineered to express tv-a receptor (139). Genes used to initiate brain tumors could be *PDGF* and *Kras* overexpression. These animals can then be crossed onto other genetic backgrounds in order to study the effects of particular mutations on tumor biology (140, 141). It has been observed that the oncogenes *Kras* and *PDGF* produce more malignant gliomas in mice with *Ink4a-Arf-/-* and *PTEN* loss backgrounds compared with those gliomas generated in wt mice, which develop lower-grade tumors (139, 142). Hambardzumyan D *et al.* described a protocol to develop gliomas in adult mice, which represent an excellent tool for studying the tumor immune microenvironment and immunotherapeutic approaches in adult gliomas (141, 143). Even though this model has not been widely used for the study of glioma's TME, it has been observed that, similar to what it is observed in the clinical setting, tumor malignancy of the gliomas generated with the RCAS system correlated with an influx of macrophages, which was influenced by tumor signal transducer and activator of transduction (STAT) 3 expression (144). In the same study, the authors report that STAT3 inhibition with WP1066 increased the MS of mice bearing brain tumors expressing PDGF-B + *Bcl-2* (144).

Another syngeneic model to generate gliomas *in situ* can be achieved by the Sleeping beauty (SB) transposon system (145). This method allows high-level stable gene transfer and sustained gene expression in many somatic cell types (146). The SB transposon system, member of the Tc1/mariner class of

transposons, is capable of recognizing inverted repeats/direct repeats (IR/DR) sites on DNA transposons and performing a cut-and-paste reaction to integrate transposable DNA segments into a host genome (145, 147). This method has been used to develop endogenous tumors that mimic gliomas by delivering DNA transposons that encode for the genetic lesions of interest. Our laboratory has developed a series of syngeneic GBM models using this method. For instance, we have engineered ATRX-deficient gliomas (148, 149), by injecting plasmids encoding SB transposase/firefly luciferase, plus other plasmids encoding for the desired genetic alterations located between IR/DR: shp53, NRASG12V, and shATRX, into the lateral ventricle of neonatal mice (148). Also, using SB transposon system, we have developed: a DIPG murine tumor model of mACVR1-G328V by injecting plasmids encoding for NRASG12V, shp53, and mACVR1-G328V (66); a mIDH1 murine tumor model by injecting plasmids encoding for NRASG12V, shp53, shATRX and IDH1-R132H (44); and a H3.3-G34R murine high grade glioma model by injecting plasmids encoding for NRASG12V, shp53, shATRX and H3.3-G34R (67, 150). This method has the advantage that the tumors developed can be resected, processed as a single cell suspension, and grown *in vitro* as neurospheres. These neurospheres can be further implanted in adult C57BL/6 mice.

Recently, Patel SM et al. described a method for in utero electroporation of neural stem cells to generate an *in situ* mouse model for DIPG tumors, a highly aggressive glioma that grows in the pons in pediatric patients (151). They used PiggyBac DNA transposon plasmids to induce the expression of different combinations of PDGFB, *Pdgfra*-D842V, or *Pdgfra*-WT, along with dominant negative *Trp53* (DNp53) and H3.3K27M expression. They report the induction of gliomas from grades IV to II, which depended on the plasmid combination (151). These tumors displayed histopathological features of the human disease and represent an invaluable tool for the modelling of the TME in DIPG, as the development of the gliomas in this model resembles their development in humans. Also, to better depict the inter-person heterogeneity in immune response and glioma genetic make-up, Aslan K et al., described the use of an hypermutated orthotopic glioma syngeneic mouse model, exhibiting more than 100 non-synonymous mutations per tumor exome. This model was used to study the dichotomy in the glioma response to immune-checkpoint blockade and to develop a method to try to predict the therapy outcomes by imaging MRI technique (152).

An alternative humanized mouse model system has also been developed to evaluate the efficacy of various GBM immunotherapies. Humanized models are generated by the engraftment of human cancer cell lines, or human patient-derived xenograft (PDX) tumors into immunodeficient NSG mice with an HLA-matched human immune system, which is achieved by the transplantation of human PBMCs, or CD34+ hematopoietic stem cells (HSCs). Transplanted CD34+ HSCs in immunocompromised mice differentiate into human helper and cytotoxic T cells, B cells, monocytes, NK cells, and DCs (153). Humanized mice can survive months post-tumor implantation with relatively stable proportions of human cells. Human microglia/macrophage-like cells have also been developed in the brain of CD34+ HSC humanized mice (154). These models have the advantage of recapitulating tumor heterogeneity and clonal diversity, which mimics the human tumor immune microenvironment and can be used to investigate the biology of GBM (109, 155). Nevertheless, the humanized mouse platform is being improved in such a way that immunotherapeutic research could become more predictive. The use of humanized mouse models in GBM preclinical and clinical studies is currently limited due to the lack of knowledge and unanswered questions, such as whether humanized mice models display the clinical features of glioblastoma patients. For instance, Ashizawa T. *et al.*, investigated the efficacy of the anti-PD-1 antibody using humanized NOG-dKO mice, generated by implanting human PBMCs and GBM cell line U87 (156). In this study, there was no rejection of the human glioma cells or the PBMCs, and T-cell and NK-cell anti-tumor immune responses were detected, thus constituting an interesting model to evaluate the effect of immunotherapeutic agents against glioma. Despite these advantages, humanized mouse models are partial in maintaining the cellular and mutational diversity of parental tumors and entail an extended generation time (157, 158). Patient-derived glioblastoma organoids (GBOs) that recapitulate the histological features, cellular diversity, gene expression, and mutational profiles of their corresponding parental tumors have recently been developed and biobanked. When GBOs are transplanted into adult rodent brains, they show rapid, aggressive infiltration and high reliability (157).

While there is no perfect murine model to study immunotherapies for glioma, syngeneic tumor models in immunocompetent mice represent a valuable resource for this purpose. The transplantable models presented are convenient because tumor location and growth can be better predicted and thus, the testing of different therapies and their relationship with the immune system can be more easily studied. Although orthotopic xenografts retain some of the human GBM features and are considered to be a useful model for therapeutic studies (159), it lacks the proper immune environment due to the use of immunocompromised mice, which is a drawback for the study of tumor immunology and anti-tumor immune-stimulatory therapies.

STRATEGIES TO OVERCOME IMMUNOSUPPRESSIVE MICROENVIRONMENT: CURRENT THERAPEUTIC MODALITIES UNDER CLINICAL TRIAL AND UNDER PRE-CLINICAL INVESTIGATION

Immune Checkpoint Blockade

Immune checkpoints (IC) are negative regulators of the immune system that maintain self-tolerance, avoid autoimmunity and adjust the extension and duration of the immune responses to prevent tissue damages (160). The mechanism involves the

interaction between IC receptors with its ligands, acting as a natural feedback loop that inhibits and reduces inflammation. Likewise, cancer cells could express IC ligands as a way to evade immune-mediated elimination. Examples of these immunomodulatory molecules, which are negative regulators of T cell activation and function, include the cytotoxic T lymphocyte antigen 4 (CTLA-4), the programmed cell death 1 (PD-1) and its ligand PD-L1, TIM-3, the enzyme indoleamine 2,3-dioxygenase (IDO), V-domain Ig suppressor of T cell activation (VISTA), killer-cell immunoglobulin-like receptor (KIR), TIGIT, B and T lymphocyte attenuator (BTLA) and LAG-3. Amongst them, CTLA-4, IDO and PD-1/PD-L1 are the most studied molecules inhibitors for which have been developed and evaluated in preclinical and clinical assays (160).

First attempts in developing IC inhibitors (ICIs) were focused in CTLA-4 molecule. CTLA-4 is a co-inhibitory receptor present on the surface of Treg that was discovered in the late 80´s (161). CTLA-4 has the B7 family of proteins (B7-1 or CD80 and B7-2 or CD86) as natural ligands, which are found at the surface of antigen presenting cells (APC). Even though CTLA-4 shares structural and biochemical similarities with CD28, a potent co-stimulatory receptor of T cells, CTLA-4 and CD28 have opposite immunoregulatory functions. Binding of CTLA-4 to B7 ligands has a 20-100 fold higher affinity than CD28, so when both are present, T cell activation is prevented and cytokine production switches to an immunosuppressive pattern, i.e. IL-10, TGFβ, and indoleamine (162).

Despite the lack of correlation between CTLA-4 ligand expression and a specific cancer cell type and the fact that *Ctla-4*-knockout mice models predicted lethal autoimmune phenotypes, it was shown that CTLA-4 inhibition produced antitumoral responses in preclinical cancer models (163). These preclinical studies showed promising results in some immunogenic tumors, using antibodies as a single agent or in combination with other agents that stimulated immune responses after tumor implantation, in the case of poorly immunogenic cancer models (163). Therefore, the development of fully humanized anti-CTLA-4 antibodies led to clinical testing of Ipilimumab and Tremelimumab. The first clinical study of CTLA-4 antibody treatment was performed in patients with advanced melanoma that were not responding to conventional therapy (164). Ipilimumab is a IgG1 monoclonal antibody that blocks the CTLA-4/CD80-CD86 interaction on APCs and T cells, promoting co-stimulatory binding of CD28 to CD80/CD86 (165). On the other hand, Tremelimumab is a monoclonal IgG2 antibody with a similar CTLA-4 blocking mechanism; but it only received orphan drug designation from the FDA for malignant mesothelioma (166).

Several pre-clinical trials evaluated the effects of CTLA-4 inhibition in GBM mouse models, showing differences in the outcomes depending on the tumor model evaluated. CTLA-4 blockade alone resulted in 80% of long survivors and abrogated Treg expansion in SMA-560 tumor-bearing mice (167). However, in other studies, the efficacy of this treatment was much lower, with 40 to 15% long term survivors (168, 169), or did not elicit antitumor efficacy (9). A significant challenge to effectively asses the efficacy of ICIs in GBM is to develop better pre-clinical animal models. In this sense, the SB28 GBM model recapitulate human GBM features, like low mutational levels and loss of MHC-I expression (170). Besides these technical issues, the sole inhibition of CTLA-4 in the immunologically suppressed microenvironment of GBM may not be effective to trigger a successful antitumoral immune response since this receptor is only present on T cells (171). In fact, our previous findings indicate that although the treatment with anti-CTLA-4 in GL26 GBM-bearing mice did not elicit antitumor effects, it boosted the efficacy of immune-stimulatory TK+Flt3L gene therapy (9). Moreover, even though preclinical data of CTLA-4 inhibition showed potential effects for GBM treatment, several adverse effects occur through a rapid and nonspecific activation of the immune system. In this regard, a Phase 1 clinical trial of Nivolumab (anti-PD-1) alone or in combination with Ipilimumab in patients with recurrent GBM showed no differences in OS but higher toxicity with the addition of anti-CTLA-4 to the treatment (172).

PD-1, which was first identified in 1992 as a putative pro-apoptotic receptor (173), plays a major role in limiting immune response and regulates T cell biology (174). While CTLA-4 acts early on T cell activation inhibition in the lymph nodes, PD-1 immune checkpoint controls the activity of T lymphocytes in peripheral tissues (175). PD1 ligand 1 (PD-L1; also known as B7-H1 and CD274) and PD-L2 (also known as B7-DC and CD273) serve as ligands for PD-1. They are present constitutively on resting T cells, dendritic cells, B cells, natural killer cells and macrophages, and can be induced in non-haematopoietic tissues by pro-inflammatory cytokines (176, 177). Specifically, tumor cells can express these ligands, protecting them from immune system eradication (178). For instance, the term "innate immune resistance" makes reference to *PDL1* gene amplification or the upregulation of PD-1 ligands by constitutively active signalling pathways on tumor cells (179–182). On the other hand, the "adaptive immune resistance" situation makes reference to PD-L1 expression by tumor cells in response to IFNγ release by T cells (183, 184).

The interaction PD-1/PD-L1 provokes effector T cells cell cycle arrest and the down-regulation of cell survival molecules like Bcl-XL, the dephosphorylation of ZAP70, and the phosphorylation of PI3K by the recruitment of SHP1 and SHP2 phosphatases (185). PD-1/PD-L1 axis disruption was thought to be a promising approach to overcome T cell inhibition and to promote an antitumoral immune response. In this regard, numerous studies have shown successful results in the treatment of metastatic melanoma (186, 187), Non-small cell lung cancer (188) and renal cell carcinoma (189). Preclinical studies using orthotopic mice models of GBM showed that PD-1 inhibition promoted NK cytotoxic effects against cancer cells when used as a single agent (190, 191) or in combination with radiotherapy (192). However, most clinical trial studies using anti-PD-1/PD-L1 monotherapy have shown limited efficacy in GBM patients (193).

Checkmate 143 was a Phase III clinical trial evaluating ICIs (Ipilimumab + Nivolumab) in GBM patients. It was concluded

that Nivolumab as monotherapy was better than the combination, due to increased adverse effects when combined with Ipilimumab, and a significant increase in OS in comparison to the current therapy with Bevacizumab was not observed (194). In the case of PD-L1 inhibitors, a Phase 1 clinical trial of Atezolizumab as monotherapy in patients with recurrent GBM have shown no improvements in survival (195).

In conclusion, anti-PD-1 immunotherapy has been extensively evaluated in mouse models, and in clinical trials as monotherapy or in combination with other treatments, offering novel approaches for the treatment of GBM (**Table 1**) (12). Additionally, anti-PD-L1 immunotherapy has also been well evaluated in clinical trials (**Table 2**). Although the efficacy of ICIs as single agents has shown no satisfactory results in GBM, it is necessary to evaluate their efficacy as complements of other active immunotherapeutic strategies, such as vaccines and/or immune-stimulating gene therapies, which promote T cell infiltration, the subsequent IFNγ production and PD-1/PD-L1 upregulation.

IDO is an enzyme with an essential role in the catabolism of tryptophan (Trp) into different metabolites, like kynurenines (Kyn). Although it is not considered as a classical checkpoint, it is included in this group of molecules because it has powerful immunosuppressive properties (196, 197). IDO expression in the context of tumor immunity has been associated to cancer and immune cells (198). IDO contributes to immunosuppression activities by increasing Kyn levels and depleting Trp, which inhibit effector T cells and NK cells, and promotes Treg proliferation (198). This enzyme has been shown to be upregulated in almost all GBM patients (199) and its high expression correlates with malignancy (200). In this sense, a pre-clinical study of TMZ in combination with an IDO inhibitor showed tumor growth reduction and an increase in long-term survival of mice with GBM (201). Encouraging preclinical results led to several clinical trials with IDO1 inhibitors, but unfortunately administration as single agent did not show significant antitumoral activity. Nowadays, several clinical trials are being conducted in order to test IDO inhibition efficacy, in combination with TMZ and radiotherapy (NCT03532295, NCT02502708 and NCT04049669). Similarly, another trial tested the combination of an IDO inhibitor (INCB024360) with Nivolumab, Anti-GITR MAb and Ipilimumab in patients with recurrent GBM (NCT03707457). However, after a failed Phase III trial in melanoma, with no differences in progression free survival (PFS) or OS, it was proposed that IDO is not an appropriated target in cancer (202). However, it is possible that more effective and specific inhibitors need to be developed in order to successfully block IDO pathway in cancer (203).

Trp degradation to Kyn by IDO1 and TDO2 provokes Trp starvation, which causes the subsequent activation of general control nonderepressible 2 (GCN2), decreasing general protein production. IDO-activated GCN2 also affects T cells proliferation and effector function, by inhibiting fatty acid synthesis, promoting T-regs activation (204), Platten, 2012 #122}. In this sense, Trp degradation has been recognized as an important microenvironmental factor with immunosuppressive properties. Particularly, the IDO/TDO-Kyn-AhR enzymatic cascade has emerged as an interesting pathway to develop novel therapeutic strategies and overcome tumour immune scape in GBM. In this regard, besides several IDO inhibitors that are being tested in preclinical and clinical trials, Kyn has been shown to be an interesting target due to its aryl hydrocarbon receptor (AhR) agonist activity. AhR activation promotes the generation of immune-tolerant DCs and T-regs (205). Thus, the approach of depleting extracellular Kyn has shown promising efficacy in mouse models. Engineered KYNase catalyses the synthesis of anthranilic acid from Kyn, promoting effector T cell infiltration into the tumour (206). Finally, several AhR antagonists are being tested in preclinical studies (207). However, due to their broadly effects inhibiting any AhR ligand (endogenous and exogenous), development of antitumoral AhR therapies is in early stages (207). In this sense, it remains to be elucidated if this approach will show anticancer activity by acting on cancer cells or by modulating immune responses, and if they achieve optimal pharmacokinetic/pharmacodynamic profiles (204).

Macrophage Reprogramming

The heterogeneous microenvironment of glioblastomas contains an enriched proportion of non-tumor cells which characterize the TME. Although the quantity of lymphocytes is very low, the tumor-associated macrophages (TAM) have been described as one of the major populations of GBM's TME. TAM comprises two main subpopulations, the microglia (MG) and the monocyte-derived macrophages (MDM) (208, 209). MGs are the resident immune cells of the central nervous system specialized to monitor and respond to pathogens or injuries (210) and MDMs are peripheral bone marrow derived cells that infiltrate the TME. Despite different origins, these two populations function as immune-suppressed cells of the TME which diminish T-cell response and promote tumor progression and invasion (209). Different studies have shown that the pro-tumorigenic role of TAM is promoted by their interaction with glioma cells through mutual paracrine signaling. Different released factors have been involved in TAM-GBM interaction and the shift of TAMs to an M2 phenotype, which is characterized by anti-inflammatory properties and reduced phagocytic activity. Several studies have demonstrated that CSF1 could act as MG chemoattractant and that TAM released factors, such as the epidermal growth factor (EGF), TGFB1, IL-10, TNF, MMP14, MMP2, can promote GBM migration and invasion (211–213). Due to the immune-suppressing role of TAM in tumor progression, this population became a novel target for antitumor immunotherapies (213).

Different strategies have been focused on the impairment of macrophage tumor recruitment and on the reprogramming of phagocyte innate immune surveillance functions of MDM and MG (**Figure 1**).

Recent studies have shown that the CSF1 ligand is expressed in glioma cells and TAM. The CSFR1R is only expressed on macrophages (214). Inhibition of CSF1R using the blood-brain barrier permeable compound BLZ945, significantly decreased tumor growth and extended survival in a mouse model of GBM and patient-derived xenografts models. Treatment efficacy was

TABLE 1 | PD-1 inhibitor treatments approved by the FDA and in clinical testing for GBM patients.

Clinical trials investigating the use of ICIs for treatment of GBM					
Drug	**Target**	**Name**	**Year**	**Clinical Phase**	**Arms**
PD-1	Nivolumab	Neoantigen-based personalized Vaccine Combined with Immune Checkpoint Blockade Therapy in Patients with Newly Diagnosed, Unmethylated GBM	Actual Study Start Date: October 31, 2018 Actual Primary Completion Date: May 25, 2020 Estimated Study Completion Date: February 26, 2021	I	Arm A: NeoVax + Nivolumab (at progression) Arm B: NeoVax + Nivolumab (at Cycle 2) Arm C: NeoVax + Nivolumab (at Cycle 1)
		GMCI, Nivolumab, and Radiation Therapy in Treating Patients with Newly Diagnosed High-grade Gliomas	Actual Study Start Date: February 27, 2018 Estimated Primary Completion Date: February 28, 2021 Estimated Study Completion Date: February 28, 2021	I	Arm A: MGMT Unmethylated patients; AdV-TK injection into resection cavity, valaciclovir 14 days, radiation after 8 days, TMZ after valaciclovir, Nivolumab every 2 weeks to 52 weeks Arm B: MGMT Methylated and undetermined patients; AdV-TK injection into resection cavity, valaciclovir 14 days, radiation after 8 days, TMZ after valaciclovir, Nivolumab every 2 weeks to 52 weeks
		Translational Study of Nivolumab in Combination with Bevacizumab for Recurrent Glioblastoma	Actual Study Start Date: October 1, 2018 Estimated Primary Completion Date: February 1, 2022 Estimated Study Completion Date: August 1, 2022	II	Arm A: Nivolumab + Bevacizumab in patients not undergoing salvage surgery Arm B: Nivolumab + Bevacizumab in patients not undergoing salvage surgery
	Pembrolizumab	Combination Adenovirus + Pembrolizumab to Trigger Immune Virus Effects (CAPTIVE)	Study Start Date: June 2016 Estimated Primary Completion Date: December 2020 Estimated Study Completion Date: June 2021	II	Intratumoral DNX-2401 (a genetically modified oncolytic adenovirus) followed by IV Pembrolizumab
		Laser Interstitial Thermotherapy (LTTI) Combined with Checkpoint Inhibitor for Recurrent GBM	Actual Study Start Date: November 29, 2017 Estimated Primary Completion Date: December 2020 Estimated Study Completion Date: January 2021	I/II	Arm A: IV Pembrolizumab 7 days pre-surgery with LITT Arm B: IV Pembrolizumab 14 days post-surgery with LITT Arm C: IV Pembrolizumab 35 days post-surgery with LITT
		PVSRIPO and Pembrolizumab in Patients With Recurrent Glioblastoma	Estimated Study Start Date: September 2020 Estimated Primary Completion Date:	I	Single Arm: PVSRIPO intratumoral infusion followed by intravenous Pembrolizumab 14 to 28 days later, and every 3 weeks, thereafter

(Continued)

TABLE 1 | Continued

Clinical trials investigating the use of ICIs for treatment of GBM					
Drug	**Target**	**Name**	**Year**	**Clinical Phase**	**Arms**
			March 2023 Estimated Study Completion Date: March 2023		

TABLE 2 | PD-L1 inhibitor treatments approved by the FDA and in clinical testing for GBM patients.

Clinical trials investigating the use of ICIs for treatment of GBM						
Target	**Drug**	**Clinical trial ID**	**Name**	**Year**	**Clinical Phase**	**Arms**
PD-L1	Avelumab	NCT03047473	Avelumab in Patients with Newly Diagnosed Glioblastoma Multiforme	Actual Study Start Date: March 10, 2017 Estimated Primary Completion Date: September 2022 Estimated Study Completion Date: September 2022	II	Addition of Avelumab to standard therapy of TMZ and radiotherapy

related to M2 macrophage polarization inhibition, but not TAM depletion in tumor treated mice. Molecular analysis of TAM showed that this population had an inhibited expression of some M2 polarization markers, such as Arg1, F13a1, Mrc1, and Adm (215). Although, different inhibitors such as BLZ945, RG 7155, PLX339 have been tested in clinical trials, blocking of CSFR1 remains challenging and requires further studies.

TAM survival is maintained by factors released by glioma cells, such as interferon-γ (IFN-γ) and granulocyte-macrophage colony stimulating factor (215, 216).

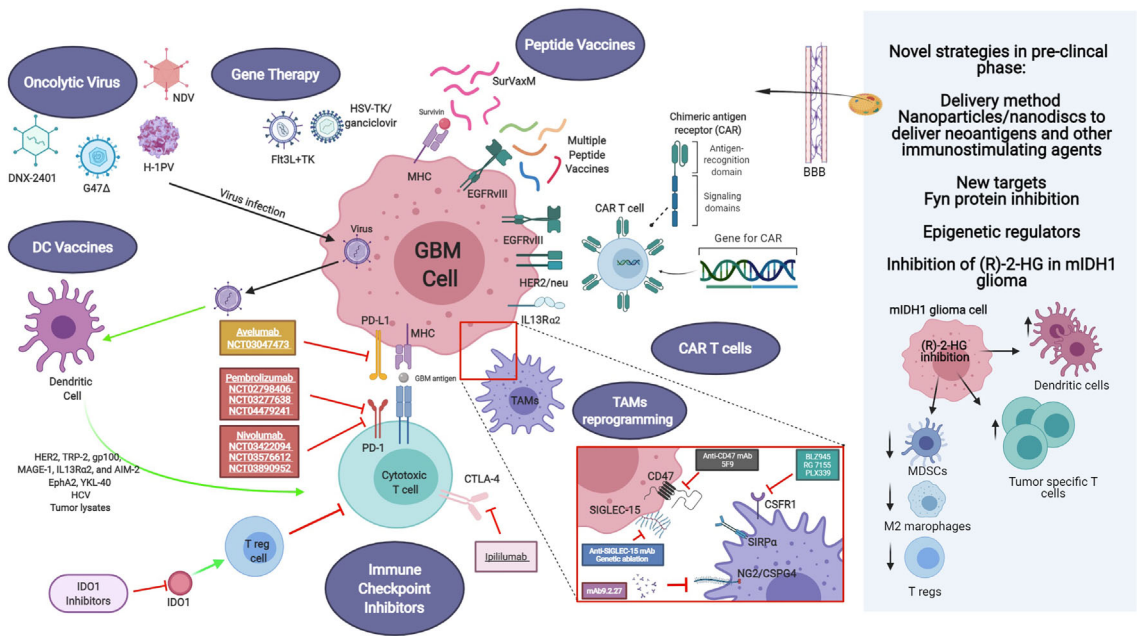

FIGURE 1 | Current and novel immunotherapeutic strategies for GBM treatment under pre-clinical and clinical investigation. Current immunotherapeutic strategies in GBM include oncolytic viruses that can destroy glioma cells through immunogenic cell death without affecting non neoplastic brain cells, TAM reprogramming and the use of CAR T cells. Activation of immune checkpoint ligands such as PD-1, CTLA-4, and IDO can help tumor cells to escape immune surveillance. Thus, inhibition of them can effectively inhibit glioma progression and improve the response to other active immunotherapeutic strategies, such as DC vaccines and immunostimulant gene therapy. GBM antigens, including IL-13Rα2, HER2/neu and EGFRvIII are present in tumor cells. These tumor-associated antigens are targets of genetically modified CAR-T cells or peptide vaccines. Also, novel strategies are being studied currently in the pre-clinical setting, addressing more efficient ways to cross the blood-brain barrier (BBB), such as nanodiscs, and the modulation of the activity of novel targets. Created with BioRender.com.

The combined treatments of CSFR1 inhibitors with PD-1 or PDL-1 monoclonal antibody are promising avenues under investigation in clinical trials (216). Also, the combination of triple therapy using checkpoint inhibitors (anti-CTLA-4 and anti-PD-1), and immune-virotherapy showed effective M1 polarization of macrophages and tumor eradication (217). Other combinational therapy approach inhibiting the Neuroglial-2/Chondroitin sulfate proteoglycan-4 (NG2/CSPG4) axes using the antibody mAb9.2.27 together with activated NK cells in preclinical animal models of gliomas decreased tumor growth, by increasing recruitment of CCR2low MDM to the TME and by amplifying ED1 and MHCII expression on MG (218).

Likewise, other studies showed that therapies using dual inhibitors of VEGF and Angiopoietin-2 (ANG-2) axes led to modifications in TAMs. A2V bi-specific antibody or dual therapies utilizing Cediranib and MEDI3617, reprogramed macrophages to antitumor M1 phenotype, inhibited TAM recruitment and delayed tumor growth and progression (219, 220).

Further research studies demonstrated that CXCR4 signaling is involved in the recruitment of TAM to the TME. Inhibition of this axis using the clinically approved drug AMD3100 prevents BMDCs infiltration, tumor revascularization, and abrogate tumor recurrence (218). Moreover, a recent phase I/II clinical trial study showed positive results in macrophage recruitment inhibition and local control of tumor recurrences after irradiation therapy using a reversible CXCR4 inhibitor Plerixafor (221).

Glioma cells redirect macrophages activating signals to a pro-inflammatory M2 state. This strategy has been related to the overexpression of Spp1 (secreted phosphoprotein 1 or osteopontin) and Mgfe8 (milk fat globule-EGF factor 8 or lactadherin) on glioma cells and human glioblastoma tissue, which prompt M2 reprogramming of MG as a result of integrin signaling activation. Furthermore, downregulation of Spp1 and Mgfe8 within glioma cells inhibits the amoeboid transformation of myeloid cells and redirect M2 microglia/macrophages phenotype impairing glioma growth (222).

The latest strategies developed have been related to the targeting of CD47/SIRPA (signal regulatory protein alpha) pathway. CD47 is a transmembrane protein overexpressed in glioma cells that binds to the receptor SIRPA on the surface of monocytes/macrophages and MG cells inhibiting phagocytic functions and allowing tumors to escape the innate immune surveillance. Transcriptomic analysis of human gliomas has shown that high expression of CD47 correlates with overall survival, which makes CD47 a novel prognostic marker (223, 224). The mechanism of activation of CD47/SIRPA includes the activation of ITIM (immune-receptor tyrosine-based inhibitory motif) and subsequent signalling through the activation of PTPN6 (protein-tyrosine phosphatase non-receptor type 6) and PTPN11, inhibiting phagocytosis (225). Moreover, preclinical studies based on orthotopic glioma models showed that blocking CD47 using antibodies decreased tumor growth and enhanced animal survival (223). Even though the major role of CD47 inhibition has been attributed to peripheral macrophage recruitment, Hutter, G. et al also demonstrated its effect on resident microglia. Using mouse glioma models which enable the differentiation of genetically labelled MDM (Ccr2 RFP) and MG (Cx3cr1 GFP), they showed that microglia associated tumor cells increase tumor cell phagocytosis in response to CD47/SIRPA axis inhibition (226). This data indicates that enhancement of MDM and MG phagocytosis phenotype is a promising avenue for glioma treatment. Recent clinical trial studies using 5F9, a CD47 inhibitor, on other solid tumors showed a positive response in combination with other anticancer treatments (227).

Another feature of malignant transformation in glioma is the protein over-glycosylation ended by charged sialic acid in glioma cells, which constitutes novel target. SIGLEC (sialic acid-binding immunoglobulin-like lectin) proteins (14 different identified variants) are receptors of sialic acid and they are mainly present on immune cells (TAMs) acting as negative regulators of phagocytosis. SIGLEC receptor activates immunosuppressive signals after binding to sialic acids through the same signalling pathways activated in the CD47/SIRPA axe as discussed above (213, 228, 229). Examination of the sialic acid/SIGLEC pathway has demonstrated that genetic and antibody ablation of SIGLEC15 expands anti-tumor immune response and obstructs tumor growth in mouse glioma models (230).

In summary, these studies show that regulation of TAM recruitment to the tumor mass or re-education to a phagocyte phenotype contributes to the anti-tumor response and inhibition of glioma progression. Due to the diversity and plasticity of TAMs, a better understanding of the mechanisms involved in TAMs recruitment and reprogramming remain a challenge to target these immune modulators of the TME for treatment. Combination of conventional therapies, immune checkpoint inhibitors together with TAMs regulation appears to be a promising alternative to improve glioma immunotherapy and halt glioma progression.

Therapies Aiming at the Stimulation of the Immune System to Develop Anti-Tumor Specific Immune Response

An additional group of immunotherapies are aimed at inducing the development of antitumor specific responses, i.e. mediated by specific T-cells or antibodies production. These therapies were discussed in detailed before, and it is not the purpose of this manuscript to review them on detail. Anti-tumor specific response-inducing therapies can be summarized in:

- Oncolytic virus-mediated therapies, where oncolytic viruses are targeted to the tumor cells to cause Immunogenic cell death (ICD), stimulating the release of tumor-associated antigens (TAA) and damage-associated molecular patterns (DAMPs), which help to overcome the immunosuppressive tumor microenvironment (231). In this way, ICD induces the recognition of tumor cells by the immune system and the development of long-term immunity (232). Furthermore, OVs induce antiviral innate immune responses triggered by pathogen-associated molecular patterns (PAMPs) (231). Additionally, OVs can be genetically engineered to deliver immunotherapeutic transgenes or to increase their tumor

selectivity, enhancing their potential for oncolytic immunotherapy (231–246).

- Suicide gene therapies, which comprises the delivery of genes encoding a conditionally cytotoxic enzyme that converts a non-toxic prodrug into a cytotoxic compound. In this way, transduced tumor cells are destroyed, sparing normal cells (247). The most evaluated suicide gene therapy for the treatment of GBM is HSV- thymidine kinase (TK) plus systemic administration of ganciclovir (GCV) (247).
- Peptide vaccines, where the main objective is to inhibit cancer progression or relapse, by producing humoral (tumor-specific antibodies) or cellular (cytotoxic T cells activation) responses against tumors (20, 248).
- Dendritic cells (DC) vaccines. DCs are professional antigen presenting cells (APCs), which function is to recognize, process and present antigens to T cells in the context of the major histocompatibility complex (MHC) I and II, in order to activate T cells and subsequently the adaptive immune response (12). Moreover, DCs are able to secrete pro and anti-inflammatory cytokines that modulate the tumor microenvironment. Autologous DCs can be loaded *ex vivo* with tumor antigens, peptides, tumor lysates, viral antigens, GSC or mRNA, among others, and then be administered back to patients as an antitumor vaccine (8, 249). These autologous DCs are usually differentiated from autologous monocytes by the incubation with specific cytokines (12).
- CAR T therapy. Chimeric antigen receptors (CARs) are recombinant receptors for specific targets found on cancer cells. They are designed to redirect the specificity and function of patient-derived cytotoxic T cells, which are *ex vivo* genetically engineered to express the CAR and re-infused to the patient (186, 250, 251).

INFLUENCE OF GENETIC ALTERATIONS PRESENT IN GLIOMA SUBTYPES ON THE RESPONSE TO IMMUNOTHERAPIES

Although the use of immune therapies to treat gliomas is still in its early stages, *i.e.*, in research and trial phases, the knowledge accumulated in the field in CNS tumors and other solid cancers indicate that the genetic makeup of the tumor is a predictive factor of the efficiency of the immune therapies. Not only the genetic information can predict if a treatment is likely to generate response or not, but also the genetic alterations present in certain subtypes of tumors can be exploited to devise tailored immunotherapies. In solid tumors, it was observed that the mutational load is a positive predictive factor of response to immunotherapy. A significant proportion of gliomas have mutations associated with DNA repair defects and genetic instability (252). As a consequence of this, higher mutational burden, has been observed, particularly in pediatric HGG patients with DNA repair-related germline mutations (252). Although a recent study found no correlation between mutational load and response to immune checkpoint inhibition in glioma (253), it is likely that the treatment in this study was inefficient due to the poor penetrance of the immune checkpoint inhibitors to the brain (254). In this respect, a patient with Lynch syndrome (a genetic condition related with mismatch DNA repair deficiency) who developed an IDH-mutant glioblastoma was treated with a PD-1 inhibitor (Nivolumab), remaining free of recurrence for 5 years (255).

Recent studies have described the peculiarities of the immune compartment in gliomas, which is strongly immunosuppressive and enriched in myeloid suppressor cells and exhausted and regulatory T-cells (209). Recently, it was demonstrated that the interactions between tumor cells and the immune microenvironment are influenced by the genetic alterations of the tumors. For instance, some studies reported that IDH mutations induce epigenetic changes that lead to establishing an immunosuppressive TME (94, 100). However, work from our team reported that infiltrating immune myeloid cells in the mutant-IDH TME are devoid of immunosuppressive properties. This highlights that it is not only important to identify the presence of a particular immune cells population using defined molecular markers, but also to assess the functional activity of these cells, to be able to describe the characteristics of the TME (15). In addition, it has been reported that mutant-IDH glioma cells express lower PD-L1 levels due to epigenetic reprogramming, suggesting a less immunosuppressive environment. All this information is pivotal to devise therapeutic approaches, *e.g.*, the concept of combining mutant-IDH inhibitors (to revert the suppressive TME) with immunotherapies. However, considerable work still needs to be done in regards to the genetic and functional characterization of immune cell populations in the TME of gliomas. Single-cell RNA-seq allows the identification of different immune cells within the glioma TME, and can inform on whether certain molecular subtypes of glioma have more immune-active or immune-suppressive environments. Another type of technologies that can shed light into the characteristics of the immune populations within glioma TME are the studies performed in *de novo* genetically engineered animal models, which can be developed in immunocompetent mice and allow to dissect the effect of particular genetic alterations in the immune TME (15, 44, 148). This type of studies will also help devising tailored immunotherapies for specific gliomas. For instance, a group of NF1-mutant low grade gliomas was demonstrated to be associated with immune activation, increased cytolytic T-cell infiltration and neoantigens production, and this group might benefit from immunotherapies (256).

Another area where immunotherapies benefit from the knowledge of the glioma genetic makeup is on the development of CAR-T therapies or peptide vaccines. CAR-T therapies require the identification of targets that are expressed on the surface of the tumor cells and that are not expressed in normal cells. Interleukin-13 receptor α2 (IL-13Rα2) was identified as a glioma specific marker, and CAR-T therapy with cells targeting this protein was evaluated in a clinical trial (257). The preliminary results of this study on a single patient reported glioma regression, but development of therapy resistance associated to the emergence of (IL-13Rα2) negative cells. Additionally, histone K27M-mutant cells show consistent expression of GD2, and its CAR-T-mediated targeting was efficient in K27M xerograph models (258). These

studies provide the foundation on future directions to develop efficient immunotherapies for glioma. CAR-T cell therapies. The identification of multiple cell surface markers with minimal off-target effects for the different molecular subtypes of gliomas is essential to target tumors and prevent antigen escape-associated resistance. In this regard, the recent genomic analysis of gliomas has led to the identification of clonal mutations that drive the different molecular subtypes. For example, IDH1/2 mutations in adult gliomas and histone H3.1 and H3.3 mutations in pediatric high grade gliomas were shown to be clonal for their respective subtypes, and developing therapies targeting these genetic alterations would reduce the risk of antigen-escape.

The epigenetic alterations induced by driver mutations such as those in IDH1/2 and H3.1 and H3.3 histones may also induce DNA repair deficiencies and/or genetic instability, and this can be associated with more immune reactive tumors. For example, cells more susceptible to DNA damage, such as H3.3-G34R mutant cells (259), undergo immunogenic cell death (ICD) upon DNA damaging conditions, which can revert the immune-suppressive TME. For this reason, acknowledging the susceptibility of the different glioma molecular subtypes to different treatments to induce ICD. For example, HDAC inhibitors were shown to target K27M HGG (260), and other tailored therapies are being explored for other subtypes (252), but the potential combinations of treatments inducing ICD and immunotherapies remain unexplored.

In summary, it is clear that the genetic alterations present in the different glioma molecular subtypes are determinant of the efficacy of immunotherapies possibilities and responses, and that the evolving information of each glioma subtype will provide opportunities for novel tailored immunotherapies.

NOVEL TARGETS AND STRATEGIES TO STIMULATE ANTI-GLIOMA IMMUNE RESPONSE

In this section, we aim to discuss about the latest glioma targets and anti-tumor strategies being studied in the pre-clinical setting (**Figure 1**).

Fyn Inhibition as a Target to Enhance Immune Response and Prevent Tumor Progression

Despite current advances in the molecular characterization of gliomas and novel therapies to target the tumor immune microenvironment, treatment of glioblastoma remains elusive (34, 261). Latest studies indicate that glioma infiltrating myeloid cells inhibit the anti-glioma immunity and enhance tumor progression and thus, the identification of the connections between tumor cells and the tumor immune suppressive microenvironment could open innovative treatment options (9, 262). Fyn, a non-receptor tyrosine kinase member of the Src family kinases (SFK), has recently emerged as a novel regulator of the tumor immune microenvironment during glioma development (20, 248). Fyn regulates several cellular functions in normal physiology and is deregulated in different cancers (263–265). It has been shown that Fyn displays important functions related to the immune system modulation, regulating the activity of T cells (266, 267); and in the development of the CNS, regulating the migration and adhesion of neurons (268, 269). Previous studies on Fyn's role in cancer, including glioma, show that Fyn is activated via NRAS dependent and independent pathways through the oncogenic receptors EGFR, PDGFR, HGF/MET or RTK/RAS/PI3K to increase cell migration, proliferation and reduce cell death (270–272). These growth factor receptors are the most common mutated driver genes in GBM tumorigenesis (34, 261). Even though Fyn is mutated in a very low percentage of human gliomas (0.1-0.4 %), it has been shown that it is overexpressed in higher grade mouse and human gliomas (20, 270).

Until recently, Fyn has been best known by its cell-autonomous functions. The majority of *in vitro* studies showed that pharmacological inhibition and genetic downregulation of Fyn in glioma cells decreased cell proliferation and migration (265, 270, 273, 274). However, *in vivo* studies had been inconclusive (275). Recently, Comba et al. demonstrated not only the effects of Fyn in increasing glioma cell proliferation and migration, but also an unusual cell-non-autonomous role of Fyn inhibiting the anti-glioma immune response (20). RNA-Seq and network bioinformatic analysis of the tumor transcriptomic landscape on glioma mouse model tumors indicated that Fyn's biological effects were related to the immune microenvironment. Using diverse genetically engineered immune-competent mouse glioma models, the study shows that genetic downregulation of Fyn increases survival and decreases glioma growth and progression. Interestingly, Fyn knockdown tumors generated in immune deficient mice (NSG, CD4-/- and CD8-/-) exhibited no differential effects on tumor growth and survival, demonstrating the relevance of the immune response in the progression of these tumors. The mechanistic analysis showed that Fyn depletion reduces the expansion of the immune suppressive myeloid cells (MDSCs) in the TME, including monocytic-MDSCs (CD45+, CD11b+, Ly6Chi, Ly6G−) or polimorphonuclear-MDSCs (CD45+, CD11b+, Ly6Clo, Ly6G+) and therefore less inhibition of T-cell activity is observed. Fyn increases tumor growth due to MDSC migration induction, their augmented expression of ARG1 and CD80, as well as their enhanced functional immunosuppressive activity (20). This work opens up new avenues for future investigations to understand glioma-immune microenvironment cross-talk and increases the potential efficacy of anti-glioma therapeutics. All these data suggest that Fyn inhibition in tumor cells is a novel therapeutic target for glioma treatment. Inhibiting Fyn's pro-tumoral activity has the combined effects of reducing tumor cell proliferation and migration, as well as inducing the anti-tumor immune response.

The incapacity of different therapeutic agents to cross the blood-brain barrier and the non-specificity of the available Fyn pharmacological inhibitors challenge the possibilities of its use as a target for glioma treatment (265). To investigate the translational implications of targeting Fyn in glioma, we propose the use of glioma pre-clinical models to test the

efficacy of nanoparticles loaded with small interfering RNA (siRNA) against *Fyn*. This strategy has the advantage of being systemically administrated, since nanoparticles have the ability to cross the brain-barrier and deliver their cargo directly into brain tumors (276, 277). Furthermore, the combination of Fyn inhibition within glioma cells and cancer immunotherapy, such as immune checkpoint blockade (PDL1 and PD1 inhibitors), IFNγ therapy, and Ad-hCMV-TK plus Ad-hCMV-Flt3L immune-stimulatory gene therapy (8, 12, 278), are promising avenues to improve the efficacy of anti-glioma immunotherapies and explore novel personalized treatment for glioma patients.

Nanoparticles as a Novel Anti-Glioma Therapy to Stimulate the Immune System

Nanotechnology is a potentially promising strategy to utilize against gliomas. It offers advantages such as (1) targeted delivery of materials to specific organs and tissues; (2) antigen and adjuvant co-delivery to antigen-presenting cells (APCs); and (3) non-invasive delivery of therapeutics; while (4) providing safe and biocompatible platforms for combinational immunotherapy, especially with immune checkpoint blockade (ICB) (279). In particular, Kuai, et al. have developed a synthetic high-density lipoprotein (sHDL) nanodisc platform composed of phospholipids and apolipoprotein A1-mimetic peptides (280). As a platform for cancer immunotherapy, sHDL has ideal properties, including multiple cargo loading sites for antigens, adjuvants, and chemotherapeutics, and its small size (10 nm) mediates efficient delivery of cargo to draining lymph nodes or directly to tumors for cytotoxic effects. In this regard, we have demonstrated strong anti-tumor efficacy of sHDL delivering GBM neoantigens or a chemotherapeutic agent docetaxel (DTX) in murine models of glioma (21, 22).

The sHDL nanodiscs using GBM neoantigens were synthesized by modifying neoantigen peptides with a reduction-sensitive cysteine-serine-serine linker, which was reacted with a dioleoyl-*sn*-glycero-3-phosphoethanolamine-*N*-[3-(2-pyridyldithio) propionate] (PDP)-modified lipid to produce neoantigen-lipid conjugates (22, 280). Loading of neoantigen-lipid conjugates and CpG (a Toll-like receptor-9 agonist) in sHDL was mediated via hydrophobic interactions after simple mixing. Nanodiscs were taken up by DCs, leading to strong localization with endosomes/lysosomes, sustained epitope-MHC I presentation, and cross-priming of CD8+ T cells against GBM. Mice were inoculated with an orthotopic GL261 model and treated with a combination of nanodiscs carrying three GBM neoantigens and anti-PD-L1. The results showed up to 100-fold higher IFNγ+ T cell responses and eradicated 30% of gliomas, compared with soluble vaccine + anti-PD-L1 treatment (22). Furthermore, there were no signs of recurrence through day 90, on which mice were re-challenged in the contralateral hemisphere and did not show any signs of neurological deficit as well (22). These results are particularly exciting as they demonstrate immunological memory and the ability of glioma-specific T cells to traverse the blood brain barrier (BBB) and exert cytotoxic effects against gliomas.

Nanodiscs carrying DTX and CpG were synthesized similarly (21). One of the main barriers of effective glioma treatment is the BBB, which provides a physical resistance to GBM chemotherapeutic treatment. By loading sHDL nanodiscs with DTX and CpG and injecting them intrathecally, the BBB was bypassed, allowing the nanodiscs to diffuse through the entire tumor (21, 281). When sHDL-DTX-CpG was administered to orthotopic GL26 tumor-bearing mice, a ~2-fold increase in survival was observed, compared with DTX, DTX-CpG, or DTX-sHDL treatment (21). sHDL-DTX-CpG triggered immunogenic cell death, as evidenced by high expression of "eat me" and "danger" signals, such as calreticulin and HMGB1 on the surface of tumor cells. sHDL-DTX-CpG also promoted recruitment of APCs as well as CD8+ T cells into GBM tumors (21). As standard therapy for GBM is normally a combination of radiation therapy and chemotherapy, GBM-bearing mice were treated with a combination of sHDL-DTX-CpG and radiation therapy, which resulted in 80% tumor regression and no tumor recurrence post tumor re-challenge (21). Exemplified by these two examples using the sHDL nanodisc platform, nanotechnology is a novel and effective therapy to stimulate a comprehensive anti-GBM immune response.

Current Therapies Aimed at Targeting Epigenetic Pathways in Glioma and Its Impact on the Immune Response

Insights into the molecular landscape of diffuse gliomas have revealed characteristic genetic and epigenetic profiles which stratified the glioma classification (38, 47). Genetic anomalies associated with gliomagenesis commonly coincide with specific epigenetic mutations (282). These include but are not limited to a mutation in histone H3 genes such as H3K27M, and H3G34R/V as well as a mutation in the epigenetic modulator gene isocitrate dehydrogenase (IDH) (38, 47). Owing to the reversibility of epigenetic modifications, the proteins and genes that regulate these changes have become new targets in the treatment of glioma (282). Epigenetic mechanisms are critical for many processes in cancer–immunity cycle. Also, epigenetic pathways can impact both tumor cells as well as immune cells resulting in a negative impact on the anti-tumor immune response. For instance, DNA methylation-associated mutagenesis is the single most important source of genetic alterations, leading to neoantigen formation in most cancers including glioma (283, 284).

Several therapies aimed at targeting epigenetic pathways are being examined for their anti-glioma abilities. Several of these therapies target proteins that mediate histone modifications. Examples of these therapies include EZH2 inhibitors, DNA methyltransferase (DNMT) inhibitors, histone deacetylase (HDAC) inhibitors, mutant IDH inhibitors, and BET inhibitors (285). The enhancer of zeste homolog 1/2 (EZH1/2) is the main subunit of PRC2 responsible for the trimethylation of Histone H3 lysine 27 (H3K27me3), which controls stem cell and oncogenic gene expression programs (282). The H3K27 mutation has been shown to inhibit polycomb repressor complex 2 (PRC2) activity which leads to hypomethylation of H3K27 and expression of potential oncogenes (282). EZH2 overexpression is associated with poor GBM prognosis, and reducing levels of EZH2 expression in vivo resulted in a reduced tumor progression, which suggests the efficacy

of EZH2 inhibitors as anti-glioma therapies (286, 287). EZH2 inhibitor, Tazemetostat, alone, and in conjunction with other therapies, is currently in clinical trials for treating pediatric glioma with EZH2, SMARCB1, or SMARCA4 mutations (ClinicalTrials.gov IDs NCT03213665, NCT03155620). These mutations affect gene expression via the regulation of chromatin remodeling.

DNA methylation is the most commonly studied epigenetic modification in cancer (285), and methylation signatures are included in glioma classification (288). Gliomas harboring mutant IDH1 display high levels of DNA hypermethylation in CpG rich domains, which are associated with increased tumor progression and altered gene expression (289, 290). Inhibitors of mutated IDH1/2 enzymes entered clinical trials and represent a novel drug class for targeted therapy of gliomas. These include AG-881, AG-120, and AG-221, all of which are being tested in preclinical and clinical settings. Preliminary results from Phase I clinical trials with IDH inhibitors demonstrated an objective response rate ranging from 31% to 40% with durable responses (>1 year) (291). To date, AG-120 showed the most clinically promising results as an orally administered, reversible, and highly selective small-molecule inhibitor of mutant IDH1/R132H cancers (292, 293).

Another group of drugs targeting the glioma methylation status are DNMT inhibitors, which are now being studied as potential anti-mIDH1 glioma therapies. DNMTs promote cancer generation by causing hypermethylation of tumor suppressor gene enhancers and promoter regions (18, 285). Early studies have shown anti-glioma efficacy of DNMT inhibitors in *vivo* and *in vitro* (294, 295). Despite the preclinical successes, a representative DNMT inhibitor, 5-aza-2′-deoxycytidine, has been shown to have minimal efficacy in early clinical trials (290). Recent studies showed a strong connection between epigenetics and cytokine production in tumor cells. One example is DNMT inhibition which can trick cancer cells into behaving as virus-infected cells, leading to activation of the interferon pathway (296, 297). In glioma, IL-6 promotes hypermethylation of the Sp1-binding site in the *miR142-3p* gene promoter, preventing binding of Sp1 and inhibiting miR-142-3p expression (298). These changes were shown to enhance the effectiveness of immune checkpoint inhibitors (296, 297). Moreover, multiple studies have shown that the PD-L1 level can be regulated by epigenetic mechanisms. For example, in IDH1 mutated glioma, we have shown that methylation in PD-L1 promoter negatively correlates with PD-L1 expression and prognosis (24).

Histone acetylation plays a role in gene expression. Whilst acetylation is generally associated with elevated transcription, deacetylated histones are generally associated with repressed genes (299). HDAC enzymes are differentially expressed in glioma and have been shown to play a role in glioma progression (18, 299). Several pre-clinical studies have shown an effective response for HDAC inhibitors via multiple mechanisms, including induction of tumor cell death, as well as increase radio-sensitivity, differentiation, and/or cell cycle arrest (300–302). Due to the promising results obtained from these studies, both Vorinostat and valproic acid, are currently being tested in clinical trials on gliomas as monotherapies and combinational therapies (18, 303–305). So far, results showed that HDAC inhibitor monotherapies are not sufficient as anti-glioma therapies, but they show promise in increasing the anti-glioma effects in combinational therapies (306).

Bromodomain and extra-terminal domain (BET) proteins are epigenetic chromatin readers that bind to acetyl marks of lysine residues to regulate gene expression (282, 285, 307). BET proteins were found to be associated with high expression of oncogenes (285, 307). BET inhibitors have been identified as possible therapies for GBM patients, as they have been found to inhibit GBM cell proliferation both *in vivo* and *in vitro* by hindering cell cycle progression and reducing oncogene expression (307, 308). Despite the promising preclinical findings, there are no clinical trials on BET inhibitors as a treatment for glioma patients.

Multiple therapeutics targeting epigenetic pathways (epidrugs) have been approved for cancer treatment which can affect the immune response. These were approved to treat hematopoietic malignancies such as T-cell lymphoma, multiple myeloma, and myelodysplastic syndromes (309, 310). Even though there is no clinical application of epidrugs targeting glioma, azemetostat, a KMT6A (EZH2) inhibitor, was approved for the treatment of epithelioid sarcoma, making it the first approved histone 'writer' inhibitor and the first epidrug to treat solid tumors (311). This demonstrates promising avenues of epidrugs to target solid tumors that have pronounced epigenetic dysregulation including glioma, which could in turn, enhance the immune response against these tumors.

Inhibition of the Oncometabolite (R)-2-HG to Enhance Anti-Glioma Immunity

Mutation in the metabolic enzyme isocitrate dehydrogenase 1 (mIDH1) at active site residue R132H occur in ~20-25% of infiltrative gliomas (40, 312, 313). The mutation leads to gain-of-function catalytic activity that converts α-ketoglutarate (αKG) to the onco-metabolite (R)-2-hydroxyglutarate ((R)-2-HG) (40, 314, 315). (R)-2-HG competitively inhibits histone demethylating enzymes ten-eleven translocation methylcytosine dioxygenases (TETs) and lysine-specific demethylases (KDMs) (289, 316). Inhibiting demethylation increases DNA and histone methylation, altering the epigenome, resulting in changes in the tumor transcriptome (289, 316). Although studies have shown that small molecule inhibitors targeting IDH1-R132H have been effective in impairing tumor progression as monotherapy in pre-clinical models (317), in phase I clinical trials they have not been effective as monotherapies (NCT02381886). We have previously shown that mIDH-R132H, in the context of *ATRX* and *TP53* inactivation, epigenetically reprograms gene regions corresponding to DNA repair proteins in human and murine glioma cell cultures (44). Treatment with AGI-5918, a small molecule inhibitor prior to radiotherapy, downregulated DNA repair gene expression, thus making the tumor cells radiosensitive. These results highlight the need for a combinatorial treatment strategy to effectively impede mIDH1 progression.

The onco-metabolite (R)-2-HG has been shown to repress expression of key immune regulatory genes, such as CCL2, CXCL-2 and C5-a, which are primarily involved in mediating lymphocytes' trafficking to the mIDH1 glioma TME (94).

Recently, one study demonstrated that combination of PD-1 inhibition and the mIDH1 inhibitor BAY1436032 extended the survival of mice implanted with GL261-IDH1R132H glioma cells by overriding the immune suppressive environment mediated by (R)-2-HG (318).

We recently demonstrated that in genetically engineered mIDH1 mouse gliomas, resembling human mutant IDH1 astrocytoma, (R)-2-HG inhibition in combination with SOC increased the infiltration of DCs and anti-tumor specific T cells in the TME, while decreasing the infiltration of immunosuppressive MDSCs, Tregs, and M2 macrophages compared to saline treated mice (24). We also observed that mIDH1 glioma cells exhibit lower levels of PD-L1 expression (24). In response to (R)-2-HG inhibition, PD-L1 expression levels on mIDH1 glioma cells significantly increased to those observed in wild type IDH gliomas (24). Numerous preclinical solid tumor models have demonstrated that the immune checkpoint blockade of PD-1/PD-L1 interaction prevents T cell exhaustion, resulting in enhanced anti-tumor immune activity and improved MS (9, 319, 320). We previously demonstrated that PD-L1 checkpoint blockade as monotherapy elicited a small increase in MS in mice bearing syngeneic glioma, with only a few long-term survivors (9). However, immune-checkpoint blockade used as monotherapy has failed in Phase III clinical trials to improve OS of patients with glioma (12). We observed that IDH1-R132H inhibition used in combination with SOC and anti-PD-L1 immune checkpoint blockade increased the frequency of tumor-specific cytotoxic CD8+ T cells and IFN-γ release within the TME (24). Strikingly, long-term survivors from IDH1-R132H inhibition in combination with SOC and anti-PD-L1 immune checkpoint treatment group remained tumor-free post mIDH1 glioma rechallenging in the contralateral hemisphere, indicating the development of anti-mIDH1 glioma immunological memory (24). This is a critical factor in determining the success of immune-therapeutic approaches in gliomas. A robust anti-tumor T cell response and the presence of anti-glioma immunological memory are required to eradicate any remnant tumor cells post-surgery and prevent recurrence.

Collectively, upon metabolic reprogramming it is possible to achieve anti-mIDH1 glioma immunity. The precise elucidation of the immune pathways affected by (R)-2-HG will lead to an understanding of the underlying biological processes and will provide better therapeutic approaches for mIDH1 glioma patients.

FUTURE PROSPECTS AND CONCLUSIONS

The path for immunotherapies against glioma has started more than a decade ago and the lack of sustained clinical beneficial outcomes demonstrates the challenge that this tumor represents (12, 17, 79, 84, 249). Malignant gliomas are tumors intrinsically difficult to target by immunotherapies due to their heterogeneity, their immunosuppressive TME and the particular cross-talk of the CNS and the immune system (6, 11). However, as tumor recurrence occurs almost always in glioma patients, since these tumors are virtually impossible to completely resect due to their infiltrative nature, anti-glioma immunological memory would be highly beneficial desirable for these patients. Also, because the immunosuppressive TME is related to glioma aggressiveness, trying to counteract this milieu represents an appealing idea for oncologists and researchers.

Research in immunotherapies against glioma developed in parallel with the broadening of our understanding regarding the molecular landscape associated to different types of glioma. These studies demonstrated that entities before defined under the same WHO group, were not as homogeneous as they were thought to be (38, 40, 321). The genetic and epigenetic data gathered so far enabled the classification of gliomas in terms of their intrinsic characteristics, in combination with the histological features, and unveiled how complex these tumors are. Also, with the advent of state-of-the-art technologies, such as scRNA-Seq, it was realized not only that gliomas have intra-tumor heterogeneity, but also, that this state could fluctuate, for example, depending on the stage of the treatment at which the biopsy is taken. Ideally, in the future, the advancements in both, sequencing methodologies and immunotherapeutic strategies, will be combined to design and apply more targeted therapies for glioma patients (**Figure 2**).

This overwhelming amount of information allowed the development of more sophisticated murine models for the pre-clinical testing of immune-mediated therapies for glioma. Mouse models that recapitulate the human disease, with animals harboring brain tumors encoding for the specific genetic and epigenetic alterations described, have been generated with techniques, such as the Sleeping Beauty method, that enable the concomitant study of the surrounding immune response.

Even though these advancements represented a milestone in the exploration of immunotherapies against glioma, the translation of pre-clinical findings to the clinical setting has not yielded consistent or sustained beneficial outcomes for patients. This drawback reveals that animal models need to be further adjusted to the genetics/biology of these tumors and that we should be cautious about generalizing the potential clinical response for a particular immune-mediated therapy. So far, the data gathered from clinical trials and the information obtained in pre-clinical models have been useful in demonstrating that the molecular features of glioma influence the anti-tumor immune response and the clinical consequences of the administration of an immunotherapy.

Despite the lack of a substantial benefit for glioma patients treated with immunotherapies, the medical-research community has learnt important lessons from these pitfalls. Currently, we know that the immune-mediated approach to treat glioma should be combinational, not only by considering more than one TAA or TSA to target, but also by integrating different immunotherapeutic strategies. For example, DC vaccines could be combined with ICI and OV therapy, to enhance the development of adaptive anti-tumor immunity. The possibility of combinational therapies is encouraging, as we have been capable of developing different immune-mediated strategies against this tumor. However, it rises the complexity of tumor treatment, as the number of combinations for drug doses, times and routes for drug administration increases exponentially.

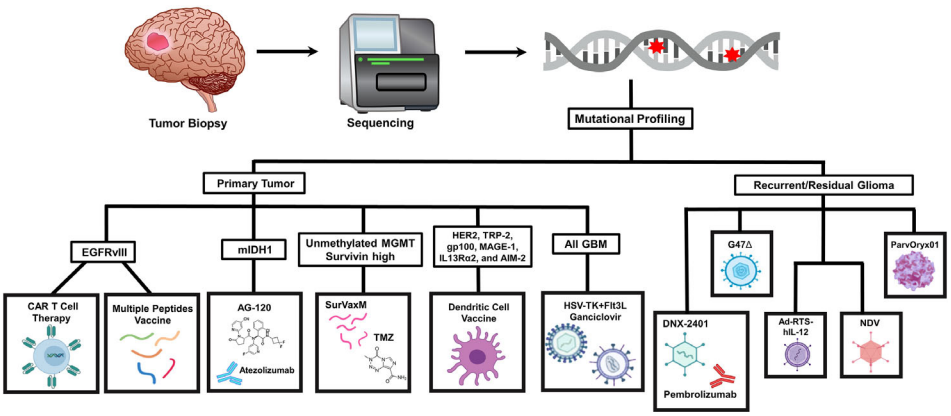

FIGURE 2 | Genomic sequencing of glioma patient tumor biopsies could guide the immunotherapy strategies selected based on the mutational profile and clinical status. Tumor biopsies obtained by surgical resection undergo high-throughput genomic sequencing to identify mutations present within the cancer cells. The genetic lesions detected could be used as a decision factor to select which immunotherapy to choose. Patients with primary tumors that express specific tumor antigens can undergo a variety of immune-based treatments that address these driver mutations directly and could be combined with chemotherapeutic agents and other approaches, such as immune checkpoint inhibitors. Patients that present with recurrent or residual glioma could also be treated with gene therapy or virotherapy-mediated approaches that directly target the glioma cells to trigger immune-stimulatory mechanisms.

The great advancements in the immune-mediated approaches for glioma therapy and the development of BBB penetrating and tumor-targeted ways of drug administration in the pre-clinical setting has demonstrated that the research community is capable of designing new alternatives to overcome the challenges that this type of tumor presents. We believe that the key for the success of immunotherapies against glioma resides in the deep understanding of the biology of this tumor and in the precise combination of diverse therapeutic approaches. It is important to carefully revise the clinical trial results and to compare them with the pre-clinical data, in order to learn from the failures and generate better animal models.

We hope that the data discussed in this review highlight the importance of taking into account the molecular features of gliomas when considering immunotherapies and that it will shed light on the aspects that we still need to tackle to successfully harness the immune system against these tumors.

AUTHOR CONTRIBUTIONS

All the authors contributed to the writing of the manuscript. MC, AS, and NG prepared **Figure 1** and tables. SC prepared **Figure 2**. All authors contributed to the article and approved the submitted version.

FUNDING

This work was supported by NIH/NINDS Grants, R37-NS094804, R01-NS105556 and 1R21NS107894 to MGC; NIH/NINDS Grants R01-NS076991, and R01-NS096756 to P.R.L.; NIH/NIBIB: R01-EB022563 grant to MGC, PL and JJM; the Department of Neurosurgery, the Rogel Cancer Center, Program in Cancer Hematopoiesis and Immunology (CHI), the ChadTough Foundation, Pediatric Brain Tumor Foundation, and Leah's Happy Hearts to MGC. and PL; RNA Biomedicine Grant F046166, Forbes Foundation Grant, University of Michigan Medical School, Rogel Cancer Center Scholar, University of Michigan Medical School to M.G.C.; T32 CA009676-26 Cancer Biology Training Grant to MAl; UL1 TR002240 for the Michigan Institute for Clinical and Health Research (MICHR), Postdoctoral Translational Scholars Program (PTSP), Project F049768 to AC and American Brain Tumor Association Basic Research Fellowship "in Memory of Bruce and Brian Jackson" to MG-F.

REFERENCES

1. Ostrom QT, Gittleman H, Fulop J, Liu M, Blanda R, Kromer C, et al. CBTRUS Statistical Report: Primary Brain and Central Nervous System Tumors Diagnosed in the United States in 2008-2012. *Neuro-Oncology* (2015) 17(Suppl 4):iv1–62. doi: 10.1093/neuonc/nov189
2. Molinaro AM, Taylor JW, Wiencke JK, Wrensch MR. Genetic and Molecular Epidemiology of Adult Diffuse Glioma. *Nat Rev Neurol* (2019) 15(7):405–17. doi: 10.1038/s41582-019-0220-2
3. Mrugala MM. Advances and Challenges in the Treatment of Glioblastoma: A Clinician's Perspective. *Discovery Med* (2013) 15(83):221–30.
4. Parrish K, Sarkaria JN, Elmquist WF. Improving Drug Delivery to Primary and Metastatic Brain Tumors: Strategies to Overcome the Blood–Brain Barrier. *Clin Pharmacol Ther* (2015) 97(4):336–46. doi: 10.1002/cpt.71
5. Mallick S, Benson R, Hakim A, Rath GK. Management of Glioblastoma After Recurrence: A Changing Paradigm. *J Egyptian Natl Cancer Institute* (2016) 28(4):199–210. doi: 10.1016/j.jnci.2016.07.001
6. Quail DF, Joyce JA. The Microenvironmental Landscape of Brain Tumors. *Cancer Cell* (2017) 31(3):326–41. doi: 10.1016/j.ccell.2017.02.009
7. Antunes ARP, Scheyltjens I, Duerinck J, Neyns B, Movahedi K, Van Ginderachter JA. Understanding the Glioblastoma Immune

Microenvironment as Basis for the Development of New Immunotherapeutic Strategies. *Elife* (2020) 9:e52176. doi: 10.7554/eLife.52176
8. Kamran N, Alghamri MS, Nunez FJ, Shah D, Asad AS, Candolfi M, et al. Current State and Future Prospects of Immunotherapy for Glioma. *Immunotherapy* (2018) 10(4):317–39. doi: 10.2217/imt-2017-0122
9. Kamran N, Kadiyala P, Saxena M, Candolfi M, Li Y, Moreno-Ayala MA, et al. Immunosuppressive Myeloid Cells' Blockade in the Glioma Microenvironment Enhances the Efficacy of Immune-Stimulatory Gene Therapy. *Mol Ther* (2017) 25(1):232–48. doi: 10.1016/j.ymthe.2016.10.003
10. Razavi S-M, Lee KE, Jin BE, Aujla PS, Gholamin S, Li G. Immune Evasion Strategies of Glioblastoma. *Front Surg* (2016) 3:11. doi: 10.3389/fsurg.2016.00011
11. Kamran N, Chandran M, Lowenstein PR, Castro MG. Immature Myeloid Cells in the Tumor Microenvironment: Implications for Immunotherapy. *Clin Immunol* (2018) 189:34–42. doi: 10.1016/j.clim.2016.10.008
12. Garcia-Fabiani MB, Ventosa M, Comba A, Candolfi M, Nicola Candia AJ, Alghamri MS, et al. Immunotherapy for Gliomas: Shedding Light on Progress in Preclinical and Clinical Development. *Expert Opin Investig Drugs* (2020) 29(7):659–84. doi: 10.1080/13543784.2020.1768528
13. Gieryng A, Pszczolkowska D, Walentynowicz KA, Rajan WD, Kaminska B. Immune Microenvironment of Gliomas. *Lab Invest* (2017) 97(5):498–518. doi: 10.1038/labinvest.2017.19
14. Lu J, Li H, Chen Z, Fan L, Feng S, Cai X, et al. Identification of 3 Subpopulations of Tumor-Infiltrating Immune Cells for Malignant Transformation of Low-Grade Glioma. *Cancer Cell Int* (2019) 19(1):1–13. doi: 10.1186/s12935-019-0972-1
15. Alghamri MS, Avvari RP, Thalla R, Kamran N, Zhang L, Ventosa M, et al. G-CSF Secreted by Epigenetically Reprogrammed Mutant IDH1 Glioma Stem Cells Reverses the Myeloid Cells'-Mediated Immunosuppressive Tumor Microenvironment. *bioRxiv* (2020) 2020.07.22.215954. doi: 10.1101/2020.07.22.215954
16. Stylli SS, Luwor RB, Ware TM, Tan F, Kaye AH. Mouse Models of Glioma. *J Clin Neurosci* (2015) 22(4):619–26. doi: 10.1016/j.jocn.2014.10.013
17. Calinescu A-A, Kamran N, Baker G, Mineharu Y, Lowenstein PR, Castro MG. Overview of Current Immunotherapeutic Strategies for Glioma. *Immunotherapy* (2015) 7(10):1073–104. doi: 10.2217/imt.15.75
18. Zang L, Kondengaden SM, Che F, Wang L, Heng X. Potential Epigenetic-Based Therapeutic Targets for Glioma. *Front Mol Neurosci* (2018) 11:408. doi: 10.3389/fnmol.2018.00408
19. Reddy RG, Bhat UA, Chakravarty S, Kumar A. Advances in Histone Deacetylase Inhibitors in Targeting Glioblastoma Stem Cells. *Cancer Chemotherapy Pharmacol* (2020) 86(2):165–79. doi: 10.1007/s00280-020-04109-w
20. Comba A, Dunn PJ, Argento AE, Kadiyala P, Ventosa M, Patel P, et al. Fyn Tyrosine Kinase, a Downstream Target of Receptor Tyrosine Kinases, Modulates Antiglioma Immune Responses. *Neuro-Oncology* (2020) 22(6):806–18. doi: 10.1093/neuonc/noaa006
21. Kadiyala P, Li D, Nuñez FM, Altshuler D, Doherty R, Kuai R, et al. High-Density Lipoprotein-Mimicking Nanodiscs for Chemo-Immunotherapy Against Glioblastoma Multiforme. *ACS Nano* (2019) 13(2):1365–84. doi: 10.1021/acsnano.8b06842
22. Scheetz L, Kadiyala P, Sun X, Son S, Hassani Najafabadi A, Aikins M, et al. Synthetic High-Density Lipoprotein Nanodiscs for Personalized Immunotherapy Against Gliomas. *Clin Cancer Res* (2020) 26(16):4369–80. doi: 10.1158/1078-0432.CCR-20-0341
23. Friedrich M, Bunse L, Wick W, Platten M. Perspectives of Immunotherapy in Isocitrate Dehydrogenase-Mutant Gliomas. *Curr Opin Oncol* (2018) 30(6):368–74. doi: 10.1097/CCO.0000000000000478
24. Kadiyala PCS, Gauss J, Garcia-Fabiani M, Núñez FJ, Nunez F, Alghamri MS, et al. Castro M Inhibition of 2-Hydroxyglutrate Elicits Metabolic-Reprograming and Mutant IDH1 Glioma Immunity. *J Clin Invest* (2020) 131(4):e139542. doi: 10.1101/2020.05.11.086371
25. Zong H, Parada LF, Baker SJ. Cell of Origin for Malignant Gliomas and its Implication in Therapeutic Development. *Cold Spring Harb Perspect Biol* (2015) 7(5):a020610. doi: 10.1101/cshperspect.a020610
26. Ostrom QT, Gittleman H, Truitt G, Boscia A, Kruchko C, Barnholtz-Sloan JS. CBTRUS Statistical Report: Primary Brain and Other Central Nervous System Tumors Diagnosed in the United States in 2011-2015. *Neuro Oncol* (2018) 20(suppl_4):iv1–86. doi: 10.1093/neuonc/noy131
27. Louis DN, Ohgaki H, Wiestler OD, Cavenee WK, Burger PC, Jouvet A, et al. The 2007 WHO Classification of Tumours of the Central Nervous System. *Acta Neuropathol* (2007) 114(2):97–109. doi: 10.1007/s00401-007-0243-4
28. Louis DN, Perry A, Reifenberger G, Von Deimling A, Figarella-Branger D, Cavenee WK, et al. The 2016 World Health Organization Classification of Tumors of the Central Nervous System: A Summary. *Acta Neuropathol* (2016) 131(6):803–20. doi: 10.1007/s00401-016-1545-1
29. Osswald M, Jung E, Sahm F, Solecki G, Venkataramani V, Blaes J, et al. Brain Tumour Cells Interconnect to a Functional and Resistant Network. *Nature* (2015) 528(7580):93–8. doi: 10.1038/nature16071
30. Perry A, Wesseling P. Histologic Classification of Gliomas. *Handb Clin Neurol* (2016) 134:71–95. doi: 10.1016/B978-0-12-802997-8.00005-0
31. Reifenberger G, Wirsching HG, Knobbe-Thomsen CB, Weller M. Advances in the Molecular Genetics of Gliomas - Implications for Classification and Therapy. *Nat Rev Clin Oncol* (2017) 14(7):434–52. doi: 10.1038/nrclinonc.2016.204
32. Masui K, Mischel PS, Reifenberger G. Molecular Classification of Gliomas. *Handb Clin Neurol* (2016) 134:97–120. doi: 10.1016/B978-0-12-802997-8.00006-2
33. Parsons DW, Jones S, Zhang X, Lin JC, Leary RJ, Angenendt P, et al. An Integrated Genomic Analysis of Human Glioblastoma Multiforme. *Science* (2008) 321(5897):1807–12. doi: 10.1126/science.1164382
34. Brennan CW, Verhaak RG, McKenna A, Campos B, Noushmehr H, Salama SR, et al. The Somatic Genomic Landscape of Glioblastoma. *Cell* (2013) 155(2):462–77. doi: 10.1016/j.cell.2013.09.034
35. Ludwig K, Kornblum HI. Molecular Markers in Glioma. *J Neuro-Oncol* (2017) 134(3):505–12. doi: 10.1007/s11060-017-2379-y
36. Masui K, Mischel PS, Reifenberger G. Molecular Classification of Gliomas. In: *Handbook of Clinical Neurology*, vol. 134. The Netherlands: Elsevier (2016). p. 97–120.
37. Wesseling P, Capper D. WHO 2016 Classification of Gliomas. *Neuropathol Appl Neurobiol* (2018) 44(2):139–50. doi: 10.1111/nan.12432
38. Sturm D, Witt H, Hovestadt V, Khuong-Quang DA, Jones DT, Konermann C, et al. Hotspot Mutations in H3F3A and IDH1 Define Distinct Epigenetic and Biological Subgroups of Glioblastoma. *Cancer Cell* (2012) 22(4):425–37. doi: 10.1016/j.ccr.2012.08.024
39. Cancer Genome Atlas Research N, Brat DJ, Verhaak RG, Aldape KD, Yung WK, Salama SR, et al. Comprehensive, Integrative Genomic Analysis of Diffuse Lower-Grade Gliomas. *N Engl J Med* (2015) 372(26):2481–98. doi: 10.1056/NEJMoa1402121
40. Ceccarelli M, Barthel FP, Malta TM, Sabedot TS, Salama SR, Murray BA, et al. Molecular Profiling Reveals Biologically Discrete Subsets and Pathways of Progression in Diffuse Glioma. *Cell* (2016) 164(3):550–63. doi: 10.1016/j.cell.2015.12.028
41. Bai H, Harmanci AS, Erson-Omay EZ, Li J, Coskun S, Simon M, et al. Integrated Genomic Characterization of IDH1-Mutant Glioma Malignant Progression. *Nat Genet* (2016) 48(1):59–66. doi: 10.1038/ng.3457
42. Cancer Genome Atlas Research N. Comprehensive Genomic Characterization Defines Human Glioblastoma Genes and Core Pathways. *Nature* (2008) 455(7216):1061–8. doi: 10.1038/nature07385
43. Dang L, White DW, Gross S, Bennett BD, Bittinger MA, Driggers EM, et al. Cancer-Associated IDH1 Mutations Produce 2-Hydroxyglutarate. *Nature* (2009) 462(7274):739–44. doi: 10.1038/nature08617
44. Núñez FJ, Mendez FM, Kadiyala P, Alghamri MS, Savelieff MG, Garcia-Fabiani MB, et al. IDH1-R132H Acts as a Tumor Suppressor in Glioma Via Epigenetic Up-Regulation of the DNA Damage Response. *Sci Trans Med* (2019) 11(479):eaaq1427. doi: 10.1126/scitranslmed.aaq1427
45. Yan H, Parsons DW, Jin G, McLendon R, Rasheed BA, Yuan W, et al. IDH1 and IDH2 Mutations in Gliomas. *New Engl J Med* (2009) 360(8):765–73. doi: 10.1056/NEJMoa0808710
46. Noushmehr H, Weisenberger DJ, Diefes K, Phillips HS, Pujara K, Berman BP, et al. Identification of a Cpg Island Methylator Phenotype That Defines a Distinct Subgroup of Glioma. *Cancer Cell* (2010) 17(5):510–22. doi: 10.1016/S1040-1741(10)79529-4
47. Wiestler B, Capper D, Sill M, Jones DT, Hovestadt V, Sturm D, et al. Integrated DNA Methylation and Copy-Number Profiling Identify Three Clinically and Biologically Relevant Groups of Anaplastic Glioma. *Acta Neuropathol* (2014) 128(4):561–71. doi: 10.1007/s00401-014-1315-x

48. Zhang YH, Li Z, Zeng T, Pan X, Chen L, Liu D, et al. Distinguishing Glioblastoma Subtypes by Methylation Signatures. *Front Genet* (2020) 11:604336. doi: 10.3389/fgene.2020.604336
49. Capper D, Jones DTW, Sill M, Hovestadt V, Schrimpf D, Sturm D, et al. DNA Methylation-Based Classification of Central Nervous System Tumours. *Nature* (2018) 555(7697):469–74. doi: 10.1038/nature26000
50. Wick W, Weller M, van den Bent M, Sanson M, Weiler M, von Deimling A, et al. MGMT Testing–the Challenges for Biomarker-Based Glioma Treatment. *Nat Rev Neurol* (2014) 10(7):372–85. doi: 10.1038/nrneurol.2014.100
51. Jones T, Holland E. Standard of Care Therapy for Malignant Glioma and its Effect on Tumor and Stromal Cells. *Oncogene* (2012) 31(16):1995–2006. doi: 10.1038/onc.2011.398
52. Jones C, Perryman L, Hargrave D. Paediatric and Adult Malignant Glioma: Close Relatives or Distant Cousins? *Nat Rev Clin Oncol* (2012) 9(7):400–13. doi: 10.1038/nrclinonc.2012.87
53. Mackay A, Burford A, Carvalho D, Izquierdo E, Fazal-Salom J, Taylor KR, et al. Integrated Molecular Meta-Analysis of 1,000 Pediatric High-Grade and Diffuse Intrinsic Pontine Glioma. *Cancer Cell* (2017) 32(4):520–37.e5. doi: 10.1016/j.ccell.2017.08.017
54. Braunstein S, Raleigh D, Bindra R, Mueller S, Haas-Kogan D. Pediatric High-Grade Glioma: Current Molecular Landscape and Therapeutic Approaches. *J Neuro-Oncol* (2017) 134(3):541–9. doi: 10.1007/s11060-017-2393-0
55. Jones C, Karajannis MA, Jones DTW, Kieran MW, Monje M, Baker SJ, et al. Pediatric High-Grade Glioma: Biologically and Clinically in Need of New Thinking. *Neuro-oncology* (2017) 19(2):153–61. doi: 10.1093/neuonc/now101
56. Schwartzentruber J, Korshunov A, Liu XY, Jones DT, Pfaff E, Jacob K, et al. Driver Mutations in Histone H3.3 and Chromatin Remodelling Genes in Paediatric Glioblastoma. *Nature* (2012) 482(7384):226–31. doi: 10.1038/nature10833
57. Wu G, Broniscer A, McEachron TA, Lu C, Paugh BS, Becksfort J, et al. Somatic Histone H3 Alterations in Pediatric Diffuse Intrinsic Pontine Gliomas and non-Brainstem Glioblastomas. *Nat Genet* (2012) 44(3):251–3. doi: 10.1038/ng.1102
58. Vanan MI, Eisenstat DD. Management of High-Grade Gliomas in the Pediatric Patient: Past, Present, and Future. *Neurooncol Pract* (2014) 1 (4):145–57. doi: 10.1093/nop/npu022
59. Ostrom QT, Gittleman H, Truitt G, Boscia A, Kruchko C, Barnholtz-Sloan JS. CBTRUS Statistical Report: Primary Brain and Other Central Nervous System Tumors Diagnosed in the United States in 2011–2015. *Neuro-oncology* (2018) 20(suppl_4):iv1–iv86. doi: 10.1093/neuonc/noy131
60. Sturm D, Pfister SM, Jones DTW. Pediatric Gliomas: Current Concepts on Diagnosis, Biology, and Clinical Management. *J Clin Oncol* (2017) 35 (21):2370–7. doi: 10.1200/JCO.2017.73.0242
61. Blionas A, Giakoumettis D, Klonou A, Neromyliotis E, Karydakis P, Themistocleous MS. Paediatric Gliomas: Diagnosis, Molecular Biology and Management. *Ann Transl Med* (2018) 6(12):251. doi: 10.21037/atm.2018.05.11
62. Coleman C, Stoller S, Grotzer M, Stucklin AG, Nazarian J, Mueller S. Pediatric Hemispheric High-Grade Glioma: Targeting the Future. *Cancer Metastasis Rev* (2020) 39(1):245–60. doi: 10.1007/s10555-020-09850-5
63. Kramm CM, Wagner S, Van Gool S, Schmid H, Sträter R, Gnekow A, et al. Improved Survival After Gross Total Resection of Malignant Gliomas in Pediatric Patients From the HIT-GBM Studies. *Anticancer Res* (2006) 26 (5B):3773–9.
64. Pollack IF, Agnihotri S, Broniscer A. Childhood Brain Tumors: Current Management, Biological Insights, and Future Directions. *J Neurosurg Pediatr* (2019) 23(3):261–73. doi: 10.3171/2018.10.PEDS18377
65. Clarke M, Mackay A, Ismer B, Pickles JC, Tatevossian RG, Newman S, et al. Infant High Grade Gliomas Comprise Multiple Subgroups Characterized by Novel Targetable Gene Fusions and Favorable Outcomes. *Cancer Discov* (2020) 10(7):942–63. doi: 10.1158/2159-8290.CD-19-1030
66. Mendez F, Kadiyala P, Nunez FJ, Carney S, Nunez FM, Gauss JC, et al. Therapeutic Efficacy of Immune Stimulatory Thymidine Kinase and Fms-Like Tyrosine Kinase 3 Ligand (TK/Flt3L) Gene Therapy in a Mouse Model of High Grade Brainstem Glioma. *Clin Cancer Res* (2020). doi: 10.1158/1078-0432.CCR-19-3714
67. Garcia-Fabiani MB, Kadiyala P, Lowenstein PR, Castro MG. An Optimized Protocol for In Vivo Analysis of Tumor Cell Division in a Sleeping Beauty-Mediated Mouse Glioma Model. *STAR Protoc* (2020) 100044:100044. doi: 10.1016/j.xpro.2020.100044
68. Medawar PB. Immunity to Homologous Grafted Skin. III. The Fate of Skin Homographs Transplanted to the Brain, to Subcutaneous Tissue, and to the Anterior Chamber of the Eye. *Br J Exp Pathol* (1948) 29(1):58.
69. Engelhardt B, Vajkoczy P, Weller RO. The Movers and Shapers in Immune Privilege of the CNS. *Nat Immunol* (2017) 18(2):123. doi: 10.1038/ni.3666
70. Ransohoff RM, Engelhardt B. The Anatomical and Cellular Basis of Immune Surveillance in the Central Nervous System. *Nat Rev Immunol* (2012) 12 (9):623–35. doi: 10.1038/nri3265
71. Louveau A, Smirnov I, Keyes TJ, Eccles JD, Rouhani SJ, Peske JD, et al. Structural and Functional Features of Central Nervous System Lymphatic Vessels. *Nature* (2015) 523(7560):337–41. doi: 10.1038/nature14432
72. Negi N, Das BK. CNS: Not an Immunoprivilaged Site Anymore But a Virtual Secondary Lymphoid Organ. *Int Rev Immunol* (2018) 37(1):57–68. doi: 10.1080/08830185.2017.1357719
73. Ousman SS, Kubes P. Immune Surveillance in the Central Nervous System. *Nat Neurosci* (2012) 15(8):1096–101. doi: 10.1038/nn.3161
74. Norris GT, Kipnis J. Immune Cells and CNS Physiology: Microglia and Beyond. *J Exp Med* (2019) 216(1):60–70. doi: 10.1084/jem.20180199
75. Hoek RM, Ruuls SR, Murphy CA, Wright GJ, Goddard R, Zurawski SM, et al. Down-Regulation of the Macrophage Lineage Through Interaction With OX2 (CD200). *Science* (2000) 290(5497):1768–71. doi: 10.1126/science.290.5497.1768
76. Mariani MM, Kielian T. Microglia in Infectious Diseases of the Central Nervous System. *J Neuroimmune Pharmacol* (2009) 4(4):448–61. doi: 10.1007/s11481-009-9170-6
77. Weiss T, Weller M, Roth P. Immunological Effects of Chemotherapy and Radiotherapy Against Brain Tumors. *Expert Rev Anticancer Ther* (2016) 16 (10):1087–94. doi: 10.1080/14737140.2016.1229600
78. Sampson JH, Gunn MD, Fecci PE, Ashley DM. Brain Immunology and Immunotherapy in Brain Tumours. *Nat Rev Cancer* (2019) 20(1):12–25. doi: 10.1038/s41568-019-0224-7
79. Bagley SJ, Desai AS, Nasrallah MP, O'Rourke DM. Immunotherapy and Response Assessment in Malignant Glioma: Neuro-Oncology Perspective. *Topics Magn Reson Imaging* (2020) 29(2):95–102. doi: 10.1097/RMR.0000000000000233
80. Neftel C, Laffy J, Filbin MG, Hara T, Shore ME, Rahme GJ, et al. An Integrative Model of Cellular States, Plasticity, and Genetics for Glioblastoma. *Cell* (2019) 178(4):835–49. e21. doi: 10.1016/j.cell.2019.06.024
81. Dirkse A, Golebiewska A, Buder T, Nazarov PV, Muller A, Poovathingal S, et al. Stem Cell-Associated Heterogeneity in Glioblastoma Results From Intrinsic Tumor Plasticity Shaped by the Microenvironment. *Nat Commun* (2019) 10(1):1–16. doi: 10.1038/s41467-019-09853-z
82. Bernstock JD, Mooney JH, Ilyas A, Chagoya G, Estevez-Ordonez D, Ibrahim A, et al. Molecular and Cellular Intratumoral Heterogeneity in Primary Glioblastoma: Clinical and Translational Implications. *J Neurosurg* (2019) 1 (aop):1–9. doi: 10.3171/2019.5.JNS19364
83. Galea I, Bechmann I, Perry VH. What is Immune Privilege (Not)? *Trends Immunol* (2007) 28(1):12–8. doi: 10.1016/j.it.2006.11.004
84. Jackson C, Ruzevick J, Phallen J, Belcaid Z, Lim M. Challenges in Immunotherapy Presented by the Glioblastoma Multiforme Microenvironment. *Clin Dev Immunol* (2011) 2011:732413. doi: 10.1155/2011/732413
85. Chen Z, Feng X, Herting CJ, Garcia VA, Nie K, Pong WW, et al. Cellular and Molecular Identity of Tumor-Associated Macrophages in Glioblastoma. *Cancer Res* (2017) 77(9):2266–78. doi: 10.1158/0008-5472.CAN-16-2310
86. Müller S, Kohanbash G, Liu SJ, Alvarado B, Carrera D, Bhaduri A, et al. Single-Cell Profiling of Human Gliomas Reveals Macrophage Ontogeny as a Basis for Regional Differences in Macrophage Activation in the Tumor Microenvironment. *Genome Biol* (2017) 18(1):234. doi: 10.1186/s13059-017-1362-4
87. Jurga AM, Paleczna M, Kuter KZ. Overview of General and Discriminating Markers of Differential Microglia Phenotypes. *Front Cell Neurosci* (2020) 14:198. doi: 10.3389/fncel.2020.00198
88. Klemm F, Maas RR, Bowman RL, Kornete M, Soukup K, Nassiri S, et al. Interrogation of the Microenvironmental Landscape in Brain Tumors

Reveals Disease-Specific Alterations of Immune Cells. *Cell* (2020) 181 (7):1643–60.e17. doi: 10.1016/j.cell.2020.05.007
89. Gielen PR, Schulte BM, Kers-Rebel ED, Verrijp K, Bossman SA, Ter Laan M, et al. Elevated Levels of Polymorphonuclear Myeloid-Derived Suppressor Cells in Patients With Glioblastoma Highly Express S100A8/9 and Arginase and Suppress T Cell Function. *Neuro-oncology* (2016) 18(9):1253–64. doi: 10.1093/neuonc/now034
90. Alban TJ, Bayik D, Otvos B, Rabljenovic A, Leng L, Jia-Shiun L, et al. Glioblastoma Myeloid-Derived Suppressor Cell Subsets Express Differential Macrophage Migration Inhibitory Factor Receptor Profiles That can be Targeted to Reduce Immune Suppression. *Front Immunol* (2020) 11:1191. doi: 10.3389/fimmu.2020.01191
91. Cassetta L, Baekkevold ES, Brandau S, Bujko A, Cassatella MA, Dorhoi A, et al. Deciphering Myeloid-Derived Suppressor Cells: Isolation and Markers in Humans, Mice and non-Human Primates. *Cancer Immunol Immunother* (2019) 68(4):687–97. doi: 10.1007/s00262-019-02302-2
92. Deng G. Tumor-Infiltrating Regulatory T Cells: Origins and Features. *Am J Clin Exp Immunol* (2018) 7(5):81.
93. Huettner C, Czub S, Kerkau S, Roggendorf W, Tonn J-C. Interleukin 10 is Expressed in Human Gliomas In Vivo and Increases Glioma Cell Proliferation and Motility In Vitro. *Anticancer Res* (1997) 17(5A):3217–24.
94. Amankulor NM, Kim Y, Arora S, Kargl J, Szulzewsky F, Hanke M, et al. Mutant IDH1 Regulates the Tumor-Associated Immune System in Gliomas. *Genes Dev* (2017) 31(8):774–86. doi: 10.1101/gad.294991.116
95. Verhaak RG. Moving the Needle: Optimizing Classification for Glioma. *Sci Trans Med* (2016) 8(350):350fs14. doi: 10.1126/scitranslmed.aah4740
96. Verhaak RG, Hoadley KA, Purdom E, Wang V, Qi Y, Wilkerson MD, et al. Integrated Genomic Analysis Identifies Clinically Relevant Subtypes of Glioblastoma Characterized by Abnormalities in PDGFRA, IDH1, EGFR, and NF1. *Cancer Cell* (2010) 17(1):98–110. doi: 10.1016/j.ccr.2009.12.020
97. Luoto S, Hermelo I, Vuorinen EM, Hannus P, Kesseli J, Nykter M, et al. Computational Characterization of Suppressive Immune Microenvironments in Glioblastoma. *Cancer Res* (2018) 78(19):5574–85. doi: 10.1158/0008-5472.CAN-17-3714
98. Wang Q, Hu B, Hu X, Kim H, Squatrito M, Scarpace L, et al. Tumor Evolution of Glioma-Intrinsic Gene Expression Subtypes Associates With Immunological Changes in the Microenvironment. *Cancer Cell* (2017) 32 (1):42–56.e6. doi: 10.1016/j.ccell.2017.06.003
99. Rutledge WC, Kong J, Gao J, Gutman DA, Cooper LA, Appin C, et al. Tumor-Infiltrating Lymphocytes in Glioblastoma are Associated With Specific Genomic Alterations and Related to Transcriptional Class. *Clin Cancer Res* (2013) 19(18):4951–60. doi: 10.1158/1078-0432.CCR-13-0551
100. Kohanbash G, Carrera DA, Shrivastav S, Ahn BJ, Jahan N, Mazor T, et al. Isocitrate Dehydrogenase Mutations Suppress STAT1 and CD8+ T Cell Accumulation in Gliomas. *J Clin Invest* (2017) 127(4):1425–37. doi: 10.1172/JCI90644
101. Berghoff AS, Kiesel B, Widhalm G, Wilhelm D, Rajky O, Kurscheid S, et al. Correlation of Immune Phenotype With IDH Mutation in Diffuse Glioma. *Neuro-oncology* (2017) 19(11):1460–8. doi: 10.1093/neuonc/nox054
102. Plant AS, Koyama S, Sinai C, Solomon IH, Griffin GK, Ligon KL, et al. Immunophenotyping of Pediatric Brain Tumors: Correlating Immune Infiltrate With Histology, Mutational Load, and Survival and Assessing Clonal T Cell Response. *J Neuro-Oncol* (2018) 137(2):269–78. doi: 10.1007/s11060-017-2737-9
103. Griesinger AM, Birks DK, Donson AM, Amani V, Hoffman LM, Waziri A, et al. Characterization of Distinct Immunophenotypes Across Pediatric Brain Tumor Types. *J Immunol* (2013) 191(9):4880–8. doi: 10.4049/jimmunol.1301966
104. Lieberman NA, DeGolier K, Kovar HM, Davis A, Hoglund V, Stevens J, et al. Characterization of the Immune Microenvironment of Diffuse Intrinsic Pontine Glioma: Implications for Development of Immunotherapy. *Neuro-oncology* (2019) 21(1):83–94. doi: 10.1093/neuonc/noy145
105. Fabiani MG, Haase S, Kadiyala P, Alghamri M, Comba A, Nuñez F, et al. Tmod-02. Characterization of the Tumor Immune Microenvironment in a Pediatric High Grade Glioma Mouse Model Harboring the H3. 3-G34r Mutation. *Neuro-oncology* (2019) 21(Supplement_2):ii121–ii. doi: 10.1093/neuonc/noz036.241
106. Garcia-Fabiani MB, Kadiyala P, Haase S, Alghamri M, Comba A, Nunez F, et al. Pdtm-20. The Histone Mutation H3. 3-G34r Encountered in Pediatric High Grade Glioma Modifies the Tumor Immune Microenvironment Rendering it More Permissive for Immune Mediated Therapies. *Neuro-oncology* (2019) 21(Supplement_6). doi: 10.1093/neuonc/noz175.796
107. Walter RB, Press OW, Pagel JM. Pretargeted Radioimmunotherapy for Hematologic and Other Malignancies. *Cancer Biother Radiopharm* (2010) 25(2):125–42. doi: 10.1089/cbr.2010.0759
108. Fukuya Y, Ikuta S, Maruyama T, Nitta M, Saito T, Tsuzuki S, et al. Tumor Recurrence Patterns After Surgical Resection of Intracranial Low-Grade Gliomas. *J Neuro-Oncol* (2019) 144(3):519–28. doi: 10.1007/s11060-019-03250-8
109. Joo KM, Kim J, Jin J, Kim M, Seol HJ, Muradov J, et al. Patient-Specific Orthotopic Glioblastoma Xenograft Models Recapitulate the Histopathology and Biology of Human Glioblastomas in Situ. *Cell Rep* (2013) 3(1):260–73. doi: 10.1016/j.celrep.2012.12.013
110. Harder BG, Blomquist MR, Wang J, Kim AJ, Woodworth GF, Winkles JA, et al. Developments in Blood-Brain Barrier Penetrance and Drug Repurposing for Improved Treatment of Glioblastoma. *Front Oncol* (2018) 8:462. doi: 10.3389/fonc.2018.00462
111. Weiss T, Puca E, Silginer M, Hemmerle T, Pazahr S, Bink A, et al. Immunocytokines are a Promising Immunotherapeutic Approach Against Glioblastoma. *Sci Transl Med* (2020) 12(564):eabb2311. doi: 10.1126/scitranslmed.abb2311
112. DiGrande S. Is Immunotherapy the Future of Glioblastoma Treatment? *Am J Managed Care* (2019) 25(2):74–5.
113. da Hora CC, Schweiger MW, Wurdinger T, Tannous BA. Patient-Derived Glioma Models: From Patients to Dish to Animals. *Cells* (2019) 8(10):1177. doi: 10.3390/cells8101177
114. Ogawa J, Pao GM, Shokhirev MN, Verma IM. Glioblastoma Model Using Human Cerebral Organoids. *Cell Rep* (2018) 23(4):1220–9. doi: 10.1016/j.celrep.2018.03.105
115. Caretti V, Sewing AC, Lagerweij T, Schellen P, Bugiani M, Jansen MH, et al. Human Pontine Glioma Cells can Induce Murine Tumors. *Acta Neuropathol* (2014) 127(6):897–909. doi: 10.1007/s00401-014-1272-4
116. Qin H, Janowski M, Pearl MS, Malysz-Cymborska I, Li S, Eberhart CG, et al. Rabbit Model of Human Gliomas: Implications for Intra-Arterial Drug Delivery. *PloS One* (2017) 12(1):e0169656. doi: 10.1371/journal.pone.0169656
117. Lan X, Kedziorek DA, Chu C, Jablonska A, Li S, Kai M, et al. Modeling Human Pediatric and Adult Gliomas in Immunocompetent Mice Through Costimulatory Blockade. *Oncoimmunology* (2020) 9(1):1776577. doi: 10.1080/2162402X.2020.1776577
118. Badie B, Bartley B, Schartner J. Differential Expression of MHC Class II and B7 Costimulatory Molecules by Microglia in Rodent Gliomas. *J Neuroimmunol* (2002) 133(1-2):39–45. doi: 10.1016/S0165-5728(02)00350-8
119. Oh T, Fakurnejad S, Sayegh ET, Clark AJ, Ivan ME, Sun MZ, et al. Immunocompetent Murine Models for the Study of Glioblastoma Immunotherapy. *J Transl Med* (2014) 12:107. doi: 10.1186/1479-5876-12-107
120. Paul AK, Ciesielski MJ, Sajjad M, Wang X, Ferrone S, Abdel-Nabi H, et al. Expression of HMP/AN2, a Melanoma Associated Antigen, in Murine Cerebral Gliomas: Potential for Radioimmunotargeting. *J Neurooncol* (2009) 94(1):21–30. doi: 10.1007/s11060-009-9798-3
121. Chen ML, Pittet MJ, Gorelik L, Flavell RA, Weissleder R, von Boehmer H, et al. Regulatory T Cells Suppress Tumor-Specific CD8 T Cell Cytotoxicity Through TGF-Beta Signals In Vivo. *Proc Natl Acad Sci USA* (2005) 102 (2):419–24. doi: 10.1073/pnas.0408197102
122. Ueda R, Fujita M, Zhu X, Sasaki K, Kastenhuber ER, Kohanbash G, et al. Systemic Inhibition of Transforming Growth Factor-Beta in Glioma-Bearing Mice Improves the Therapeutic Efficacy of Glioma-Associated Antigen Peptide Vaccines. *Clin Cancer Res* (2009) 15(21):6551–9. doi: 10.1158/1078-0432.CCR-09-1067
123. Prins RM, Odesa SK, Liau LM. Immunotherapeutic Targeting of Shared Melanoma-Associated Antigens in a Murine Glioma Model. *Cancer Res* (2003) 63(23):8487–91.
124. Curtin JF, Candolfi M, Fakhouri TM, Liu C, Alden A, Edwards M, et al. Treg Depletion Inhibits Efficacy of Cancer Immunotherapy: Implications for Clinical Trials. *PloS One* (2008) 3(4):e1983. doi: 10.1371/journal.pone.0001983

125. Pilkington GJ, Darling JL, Lantos PL, Thomas DG. Cell Lines (Vmdk) Derived From a Spontaneous Murine Astrocytoma. Morphological and Immunocytochemical Characterization. *J Neurol Sci* (1983) 62(1-3):115–39. doi: 10.1016/0022-510X(83)90193-4
126. Sampson JH, Ashley DM, Archer GE, Fuchs HE, Dranoff G, Hale LP, et al. Characterization of a Spontaneous Murine Astrocytoma and Abrogation of its Tumorigenicity by Cytokine Secretion. *Neurosurgery* (1997) 41(6):1365–72. discussion 72-3. doi: 10.1097/00006123-199712000-00024
127. Miller J, Eisele G, Tabatabai G, Aulwurm S, von Kurthy G, Stitz L, et al. Soluble CD70: A Novel Immunotherapeutic Agent for Experimental Glioblastoma. *J Neurosurg* (2010) 113(2):280–5. doi: 10.3171/2009.11.JNS09901
128. Sampson JH, Choi BD, Sanchez-Perez L, Suryadevara CM, Snyder DJ, Flores CT, et al. Egfrviii Mcar-Modified T-Cell Therapy Cures Mice With Established Intracerebral Glioma and Generates Host Immunity Against Tumor-Antigen Loss. *Clin Cancer Res* (2014) 20(4):972–84. doi: 10.1158/1078-0432.CCR-13-0709
129. Martinez-Murillo R, Martinez A. Standardization of an Orthotopic Mouse Brain Tumor Model Following Transplantation of CT-2A Astrocytoma Cells. *Histol Histopathol* (2007) 22(12):1309–26. doi: 10.14670/HH-22.1309
130. Binello E, Qadeer ZA, Kothari HP, Emdad L, Germano IM. Stemness of the CT-2A Immunocompetent Mouse Brain Tumor Model: Characterization In Vitro. *J Cancer* (2012) 3:166–74. doi: 10.7150/jca.4149
131. Shelton LM, Mukherjee P, Huysentruyt LC, Urits I, Rosenberg JA, Seyfried TN. A Novel Pre-Clinical In Vivo Mouse Model for Malignant Brain Tumor Growth and Invasion. *J Neurooncol* (2010) 99(2):165–76. doi: 10.1007/s11060-010-0115-y
132. Lee J, Kotliarova S, Kotliarov Y, Li A, Su Q, Donin NM, et al. Tumor Stem Cells Derived From Glioblastomas Cultured in Bfgf and EGF More Closely Mirror the Phenotype and Genotype of Primary Tumors Than do Serum-Cultured Cell Lines. *Cancer Cell* (2006) 9(5):391–403. doi: 10.1016/j.ccr.2006.03.030
133. Marsh J, Mukherjee P, Seyfried TN. Akt-Dependent Proapoptotic Effects of Dietary Restriction on Late-Stage Management of a Phosphatase and Tensin Homologue/Tuberous Sclerosis Complex 2-Deficient Mouse Astrocytoma. *Clin Cancer Res* (2008) 14(23):7751–62. doi: 10.1158/1078-0432.CCR-08-0213
134. Waldron JS, Yang I, Han S, Tihan T, Sughrue ME, Mills SA, et al. Implications for Immunotherapy of Tumor-Mediated T-Cell Apoptosis Associated With Loss of the Tumor Suppressor PTEN in Glioblastoma. *J Clin Neurosci* (2010) 17(12):1543–7. doi: 10.1016/j.jocn.2010.04.021
135. Weiner NE, Pyles RB, Chalk CL, Balko MG, Miller MA, Dyer CA, et al. A Syngeneic Mouse Glioma Model for Study of Glioblastoma Therapy. *J Neuropathol Exp Neurol* (1999) 58(1):54–60. doi: 10.1097/00005072-199901000-00007
136. Dyer CA, Philibotte T. A Clone of the MOCH-1 Glial Tumor in Culture: Multiple Phenotypes Expressed Under Different Environmental Conditions. *J Neuropathol Exp Neurol* (1995) 54(6):852–63. doi: 10.1097/00005072-199511000-00012
137. Higgins RJ, McKisic M, Dickinson PJ, Jimenez DF, Dow SW, Tripp LD, et al. Growth Inhibition of an Orthotopic Glioblastoma in Immunocompetent Mice by Cationic Lipid-DNA Complexes. *Cancer Immunol Immunother* (2004) 53(4):338–44. doi: 10.1007/s00262-003-0447-y
138. Markert JM, Cody JJ, Parker JN, Coleman JM, Price KH, Kern ER, et al. Preclinical Evaluation of a Genetically Engineered Herpes Simplex Virus Expressing Interleukin-12. *J Virol* (2012) 86(9):5304–13. doi: 10.1128/JVI.06998-11
139. Becher OJ, Holland EC. Genetically Engineered Models Have Advantages Over Xenografts for Preclinical Studies. *Cancer Res* (2006) 66(7):3355–9. doi: 10.1158/0008-5472.CAN-05-3827
140. Ahronian LG, Lewis BC. Using the RCAS-TVA System to Model Human Cancer in Mice. *Cold Spring Harbor Protoc* (2014) 2014(11):pdb.top069831. doi: 10.1101/pdb.top069831
141. Hambardzumyan D, Amankulor NM, Helmy KY, Becher OJ, Holland EC. Modeling Adult Gliomas Using RCAS/T-Va Technology. *Trans Oncol* (2009) 2(2):89–IN6. doi: 10.1593/tlo.09100
142. Fomchenko EI, Holland EC. Mouse Models of Brain Tumors and Their Applications in Preclinical Trials. *Clin Cancer Res* (2006) 12(18):5288–97. doi: 10.1158/1078-0432.CCR-06-0438
143. Holland EC, Hively WP, DePinho RA, Varmus HE. A Constitutively Active Epidermal Growth Factor Receptor Cooperates With Disruption of G1 Cell-Cycle Arrest Pathways to Induce Glioma-Like Lesions in Mice. *Genes Dev* (1998) 12(23):3675–85. doi: 10.1101/gad.12.23.3675
144. Kong L-Y, Wu AS, Doucette T, Wei J, Priebe W, Fuller GN, et al. Intratumoral Mediated Immunosuppression is Prognostic in Genetically Engineered Murine Models of Glioma and Correlates to Immunotherapeutic Responses. *Clin Cancer Res* (2010) 16(23):5722–33. doi: 10.1158/1078-0432.CCR-10-1693
145. Izsvak Z, Ivics Z. Sleeping Beauty Transposition: Biology and Applications for Molecular Therapy. *Mol Ther* (2004) 9(2):147–56. doi: 10.1016/j.ymthe.2003.11.009
146. Kebriaei P, Izsvak Z, Narayanavari SA, Singh H, Ivics Z. Gene Therapy With the Sleeping Beauty Transposon System. *Trends Genet* (2017) 33(11):852–70. doi: 10.1016/j.tig.2017.08.008
147. Calinescu AA, Núñez FJ, Koschmann C, Kolb BL, Lowenstein PR, Castro MG. Transposon Mediated Integration of Plasmid DNA Into the Subventricular Zone of Neonatal Mice to Generate Novel Models of Glioblastoma. *J Vis Exp* (2015) 96:52443. doi: 10.3791/52443
148. Koschmann C, Calinescu AA, Nunez FJ, Mackay A, Fazal-Salom J, Thomas D, et al. ATRX Loss Promotes Tumor Growth and Impairs Nonhomologous End Joining DNA Repair in Glioma. *Sci Transl Med* (2016) 8(328):328ra28. doi: 10.1126/scitranslmed.aac8228
149. Koschmann C, Lowenstein PR, Castro MG. ATRX Mutations and Glioblastoma: Impaired DNA Damage Repair, Alternative Lengthening of Telomeres, and Genetic Instability. *Mol Cell Oncol* (2016) 3(3):e1167158. doi: 10.1080/23723556.2016.1167158
150. Garcia-Fabiani MB, Comba A, Kadiyala P, Haase S, Núñez FJ, Altshuler D, et al. Isolation and Characterization of Immune Cells From the Tumor Microenvironment of Genetically Engineered Pediatric High-Grade Glioma Models Using the Sleeping Beauty Transposon System. *Methods Enzymol* (2020) 632:369–88. doi: 10.1016/bs.mie.2019.05.023
151. Patel SK, Hartley RM, Wei X, Furnish R, Escobar-Riquelme F, Bear H, et al. Generation of Diffuse Intrinsic Pontine Glioma Mouse Models by Brainstem-Targeted In Utero Electroporation. *Neuro-oncology* (2020) 22(3):381–92. doi: 10.1093/neuonc/noz197
152. Aslan K, Turco V, Blobner J, Sonner JK, Liuzzi AR, Núñez NG, et al. Heterogeneity of Response to Immune Checkpoint Blockade in Hypermutated Experimental Gliomas. *Nat Commun* (2020) 11(1):931. doi: 10.1038/s41467-020-14642-0
153. Zhao Y, Shuen TWH, Toh TB, Chan XY, Liu M, Tan SY, et al. Development of a New Patient-Derived Xenograft Humanised Mouse Model to Study Human-Specific Tumour Microenvironment and Immunotherapy. *Gut* (2018) 67(10):1845–54. doi: 10.1136/gutjnl-2017-315201
154. Mathews S, Branch Woods A, Katano I, Makarov E, Thomas MB, Gendelman HE, et al. Human Interleukin-34 Facilitates Microglia-Like Cell Differentiation and Persistent HIV-1 Infection in Humanized Mice. *Mol Neurodegener* (2019) 14(1):12. doi: 10.1186/s13024-019-0311-y
155. Klein E, Hau AC, Oudin A, Golebiewska A, Niclou SP. Glioblastoma Organoids: Pre-Clinical Applications and Challenges in the Context of Immunotherapy. *Front Oncol* (2020) 10:604121. doi: 10.3389/fonc.2020.604121
156. Ashizawa T, Iizuka A, Nonomura C, Kondou R, Maeda C, Miyata H, et al. Antitumor Effect of Programmed Death-1 (PD-1) Blockade in Humanized the NOG-MHC Double Knockout Mouse. *Clin Cancer Res* (2017) 23(1):149–58. doi: 10.1158/1078-0432.CCR-16-0122
157. Jacob F, Ming GL, Song H. Generation and Biobanking of Patient-Derived Glioblastoma Organoids and Their Application in CAR T Cell Testing. *Nat Protoc* (2020) 15(12):4000–33. doi: 10.1038/s41596-020-0402-9
158. Jacob F, Salinas RD, Zhang DY, Nguyen PTT, Schnoll JG, Wong SZH, et al. A Patient-Derived Glioblastoma Organoid Model and Biobank Recapitulates Inter- and Intra-Tumoral Heterogeneity. *Cell* (2020) 180(1):188–204.e22. doi: 10.1016/j.cell.2019.11.036
159. Richmond A, Su Y. Mouse Xenograft Models vs GEM Models for Human Cancer Therapeutics. *Dis Model Mech* (2008) 1(2-3):78–82. doi: 10.1242/dmm.000976
160. Topalian SL. Targeting Immune Checkpoints in Cancer Therapy. *JAMA* (2017) 318(17):1647–8. doi: 10.1001/jama.2017.14155

161. Brunet JF, Denizot F, Luciani MF, Roux-Dosseto M, Suzan M, Mattei MG, et al. A New Member of the Immunoglobulin Superfamily–CTLA-4. *Nature* (1987) 328(6127):267–70. doi: 10.1038/328267a0
162. Waldman AD, Fritz JM, Lenardo MJ. A Guide to Cancer Immunotherapy: From T Cell Basic Science to Clinical Practice. *Nat Rev Immunol* (2020) 20 (11):651–68. doi: 10.1038/s41577-020-0306-5
163. Leach DR, Krummel MF, Allison JP. Enhancement of Antitumor Immunity by CTLA-4 Blockade. *Science* (1996) 271(5256):1734–6. doi: 10.1126/science.271.5256.1734
164. Hodi FS, Mihm MC, Soiffer RJ, Haluska FG, Butler M, Seiden MV, et al. Biologic Activity of Cytotoxic T Lymphocyte-Associated Antigen 4 Antibody Blockade in Previously Vaccinated Metastatic Melanoma and Ovarian Carcinoma Patients. *Proc Natl Acad Sci USA* (2003) 100(8):4712–7. doi: 10.1073/pnas.0830997100
165. Quezada SA, Peggs KS. Exploiting CTLA-4, PD-1 and PD-L1 to Reactivate the Host Immune Response Against Cancer. *Br J Cancer* (2013) 108(8):1560–5. doi: 10.1038/bjc.2013.117
166. Calabro L, Morra A, Fonsatti E, Cutaia O, Amato G, Giannarelli D, et al. Tremelimumab for Patients With Chemotherapy-Resistant Advanced Malignant Mesothelioma: An Open-Label, Single-Arm, Phase 2 Trial. *Lancet Oncol* (2013) 14(11):1104–11. doi: 10.1016/S1470-2045(13)70381-4
167. Fecci PE, Ochiai H, Mitchell DA, Grossi PM, Sweeney AE, Archer GE, et al. Systemic CTLA-4 Blockade Ameliorates Glioma-Induced Changes to the CD4+ T Cell Compartment Without Affecting Regulatory T-Cell Function. *Clin Cancer Res* (2007) 13(7):2158–67. doi: 10.1158/1078-0432.CCR-06-2070
168. Reardon DA, Gokhale PC, Klein SR, Ligon KL, Rodig SJ, Ramkissoon SH, et al. Glioblastoma Eradication Following Immune Checkpoint Blockade in an Orthotopic, Immunocompetent Model. *Cancer Immunol Res* (2016) 4 (2):124–35. doi: 10.1158/2326-6066.CIR-15-0151
169. Wang Z, Zhang C, Liu X, Wang Z, Sun L, Li G, et al. Molecular and Clinical Characterization of PD-L1 Expression at Transcriptional Level Via 976 Samples of Brain Glioma. *Oncoimmunology* (2016) 5(11):e1196310. doi: 10.1080/2162402X.2016.1196310
170. Genoud V, Marinari E, Nikolaev SI, Castle JC, Bukur V, Dietrich PY, et al. Responsiveness to Anti-PD-1 and Anti-CTLA-4 Immune Checkpoint Blockade in SB28 and GL261 Mouse Glioma Models. *Oncoimmunology* (2018) 7(12):e1501137. doi: 10.1080/2162402X.2018.1501137
171. Sanders S, Debinski W. Challenges to Successful Implementation of the Immune Checkpoint Inhibitors for Treatment of Glioblastoma. *Int J Mol Sci* (2020) 21(8):2759. doi: 10.3390/ijms21082759
172. Omuro A, Vlahovic G, Lim M, Sahebjam S, Baehring J, Cloughesy T, et al. Nivolumab With or Without Ipilimumab in Patients With Recurrent Glioblastoma: Results From Exploratory Phase I Cohorts of Checkmate 143. *Neuro Oncol* (2018) 20(5):674–86. doi: 10.1093/neuonc/nox208
173. Ishida Y, Agata Y, Shibahara K, Honjo T. Induced Expression of PD-1, a Novel Member of the Immunoglobulin Gene Superfamily, Upon Programmed Cell Death. *EMBO J* (1992) 11(11):3887–95. doi: 10.1002/j.1460-2075.1992.tb05481.x
174. Carreno BM, Collins M. The B7 Family of Ligands and its Receptors: New Pathways for Costimulation and Inhibition of Immune Responses. *Annu Rev Immunol* (2002) 20:29–53. doi: 10.1146/annurev.immunol.20.091101.091806
175. Fife BT, Bluestone JA. Control of Peripheral T-Cell Tolerance and Autoimmunity Via the CTLA-4 and PD-1 Pathways. *Immunol Rev* (2008) 224:166–82. doi: 10.1111/j.1600-065X.2008.00662.x
176. Liang SC, Latchman YE, Buhlmann JE, Tomczak MF, Horwitz BH, Freeman GJ, et al. Regulation of PD-1, PD-L1, and PD-L2 Expression During Normal and Autoimmune Responses. *Eur J Immunol* (2003) 33(10):2706–16. doi: 10.1002/eji.200324228
177. Sharpe AH, Freeman GJ. The B7-CD28 Superfamily. *Nat Rev Immunol* (2002) 2(2):116–26. doi: 10.1038/nri727
178. Xu S, Tang L, Li X, Fan F, Liu Z. Immunotherapy for Glioma: Current Management and Future Application. *Cancer Lett* (2020) 476:1–12. doi: 10.1016/j.canlet.2020.02.002
179. Marzec M, Zhang Q, Goradia A, Raghunath PN, Liu X, Paessler M, et al. Oncogenic Kinase NPM/ALK Induces Through STAT3 Expression of Immunosuppressive Protein CD274 (PD-L1, B7-H1). *Proc Natl Acad Sci USA* (2008) 105(52):20852–7. doi: 10.1073/pnas.0810958105
180. Green MR, Rodig S, Juszczynski P, Ouyang J, Sinha P, O'Donnell E, et al. Constitutive AP-1 Activity and EBV Infection Induce PD-L1 in Hodgkin Lymphomas and Posttransplant Lymphoproliferative Disorders: Implications for Targeted Therapy. *Clin Cancer Res* (2012) 18(6):1611–8. doi: 10.1158/1078-0432.CCR-11-1942
181. Jiang X, Zhou J, Giobbie-Hurder A, Wargo J, Hodi FS. The Activation of MAPK in Melanoma Cells Resistant to BRAF Inhibition Promotes PD-L1 Expression That is Reversible by MEK and PI3K Inhibition. *Clin Cancer Res* (2013) 19(3):598–609. doi: 10.1158/1078-0432.CCR-12-2731
182. Crane C, Panner A, Pieper RO, Arbiser J, Parsa AT. Honokiol-Mediated Inhibition of PI3K/Mtor Pathway: A Potential Strategy to Overcome Immunoresistance in Glioma, Breast, and Prostate Carcinoma Without Impacting T Cell Function. *J Immunother* (2009) 32(6):585–92. doi: 10.1097/CJI.0b013e3181a8efe6
183. Pardoll DM. The Blockade of Immune Checkpoints in Cancer Immunotherapy. *Nat Rev Cancer* (2012) 12(4):252–64. doi: 10.1038/nrc3239
184. Ribas A. Adaptive Immune Resistance: How Cancer Protects From Immune Attack. *Cancer Discovery* (2015) 5(9):915–9. doi: 10.1158/2159-8290.CD-15-0563
185. Arasanz H, Gato-Canas M, Zuazo M, Ibanez-Vea M, Breckpot K, Kochan G, et al. PD1 Signal Transduction Pathways in T Cells. *Oncotarget* (2017) 8 (31):51936–45. doi: 10.18632/oncotarget.17232
186. Grupp SA, Kalos M, Barrett D, Aplenc R, Porter DL, Rheingold SR, et al. Chimeric Antigen Receptor-Modified T Cells for Acute Lymphoid Leukemia. *N Engl J Med* (2013) 368(16):1509–18. doi: 10.1056/NEJMoa1215134
187. Larkin J, Chiarion-Sileni V, Gonzalez R, Grob JJ, Cowey CL, Lao CD, et al. Combined Nivolumab and Ipilimumab or Monotherapy in Untreated Melanoma. *N Engl J Med* (2015) 373(1):23–34. doi: 10.1056/NEJMoa1504030
188. Brahmer J, Reckamp KL, Baas P, Crinò L, Eberhardt WE, Poddubskaya E, et al. Nivolumab Versus Docetaxel in Advanced Squamous-Cell non-Small-Cell Lung Cancer. *N Engl J Med* (2015) 373(2):123–35. doi: 10.1056/NEJMoa1504627
189. Motzer RJ, Escudier B, McDermott DF, George S, Hammers HJ, Srinivas S, et al. Nivolumab Versus Everolimus in Advanced Renal-Cell Carcinoma. *N Engl J Med* (2015) 373(19):1803–13. doi: 10.1056/NEJMoa1510665
190. Huang BY, Zhan YP, Zong WJ, Yu CJ, Li JF, Qu YM, et al. The PD-1/B7-H1 Pathway Modulates the Natural Killer Cells Versus Mouse Glioma Stem Cells. *PloS One* (2015) 10(8):e0134715. doi: 10.1371/journal.pone.0134715
191. Wainwright DA, Chang AL, Dey M, Balyasnikova IV, Kim CK, Tobias A, et al. Durable Therapeutic Efficacy Utilizing Combinatorial Blockade Against IDO, CTLA-4, and PD-L1 in Mice With Brain Tumors. *Clin Cancer Res* (2014) 20(20):5290–301. doi: 10.1158/1078-0432.CCR-14-0514
192. Zeng J, See AP, Phallen J, Jackson CM, Belcaid Z, Ruzevick J, et al. Anti-PD-1 Blockade and Stereotactic Radiation Produce Long-Term Survival in Mice With Intracranial Gliomas. *Int J Radiat Oncol Biol Phys* (2013) 86(2):343–9. doi: 10.1016/j.ijrobp.2012.12.025
193. Ott PA, Bang Y-J, Piha-Paul SA, Razak ARA, Bennouna J, Soria J-C, et al. T-Cell–Inflamed Gene-Expression Profile, Programmed Death Ligand 1 Expression, and Tumor Mutational Burden Predict Efficacy in Patients Treated With Pembrolizumab Across 20 Cancers: KEYNOTE-028. *J Clin Oncol* (2019) 37:(4):318–27. doi: 10.1200/JCO.2018.78.2276
194. Reardon DA, Omuro A, Brandes AA, Rieger J, Wick A, Sepulveda J, et al. OS10.3 Randomized Phase 3 Study Evaluating the Efficacy and Safety of Nivolumab vs Bevacizumab in Patients With Recurrent Glioblastoma: Checkmate 143. *Neuro-Oncology* (2017) 19(suppl_3):iii21–iii. doi: 10.1093/neuonc/nox036.071
195. Lukas RV, Rodon J, Becker K, Wong ET, Shih K, Touat M, et al. Clinical Activity and Safety of Atezolizumab in Patients With Recurrent Glioblastoma. *J Neurooncol* (2018) 140(2):317–28. doi: 10.1007/s11060-018-2955-9
196. Platten M, Wick W, Van den Eynde BJ. Tryptophan Catabolism in Cancer: Beyond IDO and Tryptophan Depletion. *Cancer Res* (2012) 72(21):5435–40. doi: 10.1158/0008-5472.CAN-12-0569
197. Prendergast GC, Smith C, Thomas S, Mandik-Nayak L, Laury-Kleintop L, Metz R, et al. Indoleamine 2,3-Dioxygenase Pathways of Pathogenic Inflammation and Immune Escape in Cancer. *Cancer Immunol Immunother* (2014) 63(7):721–35. doi: 10.1007/s00262-014-1549-4

198. Toor SM, Sasidharan Nair V, Decock J, Elkord E. Immune Checkpoints in the Tumor Microenvironment. *Semin Cancer Biol* (2020) 65:1–12. doi: 10.1016/j.semcancer.2019.06.021
199. Uyttenhove C, Pilotte L, Théate I, Stroobant V, Colau D, Parmentier N, et al. Evidence for a Tumoral Immune Resistance Mechanism Based on Tryptophan Degradation by Indoleamine 2,3-Dioxygenase. *Nat Med* (2003) 9(10):1269–74. doi: 10.1038/nm934
200. Mitsuka K, Kawataki T, Satoh E, Asahara T, Horikoshi T, Kinouchi H. Expression of Indoleamine 2,3-Dioxygenase and Correlation With Pathological Malignancy in Gliomas. *Neurosurgery* (2013) 72(6):1031–9. doi: 10.1227/NEU.0b013e31828cf945
201. Hanihara M, Kawataki T, Oh-Oka K, Mitsuka K, Nakao A, Kinouchi H. Synergistic Antitumor Effect With Indoleamine 2,3-Dioxygenase Inhibition and Temozolomide in a Murine Glioma Model. *J Neurosurg* (2016) 124 (6):1594–601. doi: 10.3171/2015.5.JNS141901
202. Long GV, Dummer R, Hamid O, Gajewski TF, Caglevic C, Dalle S, et al. Epacadostat Plus Pembrolizumab Versus Placebo Plus Pembrolizumab in Patients With Unresectable or Metastatic Melanoma (ECHO-301/ KEYNOTE-252): A Phase 3, Randomised, Double-Blind Study. *Lancet Oncol* (2019) 20(8):1083–97. doi: 10.1016/S1470-2045(19)30274-8
203. Weenink B, French PJ, Sillevis Smitt PAE, Debets R, Geurts M. Immunotherapy in Glioblastoma: Current Shortcomings and Future Perspectives. *Cancers (Basel)* (2020) 12(3):751. doi: 10.3390/cancers12030751
204. Cheong JE, Sun L. Targeting the IDO1/TDO2-KYN-Ahr Pathway for Cancer Immunotherapy - Challenges and Opportunities. *Trends Pharmacol Sci* (2018) 39(3):307–25. doi: 10.1016/j.tips.2017.11.007
205. Gutiérrez-Vázquez C, Quintana FJ. Regulation of the Immune Response by the Aryl Hydrocarbon Receptor. *Immunity* (2018) 48(1):19–33. doi: 10.1016/j.immuni.2017.12.012
206. Kulasinghe A, Kapeleris J, Kenny L, Warkiani M, Vela I, Thiery J-P, et al. Abstract 1333: Isolation, Characterization and Expansion of Circulating Tumor Cells in Solid Cancers. *Cancer Res* (2019) 79(13 Supplement):1333–. doi: 10.1158/1538-7445.AM2019-1333
207. Perepechaeva ML, Grishanova AY. The Role of Aryl Hydrocarbon Receptor (Ahr) in Brain Tumors. *Int J Mol Sci* (2020) 21(8):2863. doi: 10.3390/ijms21082863
208. Graeber MB, Scheithauer BW, Kreutzberg GW. Microglia in Brain Tumors. *Glia* (2002) 40(2):252–9. doi: 10.1002/glia.10147
209. Thorsson V, Gibbs DL, Brown SD, Wolf D, Bortone DS, Ou Yang TH, et al. The Immune Landscape of Cancer. *Immunity* (2018) 48(4):812–30.e14. doi: 10.1016/j.immuni.2018.03.023
210. Hanisch UK, Kettenmann H. Microglia: Active Sensor and Versatile Effector Cells in the Normal and Pathologic Brain. *Nat Neurosci* (2007) 10(11):1387–94. doi: 10.1038/nn1997
211. Sielska M, Przanowski P, Wylot B, Gabrusiewicz K, Maleszewska M, Kijewska M, et al. Distinct Roles of CSF Family Cytokines in Macrophage Infiltration and Activation in Glioma Progression and Injury Response. *J Pathol* (2013) 230(3):310–21. doi: 10.1002/path.4192
212. Bettinger I, Thanos S, Paulus W. Microglia Promote Glioma Migration. *Acta Neuropathol* (2002) 103(4):351–5. doi: 10.1007/s00401-001-0472-x
213. Martins TA, Schmassmann P, Shekarian T, Boulay JL, Ritz MF, Zanganeh S, et al. Microglia-Centered Combinatorial Strategies Against Glioblastoma. *Front Immunol* (2020) 11:571951. doi: 10.3389/fimmu.2020.571951
214. Garris C, Pittet MJ. Therapeutically Reeducating Macrophages to Treat GBM. *Nat Med* (2013) 19(10):1207–8. doi: 10.1038/nm.3355
215. Pyonteck SM, Akkari L, Schuhmacher AJ, Bowman RL, Sevenich L, Quail DF, et al. CSF-1R Inhibition Alters Macrophage Polarization and Blocks Glioma Progression. *Nat Med* (2013) 19(10):1264–72. doi: 10.1038/nm.3337
216. Morisse MC, Jouannet S, Dominguez-Villar M, Sanson M, Idbaih A. Interactions Between Tumor-Associated Macrophages and Tumor Cells in Glioblastoma: Unraveling Promising Targeted Therapies. *Expert Rev Neurother* (2018) 18(9):729–37. doi: 10.1080/14737175.2018.1510321
217. Saha D, Martuza RL, Rabkin SD. Macrophage Polarization Contributes to Glioblastoma Eradication by Combination Immunovirotherapy and Immune Checkpoint Blockade. *Cancer Cell* (2017) 32(2):253–67.e5. doi: 10.1016/j.ccell.2017.07.006
218. Poli A, Wang J, Domingues O, Planagumà J, Yan T, Rygh CB, et al. Targeting Glioblastoma With NK Cells and Mab Against NG2/CSPG4 Prolongs Animal Survival. *Oncotarget* (2013) 4(9):1527–46. doi: 10.18632/oncotarget.1291
219. Kloepper J, Riedemann L, Amoozgar Z, Seano G, Susek K, Yu V, et al. Ang-2/VEGF Bispecific Antibody Reprograms Macrophages and Resident Microglia to Anti-Tumor Phenotype and Prolongs Glioblastoma Survival. *Proc Natl Acad Sci USA* (2016) 113(16):4476–81. doi: 10.1073/pnas.1525360113
220. Peterson TE, Kirkpatrick ND, Huang Y, Farrar CT, Marijt KA, Kloepper J, et al. Dual Inhibition of Ang-2 and VEGF Receptors Normalizes Tumor Vasculature and Prolongs Survival in Glioblastoma by Altering Macrophages. *Proc Natl Acad Sci USA* (2016) 113(16):4470–5. doi: 10.1073/pnas.1525349113
221. Thomas RP, Nagpal S, Iv M, Soltys SG, Bertrand S, Pelpola JS, et al. Macrophage Exclusion After Radiation Therapy (MERT): A First in Human Phase I/II Trial Using a CXCR4 Inhibitor in Glioblastoma. *Clin Cancer Res* (2019) 25(23):6948–57. doi: 10.1158/1078-0432.CCR-19-1421
222. Ellert-Miklaszewska A, Wisniewski P, Kijewska M, Gajdanowicz P, Pszczolkowska D, Przanowski P, et al. Tumour-Processed Osteopontin and Lactadherin Drive the Protumorigenic Reprogramming of Microglia and Glioma Progression. *Oncogene* (2016) 35(50):6366–77. doi: 10.1038/onc.2016.55
223. Willingham SB, Volkmer JP, Gentles AJ, Sahoo D, Dalerba P, Mitra SS, et al. The CD47-Signal Regulatory Protein Alpha (Sirpa) Interaction is a Therapeutic Target for Human Solid Tumors. *Proc Natl Acad Sci USA* (2012) 109(17):6662–7. doi: 10.1073/pnas.1121623109
224. Edris B, Weiskopf K, Volkmer AK, Volkmer JP, Willingham SB, Contreras-Trujillo H, et al. Antibody Therapy Targeting the CD47 Protein is Effective in a Model of Aggressive Metastatic Leiomyosarcoma. *Proc Natl Acad Sci USA* (2012) 109(17):6656–61. doi: 10.1073/pnas.1121629109
225. Barclay AN, Van den Berg TK. The Interaction Between Signal Regulatory Protein Alpha (Sirpα) and CD47: Structure, Function, and Therapeutic Target. *Annu Rev Immunol* (2014) 32:25–50. doi: 10.1146/annurev-immunol-032713-120142
226. Hutter G, Theruvath J, Graef CM, Zhang M, Schoen MK, Manz EM, et al. Microglia are Effector Cells of CD47-Sirpα Antiphagocytic Axis Disruption Against Glioblastoma. *Proc Natl Acad Sci USA* (2019) 116(3):997–1006. doi: 10.1073/pnas.1721434116
227. Sikic BI, Lakhani N, Patnaik A, Shah SA, Chandana SR, Rasco D, et al. First-in-Human, First-in-Class Phase I Trial of the Anti-CD47 Antibody Hu5F9-G4 in Patients With Advanced Cancers. *J Clin Oncol* (2019) 37(12):946–53. doi: 10.1200/JCO.18.02018
228. Dall'Olio F, Malagolini N, Trinchera M, Chiricolo M. Sialosignaling: Sialyltransferases as Engines of Self-Fueling Loops in Cancer Progression. *Biochim Biophys Acta* (2014) 1840(9):2752–64. doi: 10.1016/j.bbagen.2014.06.006
229. Li GZ, Zhang KN, Wang Z, Hu HM, Wang ZL, Huang RY, et al. Siglecs, Novel Immunotherapy Targets, Potentially Enhance the Effectiveness of Existing Immune Checkpoint Inhibitors in Glioma Immunotherapy. *Onco Targets Ther* (2019) 12:10263–73. doi: 10.2147/OTT.S223406
230. Wang J, Sun J, Liu LN, Flies DB, Nie X, Toki M, et al. Siglec-15 as an Immune Suppressor and Potential Target for Normalization Cancer Immunotherapy. *Nat Med* (2019) 25(4):656–66. doi: 10.1038/s41591-019-0374-x
231. Lang FF, Conrad C, Gomez-Manzano C, Yung WKA, Sawaya R, Weinberg JS, et al. Phase I Study of DNX-2401 (Delta-24-RGD) Oncolytic Adenovirus: Replication and Immunotherapeutic Effects in Recurrent Malignant Glioma. *J Clin Oncol* (2018) 36(14):1419–27. doi: 10.1200/JCO.2017.75.8219
232. Jiang H, Clise-Dwyer K, Ruisaard KE, Fan X, Tian W, Gumin J, et al. Delta-24-RGD Oncolytic Adenovirus Elicits Anti-Glioma Immunity in an Immunocompetent Mouse Model. *PloS One* (2014) 9(5):e97407. doi: 10.1371/journal.pone.0097407
233. van den Bossche WBL, Kleijn A, Teunissen CE, Voerman JSA, Teodosio C, Noske DP, et al. Oncolytic Virotherapy in Glioblastoma Patients Induces a Tumor Macrophage Phenotypic Shift Leading to an Altered Glioblastoma Microenvironment. *Neuro Oncol* (2018) 20(11):1494–504. doi: 10.1093/neuonc/noy082
234. Mahasa KJ, de Pillis L, Ouifki R, Eladdadi A, Maini P, Yoon AR, et al. Mesenchymal Stem Cells Used as Carrier Cells of Oncolytic Adenovirus Results in Enhanced Oncolytic Virotherapy. *Sci Rep* (2020) 10(1):425. doi: 10.1038/s41598-019-57240-x

235. Jiang H, Rivera-Molina Y, Gomez-Manzano C, Clise-Dwyer K, Bover L, Vence LM, et al. Oncolytic Adenovirus and Tumor-Targeting Immune Modulatory Therapy Improve Autologous Cancer Vaccination. *Cancer Res* (2017) 77(14):3894. doi: 10.1158/0008-5472.CAN-17-0468
236. Zadeh G, Lang F, Daras M, Cloughesy T, Colman H, Ong S, et al. Atim-24. Interim Results of a Phase Ii Multicenter Study of the Conditionally Replicative Oncolytic Adenovirus Dnx-2401 With Pembrolizumab (Keytruda) for Recurrent Glioblastoma; Captive Study (Keynote-192). *Neuro Oncol* (2018) 20(Suppl 6):vi6–vi. doi: 10.1093/neuonc/noy148.019
237. Saha D, Martuza RL, Rabkin SD. Oncolytic Herpes Simplex Virus Immunovirotherapy in Combination With Immune Checkpoint Blockade to Treat Glioblastoma. *Immunotherapy* (2018) 10(9):779–86. doi: 10.2217/imt-2018-0009
238. Todo T, Martuza RL, Rabkin SD, Johnson PA. Oncolytic Herpes Simplex Virus Vector With Enhanced MHC Class I Presentation and Tumor Cell Killing. *Proc Natl Acad Sci U S A* (2001) 98(11):6396–401. doi: 10.1073/pnas.101136398
239. Cheema TA, Wakimoto H, Fecci PE, Ning J, Kuroda T, Jeyaretna DS, et al. Multifaceted Oncolytic Virus Therapy for Glioblastoma in an Immunocompetent Cancer Stem Cell Model. *Proc Natl Acad Sci USA* (2013) 110(29):12006–11. doi: 10.1073/pnas.1307935110
240. Cheema TA, Fecci PE, Ning J, Rabkin SD. Immunovirotherapy for the Treatment of Glioblastoma. *Oncoimmunology* (2014) 3(1):e27218. doi: 10.4161/onci.27218
241. Todo T. Atim-14. Results of Phase Ii Clinical Trial of Oncolytic Herpes Virus G47Δ in Patients With Glioblastoma. *Neuro Oncol* (2019) 21 (Supplement_6):vi4–vi. doi: 10.1093/neuonc/noz175.014
242. Freeman AI, Zakay-Rones Z, Gomori JM, Linetsky E, Rasooly L, Greenbaum E, et al. Phase I/II Trial of Intravenous NDV-HUJ Oncolytic Virus in Recurrent Glioblastoma Multiforme. *Mol Ther* (2006) 13(1):221–8. doi: 10.1016/j.ymthe.2005.08.016
243. Angelova AL, Barf M, Geletneky K, Unterberg A, Rommelaere J. Immunotherapeutic Potential of Oncolytic H-1 Parvovirus: Hints of Glioblastoma Microenvironment Conversion Towards Immunogenicity. *Viruses* (2017) 9(12):382. doi: 10.3390/v9120382
244. Geletneky K, Kiprianova I, Ayache A, Koch R, Herrero YCM, Deleu L, et al. Regression of Advanced Rat and Human Gliomas by Local or Systemic Treatment With Oncolytic Parvovirus H-1 in Rat Models. *Neuro Oncol* (2010) 12(8):804–14. doi: 10.1093/neuonc/noq023
245. Grekova SP, Raykov Z, Zawatzky R, Rommelaere J, Koch U. Activation of a Glioma-Specific Immune Response by Oncolytic Parvovirus Minute Virus of Mice Infection. *Cancer Gene Ther* (2012) 19(7):468–75. doi: 10.1038/cgt.2012.20
246. Lim M, Xia Y, Bettegowda C, Weller M. Current State of Immunotherapy for Glioblastoma. *Nat Rev Clin Oncol* (2018) 15(7):422–42. doi: 10.1038/s41571-018-0003-5
247. Hossain JA, Marchini A, Fehse B, Bjerkvig R, Miletic H. Suicide Gene Therapy for the Treatment of High-Grade Glioma: Past Lessons, Present Trends, and Future Prospects. *Neuro-Oncol Adv* (2020) 2(1):vdaa013. doi: 10.1093/noajnl/vdaa013
248. Bais SS, Chheda MG. A Fyn Romance: Tumor Cell Fyn Kinase Suppresses the Immune Microenvironment. *Neuro-Oncology* (2020) 22(6):746–7. doi: 10.1093/neuonc/noaa082
249. Young JS, Dayani F, Morshed RA, Okada H, Aghi MK. Immunotherapy for High Grade Gliomas: A Clinical Update and Practical Considerations for Neurosurgeons. *World Neurosurg* (2019) S1878–8750(19):30106–8. doi: 10.1016/j.wneu.2018.12.222
250. Park JH, Riviere I, Wang X, Bernal Y, Purdon T, Halton E, et al. Efficacy and Safety of CD19-Targeted 19-28z CAR Modified T Cells in Adult Patients With Relapsed or Refractory B-ALL. *J Clin Oncol* (2015) 33(15_suppl):7010. doi: 10.1200/jco.2015.33.15_suppl.7010
251. Sommermeyer D, Hudecek M, Kosasih PL, Gogishvili T, Maloney DG, Turtle CJ, et al. Chimeric Antigen Receptor-Modified T Cells Derived From Defined CD8+ and CD4+ Subsets Confer Superior Antitumor Reactivity In Vivo. *Leukemia* (2016) 30(2):492–500. doi: 10.1038/leu.2015.247
252. Haase S, Nuñez FM, Gauss JC, Thompson S, Brumley E, Lowenstein P, et al. Hemispherical Pediatric High-Grade Glioma: Molecular Basis and Therapeutic Opportunities. *Int J Mol Sci* (2020) 21(24):9654. doi: 10.3390/ijms21249654
253. Samstein RM, Lee C-H, Shoushtari AN, Hellmann MD, Shen R, Janjigian YY, et al. Tumor Mutational Load Predicts Survival After Immunotherapy Across Multiple Cancer Types. *Nat Genet* (2019) 51(2):202–6. doi: 10.1038/s41588-018-0312-8
254. Wang SS, Bandopadhayay P, Jenkins MR. Towards Immunotherapy for Pediatric Brain Tumors. *Trends Immunol* (2019) 40(8):748–61. doi: 10.1016/j.it.2019.05.009
255. Sherman WJ, Vitaz TW. Nivolumab With Radiation Therapy in a Glioblastoma Patient With Lynch Syndrome. *BMJ Case Rep* (2021) 14(4): e241026. doi: 10.1136/bcr-2020-241026
256. D'Angelo F, Ceccarelli M, Tala, Garofano L, Zhang J, Frattini V, et al. The Molecular Landscape of Glioma in Patients With Neurofibromatosis 1. *Nat Med* (2019) 25(1):176–87. doi: 10.1038/s41591-018-0263-8
257. Brown CE, Alizadeh D, Starr R, Weng L, Wagner JR, Naranjo A, et al. Regression of Glioblastoma After Chimeric Antigen Receptor T-Cell Therapy. *N Engl J Med* (2016) 375(26):2561–9. doi: 10.1056/NEJMoa1610497
258. Mount CW, Majzner RG, Sundaresh S, Arnold EP, Kadapakkam M, Haile S, et al. Potent Antitumor Efficacy of Anti-GD2 CAR T Cells in H3-K27M(+) Diffuse Midline Gliomas. *Nat Med* (2018) 24(5):572–9. doi: 10.1038/s41591-018-0006-x
259. Haase S, Belén Garcia-Fabiani M, Nunez F, Kadiyala P, Nunez F, Lowenstein P, et al. Pdtm-20. Elucidating Molecular Pathogenic Mechanisms of the Histone H3.3 G34r Mutation in Pediatric High-Grade Gliomas (Hggs). *Neuro Oncol* (2018) 20(Suppl 6):vi208. doi: 10.1093/neuonc/noy148.862
260. Vitanza NA, Biery MC, Myers C, Ferguson E, Zheng Y, Girard EJ, et al. Optimal Therapeutic Targeting by HDAC Inhibition in Biopsy-Derived Treatment-Naïve Diffuse Midline Glioma Models. *Neuro Oncol* (2021) 23 (3):376–86. doi: 10.1093/neuonc/noaa249
261. Herting CJ, Chen Z, Pitter KL, Szulzewsky F, Kaffes I, Kaluzova M, et al. Genetic Driver Mutations Define the Expression Signature and Microenvironmental Composition of High-Grade Gliomas. *Glia* (2017) 65 (12):1914–26. doi: 10.1002/glia.23203
262. Gabrilovich DI. Myeloid-Derived Suppressor Cells. *Cancer Immunol Res* (2017) 5(1):3–8. doi: 10.1158/2326-6066.CIR-16-0297
263. Elias D, Ditzel HJ. Fyn is an Important Molecule in Cancer Pathogenesis and Drug Resistance. *Pharmacol Res* (2015) 100:250–4. doi: 10.1016/j.phrs.2015.08.010
264. Lee GH, Yoo KC, An Y, Lee HJ, Lee M, Uddin N, et al. FYN Promotes Mesenchymal Phenotypes of Basal Type Breast Cancer Cells Through STAT5/NOTCH2 Signaling Node. *Oncogene* (2018) 37(14):1857–68. doi: 10.1038/s41388-017-0114-y
265. Schenone S, Brullo C, Musumeci F, Biava M, Falchi F, Botta M. Fyn Kinase in Brain Diseases and Cancer: The Search for Inhibitors. *Curr Med Chem* (2011) 18(19):2921–42. doi: 10.2174/092986711796150531
266. Palacios EH, Weiss A. Function of the Src-Family Kinases, Lck and Fyn, in T-Cell Development and Activation. *Oncogene* (2004) 23(48):7990–8000. doi: 10.1038/sj.onc.1208074
267. Sugie K, Jeon MS, Grey HM. Activation of Naive CD4 T Cells by Anti-CD3 Reveals an Important Role for Fyn in Lck-Mediated Signaling. *Proc Natl Acad Sci USA* (2004) 101(41):14859–64. doi: 10.1073/pnas.0406168101
268. Yamauchi J, Miyamoto Y, Torii T, Takashima S, Kondo K, Kawahara K, et al. Phosphorylation of Cytohesin-1 by Fyn is Required for Initiation of Myelination and the Extent of Myelination During Development. *Sci Signaling* (2012) 5(243):ra69. doi: 10.1126/scisignal.2002802
269. Matrone C, Petrillo F, Nasso R, Ferretti G. Fyn Tyrosine Kinase as Harmonizing Factor in Neuronal Functions and Dysfunctions. *Int J Mol Sci* (2020) 21(12):4444. doi: 10.3390/ijms21124444
270. Lu KV, Zhu S, Cvrljevic A, Huang TT, Sarkaria S, Ahkavan D, et al. Fyn and SRC are Effectors of Oncogenic Epidermal Growth Factor Receptor Signaling in Glioblastoma Patients. *Cancer Res* (2009) 69(17):6889–98. doi: 10.1158/0008-5472.CAN-09-0347
271. Yadav V, Denning MF. Fyn is Induced by Ras/PI3K/Akt Signaling and is Required for Enhanced Invasion/Migration. *Mol Carcinog* (2011) 50(5):346–52. doi: 10.1002/mc.20716
272. Jensen AR, David SY, Liao C, Dai J, Keller ET, Al-Ahmadie H, et al. Fyn is Downstream of the HGF/MET Signaling Axis and Affects Cellular Shape and Tropism in PC3 Cells. *Clin Cancer Res* (2011) 17(10):3112–22. doi: 10.1158/1078-0432.CCR-10-1264

273. Guo S, Ran H, Xiao D, Huang H, Mi L, Wang X, et al. NT5DC2 Promotes Tumorigenicity of Glioma Stem-Like Cells by Upregulating Fyn. *Cancer Lett* (2019) 454:98–107. doi: 10.1016/j.canlet.2019.04.003
274. Han X, Zhang W, Yang X, Wheeler CG, Langford CP, Wu L, et al. The Role of Src Family Kinases in Growth and Migration of Glioma Stem Cells. *Int J Oncol* (2014) 45(1):302–10. doi: 10.3892/ijo.2014.2432
275. Lewis-Tuffin LJ, Feathers R, Hari P, Durand N, Li Z, Rodriguez FJ, et al. Src Family Kinases Differentially Influence Glioma Growth and Motility. *Mol Oncol* (2015) 9(9):1783–98. doi: 10.1016/j.molonc.2015.06.001
276. Masserini M. Nanoparticles for Brain Drug Delivery. *ISRN Biochem* (2013) 2013. doi: 10.1155/2013/238428
277. Gregory JV, Kadiyala P, Doherty R, Cadena M, Habeel S, Ruoslahti E, et al. Systemic Brain Tumor Delivery of Synthetic Protein Nanoparticles for Glioblastoma Therapy. *Nat Commun* (2020) 11(1):5687. doi: 10.1038/s41467-020-19225-7
278. Ivashkiv LB. Ifngamma: Signalling, Epigenetics and Roles in Immunity, Metabolism, Disease and Cancer Immunotherapy. *Nat Rev Immunol* (2018) 18(9):545–58. doi: 10.1038/s41577-018-0029-z
279. Mi Y, Hagan CTIV, Vincent BG, Wang AZ. Emerging Nano-/Microapproaches for Cancer Immunotherapy. *Adv Sci* (2019) 6 (6):1801847. doi: 10.1002/advs.201801847
280. Kuai R, Ochyl LJ, Bahjat KS, Schwendeman A, Moon JJ. Designer Vaccine Nanodiscs for Personalized Cancer Immunotherapy. *Nat Mater* (2017) 16 (4):489–96. doi: 10.1038/nmat4822
281. Kuai R, Li D, Chen YE, Moon JJ, Schwendeman A. High-Density Lipoproteins: Nature's Multifunctional Nanoparticles. *ACS Nano* (2016) 10(3):3015–41. doi: 10.1021/acsnano.5b07522
282. Vanan MI, Underhill DA, Eisenstat DD. Targeting Epigenetic Pathways in the Treatment of Pediatric Diffuse (High Grade) Gliomas. *Neurotherapeutics* (2017) 14(2):274–83. doi: 10.1007/s13311-017-0514-2
283. Alexandrov LB, Nik-Zainal S, Wedge DC, Aparicio SAJR, Behjati S, Biankin AV, et al. Signatures of Mutational Processes in Human Cancer. *Nature* (2013) 500:415. doi: 10.1038/nature12477
284. Ilyas S, Yang JC. Landscape of Tumor Antigens in T Cell Immunotherapy. *J Immunol (Baltimore Md: 1950)* (2015) 195(11):5117–22. doi: 10.4049/jimmunol.1501657
285. Gusyatiner O, Hegi ME. Glioma Epigenetics: From Subclassification to Novel Treatment Options. *Semin Cancer Biol* (2018) 51:50–8. doi: 10.1016/j.semcancer.2017.11.010
286. Cheng T, Xu Y. Effects of Enhancer of Zeste Homolog 2 (EZH2) Expression on Brain Glioma Cell Proliferation and Tumorigenesis. *Med Sci Monit* (2018) 24:7249–55. doi: 10.12659/MSM.909814
287. Orzan F, Pellegatta S, Poliani PL, Pisati F, Caldera V, Menghi F, et al. Enhancer of Zeste 2 (EZH2) is Up-Regulated in Malignant Gliomas and in Glioma Stem-Like Cells. *Neuropathol Appl Neurobiol* (2011) 37(4):381–94. doi: 10.1111/j.1365-2990.2010.01132.x
288. Olar A, Aldape KD. Using the Molecular Classification of Glioblastoma to Inform Personalized Treatment. *J Pathol* (2014) 232(2):165–77. doi: 10.1002/path.4282
289. Turcan S, Rohle D, Goenka A, Walsh LA, Fang F, Yilmaz E, et al. IDH1 Mutation is Sufficient to Establish the Glioma Hypermethylator Phenotype. *Nature* (2012) 483(7390):479–83. doi: 10.1038/nature10866
290. Federici L, Capelle L, Annereau M, Bielle F, Willekens C, Dehais C, et al. 5-Azacitidine in Patients With IDH1/2-Mutant Recurrent Glioma. *Neuro-Oncology* (2020) 22(8):1226–8. doi: 10.1093/neuonc/noaa074
291. DiNardo C, de Botton S, Pollyea DA, Stein EM, Fathi AT, Roboz GJ, et al. Molecular Profiling and Relationship With Clinical Response in Patients With IDH1 Mutation-Positive Hematologic Malignancies Receiving AG-120, a First-in-Class Potent Inhibitor of Mutant IDH1, in Addition to Data From the Completed Dose Escalation Portion of the Phase 1 Study. *Blood* (2015) 126(23):1306–. doi: 10.1182/blood.V126.23.1306.1306
292. Golub D, Iyengar N, Dogra S, Wong T, Bready D, Tang K, et al. Mutant Isocitrate Dehydrogenase Inhibitors as Targeted Cancer Therapeutics. *Front Oncol* (2019) 9:417–. doi: 10.3389/fonc.2019.00417
293. Popovici-Muller J, Lemieux RM, Artin E, Saunders JO, Salituro FG, Travins J, et al. Discovery of AG-120 (Ivosidenib): A First-in-Class Mutant IDH1 Inhibitor for the Treatment of IDH1 Mutant Cancers. *ACS Med Chem Lett* (2018) 9(4):300–5. doi: 10.1021/acsmedchemlett.7b00421
294. Borodovsky A, Salmasi V, Turcan S, Fabius AW, Baia GS, Eberhart CG, et al. 5-Azacytidine Reduces Methylation, Promotes Differentiation and Induces Tumor Regression in a Patient-Derived IDH1 Mutant Glioma Xenograft. *Oncotarget* (2013) 4(10):1737–47. doi: 10.18632/oncotarget.1408
295. Turcan S, Fabius AW, Borodovsky A, Pedraza A, Brennan C, Huse J, et al. Efficient Induction of Differentiation and Growth Inhibition in IDH1 Mutant Glioma Cells by the DNMT Inhibitor Decitabine. *Oncotarget* (2013) 4(10):1729–36. doi: 10.18632/oncotarget.1412
296. Mackenzie KJ, Carroll P, Martin C-A, Murina O, Fluteau A, Simpson DJ, et al. Cgas Surveillance of Micronuclei Links Genome Instability to Innate Immunity. *Nature* (2017) 548(7668):461–5. doi: 10.1038/nature23449
297. Cao J, Yan Q. Cancer Epigenetics, Tumor Immunity, and Immunotherapy. *Trends Cancer* (2020) 6(7):580–92. doi: 10.1016/j.trecan.2020.02.003
298. Chiou G-Y, Chien C-S, Wang M-L, Chen M-T, Yang Y-P, Yu Y-L, et al. Epigenetic Regulation of the Mir142-3p/Interleukin-6 Circuit in Glioblastoma. *Mol Cell* (2013) 52(5):693–706. doi: 10.1016/j.molcel.2013.11.009
299. West AC, Johnstone RW. New and Emerging HDAC Inhibitors for Cancer Treatment. *J Clin Invest* (2014) 124(1):30–9. doi: 10.1172/JCI69738
300. Camphausen K, Cerna D, Scott T, Sproull M, Burgan WE, Cerra MA, et al. Enhancement of In Vitro and In Vivo Tumor Cell Radiosensitivity by Valproic Acid. *Int J Cancer* (2005) 114(3):380–6. doi: 10.1002/ijc.20774
301. Was H, Krol SK, Rotili D, Mai A, Wojtas B, Kaminska B, et al. Histone Deacetylase Inhibitors Exert Anti-Tumor Effects on Human Adherent and Stem-Like Glioma Cells. *Clin Epigenet* (2019) 11(1):11. doi: 10.1186/s13148-018-0598-5
302. Bolden JE, Peart MJ, Johnstone RW. Anticancer Activities of Histone Deacetylase Inhibitors. *Nat Rev Drug Discovery* (2006) 5(9):769–84. doi: 10.1038/nrd2133
303. Chinnaiyan P, Chowdhary S, Potthast L, Prabhu A, Tsai Y-Y, Sarcar B, et al. Phase I Trial of Vorinostat Combined With Bevacizumab and CPT-11 in Recurrent Glioblastoma. *Neuro-oncology* (2012) 14(1):93–100. doi: 10.1093/neuonc/nor187
304. Friday BB, Anderson SK, Buckner J, Yu C, Giannini C, Geoffroy F, et al. Phase II Trial of Vorinostat in Combination With Bortezomib in Recurrent Glioblastoma: A North Central Cancer Treatment Group Study. *Neuro-Oncology* (2012) 14(2):215–21. doi: 10.1093/neuonc/nor198
305. Krauze AV, Myrehaug SD, Chang MG, Holdford DJ, Smith S, Shih J, et al. A Phase 2 Study of Concurrent Radiation Therapy, Temozolomide, and the Histone Deacetylase Inhibitor Valproic Acid for Patients With Glioblastoma. *Int J Radiat Oncol Biol Phys* (2015) 92(5):986–92. doi: 10.1016/j.ijrobp.2015.04.038
306. Lee DH, Ryu HW, Won HR, Kwon SH. Advances in Epigenetic Glioblastoma Therapy. *Oncotarget* (2017) 8(11):18577–89. doi: 10.18632/oncotarget.14612
307. Pastori C, Daniel M, Penas C, Volmar CH, Johnstone AL, Brothers SP, et al. BET Bromodomain Proteins are Required for Glioblastoma Cell Proliferation. *Epigenetics* (2014) 9(4):611–20. doi: 10.4161/epi.27906
308. Cheng Z, Gong Y, Ma Y, Lu K, Lu X, Pierce LA, et al. Inhibition of BET Bromodomain Targets Genetically Diverse Glioblastoma. *Clin Cancer Res* (2013) 19(7):1748–59. doi: 10.1158/1078-0432.CCR-12-3066
309. Agrawal K, Das V, Vyas P, Hajdúch M. Nucleosidic DNA Demethylating Epigenetic Drugs - a Comprehensive Review From Discovery to Clinic. *Pharmacol Ther* (2018) 188:45–79. doi: 10.1016/j.pharmthera.2018.02.006
310. McClure JJ, Li X, Chou CJ. Advances and Challenges of HDAC Inhibitors in Cancer Therapeutics. *Adv Cancer Res* (2018) 138:183–211. doi: 10.1016/bs.acr.2018.02.006
311. First EZH2 Inhibitor Approved—for Rare Sarcoma. *Cancer Discov* (2020) 10 (3):333. doi: 10.1158/2159-8290.CD-NB2020-006
312. Iorgulescu JB, Torre M, Harary M, Smith TR, Aizer AA, Reardon DA, et al. The Misclassification of Diffuse Gliomas: Rates and Outcomes. *Clin Cancer Res* (2019) 25(8):2656–63. doi: 10.1158/1078-0432.CCR-18-3101
313. Robinson C, Kleinschmidt-DeMasters B. IDH1-Mutation in Diffuse Gliomas in Persons Age 55 Years and Over. *J Neuropathol Exp Neurol* (2017) 76 (2):151–4. doi: 10.1093/jnen/nlw112
314. Lai A, Kharbanda S, Pope WB, Tran A, Solis OE, Peale F, et al. Evidence for Sequenced Molecular Evolution of IDH1 Mutant Glioblastoma From a Distinct Cell of Origin. *J Clin Oncol* (2011) 29(34):4482. doi: 10.1200/JCO.2010.33.8715
315. Lass U, Nümann A, von Eckardstein K, Kiwit J, Stockhammer F, Horaczek JA, et al. Clonal Analysis in Recurrent Astrocytic, Oligoastrocytic and Oligodendroglial

Tumors Implicates IDH1-Mutation as Common Tumor Initiating Event. *PloS One* (2012) 7(7):e41298. doi: 10.1371/journal.pone.0041298
316. Lu C, Ward PS, Kapoor GS, Rohle D, Turcan S, Abdel-Wahab O, et al. IDH Mutation Impairs Histone Demethylation and Results in a Block to Cell Differentiation. *Nature* (2012) 483(7390):474–8. doi: 10.1038/nature10860
317. Urban DJ, Martinez NJ, Davis MI, Brimacombe KR, Cheff DM, Lee TD, et al. Assessing Inhibitors of Mutant Isocitrate Dehydrogenase Using a Suite of Pre-Clinical Discovery Assays. *Sci Rep* (2017) 7(1):1–15. doi: 10.1038/s41598-017-12630-x
318. Bunse L, Pusch S, Bunse T, Sahm F, Sanghvi K, Friedrich M, et al. Suppression of Antitumor T Cell Immunity by the Oncometabolite (R)-2-Hydroxyglutarate. *Nat Med* (2018) 24(8):1192–203. doi: 10.1038/s41591-018-0095-6
319. Maxwell R, Jackson CM, Lim M. Clinical Trials Investigating Immune Checkpoint Blockade in Glioblastoma. *Curr Treat Options Oncol* (2017) 18 (8):51. doi: 10.1007/s11864-017-0492-y
320. Yeo AT, Charest A. Immune Checkpoint Blockade Biology in Mouse Models of Glioblastoma. *J Cell Biochem* (2017) 118(9):2516–27. doi: 10.1002/jcb.25948
321. Paugh BS, Qu C, Jones C, Liu Z, Adamowicz-Brice M, Zhang J, et al. Integrated Molecular Genetic Profiling of Pediatric High-Grade Gliomas Reveals Key Differences With the Adult Disease. *J Clin Oncol* (2010) 28 (18):3061–8. doi: 10.1200/JCO.2009.26.7252

Conflict of Interest: The authors declare that the research was conducted in the absence of any commercial or financial relationships that could be construed as a potential conflict of interest.

frontiers in Immunology

ORIGINAL RESEARCH
published: 29 June 2021
doi: 10.3389/fimmu.2021.670131

CD206 Expression in Induced Microglia-Like Cells From Peripheral Blood as a Surrogate Biomarker for the Specific Immune Microenvironment of Neurosurgical Diseases Including Glioma

Shunya Tanaka[1†], Masahiro Ohgidani[2†], Nobuhiro Hata[1], Shogo Inamine[2], Noriaki Sagata[2], Noritoshi Shirouzu[1], Nobutaka Mukae[1], Satoshi O. Suzuki[3], Hideomi Hamasaki[3], Ryusuke Hatae[1], Yuhei Sangatsuda[1], Yutaka Fujioka[1], Kosuke Takigawa[1], Yusuke Funakoshi[1], Toru Iwaki[3], Masako Hosoi[4], Koji Iihara[1], Masahiro Mizoguchi[1] and Takahiro A. Kato[2]*

[1] Department of Neurosurgery, Graduate School of Medical Sciences, Kyushu University, Fukuoka, Japan, [2] Department of Neuropsychiatry, Graduate School of Medical Sciences, Kyushu University, Fukuoka, Japan, [3] Department of Neuropathology, Graduate School of Medical Sciences, Kyushu University, Fukuoka, Japan, [4] Department of Psychosomatic Medicine, Kyushu University Hospital, Fukuoka, Japan

Targeting the unique glioma immune microenvironment is a promising approach in developing breakthrough immunotherapy treatments. However, recent advances in immunotherapy, including the development of immune checkpoint inhibitors, have not improved the outcomes of patients with glioma. A way of monitoring biological activity of immune cells in neural tissues affected by glioma should be developed to address this lack of sensitivity to immunotherapy. Thus, in this study, we sought to examine the feasibility of non-invasive monitoring of glioma-associated microglia/macrophages (GAM) by utilizing our previously developed induced microglia-like (iMG) cells. Primary microglia (pMG) were isolated from surgically obtained brain tissues of 22 patients with neurological diseases. iMG cells were produced from monocytes extracted from the patients' peripheral blood. Quantitative reverse transcription-polymerase chain reaction (qRT-PCR) revealed a significant correlation of the expression levels of representative markers for M1 and M2 microglia phenotypes between pMG and the corresponding iMG cells in each patient (Spearman's correlation coefficient = 0.5225, P <0.0001). Synchronous upregulation of CD206 expression levels was observed in most patients with glioma (6/9, 66.7%) and almost all patients with glioblastoma (4/5, 80%). Therefore, iMG cells can be used as a minimally invasive tool for monitoring the disease-related immunological state of GAM in various brain diseases, including glioma. CD206 upregulation detected in iMG cells can be used as a surrogate biomarker of glioma.

Keywords: microglia, glioma, CD206, surrogate biomarker, induced microglia-like cells

OPEN ACCESS

Edited by:
Valérie Dutoit, Université de Genève, Switzerland

Reviewed by:
Michael Rückert, University Hospital Erlangen, Germany
Michel Guy André Mittelbronn, National Health Laboratory, Luxembourg

***Correspondence:**
Takahiro A. Kato
takahiro@npsych.med.kyushu-u.ac.jp

[†]These authors have contributed equally to this work

Specialty section:
This article was submitted to Cancer Immunity and Immunotherapy, a section of the journal Frontiers in Immunology

Received: *20 February 2021*
Accepted: *04 June 2021*
Published: *29 June 2021*

Citation:
Tanaka S, Ohgidani M, Hata N, Inamine S, Sagata N, Shirouzu N, Mukae N, Suzuki SO, Hamasaki H, Hatae R, Sangatsuda Y, Fujioka Y, Takigawa K, Funakoshi Y, Iwaki T, Hosoi M, Iihara K, Mizoguchi M and Kato TA (2021) CD206 Expression in Induced Microglia-Like Cells From Peripheral Blood as a Surrogate Biomarker for the Specific Immune Microenvironment of Neurosurgical Diseases Including Glioma. Front. Immunol. 12:670131. doi: 10.3389/fimmu.2021.670131

INTRODUCTION

Gliomas are tumors of the central nervous system (CNS) derived from neural tissues. Among them, glioblastoma (GBM) has a highly aggressive phenotype and accounts for most gliomas. Despite advances in surgical resection, chemotherapy, and radiation therapy, GBM prognosis remains poor, and <5% of patients survive beyond five years post-diagnosis (1).

Among the recent attempts to develop multimodal treatment strategies to modify the extremely poor survival of GBM patients, immune checkpoint inhibitors were expected to bring about a paradigm shift, similar to that achieved in the treatment of other malignancies, such as melanoma (2, 3). However, clinical trials have failed to observe significant therapeutic benefits of immune checkpoint inhibitors in patients with GBM (4, 5). Such unfavorable results may be partly due to the peculiar state of the immune system in glioma tissues and the CNS in general.

Microglia are the brain's immune system cells responsible for maintaining brain homeostasis (6). Microglia exhibit a spectrum of phenotypes. The classically activated microglia/macrophages stimulate anti-tumor immune responses through the secretion of pro-inflammatory cytokines, such as tumor necrosis factor-alpha (TNF-α), interleukin (IL)-1β, and inducible nitric oxide synthase, defined as M1 markers. However, the alternatively activated microglia/macrophages promote tumor survival by producing anti-inflammatory cytokines such as IL-4, transforming growth factor-beta (TGF-β), and IL-10, defined as M2 markers (7–10). Microglia and peripheral macrophages recruited by glioma cells, defined as glioma-associated microglia/macrophages (GAM), were shown to contribute to tumor growth and invasion (11).

GBM is a complex solid tumor containing neoplastic and non-neoplastic cells, and the majority of the non-neoplastic cells are GAM, which account for 30%-50% of the cells in GBM (12, 13). GAM have been reported to play various roles in the malignancy features of GBM, including proliferation, growth, invasion, and immunosuppression (14–17). GAM are recruited to GBM microenvironment, where they release a wide array of chemokines and cytokines in response to the factors secreted by the tumor cells (14). Recently, small extracellular vesicles secreted by GAM have been reported to promote the progression of glioma (18). Within the tumor microenvironment, GAM are forced to transform to M2 phenotypes by GBM cells that secrete factors such as IL-10, IL-4, IL-6, macrophage colony-stimulating factor, macrophage inhibitory factor, TGFβ, and prostaglandin E_2, which subsequently supports tumor growth and invasion (19). Several studies of tumor tissue samples have documented a correlation between GAM characteristics and pathological grade/prognosis of gliomas (20, 21).

Abbreviations: CNS, Central nervous system; GAM, Glioma-associated microglia/macrophages; GBM, Glioblastoma; GLI group, Glioma group; GM-CSF, Granulocyte macrophage colony-stimulating factor; IL, Interleukin; iMG cells, Induced microglia-like cells; PBMCs, Peripheral blood mononuclear cells; pMG, Primary microglia; qRT-PCR, Quantitative reverse transcription-polymerase chain reaction; RGM group, radiographic glioma-like mass lesion group; TGF-β, Transforming growth factor-beta; TNF-α, Tumor necrosis factor-alpha.

We have previously developed a technique to generate induced microglia-like (iMG) cells from peripheral blood (22). We reported that iMG cells expressed the essential characteristics of human microglia, such as surface markers and drug responses, phagocytosis, and cytokine production (22). We applied this technique for translational research focusing on neurological, psychiatric, and pain-related disorders (23, 24). Other research groups and ours have revealed that iMG cells express microglia-specific surface markers (CX3CR1, P2RY12, TMEM119, and others) and possess phagocytic activity (22, 25, 26). Recently, iMG cells have been reported to be distinct from monocytes and macrophages but clustered closer with human brain microglia [Ohgidani 2020 under review] (25). These results suggest that iMG cells are a promising research tool for less-invasive monitoring of the immunological state of microglia in the CNS.

CD206 is a 175 kDa transmembrane protein encoded by the mannose receptor C-type 1 gene (*MRC1*). It is mostly expressed in macrophages, dendritic cells, and endothelial cells, where it functions as a receptor for mannosylated ligands, such as microbial antigens (27). In neural tissues, expression of CD206 is observed in microglia (28, 29) and astrocytes (30, 31). CD206 is widely recognized as a representative M2 microglial marker (29, 32). CD206 is involved in important cellular functions, especially in pinocytosis and phagocytosis (28, 31, 33). Therefore, CD206 is suggested to play a critical role in the first step of the recognition and capture of pathogens in neural tissues (31). A recent study has suggested a positive correlation between the World Health Organization pathological grades and the numbers of CD206-positive GAM in human glioma tumor tissues (21). Interestingly, we reported that CD206 expression in iMG cells was downregulated in patients with bipolar disorder during the manic state (34). Based on that study, we proposed that iMG cells could be candidate surrogate cells to monitor the immune environment that comprises other CD206-expressing cells in CNS diseases.

We hypothesized further that iMG cells from patients with glioma might reflect the immune properties of GAM and thereby serve as a novel biomarker of glioma. To clarify this hypothesis, we compared the immunological states of blood-derived iMG cells with those of brain-derived microglia. Further, we investigated the specificity of biological properties of these cells, which were isolated from glioma patients.

MATERIALS AND METHODS

Patients

Microglia were isolated from the residual resected brain tissue after sampling for the pathological diagnosis from the surgical removal of subcortical or deeply located mass lesions (N = 15) or following epileptic surgery (N = 7) in a total of 22 patients (**Table 1**). During surgeries for the removal of nine gliomas (grade II, N = 2; grade III, N = 2; grade IV, N = 5) and six radiographic glioma-like mass lesions (meningioma, N = 1; metastatic tumor, N = 2; brain abscess, N = 1; encephalitis, N = 1; radiation necrosis, N = 1), the samples for microglia isolation were obtained from the surgical corridor during

TABLE 1 | Summary of the pathological characteristics of samples and period from subdural electrode placements.

Case No.	Sex	Diagnosis	since placement of subdural electrodes	inflammatory infiltrates due to subdural electrode placements	collect blood for Induction of iMG cells
1	Male	Tuberous sclerosis	none	n/a	–
2	Male	Epilepsy (Old cerebral contusion)	14 days	–	+
3	Female	Epilepsy	none	n/a	+
4	Male	Epilepsy	14 days	+	–
5	Male	Focal cortical dysplasia	14 days	+	+
6	Male	Focal cortical dysplasia	9 days	+	+
7	Male	Focal cortical dysplasia	7 days	–	–
8	Male	Secretory meningioma	none	n/a	+
9	Female	Radiation necrosis (chronic encapsulated expanding hematoma)	none	n/a	+
10	Male	Suspected encephalitis	none	n/a	+
11	Male	Brain abscess	none	n/a	+
12	Female	Metastatic brain tumor	none	n/a	+
13	Female	Metastatic brain tumor	none	n/a	+
14	Female	Diffuse astrocytoma (WHO grade II)	none	n/a	+
15	Male	Diffuse astrocytoma (WHO grade II)	none	n/a	+
16	Female	Anaplastic astrocytoma (WHO grade III)	none	n/a	+
17	Male	Anaplastic ganglioglioma (WHO grade III)	none	n/a	+
18	Female	Glioblastoma (WHO grade IV)	none	n/a	+
19	Female	Glioblastoma (WHO grade IV)	none	n/a	+
20	Female	Glioblastoma (WHO grade IV)	none	n/a	+
21	Male	Glioblastoma (WHO grade IV)	none	n/a	+
22	Female	Glioblastoma (WHO grade IV)	none	n/a	+

n/a, not applicable.

the approach to the lesion. In five of the seven patients with epilepsy, sampling for microglia isolation was performed at the resected epileptogenic lesion detected using chronic subdural electrodes placed during a prior surgery 1 or 2 weeks before. Resected brain tissues were immediately placed on ice and transferred to the laboratory for microglia isolation within 2 h of resection.

Primary Microglia Isolation

Human tissue samples were dissociated using a Neural Tissue Dissociation Kit (Miltenyi Biotec, Bergisch-Gladbach, Germany), according to the manufacturer's instructions (**Figure 1**). The cell suspension was incubated with CD11b microbeads (Miltenyi Biotec) in the MACS buffer (Miltenyi Biotec) for 15 min at 4°C. Afterward, the cells were washed, resuspended, and transferred to an LS column (Miltenyi Biotec) within a magnetic field. The positively selected ($CD11b^+$) microglia were collected and resuspended in the Microglia Medium (ScienCell, Carlsbad, CA, USA). Primary microglia (pMG) were plated on culture dishes at a density of 3×10^5 cells/mL and cultured overnight in standard culture conditions (37 °C, 5% CO_2). After overnight incubation, culture supernatant and non-adherent cells were removed. Microglia were cultured in RPMI-1640 Glutamax (Invitrogen, Carlsbad, CA, USA) supplemented with 1% antibiotic/antimycotic, recombinant human granulocyte macrophage colony-stimulating factor (GM-CSF) (10 ng/mL; R&D Systems, Minneapolis, MN, USA) and recombinant human IL-34 (100 ng/mL; R&D Systems) for 5 days.

Preparation of iMG Cells From Human Peripheral Blood

Peripheral blood was collected into a heparinized tube from patients with brain tumors, epilepsy, or other brain diseases (**Figure 1**). In three patients with epilepsy, consent to collect blood was not obtained. Peripheral blood mononuclear cells (PBMCs) were isolated using Histopaque-1077 (Sigma Chemical Co., St. Louis, MO, USA) density gradient centrifugation. PBMCs were resuspended in RPMI-1640 (Nacalai Tesque, Kyoto, Japan) supplemented with 10% heat-inactivated fetal bovine serum (Japan Bio Serum, Hiroshima, Japan) and 1% antibiotic/antimycotic (Invitrogen). PBMCs were plated on culture dishes at a density of 4×10^5 cells/mL and cultured overnight in standard culture conditions (37 °C, 5% CO_2). After overnight incubation, culture supernatant and non-adherent cells were removed. Adherent cells (monocytes) were cultured in RPMI-1640 Glutamax supplemented with 1% antibiotic/antimycotic, recombinant human GM-CSF (10 ng/mL), and recombinant human IL-34 (100 ng/mL) for 14 days to obtain iMG cells (22, 23).

Quantitative Reverse Transcription-Polymerase Chain Reaction

To assess gene expression patterns in microglia and iMG cells, qRT-PCR was performed using a LightCycler 480 system (Roche Diagnostics, Mannheim, Germany). Microglia and iMG cells were washed. Total RNA was extracted using a High Pure RNA Isolation kit (Roche Diagnostics) according to the manufacturer's protocol and used for cDNA synthesis using a Transcriptor First Strand cDNA Synthesis kit (Roche Diagnostics). qRT-PCR for representative markers of M1 and M2 microglia phenotypes was performed using their respective primers (**Table 2**). Normalization was performed using the reference gene glyceraldehyde-3-phosphate dehydrogenase (*GAPDH*) from the Universal ProbeLibrary (Roche Diagnostics) and the ΔΔCt method.

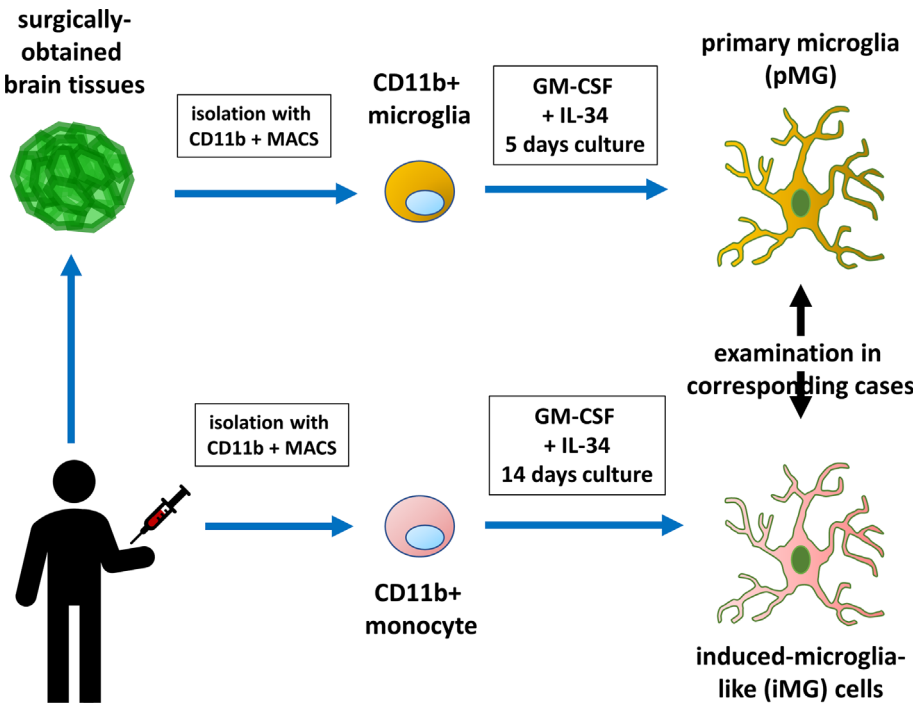

FIGURE 1 | Diagram illustrating primary microglia and induced microglia-like cell collection and experiment. Monocytes isolated from the patients were induced to develop into microglia-like (iMG) cells. The biological properties of iMG cells were compared with those of brain-derived primary microglia.

Immunohistochemistry

The resected brain tissues around the tumors were fixed in 10% neutral buffered formalin, embedded in paraffin, and processed for immunohistochemistry. The expression levels of the following microglia/macrophage markers were investigated in 4 μm serial paraffin sections: Iba-1 (pan-microglia/macrophage marker), CD68 (lysosomal protein; highly expressed by macrophages and activated microglia), and CD206 (mannose receptor, M2 marker). Goat antibody for Iba-1 (Cat. #ab5076, Abcam, Cambridge, MA, USA; 1:500 dilution, RRID: AB_2224402), rabbit antibody for CD206 (Cat. #ab64693, Abcam, Cambridge, MA, USA; 1:1000 dilution, RRID: AB_1523910), and mouse antibody for CD68 (Cat. #M0814, Dako, Carpinteria, CA, USA; 1:200 dilution, RRID: AB_2314148) were used as the primary antibodies. The sections were incubated with primary antibodies at 4°C overnight. Immunoreaction products were detected using the polymer immunocomplex method by an Envision system (Dako). The sections were counterstained with hematoxylin. Immunoreactivity was detected using 3,3′-diaminobenzidine (Dojindo, Kumamoto, Japan). The negative control experiments for CD 206, Iba-1, and CD68 were performed without primary antibodies (**Supplementary Figure S1**).

Statistical Analyses

Results are expressed as the mean ± standard deviation (SD). The Spearman's correlation coefficient was used for analyzing the correlation between parameters in pMG and iMG cells. Statistical significance was determined at $\alpha = 0.05$ level. Differences were considered statistically significant when *P*-values were <0.05. Each experiment was conducted with four independent cell cultures; however, in some cases, the number of pMG or iMG cells was small and the number of samples was <4 [N = 3.68 (SD ±0.7790)].

RESULTS

Gene Expression in Human GAM and iMG Cells

Total RNA was isolated from these paired samples to investigate the expression profiles of pMG cells isolated from brain tissue and the corresponding blood-derived iMG cells. PCR was performed to determine the expression levels of inflammation-related genes known as representative markers for M1 microglia and macrophage phenotype (CD45, CD80, HLA-DR, TNF-α, IL-1β, and IL-23) and M2 phenotype (CD206, CD209, CD23, BDNF, IL-10, and CCL18) (**Supplementary Table S1**). Spearman's correlation analysis revealed that expression levels of inflammation-related genes in the paired pMG and iMG cells derived from the same patient significantly correlated (Spearman's correlation coefficient = 0.5225, $P < 0.0001$), indicating that iMG cells exhibited disease-related phenotypes and were regulated synchronously with the corresponding pMG (**Figure 2**).

TABLE 2 | Primer sequences used for qRT-PCR.

M1 marker	
CD80	
L	GAAGCAAGGGGCTGAAAAG
R	GGAAGTTCCCAGAAGAGGTCA
CD45	
L	AGTCAAAGTTATTGTTATGCTGACAGA
R	TGCTTTCCTTCTCCCCAGTA
HLA-DR	
L	CCCAGGGAAGACCACCTTT
R	CACCCTGCAGTCGTAAACGT
TNF-α	
L	CAGCCTCTTCTCCTTCCTGAT
R	GCCAGAGGGCTGATTAGAGA
IL-1β	
L	TACCTGTCCTGCGTGTTGAA
R	TCTTTGGGTAATTTTTGGGATCT
IL-23	
L	AGCTTCATGCCTCCCTACTG
R	CTGCTGAGTCTCCCAGTGGT
M2 marker	
CD206	
L	CACCATCGAGGAATTGGACT
R	ACAATTCGTCATTTGGCTCA
CD209	
L	AGCTGACCTGGCTGAAGG
R	GTTTCCTTGGAAGAATGTCCA
BDNF	
L	GTAACGGCGGCAGACAAA
R	GACCTTTTCAAGGACTGTGACC
CD23	
L	ACAGGAACTTGGAACAAGCAG
R	CCAGCAGCACGATCTGAGT
CCL18	
L	ATGGCCCTCTGCTCCTGT
R	AATCTGCCAGGAGGTATAGACG
IL-10	
L	GATGCCTTCAGCAGAGTGAA
R	GCAACCCAGGTAACCCTTAAA

Next, to identify glioma-specific transcripts in GAM, the qPCR results were compared between the glioma group (GLI group; N = 9) and radiographic glioma-like mass lesion group (RGM group, N = 6; meningioma, N = 1; metastatic tumor, N = 2; brain abscess, N = 1; encephalitis, N = 1; and radiation necrosis, N = 1). Among the analyzed markers, the expression of CD206, known as an M2 marker, was synchronously upregulated in pMG and iMG cells in six of the nine patients (67%) in the GLI group (**Figure 3A**). Upregulation of CD206 expression in pMG and iMG cells was particularly pronounced in individuals with GBM, as this phenomenon was observed in four of the five patients studied (80%). The characteristics of the patients from the GLI group are summarized in **Table 3**, revealing no clear predictive biomarker or background characteristics correlating with CD206 upregulation. In the RGM group, synchronous upregulation of CD206 expression was detected only in two (meningioma and brain abscess) of the six (33%) patients (**Figure 3B**). The brain tissue around the tumor of the patient with meningioma showed reactive astrocytes and edematous change probably because of the physical compression (**Supplementary Figure S2**). The surrounding tissue of the patient with brain abscess showed edematous change and infiltration of inflammatory cells. There was no increment in CD206 expression level in two patients with metastatic tumor and two patients who underwent removal of tumor-suspected lesions (radiation necrosis) and encephalitis suspected lesion. Altogether, CD206 upregulation in microglia shown in the surrounding tissue might be a hallmark of glioma, especially in GBM, and can be detected by isolating iMG cells from the peripheral blood of patients.

Expression CD206, Iba-1, and CD68 in Human Brain Tumor Samples

To assess the invasion of microglia/macrophages in the brain tissue around the tumor, tissue samples of grade II–IV glioma and metastatic tumor were analyzed using immunohistochemistry (**Figures 4A–D**). Interestingly, the Iba1-positive GAM fraction was the most predominant in all tumors, followed by a slightly lower proportion of cells positive for CD68, a marker for the activated microglia. CD206 tended to be highly expressed in brain tissue surrounding GBM, and conversely, it was weakly expressed in all metastatic brain tumors and grade III gliomas. In grade II gliomas, CD206-positive GAM were present in high numbers. These results were consistent with the PCR results in all tumor cases.

DISCUSSION

Our study demonstrates that some immune properties of GAM can be monitored using iMG cells isolated from peripheral blood. In recent years, the development of drugs targeting tumor immunity has progressed rapidly. In particular, immune checkpoint inhibitors have already been confirmed to be effective in clinical trials for tumors such as melanoma (2); however, these drugs have not been proven effective for GBM. Mounting evidence has demonstrated that immune response is involved in the development and progression of GBM (14); therefore, a thorough investigation of the underlying molecular and immunologic mechanisms of GBM tumorigenesis is important for developing novel interventions. Our study demonstrated that the specific immune status of glioma might be monitored using peripheral iMG cells, which can be utilized as an effective research tool for the elucidation of immunologic mechanisms of tumorigenesis. Furthermore, GAM that play a role in supporting tumor invasion (35) may become a new target for immunotherapy of GBM in the future.

Our study revealed the specific upregulation of CD206 in iMG cells isolated from the peripheral blood of patients with glioma. These findings indicate that our technique can be used to develop a diagnostic marker for glioma. Although neuroradiological examinations, such as computed tomography and magnetic resonance imaging, are mainly performed as standard clinical examinations for the preoperative diagnosis of GBM, radiographic characteristics of GBM are similar to those of other neuronal

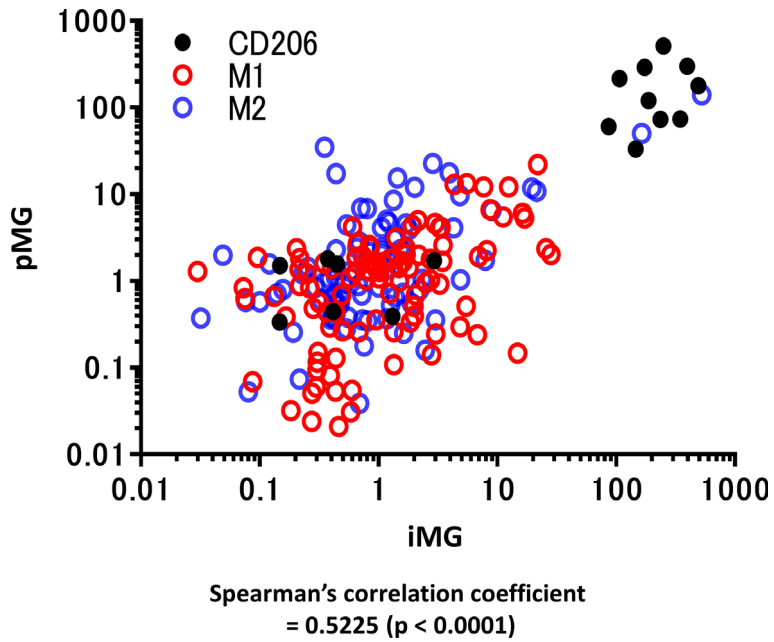

FIGURE 2 | qRT-PCR for representative M1 and M2 microglial markers in primary microglia and induced microglia-like cells. mRNA levels of M1 and M2 microglia markers (12 types in total) were measured using qRT-PCR in 19 cases in which total mRNA was extracted from both induced microglia-like (iMG) cells and primary microglia (pMG). Each value was compared with the control (epilepsy cases without inflammatory infiltrates due to subdural electrode placements, N = 2) to investigate the correlation between iMG and pMG parameters. The expression levels of inflammation-related genes significantly correlated in pMG and iMG cells from the same patients (Spearman's correlation coefficient = 0.5225, $P < 0.0001$). Red circles indicate M1 markers, M2 markers are indicated by blue circles, and CD206 is indicated by black dots. qRT-PCR was performed in four independent cell cultures; however, in some cases, the number of pMG or iMG cells was small, and the number of samples was <4 [N = 3.68 (SD ±0.7790)].

diseases, including metastatic brain tumor, brain abscess, and primary CNS lymphoma. Therefore, the development of a tumor-specific marker for GBM would greatly facilitate the presurgical confirmation of diagnosis. There have been several recent attempts of molecular diagnosis of gliomas using cerebrospinal fluid (36, 37); however, those techniques have not achieved the detection of glioma-specific mutations in peripheral blood cells. Recently, several reports on serum microRNAs can distinguish patients with gliomas from healthy controls with high sensitivity and specificity (38, 39). Zhou et al. (40) reviewed 28 reports on the diagnosis of glioma using microRNAs and reported overall sensitivity of 85% and specificity of 90%. Although these studies suggested that microRNA levels are useful for distinguishing glioma and non-glioma cases, a complete consensus has not been reached to date. Our report provides a novel alternative approach for developing a non-invasive diagnostic tool for brain tumors based on a peripheral blood test.

We have previously reported that CD206 expression in iMG cells was downregulated in manic patients with bipolar disorder (34). We hypothesized that psychiatric states change microglial polarization and affect the immune environment, associated with changes in CD206 expression levels. The present study extends the significance of CD206 expression in iMG cells as a marker to glioma, another CNS disease.

Our study revealed the upregulation of CD206 expression using qRT-PCR of microglia extracted from brain tissues around GBM in four of the five studied cases. Few studies have reported that GAM are associated with the pathological grade and prognosis of gliomas. A positive correlation between the World Health Organization pathological grades and the expression of CD206-positive GAM has been reported in human glioma tumor tissues (21). GAM may be induced to M2 polarization by glioma-secreted factors, thereby supporting tumor invasion and growth (35). In low-grade gliomas, Lee et al. reported correlations between malignant transformation, *CX3CR1* V249I gene polymorphisms, and tumor immune microenvironment. Tumors from patients that were heterozygous or homozygous for *CX3CR1* V249I polymorphisms showed less infiltration of M2 macrophages and had a better prognosis than those in patients without these mutations (41).

We found that iMG cells derived from the peripheral blood showed similar CD206 profiles to pMG in the brain. Recently, some reports have shown that extracellular vesicles derived from GBM can change the phenotype of GAM to an M2-like anti-inflammatory phenotype (42, 43). Gabrusiewicz et al. showed that exosomes secreted from GBM stem cells mainly targeted peripheral blood monocytes to induce immune suppressive M2 phenotype by secreting cytokines such as monocyte chemotactic protein-3 and chemokine (C-X-C motif) ligand 1 (44). Thus, not only the interaction between GBM and GAM, but also between GBM and peripheral blood monocytes through humoral factors and/or extracellular vesicles may reflect the microenvironment of

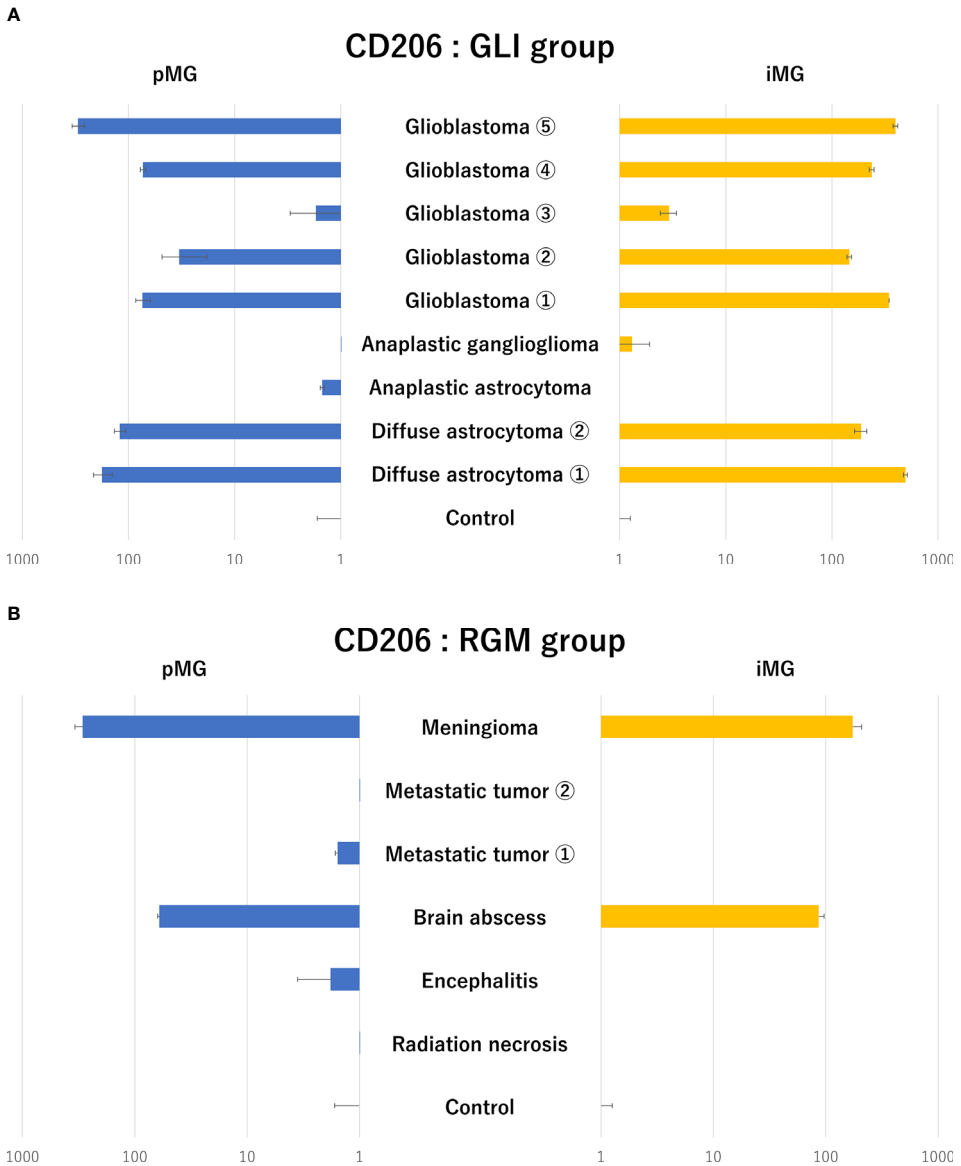

FIGURE 3 | Expression levels of CD206 in primary microglia and induced microglia-like cells in patients with glioma and radiographic glioma-like mass lesions. **(A)** CD206 expression levels in primary microglia (pMG) and induced microglia-like (iMG) cells in patients with glioma (GLI group) compared to those in control samples. Synchronous upregulation in CD206 expression was detected in pMG and iMG cells in six of the nine (66%) patients, and especially in four of the five (80%) patients with GBM. **(B)** CD206 expression levels in pMG and iMG cells in patients with a radiographic glioma-like mass lesion (RGM group) compared to those in control samples. Synchronous upregulation of CD206 expression was detected in two of the six (33%) patients. We compared CD206 expression levels in the GLI and RGM groups with those from epilepsy patients as control due to the lack of samples from healthy individuals.

gliomas and can be detected by analyzing iMG cells derived from peripheral monocytes.

Limitations

Studying human GAM has two major challenges. Control tissues are derived from post-mortem tissues or diseased non-tumor patients and, most notably, from epileptic patients because of the lack of naive control samples. However, the brain tissues obtained from patients with epilepsy are not completely normal. The second challenge is the current lack of reliable surface markers for distinguishing brain-resident microglia from infiltrating myeloid cells in the human brain. Experiments with functional assays and flow cytometry would be required to evaluate how closely iMG cells reflect the immunological activity of GAM. However, these experiments could not be performed in this study because the number of cells collected was limited. In several epilepsy patients, non-specific upregulation of microglial markers, including CD206, were observed in tissue samples

TABLE 3 | Summary of the pathological characteristics and genetic mutations in patients from the glioma group.

Case No.	14	15	16	17	18	19	20	21	22
Diagnosis	DA	DA	AA	AG	GBM	GBM	GBM	GBM	GBM
CD206 upregulation	+	+	–	–	+	+	–	+	+
ATRX	loss	loss	loss	retained	retained	loss	retained	retained	retained
Ki-67	11.10%	2.40%	4.60%	19.50%	40.90%	36%	17.60%	56.40%	60.00%
IDH1 or 2	wild type	mutant	mutant	wild type	wild type	mutant	wild type	wild type	wild type
BRAF	wild type	wild type	wild type	wild type	wild type	wild type	wild type	wild type	wild type
H3F3A	wild type	wild type	wild type	mutant	wild type	wild type	wild type	wild type	wild type
MGMT	methylated	methylated	methylated	unmethylated	unmethylated	methylated	methylated	methylated	unmethylated
TERT-p	wild type	wild type	wild type	wild type	wild type	wild type	wild type	mutant	wild type
EGFR	wild type	gain	wild type	wild type	wild type	wild type	gain	gain	gain
CDKN2A/B	wild type	wild type	wild type	wild type	wild type	wild type	wild type	wild type	hemizygous deletion
PTEN	wild type	wild type	wild type	wild type	wild type	wild type	wild type	loss	loss
p53	wild type	heterozygous	wild type	loss	loss	heterozygous	loss	loss	loss
chr10 LOH	retained	retained	partial	retained	total	retained	retained	total	total
CDK4	wild type	wild type	loss	wild type	wild type	wild type	wild type	amplified	wild type
PDGFRA	wild type	wild type	wild type	wild type	wild type	wild type	wild type	amplified	wild type

DA, Diffuse astrocytoma (WHO grade II); AA, Anaplastic astrocytoma (WHO grade III); AG, Anaplastic ganglioglioma (WHO grade III); GBM, Glioblastoma (WHO grade IV).

obtained by the second look surgeries performed approximately 1 or 2 weeks after craniotomies for subdural electrode placements. Histopathological examination of such tissue samples revealed infiltration of chronic inflammatory cells in the subarachnoid space. Physical brain damage caused the infiltration of inflammatory cells, which was thought to have affected the upregulation of CD206 expression (45–47).

In this study, synchronous upregulation of CD206 expression levels was observed in most patients with glioma; however, patients with meningioma and brain abscess showed similar levels. Identifying differences in the properties of microglia and iMG cells between glioma, meningioma, and brain abscess is recommended for future studies. As recent attempts to identify markers distinguishing microglia and monocytes/macrophages have not reached any consensus (48, 49), we analyzed human data using a sorting method based on $CD11b^+$ MACS: this approach assesses all myeloid cells, including monocytes, macrophages, dendritic cells, and neutrophils, besides microglia. Our findings were based on a limited number of patients with brain tumors, including GBM, and a limited number of epilepsy patients as control. Therefore, future studies with a larger number of patients will be necessary to confirm our results.

CONCLUSION

In summary, our study revealed that peripheral iMG cells obtained by our previously developed technique can be used to gauge the properties of pMG from the tumor lesion microenvironment in the CNS. Therefore, iMG cells are novel, less-invasive tools for monitoring the disease-related immunological state of microglia. They can be used to investigate the roles of microglia in various brain diseases, including glioma. The upregulation of CD206 expression detected using iMG cells has the potential to be used as a glioma biomarker. Our study represents the first step towards understanding the contribution of GAM to the proliferation and invasion of GBM cells. Further studies are needed for investigating the role of microglia in GBM as a better understanding of GAM roles in GBM may provide a new therapeutic target for GBM treatment.

DATA AVAILABILITY STATEMENT

The original contributions presented in the study are included in the article/**Supplementary Material**, further inquiries can be directed to the corresponding author/s.

ETHICS STATEMENT

The studies involving human participants were reviewed and approved by The ethics committee of the Graduate School of Medical Sciences, Kyushu University (application number: 26-406 and 29-624). Written informed consent to participate in this study was provided by the participants' legal guardian/next of kin. Informed consent was obtained from the patients whose brain tissues had to be resected during the operative procedure for the treatment of brain diseases under a protocol approved by the Ethics Committee of the Graduate School of Medical Sciences at the Kyushu University (application number: 26-406 and 29-624). Freshly resected patient samples and blood samples were provided by the Department of Neurosurgery of the Kyushu University Hospital. Consent to collect blood was not obtained in three patients with epilepsy due to their young age and low body weight. Handling and analysis of these tissues were performed with the approval of the Ethical Committee and according to the principles of the Declaration of Helsinki.

AUTHOR CONTRIBUTIONS

ST, MO, NH, and TK designed the study. ST and MO conducted the experiments, analyzed the results, and wrote the manuscript.

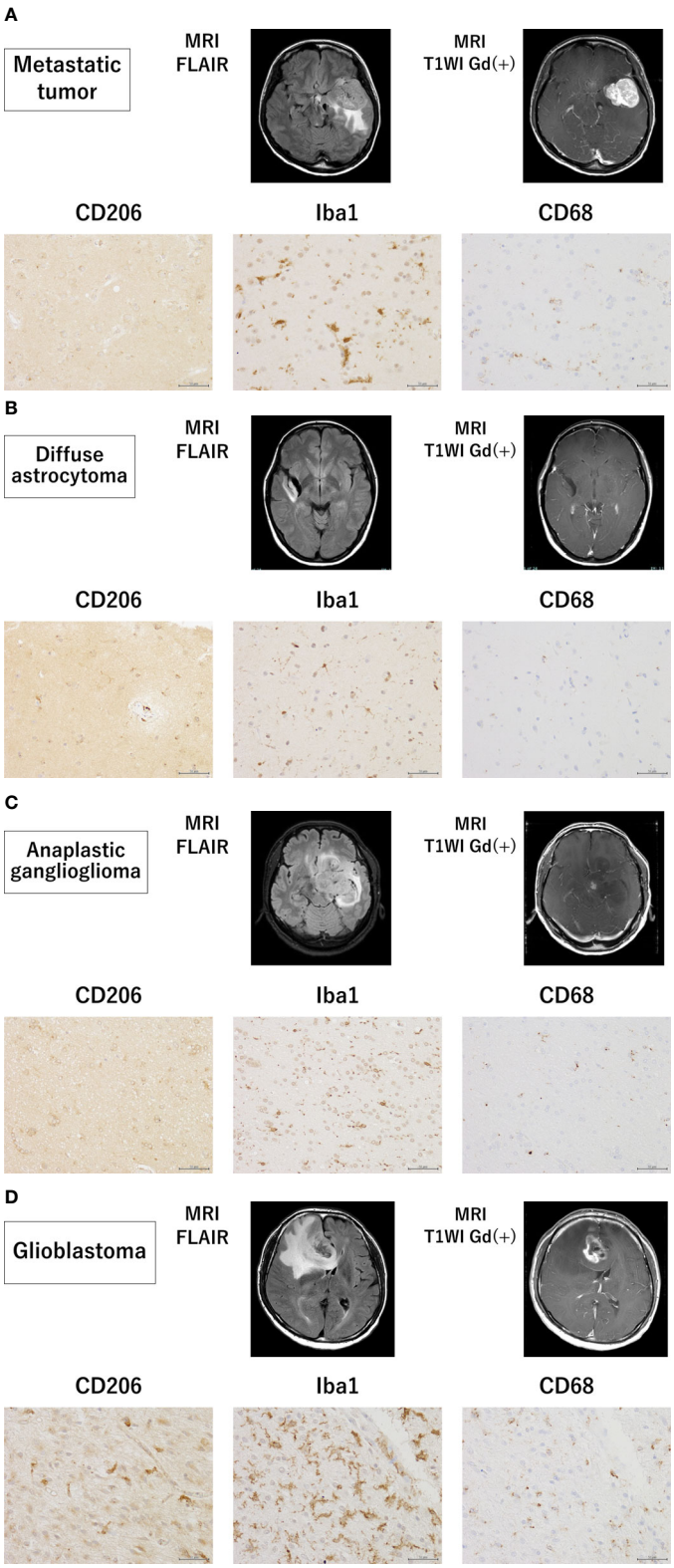

FIGURE 4 | Magnetic resonance imaging findings and immunohistochemistry staining in samples from patients with grade II–IV glioma and metastatic tumor. Magnetic resonance imaging findings and representative immunohistochemical staining for CD206, Iba-1, and CD68 of the brain tissues surrounding a metastatic tumor **(A)** and glioma (WHO grade II–IV) **(B–D)** (scale bars = 50 μm).

SI, NSa, NSh, YFuj, KT, and YFun performed the experiments. SS and HH analyzed the data. NH, NM, RH, YS, TI, MH, KI, MM, and TK critically revised the manuscript. All authors contributed to the article and approved the submitted version.

FUNDING

This work was partially supported by Grants-in-Aid for Scientific Research from (1) The Japan Agency for Medical Research and Development (Syogaisya-Taisaku-Sogo-Kenkyu-Kaihatsu-Jigyo to TK (JP18dk0307075), Yugo-No to TK (JP19dm0107095), and MH (JP19ek0610015)), (2) KAKENHI - the Japan Society for the Promotion of Science (JP26713039, JP15K15431, JP16H03741, JP16H06403, JP18H04042 & JP19K21591 to TK, JP19K17065 to MO, JP20K09392 to NH, JP21H03044 to MM), and (3) SENSHIN Medical Research Foundation (to TK). The funders had no role in study design, data collection, and analysis, decision to publish, or manuscript preparation.

ACKNOWLEDGMENTS

We thank Ms. Aki Sako and Ms. Aya Yamada for their technical assistance. We would like to thank Editage (www.editage.com) for English language editing.

SUPPLEMENTARY MATERIAL

The Supplementary Material for this article can be found online at: https://www.frontiersin.org/articles/10.3389/fimmu.2021.670131/full#supplementary-material

Supplementary Figure 1 | Negative control staining for CD 206, Iba-1, and CD68 in patients with grade II–IV glioma and metastatic tumor. The negative controls for CD 206, Iba-1, and CD68 of the brain tissues surrounding metastatic tumor **(A)** and glioma (WHO grade II–IV) **(B–D)** (scale bars = 50 μm).

Supplementary Figure 2 | Hematoxylin and eosin staining of the brain tissue around the tumor of a patient with secretory meningioma. The brain tissue around the tumor of a patient with secretory meningioma showed reactive astrocytes and edematous change (scale bars = 50 μm).

REFERENCES

1. Dolecek TA, Propp JM, Stroup NE, Kruchko C. CBTRUS Statistical Report: Primary Brain and Central Nervous System Tumors Diagnosed in the United States in 2005-2009. *Neuro Oncol* (2012) 14 Suppl 5:v1–49. doi: 10.1093/neuonc/nos218
2. Robert C, Ribas A, Schachter J, Arance A, Grob J-J, Mortier L, et al. Pembrolizumab Versus Ipilimumab in Advanced Melanoma (KEYNOTE-006): Post-Hoc 5-Year Results From an Open-Label, Multicentre, Randomised, Controlled, Phase 3 Study. *Lancet Oncol* (2019) 20(9):1239–51. doi: 10.1016/s1470-2045(19)30388-2
3. Wolchok JD, Chiarion-Sileni V, Gonzalez R, Rutkowski P, Grob JJ, Cowey CL, et al. Overall Survival With Combined Nivolumab and Ipilimumab in Advanced Melanoma. *N Engl J Med* (2017) 377(14):1345–56. doi: 10.1056/NEJMoa1709684
4. Omuro A, Vlahovic G, Lim M, Sahebjam S, Baehring J, Cloughesy T, et al. Nivolumab With or Without Ipilimumab in Patients With Recurrent Glioblastoma: Results From Exploratory Phase I Cohorts of CheckMate 143. *Neuro Oncol* (2018) 20(5):674–86. doi: 10.1093/neuonc/nox208
5. Filley AC, Henriquez M, Dey M. Recurrent Glioma Clinical Trial, CheckMate-143: The Game is Not Over Yet. *Oncotarget* (2017) 8(53):91779–94. doi: 10.18632/oncotarget.21586
6. Wolf SA, Boddeke HW, Kettenmann H. Microglia in Physiology and Disease. *Annu Rev Physiol* (2017) 79:619–43. doi: 10.1146/annurev-physiol-022516-034406
7. Mosser DM, Edwards JP. Exploring the Full Spectrum of Macrophage Activation. *Nat Rev Immunol* (2008) 8(12):958–69. doi: 10.1038/nri2448
8. Kettenmann H, Hanisch UK, Noda M, Verkhratsky A. Physiology of Microglia. *Physiol Rev* (2011) 91(2):461–553. doi: 10.1152/physrev.00011.2010
9. Mantovani A, Sica A, Sozzani S, Allavena P, Vecchi A, Locati M. The Chemokine System in Diverse Forms of Macrophage Activation and Polarization. *Trends Immunol* (2004) 25(12):677–86. doi: 10.1016/j.it.2004.09.015
10. Ye XZ, Xu SL, Xin YH, Yu SC, Ping YF, Chen L, et al. Tumor-Associated Microglia/Macrophages Enhance the Invasion of Glioma Stem-Like Cells Via TGF-beta1 Signaling Pathway. *J Immunol* (2012) 189(1):444–53. doi: 10.4049/jimmunol.1103248
11. da Fonseca AC, Badie B. Microglia and Macrophages in Malignant Gliomas: Recent Discoveries and Implications for Promising Therapies. *Clin Dev Immunol* (2013) 2013:264124. doi: 10.1155/2013/264124
12. Rossi ML, Hughes JT, Esiri MM, Coakham HB, Brownell DB. Immunohistological Study of Mononuclear Cell Infiltrate in Malignant Gliomas. *Acta Neuropathol* (1987) 74(3):269–77. doi: 10.1007/BF00688191
13. Wood GW, Morantz RA. Immunohistologic Evaluation of the Lymphoreticular Infiltrate of Human Central Nervous System Tumors. *J Natl Cancer Inst* (1979) 62(3):485–91. doi: 10.1093/jnci/62.3.485
14. Hambardzumyan D, Gutmann DH, Kettenmann H. The Role of Microglia and Macrophages in Glioma Maintenance and Progression. *Nat Neurosci* (2016) 19(1):20–7. doi: 10.1038/nn.4185
15. Bettinger I, Thanos S, Paulus W. Microglia Promote Glioma Migration. *Acta Neuropathol* (2002) 103(4):351–5. doi: 10.1007/s00401-001-0472-x
16. Watters JJ, Schartner JM, Badie B. Microglia Function in Brain Tumors. *J Neurosci Res* (2005) 81(3):447–55. doi: 10.1002/jnr.20485
17. Qian J, Luo F, Yang J, Liu J, Liu R, Wang L, et al. Tlr2 Promotes Glioma Immune Evasion by Downregulating Mhc Class Ii Molecules in Microglia. *Cancer Immunol Res* (2018) 6(10):1220–33. doi: 10.1158/2326-6066.Cir-18-0020
18. Zhang Z, Xu J, Chen Z, Wang H, Xue H, Yang C, et al. Transfer of MicroRNA Via Macrophage-Derived Extracellular Vesicles Promotes Proneural-to-Mesenchymal Transition in Glioma Stem Cells. *Cancer Immunol Res* (2020) 8(7):966–81. doi: 10.1158/2326-6066.Cir-19-0759
19. Wei J, Gabrusiewicz K, Heimberger A. The Controversial Role of Microglia in Malignant Gliomas. *Clin Dev Immunol* (2013) 2013:285246. doi: 10.1155/2013/285246
20. Gjorgjevski M, Hannen R, Carl B, Li Y, Landmann E, Buchholz M, et al. Molecular Profiling of the Tumor Microenvironment in Glioblastoma Patients: Correlation of Microglia/Macrophage Polarization State With Metalloprotease Expression Profiles and Survival. *Biosci Rep* (2019) 39(6):BSR20182361. doi: 10.1042/BSR20182361
21. Ding P, Wang W, Wang J, Yang Z, Xue L. Expression of Tumor-Associated Macrophage in Progression of Human Glioma. *Cell Biochem Biophys* (2014) 70(3):1625–31. doi: 10.1007/s12013-014-0105-3
22. Ohgidani M, Kato TA, Setoyama D, Sagata N, Hashimoto R, Shigenobu K, et al. Direct Induction of Ramified Microglia-Like Cells From Human Monocytes: Dynamic Microglial Dysfunction in Nasu-Hakola Disease. *Sci Rep* (2014) 4:4957. doi: 10.1038/srep04957
23. Ohgidani M, Kato TA, Kanba S. Introducing Directly Induced Microglia-Like (iMG) Cells From Fresh Human Monocytes: A Novel Translational Research Tool for Psychiatric Disorders. *Front Cell Neurosci* (2015) 9:184. doi: 10.3389/fncel.2015.00184
24. Sato-Kasai M, Kato TA, Ohgidani M, Mizoguchi Y, Sagata N, Inamine S, et al. Aripiprazole Inhibits polyI:C-Induced Microglial Activation Possibly Via TRPM7. *Schizophr Res* (2016) 178(1-3):35–43. doi: 10.1016/j.schres.2016.08.022
25. Atoshi Banerjee YL, Do K, Mize T, Wu X, Chen X, Chen J. Validation of Induced Microglia-Like Cells (Img Cells) for Future Studies of Brain Diseases. *Front Cell Neurosci* (2021) 15:629279. doi: 10.3389/fncel.2021.629279

26. Sellgren CM, Sheridan SD, Gracias J, Xuan D, Fu T, Perlis RH. Patient-Specific Models of Microglia-Mediated Engulfment of Synapses and Neural Progenitors. *Mol Psychiatry* (2017) 22(2):170–7. doi: 10.1038/mp.2016.220
27. Stahl PD, Ezekowitz RAB. The Mannose Receptor is a Pattern Recognition Receptor Involved in Host Defense. *Curr Opin Immunol* (1998) 10(1):50–5. doi: 10.1016/S0952-7915(98)80031-9
28. Marzolo MP, von Bernhardi R, Inestrosa NC. Mannose Receptor is Present in a Functional State in Rat Microglial Cells. *J Neurosci Res* (1999) 58(3):387–95. doi: 10.1002/(Sici)1097-4547(19991101)58:3<387::Aid-Jnr4>3.0.Co;2-L
29. Durafourt BA, Moore CS, Zammit DA, Johnson TA, Zaguia F, Guiot MC, et al. Comparison of Polarization Properties of Human Adult Microglia and Blood-Derived Macrophages. *Glia* (2012) 60(5):717–27. doi: 10.1002/glia.22298
30. Burudi EME, Riese S, Stahl PD, Rgnier-Vigouroux A. Identification and Functional Characterization of the Mannose Receptor in Astrocytes. *Glia* (1999) 25(1):44–55. doi: 10.1002/(sici)1098-1136(19990101)25:1<44::Aid-glia5>3.0.Co;2-c
31. Régnier-Vigouroux A. The Mannose Receptor in the Brain. *Int Rev Cytol* (2003) 226:321–42. doi: 10.1016/s0074-7696(03)01006-4
32. Kobayashi K, Imagama S, Ohgomori T, Hirano K, Uchimura K, Sakamoto K, et al. Minocycline Selectively Inhibits M1 Polarization of Microglia. *Cell Death Dis* (2013) 4:e525. doi: 10.1038/cddis.2013.54
33. Zimmer H, Riese S, Regnier-Vigouroux A. Functional Characterization of Mannose Receptor Expressed by Immunocompetent Mouse Microglia. *Glia* (2003) 42(1):89–100. doi: 10.1002/glia.10196
34. Ohgidani M, Kato TA, Haraguchi Y, Matsushima T, Mizoguchi Y, Murakawa-Hirachi T, et al. Microglial CD206 Gene Has Potential as a State Marker of Bipolar Disorder. *Front Immunol* (2016) 7:676. doi: 10.3389/fimmu.2016.00676
35. Pyonteck SM, Akkari L, Schuhmacher AJ, Bowman RL, Sevenich L, Quail DF, et al. Csf-1R Inhibition Alters Macrophage Polarization and Blocks Glioma Progression. *Nat Med* (2013) 19(10):1264–72. doi: 10.1038/nm.3337
36. Huang SW, Ali ND, Zhong L, Shi J. MicroRNAs as Biomarkers for Human Glioblastoma: Progress and Potential. *Acta Pharmacol Sin* (2018) 39(9):1405–13. doi: 10.1038/aps.2017.173
37. Fujioka Y, Hata N, Akagi Y, Kuga D, Hatae R, Sangatsuda Y, et al. Molecular Diagnosis of Diffuse Glioma Using a Chip-Based Digital PCR System to Analyze IDH, TERT, and H3 Mutations in the Cerebrospinal Fluid. *J Neurooncol* (2021) 152(1):47–54. doi: 10.1007/s11060-020-03682-7
38. Ohno M, Matsuzaki J, Kawauchi J, Aoki Y, Miura J, Takizawa S, et al. Assessment of the Diagnostic Utility of Serum Microrna Classification in Patients With Diffuse Glioma. *JAMA Netw Open* (2019) 2(12):e1916953. doi: 10.1001/jamanetworkopen.2019.16953
39. Zhi F, Shao N, Wang R, Deng D, Xue L, Wang Q, et al. Identification of 9 Serum microRNAs as Potential Noninvasive Biomarkers of Human Astrocytoma. *Neuro Oncol* (2015) 17(3):383–91. doi: 10.1093/neuonc/nou169
40. Zhou Q, Liu J, Quan J, Liu W, Tan H, Li W. MicroRNAs as Potential Biomarkers for the Diagnosis of Glioma: A Systematic Review and Meta-Analysis. *Cancer Sci* (2018) 109(9):2651–9. doi: 10.1111/cas.13714
41. Lee S, Latha K, Manyam G, Yang Y, Rao A, Rao G. Role of CX3CR1 Signaling in Malignant Transformation of Gliomas. *Neuro Oncol* (2020) 22(10):1463–73. doi: 10.1093/neuonc/noaa075
42. van der Vos KE, Abels ER, Zhang X, Lai C, Carrizosa E, Oakley D, et al. Directly Visualized Glioblastoma-Derived Extracellular Vesicles Transfer RNA to Microglia/Macrophages in the Brain. *Neuro Oncol* (2016) 18(1):58–69. doi: 10.1093/neuonc/nov244
43. Abels ER, Maas SLN, Nieland L, Wei Z, Cheah PS, Tai E, et al. Glioblastoma-Associated Microglia Reprogramming Is Mediated by Functional Transfer of Extracellular Mir-21. *Cell Rep* (2019) 28(12):3105–19.e7. doi: 10.1016/j.celrep.2019.08.036
44. Gabrusiewicz K, Li X, Wei J, Hashimoto Y, Marisetty AL, Ott M, et al. Glioblastoma Stem Cell-Derived Exosomes Induce M2 Macrophages and PD-L1 Expression on Human Monocytes. *Oncoimmunology* (2018) 7(4):e1412909. doi: 10.1080/2162402X.2017.1412909
45. Jin X, Ishii H, Bai Z, Itokazu T, Yamashita T. Temporal Changes in Cell Marker Expression and Cellular Infiltration in a Controlled Cortical Impact Model in Adult Male C57BL/6 Mice. *PloS One* (2012) 7(7):e41892. doi: 10.1371/journal.pone.0041892
46. Loane DJ, Kumar A. Microglia in the TBI Brain: The Good, the Bad, and the Dysregulated. *Exp Neurol* (2016) 275 Pt 3:316–27. doi: 10.1016/j.expneurol.2015.08.018
47. Wang G, Zhang J, Hu X, Zhang L, Mao L, Jiang X, et al. Microglia/Macrophage Polarization Dynamics in White Matter After Traumatic Brain Injury. *J Cereb Blood Flow Metab* (2013) 33(12):1864–74. doi: 10.1038/jcbfm.2013.146
48. Butovsky O, Jedrychowski MP, Moore CS, Cialic R, Lanser AJ, Gabriely G, et al. Identification of a Unique TGF-beta-dependent Molecular and Functional Signature in Microglia. *Nat Neurosci* (2014) 17(1):131–43. doi: 10.1038/nn.3599
49. Pong WW, Walker J, Wylie T, Magrini V, Luo J, Emnett RJ, et al. F11R is a Novel Monocyte Prognostic Biomarker for Malignant Glioma. *PloS One* (2013) 8(10):e77571. doi: 10.1371/journal.pone.0077571

Conflict of Interest: The authors declare that the research was conducted in the absence of any commercial or financial relationships that could be construed as a potential conflict of interest.

frontiers in Immunology

ORIGINAL RESEARCH
published: 20 July 2021
doi: 10.3389/fimmu.2021.653711

The N^6-Methyladenosine-Modified Pseudogene HSPA7 Correlates With the Tumor Microenvironment and Predicts the Response to Immune Checkpoint Therapy in Glioblastoma

Rongrong Zhao[1,2†], Boyan Li[1,2†], Shouji Zhang[1,2], Zheng He[1,2,3], Ziwen Pan[1,2], Qindong Guo[1,2], Wei Qiu[1,2], Yanhua Qi[1,2], Shulin Zhao[1,2], Shaobo Wang[1,2], Zihang Chen[1,2], Ping Zhang[1,2], Xing Guo[1,2], Hao Xue[1,2] and Gang Li[1,2*]*

[1] Department of Neurosurgery, Qilu Hospital, Cheeloo College of Medicine and Institute of Brain and Brain-Inspired Science, Shandong University, Jinan, China, [2] Shandong Key Laboratory of Brain Function Remodeling, Qilu Hospital of Shandong University, Jinan, China, [3] Department of Neurosurgery, Qilu Hospital (Qingdao), Cheeloo College of Medicine, Shandong University, Qingdao, China

OPEN ACCESS

Edited by:
Payal Watchmaker, University of California, San Francisco, United States

Reviewed by:
Jian Zhang, Southern Medical University, China
Ekaterina Friebel, University of Zurich, Switzerland

***Correspondence:**
Gang Li
dr.ligang@sdu.edu.cn
Hao Xue
xuehao@sdu.edu.cn

[†]These authors have contributed equally to this work

Specialty section:
This article was submitted to Cancer Immunity and Immunotherapy, a section of the journal Frontiers in Immunology

Received: 15 January 2021
Accepted: 05 July 2021
Published: 20 July 2021

Citation:
Zhao R, Li B, Zhang S, He Z, Pan Z, Guo Q, Qiu W, Qi Y, Zhao S, Wang S, Chen Z, Zhang P, Guo X, Xue H and Li G (2021) The N^6-Methyladenosine-Modified Pseudogene HSPA7 Correlates With the Tumor Microenvironment and Predicts the Response to Immune Checkpoint Therapy in Glioblastoma. Front. Immunol. 12:653711. doi: 10.3389/fimmu.2021.653711

Background: Glioblastoma (GBM), one of the most aggressive tumors of the brain, has no effective or sufficient therapies. Identifying robust biomarkers for the response to immune checkpoint blockade (ICB) therapy, a promising treatment option for GBM patients, is urgently needed.

Methods: We comprehensively evaluated lncRNA m^{6}A modification patterns in m^{6}A-sequencing (m^{6}A-seq) data for GBM tissues and systematically investigated the immune and stromal regulators of these m^{6}A-regulated lncRNAs. We used the single-sample gene-set enrichment analysis (ssGSEA) algorithm to investigate the difference in enriched tumor microenvironment (TME) infiltrating cells and the functional annotation of HSPA7 in individual GBM samples. Further, we validated that HSPA7 promoted the recruitment of macrophages into GBM TME *in vitro*, as well as in our GBM tissue section. We also explored its impact on the efficacy of ICB therapy using the patient-derived glioblastoma organoid (GBO) model.

Results: Here, we depicted the first transcriptome-wide m^{6}A methylation profile of lncRNAs in GBM, revealing highly distinct lncRNA m^{6}A modification patterns compared to those in normal brain tissues. We identified the m^{6}A-modified pseudogene HSPA7 as a novel prognostic risk factor in GBM patients, with crucial roles in immunophenotype determination, stromal activation, and carcinogenic pathway activation. We confirmed that HSPA7 promoted macrophage infiltration and SPP1 expression *via* upregulating the YAP1 and LOX expression of glioblastoma stem cells (GSCs) *in vitro* and in our clinical GBM tumor samples. We also confirmed that knockdown of HSPA7 might increase the efficiency of anti-PD1 therapy utilizing the GBO model, highlighting its potential as a novel target for immunotherapy.

Conclusions: Our results indicated that HSPA7 could be a novel immunotherapy target for GBM patients.

Keywords: N^6-methyladenosine, tumor microenvironment, glioblastoma, immune checkpoint blockade, HSPA7

INTRODUCTION

Glioblastoma (GBM), one of the most aggressive brain tumors, currently has no effective and sufficient therapies due to its intratumoral heterogeneity and molecular complexity. Immune checkpoint blockade (ICB) therapy is being actively pursued as a promising treatment option for GBM. However, very few patients respond to this therapy (1–5) partly because of the contribution of prominent immunosuppressive factors in the brain tumor microenvironment (TME) in GBM, including tumor-associated macrophages (TAMs), neutrophils, and regulatory T cells (Tregs) (6–8). The development of biomarkers and identification of the definite molecular mechanism underlying resistance to ICB therapy are urgently needed to identify effective therapeutic strategies for GBM.

N^6-Methyladenosine (m^{6}A), the most abundant reversible methylation modification of mRNA, critically affects processes in mRNA metabolism, including splicing, export, translation, and decay. Dysregulation of this modification is clearly linked to diverse pathological processes and disease progression (9, 10), including GBM tumorigenesis (11–15). Recent studies have described the role of m^{6}A modification in regulating the immune response (16–19), prompting us to reveal the importance of the spectrum of m^{6}A-regulated genes and m^{6}A regulatory mechanisms in shaping the TME. Numerous studies have demonstrated that m^{6}A is also present in numerous long non-coding RNAs (15, 20–22) (lncRNAs, transcripts longer than 200 nucleotides but lacking functional coding capacity), and lncRNA m^{6}A modification has emerged as a fundamental player in cancer progression and immune regulation, suggesting a potential association between the tumor immune response and m^{6}A lncRNA modification. However, the lncRNA m^{6}A methylation profile has not been systematically clarified in GBM tumors. Additionally, none of these studies have specifically investigated the roles of m^{6}A-modified lncRNAs in the overall TME landscape in GBM. Therefore, it is worthwhile to obtain comprehensive knowledge of the cellular TME infiltration characteristics mediated by m^{6}A-modified lncRNAs, as this knowledge would contribute to our understanding of the role of m^{6}A modification in immune regulation and guide the development of more effective immunotherapeutic strategies.

Here, we depicted the first transcriptome-wide lncRNA m^{6}A methylation profile in GBM and normal brain tissues *via* m^{6}A sequencing (m^{6}A-seq) data analysis, revealing the highly distinct lncRNA m^{6}A modification patterns between these two groups. Key immune-stromal-related lncRNAs were identified by differentially expressed gene (DEG) analysis in primary GBM cohorts from The Cancer Genome Atlas (TCGA). Integrating the m^{6}A-regulated lncRNAs revealed in this study, we identified HSPA7 as a novel prognostic factor in GBM patients. Through detailed bioinformatic analyses of HSPA7, we identified its crucial role in immunophenotype determination, stromal activation and carcinogenic pathway activation and highlighted its robust capacity to predict the ICB response. We confirmed that HSPA7 facilitated macrophage infiltration *via* the YAP1–LOX axis *in vitro*. We also confirmed that HSPA7 enhanced the efficiency of anti-PD1 therapy utilizing GBM patient-derived glioblastoma organoids, an *ex vivo* model. These results demonstrated that HSPA7 could be a novel immunotherapy target for GBM patients.

MATERIALS AND METHODS

Patient Specimens and Public Patient Cohorts

Human GBM and normal brain tissues for m^{6}A-seq were obtained from patients admitted to Qilu Hospital. All participants provided written informed consent, and the research was approved by the Ethics Committee on Scientific Research of Shandong University Qilu Hospital (approval number: KYLL-2018-324).

The RNA sequencing (RNA-seq) transcriptome, somatic mutation data, and corresponding clinicopathological parameters of the TCGA GBM cohort were obtained from the TCGA database (http://cancergenome.nih.gov/). Two Chinese Glioma Genome Atlas (CGGA) GBM RNA-seq datasets and the corresponding clinicopathological parameters were obtained from the CGGA database (http://www.cgga.org.cn/). For ICB data, genomic and clinical information from the IMvigor210 cohort, complete expression data, and detailed clinical annotations were obtained from http://research-pub.Gene.com/imvigor210corebiologies based on the Creative Commons Attribution 3.0 license. For data from GBM patients treated with PD-1 inhibitors (pembrolizumab or nivolumab), clinical information was obtained from Supplementary paper data, and the sequencing data were obtained from SRA PRJNA482620 (2). For patients with melanoma treated with anti-CTLA4 therapy, the expression data were downloaded from the cBioPortal database (http://www.cbioportal.org/), and the detailed clinical characteristics of individual patients were obtained from the supplementary data of a previous paper (23). In addition, the somatic mutation data and information in **Figure S11A** were obtained from the cBioPortal database. The m^{6}A-seq sequencing data have been deposited in SRA PRJNA661159 (the data are being processed, submission ID: SUB8069560, released when the paper is published). The processed data are available from the corresponding author upon reasonable request.

Estimation of TME Cell Characterization

We used the single-sample gene set enrichment analysis (ssGSEA) algorithm to calculate the enrichment score of immune cell infiltration into the GBM TME for each sample. Immune cell-related genes were obtained from Bindea et al. (24) and Robert L (25). (**Table S1**) and included genes related to immune cell types, immune-related pathways and functions. Based on the ssGSEA results, samples from the TCGA GBM cohort were classified into the high immune cell infiltration (immune-H) group or low immune cell infiltration (immune-L) group by using the "hclust" R package.

Functional Annotation and Pathway Enrichment Analysis

To explore the differences in biological behavior among the samples with distinct HSPA7 expression levels, we used selected HALLMARK (26) and Kyoto Encyclopedia of Genes and Genomes (KEGG) (27) from gene sets from the Molecular Signatures Database (MSigDB) and other commonly used gene signatures (28–30) to estimate pathway enrichment scores for each sample (**Table S2**) by gene set variation analysis (GSVA) using the "GSVA" R package.

The terms enriched with genes positively correlated with the expression of HSPA7 and genes interacting with HSPA7 detected in NCBI (https://www.ncbi.nlm.nih.gov/gene/3311) and the starBase database (http://starbase.sysu.edu.cn/index.php) were analyzed *via* the Metascape resource (http://metascape.org/gp/index.html#/).

Cell Lines and Reagents

All patient-derived GSC cell lines, including mesenchymal (MES) subtype GSC cell lines (GSC 20 and GSC 267), proneural (PN) subtype GSC cell lines (GSC 8–11), and neural progenitor cells (NPCs) were kindly donated by Dr. Frederick F. Lang and Dr. Krishna P.L. Bhat (The University of Texas, M.D. Anderson Cancer Center, Houston, TX, USA). The cells were cultured in DMEM/F12 supplemented with B27 (Invitrogen, California, USA), 20 ng/ml EGF (R&D Systems, USA), and 20 ng/ml bFGF (R&D Systems, California, USA). The human glioma cell lines U87MG, U251MG, A172, and LN229 and the human monocyte cell line THP-1 were obtained from the Chinese Academy of Sciences Cell Bank. U87MG, U251, A172, and LN229 cells were cultured in DMEM (Thermo Fisher Scientific, USA) supplemented with 10% FBS (Thermo Fisher Scientific; Waltham, MA, USA). THP-1 cells were cultured in RPMI-1640 (Thermo Fisher Scientific) supplemented with 10% FBS (Thermo Fisher Scientific). THP-1 cells were incubated with 100 ng/ml PMA (Sigma-Aldrich; St. Louis, MO, USA) for 24 h *in vitro* to induce their differentiation into macrophages. Cells were cultured in a standard humidified atmosphere of 5% CO_2 at 37°C.

Western Blot

Protein was extracted from GSC cells or glioma cells. The following primary antibodies were used: GAPDH (Cell Signaling Technology, Boston, USA, 5174), YAP1 (Cell Signaling Technology, 14074), CD44 (Cell Signaling Technology, 3570), LOX (Abcam, Cambridge, UK, ab174316), and YKL40 (Cell Signaling Technology, 47066).

Antisense Oligonucleotides, Lentivirus Transfection

ASOs were synthesized by RiboBio (Guangzhou, China). HSPA7/FTO overexpression, METTL3 shRNA and corresponding control lentiviruses were synthesized by GeneChem (Shanghai, China). Target sequences for HSPA7 were as follows: ASO#1: 5′-GGAAGCGGAGCTGAGCAGAT-3′; ASO#2: 5′-CTAACAAGATCACCAATGAC-3′. Target sequences for METTL3 were as follows: 5′-GCCAAGGAACAATCCATTGTT-3′.

Immunofluorescence

The slides were washed with PBS for 15 min and blocked with 10% goat serum in PBS. The slides were incubated overnight in a humidified chamber at 4°C with the following primary antibodies: LOX (Abcam, ab174316); YAP1 (Cell Signaling Technology, 14074), CD68 (Abcam, ab213363), CD44 (Cell Signaling Technology, 3570), Ki67 (Cell Signaling Technology, 9449), PD-L1 (Abcam, ab213524), and SPP1 (Abcam, ab8448). After primary antibody incubation, the samples were washed with PBS and incubated with the matching fluorescent-conjugated secondary antibody (1:500 dilution, Thermo Fisher) at room temperature for 1 h. Images were captured using a LeicaSP8 confocal microscope (Leica Microsystems, Wetzlar, Germany)

Fluorescence *In Situ* Hybridization

RNA-FISH was performed according to the instructions of the manufacturer (GenePharma, Shanghai, China). Incubated with a cy3-labeled HSPA7 probe, nuclei were counterstained with DAPI. Images were captured using a LeicaSP8 confocal microscope. Probe sequence: ATCCTTTTGCACCTCCCCGACCC; AACCTTCCCGCACCTTCCCGCCCAGTC.

Glioblastoma Organoid Model

Glioblastoma organoid models were generated as previously described (31). GBO medium containing 50% DMEM:F12 (Thermo Fisher Scientific), 50% Neurobasal (Thermo Fisher Scientific), 1× GlutaMax (Thermo Fisher Scientific), 1× NEAAs (Thermo Fisher Scientific), 1× PenStrep (Thermo Fisher Scientific), 1× N2 supplement (Thermo Fisher Scientific), 1× B27 w/o vitamin A supplement (Thermo Fisher Scientific), 1× 2-mercaptoethanol (Thermo Fisher Scientific), and 2.5 μg/ml human insulin (Sigma) per well was placed on an orbital shaker rotating at 120 rpm within a 37°C, 5% CO_2, and 90% humidity sterile incubator.

Transwell Assay

Transwell assays were performed in 24-well multiwell insert systems according to the protocol of the manufacturer. THP-1 cells were incubated with 100 ng/ml PMA (Sigma-Aldrich) for 24 h *in vitro* to induce their differentiation into macrophages and then added to the top chamber in serum-free media. The bottom chamber was filled with 10% FBS 1640 and GSC growth media.

After 24 h of incubation, the top chamber cells were removed using a cotton swab, and the membrane was fixed in 4% paraformaldehyde for 15 min and stained with crystal violet for 15 min. Five fields of adherent cells in each well were photographed randomly.

Statistical Analysis

Kaplan–Meier survival analysis was performed using GraphPad Prism 7.04, and significant differences between two groups were compared by the log-rank (Mantel–Cox) test. The waterfall function in the "maftools" package was used to visualize the mutational landscape in patients in the high- and low-HSPA7 groups or the high- and low-tumor mutation burden (TMB) groups. Student's *t*-test was used for two-group comparisons. For comparisons among more than two groups, the Wilcoxon test and one-way ANOVA were used for non-parametric and parametric data (32). $P > 0.05$ was considered nonsignificance (ns), $P \leq 0.05$ was considered statisticallysignificant (*$P < 0.05$; **$P < 0.01$; ***$P < 0.001$, ****$P < 0.0001$). All data processing with R packages was performed using R Studio (version 3.6.3)

RESULTS

Overview of Transcriptome-Wide m^{6}A Methylation in lncRNAs in GBM and Normal Brain Tissues

To understand the pattern of the lncRNA m^{6}A modification profiles in GBM, three human GBM tumor tissues and three normal brain tissues were subjected to transcriptome m^{6}A-seq, which revealed that a considerable proportion of lncRNAs were extensively m^{6}A-modified. In addition, 2,113 m^{6}A peaks were identified in the normal group, corresponding to the transcripts of 1,538 genes, including 544 long intergenic ncRNAs (lincRNAs), 720 antisense lncRNAs, 262 pseudogenes, and 12 others. In the GBM group, 2,412 m^{6}A peaks were identified, corresponding to the transcripts of 1,508 genes, namely, 445 lincRNAs, 771 antisense lncRNAs, 283 pseudogenes, and 9 other genes (**Figure 1A**). Further analysis showed that most of the lncRNAs (74.5% of the m^{6}A-methylated genes in the normal group but 65.3% of the methylated genes in the GBM group) in both groups contained only one peak, while a relatively small number of lncRNAs contained two peaks, and very few lncRNAs contained three or more peaks (**Figure 1B**). Upon further analysis of the distribution profiles of m^{6}A peaks within lncRNAs, we found that m^{6}A sites were distributed in almost the same proportion in intronic and exonic regions in the normal group but exhibited a slightly increased tendency to be distributed in exonic regions in GBM tissues (**Figure 1C**).

To reveal the significance of m^{6}A-methylated lncRNAs in GBM, the differences and overlaps in the m^{6}A-modified lncRNAs between the GBM and normal brain groups were analyzed by constructing a Venn diagram. As shown in **Figure 1D**, 781 m^{6}A-modified lncRNAs were common to both groups. A total of 727 new genes were expressed, and the expression of 757 genes was lost in the GBM group compared with the normal group, indicating a significant difference in global lncRNA m^{6}A modification patterns between the GBM and normal groups. To explore the effect of m^{6}A on lncRNA expression, the differentially expressed lncRNAs between 153 primary GBM and five normal brain tissues in the TCGA GBM cohort were compared. Compared with normal samples, GBM tissues exhibited 4,375 differentially expressed lncRNAs (LogFC ≥ 1 and padj ≤ 0.05), with 2,614 upregulated and 1,761 downregulated (**Table S3**). In addition, the global abundance of m^{6}A peaks between GBM and normal brain tissues was also compared. Furthermore, integrated analysis of these differentially m^{6}A-modified lncRNAs and differentially regulated lncRNAs from the TCGA dataset was conducted. The distribution of genes with a significant change in both the m^{6}A level ($|FC| \geq 1.2$, $P \leq 0.05$) and the overall transcript expression level ($|FC| \geq 2$, padj ≤ 0.05) is shown in **Figure 1E**. These genes were divided into four main groups: 208 were hypermethylated and upregulated ("hyperup"), 394 were hypomethylated and downregulated ("hypodown"), 56 were hypermethylated but downregulated ("hyperdown") and 64 were hypomethylated but upregulated ("hypoup") in GBM tissues relative to normal brain tissues. We also discovered a positive correlation between differentially methylated m^{6}A peaks and the expression levels of their corresponding genes [**Figure 1E**, Pearson correlation coefficient (r) = 0.495, P<0.0001], and the m^{6}A modification sites in all of the above four groups of genes were distributed in exonic regions, reconfirming that m^{6}A modification can regulate the expression of mature lncRNAs. These results revealed obviously distinct m^{6}A modification patterns between GBM and normal brain tissues. Moreover, m^{6}A modification could regulate numerous lncRNAs, possibly by regulating their stability, degradation or other functions, as reported previously.

Identification of the Immune-Stromal-m^{6}A-Related Pseudogene HSPA7 as a Novel Prognostic Risk Factor in GBM

To investigate the effects of these m^{6}A-regulated lncRNAs on cell infiltration into the TME, we assessed the tumor purity, stromal score, and immune score of 153 primary GBM cases in the TCGA GBM cohort using the ESTIMATE algorithm (see *Materials and Methods*, **Table S4**). Then, we performed differential analysis of all RNA-seq data from these 153 GBM samples in the TCGA database based on the median cutoff immune/stromal scores. The volcano plot of the high/low stromal/immune scores revealed differential gene expression profiles between the samples. A total of 791 upregulated lncRNAs and 459 downregulated lncRNAs ($|FC| \geq 1.5$, padj ≤ 0.05) were identified based on the difference in immune scores (**Supplementary Figure S1A** and **Table S5**). Simultaneously, 734 upregulated lncRNAs and 269 downregulated lncRNAs ($|FC| \geq 1.5$, padj ≤ 0.05) were identified based on the differential analysis of stromal scores (**Figure S1B** and **Table S6**). As the Venn diagram (**Supplementary Figures S1C, D**) indicates, four identical upregulated genes and 11 identical downregulated genes were related to immune activation, stromal activation, and m^{6}A modification. Then, we performed Kaplan–Meier analysis on patients stratified by the expression levels of these

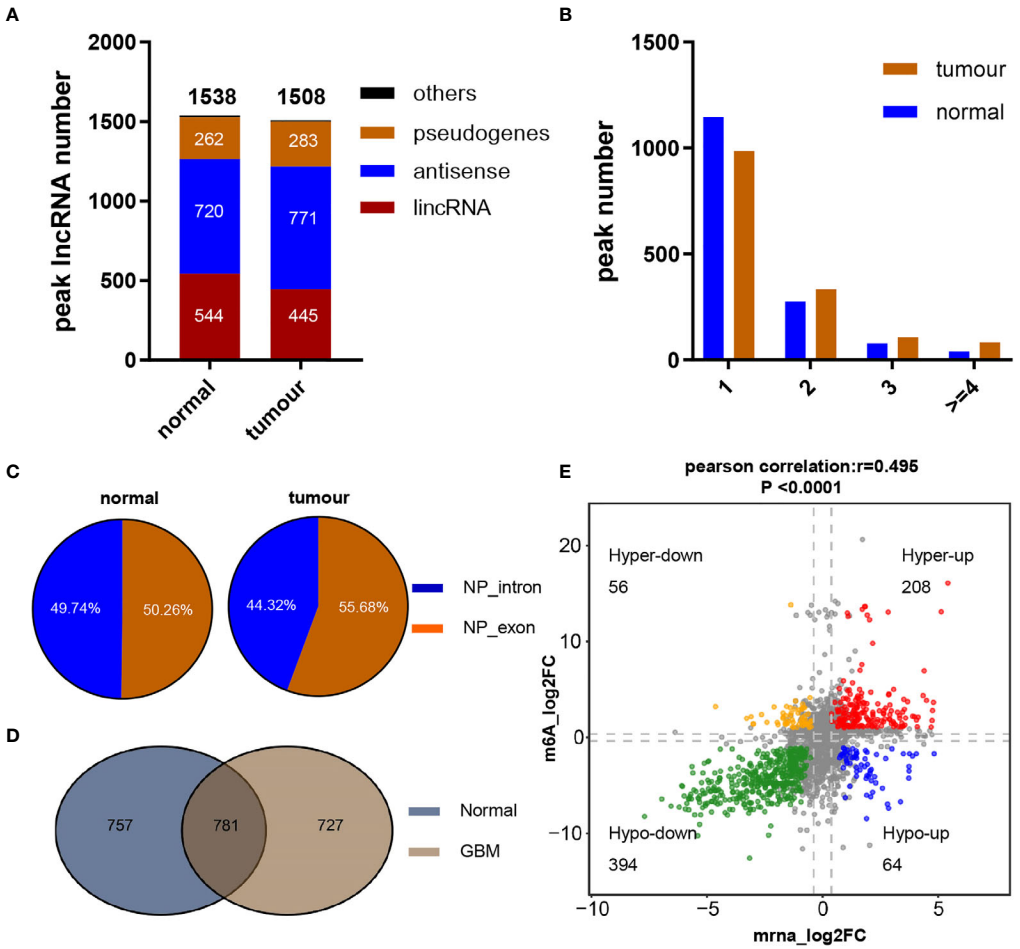

FIGURE 1 | Overview of m^{6}A methylation within lncRNAs in GBM and normal brain tissues. **(A)** Numbers and gene types of lncRNAs identified in normal brain and GBM tissue samples as identified by m^{6}A-seq. **(B)** The number of m^{6}A-modified peaks per lncRNA transcript. **(C)** Distribution of m^{6}A peaks across lncRNA transcripts. **(D)** Numbers of common and tissue-specific m^{6}A lncRNAs in normal and GBM brain tissues. **(E)** Dot plot of Log2FC (lncRNA expression) *versus* Log2FC (differential m^{6}A methylation) values showing a positive correlation between the overall m^{6}A methylation level and the lncRNA expression level (Pearson's r = 0.495; P < 0.0001) and the distribution of genes with significant changes in both the m^{6}A (FC ≥ 1.2, P ≤ 0.05) and corresponding lncRNA expression levels in GBM samples compared with normal brain tissues (FC ≥ 2, padj ≤ 0.05).

15 differentially expressed genes, and only HSPA7 (**Figure 2B**) and AC011899.9 (**Supplementary Figure S2B**) were found to have prognostic significance (P ≤ 0.05) in the 153 TCGA GBM samples based on the median expression levels. The Gene Expression Profiling Interactive Analysis (GEPIA) database was used to show that HSPA7 was significantly overexpressed in GBM tissues compared with normal brain tissues in the Genotype-Tissue Expression (GTEx) database (**Figure 2A**), while AC011899.9 was not (**Supplementary Figure S2A**). Thus, we focused only on HSPA7 in the following work.

We then tested the RNA expression level of HSPA7 in GBM cell lines (U87MG, U251MG, A172, and LN229 cells), and discovered that its expression was significantly higher in GBM cell lines than in normal human astrocyte (NHA) cells (**Figure 2C**). The m^{6}A methylation peak distribution and abundance in HSPA7 transcripts from GBM and normal brain tissues, as detected by m^{6}A-seq, were visualized using IGV software (**Figure 2D**). We found that HSPA7 was highly enriched in the m^{6}A-precipitated fraction, and the m^{6}A modification enrichment level could be regulated by methyltransferase-like 3 (METTL3), which contains a catalytic activity domain to catalyze m^{6}A formation (**Figure 2E**). Additionally, the expression of HSPA7 was significantly inhibited by knocking down METTL3 (**Figure 2F**) and overexpressing FTO, an m^{6}A demethylase (**Figure 2G**). These results provided evidence that HSPA7 harbored high m^{6}A modification levels and thus could be regulated in an m^{6}A-dependent manner.

To explore the association between HSPA7 expression and clinical characteristics, we first compared HSPA7 expression levels in patients in the TCGA GBM cohort stratified separately by molecular subtype, IDH1 status, CpG island methylator phenotype (G-CIMP) status, MGMT promoter status, age, and sex. As shown in **Figure 2H**, HSPA7 expression in the PN subtype was significantly lower than the HSPA7 expression in the classical (CL) and MES subtypes and was highest in mesenchymal samples.

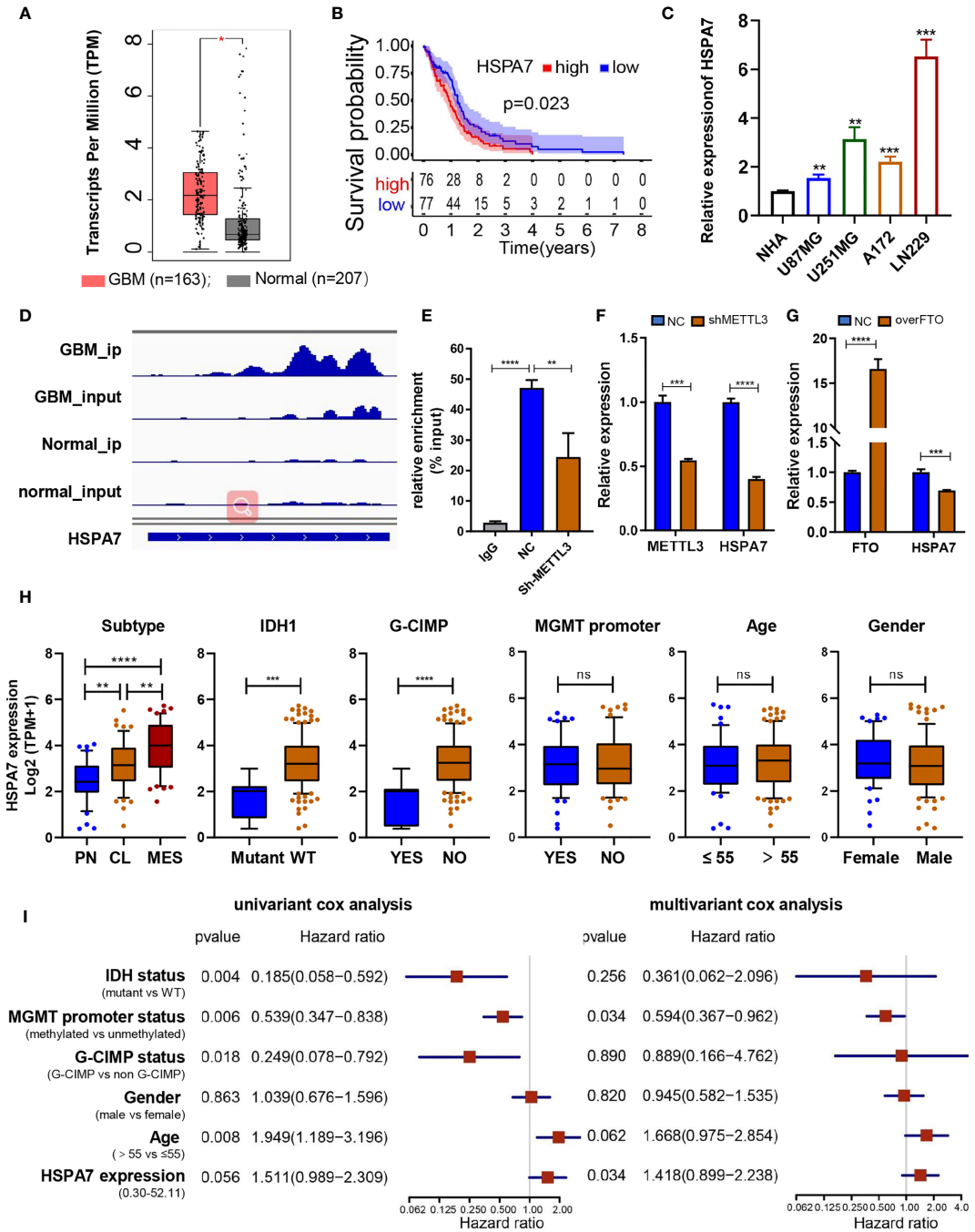

FIGURE 2 | Identification of the immune-stromal-m^{6}A-related pseudogene HSPA7 as a novel prognostic factor in GBM. **(A)** The GEPIA database showed that HSAP7 was overexpressed significantly in GBM tissues compared with GETx normal brain tissues. **(B)** Kaplan–Meier survival curves show that HSPA7 is a prognostic risk factor in GBM. **(C)** qPCR assays showing that HSPA7 expression was significantly higher in GBM cells than in NHA cells. Data are presented as the mean ± SD, n = 3. Means were compared with one-way ANOVA, and the NC group is indicated as the control. **(D)** The gene IGV plots of HSPA7 in the m^{6}A-seq. **(E)** MeRIP assay showing that HSPA7 was highly enriched by the m^{6}A antibody, and the modification can be regulated by the m^{6}A methyltransferase METTL3. Data represent mean ± S.D. from three independent experiments. qPCR assay showing that the expression of HSPA7 can be regulated by **(F)** m^{6}A methyltransferase METTL3 and **(G)** demethylase FTO. Data represent mean ± S.D. from three independent experiments. **(H)** Distribution of HSPA7 expression in different cohorts stratified by molecular subtype (CL, n = 56; MES, n = 51; PN, n = 44; PN *vs* MES, P < 0.0001; CL *vs* MES, P = 0.0020; PN *vs* CL, P = 0.0013), IDH1 status (mutant, n = 8; WT, n = 141; P = 0.0002), G-CIMP status (G-CIMP, n = 9; non-G-CIMP, n = 142; P < 0.0001), MGMT promoter status (methylated, n = 55; unmethylated, n = 67; P = 0.7445), age (high, age > 55, n = 100; low, age ≤ 55, n = 53; P = 0.5114), and sex (female, n = 54; male, n = 99; P = 0.3996). **(I)** Univariate and multivariate Cox regression analyses of HSPA7 and other clinical features in the overall survival of GBM samples. The statistical significance is shown as: ns, P > 0.05; *P < 0.05; **P < 0.01; ***P < 0.001; ****P < 0.0001.

HSPA7 expression was lower in samples with IDH mutations than in samples with wild-type IDH1. Regarding the G-CIMP status, HSPA7 expression was lower in patients with G-CIMP tumors than in those without G-CIMP tumors. No obvious correlations between HSPA7 expression and MGMT promoter methylation, age, or sex were observed. Furthermore, univariate Cox regression analysis of the overall survival of GBM patients in the TCGA cohort showed that high HSPA7 expression (HR: 1.511, P = 0.056) was an independent risk factor associated with the prognosis of GBM. Moreover, high HSPA7 expression (HR: 1.418, P = 0.034) remained a statistically significant factor in GBM patients after adjustment for age, sex, IDH status, MGMT promoter methylation status, and G-CIMP status in subsequent multivariate Cox regression analysis (**Figure 2I**). These results indicated that the pseudogene HSPA7 is a novel risk prognostic biomarker and indicates therapeutic outcomes of GBM patients.

HSPA7 Is Correlated With Immunophenotypes and TME Landscapes

To gain further insight into the exact role of HSPA7 in immunophenotype determination, we analyzed 31 immune-associated gene sets representing diverse immune cell types, functions, and pathways (see *Materials and Methods*). As shown in **Figures 3A, B**, the HSPA7-high expression group had significantly greater cell infiltration into the TME, higher immune and stromal scores, and lower tumor purity than the HSPA7-low expression group, confirming that HSPA7 could indeed regulate immune cell infiltration and immune-related gene expression. We then explored the specific differences in 31 immune cell phenotypes with high and low HSPA7 expression. Compared to tumors with low HSPA7 expression, tumors with high HSPA7 expression exhibited significantly increased infiltration of immunosuppressive cell populations, such as macrophages, neutrophils, and Tregs. However, some immune-activating cells, including activated dendritic cells (aDCs), immature DCs (iDCs), plasmacytoid DCs (pDCs), and tumor-infiltrating lymphocytes (TILs), were also enriched (**Supplementary Figure S3A**), indicating the complexity of the TME, in which GBM cells elicit multiple biological behavioral changes through direct or indirect interactions with other TME components. Two recent publications (7, 8) on single-cell mapping of human brain cancer reported that tumor-associated macrophages (TAMs) are the most abundant cellular components in brain TMEs, which can be subdivided ontogenetically into tissue-resident microglia (MGs) and macrophages of embryonic origin, and bone marrow-derived macrophages (BMDMs), showing tumor-promoting and immunosuppressive functions. To identify specific macrophage cell populations linked to HSPA7 expression in GBM, we examined the TCGA GBM dataset for TAM MG and TAM BMDM using validated gene set signatures (25), which demonstrated that tumors with high HSPA7 expression exhibited significantly increased infiltration of TAM BMDMs, while TAM MG was significantly decreased (**Figure 3A** and **Supplementary Figure S3A**), suggesting that HSPA7 enhanced recruitment of tumor-promoting BMDMs into the GBM TME rather than MG. These studies also showed that both activation and exhaustion of lymphocytes were prevalent, with increased relative frequencies of Tregs in the brain tumor TME. Moreover, we found elevated neutrophil infiltration in tumor tissues, revealing the complexity and multifaceted functions of the brain TME. We found that HSPA7 had a significant positive correlation with the enrichment scores of the three immunosuppressive immune cells and immune checkpoints (**Figure 3C**). We next investigated chemokines and immune modulators associated with immune suppression states. We then explored the specific differences in markers of myeloid lineages with suppressive functions (CD33, NOS2, CD163, CD68, SPP1, CD14, CD206), immune inhibitory checkpoints (LAG3, CTLA4, HAVCR2, PDCD1, PDCD1LG2, CD27, TIGIT, CD274, and TNFRSF9), and major neutrophil-recruiting chemokines and their receptors (ITGA3, CD177, MET, and CXCL8) between patients with high and low HSPA7 expression. Tumors with high HSPA7 expression exhibited significantly increased expression levels of these markers compared to tumors with low HSPA7 expression (**Figures 3D–F**), and positive correlations were found between HSPA7 expression and these molecules (**Supplementary Figures S4A–C**). Furthermore, to explore the direct involvement of the HSPA7 in the biological pathway causing immune suppression, we then analyzed myeloid cell-derived macrophage-restricted chemokines, which were the main factors that cause immunosuppression in GBM. We found that compared to tumors with low HSPA7 expression, tumors with high HSPA7 expression exhibited significantly increased myeloid cell-derived macrophage-restricted chemokines (8, 25) (**Supplementary Figures S4D, E**), including CCL17, CXCL2, CXCL3, and CXCL16 (involved in wound healing); immunosuppressive cytokines IL-10, CTSB, and CTSW (participating in multiple tumor-promoting processes, including invasion and metastasis); CCL2 and CCR2 (involved in macrophage chemotaxis); and other chemokine contributions of myeloid cell populations to the inflammatory TME milieu, indicating that HSPA7 could promote immunosuppressive phenotypes and suppress intratumoral antitumor immune responses.

To further understand the exact role of HSPA7 in determining the TME profile and immunophenotype, we performed unsupervised consensus clustering based on the TME cell populations and immune-related functional gene sets identified by Bindea et al. (24). This analysis identified a TME pattern with two clusters corresponding to a TME immune-low (immune-L) and a TME immune-high (immune-H) phenotype (**Supplementary Figure S3B**). Patients in the immune-H group (n = 51) exhibited poorer prognosis (**Figure 3G**) and higher HSPA7 expression levels (**Figure 3H**) than patients in the immune-L group (n = 102). The PN, CL, and MES subtypes of GBM have been most consistently described in the literature; the PN subtype is related to a more favorable outcome, and the MES subtype is related to poorer survival (23). The association between the MES gene expression signature, characterized by NF1 mutation, with reduced tumor purity, elevated invasion, enhanced migration capacity, and infiltration of immunosuppressive cells (macrophages, microglia, mesenchymal stem cells, or other cells) has been identified as a common theme across cancers (33, 34). Our results showed that most MES GBM samples had high expression of HSPA7 as well as the immune-H phenotype (**Figures 3I, J**). Moreover, we observed the same results as all GBM samples by analyzing MES glioblastoma alone, in which tumors with high HSPA7 expression exhibited

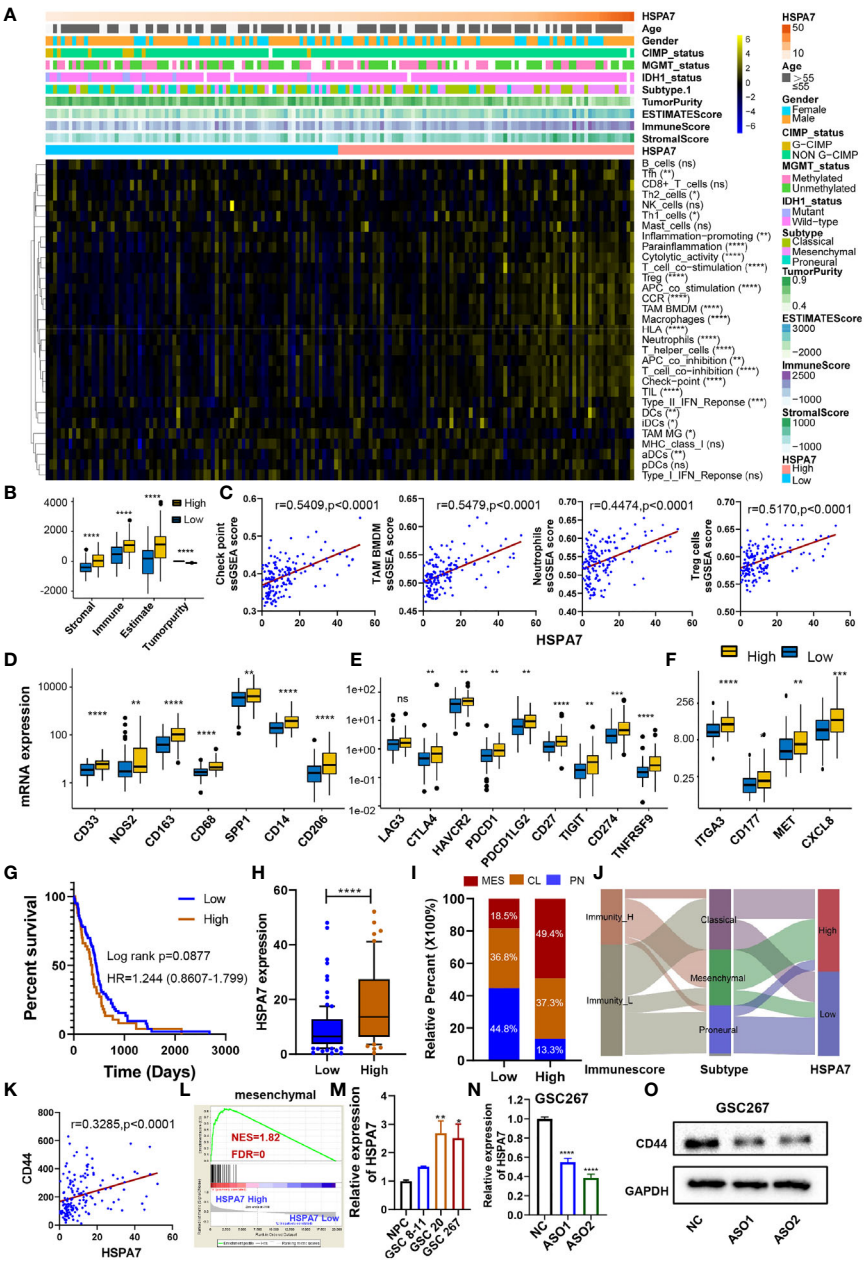

FIGURE 3 | HSPA7 is correlated with immunophenotypes and TME landscapes. **(A)** The enrichment scores of immune cell types and immune-related function-related gene sets were calculated *via the* ssGSEA algorithm. A heatmap was used to visualize these immune characteristics between the HSAP7 high and low expression groups; yellow represents a high enrichment level, black represents a median enrichment level, and blue represents a low enrichment level. **(B)** High expression of HSPA7 presented significantly increased stromal, immune, and ESTIMATE scores and decreased tumorigenicity. **(C)** HSPA7 positively correlated with immunosuppression regulators (checkpoints, macrophages, neutrophils, and Tregs). High expression of HSPA7 presented significantly increased markers of **(D)** suppressor function of myeloid lineages, **(E)** immune inhibitory checkpoints and **(F)** major neutrophil-recruiting chemokines and their receptors. The asterisks indicate a significant statistical p-value calculated using the non-parametric Wilcoxon test (*P < 0.05; **P < 0.01; ***P < 0.001, ****P < 0.0001). **(G)** Compared to the immune-L group (102 patients), patients in the immune-H group (51 patients) experienced poorer prognoses. **(H)** HSPA7 expression was higher in the immune-H group than in the immune-L group. **(I)** The proportion of GBM molecular subtypes in the low and high HSPA7 groups. MES subtype, red; CL subtype, orange; PN subtype, blue. **(J)** Alluvial diagram showing the changes in immune phenotypes, GBM molecular subtypes, and HSPA7 expression. **(K)** HSPA7 positively correlated with CD44, a marker of the MES subtype. **(L)** GSEA of mesenchymal signatures showed that GBM samples with high HSPA7 expression were enriched in the MES subtype compared to GBM samples with low HSPA7 expression. NES, normalized enrichment score; FDR, false discovery rate. **(M)** qPCR assays showed that HSPA7 expression was higher in MES subtype GSCs (GSCs 20 and 267) than in PN subtype GSCs (GSCs 8–11) and neural stem cells (NPCs). **(N)** qPCR assays verified the knockdown efficiency of HSPA7. **(O)** Western blot assays showed that HSPA7 promoted the expression of CD44. The statistical significance is shown as: ns, P > 0.05; *P < 0.05; **P < 0.01; ***P < 0.001; ****P < 0.0001.

significantly increased infiltration of immunosuppressive cell populations and regulators, such as macrophages, TAM BMDMs, neutrophils, Tregs, and immune checkpoints (**Supplementary Figures S5A, B**). As MES glioblastomas are strongly associated with higher immunosuppressive cell infiltration, we hypothesized that HSPA7 activated the immune microenvironment by promoting the phenotypic transformation of the GBM MES subtype. As shown in **Supplementary Figure S5C**, compared to tumors with low HSPA7 expression, tumors with high HSPA7 expression exhibited significantly increased expression levels of genes in the MES phenotype signature genes (33). Furthermore, HSPA7 positively correlated with CD44, a marker of the MES subtype (**Figure 3K**). GSEA also showed that GBM samples with high HSPA7 expression were enriched in the MES subtype compared to GBM samples with low HSPA7 expression (**Figure 3L**). In addition, we found that HSPA7 expression was higher in MES GSCs than in PN GSCs (**Figure 3M**). Moreover, Western blot assays revealed that knockdown of HSPA7 reduced the expression of CD44 (**Figures 3N, O**). Overall, these results indicated that in GBM, HSPA7 may be a robust indicator of the immunophenotype and be significantly correlated with a poorer immune response.

HSPA7 Is Correlated With Stromal and Carcinogenic Activation Pathways

To explore the differences in biological behaviors among these samples with distinct HSPA7 expression levels, we used the GSVA algorithm to estimate pathway enrichment scores for each sample (see *Materials and Methods*). Compared to the low HSPA7 expression group, the high HSPA7 expression group exhibited marked enrichment of stromal activation pathways [angiogenesis, epithelial–mesenchymal transition (EMT), VEGF, and TGF-β signaling pathways], oncogenic signaling pathways (hypoxia, apoptosis, PI3K Akt MTOR signaling, glycolysis, KRAS signaling, and other pathways), and immune responses (IL6 Jak stat3 signaling, which exerts immunosuppressive effects on T cell function and mediates ICB resistance in cancers (35), inflammatory response; interferon response; complement; and other pathways). However, the high HSPA7 expression group exhibited lower enrichment in pathways related to DNA replication- and DNA damage response-related functions (**Figure 4A**). Previous studies demonstrated that activation of stromal cells in the TME can induce T cell suppression and oncogenic signaling pathway activation *via* complex cellular and biological reconfiguration mechanisms (36, 37), attenuating the tumor response to PD-L1 blockade (28). As shown in **Figure 4B**, stromal activation pathways were positively correlated with carcinogenic signaling pathways and immune suppression pathways but negatively correlated with DNA damage response and repair pathways in TCGA GBM samples. Further analyses of the activity of stroma-related pathways indicated that high HSPA7 expression was significantly associated with higher stromal activation signatures (**Figure 4C**), as constructed by Mariathasan et al. (28), positively correlated with fibroblast enrichment (**Figure 4D**), as calculated by the MCP-counter method (38), and positively correlated with typical stromal cell activation-related pathways (**Figure 4E**). Furthermore, TGF-β is a pleiotropic cytokine associated with poor prognosis in GBM, playing a protumorigenic role by promoting immunosuppression, angiogenesis, metastasis, mesenchymal transition, and fibroblast activation (28, 39–41), and has been proven to promote the progression of GBM *via* an autocrine signaling loop (42). In our analysis, a TGF-β ligand (TGFB1) and a TGF-β receptor (TGFBR2), two key regulators in stromal activation and EMT pathways (28), and other genes encoding ECM and matricellular proteins (COLA4A1, COLA4A2, ECM1, and FN1) (8), which form a barrier to lymphocyte infiltration, showed increased expression in the high-HSPA7 group compared to the low-HSPA7 group (**Figure 4F**). These results suggested that immune cells and stromal cells in the TME can cooperate to synergistically regulate the immunosuppressive microenvironment, thereby promoting tumor immune escape.

Then, we explored the pathways enriched with genes positively correlated with HSPA7 (Pearson's $r \geq 0.3$, $P \leq 0.05$, **Table S7**) *via* the Metascape database (see *Materials and Methods*). These genes were significantly enriched in pathways related to the immune response, including cytokine-mediated signaling pathways, leukocyte migration, differentiation, and other immune-related pathways. Additionally, they were enriched in pathways involving stromal activation such as extracellular structure organization and response to wounding. These enriched pathways interacted with each other to form a protein–protein interaction network (**Figure 5A**). Furthermore, enrichment analysis in the PaGenBase (43) showed that these genes were almost completely specifically expressed in spleen, blood, bone marrow, and some other tissues with peripheral immune cell aggregation (**Figure 5B**), suggesting that HSPA7 can indeed promote the infiltration of immune cells into tumor tissues. In addition, enrichment analysis in the TF-target interaction database Transcriptional Regulatory Relationships Unraveled by Sentence-based Text mining (TRRUST) (44) showed that the genes were substantially transcriptionally regulated by NF-κB1 and RELA, two important transcription factors involved in NF-κB signaling pathways (**Figure 5C**). Further GSEA using the Gene Ontology (GO) and KEGG databases also showed that HSPA7 expression was positively correlated with the immune response and extracellular structure organization (**Figure 5D**).

Verification of the Functions of HSPA7 in Two CGGA Cohorts

To further validate the function of HSPA7 in GBM, we explored its expression pattern in two CGGA RNA-seq cohorts. The expression of HSPA7 was highest in GBM (WHO IV) among the glioma specimens with three different WHO grades (**Supplementary Figures S6A**, **S7A**). Kaplan–Meier survival analysis showed that GBM patients in both cohorts with high HSPA7 expression had poor survival outcomes (**Supplementary Figures S6B**, **S7B**). Further GSVA enrichment analysis also showed that HSPA7 expression was correlated with the immunophenotype, stromal activation, and oncogenic pathway activation in GBM samples (**Supplementary Figures S6C**, **S7C**). These results confirmed that HSPA7 can be used as an independent prognostic risk biomarker in GBM patients. Moreover, HSPA7 can regulate the TME immune response and stromal activation, promoting malignant progression of GBM tumors.

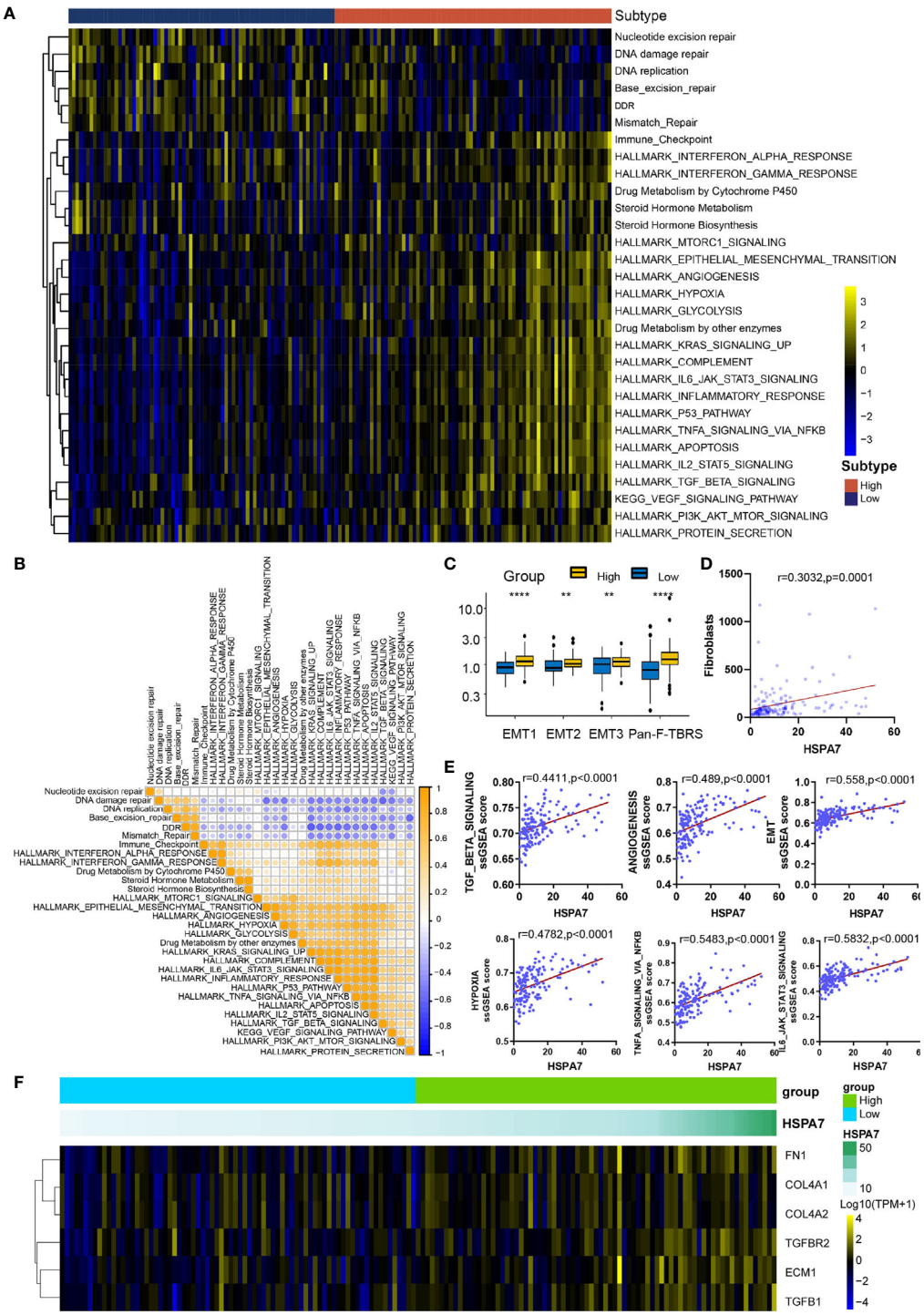

FIGURE 4 | HSPA7 is correlated with stromal and carcinogenic activation pathways. **(A)** GSVA enrichment analysis showing the activation status of biological pathways in the HSPA7-high and HSPA7-low groups. A heatmap was used to visualize these biological processes. Yellow represents activated pathways, black represents moderately activated pathways, and blue represents inhibited pathways. **(B)** Correlations between each known gene signature in the TCGA GBM cohort using Pearson correlation analysis. Negative correlations are marked with blue, and positive correlations are marked with orange. **(C)** Differences in stromal activation-related pathways between the HSPA7-high and HSPA7-low groups. EMT, epithelial–mesenchymal transition; Pan-FTBRS, panfibroblast TGF-β response signature. **(D)** HSPA7 expression was positively correlated with fibroblast enrichment, as calculated by MCP-counter. **(E)** HSPA7 expression was positively correlated with stromal activation-related pathways. **(F)** A heatmap was used to visualize the expression of stromal activation-related genes. Yellow represents high expression, black represents the median expression, and blue represents low expression. The statistical significance is shown as: **P < 0.01; ****P < 0.0001.

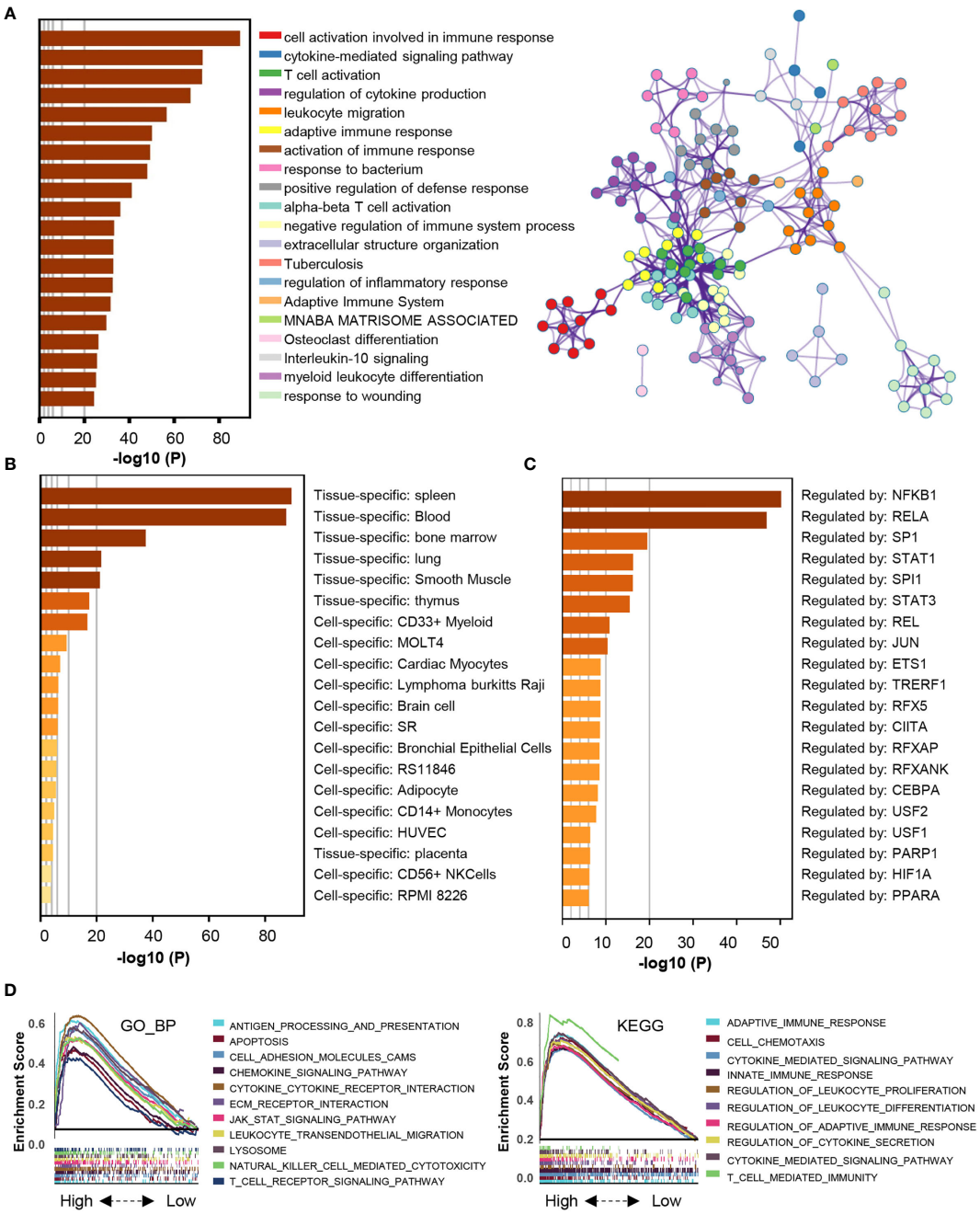

FIGURE 5 | The genes that were positively correlated with HSPA7 were enriched in immune response- and stromal-related pathways. **(A)** Bar graph of enriched terms, colored by p-values, and corresponding network of enriched terms. **(B)** Summary of enrichment analysis in PaGenBase and **(C)** summary of enrichment analysis in TRRUST across HSPA7 positively correlated genes. **(D)** GSEA analyses displayed key immune-regulated pathways enriched in the high (up) and low (down) HSPA7 groups, both in the GO biological process (left) and KEGG datasets (right), and each line is for one pathway.

M^{6}A-Modified HSPA7 Is Potentially Regulated by the Methyltransferase WTAP

To explore the potential molecular mechanism regulating HSPA7 RNA metabolism, we first screened HSPA7-interacting proteins *via* the NCBI database (**Table S8**). We verified that WTAP (45), a regulatory subunit of the m^{6}A methyltransferase (46, 47), is required for the localization of the m6A methyltransferase into nuclear speckles as a putative HSPA7-binding regulator. To better map the association between WTAP and HSPA7, we explored the expression pattern in different grades of glioma in the TCGA, CGGA, Gravendeel and Rembrandt datasets. As shown in **Supplementary Figure S8A**,

the expression of WTAP was highest in the WHO IV (GBM) group among glioma samples of three WHO grades and normal brain samples. Furthermore, overexpression of WTAP correlated with poor overall survival of GBM patients in all four datasets (**Supplementary Figure S8B**). Moreover, the expression of WTAP was positively correlated with the expression of HSPA7 in the TCGA GBM dataset (as calculated *via* the GEPIA database) and two CGGA GBM datasets (**Supplementary Figure S8C**). Further GSVA enrichment analysis showed that compared to the WTAP-low group, the WTAP-high group showed increased immune cell infiltration into the TME, stromal activation and oncogenic pathway activation, accompanied by higher immune and stromal scores and lower tumor purity, in the TCGA GBM cohort (**Supplementary Figure S8D**), CGGA GBM cohort 1 (**Supplementary Figure S9A**) and CGGA GBM cohort 2 (**Supplementary Figure S9B**). These patterns were the same as the patterns observed for HSPA7 expression. The above findings indicate that m^6A methylation of HSPA7 is regulated by WTAP, although this conclusion and the functional mechanisms need further demonstration. Subsequent pathway and process enrichment analyses of HSPA7-interacting proteins showed that they can mediate many biological behaviors, such as mitotic cell cycle phase transition, neddylation, proteasome-mediated ubiquitin-dependent protein catabolism, HIF1α pathway activity, and other functions (**Supplementary Figure S10A**, **Table S8**). Then, we further explored the enriched terms across the RNA-binding proteins (RBPs) detected by crosslinking immunoprecipitation coupled with sequencing (CLIP-seq) from data deposited in the starBase database. These RBPs were enriched mainly in terms such as mRNA processing, nucleic acid transport, and RNA catabolic process (**Supplementary Figure S10B** and **Table S9**). However, the exact mechanism by which HSPA7 regulates the GBM TME requires further clarification.

HSPA7 Holds Promise for Predicting the Therapeutic Response to ICB Therapy

We desired to further investigate the capacity of HSPA7 to predict the response to immune checkpoint therapy in GBM. However, few published immunotherapy datasets include GBM patients who received ICB therapy. Thus, we used a cohort of melanoma patients who received anti-CTLA4 therapy (23) and urothelial cancer cohorts of patients who received anti-PD-1 therapy (IMvigor210) to perform a complementary evaluation of the ability of HSPA7 to predict the immunotherapy response. Patients in the anti-CTLA4 cohort with low HSPA7 expression exhibited significant clinical benefits [**Figure 6A**, anti-CTLA cohort, HR 1.927 (0.8997–4.129)]. Furthermore, compared to the HSPA7-high group, the HSPA7-low group exhibited a significant therapeutic benefit and clinical response to antiCTLA-4 immunotherapy (**Figures 6B, C**). Similar results were found in the anti-PD-L1 cohort. Kaplan–Meier analysis showed that the patients with the 50 lowest HSPA7 expression levels exhibited markedly prolonged survival compared to the patients with the 50 highest HSPA7 expression levels [**Figure 6D**, HR 1.670 (1.022–2.792)]. Additionally, the HSPA7-low group exhibited significantly better therapeutic and clinical responses to anti-PD-L1 immunotherapy than the HSPA7-high group (**Figures 6E, F**).

Further GSVA enrichment analysis showed that compared to the HSPA7-low group, the HSPA7-high group exhibited higher TME immune cell infiltration with higher immune and stromal scores, lower tumor purity (**Supplementary Figure S11A**), higher stromal activation, higher oncogenic pathway activation, and lower MMR pathway activation (**Supplementary Figure S11B**), completely consistent with the functional enrichment patterns in GBM (**Figures 3A**, **4A** and **Supplementary Figures S5C**, **S6C**). PD-L1 expression in immune cells (ICs) and tumor cells (TCs) was also assessed in the IMvigor210 cohort, and we examined the difference in HSPA7 expression among groups with different PD-L1 expression levels. As indicated in **Figures 6G, H**, patients with higher PD-L1 expression levels in either immune cells or tumor cells exhibited higher HSPA7 expression levels (ANOVA summary IC: P = 0.0001, TC: P = 0.0009), indicating that HSPA7 can upregulate PD-L1 expression, suppressing immune activation. Moreover, previous studies indicated that F-box and WD repeat domain containing 7 (FBXW7) is a vital tumor suppressor in various cancers, controlling proteasome-mediated degradation of oncoproteins such as cyclin E, c-Myc, Mcl-1, mTOR, Jun, and Notch (48) and that its loss-of-function mutation promotes resistance to anti-PD-1 therapy through downregulation of vital sensing pathways (49). Compared to the FBXW7 wild-type group, HSPA7 expression was obviously decreased in the FBXW7 mutant group (**Figure 6I**). Fibroblast growth factor receptor 1 (FGFR1) is frequently mutated in various tumors, and inhibitors of FGFR1 have shown promising therapeutic value in several preclinical models (50). Palakurthi S. et al. (51) found that the combination of FGFR inhibition and PD-1 blockade can promote tumor-intrinsic induction of antitumor immunity. We also found that HSPA7 expression was significantly higher in the FGFR mutant group than in the FGFR wild-type group (**Figure 6J**). Collectively, our work strongly indicates that HSPA7 expression contributes to predicting the response to immune checkpoint therapy.

HSPA7 Facilitated Macrophage Infiltration and Could Be a Potential Immunotherapy Target for GBM Patients

We then analyzed the differences in the distribution of somatic mutations between the low and high HSPA7 expression groups in the TCGA GBM cohort using the "maftools" package and found that the PTEN mutation rate was significantly increased in the HSPA7-high group compared to the HSPA7-low group (**Figure 6K**; low: 20%, high: 36%). Additionally, the NF1 mutation rate, which often occurs in the MES subtype and drives recruitment and activation of TAMs (33), was also obviously elevated in the HSPA7-high group compared to the HSPA7-low group (**Figure 6K**; low: 8%, high: 11%). Chen et al. (52) found that PTEN deficiency in GBM increases macrophage infiltration by activating YAP1 signaling, which directly upregulates lysyl oxidase (LOX) expression, an MES subtype

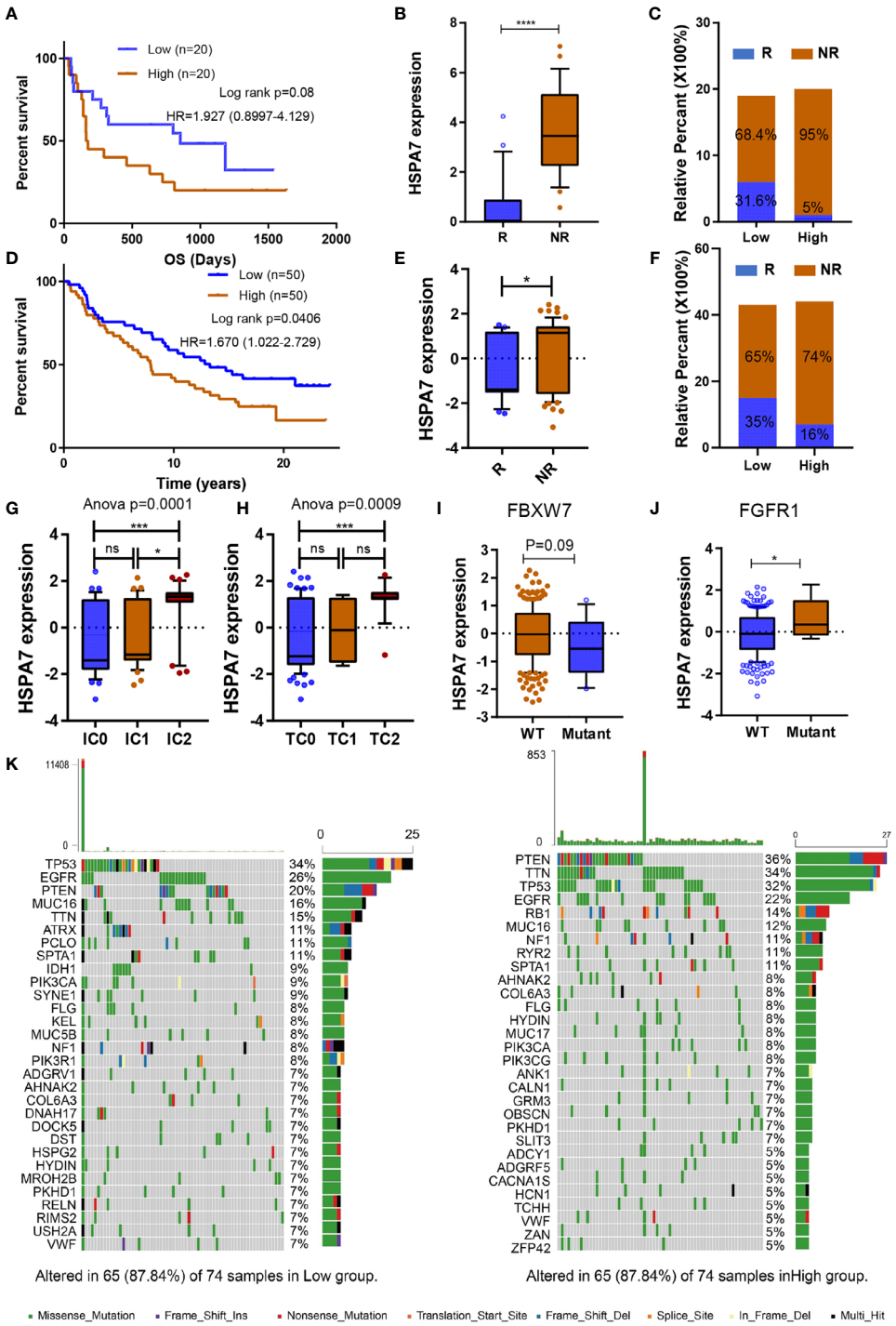

FIGURE 6 | HSPA7 holds promise for predicting the therapeutic response to ICB. **(A)** The Kaplan–Meier survival curves showed that HSPA7 was a prognostic risk factor in the melanoma cohort that received anti-CTLA4 therapy. **(B)** Expression of HSPA7 in distinct anti-CTLA4 clinical response groups, R, response; NR, no response. **(C)** The proportion of patients who responded to CTLA4 blockade immunotherapy in the low or high HSPA7 expression groups. **(D)** The Kaplan–Meier survival curves showed that HSPA7 is a prognostic risk factor in the anti-PD-L1 cohort (IMvigor210). **(E)** Expression of HSPA7 in distinct anti-PD-L1 clinical response groups, R, response; NR, no response. **(F)** The proportion of patients who responded to PD-L1 blockade immunotherapy in the low or high HSPA7 expression groups. PD-L1 expression in both ICs **(G)** and TCs **(H)** was associated with HSPA7 expression, with the highest PD-L1 expression level in cells showing the highest HSPA7 expression. (ANOVA, p = 0.0001, p = 0.0009, respectively). HSAP7 expression between **(I)** FBXW7 wild-type (WT) and mutant status and **(J)** FGFR1 wild-type (WT) and mutant status. **(K)** The waterfall plot of tumor somatic mutations established by those with high HSPA7 expression (right) and low HSPA7 expression (left). The statistical significance is shown as: ns, P > 0.05; *P < 0.05; ***P < 0.001; ****P < 0.0001.

marker and a macrophage chemoattractant (33), in turn inducing SPP1 secretion to support GBM survival. We found that YAP1 signaling was significantly upregulated in the HSPA7-high group compared to the HSPA7-low group (**Figure 7A**). We also confirmed that LOX and YAP1 were higher in MES GSCs than in PN GSCs (**Figure 7B**). Moreover, LOX and YAP1 expression levels were enhanced upon overexpression of HSPA7 in PN subtype GSCs 8–11 (**Figures 7C, D**) but decreased significantly upon knockdown of HSPA7 in MES subtype GSCs 267 (**Figure 7D**), suggesting that HSPA7 may facilitate tumor promoting macrophage infiltration by enhancing LOX expression, which could promote macrophage migration into the GBM TME and enhance angiogenesis by upregulating TAM-derived SPP1 (52). Finally, to further confirm the role of HSPA7 in facilitating macrophage migration by enhancing the YAP1-LOX axis, using the transwell assay, we found that conditioned medium from HSPA7 knockdown GSCs 267 inhibited THP1-differentiated macrophage migration significantly compared to the NC group (**Figure 7E**). Then, THP1-differentiated macrophages were cultured in conditioned medium collected from GSCs 267 transfected with HSPA7 ASO or NC. As shown in **Figure 7F**, conditioned medium from HSPA7-knockdown GSCs inhibited SPP1 expression in macrophages compared to the NC group. The immunofluorescent staining of our local clinical tumor tissue section analyses also showed that the expression of YAP1, LOX, CD68 (human macrophage marker), SPP1, and PD-L1 was enhanced in HSPA7-high GBM tissues compared to HSPA7-low tissues (**Figure 7G**).

Moreover, Robert M. Samstein et al. (53) found that TMB predicted survival after immunotherapy across multiple cancer types (including GBM). Thus, we downloaded the mutation data of 82 GBM samples and then analyzed the differences in the distribution of somatic mutations between the samples with the 30 lowest TMBs and the 30 highest TMBs. The PTEN and NF1 mutation rates were significantly increased in low-TMB samples compared to the high-TMB samples, and the same results were found for the HSPA7 expression level (**Supplementary Figure S12A**). We further explored the association between the HSPA7 expression level and TMB. As shown in **Supplementary Figure S12B**, HSPA7 expression was statistically negatively correlated with TMB. In addition, Touat M. et al. (54) recently found that mismatch repair (MMR)-deficient gliomas were characterized by a lack of prominent T cell infiltration, extensive intratumoral heterogeneity, poor patient survival, and a low rate of response to PD-1 blockade therapy. Our data also showed that the high HSPA7 expression group showed reduced activation of MMR-associated pathways (**Figure 4A**), which was negatively correlated with immunosuppression, stromal activation, and oncogene pathway activation (**Figure 4B**). Other studies have also shown the same results (28, 55). Furthermore, HSPA7 expression was negatively correlated with the expression of MMR genes such as MLH1, MSH2, MSH6, and PMS2 (**Supplementary Figure S12C**). Previous studies indicated that GBM patients exhibit resistance to immune checkpoint inhibitors (ICIs) due to the low mutation rate, the PTEN-deficient immunosuppressive microenvironment, infiltration by myeloid-derived suppressor cells (including TAMs, prominent players in brain cancers), and activation of tumor stromal cells (56, 57), indicating that knockdown of HSPA7 may enhance the efficacy of ICIs such as PD1 inhibitors in GBM. To illustrate this function, we generated patient-derived glioblastoma organoids (GBOs), which maintain cell-type heterogeneity (including macrophages, T cells, and vascular cells) and molecular signatures of their respective parental tumors, according to experimental protocols already reported by Jacob F. et al. (31). Immunofluorescence assays of our GBO sections also confirmed the presence of macrophages and vascular cells, as detected by CD68 and CD31 markers, respectively (**Supplementary Figure S13A**), supporting the use of three-dimensional GBO models for holistic study of the TME of GBM and evaluating the efficacy of PD1 inhibitors. We next applied our GBO model to test treatment responses *in vitro*. To mimic the postsurgical standard of care treatment, we subjected GBO samples from patient whose GBM tissues expressed high CD68 and SPP1 (**Supplementary Figure S13B**) to a single exposure conditioned medium from HSPA7-knockdown GSCs or with PD1 inhibitor (5 μM) treatment for 5 days. The therapeutic response was evaluated by quantifying the percentage of cells expressing Ki67 (proliferation index) and CD44 (invasion index). As shown in **Figure 7H**, knockdown of HSPA7 significantly enhanced the efficacy of the PD1 inhibitor in GBM. In summary, HSPA7 facilitated tumor promoting macrophage migration into the GBM TME by activating the YAP1–LOX axis, and our results indicated that HSPA7 might be a potential immunotherapy target for GBM patients.

Characterization of HSPA7 Across 33 Cancer Types

We investigated whether HSPA7 expression is correlated with prognosis in a pancancer patient cohort. The expression of HSPA7 in tumor tissues and GTEx normal brain tissues was determined in the GEPIA database. As shown in **Supplementary Figure S14**, the expression of HSPA7 was significantly lower in tumor tissues in the ACC, COAD, DLBC, LAML, LUAD, LUSC, READ, THCA, and THYM cohorts but significantly higher in tumor tissues in the GBM, KIRC, KIRP, and PAAD cohorts than in the corresponding normal tissues. Genetic alterations were also observed in many other tumors, although these alterations were not significant. In addition, Cox regression analysis of survival rates and Kaplan–Meier analysis were conducted using the SangerBox tool. The relationships between HSPA7 expression levels and the prognoses of different tumors are shown in **Supplementary Figures S15**-**S17**. Statistically, HSPA7 is a risk factor in most cancers (such as ACC, LDBC, and CESC). However, we found that it is a relatively favorable factor in several cancer types such as SKCM, KIRP, and SARC. We next evaluated the immune score and stromal score across 33 cancers in the TCGA database. HSPA7 expression was significantly positively correlated with the immune score (**Supplementary Figure S18**) and stromal score (**Supplementary Figure S19**) in all 33 cancer types. Moreover, HSPA7 was significantly positively correlated with immune checkpoint expression (**Supplementary Figure S20A**) and the immune response (**Supplementary Figure S20B**) in most cancer

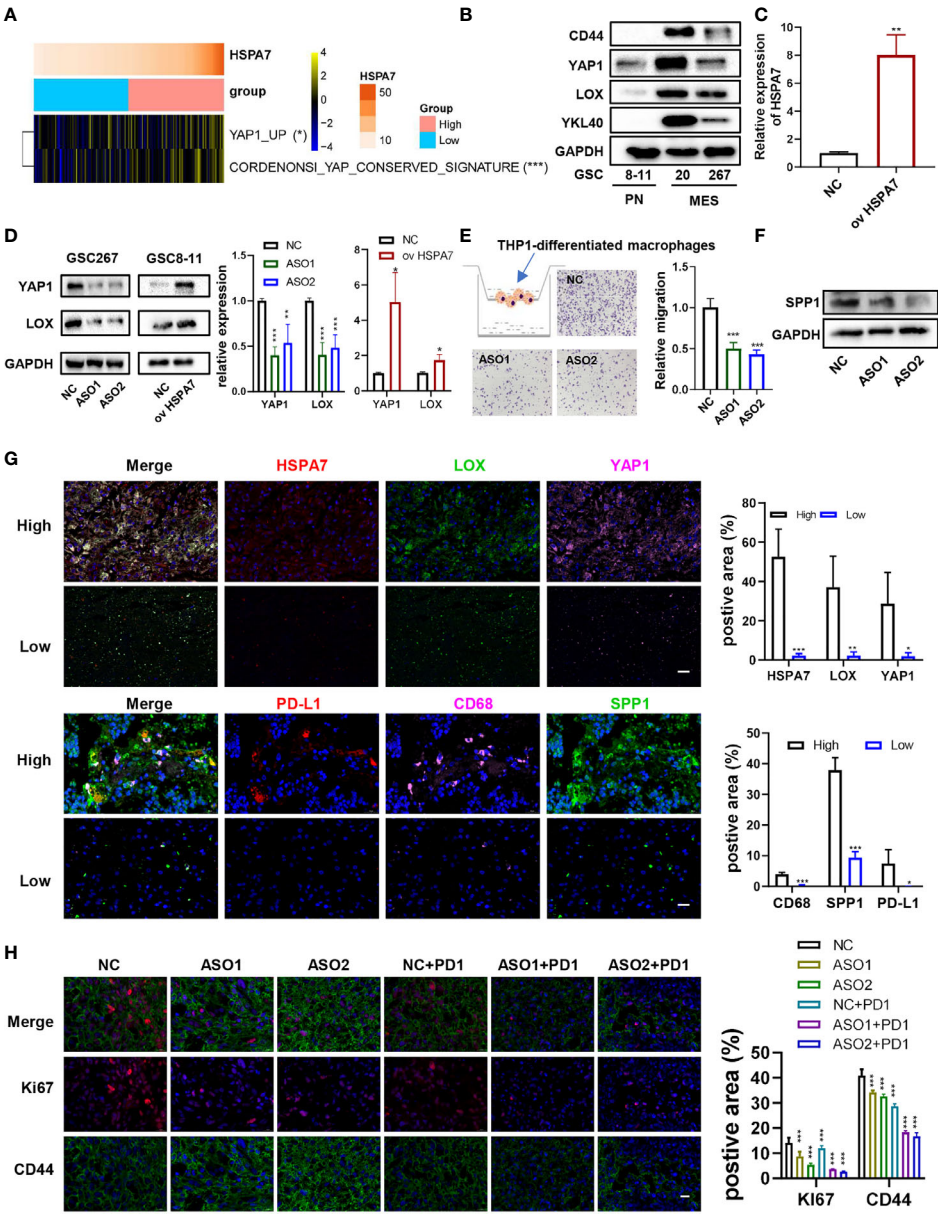

FIGURE 7 | HSPA7 facilitated macrophage infiltration and might be a novel immunotherapy target for GBM patients. **(A)** The heatmap shows that HSPA7 activated YAP1 signaling. The asterisks indicate a significant statistical p-value calculated using the non-parametric Wilcoxon test (*P < 0.05; **P < 0.01; ***P < 0.001). **(B)** The protein expression of CD44, YAP1, LOX, and YKL40 in PN subtype GSCs (GSCs 8–11) and MES subtype GSCs (GSCs 20 and 267). **(C)** qPCR assays verified the overexpression efficiency of HSPA7. **(D)** Representative Western blot assays showed that HSPA7 promoted the expression of YAP1 and LOX, a macrophage chemoattractant (left), and quantification histogram represented the relative protein expression of LOX and YAP1 (right); data are presented as the mean ± SD, n = 3. *p < 0.05, **p < 0.01, ***p < 0.001. Means were compared with Student's *t*-test for two groups and one-way ANOVA for three groups, and the NC group is indicated as the control. **(E)** Representative transwell migration assays showed that HSPA7 inhibited human THP1-differentiated macrophage migration by exposing them to conditioned medium from GSC 267 cells transfected with NC, HSPA7 ASO1, or ASO2 for 24 h. Original magnification, ×100 (left), and quantification histogram represented relative migration of THP-1 macrophages (right); data are presented as the mean ± SD, n = 3. *p < 0.05, **p < 0.01, ***p < 0.001. Means were compared with one-way ANOVA, and the NC group is indicated as the control. **(F)** Western blot assays showed that HSPA7 inhibited the expression of SPP1 in THP1-differentiated macrophages by exposing them to conditioned medium from GSC 267 cells transfected with NC, HSPA7 ASO1, or ASO2 for 48 h. **(G)** IF staining in a human GBM tissue microarray showed that the expression of LOX, YAP1, PD-L1, CD68, and SPP1 was higher in the HSPA7 high group than in the low group. Histogram representing statistical proportion data of positive area; data are presented as the mean ± SD, n = 3. *p < 0.05, **p < 0.01, ***p < 0.001, means were compared with Student's *t*-test. **(H)** GBOs at 2 weeks were cocultured with conditioned medium from GSC 267 cells, transfected with NC, HSPA7 ASO1, or ASO2 at 48 h, and PD1 antibody (5 μM) for 5 days as indicated. IF staining for Ki67 and CD44 in GBO sections showed that knockdown of HSPA7 enhanced the effect of anti-PD1 therapy, original magnification, ×630 (scale bars: 20 μm). Histogram representing statistical proportion data of positive area; data are presented as the mean ± SD, n = 3. *p < 0.05, **p < 0.01, ***p < 0.001. Means were compared with one-way ANOVA, and the NC group is indicated as the control.

types such as GBM, LGG, OV, and LUAD. However, no relationship was found in other cancers such as SKCM, UVM, TGCT, and PAAD, indicating that HSPA7 may act *via* a mechanism other than TME regulation in these cancers. Thus, the molecular mechanisms of this gene need further study in specific tumors. Collectively, these data emphasize that HSPA7 may be a key factor in facilitating the acquisition of various immunophenotypes in various cancers and may be considered in the development of more effective immunotherapies for GBM and other immunotherapy-resistant tumors. Because different immune cells may play different roles in different tumors, the functions of HSPA7 in specific tumors must be explored.

DISCUSSION

GBM, one of the most aggressive brain tumors, currently has no effective and sufficient therapies due to its intratumoral heterogeneity and molecular plasticity. ICB therapy is being actively pursued as a promising treatment option for GBM, but very few patients respond to ICB therapy. Thus, identifying markers regulating the brain TME that are prominent players in ICB therapy for cancer could reveal promising new targets for therapeutic intervention. LncRNAs and m^6A modifications are emerging as indispensable regulators of the TME. However, the overall TME infiltration characteristics mediated by m^6A-modified lncRNAs have not been comprehensively recognized. Therefore, it is worth obtaining comprehensive knowledge of the cellular TME infiltration characteristics mediated by m^6A-regulated lncRNAs.

Here, based on our m^6A-seq data, we revealed highly distinct lncRNA m^6A methylation modification patterns between GBM and normal brain tissues. In addition, we identified immune-stromal-m^6A-related HSPA7 as a novel prognostic risk factor in GBM patients; this gene plays a crucial role in immunophenotype determination, stromal activation, and oncogenic pathway activation and has a robust capacity to predict the ICB response. Furthermore, in this study, WTAP, a methyltransferase mediating m^6A modification, was identified as a potential regulator of HSPA7 expression. Further analysis showed that WTAP, like HSPA7, can also regulate immunophenotype determination and stromal activation-related pathways (**Supplementary Figures S8**, **S9**). This finding again demonstrated that m^6A modification is highly important in shaping the TME landscape. Many studies have reported that stromal cell activation in the TME can suppress immune infiltration or facilitate an immunosuppressive response in the TME, mediating therapeutic resistance to ICB (28, 58). Our data also revealed a markedly negative correlation between HSPA7 expression and TMB, a marker of the response to ICB therapy, in a TCGA GBM cohort (**Figure 6B**). In addition, another study showed that PTEN mutations were associated with immunosuppressive expression signatures in non-responders to anti-PD-1 immunotherapy in GBM (2). Chen et al. (52) found that PTEN deficiency in GBM increases the infiltration of $SPP1^+$ macrophages, which can interact with fibroblasts and vascular endothelial cells, inducing angiogenesis, EMT, and some other stromal activation-related pathways in colon cancer and are characterized by expression of the pattern recognition receptor MARCO (59) *via* a YAP1–LOX-β1 integrin–PYK2 axis. Intriguingly, antibody-mediated depletion of MARCO inhibits cancer progression and metastasis, enhancing ICB efficacy (60), suggesting that $SPP1^+$ macrophages play a non-negligible role in the immunorepressive response and immunotherapeutic resistance. We then analyzed myeloid cell-derived macrophage-restricted chemokines, which were the main factors that cause immunosuppression in GBM. We found that compared to tumors with low HSPA7 expression, tumors with high HSPA7 expression exhibited significantly increased myeloid cell-derived macrophage-restricted chemokines (8, 25) (**Supplementary Figures S4D, E**); we also confirmed that HSPA7 could facilitate the macrophage infiltration into the GBM TME *via* YAP1–LOX axis *in vitro*, as well as into our local GBM tissue sections (**Figures 7A–G**). Furthermore, we found that HSPA7 can interact with YAP1 (61), which can induce the secretion of CCL2/CSF1 to recruit monocytes (62), suggesting that HSPA7 may be a target that synergistically regulates $SPP1^+$ macrophages, which then induce stromal activation in the TME. Moreover, we found that HSPA7 and YAP are also contained in GBM extracellular exosomes (63), a fundamental regulator of TME cells. Numerous research reports have indicated that YAP is a hub in the network of signals exchanged within the TME (64), thus regulating the immune response and stromal activation. However, the specific mechanism of HSPA7 needs to be proven by a large number of experiments. We also confirmed the predictive value of HSPA7 in a cohort of melanoma patients who received anti-CTLA4 therapy and an IMvigor210 cohort of patients treated with anti-PD-L1 therapy. A statistically significant difference in HSPA7 expression was found between non-responders and responders. MMR deficiency has recently emerged as a beneficial indicator of the response to PD-1 blockade in patients with cancer (65, 66), whereas we found that HSPA7 was negatively correlated with MMR-related pathway activity (**Figure 4A**), which in turn was negatively correlated with stromal activation and oncogenic pathway activation (**Figure 4B** and **Supplementary Figure S11**). This pattern suggests that MMR deficiency is an unfavorable factor for the response to ICB therapy. Other studies have shown the same results (28, 55). By comprehensive analysis of data for 10,294 samples, a recent study showed that MMR-deficient gliomas are characterized by a lack of prominent T cell infiltration, extensive intratumoral heterogeneity, poor patient survival, and a low rate of response to PD-1 blockade (54), reconfirming the ability of HSPA7 to predict the response to immunotherapy. We also explored the function of HSPA7 in various cancer types. As shown in **Figures S13**-**S19**, HSPA7 expression had prognostic significance in most cancers; in addition, it can regulate the expression of immune checkpoint genes and the activity of immune response pathways and was positively correlated with the immune score and stromal score in the majority of tumor types. HSPA7 was found to be a risk factor in the cohort of melanoma patients who received anti-CTLA4 therapy (**Figures 6A–C**) but was found to be a beneficial prognostic factor in the TCGA SKCM cohort (23) (**Supplementary Figures S14**, **S16**), exhibiting no obvious correlation with immune

checkpoint expression (**Supplementary Figure S20A**) or the immune response (**Supplementary Figure S20B**). The mechanisms underlying this discrepancy need future exploration.

In summary, *via* integrated analysis of our own m^{6}A-seq data and public clinical data, we found highly distinct lncRNA m^{6}A methylation modification patterns between GBM and normal brain tissues and determined that HSPA7 could be used to evaluate the prognosis of GBM patients, as well as the corresponding cellular TME infiltration and activation characteristics of individual patients, and could predict the clinical efficacy of anti-PD-1/-PD-L1 immunotherapy in patients. More importantly, this study offers several novel insights regarding cancer immunotherapy; for example, targeting m^{6}A regulators to change the m^{6}A modification patterns of key immune-regulating targets may reverse unfavorable cellular TME infiltration characteristics. This study contributes to future exploration of novel drug combination strategies or novel immunotherapeutic agents.

DATA AVAILABILITY STATEMENT

The datasets presented in this study can be found in online repositories. The names of the repository/repositories and accession number(s) can be found below: https://www.ncbi.nlm.nih.gov/, SRA PRJNA661159.

ETHICS STATEMENT

The studies involving human participants were reviewed and approved by Ethical Committee on Scientific Research of Shandong University Qilu Hospital (approval number: KYLL-2018-324). The patients/participants provided their written informed consent to participate in this study.

AUTHOR CONTRIBUTIONS

GL and HX supervised the project. RRZ designed the research and performed all experiments. BYL completed the basic experiment part. ZH performed statistical analysis with the R language. SJZ, QDG, PZ, WQ, SBW and ZHC were responsible for clinical sample collection and subsequent sample delivery. XG, YHQ, ZWP helped to revise the manuscript. All authors contributed to the article and approved the submitted version.

FUNDING

This work was supported by grants from the National Natural Science Foundation of China (Nos. 81874083; 82072776; 82072775; 81702468; 81802966; 81902540; 81874082; 81472353), Natural Science Foundation of Shandong Province of China (Nos. ZR2019BH057; ZR2020QH174), Key clinical Research project of Clinical Research Center of Shandong University (2020SDUCRCA011) and Taishan Pandeng Scholar Program of Shandong Province (No. tspd20210322).

ACKNOWLEDGMENTS

We are grateful to Dr. Frederick F. Lang and Dr. Krishna P.L. Bhat for providing GSC cell lines used in our study. We thank the surgeons and patients who participated in these studies; Novogene Co., Ltd.; and Tianjin Novogene Bioinformatics Technology Co., Ltd. for m6A technical development and support.

SUPPLEMENTARY MATERIAL

The Supplementary Material for this article can be found online at: https://www.frontiersin.org/articles/10.3389/fimmu.2021.653711/full#supplementary-material

REFERENCES

1. Jackson C, Lim M. Immunotherapy for Glioblastoma: Playing Chess, Not Checkers. *Clin Cancer Res: Off J Am Assoc Cancer Res* (2018) 24(17):4059–61. doi: 10.1158/1078-0432.ccr-18-0491
2. Zhao J, Chen A, Gartrell R, Silverman A, Aparicio L, Chu T, et al. Immune and Genomic Correlates of Response to Anti-PD-1 Immunotherapy in Glioblastoma. *Nat Med* (2019) 25(3):462–9. doi: 10.1038/s41591-019-0349-y
3. Daniel P, Sabri S, Chaddad A, Meehan B, Jean-Claude B, Rak J, et al. Temozolomide Induced Hypermutation in Glioma: Evolutionary Mechanisms and Therapeutic Opportunities. *Front Oncol* (2019) 9:41. doi: 10.3389/fonc.2019.00041
4. Johanns T, Miller C, Dorward I, Tsien C, Chang E, Perry A, et al. Immunogenomics of Hypermutated Glioblastoma: A Patient With Germline POLE Deficiency Treated With Checkpoint Blockade Immunotherapy. *Cancer Discovery* (2016) 6(11):1230–6. doi: 10.1158/2159-8290.cd-16-0575
5. Bouffet E, Larouche V, Campbell B, Merico D, de Borja R, Aronson M, et al. Immune Checkpoint Inhibition for Hypermutant Glioblastoma Multiforme Resulting From Germline Biallelic Mismatch Repair Deficiency. *J Clin Oncol: Off J Am Soc Clin Oncol* (2016) 34(19):2206–11. doi: 10.1200/jco.2016.66.6552
6. Gutmann D, Kettenmann H. Microglia/Brain Macrophages as Central Drivers of Brain Tumor Pathobiology. *Neuron* (2019) 104(3):442–9. doi: 10.1016/j.neuron.2019.08.028
7. Friebel E, Kapolou K, Unger S, Núñez N, Utz S, Rushing E, et al. Single-Cell Mapping of Human Brain Cancer Reveals Tumor-Specific Instruction of Tissue-Invading Leukocytes. *Cell* (2020) 181(7):1626–42.e20. doi: 10.1016/j.cell.2020.04.055
8. Klemm F, Maas R, Bowman R, Kornete M, Soukup K, Nassiri S, et al. Interrogation of the Microenvironmental Landscape in Brain Tumors Reveals Disease-Specific Alterations of Immune Cells. *Cell* (2020) 181(7):1643–60.e17. doi: 10.1016/j.cell.2020.05.007
9. Deng X, Su R, Weng H, Huang H, Li Z, Chen J. RNA N-Methyladenosine Modification in Cancers: Current Status and Perspectives. *Cell Res* (2018) 28 (5):507–17. doi: 10.1038/s41422-018-0034-6
10. Yang Y, Hsu P, Chen Y, Yang Y. Dynamic Transcriptomic mA Decoration: Writers, Erasers, Readers and Functions in RNA Metabolism. *Cell Res* (2018) 28(6):616–24. doi: 10.1038/s41422-018-0040-8
11. Xu C, Yuan B, He T, Ding B, Li S. Prognostic Values of YTHDF1 Regulated Negatively by Mir-3436 in Glioma. *J Cell Mol Med* (2020) 24(13):7538–49. doi: 10.1111/jcmm.15382
12. Dong Z, Cui H. The Emerging Roles of RNA Modifications in Glioblastoma. *Cancers* (2020) 12(3):736. doi: 10.3390/cancers12030736
13. Chai R, Wu F, Wang Q, Zhang S, Zhang K, Liu Y, et al. mA RNA Methylation Regulators Contribute to Malignant Progression and Have Clinical Prognostic Impact in Gliomas. *Aging* (2019) 11(4):1204–25. doi: 10.18632/aging.101829
14. Visvanathan A, Patil V, Arora A, Hegde A, Arivazhagan A, Santosh V, et al. Essential Role of METTL3-Mediated mA Modification in Glioma Stem-Like

Cells Maintenance and Radioresistance. *Oncogene* (2018) 37(4):522–33. doi: 10.1038/onc.2017.351
15. Zhang S, Zhao B, Zhou A, Lin K, Zheng S, Lu Z, et al. mA Demethylase ALKBH5 Maintains Tumorigenicity of Glioblastoma Stem-Like Cells by Sustaining FOXM1 Expression and Cell Proliferation Program. *Cancer Cell* (2017) 31(4):591–606.e6. doi: 10.1016/j.ccell.2017.02.013
16. Zheng Q, Hou J, Zhou Y, Li Z, Cao X. The RNA Helicase DDX46 Inhibits Innate Immunity by Entrapping mA-Demethylated Antiviral Transcripts in the Nucleus. *Nat Immunol* (2017) 18(10):1094–103. doi: 10.1038/ni.3830
17. Gao Y, Vasic R, Song Y, Teng R, Liu C, Gbyli R, et al. mA Modification Prevents Formation of Endogenous Double-Stranded RNAs and Deleterious Innate Immune Responses During Hematopoietic Development. *Immunity* (2020) 52(6):1007–21.e8. doi: 10.1016/j.immuni.2020.05.003
18. Han D, Liu J, Chen C, Dong L, Liu Y, Chang R, et al. Anti-Tumour Immunity Controlled Through mRNA mA Methylation and YTHDF1 in Dendritic Cells. *Nature* (2019) 566(7743):270–4. doi: 10.1038/s41586-019-0916-x
19. Li H, Tong J, Zhu S, Batista P, Duffy E, Zhao J, et al. mA mRNA Methylation Controls T Cell Homeostasis by Targeting the IL-7/STAT5/SOCS Pathways. *Nature* (2017) 548(7667):338–42. doi: 10.1038/nature23450
20. Patil D, Chen C, Pickering B, Chow A, Jackson C, Guttman M, et al. M(6)A RNA Methylation Promotes XIST-Mediated Transcriptional Repression. *Nature* (2016) 537(7620):369–73. doi: 10.1038/nature19342
21. Ni W, Yao S, Zhou Y, Liu Y, Huang P, Zhou A, et al. Long Noncoding RNA GAS5 Inhibits Progression of Colorectal Cancer by Interacting With and Triggering YAP Phosphorylation and Degradation and is Negatively Regulated by the mA Reader YTHDF3. *Mol Cancer* (2019) 18(1):143. doi: 10.1186/s12943-019-1079-y
22. Huang H, Weng H, Chen J. mA Modification in Coding and Non-Coding RNAs: Roles and Therapeutic Implications in Cancer. *Cancer Cell* (2020) 37 (3):270–88. doi: 10.1016/j.ccell.2020.02.004
23. Van Allen E, Miao D, Schilling B, Shukla S, Blank C, Zimmer L, et al. Genomic Correlates of Response to CTLA-4 Blockade in Metastatic Melanoma. *Sci (New York NY)* (2015) 350(6257):207–11. doi: 10.1126/science.aad0095
24. Bindea G, Mlecnik B, Tosolini M, Kirilovsky A, Waldner M, Obenauf A, et al. Spatiotemporal Dynamics of Intratumoral Immune Cells Reveal the Immune Landscape in Human Cancer. *Immunity* (2013) 39(4):782–95. doi: 10.1016/j.immuni.2013.10.003
25. Bowman R, Klemm F, Akkari L, Pyonteck S, Sevenich L, Quail D, et al. Macrophage Ontogeny Underlies Differences in Tumor-Specific Education in Brain Malignancies. *Cell Rep* (2016) 17(9):2445–59. doi: 10.1016/j.celrep.2016.10.052
26. Liberzon A, Birger C, Thorvaldsdóttir H, Ghandi M, Mesirov J, Tamayo P. The Molecular Signatures Database (MSigDB) Hallmark Gene Set Collection. *Cell Syst* (2015) 1(6):417–25. doi: 10.1016/j.cels.2015.12.004
27. Kanehisa M, Sato Y, Kawashima M, Furumichi M, Tanabe M. KEGG as a Reference Resource for Gene and Protein Annotation. *Nucleic Acids Res* (2016) 44:D457–62. doi: 10.1093/nar/gkv1070
28. Mariathasan S, Turley S, Nickles D, Castiglioni A, Yuen K, Wang Y, et al. Tgfβ Attenuates Tumour Response to PD-L1 Blockade by Contributing to Exclusion of T Cells. *Nature* (2018) 554(7693):544–8. doi: 10.1038/nature25501
29. Zeng D, Ye Z, Wu J, Zhou R, Fan X, Wang G, et al. Macrophage Correlates With Immunophenotype and Predicts Anti-PD-L1 Response of Urothelial Cancer. *Theranostics* (2020) 10(15):7002–14. doi: 10.7150/thno.46176
30. Schalper K, Rodriguez-Ruiz M, Diez-Valle R, López-Janeiro A, Porciuncula A, Idoate M, et al. Neoadjuvant Nivolumab Modifies the Tumor Immune Microenvironment in Resectable Glioblastoma. *Nat Med* (2019) 25(3):470–6. doi: 10.1038/s41591-018-0339-5
31. Jacob F, Salinas R, Zhang D, Nguyen P, Schnoll J, Wong S, et al. A Patient-Derived Glioblastoma Organoid Model and Biobank Recapitulates Inter- and Intra-Tumoral Heterogeneity. *Cell* (2020) 180(1):188–204.e22. doi: 10.1016/j.cell.2019.11.036
32. Hazra A, Gogtay N. Biostatistics Series Module 3: Comparing Groups: Numerical Variables. *Indian J Dermatol* (2016) 61(3):251–60. doi: 10.4103/0019-5154.182416
33. Wang Q, Hu B, Hu X, Kim H, Squatrito M, Scarpace L, et al. Tumor Evolution of Glioma-Intrinsic Gene Expression Subtypes Associates With Immunological Changes in the Microenvironment. *Cancer Cell* (2017) 32 (1):42–56.e6. doi: 10.1016/j.ccell.2017.06.003
34. Wu A, Wei J, Kong L, Wang Y, Priebe W, Qiao W, et al. Glioma Cancer Stem Cells Induce Immunosuppressive Macrophages/Microglia. *Neuro-oncology* (2010) 12(11):1113–25. doi: 10.1093/neuonc/noq082
35. Tsukamoto H, Fujieda K, Miyashita A, Fukushima S, Ikeda T, Kubo Y, et al. Combined Blockade of IL6 and PD-1/PD-L1 Signaling Abrogates Mutual Regulation of Their Immunosuppressive Effects in the Tumor Microenvironment. *Cancer Res* (2018) 78(17):5011–22. doi: 10.1158/0008-5472.can-18-0118
36. Tomaszewski W, Sanchez-Perez L, Gajewski T, Sampson J. Brain Tumor Microenvironment and Host State: Implications for Immunotherapy. *Clin Cancer Res: Off J Am Assoc Cancer Res* (2019) 25(14):4202–10. doi: 10.1158/1078-0432.ccr-18-1627
37. Chen D, Mellman I. Elements of Cancer Immunity and the Cancer-Immune Set Point. *Nature* (2017) 541(7637):321–30. doi: 10.1038/nature21349
38. Becht E, Giraldo N, Lacroix L, Buttard B, Elarouci N, Petitprez F, et al. Estimating The Population Abundance of Tissue-Infiltrating Immune and Stromal Cell Populations Using Gene Expression. *Genome Biol* (2016) 17 (1):218. doi: 10.1186/s13059-016-1070-5
39. Lin R, Zhao L. Mechanistic Basis and Clinical Relevance of the Role of Transforming Growth Factor-β in Cancer. *Cancer Biol Med* (2015) 12(4):385–93. doi: 10.7497/j.issn.2095-3941.2015.0015
40. Massagué J. TGFbeta in Cancer. *Cell* (2008) 134(2):215–30. doi: 10.1016/j.cell.2008.07.001
41. Flavell R, Sanjabi S, Wrzesinski S, Licona-Limón P. The Polarization of Immune Cells in the Tumour Environment by TGFbeta. *Nat Rev Immunol* (2010) 10(8):554–67. doi: 10.1038/nri2808
42. Rodón L, Gonzàlez-Juncà A, Inda MM, Sala-Hojman A, Martínez-Sáez E, Seoane J. Active CREB1 Promotes a Malignant Tgfβ2 Autocrine Loop in Glioblastoma. *Cancer Discov* (2014) 4(10):1230–41. doi: 10.1158/2159-8290.cd-14-0275
43. Pan J, Hu S, Shi D, Cai M, Li Y, Zou Q, et al. PaGenBase: A Pattern Gene Database for the Global and Dynamic Understanding of Gene Function. *PloS One* (2013) 8(12):e80747. doi: 10.1371/journal.pone.0080747
44. Han H, Cho J, Lee S, Yun A, Kim H, Bae D, et al. TRRUST V2: An Expanded Reference Database of Human and Mouse Transcriptional Regulatory Interactions. *Nucleic Acids Res* (2018) 46:D380–D6. doi: 10.1093/nar/gkx1013
45. Yue Y, Liu J, Cui X, Cao J, Luo G, Zhang Z, et al. VIRMA Mediates Preferential mA mRNA Methylation in 3'UTR and Near Stop Codon and Associates With Alternative Polyadenylation. *Cell Discov* (2018) 4:10. doi: 10.1038/s41421-018-0019-0
46. Ping X, Sun B, Wang L, Xiao W, Yang X, Wang W, et al. Mammalian WTAP is a Regulatory Subunit of the RNA N6-Methyladenosine Methyltransferase. *Cell Res* (2014) 24(2):177–89. doi: 10.1038/cr.2014.3
47. Liu J, Yue Y, Han D, Wang X, Fu Y, Zhang L, et al. A METTL3-METTL14 Complex Mediates Mammalian Nuclear RNA N6-Adenosine Methylation. *Nat Chem Biol* (2014) 10(2):93–5. doi: 10.1038/nchembio.1432
48. Yeh C, Bellon M, Nicot C. FBXW7: A Critical Tumor Suppressor of Human Cancers. *Mol Cancer* (2018) 17(1):115. doi: 10.1186/s12943-018-0857-2
49. Gstalder C, Liu D, Miao D, Lutterbach B, DeVine A, Lin C, et al. Inactivation of Fbxw7 of Impairs dsRNA Sensing and Confers Resistance to PD-1 Blockade. *Cancer Discov* (2020) 10(9):1296–311. doi: 10.1158/2159-8290.cd-19-1416
50. Peng R, Chen Y, Wei L, Li G, Feng D, Liu S, et al. Resistance to FGFR1-Targeted Therapy Leads to Autophagy *via* TAK1/AMPK Activation in Gastric Cancer. *Gastric Cancer: Off J Int Gastric Cancer Assoc Jpn Gastric Cancer Assoc* (2020) 23(6):988–1002. doi: 10.1007/s10120-020-01088-y
51. Palakurthi S, Kuraguchi M, Zacharek S, Zudaire E, Huang W, Bonal D, et al. The Combined Effect of FGFR Inhibition and PD-1 Blockade Promotes Tumor-Intrinsic Induction of Antitumor Immunity. *Cancer Immunol Res* (2019) 7(9):1457–71. doi: 10.1158/2326-6066.cir-18-0595
52. Chen P, Zhao D, Li J, Liang X, Li J, Chang A, et al. Symbiotic Macrophage-Glioma Cell Interactions Reveal Synthetic Lethality in PTEN-Null Glioma. *Cancer Cell* (2019) 35(6):868–84.e6. doi: 10.1016/j.ccell.2019.05.003
53. Samstein R, Lee C, Shoushtari A, Hellmann M, Shen R, Janjigian Y, et al. Tumor Mutational Load Predicts Survival After Immunotherapy Across Multiple Cancer Types. *Nat Genet* (2019) 51(2):202–6. doi: 10.1038/s41588-018-0312-8
54. Touat M, Li Y, Boynton A, Spurr L, Iorgulescu J, Bohrson C, et al. Mechanisms and Therapeutic Implications of Hypermutation in Gliomas. *Nature* (2020) 580(7804):517–23. doi: 10.1038/s41586-020-2209-9

55. Zhang B, Wu Q, Li B, Wang D, Wang L, Zhou Y. mA Regulator-Mediated Methylation Modification Patterns and Tumor Microenvironment Infiltration Characterization in Gastric Cancer. *Mol Cancer* (2020) 19(1):53. doi: 10.1186/s12943-020-01170-0
56. Jackson C, Choi J, Lim M. Mechanisms of Immunotherapy Resistance: Lessons From Glioblastoma. *Nat Immunol* (2019) 20(9):1100–9. doi: 10.1038/s41590-019-0433-y
57. Lim M, Xia Y, Bettegowda C, Weller M. Current State of Immunotherapy for Glioblastoma. *Nat Rev Clin Oncol* (2018) 15(7):422–42. doi: 10.1038/s41571-018-0003-5
58. Afik R, Zigmond E, Vugman M, Klepfish M, Shimshoni E, Pasmanik-Chor M, et al. Tumor Macrophages are Pivotal Constructors of Tumor Collagenous Matrix. *J Exp Med* (2016) 213(11):2315–31. doi: 10.1084/jem.20151193
59. Zhang L, Li Z, Skrzypczynska K, Fang Q, Zhang W, O'Brien S, et al. Single-Cell Analyses Inform Mechanisms of Myeloid-Targeted Therapies in Colon Cancer. *Cell* (2020) 181(2):442–59.e29. doi: 10.1016/j.cell.2020.03.048
60. Georgoudaki A, Prokopec K, Boura V, Hellqvist E, Sohn S, Östling J, et al. Reprogramming Tumor-Associated Macrophages by Antibody Targeting Inhibits Cancer Progression and Metastasis. *Cell Rep* (2016) 15(9):2000–11. doi: 10.1016/j.celrep.2016.04.084
61. Liu Y, Zhang X, Lin J, Chen Y, Qiao Y, Guo S, et al. CCT3 Acts Upstream of YAP and TFCP2 as a Potential Target and Tumour Biomarker in Liver Cancer. *Cell Death Dis* (2019) 10(9):644. doi: 10.1038/s41419-019-1894-5
62. Zhang Y, Zhang H, Zhao B. Hippo Signaling in the Immune System. *Trends Biochem Sci* (2018) 43(2):77–80. doi: 10.1016/j.tibs.2017.11.009
63. Choi D, Montermini L, Kim D, Meehan B, Roth F, Rak J. The Impact of Oncogenic EGFRvIII on the Proteome of Extracellular Vesicles Released From Glioblastoma Cells. *Mol Cell Proteomics: MCP* (2018) 17(10):1948–64. doi: 10.1074/mcp.RA118.000644
64. Zanconato F, Cordenonsi M, Piccolo S. YAP and TAZ: A Signalling Hub of the Tumour Microenvironment. *Nat Rev Cancer* (2019) 19(8):454–64. doi: 10.1038/s41568-019-0168-y
65. Teo M, Seier K, Ostrovnaya I, Regazzi A, Kania B, Moran M, et al. Alterations in DNA Damage Response and Repair Genes as Potential Marker of Clinical Benefit From PD-1/PD-L1 Blockade in Advanced Urothelial Cancers. *J Clin Oncol: Off J Am Soc Clin Oncol* (2018) 36(17):1685–94. doi: 10.1200/jco.2017.75.7740
66. Plimack E, Dunbrack R, Brennan T, Andrake M, Zhou Y, Serebriiskii I, et al. Defects in DNA Repair Genes Predict Response to Neoadjuvant Cisplatin-Based Chemotherapy in Muscle-Invasive Bladder Cancer. *Eur Urol* (2015) 68 (6):959–67. doi: 10.1016/j.eururo.2015.07.009

Conflict of Interest: The authors declare that the research was conducted in the absence of any commercial or financial relationships that could be construed as a potential conflict of interest.

frontiers in Oncology

ORIGINAL RESEARCH
published: 24 August 2021
doi: 10.3389/fonc.2021.703465

A Novel Oral Arginase 1/2 Inhibitor Enhances the Antitumor Effect of PD-1 Inhibition in Murine Experimental Gliomas by Altering the Immunosuppressive Environment

*Paulina Pilanc[1], Kamil Wojnicki[1], Adria-Jaume Roura[1], Salwador Cyranowski[1,2], Aleksandra Ellert-Miklaszewska[1], Natalia Ochocka[1], Bartłomiej Gielniewski[1], Marcin M. Grzybowski[3], Roman Błaszczyk[3], Paulina S. Stańczak[3], Paweł Dobrzański[3] and Bozena Kaminska[1]**

[1] Laboratory of Molecular Neurobiology, Nencki Institute of Experimental Biology of the Polish Academy of Sciences, Warsaw, Poland, [2] Postgraduate School of Molecular Medicine, Medical University of Warsaw, Warsaw, Poland, [3] OncoArendi Therapeutics SA, Warsaw, Poland

OPEN ACCESS

Edited by:
Lukas Bunse,
German Cancer Research Center (DKFZ), Germany

Reviewed by:
Michael C. Burger,
Goethe University Frankfurt, Germany
Xin Yu,
Amgen, United States
Katharina Sahm,
University of Heidelberg, Germany

***Correspondence:**
Bozena Kaminska
b.kaminska@nencki.edu.pl

Specialty section:
This article was submitted to Cancer Immunity and Immunotherapy, a section of the journal Frontiers in Oncology

Received: 30 April 2021
Accepted: 02 August 2021
Published: 24 August 2021

Citation:
Pilanc P, Wojnicki K, Roura A-J, Cyranowski S, Ellert-Miklaszewska A, Ochocka N, Gielniewski B, Grzybowski MM, Błaszczyk R, Stańczak PS, Dobrzański P and Kaminska B (2021) A Novel Oral Arginase 1/2 Inhibitor Enhances the Antitumor Effect of PD-1 Inhibition in Murine Experimental Gliomas by Altering the Immunosuppressive Environment. Front. Oncol. 11:703465. doi: 10.3389/fonc.2021.703465

Glioblastomas (GBM) are the common and aggressive primary brain tumors that are incurable by conventional therapies. Immunotherapy with immune checkpoint inhibitors is not effective in GBM patients due to the highly immunosuppressive tumor microenvironment (TME) restraining the infiltration and activation of cytotoxic T cells. Clinical and experimental studies showed the upregulation of expression of the arginase 1 and 2 (ARG1 and ARG2, respectively) in murine and human GBMs. The elevated arginase activity leads to the depletion of L-arginine, an amino-acid required for the proliferation of T lymphocytes and natural killer cells. Inhibition of ARG1/2 in the TME may unblock T cell proliferation and activate effective antitumor responses. To explore the antitumor potential of ARG1/2 inhibition, we analyzed bulk and single-cell RNA sequencing (scRNA-seq) data from human and murine gliomas. We found the upregulation of *ARG1/2* expression in GBMs, both in tumor cells and in tumor infiltrating microglia and monocytes/macrophages. We employed selective arginase inhibitors to evaluate if ARG1/2 inhibition *in vitro* and *in vivo* exerts the antitumor effects. A novel, selective ARG1/2 inhibitor - OAT-1746 blocked microglia-dependent invasion of U87-MG and LN18 glioma cells in a Matrigel invasion assay better than reference compounds, without affecting the cell viability. OAT-1746 effectively crossed the blood brain barrier in mice and increased arginine levels in the brains of GL261 glioma bearing mice. We evaluated its antitumor efficacy against GL261 intracranial gliomas as a monotherapy and in combination with the PD-1 inhibition. The oral treatment with OAT-1746 did not affect the immune composition of TME, it induced profound transcriptomic changes in $CD11b^+$ cells immunosorted from tumor-bearing brains as demonstrated by RNA sequencing analyses. Treatment with OAT-1746 modified the TME resulting in reduced glioma growth and increased antitumor effects of the anti-PD-1 antibody. Our findings provide the evidence that inhibition of

ARG1/2 activity in tumor cells and myeloid cells in the TME unblocks antitumor responses in myeloid cells and NK cells, and improves the efficacy of the PD-1 inhibition.

Keywords: arginase inhibitor, tumor microenvironment, glioma associated microglia and macrophages, immune checkpoint inhibitor, immunotherapy

INTRODUCTION

Glioblastoma (GBM, WHO grade IV glioma) is the most common and aggressive primary brain tumor in adults. While the available treatments may slow down the progression of GBM and reduce neurological symptoms, the disease remains incurable. The standard treatment for GBM patients is surgical resection followed by radiation and oral chemotherapy with temozolomide (TMZ). Despite improvements in imaging, surgical techniques, radiotherapy and chemotherapy, GBM inevitably recurs and the prognosis of patients with GBM remains poor, with a median overall survival of 15 months (1, 2). The ability of tumors to modify the surrounding microenvironment and evade the immune system is increasingly recognized as an important determinant of cancer progression and patient prognosis (3). GBMs are infiltrated with various myeloid cells which do not activate their proper functions but instead they are tumor supportive and create the immunosuppressive tumor microenvironment (TME), poorly infiltrated with cytotoxic T lymphocytes and natural killer (NK) cells being frequently deficient in their antitumor activity (4).

Immune checkpoint inhibitor-based therapies provided an effective strategy to enhance antitumor immune responses in many solid cancers (5). Programmed cell death 1 (PD-1, CD279), an immune checkpoint surface receptor expressed on lymphocytes, is a mediator of immune suppression in a variety of tumors, including GBM (6). Binding of PD-1 with its ligands B7-H1 (PD-L1) or B7-DC (PD-L2) induces apoptosis or exhaustion of activated immune cells. Blockade of this interaction enhances the antitumor activity of the immune system (7). While first studies of the adjuvant therapy with pembrolizumab (a monoclonal antibody against human PD-1) in GBM patients demonstrated some benefits (8), further studies showed no survival improvement (9, 10). The recent results from a randomized phase III trial CheckMate143 with nivolumab (an anti-PD-1 antibody) did not show the improved survival of patients with recurrent GBMs compared to those treated with bevacizumab, an anti-VEGF-A antibody (11). Genomic and transcriptomic analysis of GBM patients treated with anti-PD-1 antibodies revealed a significant enrichment of the immunosuppressive transcriptomic signature in non-responders, along with differences in T cell clonal diversity and tumor microenvironment profiles (12). Growing evidence suggests that the clinical response to immunotherapies is restricted by various resistance mechanisms, such as a strong immunosuppression induced by the tumor infiltrating myeloid cells (13, 14).

Glioma-associated microglia and macrophages (GAMs) accumulate in malignant gliomas and are key drivers of tumor invasion and immunosuppression. GAMs promote tumor progression and jointly with myeloid-derived suppressor cells (MDSCs) modulate antitumor immune responses in multiple ways (15).

Both malignant cells and tumor-infiltrating myeloid cells in murine and human gliomas upregulate the expression of arginase (16, 17) and the resulting changes in the L-arginine metabolism are one of the most prominent mechanisms contributing to immunosuppression (18). There are two arginase isoforms (ARG1 and ARG2), catalyzing the same biochemical reaction, but differing in subcellular localization, expression, and regulation. ARG1 is a cytosolic protein, while ARG2 is mainly localized in the mitochondria (19). Arginase catalyzes the hydrolysis of L-arginine to urea and L-ornithine, thereby depleting extracellular L-arginine (20). T cells are auxotrophic for L-arginine and require this amino acid for the rapid and successive proliferation that follows T cell receptor activation of effector cells (21). Expression of ARG1 is a defining feature of immunosuppressive myeloid cells that are highly enriched in the TME, and the role of ARG1-expressing MDSCs in altering T-cell responses in cancer patients is well established (22, 23). CB-1158, an arginase 1 inhibitor synthesized at Calithera Biosciences blocked myeloid cell-mediated suppression of T cell proliferation *in vitro* and reduced tumor growth in several mouse models of non-CNS tumors (CT26, LLC, B16, and 4T1 tumors). The ARG1 inhibitor was effective as a single agent or in combination with checkpoint blockade (anti-PD-L1), adoptive T cell and NK cell transfer, and chemotherapy with gemcitabine. The treatment with CB-1158 increased tumor-infiltrating $CD8^+$ T cells and NK cells, inflammatory cytokines, and expression of several interferon-inducible genes (24). CB-1158 advanced to clinical trials for patients with non-CNS malignancies (NCT02903914).

In the present study, we provide the compelling evidence that OAT-1746, a novel and oral small-molecule inhibitor of ARG1/2, affects glioma-microglia interactions *in vitro*, accumulates in the brain and modulates the TME of murine intracranial gliomas. We demonstrate that OAT-1746 works synergistically with PD-1 blockade and improves antitumor immune responses against gliomas.

MATERIALS AND METHODS

Glioma Cell Cultures

Human glioblastoma cell lines LN18, U87-MG (U87) (ATCC, Manassas, VA) were cultured in Dulbecco's modified Eagle's medium (DMEM) supplemented with 10% fetal bovine serum (FBS) (Gibco, MD, USA) and antibiotics (100 U/mL penicillin,

100 µg/mL streptomycin). GL261 tdTomato^{+}luc^{+} murine glioma cells were cultured in DMEM with the addition of 10% FBS, antibiotics and 100 µg/mL G418 (Invivogen, San Diego, CA, USA). Cells were cultured in a humidified atmosphere CO_2/air (5%/95%) at 37°C (Heraeus, Hanau, Germany).

Microglial Cell Cultures

Mouse immortalized microglial BV2 cells were cultured in Dulbecco's modified Eagle's medium GlutaMAX™ (DMEM GlutaMAX™) supplemented with 2% fetal bovine serum (Gibco, MD, USA) and antibiotics (100 U/mL penicillin, 100 µg/mL streptomycin) in a humidified atmosphere CO_2/air (5%/95%) at 37°C (Heraeus, Hanau, Germany).

Primary microglial cultures were prepared from cerebral cortices of P0–P2 C57BL/6J mice as described (25). Briefly, after stripping off the meninges and enzymatic brain dissociation the cells were collected and seeded onto the culture flasks. After 48 h, cell cultures were washed three times with phosphate-buffered saline (PBS) to remove debris. Primary cultures were kept in DMEM supplemented with 10% FBS, 2 mM L-glutamine, 100 U/mL penicillin, and 100 µg/mL streptomycin (Gibco, MD, USA). Microglia were isolated by gentle shaking for 1 h at 100 RPM at 37°C. Detached microglia were collected by centrifugation, counted, and checked for viability. Microglia cultures were used for experiments 48 h after seeding to ensure that the cells were quiescent.

Recombinant Arginase Activity Assays

The inhibitory activity towards hARG1 and hARG2 enzymes was assessed using recombinant enzymes biosynthesized using a prokaryotic expression system (*E. coli*) and purified by fast protein liquid chromatography (FPLC). Briefly, recombinant enzymes were incubated with the tested compounds for 1 h at 37°C in the reaction buffer (100 mM sodium phosphate buffer, 130 mM NaCl, 1 mg/mL BSA, pH 7.4) containing substrate (10 mM L-arginine hydrochloride) and cofactor (200 µM $MnCl_2$). The assay is based on the detection of urea, which is generated during the conversion of L-arginine into L-ornithine catalyzed by arginases. To visualize the product, we adding a mixture of reagent A (4 mM oPA, 50 mM boric acid, 1 M sulfuric acid, 0.03% Brij-35) and reagent B (4 mM NED, 50 mM boric acid, 1 M sulfuric acid, 0.03% Brij-35) in equal proportions. The absorbance was measured at 515 nm. The urea production in the absence of any tested compound was considered as maximal enzyme activity. The absorbance in the absence of arginase (background) was considered as zero activity. Two reference compounds OAT-81 (ABH, no. 222638-65-5) and OAT-90 (2-amino-6-borono-2-(2-(3-(2,4-dichlorophenyl) propyloamino)ethyl) hexanoic acid, and two novel inhibitors OAT-1617 and OAT-1746 (the last three synthesized at OncoArendi Therapeutics) were tested. Normalized values were analyzed using GraphPad Prism 7.0 software and the IC_{50} values were determined.

Invasion Assays

BV2 cells were plated onto a 24-well plate at the density of 4×10^4. After 24 h, the invasion assay was performed with tissue culture inserts (6.5 mm Transwell® with 8.0 µm Pore Polycarbonate Membrane Insert, Corning, NY, USA) coated with the Growth Factor Reduced Matrigel™ Matrix (BD Biosciences, San Diego. CA, USA). The Matrigel™ Matrix (50 µL of 1 mg/mL stock solution diluted in fresh DMEM) was dried under sterile conditions (37°C) for 5–6 h. The medium in BV2 cultures was replaced with fresh one 1 h before seeding glioblastoma cells onto the inserts, then LN18 and U87 glioblastoma cells were seeded at 2×10^4/insert on Matrigel-covered membranes in a serum-reduced medium (2% FBS). Untreated glioblastoma cells co-cultured with or without BV2 cells served as positive and negative controls, respectively. Cells were treated with the arginase-1 inhibitors OAT-90, OAT-1617 and OAT-1746 solved in PBS. The cultures were kept in incubator at 37°C with humidified air containing 5% CO_2. After 18 h cells were fixed in ice-cold methanol and cell nuclei stained with DAPI (4′,6-Diamidino-2-Phenylindole; 1 µg/mL, Sigma). The membranes from Transwell® inserts were cut out and images were acquired using a fluorescence microscope (Leica DM4000B, 10x lens) from the 5 independent fields (bottom; top; left; right side and the middle). Numbers of invading cells were counted using the ImageJ software (NIH, Bethesda, MD, USA). All experiments were performed three times, in duplicates.

Viability Assay

Cell viability was assessed using MTT metabolism assay (U87 and BV2 cells) or MTS CellTiter 96® AQueous One Solution Cell Proliferation Assay (Promega) for the primary murine microglia cultures. Cells were cultured either in 96-well plates (U87 at density of 1×10^4) or 24-well plates (BV2 at density of 4×10^4 and primary microglia 8×10^4) with the indicated concentrations of the inhibitor or H_2O (vehicle) for 24 h. MTT solution (Sigma Aldrich) was added to each well to a final concentration of 0.5 mg/mL. After 1 h of incubation at 37°C, water-insoluble dark blue formazan crystals were dissolved in DMSO. Optical densities (OD) were measured at 570 and 620 nm using a scanning multiwell spectrophotometer. The MTT assay was performed according to the manufacturer's protocol. All measurements were carried out on three independent cell passages, in triplicates.

Animals

Male C57BL/6J mice (10-12 weeks at the beginning of the study) were housed with free access to food and water, on a 12h/12h day and night cycle. All efforts have been made to minimize the number of animals and animals suffering. All research protocols conformed to the Guidelines for the Care and Use of Laboratory Animals (European and national regulations 2010/63/UE September 22, 2010 and Dz. Urz. UE L276/20.10.2010, respectively). Animals were decapitated by a qualified researcher. The First Warsaw Local Ethics Committee for Animal Experimentation approved the study (approval no. 562/2018).

Determining Plasma L-Arginine and Drug Concentration

Blood plasma, as well as the brain samples (from control and treated animals), were prepared for liquid chromatography

coupled with mass spectrometry (LC-MS) by homogenization in 5% trichloroacetic acid (TCA) and the concentration of L-arginine – the substrate of arginase – was determined. In the urea cycle, arginase cleaves arginine to produce urea and ornithine. Ornithine reacts with carbamoyl phosphate to form citrulline. The brain homogenates prepared for arginine measurements, as well as plasma samples were also analyzed by LC-MS to determine the concentration of the drug, which was administered to animals 2 h before the euthanasia.

Stereotactic Implantation of Glioma Cells

Mice were deeply anesthetized with isoflurane. After identifying the sagittal and coronal sutures on the right side, a hole was drilled at the following coordinates: 1 mm anterior and 1,5 mm lateral from bregma. GL261 tdTomato$^+$luc$^+$ glioma cells (80,000 in 1 µL of DMEM) were stereotactically injected with a Hamilton syringe to the right striatum of the mouse 3 mm deep from the surface of the brain. The skin incision was closed and mice were monitored until they completely recovered from anesthesia. Mice were randomly allocated to the study groups. The animals were weighed weekly and observed daily for clinical symptoms and evidence of toxicity by evaluating their eating, mobility, weight loss, hair loss, and hunched posture. OAT-1746 was administered by oral gavage at 50 mg/kg twice a day from day 1 after implantation. Anti-PD-1 antibody (Biolegend, GoInVivo™ Purified anti-mouse CD279) was injected intraperitoneally (i.p.) at a dose of 2.5 mg/kg on days 8, 10, 12, 14 post-implantation. Control groups received vehicle (saline) twice a day by gavage. Animals were euthanized when they lost more than 20% of body weight compared to day 0.

Bioluminescence Imaging

To monitor tumor growth, mice were injected i.p. with 150 mg/kg body weight luciferin (D-luciferin sodium salt BC218 Synchem) and left for 8 min. Then, the animals were anesthetized with 3% isoflurane and transferred to the X-treme Imaging System (Bruker, Germany). At 10 min after the D-luciferin injection, a photonic emission was imaged. Tumors were visualized at days 14, 21 and 28 after implantation and bioluminescent images were quantified as photon/sec/mm^2. We applied the same ROI rectangle to all images (the whole head). Then we exported sum values for all images.

Cytokine Analysis

Measurement of pro- and anti-inflammatory cytokines was performed in blood from control and treated animals. Blood was quickly collected to EDTA containing tubes before perfusion and centrifuged (10,000 × g) for 10 min at room temperature. The plasma was collected and stored at -80°C. The levels of cytokines were measured using the Milliplex Kit (Merk-Millipore, Germany) according to the protocol. Cytokine levels were determined using the MAGPIX Multiplexing Instrument (Luminex, TX, USA) with XPonent software and analyzed with Milliplex Analyst 5.1 software. Results were expressed as pg/mL for each cytokine.

Immunohistochemistry on Brain Slices

The animals were sacrificed on the day 21 after GL261 tdTomato$^+$luc$^+$ cell implantation and perfused with 4% paraformaldehyde in PBS. Brains were removed, post-fixed for 48 h in the same fixative solution and placed in 30% sucrose in PBS at 4°C until the tissue sunk to the bottom of the flask. Tissue was frozen in Tissue Freezing Medium (Jung; Nussloch, Germany) and cut in 12 µm coronal sections using a cryostat. The slides were dried at room temperature for 2 h after being transferred from the -80°C storage. Cryosections were blocked in PBS containing 10% donkey serum and 0.1% Triton X-100 for 2 h and incubated overnight at 4°C with rabbit anti-Iba-1 and goat anti-Arg1 or with rabbit anti-CD8 antibodies. Next, sections were washed in PBS and incubated with corresponding secondary antibodies for 2 h at room temperature. All antibodies were diluted in 0.1% Triton X-100/PBS solution containing 3% donkey serum. Nuclei were counterstained with DAPI (1 µg/mL). Images were obtained using the Olympus microscope (Fluoview, FV10i). For reagent specifications, catalogue numbers, and concentrations, see the **Supplementary Table 1**. To quantify the tumor size, sections were stained with toluidine blue, and images were acquired using a Leica DM4000B microscope (Leica Microsystems, Wetzlar, Germany). Tumor areas were measured using ImageJ software (NIH, Bethesda, MD, USA) on every sixth brain slice, and tumor volumes were calculated as previously described (26).

Tissue Dissociation, Flow Cytometry and FACS Sorting

On day 28 after GL261 tdTomato$^+$luc$^+$ cell implantation mice were perfused transcardially with cold phosphate-buffered saline (PBS) to clear away blood cells from the brain. The tumor-bearing hemispheres were dissociated enzymatically with a Neural Tissue Dissociation Kit with papain (Miltenyi Biotec) and gentleMACS Octo Dissociator (Miltenyi Biotec), according to the manufacturer's protocol to obtain a single-cell suspension. Next, the enzymatic reaction was stopped by the addition of Hank's Balanced Salt Solution with calcium and magnesium (Gibco, Germany). The resulting cell suspension was filtered through 70 µm and 40 µm strainers, and centrifuged at 300 × g, 4°C for 10 min. Next, myelin was removed by centrifugation on a 22% Percoll gradient. Briefly, cells were suspended in 25 mL Percoll solution (18.9 mL gradient buffer containing 5.65 mM $NaH_2PO_4H_2O$, 20 mM $Na_2HPO_42(H_2O)$, 135 mM NaCl, 5 mM KCl, 10 mM glucose, 7.4 pH; 5.5 mL Percoll (GE Healthcare, Germany); 0.6 mL 1.5 M NaCl), overlayered with 5 mL DPBS (Gibco) and centrifuged for 20 min at 950 × g at 4°C, without acceleration and brakes. Next, cells were collected, washed with PBS and counted using NucleoCounter (Chemometec, Denmark).

Samples were handled on ice or at 4°C without light exposure. Prior to staining with antibodies, samples were incubated with LiveDead Fixable Violet Dead Cell Stain (ThermoFisher) in PBS for 10 min to exclude nonviable cells. Next, samples were incubated for 10 min with rat anti-mouse CD16/CD32 Fc

Block™ (BD Pharmingen) in Stain Buffer (BD Pharmingen) to block FcγRIII/II and reduce unspecific antibody binding. Then, cell suspensions were incubated for 30 min with an antibody cocktail in Stain Buffer (BD Pharmingen). For flow cytometry analysis of cell surface antigens the following anti-mouse antibodies were used: CD45 (30-F11), CD11b (M1/70) from BD Pharmingen and CD3 (REA641), NK 1.1 (PK136) from Miltenyi Biotec. For FACS sorting the cells were stained with CD11b (M1/70) antibody labeled with FITC (BD Pharmingen).

All antibodies were titrated prior to staining to establish the amount yielding the best stain index. Data were acquired using a BD LSR Fortessa Analyzer cytometer and analyzed with FlowJo software (v. 10.5.3, FlowJo LLC, BD). Gates were set based on FMO (fluorescence minus one) controls and back-gating analysis. Percentages on cytograms were given as the percentage of a parental gate. $CD11b^+$ cells were FACS sorted using Cell Sorter BD FACSAriaII. All flow cytometry experiments were performed at the Laboratory of Cytometry, Nencki Institute of Experimental Biology. For reagent specifications, catalog numbers and dilutions see the **Supplementary Table 1**.

RNA Isolation, mRNA Library Preparation and RNA-Sequencing

Immediately after sorting, $CD11b^+$ cells were centrifuged and lysed for further isolation of RNA using the RNeasy Plus Mini Kit (Qiagen, Germany). The integrity and quality of RNA were assessed on an Agilent 2100 Bioanalyzer with an RNA 6000 Pico Kit (Agilent Technologies, CA, USA). A total of 9 strand-specific RNA libraries were prepared for sequencing (2-3 biological replicates/treatment) using a KAPA Stranded mRNA-Seq Kit (Kapa Biosystems, MA, USA). Poly-A mRNAs were purified from 100 ng of total RNA using poly-T-oligo-magnetic beads (Kapa Biosystems, MA, USA). mRNAs were fragmented and a first-strand cDNA was synthesized using reverse transcriptase and random hexamers. A second-strand cDNA synthesis was performed by removing RNA templates and synthesizing replacement strands, incorporating dUTP in place of dTTP to generate double-stranded (ds) cDNA. dsDNA was then subjected to addition of "A" bases to the 3′ ends and ligation of adapters from NEB, followed by uracil digestion by USER enzyme (NEB, MA, USA). Amplification of fragments with adapters ligated on both ends was performed by PCR using primers containing TruSeq barcodes (NEB, Ipswich, MA, USA). Final libraries were analyzed using Bioanalyzer and Agilent DNA High Sensitivity chips (Agilent Technologies, Santa Clara, CA, USA) to confirm fragment sizes (~300 bp). Quantification was performed using a Quantus fluorometer and the QuantiFluor dsDNA System (Promega, Madison, Wisconsin, US). Libraries were loaded onto a rapid run flow cell at a concentration of 8,5 pM onto a rapid run flow cell and sequenced on an Illumina HiSeq 1500 paired-end.

Data Processing and Analysis

Illumina-specific adapters, short reads, and low quality 5' and 3' bases were filtered out in the FASTQ format files using Trimmomatic (27) tool (version 0.36). The resulting RNA sequencing reads were aligned to a reference mouse genome sequence (mm10) with STAR aligner (28) (version 2.6.1b) using the two pass Mode Basic option. Duplicate reads were then identified and flagged using Picard Tools (version 2.17.1) [broadinstitute.github.io/picard/]. Quantification of mapped reads and summarization by gene was performed using HTSeq-count (29) (version 0.11.1), with paired mode (-p) and reverse stranded mode (-s reverse) enabled, and only reads with MapQ values of 10 or higher were considered. Low-expressed features were filtered out and an analysis of differentially expressed genes was performed using DESeq2 (version 1.24.0) (30). Only mRNAs encoding protein-coding genes were retained for downstream analysis.

To identify transcriptomic differences between groups, differential expression analysis was performed using DESeq methods, with the control state (CTR) as the reference group and compared with the OAT-1746, anti-PD-1 and combination groups. The variance stabilizing transformation (vst function) was used for visualization. Pathway enrichment analysis was performed by selecting statistically significant genes (adjusted p-values ≤ 0.05) and correcting type I errors in multiple testing using the Bonferroni-Hochberg (BH) method. Gene Ontology Biological Processes (GO: BP) was used to better understand the mechanistic findings of the enriched gene lists. The clusterProfiler (31) and VennDiagram (32) packages were used to visualize the results.

RESULTS

ARG1 Expression Is Highly Upregulated in Human Glioblastoma Samples and in Murine Experimental Gliomas

Using transcriptomic data from The Cancer Genome Atlas (TCGA), we examined *ARG1* and *ARG2* expression in human gliomas of different WHO grades II, III, IV. The highest mRNA levels of both genes were found in GBM samples (**Figure 1A** and **Supplementary Figure 1A**). To determine a cell source of *ARG1* and *ARG2* expression, we explored the single-cell RNA sequencing (scRNA-seq) data from 10 astrocytoma samples (33) and checked the gene expression in various cell populations from the tumors using the SingleCell data portal (https://singlecell.broadinstitute.org/). High expression of *ARG1* and *ARG2* was detected in malignant cells and tumor-infiltrating microglia/macrophages (MG/MΦ) (**Figure 1B** and **Supplementary Figure 1B**). We took advantage of having in-house sc-RNA-seq data of $CD11b^+$ immunosorted from murine GL261 gliomas, which provided resolution to distinguish resident microglia from CNS-border associated macrophages (BAMs) or monocytes/macrophages (Mo/MΦ) (34). Using these data, we analyzed *Arg1* and *Arg2* expression in the discrete myeloid subpopulations. There was a low number of microglial cells expressing either *Arg1* (< 1%) or *Arg2* (< 0.1%) mRNA and both genes were more abundantly expressed in the Mo/MΦ population (11% and 6%, respectively) (**Figure 1C** and **Supplementary Figure 1C**). *Arg1* expression levels were significantly higher than *Arg2*

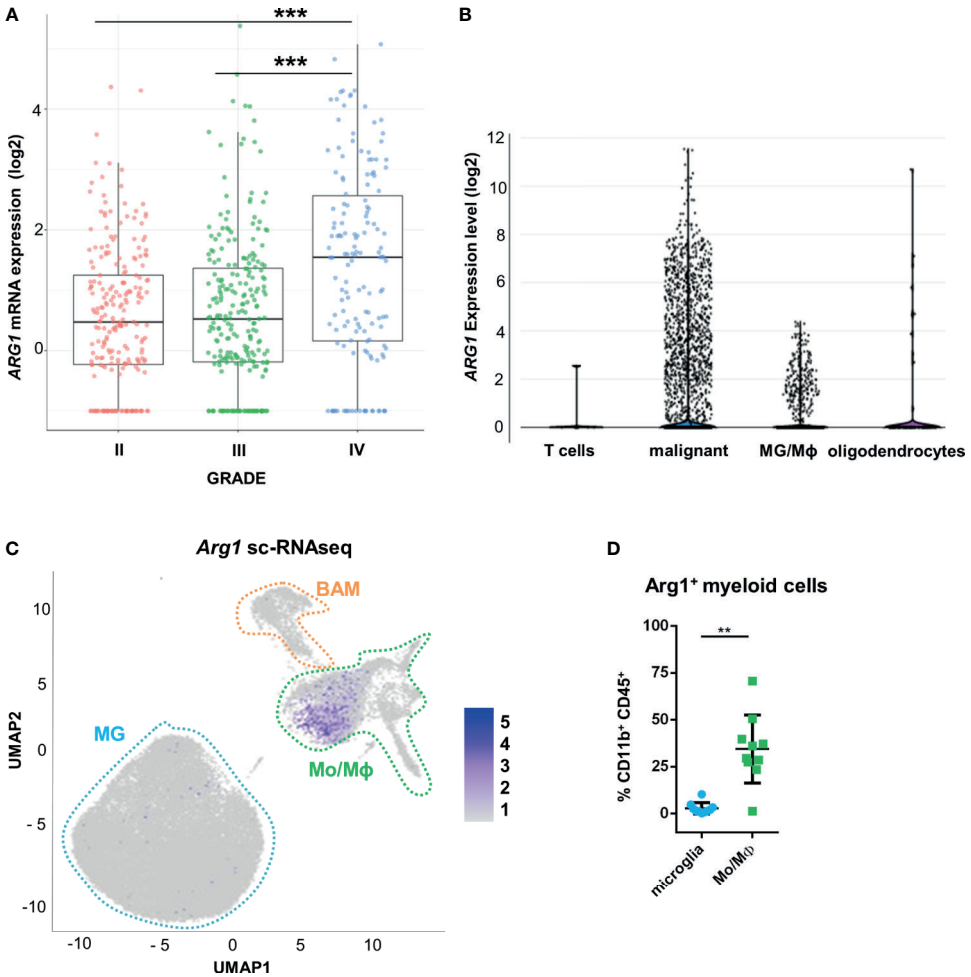

FIGURE 1 | *ARG1* expression is highly upregulated in human glioblastomas and murine experimental gliomas. **(A)** *ARG1* expression in gliomas of different WHO grades (WHO grades II- IV) in TCGA datasets. Statistical significance was determined by Tukey's Honest Significant Difference (HSD). ***$p < 0.001$. **(B)** Expression of *ARG1* in malignant cells and microglia/macrophages (MG/MΦ) in 10 samples of astrocytomas in single-cell RNA-seq datasets (public data) from Ref. (33). **(C)** UMAP plot of $CD11b^+$ cells from GL261 gliomas (n=8). Projection of cells combined from clusters identified as microglia, monocytes/macrophages (Mo/MΦ), and BAMs. Plots depicting *Arg1* mRNA which is highly expressed in infiltrating Mo/MΦ. **(D)** Flow cytometry analysis of Arg1 expressing cells among microglia ($CD11b^+CD45^{lo}$) and Mo/MΦ ($CD11b^+CD45^{high}$) cells sorted from murine gliomas (n=10); Wilcoxon matched-pairs signed rank, two-tailed, **$p < 0.01$.

mRNA levels both in microglia and Mo/MΦ immunosorted from tumor-bearing brain (**Supplementary Figure 1D**). Additionally, we assessed Arg1 levels by flow cytometry in $CD11b^+$ cells isolated from tumor-bearing hemispheres at day 21 post-implantation (**Figure 1D**). The percentage of $Arg1^+$ cells was higher in Mo/MΦ infiltrating from the periphery ($CD11b^+CD45^{high}$) than in resident microglia ($CD11b^+CD45^{low}$), which corroborated the results from scRNA-seq analysis (**Supplementary Figure 1D**). Overall, these results confirm high *ARG1* and *ARG2* expression in human malignant cells and glioma-infiltrating monocytes/macrophages. Arg1 is a predominant isoform expressed in myeloid cells in the brain of tumor-bearing mice.

The Effect of OAT Inhibitors on Human Arginase 1/2 Activity and Glioma Cell Invasion

We have previously demonstrated that *Arg1* mRNA is upregulated in microglia exposed to glioma during reprogramming of microglia into tumor-supportive, immunosuppressive cells (25, 35). Arginase inhibitors OAT-1746 and OAT-1617 were designed and synthesized by OncoArendi Therapeutics, Warsaw. OAT-1746 inhibited ARG1/2 at low nanomolar concentrations, reversed ARG1-inhibited proliferation of human and murine T cells and showed significant antitumor efficacy in various non-CNS tumor models (36).

OAT-1746 and OAT-1617 as well as two reference compounds were tested in biochemical assays for the ability to inhibit arginase activity and in cellular assays for the ability to block tumor cell invasion. OAT-1746 inhibited recombinant human ARG1 activity (IC_{50}=28 nM) and the related enzyme ARG2 (IC_{50}=49 nM) better than two reference compounds (**Figures 2A, B**). ARG2 catalyzes an identical chemical reaction and exhibits 60% sequence identity with ARG1 (37).

To evaluate the effects of these novel arginase inhibitors on glioma invasion, we performed a Matrigel invasion assay using two human glioma cell lines: U87-MG (**Figure 2C**) and LN18 (**Figure 2D**). Immortalized BV2 microglial cells, similarly to primary microglial cultures, support glioma invasion (38). In co-cultures, glioma invasion was strongly induced in the presence of BV2 microglial cells and all three arginase inhibitors significantly decreased the proportion of invading cells. OAT-1746 at a concentration of 11 μM reduced microglia-induced invasion of glioma cells more efficiently than the reference compound OAT-90 and the older generation inhibitor OAT-1617. The inhibitory effect of OAT-1746 on glioma invasion was concentration-dependent, whereas this dependence was not observed for OAT-90 (**Figure 2E**). Representative images from Matrigel invasion assays show an increased number of invading glioma cells in co-cultures with BV2 cells and the inhibitory effect of 11 μM OAT-1746 (**Figure 2F**). These results demonstrate that the inhibition of arginase activity reduced microglia-dependent invasion of human glioma cells.

To assess the potential toxicity of OAT-1746, we determined the effects of increasing drug concentrations on cell viability by performing MTT metabolism assays on human glioma cells (**Figure 2G**), murine microglial BV2 cells (**Figure 2H**), and murine primary microglia cultures (**Figure 2I**). The OAT-1746 inhibitor was not toxic towards the tested cells at concentrations up to 1000 μM; a decrease in the viability of U87-MG cells was observed at the highest concentration, which exceeds by over two folds of magnitude the effective IC_{50} concentration of the inhibitor. The results provide evidence for the efficacy of the new compound and its safety at therapeutically relevant concentrations.

OAT-1746 Treatment Increases Arginine Levels in the Brain and Plasma but Does Not Show an Antitumor Activity

To study the antitumor activity of the arginase inhibitor OAT-1746, we employed a syngeneic model of GL261 mouse glioma cells implanted into immunocompetent C57BL/6J mice. GL261 glioma cells were stably transfected with constructs allowing the expression of a red fluorophore tdTomato and luciferase to visualize tumor growth using *in vivo* imaging. Tumor-bearing mice received OAT-1746 (50 mg/kg) or saline twice a day by oral gavage.

First, we determined if the arginase inhibitor crossed the blood-brain-barrier (BBB) by measuring directly the level of the drug as well as the level of L-arginine - a substrate of arginase, in the brains and sera of mice after 14 days of OAT-1746 treatment. The brain and plasma were taken 2 h after the last drug administration. OAT-1746 was detected in the brain extracts, which confirms that it crosses the BBB and accumulates in the brain (**Figure 3A**). The administration of OAT-1746 resulted in an increase of arginine concentration, both in the brain (**Figure 3B**) and the blood plasma (**Figure 3C**).

To study the effects of arginase inhibition on the immune cells in the TME and visualize the infiltration of these cells into tumors, we performed immunohistochemical double staining for Arg1 and Iba1 (a marker of microglia/macrophages), and for CD8 (a marker of cytotoxic T cells, present also on NK cells). Mice were treated with OAT-1746 at 50 mg/kg twice a day. In parallel, we evaluated the effect of anti-PD-1 antibody which was injected intraperitoneally on days 8, 10, 12 and 14 post-implantation. The administration of OAT-1746 or anti-PD-1 treatment did not change the accumulation of $Iba1^+$ and $Arg1^+$ cells in experimental gliomas (**Figure 3D**). $CD8^+$ cells were distinctly located at the invasive tumor margin and more $CD8^+$ cells were detected in animals with smaller tumors (**Figure 3E**). As tumor cells displayed red fluorescence, evaluation of brain sections allowed quantification of a tumor growth. OAT-1746 treatment did not reduce the tumor growth when compared to the control group. However, among anti-PD-1 treated animals we noticed two groups with different tumor sizes, which is consistent with a division into responders and non-responders observed in patients (**Figure 3F**). Quantification of $CD8^+$ T cell densities at the invasive tumor margin showed an increased number of $CD8^+$ cells in responders when compared to non-responders (**Figure 3G**). Non-responders had also a lower density of $CD8^+$ T cell than OAT-1746-treated animals. These findings show that the arginase inhibitor alone is not capable of inhibiting glioma growth and anti-PD-1 treatment induces the response in a half of animals.

Combined OAT-1746 and Anti-PD-1 Treatment Reduces Glioma Growth

Antitumor immunity can be blocked by more than one suppressive mechanism, including the expression of immune checkpoint proteins and the depletion of essential nutrients from TME (39). We assumed that combining OAT-1746 with an immune-modulating agent, such as anti-PD-1 antibody, might improve drug efficacy. Tumor growth was monitored by measuring luminescence signal 14, 21 and 28 days after implantation of GL261 $tdTomato^+luc^+$ glioma cells. Representative images of gliomas at different time points are shown (**Figure 4A**). While OAT-1746 alone did not show any effect on the tumor volume and the anti-PD-1 treated animals were split into responders and non-responders, the combined treatment resulted in significantly reduced glioma growth at day 28. The combination of OAT-1746 with anti-PD-1 delayed, and in some cases abrogated, tumor growth. Effects of treatment and time of tumor progression were calculated with multifactorial ANOVA (**Figure 4B**). Both the "treatment" effect $F_{3,89}$ (4.801)=0.004 and the "time after implantation" effect $F_{2,89}$(4.726)=0.011 were significant. Tukey's honest significant difference (HDS) *post hoc* test was used to compare experimental groups and p values were as follows: CTR-OAT-1746 p=0.455, CTR-anti-PD-1 p=0.005,

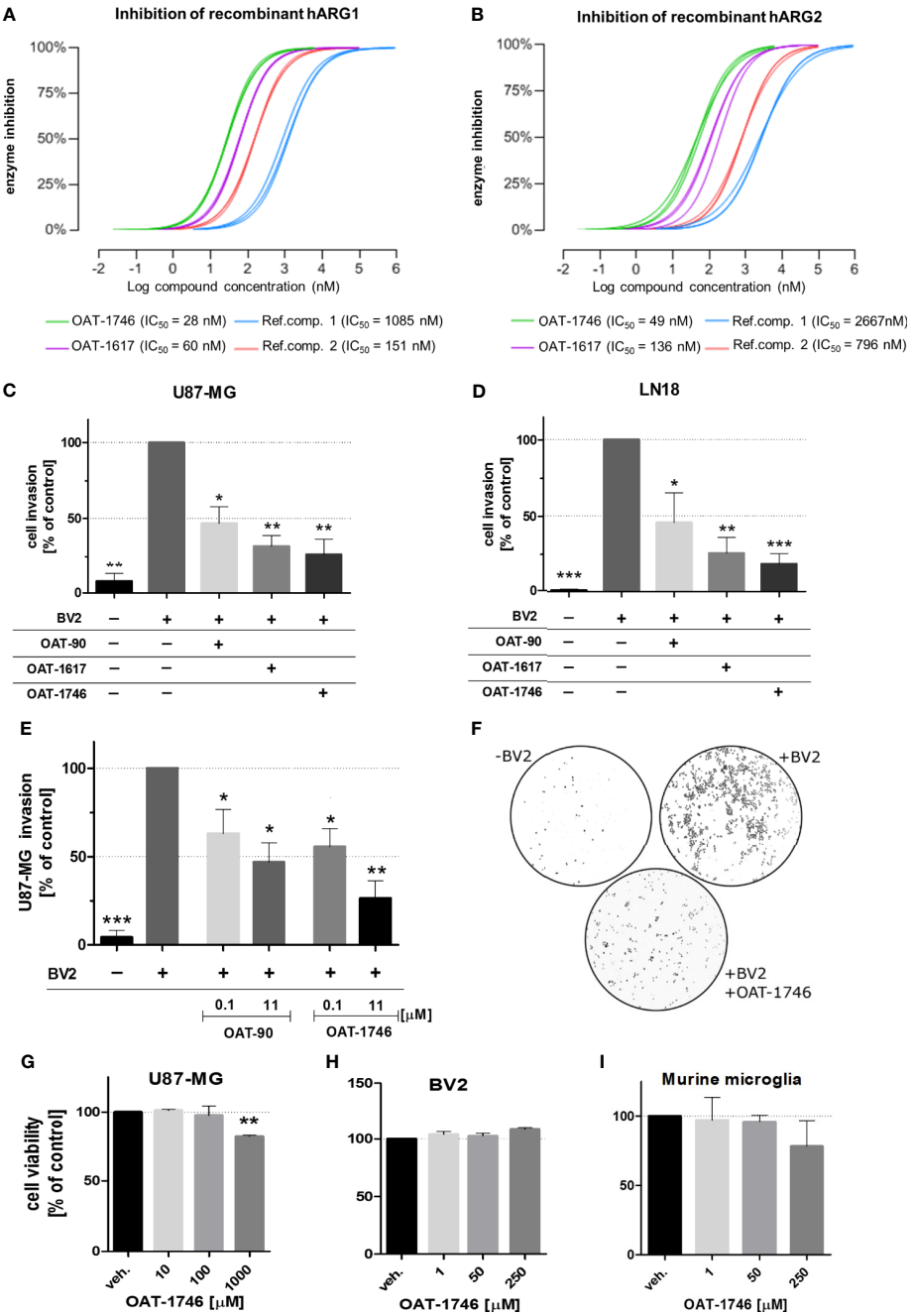

FIGURE 2 | The effect of OAT inhibitors on human arginase 1/2 activity and microglia-induced glioma invasion. **(A, B)**. The activity of two new and two reference ARG inhibitors was tested towards recombinant human ARG1 and ARG2 (hARG1 and hARG2, respectively) The IC values were determined. **(C, D)** Graphs represent relative invasion of **(C)** U87-MG or **(D)** LN18 cells induced by the co-culture with murine microglial cells (BV2). Tumor invasion was determined using a Matrigel matrix assay. Invasion of glioma cells co-cultured with BV2 cells is set as 100%. Three tested inhibitors (OAT-90, OAT-1617, OAT-1746) were used at 11 μM concentration and all of them effectively reduced glioma invasion. Data are expressed relatively to a basal invasion in the absence of microglial cells. **(E)** The effects of OAT-90 and the second generation inhibitor OAT-1746 applied at 0.1 and 11 μM concentration on microglia induced invasion of U87-MG cells. Data are presented as means ± S.D and were calculated from three independent biological experiments. Statistical significance was evaluated using one-sample t-test. **(F)** The representative images of DAPI-stained U87-MG glioma cells on inserts show the nuclei of invading cells in the presence or absence of BV2, and OAT-1746. **(G, I)** The effect of OAT-1746 on cell viability was determined using MTT metabolism test. Cells were incubated for 24 h with or without OAT-1746 at given concentrations. The influence of OAT-1746 on the viability of **(G)** U87-MG human glioma cells, **(H)** BV2 microglial cells and **(I)** primary murine microglia was determined. Data are presented as means ± S.D (n=3 independent biological experiments). Significance of differences between the treatments was evaluated using one-way ANOVA followed by Dunnett's post-hoc test, p-Values were considered as significant when ***$p < 0.001$; **$p < 0.01$; *$p < 0.05$.

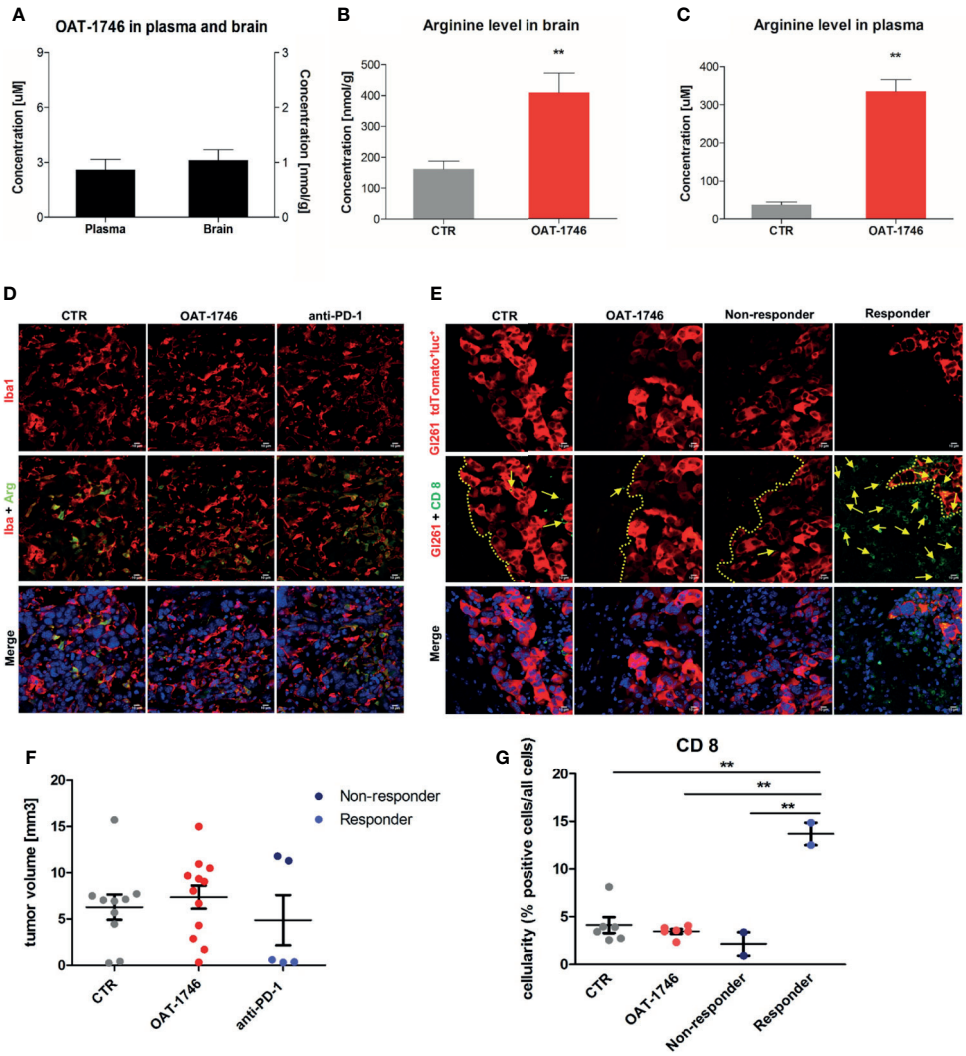

FIGURE 3 | Treatment with OAT-1746 increases arginine levels in the brain and plasma but has no antitumor activity against murine GL261 gliomas. **(A–C)** Tumor-bearing mice were treated with OAT-1746 twice a day and samples were collected 2 h after the last dosing (n = 6 per group). Concentrations of OAT-1746 **(A)** and L-arginine in tumor-bearing brains **(B)** and plasma **(C)** from the same animals were measured by LC/MS at day 14 post-implantation. The results were compared using the non-parametric Mann-Whitney test. $^{**}p < 0.01$. **(D)** Mice with implanted GL261 tdTomato^{+}luc^{+} glioma cells received orally saline CTR (n=12) or OAT-1746 50 mg/kg twice a day for 21 days (n=12). A separate group received anti-PD-1 antibody (2.5 mg/kg, i.p.) at days 8, 10, 12 and 14 (n=5). Representative images of the glioma-bearing brains (at day 21) stained with anti-Iba1 (in red) and anti-Arg1 (in green) antibodies, and co-stained with DAPI are shown. **(E)** Representative confocal microscopy images of CD8^{+} T and NK cells within the tumors after OAT-1746 or anti-PD-1 antibody administration. The yellow line separates tumor areas (with glioma cells showing red fluorescence) and the parenchyma border; cell nuclei are counterstained with DAPI (blue); magnification x60. Yellow arrows indicate the accumulation of CD8^{+} cells (in green) in the responder PD-1 inhibition but not in the non-responder. **(F)** Quantification of tumor volumes at day 21 post-implantation. Each individual from CTR (n=12), OAT-1746 (n=12) and anti-PD-1 (n=5) groups is shown. In the checkpoint inhibitor treatment group non-responders (n=2) and responders (n=3) are marked in dark and light blue, respectively. Tumor areas were measured using ImageJ in every sixth brain slice, and tumor volumes were calculated; the mean ± SEM, p values were calculated using the Mann–Whitney U-test. **(G)** Quantification of CD8^{+} cells related to the total number of cells in the area of interest. The cells were counted using ImageJ software and average values from 5 fields are presented. Significance was calculated with One-Way ANOVA, Bonferroni's multiple comparison test was used to compute p values (CTR n=6; OAT-1746 n=6, anti-PD-1 n=4); $^{**}p < 0.01$.

CTRL-COMB p=0.021, COMB-OAT-1746 p=0.46, COMB-anti-PD-1 p=0.96. These results provide evidence that combining arginase inhibition with targeting immune checkpoints could be an effective strategy to reduce glioma growth. Administration of the drug delayed tumor growth. Inhibition of glioma growth was augmented when two agents were combined. At day 14 only 2 out of 8 animals developed tumors in the COMB group, while there were 5 out of 8 mice with tumors in OAT-1746-treated cohort.

To further investigate the immune cell-mediated mechanism of action of OAT-1746 and anti-PD-1, flow cytometry was performed on cells isolated from tumors, and changes in

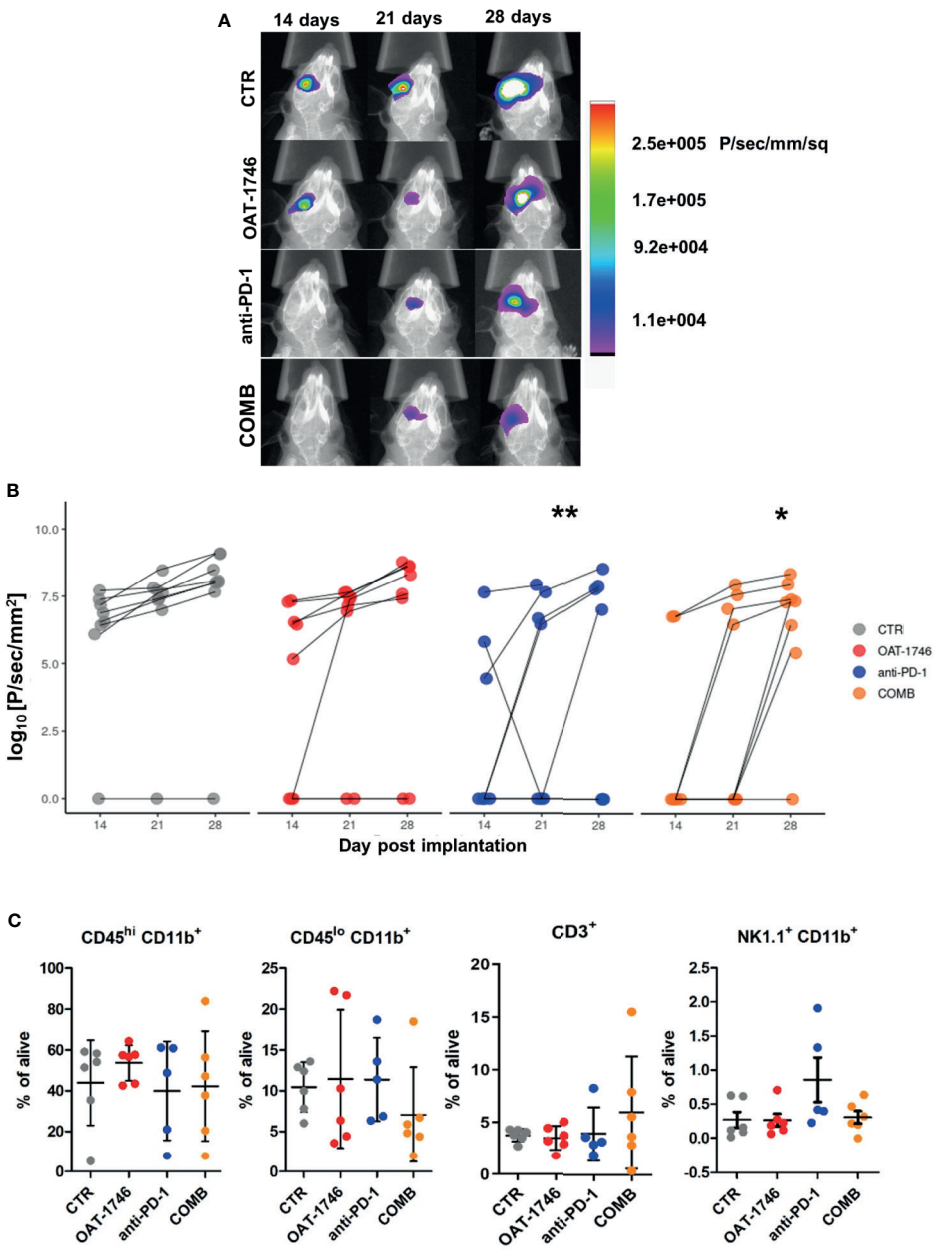

FIGURE 4 | Combined OAT-1746 and anti-PD-1 treatment reduces glioma growth. Mice were implanted with GL261 tdTomato$^+$luc$^+$ glioma cells and received saline (CTR), OAT-1746 (twice a day) alone or anti-PD-1 antibody at day 8, 10, 12 and 14 alone or in combination (COMB). **(A)** Representative images of tumor bioluminescence with Bruker Xtreme imaging. Color intensity represents a relative luciferase signal. Bioluminescence signals are plotted as photon/sec/mm^2 against time at indicated days post-implantation. **(B)** Tumor size measured using *in vivo* bioluminescence imaging at various times post-implantation. The effect of treatment and time on tumor progression was assessed with factorial ANOVA; treatment effect $F_{3,89}$= 4.801, p=0.004, day post-implantation effect $F_{2,89}$ = 4.726, p=0.011, and Tukey HSD *post hoc* test: CTRL-OAT p_{adj}=0.455, CTRL-CHECK p_{adj}=0.005, CTRL-COMB p_{adj}=0.021, COMB-OAT-1746 p_{adj}=0.46, COMB-anti-PD-1 p_{adj}=0.96. **(C)** At day 28 post-implantation animals were perfused with PBS, control and tumor-bearing brains were removed and processed to isolate myeloid cells by FACS. Percentages of peripheral macrophages (CD11b$^+$CD45^{hi}), microglia (CD11b$^+$CD45^{lo}), CD3$^+$ and NK1.1$^+$ cells were evaluated. Significance of differences between groups was assessed with One-Way ANOVA followed by Bonferroni's multiple comparison test. p-Values were considered as significant when **p < 0.01; *p < 0.05.

specific immune cell populations were quantified. Gating strategy is shown in the **Supplementary Figure 2**. The administration of OAT-1746 or anti-PD-1 treatment did not change the percentage of microglia (CD11b$^+$CD45^{low}) and blood-derived macrophages (CD11b$^+$CD45^{high}) in experimental gliomas. We noticed an increase in NK cells, however it did not reach statistical significance in anti-PD-1-treated animals compared to control group. An increased

percentage of $CD3^+$ T cells was observed in the majority of animals in the COMB group (**Figure 4C**). These results provide evidence that combining arginase inhibition with targeting the immune checkpoint, could be an effective strategy to improve immunotherapy outcome.

To obtain more insights regarding the enhancement of immunotherapy, we determined the levels of pro- and anti-inflammatory cytokines in the blood (plasma) collected 2 h after the last administration of OAT-1746. The levels of CCL5 (C-C Motif Chemokine Ligand 5) were reduced in both OAT-1746 or anti-PD-1 treated animals but the observed decrease was much stronger in animals treated with the combination of two agents (**Figure 5**). Interestingly, both OAT-1746 and anti-PD-1 treated animals showed higher levels of the cytokine CCL2 and this effect was abrogated in animals receiving the combination (**Figure 5**). The levels of CCL3 and M-CSF (macrophage colony stimulating factor, Csf1) were not changed by the treatments. C–C motif chemokine ligand 2 (CCL2) and CCL5 are the main chemokines involved in monocyte migration to tumors (40). CCL2 *via* its receptor CCR2 controls the migration of regulatory T cells (Treg) and myeloid suppressor cells (41), as well as their ability to promote tumor growth (42). The CCL5/CCR5 axis directs infiltration and interactions between monocytes/macrophages and mesenchymal stem cells. CCR5 is highly expressed in glioblastoma, controls glioma invasion and its expression is associated with the poor prognosis of GBM patients (43, 44).

Transcriptomic Profiles of $CD11b^+$ From OAT-1746 Treated Animals Show Reduced Expression of Tumor Supportive Genes

While OAT-1746 treatment alone showed no antitumor activity, it increased the therapeutic efficacy of PD-1 inhibition in murine gliomas. To gain insights into potential mechanisms of the observed phenomenon, we compared the transcriptomic profiles of glioma-associated $CD11b^+$ cells isolated from control mice (CTR), mice treated with anti-PD-1, OAT-1746 or a combination of both (COMB). $CD11b^+$ cells were sorted from tumor-bearing hemispheres as previously described (34)

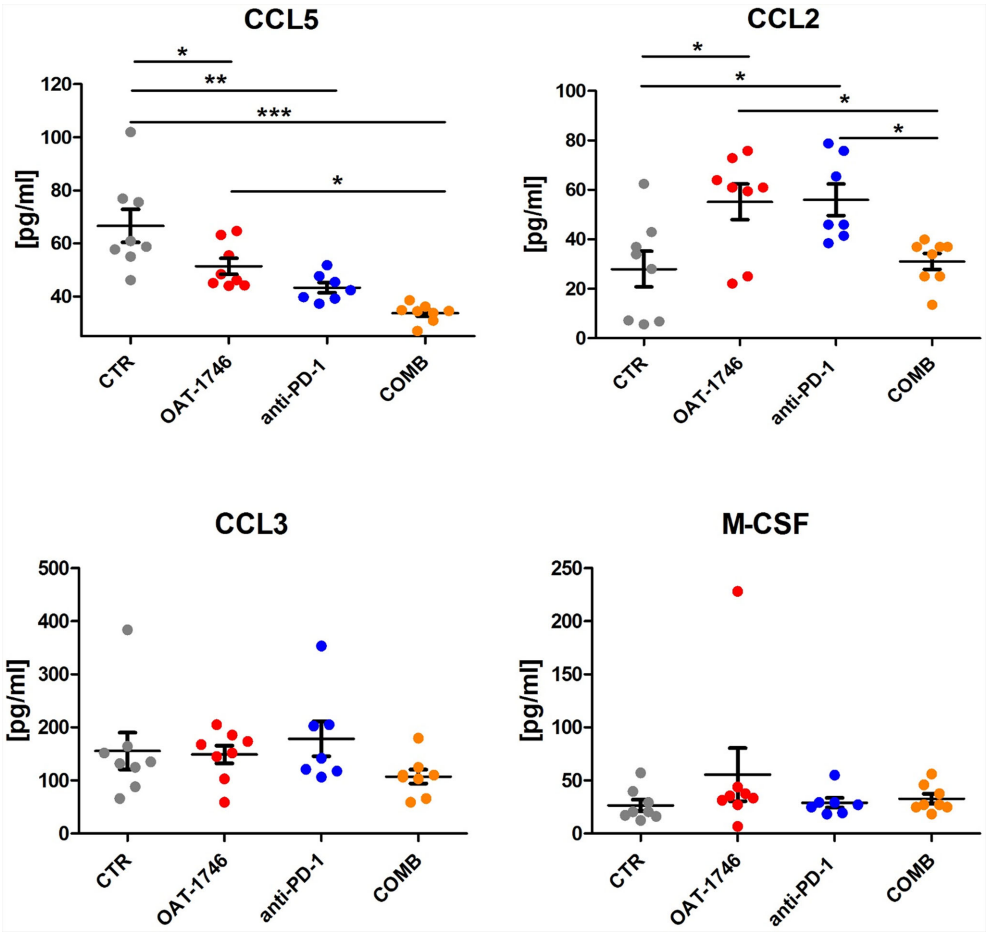

FIGURE 5 | The effect of treatment on the levels of pro- and anti-inflammatory cytokines. The levels of pro/anti-inflammatory cytokines were determined in blood plasma of the animals from the experimental groups described above using a multiplexed bead-based assay and Luminex technology (MAGPIX). Histograms show the levels of tested cytokines in pg/mL; the results are shown as means ± SEM; significance was assessed with One–Way ANOVA and Bonferroni's multiple comparison test, ***$p < 0.001$; **$p < 0.01$; *$p < 0.05$.

and the gating strategy is shown in the **Supplementary Figure 3**. $CD11b^+$ cells immunosorted from GL261 tumor-bearing hemispheres encompass microglia, infiltrating monocytes/macrophages and BAMs, as well as granulocytes, certain subpopulations of dendritic cells and NK cells (34). RNA sequencing of total RNA isolated from $CD11b^+$ cells was followed by computational analyses of differentially expressed genes and detection of altered signaling pathways.

OAT-1746 had the greatest impact on the transcriptome of $CD11b^+$ cells and over 1800 genes were identified as differentially expressed genes (DEG) between the OAT-1746 and CTR groups ($p_{adj}<0.05$) (**Figure 6A**). To classify the DEGs into functional categories, we performed Gene Ontology (GO) enrichment, in which genes were assigned to biological processes. Pathway enrichment for OAT-1746 showed significant terms which are shown in **Figures 6B, C**. The number of DEGs between other groups (anti-PD-1 *vs*. CTR and COMB *vs*. CTR) was low and no significantly affected processes were identified. Among the differentially up-regulated genes in the OAT-1746 group, we found a significant overrepresentation of genes involved in GTPase-mediated signal transduction, myeloid cell differentiation, NF-κB (nuclear factor kappa B) signaling, and regulation of inflammatory responses. In contrast, the downregulated genes in the OAT-1746 group were related to ribosome biogenesis, the cell cycle and DNA replication, which indicates the decreased proliferative activity of the tumor-associated myeloid cells.

We selected several DEGs which showed statistically significant changes in at least one of these different comparisons (OAT-1746 *vs* CTR, anti-PD-1 *vs* CTR or COMB *vs* CTR) and profiled their expression in $CD11b^+$ cells from the tested groups (**Figure 6D**). Genes associated with differentiation and cytotoxic activity of NK cells were significantly upregulated under anti-PD-1 treatment and in combination with OAT-1746. This group included genes coding for NK cell surface proteins (*Klrb1f*, *Klre1*, *Klrc2*), cytotoxic granule protein (*Nkg7*), T-Box transcription factor 21 (*Tbx21*), which is involved in NK cell differentiation and regulation of IFNγ expression, as well as granzyme A (*Gzma*) and perforin (*Prf1*), which are the major cytolytic factors in antitumor response of cytotoxic NK and T cells. In parallel, *Serpinb6b* and *Serpinb9b*, which encode serine protease inhibitors, were upregulated, which may protect leukocytes from the cell death mediated by granzyme A and B, respectively. Such a signature indicates an increased intratumoral influx of activated cytotoxic NK cells.

Moreover, treatment with OAT-1746 induced the expression of genes related to NF-κB pathways (*Nfkbia*, *Nfkbid*, *Nfkbiz*) and a number of GTPases-encoding genes, including RhoB (*Rhob*), which was shown to increase NF-κB activity towards *IL-1β*, *IL-6*, and *TNF-α* genes in macrophages (45). In $CD11b^+$ cells from mice treated with OAT-1746, we found high expression of *Gpr34*, which is upregulated in microglia during inflammation, *Tgif2*, which encodes a repressor of TGFβ-mediated responses, and *Duoxa1*, which encodes dual oxidase maturation factor 1 (DUOXA1) involved in pathways generating reactive oxygen species (ROS). Effective upregulation of several genes implicated in the antitumor immune response, such as those encoding for nitric oxide synthase (*Nos2*), IFNγ (*Ifng*), Tlr4 (*Tlr4*), and CD86 (*CD86*), which provides co-stimulatory signals necessary for T-cell activation, has been demonstrated in the COMB group.

Treatment with OAT-1746 resulted in a reduced expression of genes related to DNA replication and cell cycle progression, including topoisomerase 2a (*Top2a*), cyclin B1, E1 and E2 (*Ccnb1*, *Ccne1*, *Ccne2*); spindle and kinetochore-associated complex subunit 1, 2 and 3 (*Ska1*, *Ska2*, *Ska3*), as well as mitotic checkpoint kinase Bub1b (*Bub1b*) and aurora kinase B (*Aurkb*), which are involved in chromosome segregation during mitosis. This is consistent with the requirement of arginase activity for the production of L-ornithine from arginine, which is required for cell proliferation (46).

Among downregulated genes in the OAT-1746 group, we identified those involved in lymphocyte chemotaxis, i.e. *Ccl2*, *Ccl7* and *Ccl17*, and genes related to migration and invasion (*Cme1*, *S100a4* and *Mmp14*). Ccl2 and Ccl7 (also known as monocyte chemoattractant protein 1 and 3, respectively) play a critical role in the recruitment of monocytes and neutrophils to the inflamed or tumor tissue, while Ccl17 attracts regulatory T cells (47). Metalloproteinase 14 (MMP14) participates in MMP2 activation and the degradation of the extracellular matrix (ECM). MMP14 is upregulated in GAMs, and its expression correlates with the increased tumor growth in murine glioma models (48). *Clec12a* and *Clec4a1*, encoding inhibitory receptors for dendritic cells, were downregulated in the OAT-1746 group. The expression of genes encoding factors involved in the suppression of immune responses, i.e.: ApoE – a marker of an anti-inflammatory GAMs phenotype (49), CD69 – a negative regulator of immune responses implicated in inducing the exhaustion of tumor-infiltrating T cells (50), and Cxcr4 – a receptor for the immunosuppressive chemokine Cxcl12, were downregulated in the OAT-1746 and COMB groups. The decreased expression of these genes together with the upregulation of genes encoding mediators of the pro-inflammatory response suggests reprogramming of myeloid cells and restoration of the antitumor immunity.

DISCUSSION

Current therapies are not effective in glioblastoma patients as gross resection does not completely remove tumor cells, and the inactivation of tumor suppressors and enhanced DNA repair result in tumor cell resistance to radiotherapy and TMZ. Approximately 40% of patients with GBM do not or poorly respond to therapy and patients frequently experience fast tumor recurrence (51). While immunotherapy has been effective in many solid tumors, the results in GBM are disappointing despite the fact that PD-1 is an important checkpoint inhibitor in GBM (11). The failure of GBM to respond to anti-PD-1 is attributed to the immunosuppressive TME, which as in other "cold" tumors is characterized by a paucity of tumor infiltrating lymphocytes and a predominance of immunosuppressive myeloid cells (52–54). GAMs produce CCL2, a chemokine recruiting $CCR4^+$ Treg and

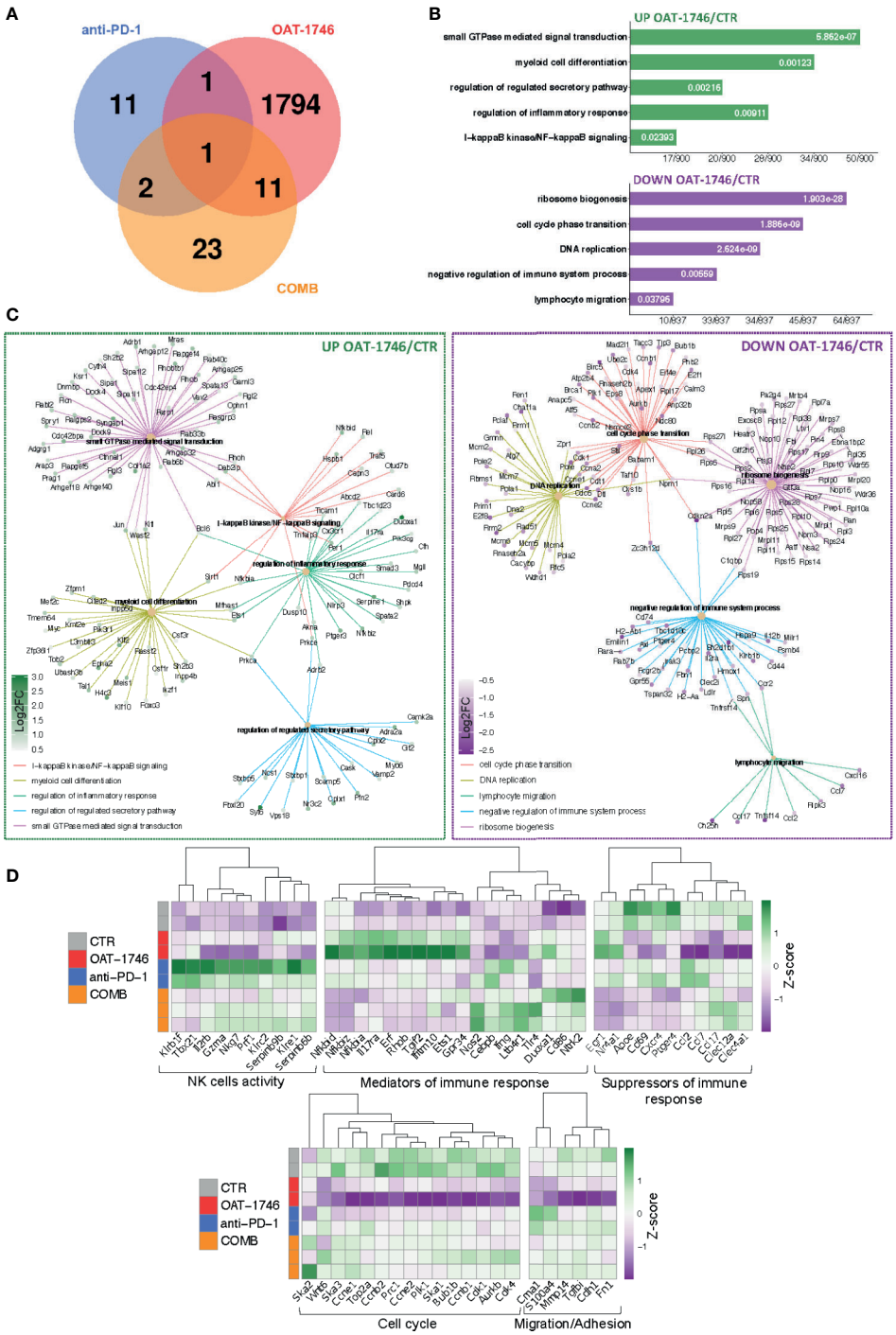

FIGURE 6 | Transcriptomic profiles of CD11b$^+$ from OAT-1746-treated mice show reduction of the pro-tumor phenotype genes and upregulation of gene expression indicative of antitumor responses. **(A–D)** Gene expression profiling was performed by RNA-seq of CD11b$^+$ cells from the tumor-bearing hemispheres of mice from the experimental groups at day 21 post-implantation. **(A)** Venn diagram showing the number of differentially expressed genes (DEG) between OAT-1746, anti-PD-1 and COMB compared to the CTR group (p_{adj}<0.05). **(B)** Functional enrichment analysis with Gene Ontology (GO) biological processes for up- and downregulated genes in OAT-1746 compared to CTR. Enriched GO pathway names are shown, the size of the bars indicates the ratio of genes (a number of genes annotated to the pathway/total number of DEGs with adjusted p-values < 0.05). **(C)** Graphical representation of selected overrepresented categories among DEGs in the OAT-1746 *versus* the CTR group **(D)** Z-score heatmaps for selected genes represent the relative change in gene expression in the CD11b$^+$ cells from OAT-1746, anti-PD-1 or COMB treated animals.

$CCR2^+Ly\text{-}6C^+$ monocytic MDSCs in murine gliomas (41). The combination of PD-1 blockade and CCR2 inhibition (both genetic and pharmacological with the CCR2 agonist CCX872) improved survival of KR158 glioma-bearing mice, and reduced accumulation of $CD11b^+/Ly6C^{hi}/PD\text{-}L1^+$ MDSCs in gliomas. The combined treatment resulted in increased TILs infiltration, IFNγ expression and the decreased expression of exhaustion markers in $CD4^+$ and $CD8^+$ T cells (55).

Exploring various public datasets we found the elevated expression of *ARG1* and *ARG2* in high grade gliomas, in particular in highly aggressive GBMs. Interrogation of single-cell sequencing data from gliomas shows *ARG1* and *ARG2* expression in both malignant cells and microglia/macrophages in human high grade gliomas. Both arginase isoforms are expressed in myeloid cells in murine experimental gliomas, however *Arg1* mRNA levels are significantly higher than *Arg2*. Moreover, *Arg1*, a phenotypic marker of immunosuppressive myeloid cells, is expressed mainly in infiltrating monocytes as compared to microglia.

Newly developed ARG1/2 inhibitors showed a comparable inhibitory efficacy towards recombinant proteins *in vitro* as two reference inhibitors and several compounds described in the literature (56). In microglia-glioma co-cultures, which are used to model microglia-induced glioma invasion, OAT-1746 at micromolar concentrations strongly reduced glioma invasion, and this effect was concentration dependent. The reference compound was less effective and did not show any dose dependency. OAT-1746 up to the concentration of 1 mM was not toxic to two types of microglial cells and glioma cells, only a 20% reduction of the cell viability was detected in U87-MG glioma cells treated with this high dose of the drug. The concentration that showed toxicity exceeds by over two orders of magnitude the effective concentration of the inhibitor. The results provide evidence for the efficacy of a new compound and its safety in therapeutically relevant concentrations. Moreover, in the previous studies OAT-1746 showed no toxicity in experimental animals after multiple oral dosing in mono- or combinatorial therapies in other tumor models (36, 57). The presented data provide a strong rationale for using an ARG1 inhibitor OAT-1746 to block the pro-tumor activity of GAMs. OAT-1746 penetrated BBB and significantly increased the concentration of arginine in the brain and plasma of the receiving mice. While OAT-1746 did not affect the accumulation of microglia/macrophages ($Iba1^+$ cells) and $CD8^+$ cells, it considerably changed the transcriptomic profiles in $CD11b^+$ immunosorted from tumor-bearing brains.

OAT-1746 had the highest impact on the transcriptome of $CD11b^+$ cells in comparison to other treatments. Gene Ontology (GO) term enrichment revealed a significant overrepresentation of genes involved in GTPase-mediated signal transduction, myeloid cell differentiation, NF-κB signaling and the regulation of inflammatory responses, with simultaneous significant downregulation of genes related to ribosome biogenesis, the cell cycle and DNA replication. These changes in transcriptome are consistent with the decreased proliferation of GAMs (*Top2a*, *Ccnb1*, *Ccne1*, *Ccne2*, *Ska1*, *Ska2*, *Ska3, Bub1b, Aurkb*) and changes in their functions. High expression of inflammation mediators such as genes coding for *Gpr34* and *Duoxa1* indicates a switch to the pro-inflammatory phenotype. This is consistent with the requirement of the arginase activity for the production of L-ornithine and polyamines for cell proliferation (46).

Moreover, OAT-1746 treatment affects the expression of genes involved in leukocyte chemotaxis (*Ccl2*, *Ccl7*, *Ccl17)* and supporting glioma migration and invasion (*Cme1*, *S100a4* and *Mmp14)*. Ccl2 and Ccl7 control the recruitment of monocytes and neutrophils to the inflamed or tumor tissues, while Ccl17 attracts regulatory T cells (47). MMP14 (MT1MMP) is a metalloproteinase upregulated in GAMs, which activates MMP2 and ECM degradation (48). *Clec12a* and *Clec4a1*, which encode dendritic cell inhibitory receptors, were downregulated in the OAT-1746 group.

Ccl2 is released by many cells present in the tumor microenvironment, including stromal cells, leukocytes, endothelial cells, and malignant cells, which results in augmentation of the plasma chemokine levels (58). Despite decreased expression of *Ccl2* mRNA in $CD11b^+$ cells immunosorted from the tumor-bearing brains of OAT-1746-treated animals, the other cells in the tumor microenvironment could still be the source of the cytokine and augment Ccl2 plasma levels. In humans and in animal glioma models, increased CCL2 expression has been associated with high number of GAMs infiltrating tumor tissues, increased angiogenesis and tumor invasion, and poor clinical prognosis (59–61). Impact of increased Ccl2 and decreased Ccl5 plasma levels in OAT-1746 treated animals on the outcome of potential treatment requires further investigation. Measuring the levels of cytokines in the brain or tumor tissue would provide additional insights into the mechanism of action of mono- and combined therapies

Interestingly, the transcriptomic analysis showed the upregulation of several genes implicated in antitumor immune responses such as *Nos2*, *Ifng*, *Tlr4* and *CD86* upon the combinatorial therapy. Genes associated with differentiation and cytotoxic activity of NK cells were significantly upregulated upon anti-PD-1 treatment and COMB therapy. The $CD11b^+$ population encompasses NK cells. The upregulation of genes encoding NK surface proteins (*Klrb1f*, *Klre1*, *Klrc2*), cytotoxic granule protein (*Nkg7*), T-Box transcription factor 21 (*Tbx21*), granzyme A (*Gzma*) and perforin (*Prf1*), along with the upregulation of *Serpinb6b* and *Serpinb9b* that protect leukocytes from the granzyme-mediated cell death, suggests the restoration of NK cell functions. Downregulation of genes encoding proteins acting as the suppressors of the immune responses: ApoE, CD69 (50), and Cxcr4 in OAT-1746 and COMB groups indicates the restoration of antitumor functions of $CD11b^+$ cells, which may explain the antitumor effect of the combination therapy. These results indicate how important for the effective immunotherapy is the reprogramming of TME. Altogether, our results demonstrate that combining OAT-1746 with PD-1 inhibition may be a promising strategy for the therapy of GBM patients. The complexity of interactions in the tumor microenvironment,

arginase inhibition in different cells and anti-PD-1 inhibition resulting in changes of the immune compartment may explain a low number of differentially expressed genes in the COMB group and a small overlap of OAT-1746 mono and combined treatment Future testing of the drug efficacy on established tumors, alternatively to the currently studied preventive treatment regimen, would provide additional information on a mode of action and a translational potential of OAT-1746. ARG1 expression is substantially elevated in myeloid cells in cancer and mitigates antitumor responses *via* multiple mechanisms. Arginase production by macrophages not only leads to the inhibition of antitumor response *via* L-arginine degradation, but also increases the proliferation of tumor cells, which is associated with the production of L-ornithine and then polyamines. Moreover, L-arginine depletion in the tumor microenvironment attenuates nitric oxide (NO) production and reduces its cytotoxic effects on tumor cells (62).

Cytotoxic lymphocytes require exogenous arginine for proliferation (19, 21, 63) and low plasma arginine levels are linked to immunosuppression in cancer patients (64). Arginase 1 expression in malignant cells and myeloid cells in the TME represents a powerful mechanism for tumor immune evasion (65). Dietary supplementation with L-arginine altered the spectrum of TILs and enhanced cytotoxicity in human colorectal and breast cancers (66, 67). Elevation of arginine levels exerted immune-stimulatory effects in various cancers, for example blocking arginase activity with nor-NOHA in leukemic cells induced cell death (68) and treatment with another inhibitor CB-1158 had antitumor effects in several non-CNS cancers in mice (24). Here we demonstrate that a novel, oral ARG1/2 inhibitor, which increases L-arginine levels in the brain and restores the functionality of GAMs and NK cells, sensitizes murine gliomas to the PD-1 inhibition. The combination of OAT-1746 and anti-PD1 leads to the elevation of a number of $CD3^+$ T cells in the majority of tumors. Our results support a rationale of combining compounds targeting TME (such as OAT-1746) with PD-1 inhibition as a potential strategy to treat GBM patients.

DATA AVAILABILITY STATEMENT

The original contributions presented in the study are publicly available. This data can be found here: National Center for Biotechnology Information (NCBI) Gene Expression Omnibus under accession number GSE173865.

ETHICS STATEMENT

The animal study was reviewed and approved by The First Warsaw Local Ethics Committee for Animal Experimentation (approval no 562/2018).

AUTHOR CONTRIBUTIONS

BK, PP, and AE-M designed the experiments, evaluated the data, and wrote the manuscript. PP, KW, SC, AE-M, and NO performed the experiments, data interpretation and wrote the manuscript. BG performed RNA-seq and A-JR performed computational analyses, data interpretation and edited the manuscript. MG, PS, RB, and PD synthesized the ARG1/2 inhibitors, performed enzyme inhibition tests and determination of the inhibitor and arginine concentrations, contributed to the data interpretation and edited the manuscript. All authors contributed to the article and approved the submitted version.

FUNDING

Studies were supported by the project DIMUNO "Development of new cancer therapies based on selective antitumor immunomodulators"- co-financed by the National Centre for Research and Development, Poland and the Foundation for Polish Science TEAM-TECH Core Facility project "NGS platform for comprehensive diagnostics and personalized therapy in neuro-oncology" (KW, AJ-R, BG, BK).

ACKNOWLEDGMENTS

We thank Beata Kaza for technical assistance, Julian Swatler for help with flow cytometry.

SUPPLEMENTARY MATERIAL

The Supplementary Material for this article can be found online at: https://www.frontiersin.org/articles/10.3389/fonc.2021.703465/full#supplementary-material

REFERENCES

1. Jemal A, Murray T, Ward E, Samuels A, Tiwari RC, Ghafoor A, et al. Cancer Statistics, 2005. *CA Cancer J Clin* (2005) 55(1):10–30. doi: 10.3322/canjclin.55.1.10
2. Stupp R, Hegi ME, Mason WP, van den Bent MJ, Taphoorn MJ, Janzer RC, et al. Effects of Radiotherapy With Concomitant and Adjuvant Temozolomide *Versus* Radiotherapy Alone on Survival in Glioblastoma in a Randomised Phase III Study: 5-Year Analysis of the EORTC-NCIC Trial. *Lancet Oncol* (2009) 10(5):459–66. doi: 10.1016/S1470-2045(09)70025-7
3. Galon J, Angell HK, Bedognetti D, Marincola FM. The Continuum of Cancer Immunosurveillance: Prognostic, Predictive, and Mechanistic Signatures. *Immunity* (2013) 39(1):11–26. doi: 10.1016/j.immuni.2013.07.008
4. Woroniecka KI, Rhodin KE, Chongsathidkiet P, Keith KA, Fecci PE. T-Cell Dysfunction in Glioblastoma: Applying a New Framework. *Clin Cancer Res* (2018) 24(16):3792–802. doi: 10.1158/1078-0432.CCR-18-0047
5. Webster RM. The Immune Checkpoint Inhibitors: Where Are We Now? *Nat Rev Drug Discov* (2014) 13(12):883–4. doi: 10.1038/nrd4476
6. Scheffel TB, Grave N, Vargas P, Diz FM, Rockenbach L, Morrone FB. Immunosuppression in Gliomas *via* PD-1/PD-L1 Axis and Adenosine Pathway. *Front Oncol* (2020) 10:617385. doi: 10.3389/fonc.2020.617385

7. Parsa AT, Waldron JS, Panner A, Crane CA, Parney IF, Barry JJ, et al. Loss of Tumor Suppressor PTEN Function Increases B7-H1 Expression and Immunoresistance in Glioma. *Nat Med* (2007) 13(1):84–8. doi: 10.1038/nm1517
8. Cloughesy TF, Mochizuki AY, Orpilla JR, Hugo W, Lee AH, Davidson TB, et al. Neoadjuvant Anti-PD-1 Immunotherapy Promotes a Survival Benefit With Intratumoral and Systemic Immune Responses in Recurrent Glioblastoma. *Nat Med* (2019) 25(3):477–86. doi: 10.1038/s41591-018-0337-7
9. Lombardi G, Barresi V, Indraccolo S, Simbolo M, Fassan M, Mandruzzato S, et al. Pembrolizumab Activity in Recurrent High-Grade Gliomas With Partial or Complete Loss of Mismatch Repair Protein Expression: A Monocentric, Observational and Prospective Pilot Study. *Cancers (Basel)* (2020) 12(8):2283. doi: 10.3390/cancers12082283
10. Nayak L, Molinaro AM, Peters K, Clarke JL, Jordan JT, de Groot J, et al. Randomized Phase II and Biomarker Study of Pembrolizumab Plus Bevacizumab *Versus* Pembrolizumab Alone for Patients With Recurrent Glioblastoma. *Clin Cancer Res* (2021) 27(4):1048–57. doi: 10.1158/1078-0432.CCR-20-2500
11. Reardon DA, Brandes AA, Omuro A, Mulholland P, Lim M, Wick A, et al. Effect of Nivolumab *vs* Bevacizumab in Patients With Recurrent Glioblastoma: The Checkmate 143 Phase 3 Randomized Clinical Trial. *JAMA Oncol* (2020) 6(7):1003–10. doi: 10.1001/jamaoncol.2020.1024
12. Zhao J, Chen AX, Gartrell RD, Silverman AM, Aparicio L, Chu T, et al. Author Correction: Immune and Genomic Correlates of Response to Anti-PD-1 Immunotherapy in Glioblastoma. *Nat Med* (2019) 25(6):1022. doi: 10.1038/s41591-019-0449-8
13. Jenkins RW, Barbie DA, Flaherty KT. Mechanisms of Resistance to Immune Checkpoint Inhibitors. *Br J Cancer* (2018) 118(1):9–16. doi: 10.1038/bjc.2017.434
14. de Groot J, Penas-Prado M, Alfaro-Munoz K, Hunter K, Pei BL, O'Brien B, et al. Window-of-Opportunity Clinical Trial of Pembrolizumab in Patients With Recurrent Glioblastoma Reveals Predominance of Immune-Suppressive Macrophages. *Neuro Oncol* (2020) 22(4):539–49. doi: 10.1093/neuonc/noz185
15. Locarno CV, Simonelli M, Carenza C, Capucetti A, Stanzani E, Lorenzi E, et al. Role of Myeloid Cells in the Immunosuppressive Microenvironment in Gliomas. *Immunobiology* (2020) 225(1):151853. doi: 10.1016/j.imbio.2019.10.002
16. Gieryng A, Pszczolkowska D, Bocian K, Dabrowski M, Rajan WD, Kloss M, et al. Immune Microenvironment of Experimental Rat C6 Gliomas Resembles Human Glioblastomas. *Sci Rep* (2017) 7(1):17556. doi: 10.1038/s41598-017-17752-w
17. Zhang I, Alizadeh D, Liang J, Zhang L, Gao H, Song Y, et al. Characterization of Arginase Expression in Glioma-Associated Microglia and Macrophages. *PLoS One* (2016) 11(12):e0165118. doi: 10.1371/journal.pone.0165118
18. Gabrilovich DI, Ostrand-Rosenberg S, Bronte V. Coordinated Regulation of Myeloid Cells by Tumours. *Nat Rev Immunol* (2012) 12(4):253–68. doi: 10.1038/nri3175
19. Munder M, Schneider H, Luckner C, Giese T, Langhans CD, Fuentes JM, et al. Suppression of T-Cell Functions by Human Granulocyte Arginase. *Blood* (2006) 108(5):1627–34. doi: 10.1182/blood-2006-11-010389
20. Morris SMJr. Recent Advances in Arginine Metabolism: Roles and Regulation of the Arginases. *Br J Pharmacol* (2009) 157(6):922–30. doi: 10.1111/j.1476-5381.2009.00278.x
21. Rodriguez PC, Zea AH, DeSalvo J, Culotta KS, Zabaleta J, Quiceno DG, et al. L-Arginine Consumption by Macrophages Modulates the Expression of CD3 Zeta Chain in T Lymphocytes. *J Immunol* (2003) 171(3):1232–9. doi: 10.4049/jimmunol.171.3.1232
22. Raber P, Ochoa AC, Rodriguez PC. Metabolism of L-Arginine by Myeloid-Derived Suppressor Cells in Cancer: Mechanisms of T Cell Suppression and Therapeutic Perspectives. *Immunol Invest* (2012) 41(6-7):614–34. doi: 10.3109/08820139.2012.680634
23. Rodriguez PC, Ochoa AC, Al-Khami AA. Arginine Metabolism in Myeloid Cells Shapes Innate and Adaptive Immunity. *Front Immunol* (2017) 8:93. doi: 10.3389/fimmu.2017.00093
24. Steggerda SM, Bennett MK, Chen J, Emberley E, Huang T, Janes JR, et al. Inhibition of Arginase by CB-1158 Blocks Myeloid Cell-Mediated Immune Suppression in the Tumor Microenvironment. *J Immunother Cancer* (2017) 5(1):101. doi: 10.1186/s40425-017-0308-4
25. Walentynowicz KA, Ochocka N, Pasierbinska M, Wojnicki K, Stepniak K, Mieczkowski J, et al. In Search for Reliable Markers of Glioma-Induced Polarization of Microglia. *Front Immunol* (2018) 9:1329. doi: 10.3389/fimmu.2018.01329
26. Gabrusiewicz K, Ellert-Miklaszewska A, Lipko M, Sielska M, Frankowska M, Kaminska B. Characteristics of the Alternative Phenotype of Microglia/Macrophages and Its Modulation in Experimental Gliomas. *PLoS One* (2011) 6(8):e23902. doi: 10.1371/journal.pone.0023902
27. Bolger AM, Lohse M, Usadel B. Trimmomatic: A Flexible Trimmer for Illumina Sequence Data. *Bioinformatics* (2014) 30(15):2114–20. doi: 10.1093/bioinformatics/btu170
28. Dobin A, Davis CA, Schlesinger F, Drenkow J, Zaleski C, Jha S, et al. STAR: Ultrafast Universal RNA-Seq Aligner. *Bioinformatics* (2013) 29(1):15–21. doi: 10.1093/bioinformatics/bts635
29. Anders S, Pyl PT, Huber W. Htseq–A Python Framework to Work With High-Throughput Sequencing Data. *Bioinformatics* (2015) 31(2):166–9. doi: 10.1093/bioinformatics/btu638
30. Love MI, Huber W, Anders S. Moderated Estimation of Fold Change and Dispersion for RNA-Seq Data With Deseq2. *Genome Biol* (2014) 15(12):550. doi: 10.1186/s13059-014-0550-8
31. Yu G, Wang LG, Han Y, He QY. Clusterprofiler: An R Package for Comparing Biological Themes Among Gene Clusters. *OMICS* (2012) 16(5):284–7. doi: 10.1089/omi.2011.0118
32. Chen H, Boutros PC. Venndiagram: A Package for the Generation of Highly-Customizable Venn and Euler Diagrams in R. *BMC Bioinf* (2011) 12:35. doi: 10.1186/1471-2105-12-35
33. Venteicher AS, Tirosh I, Hebert C, Yizhak K, Neftel C, Filbin MG, et al. Decoupling Genetics, Lineages, and Microenvironment in IDH-Mutant Gliomas by Single-Cell RNA-Seq. *Science* (2017) 355(6332):eaai8478. doi: 10.1126/science.aai8478
34. Ochocka N, Segit P, Walentynowicz KA, Wojnicki K, Cyranowski S, Swatler J, et al. Single-Cell RNA Sequencing Reveals Functional Heterogeneity of Glioma-Associated Brain Macrophages. *Nat Commun* (2021) 12(1):1151. doi: 10.1038/s41467-021-21407-w
35. Ellert-Miklaszewska A, Wisniewski P, Kijewska M, Gajdanowicz P, Pszczolkowska D, Przanowski P, et al. Tumour-Processed Osteopontin and Lactadherin Drive the Protumorigenic Reprogramming of Microglia and Glioma Progression. *Oncogene* (2016) 35(50):6366–77. doi: 10.1038/onc.2016.55
36. Czystowska-Kuzmicz M, Sosnowska A, Nowis D, Ramji K, Szajnik M, Chlebowska-Tuz J, et al. Small Extracellular Vesicles Containing Arginase-1 Suppress T-Cell Responses and Promote Tumor Growth in Ovarian Carcinoma. *Nat Commun* (2019) 10(1):3000. doi: 10.1038/s41467-019-10979-3
37. Ash DE. Structure and Function of Arginases. *J Nutr* (2004) 134(10 Suppl):2760S–4Sdiscussion 2765S–2767S. doi: 10.1093/jn/134.10.2765S
38. Sielska M, Przanowski P, Pasierbinska M, Wojnicki K, Poleszak K, Wojtas B, et al. Tumour-Derived CSF2/Granulocyte Macrophage Colony Stimulating Factor Controls Myeloid Cell Accumulation and Progression of Gliomas. *Br J Cancer* (2020) 123(3):438–48. doi: 10.1038/s41416-020-0862-2
39. Spranger S, Gajewski T. Rational Combinations of Immunotherapeutics That Target Discrete Pathways. *J Immunother Cancer* (2013) 1:16. doi: 10.1186/2051-1426-1-16
40. Kumar V, Patel S, Tcyganov E, Gabrilovich DI. The Nature of Myeloid-Derived Suppressor Cells in the Tumor Microenvironment. *Trends Immunol* (2016) 37(3):208–20. doi: 10.1016/j.it.2016.01.004
41. Chang AL, Miska J, Wainwright DA, Dey M, Rivetta CV, Yu D, et al. CCL2 Produced by the Glioma Microenvironment Is Essential for the Recruitment of Regulatory T Cells and Myeloid-Derived Suppressor Cells. *Cancer Res* (2016) 76(19):5671–82. doi: 10.1158/0008-5472.CAN-16-0144
42. From the American Association of Neurological Surgeons ASoNC, Interventional Radiology Society of Europe CIRACoNSESoMINTESoNESOSfCA, Interventions SoIRSoNS, World Stroke O, Sacks D, Baxter B, Campbell BCV, Carpenter JS, Cognard C, et al. Multisociety Consensus Quality Improvement Revised Consensus Statement for Endovascular Therapy of Acute Ischemic Stroke. *Int J Stroke* (2018) 13(6):612–32. doi: 10.1016/j.jvir.2017.11.026

43. Kranjc MK, Novak M, Pestell RG, Lah TT. Cytokine CCL5 and Receptor CCR5 Axis in Glioblastoma Multiforme. *Radiol Oncol* (2019) 53(4):397–406. doi: 10.2478/raon-2019-0057
44. Yu-Ju Wu C, Chen CH, Lin CY, Feng LY, Lin YC, Wei KC, et al. CCL5 of Glioma-Associated Microglia/Macrophages Regulates Glioma Migration and Invasion *via* Calcium-Dependent Matrix Metalloproteinase 2. *Neuro Oncol* (2020) 22(2):253–66. doi: 10.1093/neuonc/noz189
45. Huang B, Lei Z, Zhao J, Gong W, Liu J, Chen Z, et al. CCL2/CCR2 Pathway Mediates Recruitment of Myeloid Suppressor Cells to Cancers. *Cancer Lett* (2007) 252(1):86–92. doi: 10.1016/j.canlet.2006.12.012
46. Caldwell RW, Rodriguez PC, Toque HA, Narayanan SP, Caldwell RB. Arginase: A Multifaceted Enzyme Important in Health and Disease. *Physiol Rev* (2018) 98(2):641–65. doi: 10.1152/physrev.00037.2016
47. Hirata A, Hashimoto H, Shibasaki C, Narumi K, Aoki K. Intratumoral IFN-Alpha Gene Delivery Reduces Tumor-Infiltrating Regulatory T Cells Through the Downregulation of Tumor CCL17 Expression. *Cancer Gene Ther* (2019) 26(9-10):334–43. doi: 10.1038/s41417-018-0059-5
48. Markovic DS, Vinnakota K, Chirasani S, Synowitz M, Raguet H, Stock K, et al. Gliomas Induce and Exploit Microglial MT1-MMP Expression for Tumor Expansion. *Proc Natl Acad Sci USA* (2009) 106(30):12530–5. doi: 10.1073/pnas.0804273106
49. Baitsch D, Bock HH, Engel T, Telgmann R, Muller-Tidow C, Varga G, et al. Apolipoprotein E Induces Antiinflammatory Phenotype in Macrophages. *Arterioscler Thromb Vasc Biol* (2011) 31(5):1160–8. doi: 10.1161/ATVBAHA.111.222745
50. Mita Y, Kimura MY, Hayashizaki K, Koyama-Nasu R, Ito T, Motohashi S, et al. Crucial Role of CD69 in Anti-Tumor Immunity Through Regulating the Exhaustion of Tumor-Infiltrating T Cells. *Int Immunol* (2018) 30(12):559–67. doi: 10.1093/intimm/dxy050
51. Weller M, Cloughesy T, Perry JR , Wick W. Standards of Care for Treatment of Recurrent Glioblastoma–Are We There Yet? *Neuro Oncol* (2013) 15(1):4–27. doi: 10.1093/neuonc/nos273
52. Kim JE, Patel MA, Mangraviti A, Kim ES, Theodros D, Velarde E, et al. Combination Therapy With Anti-PD-1, Anti-TIM-3, and Focal Radiation Results in Regression of Murine Gliomas. *Clin Cancer Res* (2017) 23(1):124–36. doi: 10.1158/1078-0432.CCR-15-1535
53. Wu A, Maxwell R, Xia Y, Cardarelli P, Oyasu M, Belcaid Z, et al. Combination Anti-CXCR4 and Anti-PD-1 Immunotherapy Provides Survival Benefit in Glioblastoma Through Immune Cell Modulation of Tumor Microenvironment. *J Neurooncol* (2019) 143(2):241–9. doi: 10.1007/s11060-019-03172-5
54. Arlauckas SP, Garris CS, Kohler RH, Kitaoka M, Cuccarese MF, Yang KS, et al. *In Vivo* Imaging Reveals a Tumor-Associated Macrophage-Mediated Resistance Pathway in Anti-PD-1 Therapy. *Sci Transl Med* (2017) 9(389):eaal3604. doi: 10.1126/scitranslmed.aal3604
55. Flores-Toro JA, Luo D, Gopinath A, Sarkisian MR, Campbell JJ, Charo IF, et al. CCR2 Inhibition Reduces Tumor Myeloid Cells and Unmasks a Checkpoint Inhibitor Effect to Slow Progression of Resistant Murine Gliomas. *Proc Natl Acad Sci USA* (2020) 117(2):1129–38. doi: 10.1073/pnas.1910856117
56. Grobben Y, Uitdehaag JCM, Willemsen-Seegers N, Tabak WWA, de Man J, Buijsman RC, et al. Structural Insights Into Human Arginase-1 Ph Dependence and Its Inhibition by the Small Molecule Inhibitor CB-1158. *J Struct Biol X* (2020) 4:100014. doi: 10.1016/j.yjsbx.2019.100014
57. Stanczak PS, Grzybowski MM, Wolska P, Zdziarska AM, Mazurkiewicz M, Blaszczyk R, et al. Development of OAT-1746, a Novel Arginase 1 and 2 Inhibitor for Cancer Immunotherapy. *Ann Oncol* (2017) 28(Supplement 5):V418–9. doi: 10.1093/annonc/mdx376.046
58. Kohli K, Pillarisetty VG, Kim TS. Key Chemokines Direct Migration of Immune Cells in Solid Tumors. *Cancer Gene Ther* (2021). doi: 10.1038/s41417-021-00303-x
59. Kuratsu J, Yoshizato K, Yoshimura T, Leonard EJ, Takeshima H, Ushio Y. Quantitative Study of Monocyte Chemoattractant Protein-1 (MCP-1) in Cerebrospinal Fluid and Cyst Fluid From Patients With Malignant Glioma. *J Natl Cancer Inst* (1993) 85(22):1836–9. doi: 10.1093/jnci/85.22.1836
60. Platten M, Kretz A, Naumann U, Aulwurm S, Egashira K, Isenmann S, et al. Monocyte Chemoattractant Protein-1 Increases Microglial Infiltration and Aggressiveness of Gliomas. *Ann Neurol* (2003) 54(3):388–92. doi: 10.1002/ana.10679
61. Zhang J, Sarkar S, Cua R, Zhou Y, Hader W, Yong VW. A Dialog Between Glioma and Microglia That Promotes Tumor Invasiveness Through the CCL2/CCR2/Interleukin-6 Axis. *Carcinogenesis* (2012) 33(2):312–9. doi: 10.1093/carcin/bgr289
62. Chang CI, Liao JC, Kuo L. Macrophage Arginase Promotes Tumor Cell Growth and Suppresses Nitric Oxide-Mediated Tumor Cytotoxicity. *Cancer Res* (2001) 61(3):1100–6.
63. Lamas B, Vergnaud-Gauduchon J, Goncalves-Mendes N, Perche O, Rossary A, Vasson MP, et al. Altered Functions of Natural Killer Cells in Response to L-Arginine Availability. *Cell Immunol* (2012) 280(2):182–90. doi: 10.1016/j.cellimm.2012.11.018
64. Zea AH, Rodriguez PC, Atkins MB, Hernandez C, Signoretti S, Zabaleta J, et al. Arginase-Producing Myeloid Suppressor Cells in Renal Cell Carcinoma Patients: A Mechanism of Tumor Evasion. *Cancer Res* (2005) 65(8):3044–8. doi: 10.1158/0008-5472.CAN-04-4505
65. Rodriguez PC, Quiceno DG, Zabaleta J, Ortiz B, Zea AH, Piazuelo MB, et al. Arginase I Production in the Tumor Microenvironment by Mature Myeloid Cells Inhibits T-Cell Receptor Expression and Antigen-Specific T-Cell Responses. *Cancer Res* (2004) 64(16):5839–49. doi: 10.1158/0008-5472.CAN-04-0465
66. Heys SD, Segar A, Payne S, Bruce DM, Kernohan N, Eremin O. Dietary Supplementation With L-Arginine: Modulation of Tumour-Infiltrating Lymphocytes in Patients With Colorectal Cancer. *Br J Surg* (1997) 84(2):238–41. doi: 10.1046/j.1365-2168.1997.02528.x
67. Heys SD, Ogston K, Miller I, Hutcheon AW, Walker LG, Sarker TK, et al. Potentiation of the Response to Chemotherapy in Patients With Breast Cancer by Dietary Supplementation With L-Arginine: Results of a Randomised Controlled Trial. *Int J Oncol* (1998) 12(1):221–5. doi: 10.3892/ijo.12.1.221
68. Ng KP, Manjeri A, Lee LM, Chan ZE, Tan CY, Tan QD, et al. The Arginase Inhibitor Nomega-Hydroxy-Nor-Arginine (Nor-NOHA) Induces Apoptosis in Leukemic Cells Specifically Under Hypoxic Conditions But CRISPR/Cas9 Excludes Arginase 2 (ARG2) as the Functional Target. *PLoS One* (2018) 13(10):e0205254. doi: 10.1371/journal.pone.0205254

Conflict of Interest: MG, PS, and RB are employees of OncoArendi Therapeutics. PD is a former employee of OncoArendi Therapeutics.

The remaining authors declare that the research was conducted in the absence of any commercial or financial relationships that could be construed as a potential conflict of interest.

Publisher's Note: All claims expressed in this article are solely those of the authors and do not necessarily represent those of their affiliated organizations, or those of the publisher, the editors and the reviewers. Any product that may be evaluated in this article, or claim that may be made by its manufacturer, is not guaranteed or endorsed by the publisher.

frontiers in Oncology

REVIEW
published: 31 August 2021
doi: 10.3389/fonc.2021.682129

Immune Modulatory Short Noncoding RNAs Targeting the Glioblastoma Microenvironment

Jun Wei[1], *Eli Gilboa*[2], *George A. Calin*[3] *and Amy B. Heimberger*[4*]

[1] Department of Immunology, The University of Texas MD Anderson Cancer Center, Houston, TX, United States, [2] Department of Microbiology & Immunology, Dodson Interdisciplinary Immunotherapy Institute, Sylvester Comprehensive Cancer Center, University of Miami, Miami, FL, United States, [3] Departments of Translational Molecular Pathology, The University of Texas MD Anderson Cancer Center, Houston, TX, United States, [4] Department of Neurological Surgery, Feinberg School of Medicine, Northwestern University, Chicago, IL, United States

Glioblastomas are heterogeneous and have a poor prognosis. Glioblastoma cells interact with their neighbors to form a tumor-permissive and immunosuppressive microenvironment. Short noncoding RNAs are relevant mediators of the dynamic crosstalk among cancer, stromal, and immune cells in establishing the glioblastoma microenvironment. In addition to the ease of combinatorial strategies that are capable of multimodal modulation for both reversing immune suppression and enhancing antitumor immunity, their small size provides an opportunity to overcome the limitations of blood-brain-barrier (BBB) permeability. To enhance glioblastoma delivery, these RNAs have been conjugated with various molecules or packed within delivery vehicles for enhanced tissue-specific delivery and increased payload. Here, we focus on the role of RNA therapeutics by appraising which types of nucleotides are most effective in immune modulation, lead therapeutic candidates, and clarify how to optimize delivery of the therapeutic RNAs and their conjugates specifically to the glioblastoma microenvironment.

Keywords: noncoding RNAs, tumor microenvironment, microRNA, siRNA, aptamer, antisense oligonucleotide, glioblastoma

OPEN ACCESS

Edited by:
Payal Watchmaker, University of California, San Francisco, United States

Reviewed by:
Songguang Ju, Soochow University, China
Lisa Sevenich, Georg Speyer Haus, Germany

***Correspondence:**
Amy B. Heimberger
amy.heimberger@northwestern.edu

Specialty section:
This article was submitted to Cancer Immunity and Immunotherapy, a section of the journal Frontiers in Oncology

Received: *17 March 2021*
Accepted: *11 August 2021*
Published: *31 August 2021*

Citation:
Wei J, Gilboa E, Calin GA and Heimberger AB (2021) Immune Modulatory Short Noncoding RNAs Targeting the Glioblastoma Microenvironment. Front. Oncol. 11:682129. doi: 10.3389/fonc.2021.682129

INTRODUCTION

Glioblastoma cells would not survive without close connection and dependence on their adjacent molecular and cellular components. Multilevel and complicated communication between glioblastoma cells and nonmalignant cells promotes a permissive microenvironment for gliomagenesis. The glioblastoma microenvironment can be taken as a local niche comprising glioma cells, immune cells, parenchymal cells, and their associated molecular factors and subcellular vesicles. Microglia, a major type of parenchymal cells, contribute significantly to the brain tumor mass and immunosuppressive microenvironment. In addition, these cells can secrete a number of factors together with glioblastoma cells and nonneoplastic astrocytes that have an effect on glioblastoma progression.

Heterogenous molecular factors contribute to the complexity of the glioblastoma microenvironment and emphasize the importance of local niche influence to the tumor cells.

An important contributor to these molecular factors is short noncoding RNAs (ncRNAs) including small noncoding microRNAs (miRNAs) and small interfering RNAs (siRNAs) carried by extracellular vehicles (EVs). miRNAs account for a large portion of the human transcriptome in the glioblastoma cells and their surrounding cells, and these miRNAs regulate numerous hallmarks of glioblastoma such as proliferation, invasion, immune escape and resistance to treatment (1). The development of various RNA agents including siRNA, antisense oligonucleotides (ASO), and aptamers for specific gene targeting and knockdown offers enormous therapeutic potential (2). In this manuscript, we discuss the current state of knowledge of miRNA immune regulatory functions and the impact of immunomodulatory miRNAs on the glioblastoma microenvironment. Next, we will review possible use of miRNAs, their analogue siRNAs, and aptamers as antiglioblastoma therapeutics. Finally, we will discuss potential RNA nucleotide therapeutics targeting immunomodulatory pathways and survey effective strategies for delivery to the glioblastoma microenvironment.

MIRNAS IN THE GLIOBLASTOMA MICROENVIRONMENT

miRNA Roles in Glioblastoma Pathobiology

Our understanding of gene expression modulation evolved upon the discovery of the role of miRNA as an epigenetic regulator. miRNAs at 21–23 nucleotide long can suppress target gene expression by binding to the 3′ untranslated regions (UTRs) of mRNA with partial complementarity base-pairing (3). At present, around 2,500 human miRNAs have been identified that act in this capacity (4). miRNA and mRNA interactions can be complex: a mRNA can be modulated by multiple miRNAs and a miRNA can target many different mRNAs. Thus, it is not surprising that miRNAs play important roles in glioblastoma initiation and progression. miRNAs have been indicated as critical regulators of glioblastoma stem cell maintenance (5), epigenetic regulation (6), tumorigenesis (7), oncogenic pathways, and migration (8, 9). Furthermore, miRNA is involved in regulating radio- and chemotherapy resistance and sensitivity and may serve as biomarkers for diagnosis and outcome (10, 11).

Glioblastoma Cell-Associated miRNAs

Upregulated miRNAs in glioblastoma cells can act as oncogenes (oncomiRs) and silence onco-suppressor genes. A prototypical example and one of the first oncomiRs identified is miR-21 which is involved in malignant processes by targeting genes important for proliferation, cell survival, invasion, and treatment resistance (12). Other upregulated miRNAs such as the miR-17-92 cluster, miR-10b, and miR-15b have been investigated in preclinical studies and shown to be indispensable for tumor initiation. As such, oncomiR blockade in glioma cells could activate numerous tumor suppressor genes (13) and also restore immune surveillance of the glioblastoma (14, 15). Liu et al., for example, demonstrated that miR-340-5p suppression in glioblastoma cell enhanced M2 macrophage polarization and macrophage recruitment to the glioblastoma microenvironment (16), suggesting restoration of miR-340-5p could be a potential strategy to reverse immune suppression mediated by M2 macrophages.

In contrast, some miRNAs may function as tumor suppressors and could be therapeutically reconstituted. For instance, the miR-1, miR-7, miR-34a, miR-124, miR-128, miR-138, and miR-181 family are a group of suppressor miRNAs inhibiting glioblastoma progression when they are overexpressed (8, 17, 18). These miRNAs not only directly target oncogenic/tumor suppressor pathways in glioma cells but also exert broad regulatory effects on the immune system. Our group found that miR-124 inhibited multiple targets in the signal transducer and activator of transcription 3 (STAT3) signaling pathway and reversed immune dysfunction of T cells induced by glioblastoma stem cells (GSCs) (19). We also showed that miR-138 can target multiple immune checkpoint molecules such as CTLA-4 and programmed cell death protein 1 (PD-1) to inhibit tumor-infiltrating Tregs. *In vivo* administration of miR-138 suppressed tumor development and significantly prolonged survival time of immune-competent glioma-bearing mice, but not immune-deficient mice (20), indicating the pivotal role of miR-138 in immunological tumor surveillance.

One of the key mechanisms for intercellular communication in the tumor microenvironment are exosomes that contain a wide variety of miRNAs (12–16, 21). Exosomal miR-21 has been shown to be an important mediator of immune cell reprogramming by glioblastoma cells to create a niche favorable for cancer progression (14). miR-1246 has been identified as the most enriched miRNA in glioblastoma-derived exosomes and mediates glioblastoma-induced protumorigenic macrophage formation by targeting TERF2IP and subsequently activating the STAT3 pathway (22). miR-214-5p, another glioblastoma-derived exosomal miRNA, mediates proinflammatory responses by targeting CXCR5 in primary microglia upon lipopolysaccharide stimulation (23). Furthermore, exosomal miR-29a and miR-92a from glioblastoma cells promotes the proliferation and immunosuppressive phenotype of glioblastoma-infiltrating macrophages (GIMs) by targeting protein kinase cAMP-dependent type I regulatory subunit alpha and high-mobility group box transcription factor 1 (24). Given this is an emerging area of investigation, it is likely that almost every key pathway and mechanism elucidated for gliomagenesis will have a network of miRNA control.

Glioblastoma-Infiltrating Macrophages Associated miRNAs

Secondary to an immunosuppressive microenvironment, glioblastoma patients are deficient in antitumor immunity leading to malignant progression and resistance to treatment. GIMs, the most frequent infiltrating immune cell subset (25), originate from peripheral blood monocytes in response to tumor-derived chemokines. Upon entry into the glioblastoma, the macrophages adopt a M0/M2 phenotype with the capacity to promote tumor cell invasion and exert immune suppression through factors like tumor growth factor-β (TGFβ) (26, 27).

We have shown that miR-142-3p, by modulating the TGFβ signaling, inhibits the M2 phenotype of GIMs, and systemic *in vivo* administration of miR-142-3p induces antiglioma immune function (28). Ishii et al. reported that exogenous expression of miR-130a and miR-145 in myeloid-derived suppressor cells (MDSCs) decreased tumor metastasis through downregulation of TGFβ receptor II (TβRII) and related immune suppressive cytokines (29). Reciprocally, GIM-derived exosomal miR-22-3p, miR-27a-3p, and miR-221-3p can promote the proneural-to-mesenchymal transition of GSCs by simultaneously targeting CHD7 (30). miR-21 is also enriched in GIM-derived exosomes and mediates temozolomide (TMZ) resistance for which the STAT3 inhibitor pacritinib could overcome this resistance by downregulating miR-21 (31). Moreover, the downregulation of miR-21 promotes M1 macrophage polarization (32). As such, miR-21 deregulation is an operational mechanism in both GIMs and glioblastoma cells that modulates multiple oncogenic molecules, and signaling pathway such as STAT3 and anti-miR-21 strategies could be therapeutically developed.

Astrocyte-Associated miRNAs

In addition to the crosstalk between glioblastoma and immune cells, astrocytes also contribute to tumor growth, invasion, and immune suppression (33). For example, miR-19a is transferred from astrocytes to metastatic cancer cells in the central nervous system (CNS). Zhang et al. have demonstrated that exosomal transfer of miR-19a downregulates PTEN and subsequently promotes cytokine chemokine ligand 2 (CCL2) secretion. CCL2 recruits macrophages that contribute to immune resistance (34). Another astrocyte-associated miRNA, miR-10b, is overexpressed in gliomas and brain metastasis, and this miRNA can induce astrocyte transformation (13). Targeting astrocytes and their associated miRNAs is an emerging strategy for potentially treating CNS tumors.

Oligodendrocyte-Associated miRNAs

Oligodendrocytes have important protecting roles because they produce myelin for neuron protection. Being a major cell population in the glioblastoma microenvironment, oligodendrocytes interact with astrocytes and microglia and participate in the formation of a tumor permissive niche (35, 36). Oligodendrocyte progenitor cells (OPCs) are the largest proliferating population in the CNS, and together with GIMs, are enriched at the infiltrating edge (37). Several miRNAs such as miR-219, miR-129-2, and miR-338 have higher expression at the infiltrating edge and are involved in oligodendrocyte differentiation (38). Negative regulators of oligodendrocyte differentiation such as SOX6, HES5, PDGFRA, and ZFP238 are suppressed by these miRNAs (39). One of the important functions of miR-219 is to mediate OPC differentiation to oligodendrocytes (40). Additionally, miR-219 indirectly promotes receptor tyrosine kinase signaling activity by targeting and inhibiting epidermal growth factor receptor expression. Thus, the evidence points to the involvement of oligodendrocyte-associated miRNAs in the glioblastoma microenvironment and warrants further study to determine their exact targets mediating the crosstalk of the OPCs and tumor cells.

Endothelial Cell-Associated miRNAs

Glioblastoma is highly vascularized, and its invasion and outgrowth rely on a nutrient supply by acquiring new blood vessel formation (41). Endothelial cell proliferation from the tumor is a direct measure of its malignancy. GSC-associated exosomes are capable of inducing angiogenesis of endothelia cells mediated by miR-21 (42). Some endothelial cell-associated miRNAs such as miR-145-5p and miR-5096 can transfer between human microvascular endothelial cells (HMECs) and glioblastoma cells through gap junctions. In the process, miR-145-5p is downregulated in early gliomagenesis and acts as a tumor suppressor when passing from HMECs into glioma cells, whereas miR-5096 is transferred from glioma cells into HMECs and promotes angiogenesis (43). Finally, the miR-221/222 cluster has also been shown to enhance angiogenesis and silencing attenuates angiogenesis by inhibiting the JAK/STAT pathway (44). All these targetable miRNAs associated with the various cell lineages in the glioblastoma microenvironment are depicted in **Figure 1**.

SMALL INTERFERING RNAS AND ANTISENSE OLIGONUCLEOTIDES

In addition to the use of miRNAs, siRNA, which are 21–27 base pair double-stranded oligonucleotides, are another treatment modality for inhibiting protein synthesis at the posttranscriptional level. Although both miRNA and siRNA strategies are capable of BBB penetration, miRNA has the therapeutic advantage of target networks which would be beneficial in complex heterogenous cancers such as glioblastoma. However, miRNA off target effects remains a substantial concern. In contrast, siRNA approaches have much greater specificity that is counterbalanced by tumor plasticity and escape mechanisms.

Potential Candidates of Immune Modulatory siRNAs Targeting the Glioblastoma Microenvironment

Vascular Endothelial Growth Factor

Abnormal vasculature is enriched in glioblastoma as a consequence of upregulated angiogenic factors such as VEGF. Increased VEGF causes new blood vessels to form within the tumor *via* angiogenesis and the associated proliferation of endothelial cells (45). The resulting vascular networks display increased vessel permeability and enlarged vessel size that results in plasma leakage into the tumor tissue and disruption to the BBB. Together, these abnormalities induce inflammation, cerebral edema, and increased interstitial pressure. Thus, antiangiogenic VEGF treatments have been extensively investigated including monoclonal antibodies such as bevacizumab and small molecules targeting its receptor VEGFR (46). These agents have limitations based on short half-life, limited efficacy in patient overall survival

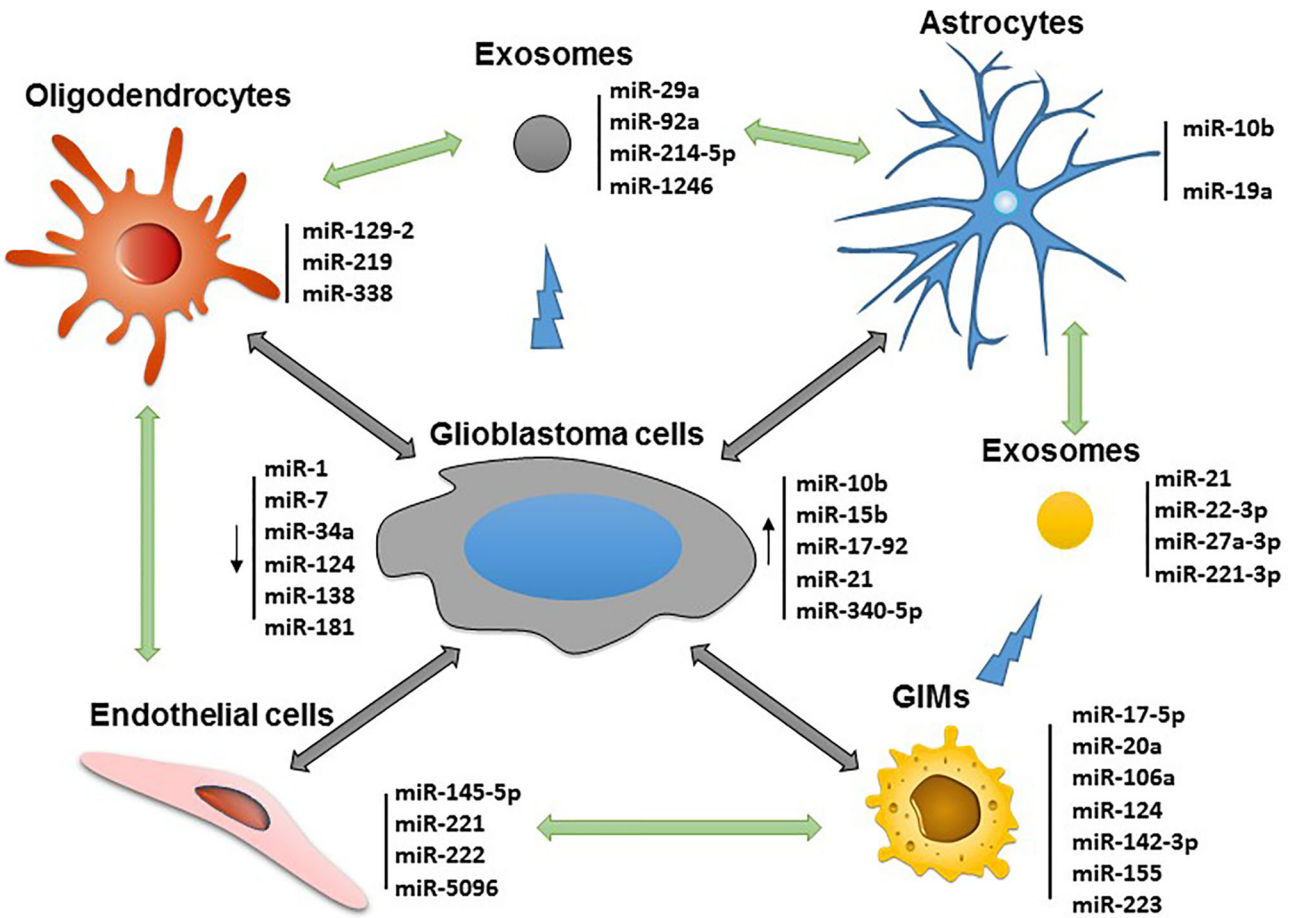

FIGURE 1 | Potential miRNAs that can be targeted for immune modulation and therapeutic application in the glioblastoma microenvironment.

improvement, and systemic toxicity. Some siRNA formulations targeting VEGF have been evaluated in early stage clinical trials, but this have not been advanced further (47, 48).

Programmed Cell Death Protein 1

T cells are present in the glioblastoma microenvironment, although at lower frequencies than GIMs (25). They have a profoundly exhausted phenotype characterized by expression of multiple immune checkpoint ligands (49, 50) likely accounting for their inability to control tumor growth. The lack of effective T-cell response is also highlighted by the ineffectiveness of checkpoint blockade immunotherapy in glioblastoma. Nonetheless, anti-PD-1 therapy achieves potent antiglioma activity in mouse glioma activity possibly through the depletion of PD-1+ macrophages and proinflammatory polarization in the glioblastoma microenvironment (51). A RNAi specific to the PD-1/PD-L1 pathway was delivered by a hemagglutinating virus of Japan-envelope—a nonreplicating viral vector that was capable of inhibiting immune suppression and eliciting antiglioma immune responses (52). Similarly, we showed that miR-138 could downregulate both CTLA-4 and PD-1 to inhibit tumor-infiltrating regulatory T cells (Tregs) and *in vivo* administration induced tumor reduction and prolonged the survival of immune syngeneic glioma-bearing mice (20).

Neuroligin 3

Neuronal activity is involved in glioblastoma growth and progression (53). In the normal brain microenvironment, neurons are strong mitogenic signalers stimulating the growth of neural and oligodendrocyte precursor cells—an important consideration in the role of stem/progenitor cells in glioblastoma (54). Elegant studies of neuronal activity conducted by Venkatesh et al. in xenograft glioma mouse models show that presynaptic and postsynaptic function is disrupted in the presence of glioma with microenvironmental neurolignin 3 (NLGN3) being hijacked to induce signaling through the PI3K/PTEN/AKT/mTOR pathway (55). Neurons and OPCs produce NLGN3 by cleavage of ADAM10 sheddase, so the inhibition of this enzyme blocks NLGN3 secretion into the tumor microenvironment and suppresses glioma outgrowth in preclinical models. Therefore, siRNAs targeting NLGN3/ADAM10 are promising for treating glioblastoma by modulating the interaction between neuronal cells and tumor cells (56).

Growth Differentiation Factor

Growth differentiation factor (GDF15) is highly expressed in glioblastoma as a secreted cytokine participate in regulating tumor cell proliferation and immunosuppression (57). GDF15 promotes GSC stemness by activating the leukemia inhibitor factor–STAT3 pathway (58). Thus, it represents a potential therapeutic target in glioblastoma treatment by siRNA targeting GDF15 or its cognate receptor GFRAL (the GDNF family receptor alpha like) (59).

O^6-Methylguanine-DNA Methyltransferase

Temozolomide (TMZ) is the standard-of-care for glioblastoma and the other brain tumors, but many patients show limited response due to unmethylated O^6-methylguanine-DNA methyltransferase (MGMT). Efforts to inhibit MGMT activity by systemic delivery of a siRNA have been made to silence the TMZ resistance gene MGMT. Wang et al. developed a MGMT siRNA nanoparticle that when combined with TMZ was found to reduce tumor growth and significantly extending survival in a GSC xenograft model relative to TMZ monotherapy (60). Like MGMT, other DNA damage response mediators such as ataxia-telangiectasia-mutated, ataxia-terlangiectasia-Rad3-related, DNA-dependent protein kinase, and poly-ADP-ribose polymerase could also be targeted with a siRNAs, which represent novel strategies for overcoming chemotherapy resistance (61–64).

c-MET

The immunosuppressive potency of the glioblastoma microenvironment may be a function of tumor invasiveness and epithelial-mesenchymal transition (EMT), in which c-MET plays a key role. c-MET was recently shown to mediate EMT *via* activation of Wnt/β-catenin signaling (65). MiR-128-3p targeting c-MET inhibited glioblastoma migration and invasion and enhanced TMZ therapeutic efficacy *in vivo* (66). Other miRNAs such as miR-34a, miR-144-3p, and miR-562 have been reported to exert activity against glioblastoma proliferation and invasion by also targeting c-MET (66–68). Hence, these therapeutic miRNAs and c-MET siRNAs could be used to treat glioblastoma by means of suppressing tumor invasion and EMT.

Chitinase-3-Like-1

GIM mediate immunosuppression is mediated by the chitinase-3-like-1 (CHI3L1)/Gal3-PI3K/ATK/mTOR axis. Chen et al. showed that inhibiting CHI3L1 complexes reversed GIM immunosuppression and delayed tumor progression (69). In other cancer models, genetic ablation of CHI3L1 *in vivo* reduced macrophage recruitment and increased effector T-cell infiltration in the tumor (70). Thus, siRNA targeting CHI3L1 is another potential therapy that could be beneficial to glioblastoma patients.

TGFβ

Overactivation of TGFβ signaling plays a critical role in reprogramming the glioblastoma to be immune suppressive and mediates immune escape and treatment resistance. In the glioblastoma microenvironment, a variety of dysfunctional cellular components and their interaction such as tumor, T, myeloid and NK cells are governed by the TGFβ signaling pathway. Consequently, the anti-TGFβ latency-associated peptide antibody can enhance antitumor immune responses in murine glioblastoma models (71); miR-142-3p targeting the TGFβR1 on M2 macrophages results in glioblastoma growth inhibition (28), and targeting the TGFβ-integrin axis improves NK cell antiglioblastoma activity (72). Anti-TGFβ RNA therapeutic represents a promising treatment avenue to be investigated in glioblastoma patients. A recent study showed that antisense oligonucleotides specifically targeting $TGF\beta_1$ and $TGF\beta_2$ exerts strong antiglioblastoma activity *in vitro* and *in vivo* (73).

S100A

S100A gene family members can modulate EMT, GSC stemness, and immune cell infiltration and are candidate therapeutic targets for glioblastoma patients (74). S100A4 is the most studied as a central player controlling EMT, stemness, and neutrophil infiltration. Its depletion downregulates the glioblastoma progression and treatment resistance (75, 76). Several microRNAs such as miR-124 (77), miR-149-3p (78), and miR-520c (79) have been identified as targeting S100A4, and their mimics resulted in antiglioblastoma activity *in vivo*. Therefore, these suppressor miRNAs and siRNAs targeting S100A4 could also be explored for therapeutic activity in glioblastoma patients.

TARGETING STRATEGIES

Antisense Oligonucleotides (ASOs)

Antisense oligonucleotides (ASOs) bind sequences specifically by Watson-Crick base pairing to the target RNA and regulate protein expression through RNase H mediated degradation and ribosome blockage by steric hindrance (80, 81). Significant advancement of oligonucleotide chemistry and numerous delivery platforms enhance ASO development and clinical application. Recently, the FDA has approved a few nucleic acid-based drugs, which stimulates greater interest in ASO therapeutic development. Currently, a variety of ASO drugs are being tested in clinical trials to treat cancer, infectious, and neurodegenerative diseases (82). Some ASO drugs target oncomiRs that promote tumorigenesis and metastasis. For example, RG-012, an anti-miR-21 ASO for Alport syndrome is being evaluated to ascertain if it decreases the rate of progression of renal fibrosis (83). Cobomarsen (MRG-106) is a miR-155 inhibitory ASO presently in phase II trials treating T cell leukemia and lymphoma (84). The anti-miR-21 and anti-miR-155 ASO strategy have been tested in preclinical models and showed potent anti-glioma efficacy (85, 86). Therefore, these anti–oncomiR ASOs can potentially be applied for the treatment of glioblastoma patients that have miR–21 and miR–155 dysregulation.

Aptamers

Aptamers are short oligonucleotides that possess a 3–D distinct structure for their target recognition and binding. Systematic

Evolution of Ligands by EXponential enrichment (SELEX) is the most used screening approach to identify specific aptamers binding a target with high affinity and selectivity. Their relatively small molecular weight (one–tenth that of monoclonal antibody) makes them more accessible to the glioblastoma microenvironment (87). In addition, aptamers are called chemical antibodies since they can be derived completely using chemical synthesis. Moreover, the low immunogenicity and long shelf life are advantageous features of aptamers for clinical application. Oligonucleotide aptamers are synthesized and assembled with cell–free automation enabling rapid and cost–effective production with minimal variation between batches. However, for clinical utility, they require further chemical modification for improving their *in vivo* half–life because of fast renal excretion and nuclease degradation. These modifications should have minimal effect on the affinity and specificity of the aptamers, and simultaneously improve their stability. Some promising modifications include inverted thymidine capping on the terminals, two hydroxyl group modifications in the ribose ring, the phosphodiester bond replacement and PEGylation (88). De La Fuente et al. identified several human and mouse specific RNA aptamers using tumor–associated myeloid cells as the targets *via* SELEX. These aptamers were specific to tumor–associated MDSCs in several cancer lineages including glioblastoma and had high binding affinity—highlighting their application as therapeutics targeting to the tumor microenvironment (89). Conjugating these MDSC–specific aptamers to a tumoricidal agent could significantly improve their potency.

Conjugates of Aptamer and siRNA

Nucleotide aptamers and siRNAs share the same nucleic acid units, so base pair annealing, or covalent linkage can create an aptamer–siRNA chimera. These chimeras have great advantages over protein and cellular products: single component simplicity, small size, and easy manufacturing (90, 91). They also have less immunogenicity because the human immune system does not recognize nucleic acids as foreign molecules (92). Additionally, the siRNA portion in the chimeras can still be recognized and processed by Dicer with no compromised efficacy, resulting in their target mRNA degradation and protein depletion (93). The first aptamer–siRNA chimera designated PSMA aptamer–Plk1 siRNA was constructed in 2006. Since then, a number of aptamer–siRNA chimeras have been made with improved stability, targetting specificity and *in vivo* efficacy (94). A list of the examples for targeted RNAi potentially applicable to the glioblastoma and its associated microenvironment are presented in **Table 1**.

Aptamer–siRNA Therapeutic Overcoming Resistance to Immune Checkpoint Blockade

In spite of significant successes of immune checkpoint blockade (ICB) in treating cancer patients, thus far, this immunotherapy approach has minimal efficacy for the vast majority of glioblastoma patients secondary to a wide variety of mechanisms such as mutations in the antigen presentation pathway and the IFN–γ signaling pathway (106). Protein tyrosine phosphatase (PTPN2) has been identified by *in vivo* CRISPR screening as a new target–mediating resistance to ICB immunotherapy. Knockdown of PTPN2 results in enhanced ICB therapeutic efficacy by promoting antigen presentation and IFN–γ signaling in tumor cells (107). PTPN2 is overexpressed in glioblastoma and its expression associates with IDH wild–type expression and the mesenchymal subtype that indicates a worse prognosis. Furthermore, there is an inverse relationship between PTPN2 and an inflammatory response in glioblastoma (108). Thus, we believe that a PTPN2 siRNA–tumor–specific aptamer

TABLE 1 | Summary of aptamer–siRNA chimeras potentially applicable to the glioblastoma.

Formulation	Aptamer target	Target gene	Outcome	Reference
Aptamer–siRNA chimera	CTLA4	STAT3	Apoptosis of tumor cells and suppression of T–cell lymphoma outgrowth in immunodeficient mice	Hermann (95)
Aptamer–siRNA chimera	EpCAM	PLK1	Inhibition of EpCAM+ breast cancer growth in xenograft models	Gilboa–Geffen (96)
Aptamer dimer–siRNA chimera	4–1BB	mTOR complex 1 (mTORC1)	Inhibition of mTORC1 signaling in CD8+ effector T cells to induce a T–cell memory response and protective immunity by 4–1BB aptamer dimer activation	Berezhnoy (97)
Aptamer–siRNA chimera	αvβ3 integrin	Elongation factor 2	Inhibition of cell proliferation and the induction of apoptosis specifically in multiple cancer lineages including glioblastoma	Hussain (98)
Aptamer dimer–siRNA	4–1BB	CD25, Axin–1	Anti–tumor activity mediated by enhanced CD8+ T cell memory response in multiple syngeneic mouse models	Rajagopalan (99)
Aptamer–siRNA chimera	Nucleolin	SLUG/NRP1	Suppression of tumor cell invasion, growth, and angiogenesis	Lai (100)
Dox–aptamer–siRNA chimera	EpCAM	Survivin	Prolonged survival in mice bearing chemoresistant breast tumor	Wang (101) and Subramanian (102)
Aptamer–siRNA chimera	PDGFRβ	STAT3	Inhibition of glioma cell growth and angiogenesis *in vivo* in a xenograft mouse model	Esposito (103)
Aptamer–siRNA chimera	PDGFRα	STAT3	Inhibition of glioma cell viability	Yoon (104)
Aptamer–siRNA chimera	EpCAM	PKC_I	Inhibition of PRKCI amplified ovarian cancer cell proliferation and xenograft model tumor growth	Rehmani (105)

therapeutic may provide an important strategy to overcome ICB resistance of glioblastoma patients.

Another target mediating ICB resistance is A–to–I editing of interferon–inducible RNA species (ADAR1) that encodes an adenosine deaminase that inhibits the sensing of endogenous double–stranded RNAs (dsRNAs), and subsequently hinders antitumor immunity. Thus, ADAR1 inhibition can improve patient responses when combined with PD–1 blockade by overcoming the resistance mechanism of nonresponding to endogenous dsRNAs (109). ADAR1 is found highly active in glioma tissues and cells and essential for the maintenance of gliomagenesis (110), so we propose that ADAR1 can be a potential target inhibited by tumor cell specific aptamer–ADAR1 siRNA conjugates.

Neoantigen Induction in Glioma Cells by Aptamer–siRNA

One of the major challenges in developing effective cancer immunotherapy is to identify tumor–specific and immunogenic neoantigens to stimulate a robust and durable immune response. There are several approaches to induce neoantigens in tumor cells *in situ* by aptamer–siRNAs specific to unique pathways that trigger the expression of neoantigens. The first pathway is nonsense–mediated messenger RNA decay (NMD), which is a highly conserved surveillance mechanism in mammal cells that prevents the translation of mRNAs with a premature stopping codon. NMD inhibition using tumor–specific oligonucleotide aptamer–targeted delivery of siRNAs to NMD–associated molecules such as SMG1 and UPF2 results in the expression of *de novo* antigens encoded by the premature stopping codon–containing mRNAs and their immune–mediated tumor rejection in metastatic and subcutaneous tumor models (111). This strategy is readily applicable to human glioblastoma as NMD pathway is important for gliomagenesis detection (112) and SMG1 mRNA expression is present in glioma cells (TCGA_GBM data). The second one is to target the transporter associated with antigen processing (TAP). Genetic ablation results in drastically enhanced presentation of new MHC class I–restricted epitopes independent of TAP. These induced new antigen epitopes form MHC–peptide complexes for engaging and activating CD8+ T cells capable of killing TAP–deficient tumor cells. Administration of TAP siRNAs conjugated to a tumor–targeting nucleolin aptamer (AS1411) has been shown to exert antitumor activity in multiple mouse tumor models (113). Both TAP and nucleolin are expressed in gliomas, making AS1411 and TAP siRNA conjugates an appealing candidate of the RNA–based immune therapy for treating glioblastoma patients with preclinical efforts underway by our group.

Aptamer–siRNA Targeting STAT3 Signaling in the Tumor Microenvironment

STAT3 has been shown to be a signaling hub in tumor cells as well as tumor–associated immune cells (114, 115). In the glioblastoma microenvironment, STAT3 is persistently activated in glioma cells, myeloid, and T cells and promotes tumor cell survival, proliferation, invasion, and immunosuppression (26, 116, 117). Due to CTLA4 upregulation on tumor–infiltrating CD8+ T cells, a CTLA4-targeting aptamer STAT3 siRNA chimera was created that triggers CD8+ T cell reactivation in the tumor microenvironment. Additionally, this chimera inhibits tumor–infiltrating Tregs and shows significant antitumor efficacy in multiple primary and metastatic tumor models (95). The Yu group has generated a DNA aptamer CpG1668–STAT3 siRNA chimera linked by a C3 carbon chain, which preserved the immunostimulatory properties of CpG1668 and at the same time does not interfere with Dicer processing of siRNA, thereby contributing to synergistic antitumor effects (118). Other aptamers have been tested including: (1) a STAT3 siRNA that successfully induces antitumor effects in glioblastoma when conjugated with a PDR3 aptamer against PDGFRα (104), and (2) a PDGFRβ–specific aptamer–siRNA chimera designated Gin4.T–STAT3 that could efficiently antagonize STAT3 in PDGFRβ+ GBM xenografts (103, 119).

Aptamer–siRNAs Targeting Highly Enriched Chemokines and Cytokines in the Glioblastoma Microenvironment

Two major cell components in the glioblastoma microenvironment responsible for tumor escape from immune surveillance include GSCs and GIMs (26, 116, 120). Osteopontin (OPN), a key molecule–mediating immune suppression in this setting, is highly expressed in both GSCs and GIMs. It is a secreted phosphoprotein chemokine that also operates intracellularly with both forms playing important roles in tumor growth and metastasis (121). Our data indicate that highly expressed OPN in the glioblastoma microenvironment is indispensable for macrophage infiltration. We have further shown that both tumor–derived OPN and nontumor–derived OPN are essential for glioblastoma development. A deficiency of OPN in either glioblastoma cells or immune cells results in a marked reduction in numbers of immune suppressive M2 macrophages and enhanced T–cell effector function (87). As such, OPN is an attractive therapeutic target specific to the glioblastoma microenvironment. Interestingly, periostin sharing the same RGD functional motif with OPN is secreted from GSCs and correlates with GIM infiltration in human glioblastoma. Periostin depletion diminishes the tumor supportive M2 type of GIMs in xenografts (122). CCL2, another chemokine highly enriched in the glioma microenvironment, is important for attracting both CCR2+Ly–6C+ monocytic MDSCs and CCR4+ Tregs. CD163+ GIMs are a major source producing CCL2 in the glioblastoma microenvironment (123). GIM–derived CCL8 contributes to the stemness maintenance and invasion of glioblastoma cells through ERK1/2 pathway and its blockade significantly decreases invasion of glioma cells (124). Boeck et al. have also shown that IL–33 is another important chemokine–mediating GIM infiltration since its expression correlates with GIM density in human and mouse glioma tissues. Furthermore, both intracellular and secreted isoforms of IL–33 upregulate other

chemokines that collectively recruit and transform peripheral innate immune cells to create an immunosuppressive environment (125). Bispecific aptamer siRNA conjugates to the aforementioned chemokines are plausible strategies and could be developed.

Bispecific Aptamers to Elicit Antitumor Immunity

Bispecific aptamers, composed of two aptamers, exhibit concurrent binding to two different entities such as antigens. Absence of costimulatory signal in the tumor microenvironment results T–cell energy (126). Accordingly, an aptamer specific to 4–1BB receptor has been developed to target and activate tumor–infiltrating T cells (127). Pastor et al. generated the first bispecific aptamers consisting of a bivalent 4–1BB aptamer and a tumor–specific PSMA aptamer, enhancing the conjugate delivery to the tumor niche and activation of costimulatory responses. Profound antitumor activity of a 4–1BB–PSMA aptamer chimera has been observed in multiple immune competent mouse models including colon cancer and melanoma lung metastasis when administered systemically (128). A similar strategy could be considered for glioblastoma but would require the selection of a subset of patients that express a given tumor antigen. Other bispecific aptamers have been engineered to specifically target CD28–expressing T cells in multidrug resistance–associated protein 1 melanoma that triggered prolonged survival of tumor–bearing mice. The associated immune mechanism included reactivation of tumor–infiltrating T cells *via* CD28 costimulation by CD28 aptamer binding and crosslinking (95). Schrand et al. synthesized another bivalent aptamer by fusing an agonistic 4–1BB aptamer with an aptamer specific to VEGF and showed effective targeting of the stroma in the tumor microenvironment. This 4–1BB–VEGF aptamer was capable of inducing the activation and expansion of CD8+ effector T cells and promoting T memory cell differentiation that prevented tumor recurrence across cancer lineages (129). Since VEGF expression is a common feature of glioblastoma, a strategy in which T cells are activated and expanded may induce glioma cell–specific killing (130), but this will require preclinical testing. A list of the examples for bispecific aptamers potentially applicable to the glioblastoma and its associated microenvironment is presented in **Table 2**.

RNA Nanocarrier Delivery Systems

Aptamer–siRNA chimeras and bispecific aptamers are one of the most efficient strategies for target delivery modules because of their high specificity and binding affinity, fully automated synthesis, and great potential for clinical application. Nonetheless, a major obstacle needs to be overcome for delivery of siRNAs into the cytoplasm of the targeted tumor and/or immune cells. One hurdle for the efficient delivery of aptamer–siRNA chimeras to the cytoplasm is the negative charge of nucleotides and endosomal degradation. A strategy that could overcome this limitation is to embed the cell–specific aptamers into siRNA encapsulating nanoparticles, which improve the delivery efficacy of naked siRNAs passing through the cellular barriers.

Natural Nanocarriers

Many cell types in the glioblastoma microenvironment interact with each other through microvesicles and exosomes (137). As a natural system of miRNA delivery, these vesicles can be secreted from genetically engineered miRNA overexpressing cells or generated from exosomes transfected with miRNAs (138, 139). Glioblastoma cells or stem cells, for example, could be genetically modified to express exogenous tumor suppressor miRNAs and the elaborated exosomes with the tumor–suppressor miRNA used as a therapeutic product. Proof–of–principal preclinical studies using this type of strategy have been shown to reduce the tumor burden and have potential clinical utility (140). Although there are other contents in the exosomes such as other RNA and protein molecules, this composition can be altered by the cell status and signaling stimuli (141). As such, these natural vesicles may be an excellent RNAi carrier system (142). Continuing efforts are warranted to improve capacity of these exosome nanocarriers

TABLE 2 | Summary of bispecific aptamers applicable to the glioblastoma treatment.

Formulation	Targeting aptamer	Effector aptamer	Outcome	Reference
Aptamer–aptamer	MRP1	CD28	Inhibition of tumor growth of melanoma–bearing mice	Soldevilla (126)
Aptamer dimer–aptamer	4–1BB	VEGF	Induction of potent antitumor immunity against multiple tumor types including glioma.	Schrand (129)
Aptamer–aptamer	EpCAM	CD44	Suppression of intraperitoneal ovarian cancer outgrowth much more significantly than single aptamers	Zheng (131)
Aptamer–aptamer	CD3	Liver cancer specific TLS11a	Effective inhibition of liver tumor growth and survival extension *via* binding hepatoma cells and T cells	Hu (132)
Aptamer dimer–aptamer	4–1BB	osteopontin	Increased median survival of glioma bearing mice with enhanced effector T cell infiltration	Wei (87)
Aptamer–siRNA chimera	Nucleolin	SLUG/NRP1	Synergistic inhibition of lung cancer cell invasion, tumor growth, and angiogenesis	Lai (100)
Aptamer dimer–aptamer dimer	CD16	Mucin 1	Recruitment of CD16+ immune cells to the MUC1+ tumor cells and enhancement of the immune cytotoxicity	Li (133) and Boltz (134)
Aptamer–aptamer	MRP1	ICOS	Strong antitumor immunity in combination with CTLA–4 blockade	Soldevilla (135)
Aptamer–aptamer	CD62L	PTK7	Linkage of T cells and tumor cells that induces tumor specific killing	Yang (130)
Aptamer–aptamer–gold nanocarrier	Nucleolin	c–MET	Enhanced anti–gastric and lung cancer efficacy	Lee (136)

for passing the BBB and efficient delivery of their siRNA cargo to the glioblastoma microenvironment.

Other types of natural modifications include conjugation to chitosan, a natural polysaccharide composed of repeating *N*–acetyl–glucosamine and glucosamine units. The cationic charge of chitosan can rapidly form complexes with negatively charged nucleic acids. Furthermore, highly reactive amino and hydroxyl groups of chitosan allow for chemical modification and linkage of cognate ligands (143). Noh et al. demonstrated that systemic administration of EGFL6 siRNA—chitosan nanoparticles were delivered to endothelial ovarian cancer cells and markedly inhibited tumor progression (144).

For effective glioblastoma therapy, nanoparticles that are delivered systemically must have tumor and/or immune specificity with little measurable side effects. More recently, RNA nanocarriers have gained attention as a versatile natural platform of nanoassembly and construction. The three–strand packaging RNA complex in the polyhedra bacteriophage phi29 is self–assembled and highly dynamic. This unique feature is utilized to generate a variety of RNA nanoparticles with a wide range of specific sizes and shapes. The pRNA–3WJ motif is a three–RNA–strand scaffold that is capable of targeting intracranial gliomas in mice (145).

Synthetic Nanocarriers

Lipid–formulated nanoparticles have intensively been utilized in laboratory studies and clinical trials for RNA therapeutics delivery because of the ease of manufacturing and high biocompatibility (146). Sun et al. developed a novel liposome system simultaneously delivering survivin siRNA and paclitaxel to the glioblastoma. Specifically, a CD133–specific RNA aptamer and a low–density lipoprotein receptor–related protein were integrated into the exterior membrane of the liposomes, resulting in dual targeting ability to bind glioblastoma cells and endothelial cells in the tumor microenvironment. This lipid nanoformulation could enrich in the tumor niche *via* efficiently binding to the low–density lipoprotein receptor expressing endothelial cells, and selectively induce apoptosis of CD133+ GSCs as well as endothelial stroma cells (147). Another similar liposome siRNA delivery carrier has been developed to treat breast cancer by means of CD44 aptamer targeting. These liposomes were found to efficiently inhibit CD44+ tumor outgrowth *in vivo* (148). CD44 is also found overexpressed in glioma cells and a common GSC surface marker (149). As such, an anti–CD44 aptamer–equipped siRNA liposome delivery system may be applicable to glioblastoma.

A critical determinant of successful delivery of RNA is the prevention of nuclease degradation. Polymeric nanocarriers have been extensively utilized for the protection of miRNAs and siRNAs due to their positive charge (150). Recently, cationic polymers were broadly used to form stable complexes with negatively charged RNA. Among them, polyethyleneimine is the most commonly used for nucleic acid delivery, but its clinical application is hampered by its inherent toxicity. One alternative approach is to use hybrid polymers such as PEI–chitosan hybrid nanocarriers that show an improved safety profile (151). Another strategy is to link polyethyleneimine polyplexes with brain–targeting rabies virus glycoprotein. These nanoparticles have shown both effective brain tumor targeting and low toxicity (152).

CONCLUSION AND FUTURE PERSPECTIVE

Despite enormous and continuous efforts for developing new and combinational treatment strategies for glioblastoma, there has been minimal improvement in survival. The brain tumor microenvironment is a key driver that promotes and regulates tumor initiation and progress and mediates the treatment resistance in both primary and metastatic brain malignancies. Molecular dissection into the protumorigenic functions of single elements of the brain tumor microenvironment has resulted in the discovery of a number of promising noncoding RNA therapeutic targets. These RNA therapeutics include miRNAs, siRNAs, and aptamers and are emerging as a novel avenue to treat brain cancer patients. Since miRNAs can act upon multiple targets and pathways regulating immune suppression and chemoresistance, they may be more effective in treating the malignancies such as glioblastoma that are highly heterogeneous. Nonetheless, one major challenge remains for clinical application for treating glioblastoma is the ability of an agent to cross the BBB. This issue is alleviated by their small molecular weight and compact size, which can be further enhanced with nanocarrier–specific targeted delivery. Increasingly sophisticated nanoparticle systems, also relying on targeting moieties for BBB penetration and/or improved target cell transfection efficacy, may provide an avenue toward clinical application. On the other hand, it should be noted that too complicated systems based on multiple components may prohibit drug approval and transition into the clinic.

The unique characteristics of aptamers make them highly attractive for targeted therapy of glioblastoma and the other malignancies. A given aptamer can be conjugated to another aptamer, siRNA or miRNA, which leads to the production of multimodal chimeric therapeutics with novel functions enabling simultaneous targeting of numerous molecules and cell subsets in the glioblastoma microenvironment. Their small size and simple structure may have key advantages superior for passing through the BBB and gaining access to the brain tumor when administered systemically.

AUTHOR CONTRIBUTIONS

JW provided ideas for the project and wrote the initial draft. ABH, GAC and EG completed the final version. All authors contributed to the article and approved the submitted version.

FUNDING

Funding was provided by the Ben and Catherine Ivy Foundation, the MD Anderson Cancer Center Provost Fund and NIH grant CA120813.

REFERENCES

1. Jethwa K, Wei J, McEnery K, Heimberger AB. miRNA–Mediated Immune Regulation and Immunotherapeutic Potential in Glioblastoma. *Clin Invest* (2011) 1:1637–50. doi: 10.4155/cli.11.159
2. Pastor F, Berraondo P, Etxeberria I, Frederick J, Sahin U, Gilboa E, et al. An RNA Toolbox for Cancer Immunotherapy. Nature reviews. *Drug Discov* (2018) 17:751–67. doi: 10.1038/nrd.2018.132
3. Rupaimoole R, Calin GA, Lopez–Berestein G, Sood AK. miRNA Deregulation in Cancer Cells and the Tumor Microenvironment. *Cancer Discovery* (2016) 6:235–46. doi: 10.1158/2159-8290.CD-15-0893
4. Acunzo M, Romano G, Wernicke D, Croce CM. MicroRNA and Cancer–a Brief Overview. *Adv Biol Regul* (2015) 57:1–9. doi: 10.1016/j.jbior.2014.09.013
5. Katsushima K, Kondo Y. Non–Coding RNAs as Epigenetic Regulator of Glioma Stem–Like Cell Differentiation. *Front Genet* (2014) 5:14. doi: 10.3389/fgene.2014.00014
6. Kreth S, Thon N, Kreth FW. Epigenetics in Human Gliomas. *Cancer Lett* (2014) 342:185–92. doi: 10.1016/j.canlet.2012.04.008
7. Nikaki A, Piperi C, Papavassiliou AG. Role of microRNAs in Gliomagenesis: Targeting miRNAs in Glioblastoma Multiforme Therapy. *Expert Opin Invest Drugs* (2012) 21:1475–88. doi: 10.1517/13543784.2012.710199
8. Bronisz A, Wang Y, Nowicki MO, Peruzzi P, Ansari K, Ogawa D, et al. Extracellular Vesicles Modulate the Glioblastoma Microenvironment *via* a Tumor Suppression Signaling Network Directed by miR–1. *Cancer Res* (2014) 74:738–50. doi: 10.1158/0008-5472.CAN-13-2650
9. Godlewski J, Bronisz A, Nowicki MO, Chiocca EA, Lawler S. microRNA–451: A Conditional Switch Controlling Glioma Cell Proliferation and Migration. *Cell Cycle (Georgetown Tex)* (2010) 9:2742–8. doi: 10.4161/cc.9.14.12248
10. Hermansen SK, Kristensen BW. MicroRNA Biomarkers in Glioblastoma. *J Neuro–Oncol* (2013) 114:13–23. doi: 10.1007/s11060-013-1155-x
11. Anfossi S, Babayan A, Pantel K, Calin GA. Clinical Utility of Circulating non–Coding RNAs – an Update. Nature Reviews. *Clin Oncol* (2018) 15:541–63. doi: 10.1038/s41571-018-0035-x
12. Møller HG, Rasmussen AP, Andersen HH, Johnsen KB, Henriksen M, Duroux M. A Systematic Review of microRNA in Glioblastoma Multiforme: Micro–Modulators in the Mesenchymal Mode of Migration and Invasion. *Mol Neurobiol* (2013) 47:131–44. doi: 10.1007/s12035-012-8349-7
13. El Fatimy R, Subramanian S, Uhlmann EJ, Krichevsky AM. Genome Editing Reveals Glioblastoma Addiction to MicroRNA–10b. *Mol Ther* (2017) 25:368–78. doi: 10.1016/j.ymthe.2016.11.004
14. Abels ER, Maas SLN, Nieland L, Wei Z, Cheah PS, Tai E, et al. Glioblastoma–Associated Microglia Reprogramming Is Mediated by Functional Transfer of Extracellular miR–21. *Cell Rep* (2019) 28:3105–19.e7. doi: 10.1016/j.celrep.2019.08.036
15. Guo X, Qiu W, Liu Q, Qian M, Wang S, Zhang Z, et al. Immunosuppressive Effects of Hypoxia–Induced Glioma Exosomes Through Myeloid–Derived Suppressor Cells *via* the miR–10a/Rora and miR–21/Pten Pathways. *Oncogene* (2018) 37:4239–59. doi: 10.1038/s41388-018-0261-9
16. Liu Y, Li X, Zhang Y, Wang H, Rong X, Peng J, et al. An miR–340–5p–Macrophage Feedback Loop Modulates the Progression and Tumor Microenvironment of Glioblastoma Multiforme. *Oncogene* (2019) 38:7399–415. doi: 10.1038/s41388-019-0952-x
17. Yang L, Ma Y, Xin Y, Han R, Li R, Hao X. Role of the microRNA 181 Family in Glioma Development. *Mol Med Rep* (2018) 17:322–9. doi: 10.3892/mmr.2017.7895
18. Banelli B, Forlani A, Allemanni G, Morabito A, Pistillo MP, Romani M. MicroRNA in Glioblastoma: An Overview. *Int J Genomics* (2017) 2017:7639084. doi: 10.1155/2017/7639084
19. Wei J, Wang F, Kong LY, Xu S, Doucette T, Ferguson SD, et al. miR–124 Inhibits STAT3 Signaling to Enhance T Cell–Mediated Immune Clearance of Glioma. *Cancer Res* (2013) 73:3913–26. doi: 10.1158/0008-5472.CAN-12-4318
20. Wei J, Nduom EK, Kong LY, Hashimoto Y, Xu S, Gabrusiewicz K, et al. MiR–138 Exerts Anti–Glioma Efficacy by Targeting Immune Checkpoints. *Neuro–oncology* (2016) 18:639–48. doi: 10.1093/neuonc/nov292
21. Anfossi S, Fu X, Nagvekar R, Calin GA. MicroRNAs, Regulatory Messengers Inside and Outside Cancer Cells. *Adv Exp Med Biol* (2018) 1056:87–108. doi: 10.1007/978-3-319-74470-4_6
22. Qian M, Wang S, Guo X, Wang J, Zhang Z, Qiu W, et al. Hypoxic Glioma–Derived Exosomes Deliver microRNA–1246 to Induce M2 Macrophage Polarization by Targeting TERF2IP *via* the STAT3 and NF–κb Pathways. *Oncogene* (2020) 39:428–42. doi: 10.1038/s41388-019-0996-y
23. Yang JK, Liu HJ, Wang Y, Li C, Yang JP, Yang L, et al. Exosomal miR–214–5p Released From Glioblastoma Cells Modulates Inflammatory Response of Microglia After Lipopolysaccharide Stimulation Through Targeting Cxcr5. *CNS Neurol Disord Drug Targets* (2019) 18:78–87. doi: 10.2174/1871527317666181105112009
24. Guo X, Qiu W, Wang J, Liu Q, Qian M, Wang S, et al. Glioma Exosomes Mediate the Expansion and Function of Myeloid–Derived Suppressor Cells Through microRNA–29a/Hbp1 and microRNA–92a/Prkar1a Pathways. *Int J Cancer* (2019) 144:3111–26. doi: 10.1002/ijc.32052
25. Hussain SF, Yang D, Suki D, Aldape K, Grimm E, Heimberger AB. The Role of Human Glioma–Infiltrating Microglia/Macrophages in Mediating Antitumor Immune Responses. *Neuro–Oncology* (2006) 8:261–79. doi: 10.1215/15228517-2006-008
26. Wu A, Wei J, Kong LY, Wang Y, Priebe W, Qiao W, et al. Glioma Cancer Stem Cells Induce Immunosuppressive Macrophages/Microglia. *Neuro–Oncology* (2010) 12:1113–25. doi: 10.1093/neuonc/noq082
27. Gabrusiewicz K, Rodriguez B, Wei J, Hashimoto Y, Healy LM, Maiti SN, et al. Glioblastoma–Infiltrated Innate Immune Cells Resemble M0 Macrophage Phenotype. *JCI Insight* (2016) 1(2):e85841. doi: 10.1172/jci.insight.85841
28. Xu S, Wei J, Wang F, Kong LY, Ling XY, Nduom E, et al. Effect of miR––3p on the M2 Macrophage and Therapeutic Efficacy Against Murine Glioblastoma. *J Natl Cancer Inst* (2014) 106:dju162. doi: 10.1093/jnci/dju162
29. Ishii H, Vodnala SK, Achyut BR, So JY, Hollander MC, Greten TF, et al. miR–130a and miR–145 Reprogram Gr–1(+)CD11b(+) Myeloid Cells and Inhibit Tumor Metastasis Through Improved Host Immunity. *Nat Commun* (2018) 9:2611. doi: 10.1038/s41467-018-05023-9
30. Zhang Z, Xu J, Chen Z, Wang H, Xue H, Yang C, et al. Transfer of MicroRNA *via* Macrophage–Derived Extracellular Vesicles Promotes Proneural–To–Mesenchymal Transition in Glioma Stem Cells. *Cancer Immunol Res* (2020) 8:966–81. doi: 10.1158/2326-6066.CIR-19-0759
31. Chuang HY, Su YK, Liu HW, Chen CH, Chiu SC, Cho DY, et al. Preclinical Evidence of STAT3 Inhibitor Pacritinib Overcoming Temozolomide Resistance *via* Downregulating miR––Enriched Exosomes From M2 Glioblastoma–Associated Macrophages. *J Clin Med* (2019) 8:959. doi: 10.20944/preprints201905.0374.v1
32. Xi J, Huang Q, Wang L, Ma X, Deng Q, Kumar M, et al. miR–21 Depletion in Macrophages Promotes Tumoricidal Polarization and Enhances PD–1 Immunotherapy. *Oncogene* (2018) 37:3151–65. doi: 10.1038/s41388-018-0178-3
33. Brandao M, Simon T, Critchley G, Giamas G. Astrocytes, the Rising Stars of the Glioblastoma Microenvironment. *Glia* (2019) 67:779–90. doi: 10.1002/glia.23520
34. Zhang L, Zhang S, Yao J, Lowery FJ, Zhang Q, Huang WC, et al. Microenvironment–Induced PTEN Loss by Exosomal microRNA Primes Brain Metastasis Outgrowth. *Nature* (2015) 527:100–4. doi: 10.1038/nature15376
35. Peferoen L, Kipp M, van der Valk P, van Noort JM, Amor S. Oligodendrocyte–Microglia Cross–Talk in the Central Nervous System. *Immunology* (2014) 141:302–13. doi: 10.1111/imm.12163
36. Hide T, Shibahara I, Kumabe T. Novel Concept of the Border Niche: Glioblastoma Cells Use Oligodendrocytes Progenitor Cells (GAOs) and Microglia to Acquire Stem Cell–Like Features. *Brain Tumor Pathol* (2019) 36:63–73. doi: 10.1007/s10014-019-00341-2
37. Hide T, Komohara Y, Miyasato Y, Nakamura H, Makino K, Takeya M, et al. Oligodendrocyte Progenitor Cells and Macrophages/Microglia Produce Glioma Stem Cell Niches at the Tumor Border. *EBioMedicine* (2018) 30:94–104. doi: 10.1016/j.ebiom.2018.02.024
38. Hide T, Komohara Y. Oligodendrocyte Progenitor Cells in the Tumor Microenvironment. *Adv Exp Med Biol* (2020) 1234:107–22. doi: 10.1007/978-3-030-37184-5_8
39. Zhao X, He X, Han X, Yu Y, Ye F, Chen Y, et al. MicroRNA–Mediated Control of Oligodendrocyte Differentiation. *Neuron* (2010) 65:612–26. doi: 10.1016/j.neuron.2010.02.018
40. Galloway DA, Moore CS. miRNAs As Emerging Regulators of Oligodendrocyte Development and Differentiation. *Front Cell Dev Biol* (2016) 4:59. doi: 10.3389/fcell.2016.00059
41. Dubois LG, Campanati L, Righy C, D'Andrea–Meira I, Spohr TC, Porto–Carreiro I, et al. Gliomas and the Vascular Fragility of the Blood Brain Barrier. *Front Cell Neurosci* (2014) 8:418. doi: 10.3389/fncel.2014.00418

42. Sun X, Ma X, Wang J, Zhao Y, Wang Y, Bihl JC, et al. Glioma Stem Cells–Derived Exosomes Promote the Angiogenic Ability of Endothelial Cells Through miR–21/VEGF Signal. *Oncotarget* (2017) 8:36137–48. doi: 10.18632/oncotarget.16661
43. Lu Y, Chopp M, Zheng X, Katakowski M, Buller B, Jiang F. MiR–145 Reduces ADAM17 Expression and Inhibits *In Vitro* Migration and Invasion of Glioma Cells. *Oncol Rep* (2013) 29:67–72. doi: 10.3892/or.2012.2084
44. Xu CH, Liu Y, Xiao LM, Chen LK, Zheng SY, Zeng EM, et al. Silencing microRNA–221/222 Cluster Suppresses Glioblastoma Angiogenesis by Suppressor of Cytokine Signaling––Dependent JAK/STAT Pathway. *J Cell Physiol* (2019) 234:22272–84. doi: 10.1002/jcp.28794
45. Weathers SP, de Groot J. VEGF Manipulation in Glioblastoma. *Oncol (Williston Park NY)* (2015) 29:720–7.
46. Kochar AS, Madhavan M, Manjila S, Scoco A, Belle VK, Geertman RT. Contemporary Updates on Clinical Trials of Antiangiogenic Agents in the Treatment of Glioblastoma Multiforme. *Asian J Neurosurg* (2018) 13:546–54. doi: 10.4103/ajns.AJNS_266_16
47. Tabernero J, Shapiro GI, LoRusso PM, Cervantes A, Schwartz GK, Weiss GJ, et al. 3rd, First–In–Humans Trial of an RNA Interference Therapeutic Targeting VEGF and KSP in Cancer Patients With Liver Involvement. *Cancer Discovery* (2013) 3:406–17. doi: 10.1158/2159-8290.CD-12-0429
48. Kaiser PK, Symons RC, Shah SM, Quinlan EJ, Tabandeh H, Do DV, et al. RNAi–Based Treatment for Neovascular Age–Related Macular Degeneration by Sirna–027. *Am J Ophthalmol* (2010) 150:33–39.e2. doi: 10.1016/j.ajo.2010.02.006
49. Ott M, Tomaszowski KH, Marisetty A, Kong LY, Wei J, Duna M, et al. Profiling of Patients With Glioma Reveals the Dominant Immunosuppressive Axis Is Refractory to Immune Function Restoration. *JCI Insight* (2020) 5(17):e134386. doi: 10.1172/jci.insight.134386
50. Woroniecka K, Chongsathidkiet P, Rhodin K, Kemeny H, Dechant C, Farber SH, et al. T–Cell Exhaustion Signatures Vary With Tumor Type and Are Severe in Glioblastoma. *Clin Cancer Res* (2018) 24:4175–86. doi: 10.1158/1078-0432.CCR-17-1846
51. Rao G, Latha K, Ott M, Sabbagh A, Marisetty A, Ling X, et al. Anti–PD–1 Induces M1 Polarization in the Glioma Microenvironment and Exerts Therapeutic Efficacy in the Absence of CD8 Cytotoxic T Cells. *Clin Cancer Res* (2020) 26:4699–712. doi: 10.1158/1078-0432.CCR-19-4110
52. Sugii N, Matsuda M, Okumura G, Shibuya A, Ishikawa E, Kaneda Y, et al. Hemagglutinating Virus of Japan–Envelope Containing Programmed Cell Death–Ligand 1 siRNA Inhibits Immunosuppressive Activities and Elicits Antitumor Immune Responses in Glioma. *Cancer Sci* (2020) 112:81–90. doi: 10.1111/cas.14721
53. Venkatesh HS, Johung TB, Caretti V, Noll A, Tang Y, Nagaraja S, et al. Neuronal Activity Promotes Glioma Growth Through Neuroligin–3 Secretion. *Cell* (2015) 161:803–16. doi: 10.1016/j.cell.2015.04.012
54. Lan X, Jörg DJ, Cavalli FMG, Richards LM, Nguyen LV, Vanner RJ, et al. Fate Mapping of Human Glioblastoma Reveals an Invariant Stem Cell Hierarchy. *Nature* (2017) 549:227–32. doi: 10.1038/nature23666
55. Venkatesh HS, Tam LT, Woo PJ, Lennon J, Nagaraja S, Gillespie SM, et al. Targeting Neuronal Activity–Regulated Neuroligin–3 Dependency in High–Grade Glioma. *Nature* (2017) 549:533–7. doi: 10.1038/nature24014
56. Kohutek ZA, diPierro CG, Redpath GT, Hussaini IM. ADAM––Mediated N–Cadherin Cleavage Is Protein Kinase C–Alpha Dependent and Promotes Glioblastoma Cell Migration. *J Neurosci* (2009) 29:4605–15. doi: 10.1523/JNEUROSCI.5126-08.2009
57. Roth P, Junker M, Tritschler I, Mittelbronn M, Dombrowski Y, Breit SN, et al. GDF–15 Contributes to Proliferation and Immune Escape of Malignant Gliomas. *Clin Cancer Res* (2010) 16:3851–9. doi: 10.1158/1078-0432.CCR-10-0705
58. Zhu S, Yang N, Guan Y, Wang X, Zang G, Lv X, et al. GDF15 Promotes Glioma Stem Cell–Like Phenotype *via* Regulation of ERK1/2–C–Fos–LIF Signaling. *Cell Death Discov* (2021) 7:3. doi: 10.1038/s41420-020-00395-8
59. Suriben R, Chen M, Higbee J, Oeffinger J, Ventura R, Li B, et al. Antibody–Mediated Inhibition of GDF15–GFRAL Activity Reverses Cancer Cachexia in Mice. *Nat Med* (2020) 26:1264–70. doi: 10.1038/s41591-020-0945-x
60. Wang K, Kievit FM, Chiarelli PA, Stephen ZR, Lin G, Silber JR, et al. siRNA Nanoparticle Suppresses Drug–Resistant Gene and Prolongs Survival in an Orthotopic Glioblastoma Xenograft Mouse Model. *Adv Funct Mater* (2021) 31. doi: 10.1002/adfm.202007166
61. Karlin J, Allen J, Ahmad SF, Hughes G, Sheridan V, Odedra R, et al. Orally Bioavailable and Blood–Brain Barrier–Penetrating ATM Inhibitor (AZ32) Radiosensitizes Intracranial Gliomas in Mice. *Mol Cancer Ther* (2018) 17:1637–47. doi: 10.1158/1535-7163.MCT-17-0975
62. Wengner AM, Siemeister G, Lücking U, Lefranc J, Wortmann L, Lienau P, et al. The Novel ATR Inhibitor BAY 1895344 Is Efficacious as Monotherapy and Combined With DNA Damage–Inducing or Repair–Compromising Therapies in Preclinical Cancer Models. *Mol Cancer Ther* (2020) 19:26–38. doi: 10.1158/1535-7163.MCT-19-0019
63. Mohiuddin IS, Kang MH. DNA–PK as an Emerging Therapeutic Target in Cancer. *Front Oncol* (2019) 9:635. doi: 10.3389/fonc.2019.00635
64. Higuchi F, Nagashima H, Ning J, Koerner MVA, Wakimoto H, Cahill DP. Restoration of Temozolomide Sensitivity by PARP Inhibitors in Mismatch Repair Deficient Glioblastoma is Independent of Base Excision Repair. *Clin Cancer Res* (2020) 26:1690–9. doi: 10.1158/1078-0432.CCR-19-2000
65. Huang M, Zhang D, Wu JY, Xing K, Yeo E, Li C, et al. Wnt–Mediated Endothelial Transformation Into Mesenchymal Stem Cell–Like Cells Induces Chemoresistance in Glioblastoma. *Sci Transl Med* (2020) 12: eaay7522. doi: 10.1126/scitranslmed.aay7522
66. Zhao C, Guo R, Guan F, Ma S, Li M, Wu J, et al. MicroRNA––3p Enhances the Chemosensitivity of Temozolomide in Glioblastoma by Targeting C–Met and EMT. *Sci Rep* (2020) 10:9471. doi: 10.1038/s41598-020-65331-3
67. Lan F, Yu H, Hu M, Xia T, Yue X. miR––3p Exerts Anti–Tumor Effects in Glioblastoma by Targeting C–Met. *J Neurochem* (2015) 135:274–86. doi: 10.1111/jnc.13272
68. Nie X, Su Z, Yan R, Yan A, Qiu S, Zhou Y. MicroRNA–562 Negatively Regulated C–MET/AKT Pathway in the Growth of Glioblastoma Cells. *OncoTargets Ther* (2019) 12:41–9. doi: 10.2147/OTT.S186701
69. Chen A, Jiang Y, Li Z, Wu L, Santiago U, Zou H, et al. Chitinase––Like–1 Protein Complexes Modulate Macrophage–Mediated Immune Suppression in Glioblastoma. *J Clin Invest* (2021) 131:e147552. doi: 10.1172/JCI147552
70. Cohen N, Shani O, Raz Y, Sharon Y, Hoffman D, Abramovitz L, et al. Fibroblasts Drive an Immunosuppressive and Growth–Promoting Microenvironment in Breast Cancer *via* Secretion of Chitinase 3–Like 1. *Oncogene* (2017) 36:4457–68. doi: 10.1038/onc.2017.65
71. Gabriely G, da Cunha AP, Rezende RM, Kenyon B, Madi A, Vandeventer T, et al. Targeting Latency–Associated Peptide Promotes Antitumor Immunity. *Sci Immunol* (2017) 2:eaaj1738. doi: 10.1126/sciimmunol.aaj1738
72. Shaim H, Shanley M, Basar R, Daher M, Gumin J, Zamler DB, et al. Targeting the αv Integrin/TGF–β Axis Improves Natural Killer Cell Function Against Glioblastoma Stem Cells. *J Clin Invest* (2021) 131:e142116. doi: 10.1172/JCI142116
73. Papachristodoulou A, Silginer M, Weller M, Schneider H, Hasenbach K, Janicot M, et al. Therapeutic Targeting of Tgfβ Ligands in Glioblastoma Using Novel Antisense Oligonucleotides Reduces the Growth of Experimental Gliomas. *Clin Cancer Res* (2019) 25:7189–201. doi: 10.1158/1078-0432.CCR-17-3024
74. Zhang Y, Yang X, Zhu XL, Bai H, Wang ZZ, Zhang JJ, et al. S100A Gene Family: Immune–Related Prognostic Biomarkers and Therapeutic Targets for Low–Grade Glioma. *Aging* (2021) 13:15459–78. doi: 10.18632/aging.203103
75. Chow KH, Park HJ, George J, Yamamoto K, Gallup AD, Graber JH, et al. S100A4 Is a Biomarker and Regulator of Glioma Stem Cells That Is Critical for Mesenchymal Transition in Glioblastoma. *Cancer Res* (2017) 77:5360–73. doi: 10.1158/0008-5472.CAN-17-1294
76. Liang J, Piao Y, Holmes L, Fuller GN, Henry V, Tiao N, et al. Neutrophils Promote the Malignant Glioma Phenotype Through S100A4. *Clin Cancer Res* (2014) 20:187–98. doi: 10.1158/1078-0432.CCR-13-1279
77. Choe N, Kwon DH, Shin S, Kim YS, Kim YK, Kim J, et al. The microRNA miR–124 Inhibits Vascular Smooth Muscle Cell Proliferation by Targeting S100 Calcium–Binding Protein A4 (S100a4). *FEBS Lett* (2017) 591:1041–52. doi: 10.1002/1873-3468.12606
78. Yang D, Du G, Xu A, Xi X, Li D. Expression of miR––3p Inhibits Proliferation, Migration, and Invasion of Bladder Cancer by Targeting S100A4. *Am J Cancer Res* (2017) 7:2209–19.
79. Mudduluru G, Ilm K, Fuchs S, Stein U. Epigenetic Silencing of miR–520c Leads to Induced S100A4 Expression and its Mediated Colorectal Cancer Progression. *Oncotarget* (2017) 8:21081–94. doi: 10.18632/oncotarget.15499
80. Ward AJ, Norrbom M, Chun S, Bennett CF, Rigo F. Nonsense–Mediated Decay as a Terminating Mechanism for Antisense Oligonucleotides. *Nucleic Acids Res* (2014) 42:5871–9. doi: 10.1093/nar/gku184

81. Rinaldi C, Wood MJA. Antisense Oligonucleotides: The Next Frontier for Treatment of Neurological Disorders. Nature Reviews. *Neurology* (2018) 14:9–21. doi: 10.1172/JCI142116
82. Dhuri K, Bechtold C, Quijano E, Pham H, Gupta A, Vikram A, et al. Antisense Oligonucleotides: An Emerging Area in Drug Discovery and Development. *J Clin Med* (2020) 9:2004. doi: 10.3390/jcm9062004
83. Shah MY, Ferrajoli A, Sood AK, Lopez–Berestein G, Calin GA. microRNA Therapeutics in Cancer – An Emerging Concept. *EBioMedicine* (2016) 12:34–42. doi: 10.1016/j.ebiom.2016.09.017
84. Seto AG, Beatty X, Lynch JM, Hermreck M, Tetzlaff M, Duvic M, et al. Cobomarsen, an Oligonucleotide Inhibitor of miR–155, Co–Ordinately Regulates Multiple Survival Pathways to Reduce Cellular Proliferation and Survival in Cutaneous T–Cell Lymphoma. *Br J Haematol* (2018) 183:428–44. doi: 10.1111/bjh.15547
85. Oh B, Song H, Lee D, Oh J, Kim G, Ihm SH, et al. Anti–Cancer Effect of R3V6 Peptide–Mediated Delivery of an anti–microRNA–21 Antisense–Oligodeoxynucleotide in a Glioblastoma Animal Model. *J Drug Target* (2017) 25:132–9. doi: 10.1080/1061186X.2016.1207648
86. Milani R, Brognara E, Fabbri E, Manicardi A, Corradini R, Finotti A, et al. Targeting Mir–155–5p and Mir–221–3p by Peptide Nucleic Acids Induces Caspase–3 Activation and Apoptosis in Temozolomide–Resistant T98G Glioma Cells. *Int J Oncol* (2019) 55:59–68. doi: 10.3892/ijo.2019.4810
87. Wei J, Marisetty A, Schrand B, Gabrusiewicz K, Hashimoto Y, Ott M, et al. Osteopontin Mediates Glioblastoma–Associated Macrophage Infiltration and is a Potential Therapeutic Target. *J Clin Invest* (2019) 129:137–49. doi: 10.1172/JCI121266
88. Ni S, Yao H, Wang L, Lu J, Jiang F, Lu A, et al. Chemical Modifications of Nucleic Acid Aptamers for Therapeutic Purposes. *Int J Mol Sci* (2017) 18:1683. doi: 10.3390/ijms18081683
89. De La Fuente A, Zilio S, Caroli J, Van Simaeys D, Mazza EMC, Ince TA, et al. Aptamers Against Mouse and Human Tumor–Infiltrating Myeloid Cells as Reagents for Targeted Chemotherapy. *Sci Transl Med* (2020) 12:eaav9760. doi: 10.1126/scitranslmed.aav9760
90. Cerchia L, de Franciscis V. Targeting Cancer Cells With Nucleic Acid Aptamers. *Trends Biotechnol* (2010) 28:517–25. doi: 10.1016/j.tibtech.2010.07.005
91. Zhou J, Rossi J. Aptamers as Targeted Therapeutics: Current Potential and Challenges. Nature reviews. *Drug Discov* (2017) 16:181–202. doi: 10.1038/nrd.2016.199
92. Song KM, Lee S, Ban C. Aptamers and Their Biological Applications. *Sensors (Basel Switzerland)* (2012) 12:612–31. doi: 10.3390/s120100612
93. McNamara JO2nd, Andrechek ER, Wang Y, Viles KD, Rempel RE, Gilboa E, et al. Cell Type–Specific Delivery of siRNAs With aptamer–siRNA Chimeras. *Nat Biotechnol* (2006) 24:1005–15. doi: 10.1038/nbt1223
94. Kruspe S, Giangrande PH. Aptamer–siRNA Chimeras: Discovery, Progress, and Future Prospects. *Biomedicines* (2017) 5:45. doi: 10.3390/biomedicines5030045
95. Herrmann A, Priceman SJ, Swiderski P, Kujawski M, Xin H, Cherryholmes GA, et al. CTLA4 Aptamer Delivers STAT3 siRNA to Tumor–Associated and Malignant T Cells. *J Clin Invest* (2014) 124:2977–87. doi: 10.1172/JCI73174
96. Gilboa–Geffen A, Hamar P, Le MT, Wheeler LA, Trifonova R, Petrocca F, et al. Gene Knockdown by EpCAM Aptamer–siRNA Chimeras Suppresses Epithelial Breast Cancers and Their Tumor–Initiating Cells. *Mol Cancer Ther* (2015) 14:2279–91. doi: 10.1158/1535-7163.MCT-15-0201-T
97. Berezhnoy A, Castro I, Levay A, Malek TR, Gilboa E. Aptamer–Targeted Inhibition of mTOR in T Cells Enhances Antitumor Immunity. *J Clin Invest* (2014) 124:188–97. doi: 10.1172/JCI69856
98. Hussain AF, Tur MK, Barth S. An aptamer–siRNA Chimera Silences the Eukaryotic Elongation Factor 2 Gene and Induces Apoptosis in Cancers Expressing αvβ3 Integrin. *Nucleic Acid Ther* (2013) 23:203–12. doi: 10.1089/nat.2012.0408
99. Rajagopalan A, Berezhnoy A, Schrand B, Puplampu–Dove Y, Gilboa E. Aptamer–Targeted Attenuation of IL–2 Signaling in CD8(+) T Cells Enhances Antitumor Immunity. *Mol Ther* (2017) 25:54–61. doi: 10.1016/j.ymthe.2016.10.021
100. Lai WY, Wang WY, Chang YC, Chang CJ, Yang PC, Peck K. Synergistic Inhibition of Lung Cancer Cell Invasion, Tumor Growth and Angiogenesis Using aptamer–siRNA Chimeras. *Biomaterials* (2014) 35:2905–14. doi: 10.1016/j.biomaterials.2013.12.054
101. Wang T, Gantier MP, Xiang D, Bean AG, Bruce M, Zhou SF, et al. EpCAM Aptamer–Mediated Survivin Silencing Sensitized Cancer Stem Cells to Doxorubicin in a Breast Cancer Model. *Theranostics* (2015) 5:1456–72. doi: 10.7150/thno.11692
102. Subramanian N, Kanwar JR, Kanwar RK, Krishnakumar S. Targeting Cancer Cells Using LNA–Modified Aptamer–siRNA Chimeras. *Nucleic Acid Ther* (2015) 25:317–22. doi: 10.1089/nat.2015.0550
103. Esposito CL, Nuzzo S, Catuogno S, Romano S, de Nigris F, de Franciscis V. STAT3 Gene Silencing by Aptamer–siRNA Chimera as Selective Therapeutic for Glioblastoma. *Mol Ther Nucleic Acids* (2018) 10:398–411. doi: 10.1016/j.omtn.2017.12.021
104. Yoon S, Wu X, Armstrong B, Habib N, Rossi JJ. An RNA Aptamer Targeting the Receptor Tyrosine Kinase Pdgfrα Induces Anti–Tumor Effects Through STAT3 and P53 in Glioblastoma. *Mol Ther Nucleic Acids* (2019) 14:131–41. doi: 10.1016/j.omtn.2018.11.012
105. Rehmani H, Li Y, Li T, Padia R, Calbay O, Jin L, et al. Addiction to Protein Kinase Cι Due to PRKCI Gene Amplification can be Exploited for an Aptamer–Based Targeted Therapy in Ovarian Cancer. *Signal Transduct Target Ther* (2020) 5:140. doi: 10.1038/s41392-020-0197-8
106. Kalbasi A, Ribas A. Tumour–Intrinsic Resistance to Immune Checkpoint Blockade. Nature reviews. *Immunology* (2020) 20:25–39. doi: 10.1038/s41577-019-0218-4
107. Manguso RT, Pope HW, Zimmer MD, Brown FD, Yates KB, Miller BC, et al. *In Vivo* CRISPR Screening Identifies Ptpn2 as a Cancer Immunotherapy Target. *Nature* (2017) 547:413–8. doi: 10.1038/nature23270
108. Wang PF, Cai HQ, Zhang CB, Li YM, Liu X, Wan JH, et al. Molecular and Clinical Characterization of PTPN2 Expression From RNA–Seq Data of 996 Brain Gliomas. *J Neuroinflamm* (2018) 15:145. doi: 10.1186/s12974-018-1187-4
109. Ishizuka JJ, Manguso RT, Cheruiyot CK, Bi K, Panda A, Iracheta–Vellve A, et al. Loss of ADAR1 in Tumours Overcomes Resistance to Immune Checkpoint Blockade. *Nature* (2019) 565:43–8. doi: 10.1038/s41586-018-0768-9
110. Yang B, Hu P, Lin X, Han W, Zhu L, Tan X, et al. PTBP1 Induces ADAR1 P110 Isoform Expression Through IRES–Like Dependent Translation Control and Influences Cell Proliferation in Gliomas. *Cell Mol Life Sci: CMLS* (2015) 72:4383–97. doi: 10.1007/s00018-015-1938-7
111. Pastor F, Kolonias D, Giangrande PH, Gilboa E. Induction of Tumour Immunity by Targeted Inhibition of Nonsense–Mediated mRNA Decay. *Nature* (2010) 465:227–30. doi: 10.1038/nature08999
112. Li F, Yi Y, Miao Y, Long W, Long T, Chen S, et al. N(6)–Methyladenosine Modulates Nonsense–Mediated mRNA Decay in Human Glioblastoma. *Cancer Res* (2019) 79:5785–98. doi: 10.1158/0008-5472.CAN-18-2868
113. Garrido G, Schrand B, Rabasa A, Levay A, D'Eramo F, Berezhnoy A, et al. Tumor–Targeted Silencing of the Peptide Transporter TAP Induces Potent Antitumor Immunity. *Nat Commun* (2019) 10:3773. doi: 10.1038/s41467-019-11728-2
114. Kortylewski M, Yu H. Role of Stat3 in Suppressing Anti–Tumor Immunity. *Curr Opin Immunol* (2008) 20:228–33. doi: 10.1016/j.coi.2008.03.010
115. Ferguson SD, Srinivasan VM, Heimberger AB. The Role of STAT3 in Tumor–Mediated Immune Suppression. *J Neuro–Oncol* (2015) 123:385–94. doi: 10.1007/s11060-015-1731-3
116. Wei J, Wu A, Kong LY, Wang Y, Fuller G, Fokt I, et al. Hypoxia Potentiates Glioma–Mediated Immunosuppression. *PloS One* (2011) 6:e16195. doi: 10.1371/journal.pone.0016195
117. Wei J, Barr J, Kong LY, Wang Y, Wu A, Sharma AK, et al. Glioblastoma Cancer–Initiating Cells Inhibit T–Cell Proliferation and Effector Responses by the Signal Transducers and Activators of Transcription 3 Pathway. *Mol Cancer Ther* (2010) 9:67–78. doi: 10.1158/1535-7163.MCT-09-0734
118. Kortylewski M, Swiderski P, Herrmann A, Wang L, Kowolik C, Kujawski M, et al. *In Vivo* Delivery of siRNA to Immune Cells by Conjugation to a TLR9 Agonist Enhances Antitumor Immune Responses. *Nat Biotechnol* (2009) 27:925–32. doi: 10.1038/nbt.1564
119. Esposito CL, Nuzzo S, Ibba ML, Ricci–Vitiani L, Pallini R, Condorelli G, et al. Combined Targeting of Glioblastoma Stem–Like Cells by Neutralizing RNA–Bio–Drugs for STAT3. *Cancers (Basel)* (2020) 12:1434. doi: 10.3390/cancers12061434
120. Wei J, Chen P, Gupta P, Ott M, Zamler D, Kassab C, et al. Immune Biology of Glioma–Associated Macrophages and Microglia: Functional and Therapeutic Implications. *Neuro–oncology* (2020) 22:180–94. doi: 10.1093/neuonc/noz212

121. Sangaletti S, Tripodo C, Sandri S, Torselli I, Vitali C, Ratti C, et al. Osteopontin Shapes Immunosuppression in the Metastatic Niche. *Cancer Res* (2014) 74:4706–19. doi: 10.1158/0008-5472.CAN-13-3334
122. Zhou W, Ke SQ, Huang Z, Flavahan W, Fang X, Paul J, et al. Periostin Secreted by Glioblastoma Stem Cells Recruits M2 Tumour–Associated Macrophages and Promotes Malignant Growth. *Nat Cell Biol* (2015) 17:170–82. doi: 10.1038/ncb3090
123. Chang AL, Miska J, Wainwright DA, Dey M, Rivetta CV, Yu D, et al. CCL2 Produced by the Glioma Microenvironment Is Essential for the Recruitment of Regulatory T Cells and Myeloid–Derived Suppressor Cells. *Cancer Res* (2016) 76:5671–82. doi: 10.1158/0008-5472.CAN-16-0144
124. Zhang X, Chen L, Dang WQ, Cao MF, Xiao JF, Lv SQ, et al. CCL8 Secreted by Tumor–Associated Macrophages Promotes Invasion and Stemness of Glioblastoma Cells *via* ERK1/2 Signaling. *Lab Invest* (2020) 100:619–29. doi: 10.1038/s41374-019-0345-3
125. De Boeck A, Ahn BY, D'Mello C, Lun X, Menon SV, Alshehri MM, et al. Glioma–Derived IL–33 Orchestrates an Inflammatory Brain Tumor Microenvironment That Accelerates Glioma Progression. *Nat Commun* (2020) 11:4997. doi: 10.1038/s41467-020-18569-4
126. Soldevilla MM, Villanueva H, Casares N, Lasarte JJ, Bendandi M, Inoges S, et al. MRP1–CD28 Bi–Specific Oligonucleotide Aptamers: Target Costimulation to Drug–Resistant Melanoma Cancer Stem Cells. *Oncotarget* (2016) 7:23182–96. doi: 10.18632/oncotarget.8095
127. McNamara JO, Kolonias D, Pastor F, Mittler RS, Chen L, Giangrande PH, et al. Multivalent 4–1BB Binding Aptamers Costimulate CD8+ T Cells and Inhibit Tumor Growth in Mice. *J Clin Invest* (2008) 118:376–86. doi: 10.1172/JCI33365
128. Pastor F, Kolonias D, McNamara JO2nd, Gilboa E. Targeting 4–1BB Costimulation to Disseminated Tumor Lesions With Bi–Specific Oligonucleotide Aptamers. *Mol Ther* (2011) 19:1878–86. doi: 10.1038/mt.2011.145
129. Schrand B, Berezhnoy A, Brenneman R, Williams A, Levay A, Kong LY, et al. Targeting 4–1BB Costimulation to the Tumor Stroma With Bispecific Aptamer Conjugates Enhances the Therapeutic Index of Tumor Immunotherapy. *Cancer Immunol Res* (2014) 2:867–77. doi: 10.1158/2326-6066.CIR-14-0007
130. Yang Y, Sun X, Xu J, Cui C, Safari Yazd H, Pan X, et al. Circular Bispecific Aptamer–Mediated Artificial Intercellular Recognition for Targeted T Cell Immunotherapy. *ACS Nano* (2020) 14:9562–71. doi: 10.1021/acsnano.9b09884
131. Zheng J, Zhao S, Yu X, Huang S, Liu HY. Simultaneous Targeting of CD44 and EpCAM With a Bispecific Aptamer Effectively Inhibits Intraperitoneal Ovarian Cancer Growth. *Theranostics* (2017) 7:1373–88. doi: 10.7150/thno.17826
132. Hu Z, He J, Gong W, Zhou N, Zhou S, Lai Z, et al. TLS11a Aptamer/CD3 Antibody Anti–Tumor System for Liver Cancer. *J Biomed Nanotechnol* (2018) 14:1645–53. doi: 10.1166/jbn.2018.2619
133. Li Z, Hu Y, An Y, Duan J, Li X, Yang XD. Novel Bispecific Aptamer Enhances Immune Cytotoxicity Against MUC1–Positive Tumor Cells by MUC1–CD16 Dual Targeting. *Molecules* (2019) 24:478. doi: 10.3390/molecules24030478
134. Boltz A, Piater B, Toleikis L, Guenther R, Kolmar H, Hock B. Bi–Specific Aptamers Mediating Tumor Cell Lysis. *J Biol Chem* (2011) 286:21896–905. doi: 10.1074/jbc.M111.238261
135. Soldevilla MM, Villanueva H, Meraviglia–Crivelli D, Menon AP, Ruiz M, Cebollero J, et al. ICOS Costimulation at the Tumor Site in Combination With CTLA–4 Blockade Therapy Elicits Strong Tumor Immunity. *Mol Ther* (2019) 27:1878–91. doi: 10.1016/j.ymthe.2019.07.013
136. Lee H, Kim TH, Park D, Jang M, Chung JJ, Kim SH, et al. Combinatorial Inhibition of Cell Surface Receptors Using Dual Aptamer–Functionalized Nanoconstructs for Cancer Treatment. *Pharmaceutics* (2020) 12:689. doi: 10.3390/pharmaceutics12070689
137. Godlewski J, Ferrer–Luna R, Rooj AK, Mineo M, Ricklefs F, Takeda YS, et al. MicroRNA Signatures and Molecular Subtypes of Glioblastoma: The Role of Extracellular Transfer. *Stem Cell Rep* (2017) 8:1497–505. doi: 10.1016/j.stemcr.2017.04.024
138. Fareh M, Almairac F, Turchi L, Burel–Vandenbos F, Paquis P, Fontaine D, et al. Cell–Based Therapy Using miR–302–367 Expressing Cells Represses Glioblastoma Growth. *Cell Death Dis* (2017) 8:e2713. doi: 10.1038/cddis.2017.117
139. Alvarez–Erviti L, Seow Y, Yin H, Betts C, Lakhal S, Wood MJ. Delivery of siRNA to the Mouse Brain by Systemic Injection of Targeted Exosomes. *Nat Biotechnol* (2011) 29:341–5. doi: 10.1038/nbt.1807
140. Deng SZ, Lai MF, Li YP, Xu CH, Zhang HR, Kuang JG. Human Marrow Stromal Cells Secrete microRNA–375–Containing Exosomes to Regulate Glioma Progression. *Cancer Gene Ther* (2020) 27:203–15. doi: 10.1038/s41417-019-0079-9
141. De Toro J, Herschlik L, Waldner C, Mongini C. Emerging Roles of Exosomes in Normal and Pathological Conditions: New Insights for Diagnosis and Therapeutic Applications. *Front Immunol* (2015) 6:203. doi: 10.3389/fimmu.2015.00203
142. Ha D, Yang N, Nadithe V. Exosomes as Therapeutic Drug Carriers and Delivery Vehicles Across Biological Membranes: Current Perspectives and Future Challenges. *Acta Pharm Sin B* (2016) 6:287–96. doi: 10.1016/j.apsb.2016.02.001
143. Steg AD, Katre AA, Goodman B, Han HD, Nick AM, Stone RL, et al. Targeting the Notch Ligand JAGGED1 in Both Tumor Cells and Stroma in Ovarian Cancer. *Clin Cancer Res* (2011) 17:5674–85. doi: 10.1158/1078-0432.CCR-11-0432
144. Noh K, Mangala LS, Han HD, Zhang N, Pradeep S, Wu SY, et al. Differential Effects of EGFL6 on Tumor Versus Wound Angiogenesis. *Cell Rep* (2017) 21:2785–95. doi: 10.1016/j.celrep.2017.11.020
145. Lee TJ, Haque F, Shu D, Yoo JY, Li H, Yokel RA, et al. RNA Nanoparticle as a Vector for Targeted siRNA Delivery Into Glioblastoma Mouse Model. *Oncotarget* (2015) 6:14766–76. doi: 10.18632/oncotarget.3632
146. Zatsepin TS, Kotelevtsev YV, Koteliansky V. Lipid Nanoparticles for Targeted siRNA Delivery – Going From Bench to Bedside. *Int J Nanomed* (2016) 11:3077–86. doi: 10.2147/IJN.S106625
147. Sun X, Chen Y, Zhao H, Qiao G, Liu M, Zhang C, et al. Dual–Modified Cationic Liposomes Loaded With Paclitaxel and Survivin siRNA for Targeted Imaging and Therapy of Cancer Stem Cells in Brain Glioma. *Drug Delivery* (2018) 25:1718–27. doi: 10.1080/10717544.2018.1494225
148. Alshaer W, Hillaireau H, Vergnaud J, Mura S, Deloménie C, Sauvage F, et al. Aptamer–Guided siRNA–Loaded Nanomedicines for Systemic Gene Silencing in CD–44 Expressing Murine Triple–Negative Breast Cancer Model. *J Controlled Rel* (2018) 271:98–106. doi: 10.1016/j.jconrel.2017.12.022
149. Wang C, Wang Z, Chen C, Fu X, Wang J, Fei X, et al. A Low MW Inhibitor of CD44 Dimerization for the Treatment of Glioblastoma. *Br J Pharmacol* (2020) 177:3009–23. doi: 10.1111/bph.15030
150. Lächelt U, Wagner E. Nucleic Acid Therapeutics Using Polyplexes: A Journey of 50 Years (and Beyond). *Chem Rev* (2015) 115:11043–78. doi: 10.1021/cr5006793
151. Adams C, Israel LL, Ostrovsky S, Taylor A, Poptani H, Lellouche JP, et al. Development of Multifunctional Magnetic Nanoparticles for Genetic Engineering and Tracking of Neural Stem Cells. *Adv Healthc Mater* (2016) 5:841–9. doi: 10.1002/adhm.201500885
152. Zaman RU, Mulla NS, Braz Gomes K, D'Souza C, Murnane KS, D'Souza MJ. Nanoparticle Formulations That Allow for Sustained Delivery and Brain Targeting of the Neuropeptide Oxytocin. *Int J Pharm* (2018) 548:698–706. doi: 10.1016/j.ijpharm.2018.07.043

Conflict of Interest: GC is one of the scientific founders of Ithax Pharmaceuticals.

The remaining authors declare that the research was conducted in the absence of any commercial or financial relationships that could be construed as a potential conflict of interest.

Publisher's Note: All claims expressed in this article are solely those of the authors and do not necessarily represent those of their affiliated organizations, or those of the publisher, the editors and the reviewers. Any product that may be evaluated in this article, or claim that may be made by its manufacturer, is not guaranteed or endorsed by the publisher.

frontiers in Oncology

ORIGINAL RESEARCH
published: 10 September 2021
doi: 10.3389/fonc.2021.664236

OPEN ACCESS

Edited by:
Payal Watchmaker, University of California, San Francisco, United States

Reviewed by:
Giedre Krenciute, St. Jude Children's Research Hospital, United States
Xuyao Zhang, Fudan University, China
Sadhak Sengupta, Triumvira Immunologics, Inc., United States

***Correspondence:**
Donald M. O'Rourke donald.orourke@pennmedicine.upenn.edu

†Present address:
Yibo Yin, Department of Neurosurgery, First Affiliated Hospital of Harbin Medical University, Harbin, China

‡These authors have contributed equally to this work and share first authorship

Specialty section:
This article was submitted to Cancer Immunity and Immunotherapy, a section of the journal Frontiers in Oncology

Received: *04 February 2021*
Accepted: *18 August 2021*
Published: *10 September 2021*

Citation:
Thokala R, Binder ZA, Yin Y, Zhang L, Zhang JV, Zhang DY, Milone MC, Ming GL, Song H and O'Rourke DM (2021) High-Affinity Chimeric Antigen Receptor With Cross-Reactive scFv to Clinically Relevant EGFR Oncogenic Isoforms. Front. Oncol. 11:664236. doi: 10.3389/fonc.2021.664236

High-Affinity Chimeric Antigen Receptor With Cross-Reactive scFv to Clinically Relevant EGFR Oncogenic Isoforms

Radhika Thokala[1,2‡], Zev A. Binder[1,2‡], Yibo Yin[1,2†], Logan Zhang[1,2], Jiasi Vicky Zhang[1,2], Daniel Y. Zhang[2,3], Michael C. Milone[2,4], Guo-li Ming[3], Hongjun Song[2,5] and Donald M. O'Rourke[1,2]*

[1] Department of Neurosurgery, Perelman School of Medicine, University of Pennsylvania, Philadelphia, PA, United States, [2] Glioblastoma Translational Center of Excellence, Abramson Cancer Center, Perelman School of Medicine, University of Pennsylvania, Philadelphia, PA, United States, [3] Biochemistry and Molecular Physics Graduate Group, Perelman School of Medicine, University of Pennsylvania, Philadelphia, PA, United States, [4] Department of Pathology and Laboratory Medicine, Perelman School of Medicine, University of Pennsylvania, Philadelphia, PA, United States, [5] Department of Neuroscience and Mahoney Institute for Neurosciences, Perelman School of Medicine, University of Pennsylvania, Philadelphia, PA, United States

Tumor heterogeneity is a key reason for therapeutic failure and tumor recurrence in glioblastoma (GBM). Our chimeric antigen receptor (CAR) T cell (2173 CAR T cells) clinical trial (NCT02209376) against epidermal growth factor receptor (EGFR) variant III (EGFRvIII) demonstrated successful trafficking of T cells across the blood–brain barrier into GBM active tumor sites. However, CAR T cell infiltration was associated only with a selective loss of EGFRvIII+ tumor, demonstrating little to no effect on EGFRvIII$^-$ tumor cells. Post-CAR T-treated tumor specimens showed continued presence of EGFR amplification and oncogenic EGFR extracellular domain (ECD) missense mutations, despite loss of EGFRvIII. To address tumor escape, we generated an EGFR-specific CAR by fusing monoclonal antibody (mAb) 806 to a 4-1BB co-stimulatory domain. The resulting construct was compared to 2173 CAR T cells in GBM, using *in vitro* and *in vivo* models. 806 CAR T cells specifically lysed tumor cells and secreted cytokines in response to amplified EGFR, EGFRvIII, and EGFR-ECD mutations in U87MG cells, GBM neurosphere-derived cell lines, and patient-derived GBM organoids. 806 CAR T cells did not lyse fetal brain astrocytes or primary keratinocytes to a significant degree. They also exhibited superior antitumor activity *in vivo* when compared to 2173 CAR T cells. The broad specificity of 806 CAR T cells to EGFR alterations gives us the potential to target multiple clones within a tumor and reduce opportunities for tumor escape *via* antigen loss.

Keywords: GBM, glioma, immunotherapy, CAR T cells, adoptive T cell therapy, EGFR

INTRODUCTION

Chimeric antigen receptor (CAR) cells targeting pediatric B cell malignancies have shown unprecedented responses and were the first CAR T cell therapies to receive FDA approval, in 2017 (1–3). The successful application of this therapeutic technology in the treatment of solid tumors, including glioblastoma (GBM), remains a significant challenge; chief among them are tumor heterogeneity, immunosuppressive tumor microenvironment, and antigen escape (4, 5). Successful strategies for overcoming these obstacles are required to advance CAR T therapy in solid tumors.

Epidermal growth factor receptor (EGFR) was one of the first oncogenes identified in GBM and presents an attractive therapeutic target, given its extracellular nature and frequent alterations in GBM. Approximately 60% of GBM specimens contain a mutation, rearrangement, splicing alteration, and/or amplification of EGFR (6). EGFR overexpression, mediated through focal amplification of the EGFR locus as double minute chromosomes, has long been recognized as the most common EGFR alteration, present in 60% of GBM patients (7, 8). Tumor-specific EGFR variant III (EGFRvIII), resulting from deletion of exon 2–7 of wild-type EGFR (wtEGFR), is present in 30% of GBM patients (9). In addition, oncogenic missense mutations $EGFR^{A289D/T/V}$, $EGFR^{R108G/K}$, and $EGFR^{G598V}$ have been identified in 12%–13% of cases in the extracellular domain (ECD) of EGFR, independent of EGFRvIII. Missense mutations and EGFRvIII often co-occur with EGFR amplification and activate EGFR receptor independent of its ligand (10). Several of the missense mutations have been shown to have a negative effect on patient survival, driving tumor proliferation and invasion (11).

Our first-in-man CAR T clinical trial (NCT02209376) against EGFRvIII in recurrent GBM demonstrated the safety of a peripheral infusion of CAR T cells and resulted in successful trafficking of the CAR T cells to active tumor sites, across the blood–brain barrier (12). After treatment, CAR T cells infiltrated the GBM tumors rapidly, proliferated *in situ*, and persisted over a prolonged period of time. However, CAR T cell infiltration was associated only with a selective loss of EGFRvIII+ GBM cells. Importantly, post-CAR T-treated tumor specimens showed the continued presence of EGFR amplification and missense mutations, despite the decrease in EGFRvIII target antigen. Persistence of EGFR amplification and ECD missense mutations in the context of loss of EGFRvIII expression suggested that tumor heterogeneity played an essential role for tumor recurrence and continued regrowth.

mAb806, originally raised against EGFRvIII, recognizes a conformationally exposed epitope of wtEGFR when it is overexpressed on tumor cells. The same epitope is not exposed in EGFR expressed on normal non-overexpressing cells (13, 14). ABT-414, an antibody–drug conjugate composed of a humanized mAb806 (ABT-806), showed early efficacy in phase I/II clinical trials with no apparent skin toxicity in treated GBM patients (15). However, a recent Phase III trial was terminated when an interim analysis failed to demonstrate a survival benefit over placebo (16). mAb806 showed an increased binding affinity for not only EGFRvIII but also EGFR ECD mutations and a low affinity for wtEGFR (11). These findings suggest that mAb806 is a viable therapeutic option for tumors harboring EGFR alterations in addition to EGFRvIII.

In the present study, we have developed EGFR-specific CAR T cells derived from the single-chain fragment variable region (scFv) of 806 mAb, using our standard 4-1BB-ζ construct (17). We then compared 806 CAR T activity with EGFRvIII-specific CAR T cells (2173 CAR T), currently in clinic, for specificity against oncogenic EGFR alterations, including amplified EGFR, EGFRvIII, and extracellular mutations *in vitro* and *in vivo*.

MATERIALS AND METHODS

CAR Constructs

806 scFvs were swapped with scFv of our standard CD19-BB-ζ lentiviral vector described previously to generate 806-BB-ζ CAR (17, 18). Briefly, the nucleotide coding sequences of 806 or C225 scFv with the huCD8 leader were synthesized by GeneArt (Thermo Fisher Scientific, Waltham, MA) with 5′ Xba1 and 3′ Nhe1 and ligated to Xba1 and Nhe1 sites of CD19-BB-ζ car construct. The C225-BB-ζ CAR was obtained from Dr. Avery Posey's lab at the University of Pennsylvania. The 2173-BB-ζ CAR T construct was obtained from Dr. Laura Johnson's Lab at the University of Pennsylvania (19, 20).

Transduction and Expansion of Primary Human T Lymphocytes

Human primary total T cells (CD4 and CD8) were isolated from normal healthy donors following leukapheresis by negative selection using RosetteSep kits (STEMCELL Technologies, Vancouver, CA, Canada). All specimens were collected with protocol approved by the University Review Board, and written informed consent was obtained from each donor. T cells were cultured in RPMI 1640 (Thermo Fisher Scientific) supplemented with 10% fetal bovine serum (FBS) (VWR, Radnor, PA, USA), 10 mM HEPES (Thermo Fisher Scientific), 100 U/mL penicillin (Thermo Fisher Scientific), and 100 g/ml streptomycin sulfate (Thermo Fisher Scientific) and stimulated with magnetic beads coated with anti-CD3/anti-CD28 (Thermo Fisher Scientific) at the 1:3 T cell-to-bead ratio. Approximately 24 h after activation, T cells were transduced with lentiviral vectors encoding the CAR transgene at an MOI of 3 to 6. On day 5, beads were removed and thereafter cells were counted and fed every 2 days, supplemented with IL 2 150 U/ml until they were either used for functional assays or cryopreserved for future use.

Cell Lines and Cell Culture

The human cell line U87MG was purchased from the American Type Culture Collection (ATCC) and maintained in MEM (Richter's modification) (Thermo Fisher Scientific) with components GlutaMAX-1 (Thermo Fisher Scientific), HEPES pyruvate, and penicillin/streptomycin supplemented with 10% FBS. Primary human keratinocytes were purchased from the Dermatology Core Facility at the University of Pennsylvania. K562 cells were purchased from ATCC and maintained in RPMI

media (Invitrogen, Carlsbad, CA, USA) supplemented with 10% FBS, 20 mM HEPES, and 1% penicillin/streptomycin. Primary astrocytes were purchased (ScienCell Research Laboratories, Carlsbad, CA, USA) and cultured according to the manufacturer's instructions. The cells from early passages were used for cytotoxicity and cytokine experiments. GSC cell lines were cultured in DMEM F-12 media (Sigma-Aldrich, St. Louis, MO, USA) supplemented with 2% B27 without vitamin A (Thermo Fisher Scientific), 20 mM HEPES, and penicillin/streptomycin.

EGFR-Mutant Cell Lines

To produce the overexpressing EGFR cell line (designated as U87MG-EGFR), the lentivirus co-expressing wtEGFR and Cyan Fluorescent Protein (CFP) under the control of the EF-1α promoter was transduced into the U87MG cell line. On post-transduction day 4, cells were sorted on an Influx cell sorter (BD, Franklin Lakes, NJ, USA) on the basis of high EGFR expression and subsequently expanded. The lentivirus co-expressing CFP and EGFR mutants $EGFR^{R108K/G}$, $EGFR^{A289D/T/V}$, or EGFRvIII was transduced into U87MG-EGFR, GSC5077 neurosphere cells (21), and K562 cell lines. CFP-positive cells were sorted by fluorescence-activated cell sorting (FACS). For luciferase killing assays and *in vivo* tracking studies, U87MG and U87MG-EGFR mutant cell lines were transduced with lentivirus click beetle green (CBG) luciferase and green fluorescent protein (GFP). Anti-GFP-positive cells were sorted by FACS.

Cytokine Analysis

CAR T cells and K562 targets expressing EGFR and its variants were cocultured in 1:2 ratio in the R10 medium in a 96-well plate, in triplicate. Plates were incubated at 37°C with 5% CO_2. After 48 h, supernatants were collected and cytokine levels were assessed by ELISA kit (R&D Systems, Minneapolis, MN, USA) for IFN-γ, TNF-α, and IL2 production, according to the manufacturer's instructions.

Chromium Release Assay

The cytolytic efficacy of CAR T cells against K562 cells was evaluated by 4-h chromium release assays using E:T ratios of 5:1, 2.5:1, and 1:1. 51Cr-labeled target cells were incubated with CAR T cells in complete medium or 0.1% Triton X-100, to determine spontaneous and maximum 51Cr release respectively, in a V-bottomed 96-well plate. The mean percentage of specific cytolysis of triplicate wells was calculated from the release of ^{51}Cr using a TopCount NXT (Perkin-Elmer Life and Analytical Sciences, Inc., Waltham, MA) as:

$$100 \times \frac{(experimental\ \ release - spontaneous\ \ release)}{(maximal\ \ release - spontaneous\ \ release)}$$

Data was reported as mean ± SD.

Luciferase-Based Cytotoxic Assay

CBG+ target cell lines (U87 variants and GSC5077 variants) were cocultured with CAR T cells at E:T ratios of 10:1, 5:1, and 2.5:1, for 24 h at 37°C. One hundred microliters of the mixture was transferred to a 96-well black luminometer plate, 100 µl of 66 µg/ml D-luciferin (GoldBio, St. Louis, MO, USA) was added, and the luminescence was immediately determined. Results were reported as percent killing based on luciferase activity in wells with tumor cells alone.

CD107a Degranulation

To assess CD107a degranulation, we plated 1×10^5 T cells and 5×10^5 stimulator target cells per well in round-bottom 96-well plates, to a final volume of 200 µl in complete R10 medium, in triplicates. The CD107a-PE antibody (BD) was added into each well and incubated at 37°C for 4 h, along with surface staining for CD8 (BioLegend, San Diego, CA, USA) and CD3 and then analyzed by flow cytometry.

Flow Cytometry

For CAR detection, cells were stained with biotinylated protein L (GenScript, Piscataway, NJ, USA), goat anti-mouse IgG, and anti-human IgG (Jackson ImmunoResearch Laboratories, West Grove, PA), followed by streptavidin-conjugated allophycocyanin (APC) (BD). The surface expression of EGFR and its mutants was detected by CFP and APC-conjugated cetuximab antibody (Novus Biologicals, Centennial, CO, USA). EGFRvIII expression was detected by anti-EGFRvIII antibody, clone DH8.3 (Santa Cruz Biotechnology, Dallas, TX, USA). Flow analysis done by LSRFortessa (BD) and data were analyzed by FlowJo software (BD).

Animal Experiments

All mouse experiments were conducted according to Institutional Animal Care and Use Committee (IACUC)–approved protocols. NSG mice were injected with 2.5×10^5 U87MG-EGFR/EGFRvIII/Luc+ tumors subcutaneously in 100 µl of PBS on day 0, seven animals per cohort. Tumor progression was evaluated by luminescence emission on an IVIS Lumina III In Vivo Imaging System (Caliper Life Sciences, Hopkinton, MA, USA) after intraperitoneal D-luciferin injection according to the manufacturer's instructions (GoldBio). Tumor size was measured by calipers in two dimensions and approximated to volume using the following calculation:

$$Volume = \frac{L \times \pi W^2}{6}$$

Seven days after tumor implantation, mice were treated with 3×10^6 CAR T cells intravenously *via* the tail vein, in 100 µl of PBS. Survival was followed over time until predetermined IACUC-approved endpoints were reached.

GBM Organoids

GBM organoids (GBOs) were established from primary patient tissue, under a University of Pennsylvania Institutional Review Board-approved protocol and with patient written informed consent, and cocultured with CAR T cells as described previously (22, 23). GBOs were fixed and stained after coculture, using anti-CD3 (BioLegend), anti-cleaved caspase 3 (Cell Signaling Technology, Danvers, MA), anti-EGFR (Thermo Fisher Scientific), anti-EGFRvIII (Cell Signaling Technology), and DAPI (Sigma). To control for tumor heterogeneity, four GBOs per condition were used. Mutational data and variant

allele fractions (VAF) were obtained from the Center for Personalized Diagnostics at the University of Pennsylvania, as described previously (24).

Statistical Analysis

All *in vitro* experiments were performed at least in triplicate. GraphPad Prism 6 software (GraphPad Software, San Diego, CA, USA) was used for statistical analyses. Data were presented as mean ± standard deviation. The differences between means were tested by appropriate tests. For the mouse experiments, changes in tumor radiance from baseline at each time point were calculated and compared between groups using the t-test or Wilcoxon rank-sum test, as appropriate. Survival determined from the time of T cell injection was analyzed by the Kaplan–Meier method, and differences in survival between groups were compared by the log-rank Mantel–Cox test.

RESULTS

Generation of 806 CARs and Cell Lines Expressing EGFR-Mutated Proteins

In the present study, we have generated CARs that target EGFR and EGFR mutants by fusing the scFv derived from mAb806 to a second-generation CAR construct containing 4-1BB-CD3ζ signaling 806 CAR, the design of which is shown schematically in **Figure 1A**. The EGFRvIII-specific 4-1BB-CD3ζ-based 2173 CAR used in our clinical trials (NCT02209376 and NCT03726515) was generated for comparative evaluation with 806 CAR. 4-1BB-based cetuximab (C225) and CD19 CARs were used as positive and negative controls. Lentiviral vectors encoding CARs were transduced into a mixture of CD4 and CD8 T cells, and surface expression was confirmed by flow cytometry (**Figure 1B**). We next turned to generating target-positive tumor cell lines, expressing the mutations $EGFR^{R108K/G}$, $EGFR^{A289D/T/V}$, $EGFR^{G598V}$, and EGFRvIII, for testing of our CAR constructs (**Figure 1C**). In order to more faithfully model the EGFR mutations, which are almost always co-expressed with amplified wtEGFR, we transduced the GBM cell line U87MG and patient-derived glioma stem cell line GSC5077 (21), both of which express low levels of wtEGFR, with a lentiviral vector encoding wtEGFR (**Figure 1D**) (resultant lines referred to as U87MG-EGFR and GSC5077-EGFR), as well as K562 chronic myelogenous leukemia (CML) cells that lack endogenous expression of EGFR, with wtEGFR (**Figure 1E**). U87MG-EGFR, GSC5077-EGFR, and K562 cells were also transduced with EGFRvIII lentivirus and expression was then analyzed by an EGFRvIII-specific antibody (**Figure 1F**). A lentiviral vector co-expressing CFP and the targeted EGFR extracellular mutants (**Figure 1D**) was transduced into U87MG-EGFR, GSC5077-EGFR, and K562 cells. The resulting CFP-positive cells were sorted by fluorescence-activated cell sorting to obtain a positively transduced cell population (**Figure 1G**).

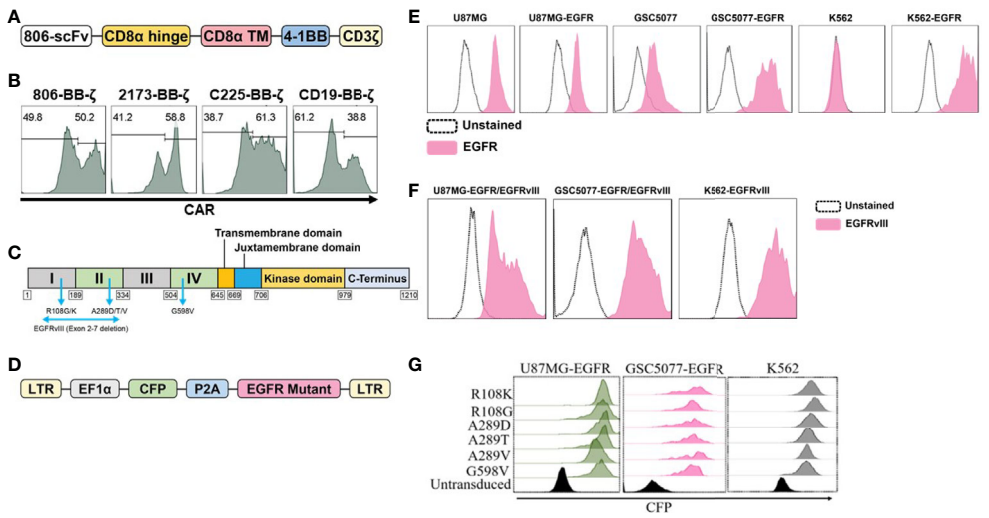

FIGURE 1 | Construction and expression of 806 CAR and EGFR mutant cell lines. **(A)** Schematic diagram of vector map of 806 CAR containing the 4-1BB co-stimulatory domain. **(B)** CAR surface expression in primary human $CD4^+$ and $CD8^+$ T cells. Human T cells were simulated for 24 h with anti-CD3/anti-CD28 T-cell activating beads and transduced with CAR transgenes, and CAR expression was analyzed by flow cytometry using biotinylated goat-anti-mouse (806, C225, and CD19 CARs) and goat-anti human F(ab)2 fragment-specific antibodies (2173 CARs) followed by secondary staining with streptavidin-APC. **(C)** Schematic showing targeted missense mutations in the extracellular domain of EGFR, $EGFR^{R108K/G}$, $EGFR^{A289D/T/V}$, $EGFR^{G598V}$, and splice variant EGFRvIII. **(D)** Schematic of lentiviral vector co-expressing CFP and wtEGFR or EGFR mutant. **(E)** Flow-based analysis of endogenous and ectopically expressed EGFR in U87MG, GSC5077, and K562 cell lines using the cetuximab antibody. **(F)** U87MG, U87MG-EGFR, and GSC5077-EGFR expression of EGFRvIII. **(G)** U87MG-EGFR, GSC5077-EGFR, and K562 cell lines were transduced with a lentiviral vector co-expressing CFP and indicated EGFR missense mutations and sorted by CFP expression using fluorescent-activated cell sorting.

In Vitro Characterization of 806 CAR T Cells

To determine the specificity of the 806 and 2173 CARs for overexpressed wtEGFR, EGFRvIII, and the EGFR-ECD mutants, 2173 and 806 EGFR BB-ζ CAR T cells were cocultured with U87MG-EGFR and GSC5077-EGFR cell lines expressing EGFRvIII and extracellular mutants $EGFR^{R108K/G}$, $EGFR^{A289D/T/V}$, and $EGFR^{G598V}$, in 24-h bioluminescence-luciferase based killing assays (**Figures 2A, B**). While 2173 CAR T cells demonstrated specificity for EGFRvIII alone, 806 CAR T cells efficiently lysed all targets and exhibited similar cytolytic potential as C225 CAR T (**Figures 2A, B**). Notably, 806 CAR T cells were able to kill U87MG cells, despite expressing only low levels of wtEGFR, at an equal level when compared to overexpressed wtEGFR and EGFRvIII. Since U87MG-EGFR mutants expressed endogenous and ectopic EGFR, we could not distinguish if the 806 scFv-binding specificity was restricted to the mutant or wtEGFR. To test the exclusive specificity to the mutants, we cocultured 806 and 2173 CAR T cells with the CML cell line K562, transduced to express wtEGFR, EGFRvIII, or EGFR mutants, as K562 does not have any endogenous EGFR (**Figure 2B**). 806 CAR T cells did not lyse untransduced K562 cells, confirming the lack of EGFR on the parental line. The 806 CAR T cells selectively targeted K562 cells expressing EGFR, EGFRvIII, or EGFR-ECD mutants and demonstrated similar efficacy as C225 CAR T cells. 2173 CAR T cells lysed K562-EGFRvIII cells but did not show any activity against either wtEGFR or the ECD mutants, as expected (**Figure 2B**). T cell activation was assessed by induction of

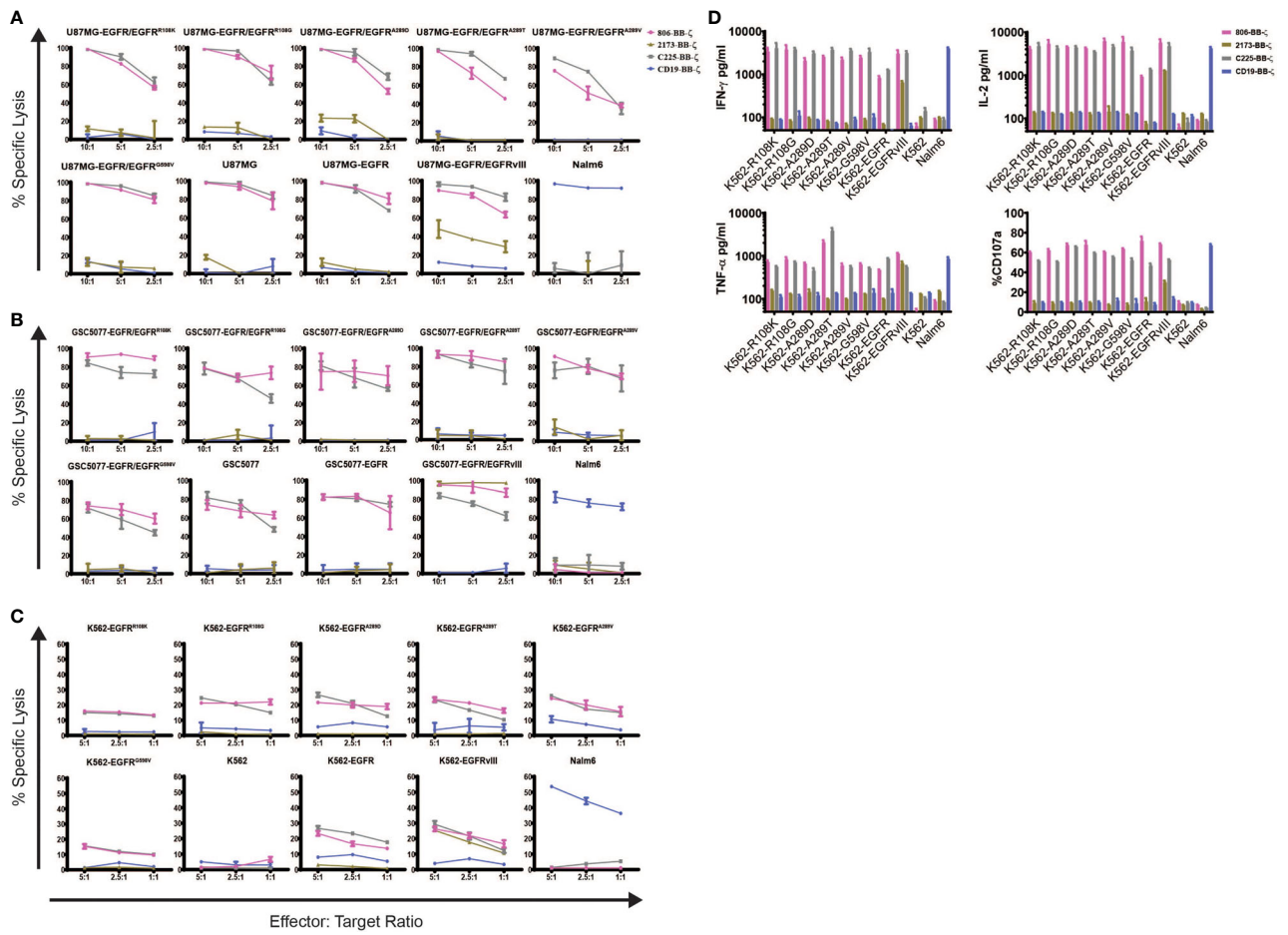

FIGURE 2 | *In vitro* characterization of 806 EGFR CAR T cells. Antigen-specific cytolytic activity of 806 and 2173 CAR T cells against cell lines expressing EGFR and its variants. **(A)** U87MG-EGFR and GSC5077-EGFR cell lines expressing EGFRvIII, $EGFR^{R108K/G}$, $EGFR^{A289D/T/V}$, and $EGFR^{G598V}$ mutant variants were stably transduced with Click Beetle Green (CBG) and cocultured with CAR T cells at indicated effector-to-target ratios for 24 h. One representative experiment from three normal donors is shown. Samples were performed in triplicates in three replicative experiments. C225-BB-ζ CAR, and CD19-BB-ζ CAR were used as positive and negative controls, respectively. **(B)** Antigen-specific cytolytic activity of 806 and 2173 CAR T cells in EGFR and its variants expressed in K562 cells in a 4-h chromium release assay at indicated effector-to-target ratios. **(C)** K562 cells expressing wtEGFR, EGFRvIII, or EGFR-mutants were cocultured with 806 CART cells for 48 h. IFN-γ, TNF-α, and IL2 secretion was measured in the supernatant by ELISA. Bar charts represent results from a single experiment, and values represent the average ± SD of triplicates. **(D)** CD107a upregulation on CAR T cells stimulated with K562 cells expressing wtEGFR, EGFRvIII, or EGFR-mutants for 4 h. The percentage of CD107a expression was quantified on CD3 cells (values represent the average of ± SD of two repeated experiments).

surface CD107a expression after coculture of CAR T cells with target-expressing cells (**Figure 2C**). Antigen-specific effector cytokine production was assessed by coculturing K562 target cells transduced with EGFR and its variants with CAR T cells. The resulting supernatants were analyzed for IFN-γ, TNF-α, and IL2 production (**Figure 2D**). Untransduced K562 and Nalm6 cells were used as negative controls. 806 and C225 CAR T cells produced similar levels of CD107 degranulation (**Figure 2C**) and IFN-γ, TNF-α, and IL2 (**Figure 2D**) in response to EGFRvIII, EGFR-ECD mutants, and EGFR overexpressing cells, while 2173 CAR T cells responded to EGFRvIII alone.

806 CAR T Cells Exhibit Low or No Affinity for EGFR Expressed on Primary Astrocytes and Keratinocytes

Having confirmed the function of the 806 CARs, we next sought to compare the reactivity of 806 and 2173 CAR T cells in response to endogenous levels of EGFR in normal cells, *in vitro*. We cultured primary human keratinocytes and astrocytes, as those cell types express wtEGFR (**Figure 3A**) and used them to stimulate CAR T cells. We observed production of IFN-γ by C225 CAR T cells, in response to EGFR presented by either astrocytes or keratinocytes, as well as U87MG-EGFR (**Figure 3B**). In contrast, 2173 CAR T cells produced IFN-γ in response to EGFRvIII antigen alone. 806 CAR T cells exhibited low or no cytotoxicity when cocultured with astrocytes or keratinocytes (**Figure 3C**), with corresponding low IFN-γ production (**Figure 3B**).

Antitumor Activity of 806 CAR T Cells *In Vivo*

Having compared the antigen-specific effector function of 806 CAR with 2173 CARs, we next sought to confirm its *in vivo* antitumor effects, using immunodeficient NSG mice bearing human GBM tumors (**Figure 4A**). On Day 0, U87MG-EGFR/EGFRvIII tumors were implanted subcutaneously, and on Day 5, tumor engraftment was confirmed by bioluminescence imaging (BLI). On Day 7, a single dose of 3×10^6 CAR-positive T cells were infused intravenously (n = 7 per cohort). Total bioluminescence (**Figure 4B**) and individual bioluminescence (**Figure 4C**) were assessed in 806 and 2173 CAR T cell-treated groups. Animals in the negative control cohort, receiving CD19 CAR T cells, demonstrated rapid tumor growth, with all mice reaching a predetermined humane experimental endpoint by 42 days after initial tumor engraftment. To be noted, all mice in the CD19, 2173, and 806 groups reached experimental endpoint by day 42, 63, and 91, respectively (**Figure 4A**).

High-Fidelity GBM Organoids Demonstrate Cross-Reactivity of 806 CAR

Given the ability of the 806 CAR to target EGFR alterations beyond EGFRvIII, we turned to patient-derived GBM organoids (GBOs) to demonstrate activity in a heterogeneous model previously characterized to be of high fidelity to human tumors (22, 23). GBOs retain the originating tumor heterogeneity to a high degree out beyond 12 weeks of culturing and maintain the expression of endogenous EGFR and its alterations, providing a valuable model platform for testing therapies aimed at addressing tumor escape. The GBOs selected for coculture experiments contained multiple EGFR mutations (**Figure 5A**). GBO 9057 had EGFR copy number gain, EGFRvIII, and two missense mutations, $EGFR^{G598V}$ and $EGFR^{C595Y}$. The missense mutation was found to have a VAF of 24%, while EGFRvIII was identified in less than 10% of the reads, based on next-generation sequencing (NGS). GBO 9066 had EGFR copy number gain, $EGFR^{A289V}$, and $EGFR^{G598V}$. Both $EGFR^{A289V}$ and $EGFR^{G598V}$ had a VAF of less than 15%, making determination of co-occurrence impossible through NGS.

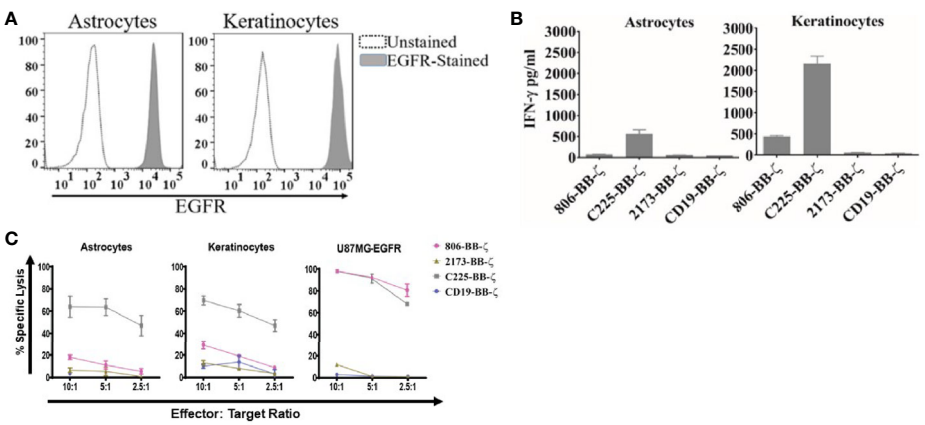

FIGURE 3 | Antitumor efficacy of 806 CAR T cells in primary astrocytes and keratinocytes. **(A)** Surface expression of EGFR assessed by flow cytometry on human primary astrocytes and keratinocytes using EGFR-specific cetuximab antibody. **(B)** Primary astrocytes and keratinocytes were cocultured with 806 CAR T cells at indicated ratios in a 4-h chromium assay, and results are representative of a single experiment showing the average ± SD of triplicates. **(C)** Levels of IFN-γ measured in supernatants by ELISA 24 h after coculturing 806 and 2173 CAR T cells with primary astrocytes and keratinocytes at an effector-to-target ratio of 1:1. Results are representative of a single experiment with the average ± SD of triplicates.

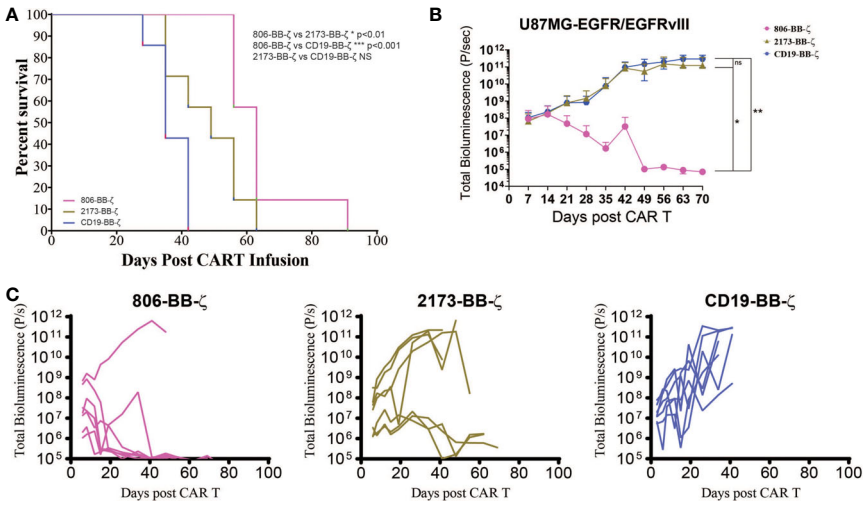

FIGURE 4 | *In vivo* antitumor effect of 806 CAR T cells in NSG mice bearing U87MG-EGFR/EGFRvIII$^+$ xenografts. Seven days after 250,000 U87MG-EGFR/EGFRvIII cells were subcutaneously implanted into mice, 3 × 10^6 T cells were injected intravenously with indicated CAR constructs. **(A)** Survival based on time to endpoint was plotted using a Kaplan–Meier curve and statistically significant differences between CAR groups were determined using the log-rank Mantel-Cox test. Tumor burden was assessed by bioluminescent imaging. Bars indicate means ± SD (n = 7 mice per group). Tumor burden was quantified as total flux **(B)** and in individual mice **(C)** in units of photons/second. Bars indicate means± SD (n = 7 mice). P = photons. ns, $p > 0.05$; *$p \leq 0.05$; **$p \leq 0.01$.

GBOs were cocultured with 806, 2173, and CD19 CAR T cells, at a 1:10 E:T ratio, for 72 h before fixation and evaluation. CAR T cell infiltration, as quantified by CD3 staining, was more significant in the 806 CAR T cell population than either the 2173 or CD19 CAR T cell population (**Figure 5B**). Cleaved caspase 3 (CC3) was used as a measure of cell death and antitumor activity. As with the CD3$^+$ cell infiltration, the 806 CAR coculture resulted in higher CC3 levels than either the 2173 or CD19 CAR cocultures (**Figure 5C**). These results highlighted the broad cross-reactivity of the 806 CAR in a heterogeneous, high-fidelity GBM model. wtEGFR staining in both GBO lines provided additional evidence of the cross-reactive nature of the 806 CAR (**Figure 5D**). Staining intensity, normalized to CD19 CAR-treated GBOs, showed consistent decreases in 806 CAR-treated GBOs, to a greater degree than the 2173 CAR-treated GBOs (**Figure 5E**).

DISCUSSION

We have shown broad cross-reactivity of 806 CAR T cells to EGFR mutant proteins resulting in enhanced anti-GBM tumor killing, along with a low on-target, off-tumor effect against both astrocytes and keratinocytes that express wild-type EGFR. Importantly, 806 CAR T cells are able to more effectively control tumor growth in a wtEGFR/EGFRvIII model. 806 CAR T cells also demonstrate greater killing in GBOs with heterogeneity of endogenous EGFR and EGFR mutants, confirming its potential to more effectively treat GBM tumors by limiting the impact of tumor escape due to antigen loss.

With regard to the CAR T trial in recurrent GBM (12), the demonstrated tumor recurrence was likely due to the exclusive specificity of the scFv employed in the trial. The 2173 construct was chosen for its selective binding to a novel glycine residue formed at the exon 2–7 deletion in EGFRvIII and for a lack of cross-reactivity to wtEGFR (20). However, the binding affinity and target repertoire were of secondary importance. Given the co-occurrence of amplified wtEGFR with EGFRvIII and most ECD missense mutations (11), there is a clinically relevant rationale for targeting multiple EGFR alterations in the GBM population (25). Dual targeting of EGFR and EGFRvIII by CAR T and NK cells has been demonstrated in recent studies using scFvs specific for both antigens (26–29). Our work expands on that, as 806 CAR T cells were able to lyse GBM (U87MG, GSC5077) and non-GBM (K562) cell lines modified to express not only wtEGFR and EGFRvIII but also EGFR extracellular mutations. In comparison, 2173 CAR T cells exhibited specificity for EGFRvIII alone (12, 20). While 806 CAR treated animals did eventually reach experimental endpoints, their loss of weight, patchy hair, and red eyes were suggestive of the development of graft-vs-host disease and not tumor growth. This hypothesis was supported by a lack of palpable or visible tumor at autopsy.

GBM tumors are significantly heterogeneous, both intratumorally (30, 31) and intertumorally (6). Intratumorally, there are mixed cytological subtypes, exhibiting regional differences in gene expression, key genetic mutations, and chromosomal alterations. This polyclonal nature contributes to therapeutic resistance and tumor escape (32). To address intratumoral heterogeneity, relevant targeted therapies would ideally be able to target larger tumor cell populations within the entire tumor bulk. Given the co-occurrence of wtEGFR amplification seen with EGFR mutations and splice variants (24), the cross-reactive EGFR-targeting 806 scFv should provide greater tumor cell coverage, resulting in better tumor control. The potential

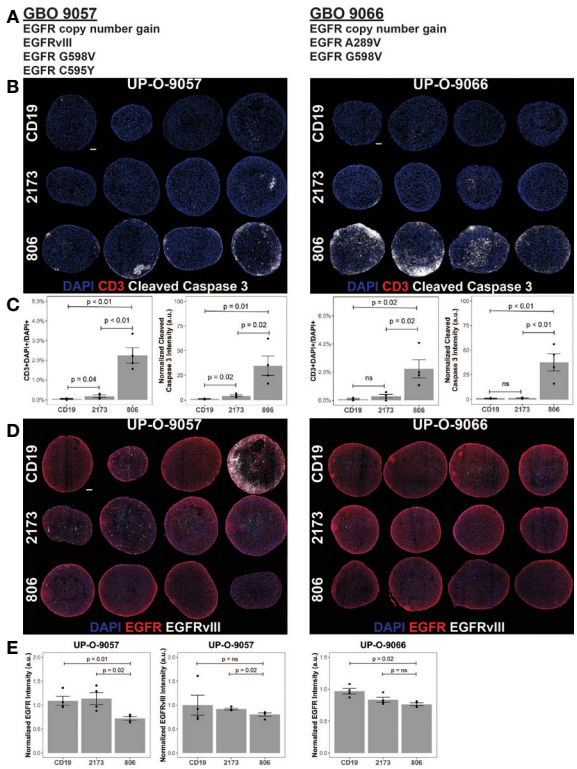

FIGURE 5 | 806 CAR T activity in heterogeneous GBOs highlights cross-reactivity of 806 binder against oncogenic EGFRs. CAR T coculture with GBOs was used to demonstrate anti-EGFR activity. **(A)** EGFR alterations identified in each GBO line. **(B)** Immunofluorescence images of CAR T cells engrafted GBOs, for four organoids per condition, 9057 (left) and 9066 (right). Blue = DAPI; red = $CD3^+$; white = cleaved caspase 3^+ ($CC3^+$), scale bar = 100 µm. **(C)** Quantification of $CD3^+$ cells (left) and $CC3^+$ cells (right) showing antitumor activity from the 806 CAR T cells. **(D)** Immunofluorescence images of CAR T cell targets in GBOs, for 9057 (left) and 9066 (right). Blue = DAPI; red = $EGFR^+$; white = $EGFRvIII^+$, scale bar = 100 µm. **(E)** Quantification of $EGFR^+$ (left) and $EGFRvIII^+$ signals (right) showing antitumor activity from the 806 CAR T cells. Error bars are ± standard error. ns, $p > 0.05$.

for broader tumor control was demonstrated through the high-fidelity, heterogeneous GBO model (22). GBOs have retained the originating tumor heterogeneity to a high degree, as assessed by both mRNA and protein levels. These "mini-tumors" provided the opportunity to test 806 CAR T cells against a target-heterogeneous tumor and showcase its ability to exert antitumor activity against a greater portion of the tumor than the compared 2173 CAR and CD19 CAR T cells. While the VAFs associated with the originating tumors of the GBOS allow for hypothesizing of independent EGFR mutant tumor populations, one caveat is that the NGS methods used do not allow for concrete determination of subpopulations. The data were subject to bias from tumor viability and number of reads of the sample. Additionally, the heterogeneity of the EGFR variants on amplified alleles is complicated by the mechanisms of amplification of EGFR. GBMs frequently harbor double minutes, extrachromosomal sequences of DNA that are acentric and lead to asymmetric distribution to daughter cells (33). This causes increased cell-to-cell heterogeneity of EGFR alterations in GBM.

Intertumoral variation, from patient to patient, reduces the applicable population for targeted therapies. However, there are gene families frequently found altered across GBM (6). In particular, EGFR amplification is found in up to 60% of GBMs. Concurrently with amplification, 30%–40% of GBM tumors express the constitutively active mutant variant, EGFRvIII (34). Combined with the intratumoral expression of EGFR variants, these data suggest that targeting the EGFR family of tumor-specific alterations may successfully address both inter- and intratumoral heterogeneity.

Several EGFRvIII-targeted agents are currently in development or in clinical trials for the treatment of GBM. Although the preclinical data from experimental studies evaluating these therapies have been promising, their efficacy in the clinic has yet to be conclusively demonstrated (35–37). In a vaccination approach to target the EGFRvIII in GBM patients, a phase III trial for newly diagnosed glioblastoma failed to show overall efficacy despite 60%–80% of recurrent tumors showing complete loss of EGFRvIII positive cells (38). Additional trials targeting EGFRvIII demonstrated similar loss of EGFRvIII concurrent with tumor recurrence (12, 39, 40). Similarly, the EGFRvIII-targeting CAR T trial illustrated the continued presence of EGFR amplification and oncogenic EGFR ECD missense mutations despite EGFRvIII antigen loss in posttreatment tumor specimens (12). These results confirm the need to target multiple EGFR alterations simultaneously.

Despite preclinical efficacy, the success of wtEGFR targeting mAbs cetuximab and panitumumab has been associated with on-target, off-tumor toxicity in other tumor types, due to their significant binding to EGFR expressed on normal tissues (41, 42). Their clinical activity in GBM has yet to be successfully demonstrated in large-scale studies. Coculture of 806 CAR T cells with basal physiologic EGFR-expressing normal tissue cell lines did not lead to significant cell killing in our work. Previous work has suggested that the 806 epitope is exposed on both mutated EGFR (EGFRvIII, $EGFR^{R108G/K}$, $EGFR^{A289D/T/V}$) as well as amplified wtEGFR found on tumors, but not accessible on wtEGFR found on normal tissue (43). The wtEGFR differences have been proposed to be due to different posttranslational mannose modifications and kinetics of EGFR trafficking in tumors compared to normal tissue (44). Multiple clinical trials with humanized mAb 806 conjugated to a microtubule inhibitor (ABT-414) have demonstrated only low levels of cutaneous toxicity (45–47). The therapeutic window of CAR T cells for tumor-associated antigens relies on the quantitative difference between antigen-overexpressing tumor and antigen-low normal tissue. Preclinical studies targeting EGFR and erbB2 with affinity-lowered CAR T cells have demonstrated potent antitumor effects against high antigen density while sparing low antigen density normal tissue (48–50). The demonstrated cross-reactivity of 806 CAR T cells for EGFR alterations, including amplified wtEGFR, EGFRvIII, and ECD missense mutations, suggests that 806 CAR T cells may be a more efficacious therapeutic strategy to achieve tumor control and prevent tumor escape *via* target antigen loss.

DATA AVAILABILITY STATEMENT

The original contributions presented in the study are included in the article/supplementary material. Further inquiries can be directed to the corresponding author.

ETHICS STATEMENT

The studies involving human participants were reviewed and approved by the University of Pennsylvania Institutional Review Board. The patients/participants provided their written informed consent to participate in this study. The animal study was reviewed and approved by University of Pennsylvania Institutional Animal Care and Use Committee.

AUTHOR CONTRIBUTIONS

RT and ZB conceived and carried out the experiments, with contributions from YY, LZ, JZ, and DZ for specific assays. MM, GLM, HS, and DO'R supervised the project. RT and ZB wrote the manuscript. All authors contributed to the article and approved the submitted version.

FUNDING

The described work was funded by the GBM Translational Center of Excellence, the Templeton Family Initiative in Neuro-Oncology, The Maria and Gabriele Troiano Brain Cancer Immunotherapy Fund, and NIH (R35NS116843 to HS and R35NS097370 to GLM).

ACKNOWLEDGMENTS

The authors thank the Human Immunology Core at the University of Pennsylvania for providing leukocytes for the described work, the Stem Cell and Xenograft Core at the University of Pennsylvania for assistance with the animal work, and the Small Animal Imaging Facility at the University of Pennsylvania for the bioluminescence imaging.

REFERENCES

1. Castellarin M, Watanabe K, June CH, Kloss CC, Posey AD Jr. Driving Cars to the Clinic for Solid Tumors. *Gene Ther* (2018) 25(3):165–75. doi: 10.1038/s41434-018-0007-x
2. Fesnak AD, June CH, Levine BL. Engineered T Cells: The Promise and Challenges of Cancer Immunotherapy. *Nat Rev Cancer* (2016) 16(9):566–81. doi: 10.1038/nrc.2016.97
3. Porter DL, Levine BL, Kalos M, Bagg A, June CH. Chimeric Antigen Receptor-Modified T Cells in Chronic Lymphoid Leukemia. *N Engl J Med* (2011) 365(8):725–33. doi: 10.1056/NEJMoa1103849
4. Jackson C, Ruzevick J, Phallen J, Belcaid Z, Lim M. Challenges in Immunotherapy Presented by the Glioblastoma Multiforme Microenvironment. *Clin Dev Immunol* (2011) 2011:732413. doi: 10.1155/2011/732413
5. Nduom EK, Weller M, Heimberger AB. Immunosuppressive Mechanisms in Glioblastoma. *Neuro Oncol* (2015) 17(Suppl 7):vii9–vii14. doi: 10.1093/neuonc/nov151
6. Brennan CW, Verhaak RG, McKenna A, Campos B, Noushmehr H, Salama SR, et al. The Somatic Genomic Landscape of Glioblastoma. *Cell* (2013) 155 (2):462–77. doi: 10.1016/j.cell.2013.09.034
7. Cominelli M, Grisanti S, Mazzoleni S, Branca C, Buttolo L, Furlan D, et al. EGFR Amplified and Overexpressing Glioblastomas and Association With Better Response to Adjuvant Metronomic Temozolomide. *J Natl Cancer Inst* (2015) 107(5). doi: 10.1093/jnci/djv041
8. Lopez-Gines C, Gil-Benso R, Ferrer-Luna R, Benito R, Serna E, Gonzalez-Darder J, et al. New Pattern of EGFR Amplification in Glioblastoma and the Relationship of Gene Copy Number With Gene Expression Profile. *Mod Pathol* (2010) 23(6):856–65. doi: 10.1038/modpathol.2010.62
9. Nishikawa R, Ji XD, Harmon RC, Lazar CS, Gill GN, Cavenee WK, et al. A Mutant Epidermal Growth Factor Receptor Common in Human Glioma Confers Enhanced Tumorigenicity. *Proc Natl Acad Sci USA* (1994) 91 (16):7727–31. doi: 10.1073/pnas.91.16.7727
10. Lee JC, Vivanco I, Beroukhim R, Huang JH, Feng WL, DeBiasi RM, et al. Epidermal Growth Factor Receptor Activation in Glioblastoma Through Novel Missense Mutations in the Extracellular Domain. *PloS Med* (2006) 3 (12):e485. doi: 10.1371/journal.pmed.0030485
11. Binder ZA, Thorne AH, Bakas S, Wileyto EP, Bilello M, Akbari H, et al. Epidermal Growth Factor Receptor Extracellular Domain Mutations in Glioblastoma Present Opportunities for Clinical Imaging and Therapeutic Development. *Cancer Cell* (2018) 34(1):163–77.e7. doi: 10.1016/j.ccell.2018.06.006
12. O'Rourke DM, Nasrallah MP, Desai A, Melenhorst JJ, Mansfield K, Morrissette JJD, et al. A Single Dose of Peripherally Infused EGFRvIII-Directed CAR T Cells Mediates Antigen Loss and Induces Adaptive

Resistance in Patients With Recurrent Glioblastoma. *Sci Transl Med* (2017) 9 (399). doi: 10.1126/scitranslmed.aaa0984
13. Gan HK, Burgess AW, Clayton AH, Scott AM. Targeting of a Conformationally Exposed, Tumor-Specific Epitope of EGFR as a Strategy for Cancer Therapy. *Cancer Res* (2012) 72(12):2924–30. doi: 10.1158/0008-5472.CAN-11-3898
14. Panousis C, Rayzman VM, Johns TG, Renner C, Liu Z, Cartwright G, et al. Engineering and Characterisation of Chimeric Monoclonal Antibody 806 (Ch806) for Targeted Immunotherapy of Tumours Expressing De2-7 EGFR or Amplified EGFR. *Br J Cancer* (2005) 92(6):1069–77. doi: 10.1038/sj.bjc.6602470
15. Phillips AC, Boghaert ER, Vaidya KS, Mitten MJ, Norvell S, Falls HD, et al. ABT-414, an Antibody-Drug Conjugate Targeting a Tumor-Selective EGFR Epitope. *Mol Cancer Ther* (2016) 15(4):661–9. doi: 10.1158/1535-7163.MCT-15-0901
16. Lassman A, Pugh S, Wang T, Aldape K, Gan H, Preusser M, et al. ACTR-21. A Randomized, Double-Blind, Placebo-Controlled Phase 3 Trial of Depatuxizumab Mafooditin (ABT-414) in Epidermal Growth Factor Receptor (EGFR) Amplified (AMP) Newly Diagnosed Glioblastosma (nGBM). *Neuro-Oncology* (2019) 21(Supplement_6):vi17–vi. doi: 10.1093/neuonc/noz175.064
17. Milone MC, Fish JD, Carpenito C, Carroll RG, Binder GK, Teachey D, et al. Chimeric Receptors Containing CD137 Signal Transduction Domains Mediate Enhanced Survival of T Cells and Increased Antileukemic Efficacy In Vivo. *Mol Ther* (2009) 17(8):1453–64. doi: 10.1038/mt.2009.83
18. Imai C, Mihara K, Andreansky M, Nicholson IC, Pui CH, Geiger TL, et al. Chimeric Receptors With 4-1BB Signaling Capacity Provoke Potent Cytotoxicity Against Acute Lymphoblastic Leukemia. *Leukemia* (2004) 18 (4):676–84. doi: 10.1038/sj.leu.2403302
19. Carpenito C, Milone MC, Hassan R, Simonet JC, Lakhal M, Suhoski MM, et al. Control of Large, Established Tumor Xenografts With Genetically Retargeted Human T Cells Containing CD28 and CD137 Domains. *Proc Natl Acad Sci USA* (2009) 106(9):3360–5. doi: 10.1073/pnas.0813101106
20. Johnson LA, Scholler J, Ohkuri T, Kosaka A, Patel PR, McGettigan SE, et al. Rational Development and Characterization of Humanized Anti-EGFR Variant III Chimeric Antigen Receptor T Cells for Glioblastoma. *Sci Transl Med* (2015) 7(275):275ra22. doi: 10.1126/scitranslmed.aaa4963
21. Yin Y, Boesteanu AC, Binder ZA, Xu C, Reid RA, Rodriguez JL, et al. Checkpoint Blockade Reverses Anergy in IL-13ralpha2 Humanized scFv-Based CAR T Cells to Treat Murine and Canine Gliomas. *Mol Ther Oncolytics* (2018) 11:20–38. doi: 10.1016/j.omto.2018.08.002
22. Jacob F, Salinas RD, Zhang DY, Nguyen PTT, Schnoll JG, Wong SZH, et al. A Patient-Derived Glioblastoma Organoid Model and Biobank Recapitulates Inter- and Intra-Tumoral Heterogeneity. *Cell* (2020) 180(1):188–204.e22. doi: 10.1016/j.cell.2019.11.036
23. Jacob F, Ming GL, Song H. Generation and Biobanking of Patient-Derived Glioblastoma Organoids and Their Application in CAR T Cell Testing. *Nat Protoc* (2020) 15(12):4000–33. doi: 10.1038/s41596-020-0402-9
24. Nasrallah MP, Binder ZA, Oldridge DA, Zhao J, Lieberman DB, Roth JJ, et al. Molecular Neuropathology in Practice: Clinical Profiling and Integrative Analysis of Molecular Alterations in Glioblastoma. *Acad Pathol* (2019) 6:2374289519848353. doi: 10.1177/2374289519848353
25. Reilly EB, Phillips AC, Buchanan FG, Kingsbury G, Zhang Y, Meulbroek JA, et al. Characterization of ABT-806, a Humanized Tumor-Specific Anti-EGFR Monoclonal Antibody. *Mol Cancer Ther* (2015) 14(5):1141–51. doi: 10.1158/1535-7163.MCT-14-0820
26. Genssler S, Burger MC, Zhang C, Oelsner S, Mildenberger I, Wagner M, et al. Dual Targeting of Glioblastoma With Chimeric Antigen Receptor-Engineered Natural Killer Cells Overcomes Heterogeneity of Target Antigen Expression and Enhances Antitumor Activity and Survival. *Oncoimmunology* (2016) 5(4): e1119354. doi: 10.1080/2162402X.2015.1119354
27. Han J, Chu J, Keung Chan W, Zhang J, Wang Y, Cohen JB, et al. CAR-Engineered NK Cells Targeting Wild-Type EGFR and EGFRvIII Enhance Killing of Glioblastoma and Patient-Derived Glioblastoma Stem Cells. *Sci Rep* (2015) 5:11483. doi: 10.1038/srep11483
28. Jiang H, Gao H, Kong J, Song B, Wang P, Shi B, et al. Selective Targeting of Glioblastoma With EGFRvIII/EGFR Bitargeted Chimeric Antigen Receptor T Cell. *Cancer Immunol Res* (2018) 6(11):1314–26. doi: 10.1158/2326-6066.CIR-18-0044
29. Ravanpay AC, Gust J, Johnson AJ, Rolczynski LS, Cecchini M, Chang CA, et al. EGFR806-CAR T Cells Selectively Target a Tumor-Restricted EGFR Epitope in Glioblastoma. *Oncotarget* (2019) 10(66):7080–95. doi: 10.18632/oncotarget.27389
30. Darmanis S, Sloan SA, Croote D, Mignardi M, Chernikova S, Samghababi P, et al. Single-Cell RNA-Seq Analysis of Infiltrating Neoplastic Cells at the Migrating Front of Human Glioblastoma. *Cell Rep* (2017) 21(5):1399–410. doi: 10.1016/j.celrep.2017.10.030
31. Patel AP, Tirosh I, Trombetta JJ, Shalek AK, Gillespie SM, Wakimoto H, et al. Single-Cell RNA-Seq Highlights Intratumoral Heterogeneity in Primary Glioblastoma. *Science* (2014) 344(6190):1396–401. doi: 10.1126/science.1254257
32. Skaga E, Kulesskiy E, Fayzullin A, Sandberg CJ, Potdar S, Kyttala A, et al. Intertumoral Heterogeneity in Patient-Specific Drug Sensitivities in Treatment-Naive Glioblastoma. *BMC Cancer* (2019) 19(1):628. doi: 10.1186/s12885-019-5861-4
33. Bailey C, Shoura MJ, Mischel PS, Swanton C. Extrachromosomal DNA-Relieving Heredity Constraints, Accelerating Tumour Evolution. *Ann Oncol* (2020) 31(7):884–93. doi: 10.1016/j.annonc.2020.03.303
34. Gan HK, Kaye AH, Luwor RB. The EGFRvIII Variant in Glioblastoma Multiforme. *J Clin Neurosci* (2009) 16(6):748–54. doi: 10.1016/j.jocn.2008.12.005
35. Choi BD, Archer GE, Mitchell DA, Heimberger AB, McLendon RE, Bigner DD, et al. EGFRvIII-Targeted Vaccination Therapy of Malignant Glioma. *Brain Pathol* (2009) 19(4):713–23. doi: 10.1111/j.1750-3639.2009.00318.x
36. Karpel-Massler G, Schmidt U, Unterberg A, Halatsch ME. Therapeutic Inhibition of the Epidermal Growth Factor Receptor in High-Grade Gliomas: Where do We Stand? *Mol Cancer Res* (2009) 7(7):1000–12. doi: 10.1158/1541-7786.MCR-08-0479
37. Rosenthal M, Curry R, Reardon DA, Rasmussen E, Upreti VV, Damore MA, et al. Safety, Tolerability, and Pharmacokinetics of Anti-EGFRvIII Antibody-Drug Conjugate AMG 595 in Patients With Recurrent Malignant Glioma Expressing EGFRvIII. *Cancer Chemother Pharmacol* (2019) 84(2):327–36. doi: 10.1007/s00280-019-03879-2
38. Heimberger AB, Sampson JH. The PEPvIII-KLH (CDX-110) Vaccine in Glioblastoma Multiforme Patients. *Expert Opin Biol Ther* (2009) 9(8):1087–98. doi: 10.1517/14712590903124346
39. Weller M, Butowski N, Tran DD, Recht LD, Lim M, Hirte H, et al. Rindopepimut With Temozolomide for Patients With Newly Diagnosed, EGFRvIII-Expressing Glioblastoma (ACT IV): A Randomised, Double-Blind, International Phase 3 Trial. *Lancet Oncol* (2017) 18(10):1373–85. doi: 10.1016/S1470-2045(17)30517-X
40. Schuster J, Lai RK, Recht LD, Reardon DA, Paleologos NA, Groves MD, et al. Multicenter Trial of Rindopepimut (CDX-110) in Newly Diagnosed Glioblastoma: The ACT III Study. *Neuro Oncol* (2015) 17(6):854–61. doi: 10.1093/neuonc/nou348
41. Saltz LB, Meropol NJ, Loehrer PJ, Needle MN, Kopit J, Mayer RJ. Phase II Trial of Cetuximab in Patients With Refractory Colorectal Cancer That Expresses the Epidermal Growth Factor Receptor. *J Clin Oncol* (2004) 22 (7):1201–8. doi: 10.1200/JCO.2004.10.182
42. Holch JW, Held S, Stintzing S, Fischer von Weikersthal L, Decker T, Kiani A, et al. Relation of Cetuximab-Induced Skin Toxicity and Early Tumor Shrinkage in Metastatic Colorectal Cancer Patients: Results of the Randomized Phase 3 Trial FIRE-3 (AIO Krk0306). *Ann Oncol* (2020) 31 (1):72–8. doi: 10.1016/j.annonc.2019.10.001
43. Orellana L, Thorne AH, Lema R, Gustavsson J, Parisian AD, Hospital A, et al. Oncogenic Mutations at the EGFR Ectodomain Structurally Converge to Remove a Steric Hindrance on a Kinase-Coupled Cryptic Epitope. *Proc Natl Acad Sci USA* (2019) 116(20):10009–18. doi: 10.1073/pnas.1821442116
44. Johns TG, Mellman I, Cartwright GA, Ritter G, Old LJ, Burgess AW, et al. The Antitumor Monoclonal Antibody 806 Recognizes a High-Mannose Form of the EGF Receptor That Reaches the Cell Surface When Cells Over-Express the Receptor. *FASEB J* (2005) 19(7):780–2. doi: 10.1096/fj.04-1766fje
45. Cleary JM, Reardon DA, Azad N, Gandhi L, Shapiro GI, Chaves J, et al. A Phase 1 Study of ABT-806 in Subjects With Advanced Solid Tumors. *Invest New Drugs* (2015) 33(3):671–8. doi: 10.1007/s10637-015-0234-6
46. Reardon DA, Lassman AB, van den Bent M, Kumthekar P, Merrell R, Scott AM, et al. Efficacy and Safety Results of ABT-414 in Combination With Radiation and Temozolomide in Newly Diagnosed Glioblastoma. *Neuro Oncol* (2017) 19(7):965–75. doi: 10.1093/neuonc/now257

47. van den Bent M, Gan HK, Lassman AB, Kumthekar P, Merrell R, Butowski N, et al. Efficacy of Depatuxizumab Mafodotin (ABT-414) Monotherapy in Patients With EGFR-Amplified, Recurrent Glioblastoma: Results From a Multi-Center, International Study. *Cancer Chemother Pharmacol* (2017) 80 (6):1209–17. doi: 10.1007/s00280-017-3451-1
48. Caruso HG, Hurton LV, Najjar A, Rushworth D, Ang S, Olivares S, et al. Tuning Sensitivity of CAR to EGFR Density Limits Recognition of Normal Tissue While Maintaining Potent Antitumor Activity. *Cancer Res* (2015) 75 (17):3505–18. doi: 10.1158/0008-5472.CAN-15-0139
49. Liu X, Jiang S, Fang C, Yang S, Olalere D, Pequignot EC, et al. Affinity-Tuned ErbB2 or EGFR Chimeric Antigen Receptor T Cells Exhibit an Increased Therapeutic Index Against Tumors in Mice. *Cancer Res* (2015) 75(17):3596–607. doi: 10.1158/0008-5472.CAN-15-0159
50. Richman SA, Milone MC. Neurotoxicity Associated With a High-Affinity GD2 CAR-Response. *Cancer Immunol Res* (2018) 6(4):496–7. doi: 10.1158/2326-6066.CIR-18-0090

Author Disclaimer: All claims expressed in this article are solely those of the authors and do not necessarily represent those of their affiliated organizations, or those of the publisher, the editors, and the reviewers. Any product that may be evaluated in this article, or claim that may be made by its manufacturer, is not guaranteed or endorsed by the publisher.

Conflict of Interest: The described work involves patent applications owned by the University of Pennsylvania. MM is an inventor on multiple issued and pending patents related to CAR T cell technology used in this study. These patents are assigned to the University of Pennsylvania and have been licensed to third parties for which royalties have or may be received.

The remaining authors declare that the research was conducted in the absence of any commercial or financial relationships that could be construed as a potential conflict of interest.

Publisher's Note: All claims expressed in this article are solely those of the authors and do not necessarily represent those of their affiliated organizations, or those of the publisher, the editors and the reviewers. Any product that may be evaluated in this article, or claim that may be made by its manufacturer, is not guaranteed or endorsed by the publisher.

Advantages of publishing in Frontiers

OPEN ACCESS
Articles are free to read for greatest visibility and readership

FAST PUBLICATION
Around 90 days from submission to decision

HIGH QUALITY PEER-REVIEW
Rigorous, collaborative, and constructive peer-review

TRANSPARENT PEER-REVIEW
Editors and reviewers acknowledged by name on published articles

Frontiers
Avenue du Tribunal-Fédéral 34
1005 Lausanne | Switzerland

Visit us: www.frontiersin.org
Contact us: frontiersin.org/about/contact

REPRODUCIBILITY OF RESEARCH
Support open data and methods to enhance research reproducibility

DIGITAL PUBLISHING
Articles designed for optimal readership across devices

FOLLOW US
@frontiersin

IMPACT METRICS
Advanced article metrics track visibility across digital media

EXTENSIVE PROMOTION
Marketing and promotion of impactful research

LOOP RESEARCH NETWORK
Our network increases your article's readership